EXPLORING THE POTENTIAL OF PSMA-PET IMAGING ON PERSONALIZED PROSTATE CANCER TREATMENT

EDITED BY: Constantinos Zamboglou, Xuefeng Qiu, Harun Ilhan and Trevor Royce

PUBLISHED IN: Frontiers in Oncology

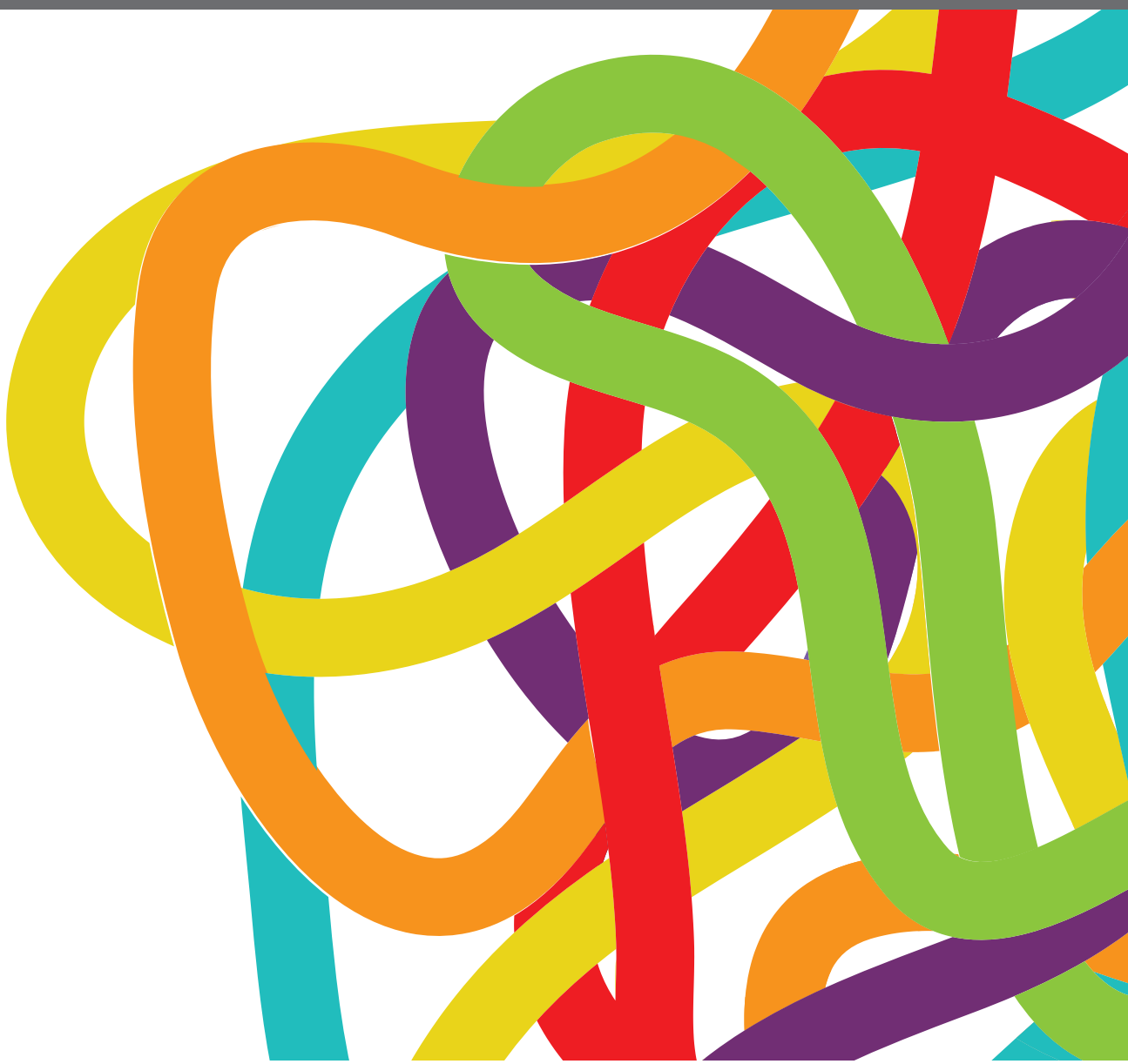

frontiers Research Topics

ISSN 1664-8714
ISBN 978-2-88974-574-6
DOI 10.3389/978-2-88974-574-6

About Frontiers

Frontiers is more than just an open-access publisher of scholarly articles: it is a pioneering approach to the world of academia, radically improving the way scholarly research is managed. The grand vision of Frontiers is a world where all people have an equal opportunity to seek, share and generate knowledge. Frontiers provides immediate and permanent online open access to all its publications, but this alone is not enough to realize our grand goals.

Frontiers Journal Series

The Frontiers Journal Series is a multi-tier and interdisciplinary set of open-access, online journals, promising a paradigm shift from the current review, selection and dissemination processes in academic publishing. All Frontiers journals are driven by researchers for researchers; therefore, they constitute a service to the scholarly community. At the same time, the Frontiers Journal Series operates on a revolutionary invention, the tiered publishing system, initially addressing specific communities of scholars, and gradually climbing up to broader public understanding, thus serving the interests of the lay society, too.

Dedication to Quality

Each Frontiers article is a landmark of the highest quality, thanks to genuinely collaborative interactions between authors and review editors, who include some of the world's best academicians. Research must be certified by peers before entering a stream of knowledge that may eventually reach the public - and shape society; therefore, Frontiers only applies the most rigorous and unbiased reviews.
Frontiers revolutionizes research publishing by freely delivering the most outstanding research, evaluated with no bias from both the academic and social point of view. By applying the most advanced information technologies, Frontiers is catapulting scholarly publishing into a new generation.

What are Frontiers Research Topics?

Frontiers Research Topics are very popular trademarks of the Frontiers Journals Series: they are collections of at least ten articles, all centered on a particular subject. With their unique mix of varied contributions from Original Research to Review Articles, Frontiers Research Topics unify the most influential researchers, the latest key findings and historical advances in a hot research area! Find out more on how to host your own Frontiers Research Topic or contribute to one as an author by contacting the Frontiers Editorial Office: frontiersin.org/about/contact

EXPLORING THE POTENTIAL OF PSMA-PET IMAGING ON PERSONALIZED PROSTATE CANCER TREATMENT

Topic Editors:
Constantinos Zamboglou, University of Freiburg Medical Center, Germany
Xuefeng Qiu, Department of Urology, Nanjing Drum Tower Hospital, China
Harun Ilhan, LMU Munich University Hospital, Germany
Trevor Royce, University of North Carolina at Chapel Hill, United States

Citation: Zamboglou, C., Qiu, X., Ilhan, H., Royce, T., eds. (2022). Exploring the Potential of PSMA-PET Imaging on Personalized Prostate Cancer Treatment. Lausanne: Frontiers Media SA. doi: 10.3389/978-2-88974-574-6

Table of Contents

frontiers in Oncology

EDITORIAL
published: 02 February 2022
doi: 10.3389/fonc.2022.832747

Editorial: Exploring the Potential of PSMA-PET Imaging on Personalized Prostate Cancer Treatment

Harun Ilhan[1]*, *Trevor Royce*[2,3], *Xuefeng Qiu*[4] and *Constantinos Zamboglou*[5,6]*

[1] Department of Nuclear Medicine, University Hospital, Ludwigs-Maximilian Universitaet (LMU) Munich, Munich, Germany, [2] Department of Radiation Oncology, University of North Carolina at Chapel Hill School of Medicine, Chapel Hill, NC, United States, [3] Flatiron Health, New York, NY, United States, [4] Department of Urology, Affiliated Drum Tower Hospital, Medical School of Nanjing University, Nanjing, China, [5] Department of Radiation Oncology, Medical Center – University of Freiburg, Faculty of Medicine, University of Freiburg, Freiburg, Germany, [6] German Oncology Center, European University Cyprus, Limassol, Cyprus

Keywords: prostate specific membrane antigen (PSMA), prostate cancer, personalized and precision medicine (PPM), surgery, radiotherapy

Editorial on the Research Topic

Exploring the Potential of PSMA-PET Imaging on Personalized Prostate Cancer Treatment

OPEN ACCESS

Edited and reviewed by:
Zaver Bhujwalla,
Johns Hopkins University,
United States

***Correspondence:**
Constantinos Zamboglou
constantinos.zamboglou@uniklinik-freiburg.de
Harun Ilhan
harun.ilhan@med.uni-muenchen.de

Specialty section:
This article was submitted to Cancer Imaging and Image-directed Interventions, a section of the journal Frontiers in Oncology

Received: *10 December 2021*
Accepted: *14 January 2022*
Published: *02 February 2022*

Citation:
Ilhan H, Royce T, Qiu X and Zamboglou C (2022) Editorial: Exploring the Potential of PSMA-PET Imaging on Personalized Prostate Cancer Treatment. Front. Oncol. 12:832747. doi: 10.3389/fonc.2022.832747

INTRODUCTION

Prostate cancer (PCa) is the second most frequent cancer diagnosis made in men worldwide (1). Accurate and reliable diagnostic medical imaging is a frequent prerequisite for personalized treatment approaches in patients with PCa by enabling, in part, (i) understanding extent of disease, (ii) accurate segmentation of PCa lesions and, (iii) non-invasive tumor characterization, for example, using radiomics or artificial intelligence tools (2).

Prostate Specific Membrane Antigen (PSMA) has been found to be selectively overexpressed in PCa cells (3) and can be traced by radio-labelled peptide ligands in positron emission tomography (PSMA-PET). First studies suggested excellent diagnostic accuracy and a major impact on therapeutic approaches for PSMA-PET in newly diagnosed (4), recurrent (5) or metastatic PCa patients (4). The goal of this Research Topic was to concentrate scientific contributions on the growing evidence of integrating PSMA-PET imaging in personalized PCa treatment concepts.

The Research Topic accepted 15 articles including a total of 126 authors, demonstrating the growing interest in the field of PSMA-PET imaging. The manuscripts of the Research Topic can be divided into the following topics.

PSMA-PET FOR PRIMARY LOCALIZED PCA

The accurate segmentation of the intraprostatic tumor mass is a prerequisite for precise targeted-biopsy and focal therapy (FT) approaches in patients with localized PCa. The current imaging gold-standard for intraprostatic tumor detection and delineation is multiparametric magnetic resonance imaging (mpMRI) (6, 7). However, mpMRI was reported to be associated with underestimation of the true intraprostatic PCa extent (Kramer et al.). Recently, it has been suggested that PSMA-PET

might give complementary information for intraprostatic tumor detection (8) and guidance of FT (9). In this Research Topic, Spohn et al. compared manual and semi-automatic methods for intraprostatic tumor delineation based on 18F-PSMA-1007 PET/CT images. By using whole-section surgery specimen as the standard of reference the authors proposed several methods with high sensitivity or high specificity. In another work by Spohn et al. the authors used the same methodology in terms of histology reference to perform an *in-silico* radiotherapy planning study (The authors simulated a focal radiotherapy dose escalation based on PSMA-PET and mpMR images and demonstrated that a dosimetric sparing of the intraprostatic urethra might increase the therapeutic ratio.

PSMA-PET FOR RECURRENT PCA

Biochemical recurrence (BCR) after primary curative intent radiotherapy or radical prostatectomy represents one of the major challenges in the management of PCa. In the recent years, multiple ^{68}Ga- and ^{18}F-labelled PSMA-targeting radiotracers have been introduced and recommended in several guidelines (10–12). Furthermore, ^{68}Ga-PSMA-11 and ^{18}F-DCFPyL received recent FDA-approval for imaging of BCR (13, 14).

This Research Topic includes two meta-analyses evaluating the value of several PET-radiopharmaceuticals for the detection of BCR. Wang et al. included 46 studies and compared the three ^{18}F-labeled radiotracers ^{18}F-choline targeting the phospholipid metabolism, the amino acid ^{8}F-Fluciclovine, and ^{18}F-labelled PSMA-targeting tracers including PSMA-1007, rhPSMA-7, and DCFPyL. Highest detection rates, even at low PSA levels were observed for ^{18}F-PSMA tracers, with a sensitivity of 58% at PSA levels of <0.5 ng/ml compared to 35% and 23% for ^{18}F-Choline and ^{18}F-Fluciclovine, respectively. In a detailed review and meta-analysis on detection rates for ^{18}F-DCFPyL, Sun et al. included 844 patients from 9 studies. With a pooled sensitivity of 88.8% at PSA levels ≥0.5 ng/ml and 47.2% at <0.5 ng/ml, ^{18}F-DCFPyL provides high detection rates for BCR despite high heterogeneity in the overall cohort.

The impact of PSMA-PET imaging on the therapeutic management of PCa patients represents another major aspect of this Research Topic. In a multicenter retrospective analysis, Schmidt-Hegemann et al. evaluated biochemical recurrence-free survival (BRFS) after salvage radiotherapy (RT) in a cohort of 459 patients without lymph node or distant metastasis determined by conventional imaging and additional ^{68}Ga-PSMA-PET or conventional imaging alone. The authors did not find any significant impact of prior ^{68}Ga-PSMA PET on BRFS despite more adverse clinical features in the PET cohort. These results indicate that salvage RT should not be postponed until a PSMA PET-positive result is observed in patients with BCR. Several work-groups all over the globe have evaluated the impact of different PSMA-PET tracers on salvage RT. The high sensitivity of PSMA-PET, specifically for small lymph node and bone metastases has a high impact on target volume definition. According the article by Bottke et al. including only patients with PSA levels ≤0.5 ng/ml, PSMA-PET has a major impact on the target volume definition in 17% and a minor impact in 11%. According to the authors, PSMA-PET based RT might have impact on patients survival. Vogel et al. evaluate the toxicity and outcome of dose escalated salvage RT (DE-SRT) after PSMA-PET compared to conventional salvage RT with. There were no significant differences regarding toxicity rates and the majority of patients should PSA response indicating the feasibility of DE-SRT for personalized RT planning.

Finally, this Research Topic also includes an article on the administrative challenges when imaging PCa patients with BCR. Young et al. provide a detailed description of a PSMA-PET registry in Ontario, Canada including the impact of PSMA-PET imaging on patient management, stakeholder perspectives and interviews. They provide data for ^{18}F-DCFPyL in more than 1700 men since 2018. The main idea is to summarize important real world data to provide improved access to novel PET radiopharmaceuticals also in the future.

PSMA-PET FOR METASTATIC PCA

Local therapy applications in the metastatic setting is one of the exciting developing frontiers of prostate cancer treatment; for example the randomized STOMP trial (15) which found an androgen deprivation therapy-free survival benefit with metastasis-directed therapy (e.g., ablation with stereotactic radiotherapy) for oligorecurrent prostate cancer. The improved performance of PSMA-based imaging techniques amplify this excitement, with the potential to detect earlier metastases. Henkenberens et al. add to the developing body of literature in this area by reporting their experience of 42 patients with oligometastatic CRPC (141 PSMA positive metastases) receiving radiation to all PSMA positive lesions. Their results further suggest such approaches may delay the need for systemic therapies (eg second-line systemic treatment free survival).

Beyond target delineation for the above local therapy applications, PSMA imaging will also likely be valuable in assessing systemic treatment response for metastatic disease. In this context it should be mentioned that PSMA theranostics may result in damage to some PSMA expressing normal tissues such as salivary glands during PSMA-radioligand therapy. Mittlmeier et al. put effort into characterizing and standardizing PSMA-measured metastatic lymph node treatment responses by correlating PSMA-based tumor volumes with a CT reference in fifty patients with metastatic prostate cancer. In their investigation, they derive a proposed SUV threshold value for this purpose. These sorts of investigations will lay the groundwork for future clinical research as PSMA-applications continue to expand. Importantly, these applications can enhance imaging performance by appropriately accounting for normal tissues (ie physiologic uptake of radiotracer). In this Research Topic, Shi et al. published their efforts into characterizing this as it relates to peripheral ganglia physiologic uptake versus pathologic lymph node metastases uptake among 138 prostate cancer patients who underwent both PSMA and FDG scans (Shi et al.; Shi et al.).

CONCLUSION

The evolving field of PSMA-targeted diagnostic imaging and therapeutics (theranostics) promise to advance the management of PCa patients in all stages of the disease. Exciting opportunities abound with PSMA-theranostics currently in the discovery pipeline. In a Mini Review by Ng et al. a vision for multidisciplinary use of PSMA theranostics was presented. We fully agree with Ng et al., who conclude by highlighting that the collaboration across the multidisciplinary prostate cancer team will be essential in maximizing the impact of these novel techniques.

AUTHOR CONTRIBUTIONS

All authors contributed to the article and approved the submitted version.

REFERENCES

1. Rawla P. Epidemiology of Prostate Cancer. *World J Oncol* (2019) 10(2):63–89. doi: 10.14740/wjon1191
2. Kostyszyn D, Fechter T, Bartl N, Grosu AL, Gratzke C, Sigle A, et al. Intraprostatic Tumor Segmentation on PSMA PET Images in Patients With Primary Prostate Cancer With a Convolutional Neural Network. *J Nucl Med* (2021) 62(6):823–8. doi: 10.2967/jnumed.120.254623
3. Bravaccini S, Puccetti M, Bocchini M, Ravaioli S, Celli M, Scarpi E, et al. PSMA Expression: A Potential Ally for the Pathologist in Prostate Cancer Diagnosis. *Sci Rep* (2018) 8(1):4254. doi: 10.1038/s41598-018-22594-1
4. Hofman MS, Lawrentschuk N, Francis RJ, Tang C, Vela I, Thomas P, et al. Prostate-Specific Membrane Antigen PET-CT in Patients With High-Risk Prostate Cancer Before Curative-Intent Surgery or Radiotherapy (proPSMA): A Prospective, Randomised, Multicentre Study. *Lancet* (2020) 395 (10231):1208–16. doi: 10.1016/S0140-6736(20)30314-7
5. Fendler WP, Calais J, Eiber M, Flavell RR, Mishoe A, Feng FY, et al. Assessment of 68Ga-PSMA-11 PET Accuracy in Localizing Recurrent Prostate Cancer: A Prospective Single-Arm Clinical Trial. *JAMA Oncol* (2019) 5(6):856–63. doi: 10.1001/jamaoncol.2019.0096
6. Kerkmeijer LGW, Groen VH, Pos FJ, Haustermans K, Monninkhof EM, Smeenk RJ, et al. Focal Boost to the Intraprostatic Tumor in External Beam Radiotherapy for Patients With Localized Prostate Cancer: Results From the FLAME Randomized Phase III Trial. *J Clin Oncol* (2021) 39(7):787–96. doi: 10.1200/JCO.20.02873
7. Ahdoot M, Wilbur AR, Reese SE, Lebastchi AH, Mehralivand S, Gomella PT, et al. MRI-Targeted, Systematic, and Combined Biopsy for Prostate Cancer Diagnosis. *N Engl J Med* (2020) 382(10):917–28. doi: 10.1056/NEJMoa1910038
8. Lam TBL, MacLennan S, Willemse PM, Mason MD, Plass K, Shepherd R, et al. EAU-EANM-ESTRO-ESUR-SIOG Prostate Cancer Guideline Panel Consensus Statements for Deferred Treatment With Curative Intent for Localised Prostate Cancer From an International Collaborative Study (DETECTIVE Study). *Eur Urol* (2019) 76(6):790–813. doi: 10.1016/j.eururo.2019.09.020
9. Zamboglou C, Thomann B, Koubar K, Bronsert P, Krauss T, Rischke HC, et al. Focal Dose Escalation for Prostate Cancer Using (68)Ga-HBED-CC PSMA PET/CT and MRI: A Planning Study Based on Histology Reference. *Radiat Oncol* (2018) 13(1):81. doi: 10.1186/s13014-018-1036-8
10. Mottet N, van den Bergh RCN, Briers E, Van den Broeck T, Cumberbatch MG, De Santis M, et al. EAU-EANM-ESTRO-ESUR-SIOG Guidelines on Prostate Cancer-2020 Update. Part 1: Screening, Diagnosis, and Local Treatment With Curative Intent. *Eur Urol* (2021) 79(2):243–62. doi: 10.1016/j.eururo.2020.09.042
11. Parker C, Castro E, Fizazi K, Heidenreich A, Ost P, Procopio G, et al. Prostate Cancer: ESMO Clinical Practice Guidelines for Diagnosis, Treatment and Follow-Up. *Ann Oncol* (2020) 31(9):1119–34. doi: 10.1016/j.annonc.2020.06.011
12. Schaeffer E, Srinivas S, Antonarakis ES, Armstrong AJ, Bekelman JE, Cheng H, et al. NCCN Guidelines Insights: Prostate Cancer, Version 1.2021. *J Natl Compr Canc Netw* (2021) 19(2):134–43. doi: 10.6004/jnccn.2021.0008
13. Liu A, Han J, Nakano A, Konno H, Moriwaki H, Abe H, et al. New Pharmaceuticals Approved by FDA in 2020: Small-Molecule Drugs Derived From Amino Acids and Related Compounds. *Chirality* (2021). doi: 10.1002/chir.23376
14. Keam SJ. Piflufolastat F 18: Diagnostic First Approval. *Mol Diagn Ther* (2021) 25(5):647–56. doi: 10.1007/s40291-021-00548-0
15. Ost P, Reynders D, Decaestecker K, Fonteyne V, Lumen N, De Bruycker A, et al. Surveillance or Metastasis-Directed Therapy for Oligometastatic Prostate Cancer Recurrence: A Prospective, Randomized, Multicenter Phase II Trial. *J Clin Oncol* (2018) 36(5):446–53. doi: 10.1200/JCO.2017.75.4853

Conflict of Interest: Authors TR was employed by Flatiron Health.

The remaining authors declare that the research was conducted in the absence of any commercial or financial relationships that could be construed as a potential conflict of interest.

frontiers in Oncology

ORIGINAL RESEARCH
published: 07 December 2020
doi: 10.3389/fonc.2020.600690

Comparison of Manual and Semi-Automatic [^{18}F]PSMA-1007 PET Based Contouring Techniques for Intraprostatic Tumor Delineation in Patients With Primary Prostate Cancer and Validation With Histopathology as Standard of Reference

Simon K. B. Spohn[1,2], Maria Kramer[1], Selina Kiefer[3], Peter Bronsert[3], August Sigle[4], Wolfgang Schultze-Seemann[4], Cordula A. Jilg[4], Tanja Sprave[1,2], Lara Ceci[1], Thomas F. Fassbender[5], Nils H. Nicolay[1,2], Juri Ruf[5], Anca L. Grosu[1,2] and Constantinos Zamboglou[1,2,6]*

[1] Department of Radiation Oncology, Medical Center–University of Freiburg, Faculty of Medicine, University of Freiburg, Freiburg, Germany, [2] German Cancer Consortium (DKTK), Partner Site Freiburg, Freiburg, Germany, [3] Institute for Surgical Pathology, Medical Center–University of Freiburg, Faculty of Medicine, University of Freiburg, Freiburg, Germany, [4] Department of Urology, Medical Center–University of Freiburg, Faculty of Medicine, University of Freiburg, Freiburg, Germany, [5] Department of Nuclear Medicine, Medical Center–University of Freiburg, Faculty of Medicine, University of Freiburg, Freiburg, Germany, [6] Berta-Ottenstein-Programme, Faculty of Medicine, University of Freiburg, Freiburg, Germany

Purpose: Accurate contouring of intraprostatic gross tumor volume (GTV) is pivotal for successful delivery of focal therapies and for biopsy guidance in patients with primary prostate cancer (PCa). Contouring of GTVs, using 18-Fluor labeled tracer prostate specific membrane antigen positron emission tomography ([^{18}F]PSMA-1007/PET) has not been examined yet.

Patients and Methods: Ten Patients with primary PCa who underwent [^{18}F]PSMA-1007 PET followed by radical prostatectomy were prospectively enrolled. Coregistered histopathological gross tumor volume (GTV-Histo) was used as standard of reference. PSMA-PET images were contoured on two ways: (1) manual contouring with PET scaling SUVmin-max: 0–10 was performed by three teams with different levels of experience. Team 1 repeated contouring at a different time point, resulting in n = 4 manual contours. (2) Semi-automatic contouring approaches using SUVmax thresholds of 20–50% were performed. Interobserver agreement was assessed for manual contouring by calculating the Dice Similarity Coefficient (DSC) and for all approaches sensitivity, specificity were calculated by dividing the prostate in each CT slice into four equal quadrants under consideration of histopathology as standard of reference.

OPEN ACCESS

Edited by:
Tiziana Rancati, Istituto Nazionale dei Tumori (IRCCS), Italy

Reviewed by:
Thomas Zilli, Université de Genève, Switzerland
Fei Yang, University of Miami School of Medicine, United States

***Correspondence:**
Simon K. B. Spohn
Simon.Spohn@uniklinik-freiburg.de

Specialty section:
This article was submitted to Radiation Oncology, a section of the journal Frontiers in Oncology

Received: *30 August 2020*
Accepted: *04 November 2020*
Published: *07 December 2020*

Citation:
Spohn SKB, Kramer M, Kiefer S, Bronsert P, Sigle A, Schultze-Seemann W, Jilg CA, Sprave T, Ceci L, Fassbender TF, Nicolay NH, Ruf J, Grosu AL and Zamboglou C (2020) Comparison of Manual and Semi-Automatic [^{18}F] PSMA-1007 PET Based Contouring Techniques for Intraprostatic Tumor Delineation in Patients With Primary Prostate Cancer and Validation With Histopathology as Standard of Reference. Front. Oncol. 10:600690. doi: 10.3389/fonc.2020.600690

Results: Manual contouring yielded an excellent interobserver agreement with a median DSC of 0.90 (range 0.87–0.94). Volumes derived from scaling SUVmin-max 0–10 showed no statistically significant difference from GTV-Histo and high sensitivities (median 87%, range 84–90%) and specificities (median 96%, range 96–100%). GTVs using semi-automatic segmentation applying a threshold of 20–40% of SUVmax showed no significant difference in absolute volumes to GTV-Histo, GTV-SUV50% was significantly smaller. Best performing semi-automatic contour (GTV-SUV20%) achieved high sensitivity (median 93%) and specificity (median 96%). There was no statistically significant difference to SUVmin-max 0–10.

Conclusion: Manual contouring with PET scaling SUVmin-max 0–10 and semi-automatic contouring applying a threshold of 20% of SUVmax achieved high sensitivities and very high specificities and are recommended for [18F]PSMA-1007 PET based focal therapy approaches. Providing high specificities, semi-automatic approaches applying thresholds of 30–40% of SUVmax are recommend for biopsy guidance.

Keywords: primary prostate cancer, focal therapy, contouring, PSMA-PET/CT, histopathology

INTRODUCTION

Accurate intraprostatic tumor contouring is pivotal for successful delivery of high precision focal therapies of primary prostate cancer (PCa) and biopsy guidance. Radiation dose escalation has been shown to be beneficial for treatment outcome (1–3) and boosting visible tumor burden is currently being investigated in phase III trials (4, 5). Besides multiparametric magnetic resonance tomography (mpMRI) (6), positron emission tomography with tracers against prostate membrane specific membrane antigen (PSMA-PET) has emerged as an excellent technique for diagnostic and staging of primary and recurrent PCa (7–10). In primary PCa results from our workgroup as well as other studies suggest that PSMA-PET shows better sensitivities with comparable specificity than mpMRI in intraprostatic lesions detection (11, 12), gives complementary information (13) and may thus be favorable for focal therapy guidance (14). Different contouring approaches for Gallium-68-labeled ([^{68}Ga]PSMA-PET) have already been validated and manual contouring applying SUVmin-max: 0–5 provided high sensitivities (11). Fluorine-18-labeled Tracers ([^{18}F]PSMA-1007) have been implemented in nuclear medicine practice, with suspected benefits due to lesser renal elimination and consequent less background signal in the bladder (15) and performed with good diagnostic accuracy (16). Since [^{68}Ga]- and [^{18}F]PSMA-1007 tracers show differences in SUV distribution scaling recommendations might not be used interchangeable (17). This prospectively designed study aims to validate [^{18}F]PSMA-1007 PET based contouring approaches for intraprostatic tumor contouring using whole mount histopathology as standard of reference, since a consensual method to accurately contour intraprostatic lesions for this tracer has not yet been established.

PATIENTS AND METHODS

Patients

Between June 2019 and February 2020, 10 patients with histopathological proven primary PCa, pre-therapeutic [^{18}F]PSMA-1007 PET scan and intended radical prostatectomy were prospectively enrolled. Exclusion criteria were neoadjuvant androgen deprivation therapy and transurethral prostate resection prior to PET imaging. See **Table 1** for patient characteristics. Written informed consent was obtained from all patients. The study was approved by the institutional review board (No. 476/19).

PET Imaging

[18F]PSMA-1007 had been synthesized according to Cardinale et al. (18). The mean injected activity of [^{18}F]PSMA-1007 was 299 MBq (min–max: 249–370 MBq). Patients underwent a whole-body PET scan starting 2 h after injection. Scans were performed with a 16-slice Gemini TF big bore in one patient and a Vereos PET/CT scanner in nine patients (all Philips Healthcare, USA). A phantom study was performed and comparable SUV values were obtained in both systems (19). Both scanners fulfilled the requirements indicated in the European Association of Nuclear Medicine (EANM) imaging guidelines and obtained EANM Research Ltd (EARL). accreditation during acquisition. At the time of the PET scan, either a contrast-enhanced or native diagnostic CT scan (120 kVp, 100–400 mAs, dose modulation) was performed for attenuation correction (depending on previous CT scans and contraindications). Please see (19) for details about reconstruction methods. All systems resulted in a PET image with a voxel size of $2 \times 2 \times 2$ mm^3. The uptake of [^{18}F]PSMA-1007 was quantified in terms of standardized uptake values (SUV) normalized body weight.

TABLE 1 | Patient characteristics.

Patient	Age (y)	PSA (ng/ml)	pT	Gleason score (specimen)
1	70	4.3	pT2a	4+3 (7b)
2	66	17.2	pT3	4+3 (7b)
3	69	103.0	pT3a	4+5 (9)
4	76	5.0	pT2c	4+3 (7b)
5	80	8.6	pT2a	4+5 (9)
6	53	72.0	pT3b	5+4 (9)
7	64	19.5	pT3a	4+4 (8)
8	72	24.8	pT2a	4+4 (8)
9	74	13.9	pT3a	4+3 (7b)
10	66	17.5	pT3b	4+5 (9)
Median	70	17.4		
95% CI	64–74	5.3–51.9		

Histopathology and PET/CT Image Coregristation

PCa lesions in whole mount histopathology specimens were transferred into 3D volumes using a published in-house coregistration protocol and served as standard of reference (11, 20, 21). Following formalin fixation, the resected prostate underwent *ex-vivo* CT scan using a customized localizer. A customized cutting device was used to cut step sections every 4 mm to guarantee equal cutting angles between tissue specimen and *ex-vivo* CT-slices. After paraffin embedding specimens were cut using a Leica microtome. Hematoxylin and eosin staining was performed following routine protocols and PCa lesions were marked by one experienced pathologist. Histopathological slices were registered on *ex-vivo*-CT images and PCa contours were transferred into the corresponding CT images. Contours were interpolated by 2 mm expansion in Z-axis directions do create a model for 3D distribution. Manual coregistration allowing elastic deformations was used to take into account non-linear transformations of the prostatic gland after resection. Subsequently in this approach, following previously used workflows, manual coregistration of *ex-vivo* CT, including 3D volumes of pathology reference on *in-vivo* CT from diagnostic PSMA-PET/CT was performed. Pre-treatment mpMRIs (T2w sequences) were co-registered to *in-vivo* CT and an experienced radiation oncologist delineated prostatic gland on the CT-images under consideration of the mpMRI information.

PET Based Contouring

Gross tumor volume (GTV) contouring of intraprostatic tumor lesions was performed in PSMA-PET images for all 10 patients using manual and semi-automatic approaches (**Figure 1**). Eclipse™ Treatment Planning System (Varian, USA) was used for both approaches. Three teams were recruited. Team 1 consisted of two readers with <1 year of experience in interpretation of PSMA-PET images. Team 2 consisted of two readers with >4 years of experience in interpretation of PSMA-PET images and team 3 consisted of one reader with <2 years of experience in interpretation of PSMA-PET images respectively. Additionally Team 1 repeated contouring blinded to previously performed segmentations after >4 months (Team 1v2).

Manual Contouring: According to recommendations for [68Ga]-PSMA-PET imaging scaling of SUVmin-max 0–5 was firstly applied for intraprostatic tumor lesion contouring (11). Due to volume overestimation and differences in SUVuptake between both tracers (17, 22), a second analysis applying individual scaling was performed to define an additional scaling range for manual contouring, which results in absolute volumes (GTV-Individual) more consistent with GTV-Histo. Therefore, PET images of each patient were scaled individually by modifying the scaling value of the upper SUV-limit, adjusting the volume to the available histological information. Based on the median applied SUVmax of 10, a second manual contouring approach with scaling SUVmin-max 0–10 was performed by all teams. Apart from PET and CT images no additional clinical information was provided.

Threshold Segmentations: A threshold of 20, 30, 40, and 50% of intraprostatic SUV max was applied for semi-automatic segmentation of GTV-20–50%, respectively.

All contours were created in the PET images and transferred to the corresponding, hardware-based, co-registered CT images. GTVs were trimmed to the prostatic gland and to the region of the prostatic gland, which was used for histopathologic examination.

Statistical Analysis

Sensitivity and specificity for all GTVs based on the histology as reference were calculated by dividing the prostate in each CT slice into four equal quadrants as performed previously by our group (11). The statistical analysis was performed on GraphPad Prism v8.4.2 (GraphPad Software). Normal distribution was tested using the Shapiro-Wilk test. Since tested variables showed no Gaussian distribution Friedman test and uncorrected Dunn's test at a significance level of 0.05 was used. Overlap of contours as well as the proportion of the GTVs to the prostatic gland was measured in the Eclipse planning software. Analyses of volumes including GTV-Histo was limited to the proportion of the prostate that was used for histopathological examination, defined by histological slices. Additionally, proportion of contoured GTVs and the whole prostate was calculated. Agreement between manual contours of team 1, team 2, team 3, and team 1v2 was assessed at voxel level using the Dice Similarity Coefficient (DSC), which is identical to the kappa index when applied at voxel level (23).

RESULTS

Table 2 gives an overview of the absolute volumes, coverage of GTV-Histo, sensitivities and specificities of the evaluated contouring approaches. GTVs from scaling SUVmin-max 0–5 were significantly larger than GTV Histo (median 3.8 ml for GTV-Histo, median 6.2–8.2 ml for all teams, p = <0.0029, see **Figure 2**). Sensitivities were very high (median ≥99%) and specificities moderate (median 54–89%) (**Figure 3**). In the second step, individual PET image scaling for manual contouring revealed a varying SUVmax of 6–20 (corresponding to a percentage of SUVmax between 15 and 60%). Median applied SUVmax was 10 (corresponding to a median percentage of SUVmax of 36%). Median volume of GTV-Individual was 3.4 ml (**Figure 2**) and

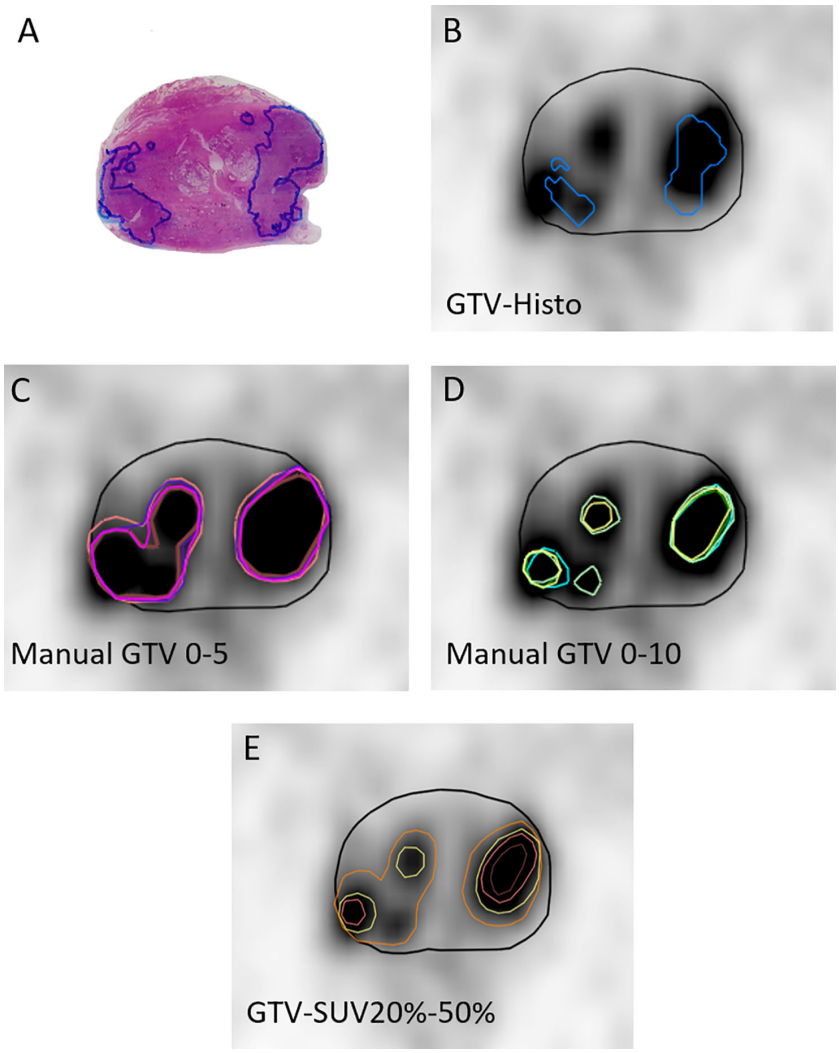

FIGURE 1 | Image segmentations. **(A)** shows the H&E stained whole-mount prostatectomy specimen with intraprostatic tumor lesions marked in blue. The other images display representative axial PSMA-PET images with the respective GTVs. PET image scaling is SUVmin-max 0–5. **(B)** shows GTV-Histo. **(C)** shows manual contouring approaches with scaling SUVmin-max 0–5 (team 1 = brown, team 2 = pink, team 3 = magenta, and team 1v2 = purple). **(D)** shows manual contouring approaches with scaling SUVmin-max 0–10 (team 1 = cyan, team 2 = green, team 3 = yellow, and team 1v2 = dark green). **(E)** shows semi-automatic contouring approaches applying a threshold of SUVmax of 20% (orange), 30% (yellow), 40% (pink), and 50% (brown). Prostatic gland is marked in black.

showed no statistically significant difference to GTV-Histo. Likewise median volumes of GTVs from scaling SUVmin-max 0–10 (median 2.6 ml, range 2.0–3.1 ml) were not statistically significant difference to GTV-Histo (**Figure 2**). Scaling SUVmin-max 0–10 and individual scaling achieved lower median sensitivities (84–90% for all teams, 89.0% for individual scaling, respectively) with higher median specificities (96–100% for all teams, 96% for individual scaling, respectively) (**Figure 3**). Sensitivities for scaling SUVmin-max 0–5 were mostly significantly higher than for scaling SUVmin-max 0–10 and individual scaling, *vice versa* specificities were mostly significantly lower (see **Table S1** for details about p = values). Analysis of the different manual segmentation methods revealed an excellent interobserver agreement with median DSCs between 0.87 and 0.94 (see **Table 3** for details). For proportion of prostate specimen, proportion of whole prostate and coverage of GTV-Histo please see **Table 2**.

Median intraprostatic SUVmax was 39.6 (range 11.6–59.8). Analysis of semi-automatic segmentation approaches provided median volumes for GTV-SUV20–50% of 3.9, 2.6, 1.7, and 1.2 ml, respectively (**Figure 2**). GTV-SUV20% showed no significant difference to GTV-Histo and a median sensitivity of 93% and median specificity of 96% (**Figure 3**). For proportion of prostate specimen, proportion of whole prostate and coverage of GTV-Histo for semi-automatic approaches please see **Table 2**. GTV-SUV20% as best performing semi-automatic contouring approach was chosen for comparison between manual and semi-automatic contouring.

TABLE 2 | Overview of different [18F]PSMA-1007 PET based segmentation approaches in comparison with histology as reference standard.

	Median volume in ml (IQR)	GTV trimmed to specimen/ prostatic specimen volume in % Median (IQR)	GTV/prostatic volume in % Median(IQR)	Coverage of GTV-Histo in % (IQR)	Median sensitivity in % (IQR)	Median specificity in % (IQR)
GTV-Histo	3.8 (0.6–9.9)	11 (3–29)				
GTV-Team 1: 0–5	6.3 (4.0–22.3)	29 (14–51)	29 (10–47)	72 (56–93)	100 (91–100)	80 (52–91)
GTV-Team 2: 0–5	6.2 (3.6–24.1)	30 (12–55)	31 (9–53)	72 (66–95)	100 (91–100)	65 (42–88)
GTV-Team 3: 0–5	8.2 (3.7–20.7)	34 (13–54)	29 (8–48)	75 (57–94)	99 (91–100)	54 (34–97)
GTV-Team 1v2: 0–5	6.7 (3.2–22.2)	32 (11–51)	30 (8–34)	78 (58–93)	100 (90–100)	89 (36–92)
GTV-Team 1: 0–10	3.1 (1.5–10.9)	11 (6–28)	12 (4–35)	59 (34–86)	88 (73–100)	96 (83–100)
GTV-Team 2: 0–10	2.1 (1.3–10.7)	10 (4–27)	8 (3-34)	56 (27–85)	84 (52–95)	100 (85–100)
GTV-Team 3: 0–10	2.2 (1.2–10.8)	11 (4–27)	8 (3–34)	53 (25–84)	86 (69–100)	96 (64–100)
GTV-Team 1v2: 0–10	3.0 (1.3–10.6)	34 (13–54)	9 (3–34)	59 (30–84)	90 (68–100)	96 (71–100)
GTV-Individual	3.4 (1.4–11.9)	13 (7–31)	10 (4–31)	56 (36–81)	89 (74–97)	96 (75–100)
GTV-SUV20%	3.9 (1.0–25.5)	19 (4–59)	21 (3–62)	69 (42–84)	93 (60–100)	96 (57–100)
GTV-SUV30%	2.6 (0.6–20.0)	11 (3–46)	15 (2–45)	58 (32–73)	86 (57–95)	97 (69–100)
GTV-SUV40%	1.7 (0.4–10.2)	7 (2–24)	9 (1–21)	36 (25–57)	70 (44–88)	97 (91–100)
GTV-SUV50%	1.2 (0.3–4.2)	4 (1–9)	6 (1–8)	25 (11–42)	60 (43–68)	97 (91–100)
Prostate specimen	29.1 (20.4–41.8)					
Prostate whole	52.3 (33.4–65.7)					

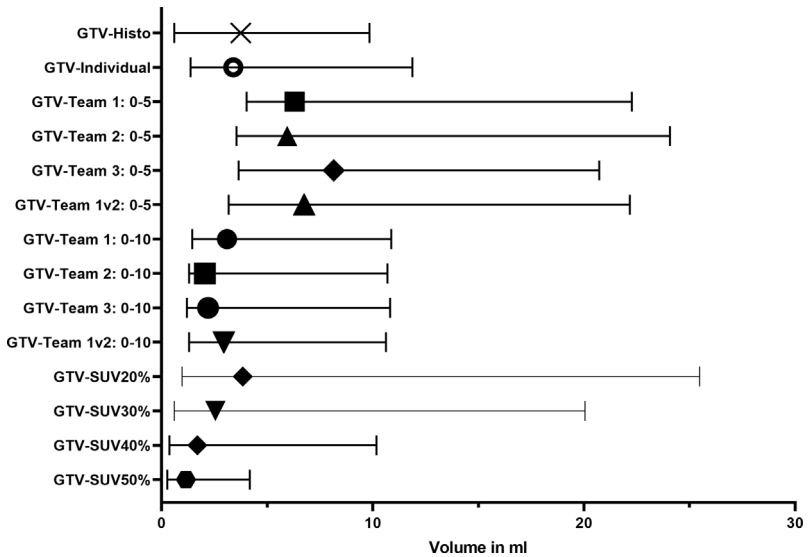

FIGURE 2 | Volumes of histology reference (GTV-Histo) and different [18F]PSMA-1007 PET based segmentation approaches. The median and interquartile ranges over all patients are shown.

Sensitivity of GTV-SUV20% was slightly, but significantly lower than manual contouring with scaling SUVmin-max 0–5 and not significantly different to scaling SUVmin-max 0–10 and individual scaling. Specificity of GTV-SUV20% was significantly higher than GTV-Team 1 with scaling SUVmin-max 0–5 and not significantly different to other manual contouring approaches. See **Table S1** for details about p-values.

Coverage of GTV Histo was significantly higher for manual scaling SUVmin-max 0–5 than for semi-automatic contouring with SUV20%max ($p < 0.024$) and for scaling SUVmin-max 0–10 ($p < 0.038$) except for team 1. There was no significant difference between manual scaling SUVmin-max 0–10 and semiautomatic contouring.

DISCUSSION

Improvements in PCa detection and contouring are requested to facilitate successful biopsy guidance and focal therapy planning. PSMA-PET/CT has been established as a promising diagnostic method for identification of intraprostatic lesions (24). [68Ga] PSMA is a widely used tracer with excellent performance (9, 11), but new tracers like [18F]PSMA-1007 have been developed in recent years with putative benefits in terms of lesser renal elimination and consequent less background signal in the bladder (15), simplified manufacturing (18), and lesion detection (16). So far, there is no consensus and no recommendations on how to accurately contour intraprostatic

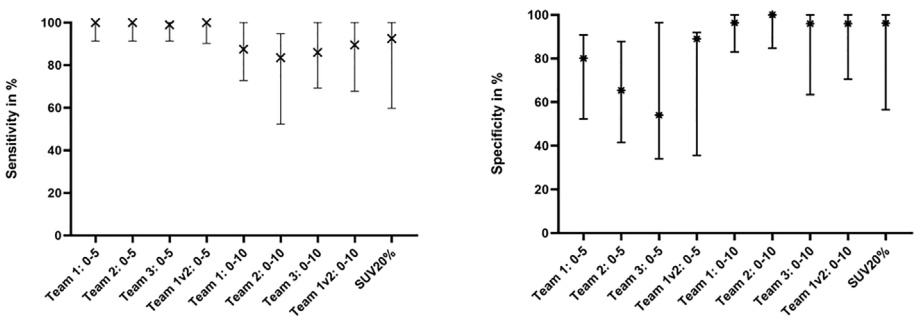

FIGURE 3 | Sensitivity and Specificity of Team 1, Team 2, Team 3, Team 1v2, and SUV20%. The median and interquartile ranges over all patients are shown.

TABLE 3 | DSC of different manual contouring techniques.

0–5 Team 1/Team 2	0–5 Team 1/Team 3	0–5 Team 1/Team 1v2	0–5 Team 2/Team 1v2	0–5 Team 3/Team 1v2
87.5 (81–90)	91.0 (80–98)	89.5 (78–97)	91.5 (81–97)	94.0 (80–99)
0–10 Team1/Team 2	**0–10 Team1/Team 3**	**0–10 Team1/Team 1v2**	**0–10 Team 2/Team 1v2**	**0–10 Team 3/Team 1v2**
88.5 (79–97)	86.5 (79–99)	88.5 (80–96)	92.0 (86–98)	90.5 (88–97)

Median and IQR are shown.

tumor mass based on [18F]PSMA-1007 PET. Following the same approach as previously conducted by our group for [68Ga]-PSMA, this study aimed to validate different contouring methods using whole mount histology as the reference standard to be used for focal therapy planning (high sensitivity) and biopsy guidance (high specificity). Likewise, we used a quadrant-based slice-by-slice analysis approach. We chose this analysis method anticipating the most accurate analysis method but still taking mismatch susceptibilities during the registration workflow into account, which would severely effect voxel-based analysis approaches. Considering advantages of mpMRI for prostate delineation, respective contours were based on available mpMRI information (25).

Previous experience with thresholds of 30% (21), 40% (26), and 50% (27) for semi-automatic PCa segmentation and a threshold of 20% showed good performance in [68Ga]-PSMA/PET (11). Consequently, these approaches were selected for validation in our study. Additionally, a previously described semi-automatic segmentation techniques using a ratio between tumor and normal tissue uptake (11, 28) was utilized at the beginning, but rejected for further analysis since the volumes filled out high percentages of the prostate and performance was expected to be low.

Manually contoured GTVs with PET image scaling SUVmin-max 0–5 were statistically significantly larger than GTV-Histo (>60% larger). Therefore, we performed a second analysis, to define an additional scaling range for manual contouring, which results in volumes more concordant with GTV-Histo. The median for SUVmax was 10 and expressed in percentage relative to SUVmax median applied SUVmax was 36%. The relatively wide range of 15% to 60% in our cohort suggest, that a general recommendable threshold for threshold-based segmentation approaches may be difficult to define. However, the applied semi-automatic approaches represent the resulted SUV-range. Anticipating a putative benefit for manual contouring approaches, which does not leave out lesions below an applied threshold we consequently performed an additional analysis with manual contouring with scaling SUVmin-max 0–10.

Interobserver agreement between all Teams, using the same SUV scaling was excellent for both scaling techniques (median DSC between 0.87 and 0.94) and undermines, that using the same scaling range leads to comparable results even for readers with different levels of experience. These results comply with previous studies (11) and are contrary to MRI, the current standard of care in prostate cancer imaging, due to challenges in interpretation of different MRI modalities (23, 29). A low interobserver agreement is a prerequisite for implementing [18F]PSMA-1007 based tumor contours in focal therapy guidance (14, 30) or for non-invasive tumor characterization (19).

Our results of manual contouring performance reveal that volumes derived from scaling with SUVmin-max 0–10 are more consistent with GTV-Histo and sill reached high sensitivities and very high specificities, without overestimating tumor volume. GTV-SUV20% was the best performing semi-automatic contouring approach with comparable results. Nevertheless, manual scaling SUVmin-max 0–10 performed in all but one patient (patient 7) similar or better than GTV-SUV20%. Analysis of patient characteristics revealed no special features. However, intraprostatic SUVmax of this patient was 11.6, thereby lower than others and close to the applied SUVmax for scaling. This results in discrepancy of volumes in all Teams (1.6–4.8 ml), a low DSC (0.36–0.61) and plausibly in low performance of manual contouring. Regarding this aspect semi-automatic contouring

possesses the advantage of easy feasibility and reproducibility. In the setting of focal therapy high sensitivities are necessary, since it's not clear which regions represent the dominant intraprostatic lesions responsible for relapse (30, 31). On the other hand, large boost volumes and inclusion of normal tissue (low specificity) lead to an increase of toxicity. Taking these aspects into account manual contouring with scaling SUVmin-max 0–10 and semi-automatic contouring with 20% of SUVmax should be considered firstly for [^{18}F]PSMA-1007-based dose escalation. In case intraprostatic SUVmax is close to the applied SUVmax for manual scaling, adjustment of the range, for instance SUVmin-max 0–5, might be considered as an appropriate alternative. Our results suggest, that the use [^{18}F]PSMA-1007 for contouring of lesions for focal therapy planning is likely to be as effective as other tracers, who's performance was evaluated in radiotherapy planning studies and showed promising results in terms of tumor control and normal tissue toxicities (14, 32).

Another requirement for sufficient tumor control is coverage of intraprostatic tumor. Manual contouring and GTV-SUV20% reached a median coverage of GTV-Histo of >50% in all patients. Coverage with scaling SUVmin-max 0–5 was significantly higher, again explainable due to the large and overestimated volumes. Comparison of remaining approaches showed no significant difference. However, the co-registration workflow bears uncertainties in the exact localization of GTV-Histo. Consequently, coverage of GTV-Histo calculated by intersection volumes is the most inaccurate parameter of this study and conclusions based on the coverage of GTV-Histo should be drawn with caution. Nevertheless, the recommended contouring approaches reveal volumes consistent with GTV-Histo. Considering the fact that PSMA-Expression shows heterogeneity with potentially low or even missing PSMA-expression (33, 34), information provided by mpMRI complements PSMA-PET for intraprostatic tumor detection (11). As previously demonstrated combination of mpMRI and PSMA-PET/CT further achieves higher sensitivity and specificity (11, 12, 35, 36). Consequently. future studies should investigate whether the addition of [^{18}F]PSMA-1007 information for focal therapy planning can be translated into increased tumor control.

Biopsy guidance in patients with PCa relies on high specificities, which increases the chance of PCa detection in the biopsy sample. As expected, specificity of manual scaling SUVmin-max 0–10 and SUVmax20% was statistically significantly higher than scaling with SUVmin-max 0–5. Volumes of GTV-50%, but not GTV-SUV20–40% were significantly smaller than GTV-Histo, however higher thresholds yielded to less coverage of GTV-Histo. Bravaccini et al. showed that PSMA-Expression correlates with Gleason Score (37), therefore targeting lesions with high SUV values might guide to more aggressive PCa regions. Semi-automatic scaling approach with 30–40% of SUVmax showed good sensitivity with excellent specificity and might be effective and feasible to target lesions that are more aggressive. Consequently, semiautomatic contouring with 30–40% of SUVmax are recommended for [^{18}F]PSMA-1007-PET guided biopsies, depending on the obtained volumes. However, scaling with SUVminmax 0–10 might be an appropriate alternative.

This study shows a trend towards higher sensitivity and specificity in intraprostatic PCa detection for [^{18}F]PSMA-1007 compared to [^{68}Ga]-PSMA. Histopathological comparison studies showed sensitivities between 64 and 89% and specificities between 71 and 95% for [^{68}Ga]-PSMA (11, 12, 36, 38, 39). Our results performed similarly well as a study by Kuten et al., which showed a sensitivity of 100% and a specificity of 90.9% for [^{18}F]PSMA-1007. In the head-to-head comparison [^{18}F]PSMA-1007 showed a higher sensitivity and lower specificity than [^{68}Ga]-PSMA (85.7 and 98.2%, respectively). Noteworthy, both tracers detected significant index lesions equally. However, identification of PCa was based on expert review with unknown scaling (16), which hampers direct comparison to our study. Kesch et al. showed lower sensitivity (71%) and specificity (81%) for [^{18}F]PSMA-1007 (35). A possible explanation for these variations might be the usage of different approaches for coregistration and analysis. Whether these aspects contribute significantly to the results has not been challenged yet. Future studies should compare these to clarify comparability. Furthermore future studies should evaluate performance of neuronal networks trained for GTV contouring in [^{18}F]PSMA-1007 images, which might circumvent the issue of proper manual scaling ranges.

The study's limitation is the imprecision in correlation of PET/CT and histopathology (e.g. non-linear shrinkage of the prostate after prostatectomy). As mentioned, low to moderate coverage of GTV-Histo might be a consequence of mismatch in coregistration or incomplete histopathological coverage. This potential bias is marginal for calculation of sensitivities and specificities, since they were not performed on a voxel-level but on a less stringent slice-by-slice level. Furthermore, the use of two different PET/CT scanners is a limitation. However, a phantom study confirmed the comparability of SUV values between the two scanning systems and rigorous reconstruction parameters were applied. Additionally, 9 of 10 patients underwent the scan in the same scanner and the single outlier patient was independent of the used scanner type. Third, the sample size in our study is relatively small, due to the elaborate pathology-imaging co-registration protocol. Lastly, we enrolled patients planned for prostatectomy to obtain histopathologic information from the specimens and thus caused a selection bias. Consequently, our results are only representative for intermediate- and high-risk PCa patients. However, these patients are likely to benefit most from focal therapy approaches, which is being investigated in phase III trials (4).

In conclusion manual contouring by using the same PET image scaling technique yields low interobserver variability even for readers with different levels of experience. Scaling PET images with SUVmin-max:0–5 showed excellent sensitivities but moderate specificity by overestimating the tumor volume. PET image scaling with SUVmin-max 0–10 showed slightly but statistically significant lower sensitivities with statistically significant higher specificities. Semi-automatic contouring with SUVmax20% similarly achieved high sensitivity and very high

specificity. In this study manual scaling with SUvmin-max 0–10 performed similar or better than SUVmax20% in all but one patient. However, semiautomatic contouring approaches possess the advantage of easy feasibility and reproducibility. Consequently, evaluating total performance manual contouring with SUVmin-max 0–10 and semiautomatic contouring applying a threshold of 20% of SUVmax are firstly recommended for [^{18}F]PSMA-1007 based focal therapy approaches. Providing very high specificities and depiction of the high-uptake areas within the tumor, semi-automatic approaches applying thresholds of SUVmax 30–40% are recommend for biopsy guidance.

DATA AVAILABILITY STATEMENT

The raw data supporting the conclusions of this article will be made available by the authors upon request without undue reservation.

ETHICS STATEMENT

The studies involving human participants were reviewed and approved by Institutional Review Board University Freiburg. The patients/participants provided their written informed consent to participate in this study.

AUTHOR CONTRIBUTIONS

SS and CZ contributed to conception and design of the study. MK and AS enrolled patients. MK and CZ performed histo/image co-registration. SS, MK, LC, CZ, and AG performed PET-contouring. SS and MK conducted metrics calculation. WS-S, CJ, and AS were responsible for surgery indication and prostatectomy. SK and PB conducted the histopathological processing and marking of tumor lesions. TF and JR were responsible for conduction and reporting of the PSMA-PET/CTs. TS, NN, and AG supervised the study and co-registration. SS wrote the first draft of the manuscript. CZ wrote sections of the manuscript. All authors contributed to the article and approved the submitted version.

FUNDING

This study was funded by the Era PerMed call 2018 (BMBF).

SUPPLEMENTARY MATERIAL

The Supplementary Material for this article can be found online at: https://www.frontiersin.org/articles/10.3389/fonc.2020.600690/full#supplementary-material

REFERENCES

1. Dearnaley DP, Sydes MR, Graham JD, Aird EG, Bottomley D, Cowan RA, et al. Escalated-dose versus standard-dose conformal radiotherapy in prostate cancer: first results from the MRC RT01 randomised controlled trial. *Lancet Oncol* (2007) 8(6):475–87. doi: 10.1016/S1470-2045(07)70143-2
2. Peeters ST, Heemsbergen WD, Koper PC, van Putten WL, Slot A, Dielwart MF, et al. Dose-response in radiotherapy for localized prostate cancer: results of the Dutch multicenter randomized phase III trial comparing 68 Gy of radiotherapy with 78 Gy. *J Clin Oncol Off J Am Soc Clin Oncol* (2006) 24 (13):1990–6. doi: 10.1200/JCO.2005.05.2530
3. Pollack A, Zagars GK, Starkschall G, Antolak JA, Lee JJ, Huang E, et al. Prostate cancer radiation dose response: results of the M. D. Anderson phase III randomized trial. *Int J Radiat Oncol Biol Phys* (2002) 53(5):1097–105. doi: 10.1016/S0360-3016(02)02829-8
4. Lips IM, van der Heide UA, Haustermans K, van Lin EN, Pos F, Franken SP, et al. Single blind randomized phase III trial to investigate the benefit of a focal lesion ablative microboost in prostate cancer (FLAME-trial): study protocol for a randomized controlled trial. *Trials* (2011) 12:255. doi: 10.1186/1745-6215-12-255
5. Monninkhof EM, van Loon JWL, van Vulpen M, Kerkmeijer LGW, Pos FJ, Haustermans K, et al. Standard whole prostate gland radiotherapy with and without lesion boost in prostate cancer: Toxicity in the FLAME randomized controlled trial. *Radiother Oncol J Eur Soc Ther Radiol Oncol* (2018) 127 (1):74–80. doi: 10.1016/j.radonc.2017.12.022
6. Kasivisvanathan V, Rannikko AS, Borghi M, Panebianco V, Mynderse LA, Vaarala MH, et al. MRI-Targeted or Standard Biopsy for Prostate-Cancer Diagnosis. *N Engl J Med* (2018) 378(19):1767–77. doi: 10.1056/NEJMoa1801993
7. Eder M, Neels O, Müller M, Bauder-Wüst U, Remde Y, Schäfer M, et al. Novel Preclinical and Radiopharmaceutical Aspects of [68Ga]Ga-PSMA-HBED-CC: A New PET Tracer for Imaging of Prostate Cancer. *Pharmaceuticals (Basel Switzerland)* (2014) 7(7):779–96. doi: 10.3390/ph7070779
8. Mhawech-Fauceglia P, Zhang S, Terracciano L, Sauter G, Chadhuri A, Herrmann FR, et al. Prostate-specific membrane antigen (PSMA) protein expression in normal and neoplastic tissues and its sensitivity and specificity in prostate adenocarcinoma: an immunohistochemical study using mutiple tumour tissue microarray technique. *Histopathology* (2007) 50(4):472–83. doi: 10.1111/j.1365-2559.2007.02635.x
9. Hofman MS, Lawrentschuk N, Francis RJ, Tang C, Vela I, Thomas P, et al. Prostate-specific membrane antigen PET-CT in patients with high-risk prostate cancer before curative-intent surgery or radiotherapy (proPSMA): a prospective, randomised, multicentre study. *Lancet (London England)* (2020) 395(10231):1208–16. doi: 10.1016/S0140-6736(20)30314-7
10. Eiber M, Maurer T, Souvatzoglou M, Beer AJ, Ruffani A, Haller B, et al. Evaluation of Hybrid ^{68}Ga-PSMA Ligand PET/CT in 248 Patients with Biochemical Recurrence After Radical Prostatectomy. *J nuclear Med Off Publication Soc Nuclear Med* (2015) 56(5):668–74. doi: 10.2967/jnumed.115.154153
11. Bettermann AS, Zamboglou C, Kiefer S, Jilg CA, Spohn S, Kranz-Rudolph J, et al. [(68)Ga-]PSMA-11 PET/CT and multiparametric MRI for gross tumor volume delineation in a slice by slice analysis with whole mount histopathology as a reference standard - Implications for focal radiotherapy planning in primary prostate cancer. *Radiother Oncol* (2019) 141:214–9. doi: 10.1016/j.radonc.2019.07.005
12. Eiber M, Weirich G, Holzapfel K, Souvatzoglou M, Haller B, Rauscher I, et al. Simultaneous (68)Ga-PSMA HBED-CC PET/MRI Improves the Localization of Primary Prostate Cancer. *Eur Urol* (2016) 70(5):829–36. doi: 10.1016/j.eururo.2015.12.053
13. Spohn S, Jaegle C, Fassbender TF, Sprave T, Gkika E, Nicolay NH, et al. Intraindividual comparison between (68)Ga-PSMA-PET/CT and mpMRI for intraprostatic tumor delineation in patients with primary prostate cancer: a retrospective analysis in 101 patients. *Eur J Nuclear Med Mol Imaging* (2020) 47:2796–803. doi: 10.1007/s00259-020-04827-6
14. Zamboglou C, Sachpazidis I, Koubar K, Drendel V, Wiehle R, Kirste S, et al. Evaluation of intensity modulated radiation therapy dose painting for localized prostate cancer using (68)Ga-HBED-CC PSMA-PET/CT: A planning study based on histopathology reference. *Radiother Oncol* (2017) 123(3):472–7. doi: 10.1016/j.radonc.2017.04.021
15. Rahbar K, Weckesser M, Ahmadzadehfar H, Schäfers M, Stegger L, Bögemann M. Advantage of (18)F-PSMA-1007 over (68)Ga-PSMA-11 PET imaging for differentiation of local recurrence vs. urinary tracer excretion. *Eur J Nuclear Med Mol Imaging* (2018) 45(6):1076–7. doi: 10.1007/s00259-018-3952-0

16. Kuten J, Fahoum I, Savin Z, Shamni O, Gitstein G, Hershkovitz D, et al. Head-to-Head Comparison of (68)Ga-PSMA-11 with (18)F-PSMA-1007 PET/CT in Staging Prostate Cancer Using Histopathology and Immunohistochemical Analysis as a Reference Standard. *J Nucl Med* (2020) 61(4):527–32. doi: 10.2967/jnumed.119.234187
17. Draulans C, De Roover R, van der Heide UA, Kerkmeijer L, Smeenk RJ, Pos F, et al. Optimal 68Ga-PSMA and 18F-PSMA PET window levelling for gross tumour volume delineation in primary prostate cancer. *Eur J Nuclear Med Mol Imaging* (2020). doi: 10.1007/s00259-020-05059-4
18. Cardinale J, Martin R, Remde Y, Schäfer M, Hienzsch A, Hübner S, et al. Procedures for the GMP-Compliant Production and Quality Control of [(18)F]PSMA-1007: A Next Generation Radiofluorinated Tracer for the Detection of Prostate Cancer. *Pharmaceuticals (Basel Switzerland)* (2017) 10(4):77. doi: 10.3390/ph10040077
19. Zamboglou C, Carles M, Fechter T, Kiefer S, Reichel K, Fassbender TF, et al. Radiomic features from PSMA PET for non-invasive intraprostatic tumor discrimination and characterization in patients with intermediate- and high-risk prostate cancer - a comparison study with histology reference. *Theranostics* (2019) 9(9):2595–605. doi: 10.7150/thno.32376
20. Zamboglou C, Drendel V, Jilg CA, Rischke HC, Beck TI, Schultze-Seemann W, et al. Comparison of (68)Ga-HBED-CC PSMA-PET/CT and multiparametric MRI for gross tumour volume detection in patients with primary prostate cancer based on slice by slice comparison with histopathology. *Theranostics* (2017) 7(1):228–37. doi: 10.7150/thno.16638
21. Zamboglou C, Schiller F, Fechter T, Wieser G, Jilg CA, Chirindel A, et al. (68)Ga-HBED-CC-PSMA PET/CT Versus Histopathology in Primary Localized Prostate Cancer: A Voxel-Wise Comparison. *Theranostics* (2016) 6(10):1619–28. doi: 10.7150/thno.15344
22. Rauscher I, Krönke M, König M, Gafita A, Maurer T, Horn T, et al. Matched-Pair Comparison of (68)Ga-PSMA-11 PET/CT and (18)F-PSMA-1007 PET/CT: Frequency of Pitfalls and Detection Efficacy in Biochemical Recurrence After Radical Prostatectomy. *J Nucl Med* (2020) 61(1):51–7. doi: 10.2967/jnumed.119.229187
23. Steenbergen P, Haustermans K, Lerut E, Oyen R, De Wever L, Van den Bergh L, et al. Prostate tumor delineation using multiparametric magnetic resonance imaging: Inter-observer variability and pathology validation. *Radiother Oncol* (2015) 115(2):186–90. doi: 10.1016/j.radonc.2015.04.012
24. Zschaeck S, Lohaus F, Beck M, Habl G, Kroeze S, Zamboglou C, et al. PSMA-PET based radiotherapy: a review of initial experiences, survey on current practice and future perspectives. *Radiation Oncol* (2018) 13(1):90. doi: 10.1186/s13014-018-1047-5
25. Pathmanathan AU, McNair HA, Schmidt MA, Brand DH, Delacroix L, Eccles CL, et al. Comparison of prostate delineation on multimodality imaging for MR-guided radiotherapy. *Br J Radiol* (2019) 92(1095):20180948–. doi: 10.1259/bjr.20180948
26. Giesel FL, Sterzing F, Schlemmer HP, Holland-Letz T, Mier W, Rius M, et al. Intra-individual comparison of 68Ga-PSMA-11-PET/CT and multi-parametric MR for imaging of primary prostate cancer. *Eur J Nuclear Med Mol Imaging* (2016) 43(8):1400–6. doi: 10.1007/s00259-016-3346-0
27. Thomas L, Kantz S, Hung A, Monaco D, Gaertner FC, Essler M, et al. 68Ga-PSMA-PET/CT imaging of localized primary prostate cancer patients for intensity modulated radiation therapy treatment planning with integrated boost. *Eur J Nuclear Med Mol Imaging* (2018) 45(7):1170–8. doi: 10.1007/s00259-018-3954-y
28. Oehlke O, Mix M, Graf E, Schimek-Jasch T, Nestle U, Götz I, et al. Amino-acid PET versus MRI guided re-irradiation in patients with recurrent glioblastoma multiforme (GLIAA)–protocol of a randomized phase II trial (NOA 10/ARO 2013-1). *BMC Cancer* (2016) 16(1):769. doi: 10.1186/s12885-016-2806-z
29. Rischke HC, Nestle U, Fechter T, Doll C, Volegova-Neher N, Henne K, et al. 3 Tesla multiparametric MRI for GTV-definition of Dominant Intraprostatic Lesions in patients with Prostate Cancer – an interobserver variability study. *Radiat Oncol* (2013) 8(1):183. doi: 10.1186/1748-717X-8-183
30. Zamboglou C, Klein CM, Thomann B, Fassbender TF, Rischke HC, Kirste S, et al. The dose distribution in dominant intraprostatic tumour lesions defined by multiparametric MRI and PSMA PET/CT correlates with the outcome in patients treated with primary radiation therapy for prostate cancer. *Radiat Oncol (London England)* (2018) 13(1):65. doi: 10.1186/s13014-018-1014-1
31. Pucar D, Hricak H, Shukla-Dave A, Kuroiwa K, Drobnjak M, Eastham J, et al. Clinically significant prostate cancer local recurrence after radiation therapy occurs at the site of primary tumor: magnetic resonance imaging and step-section pathology evidence. *Int J Radiat Oncol Biol Phys* (2007) 69(1):62–9. doi: 10.1016/j.ijrobp.2007.03.065
32. Goodman CD, Fakir H, Pautler S, Chin J, Bauman GS. Dosimetric Evaluation of PSMA PET-Delineated Dominant Intraprostatic Lesion Simultaneous Infield Boosts. *Adv Radiat Oncol* (2020) 5(2):212–20. doi: 10.1016/j.adro.2019.09.004
33. Mannweiler S, Amersdorfer P, Trajanoski S, Terrett JA, King D, Mehes G. Heterogeneity of Prostate-Specific Membrane Antigen (PSMA) Expression in Prostate Carcinoma with Distant Metastasis. *Pathol Oncol Res* (2009) 15(2):167–72. doi: 10.1007/s12253-008-9104-2
34. Paschalis A, Sheehan B, Riisnaes R, Rodrigues DN, Gurel B, Bertan C, et al. PSMA heterogeneity and DNA repair defects in prostate cancer. *J Clin Oncol* (2019) 37(15_suppl):5002–. doi: 10.1200/JCO.2019.37.15_suppl.5002
35. Kesch C, Vinsensia M, Radtke JP, Schlemmer HP, Heller M, Ellert E, et al. Intraindividual comparison of 18F-PSMA-1007 PET/CT, multiparametric MRI, and radical prostatectomy specimens in patients with primary prostate cancer: a retrospective, proof-of-concept study. *J Nucl Med* (2017) 58(11):1805–10. doi: 10.2967/jnumed.116.189233
36. Chen M, Zhang Q, Zhang C, Zhao X, Marra G, Gao J, et al. Combination of 68Ga-PSMA PET/CT and Multiparametric MRI Improves the Detection of Clinically Significant Prostate Cancer: A Lesion-by-Lesion Analysis. *J Nuc Med* (2019) 60(7):944–9. doi: 10.2967/jnumed.118.221010
37. Bravaccini S, Puccetti M, Bocchini M, Ravaioli S, Celli M, Scarpi E, et al. PSMA expression: a potential ally for the pathologist in prostate cancer diagnosis. *Scientific Reports* (2018) 8: (1):1–8. doi: 10.1038/s41598-018-22594-1
38. Rhee H, Thomas P, Shepherd B, Gustafson S, Vela I, Russell P, et al. Prostate specific membrane antigen positron emission tomography may improve the diagnostic accuracy of multiparametric magnetic resonance imaging in localized prostate cancer. *J Urol* (2016) 196(4):1261–7. doi: 10.1016/j.juro.2016.02.3000
39. Berger I, Annabattula C, Lewis J, Shetty D, Kam J, Maclean F, et al. 68 Ga-PSMA PET/CT vs. mpMRI for locoregional prostate cancer staging: correlation with final histopathology. *Prostate Cancer and Prostatic Diseases* (2018) 21(2):204–11. doi: 10.1038/s41391-018-0048-7

Conflict of Interest: The authors declare that the research was conducted in the absence of any commercial or financial relationships that could be construed as a potential conflict of interest.

The reviewer TZ declared a past co-authorship with several of the authors WS-S, CJ, and AG to the handling editor.

frontiers in Oncology

ORIGINAL RESEARCH
published: 10 March 2021
doi: 10.3389/fonc.2021.646110

Use of ^{68}Ga-PSMA-11 and ^{18}F-FDG PET-CT Dual-Tracer to Differentiate Between Lymph Node Metastases and Ganglia

Yiping Shi[1†], Lian Xu[1†], Yinjie Zhu[2†], Yining Wang[1], Ruohua Chen[1] and Jianjun Liu[1*]*

[1] Department of Nuclear Medicine, Ren Ji Hospital, School of Medicine, Shanghai Jiao Tong University, Shanghai, China, [2] Department of Urology, Ren Ji Hospital, School of Medicine, Shanghai Jiao Tong University, Shanghai, China

OPEN ACCESS

Edited by:
Xuefeng Qiu,
Nanjing Drum Tower Hospital, China

Reviewed by:
Punit Sharma,
Apollo Gleneagles Hospitals, India
Clément Morgat,
Centre Hospitalier Universitaire de Bordeaux, France

***Correspondence:**
Ruohua Chen
crh19870405@163.com
Jianjun Liu
nuclearj@163.com

[†]These authors have contributed equally to this work

Specialty section:
This article was submitted to Cancer Imaging and Image-directed Interventions, a section of the journal Frontiers in Oncology

Received: 25 December 2020
Accepted: 04 February 2021
Published: 10 March 2021

Citation:
Shi Y, Xu L, Zhu Y, Wang Y, Chen R and Liu J (2021) Use of ^{68}Ga-PSMA-11 and ^{18}F-FDG PET-CT Dual-Tracer to Differentiate Between Lymph Node Metastases and Ganglia. Front. Oncol. 11:646110. doi: 10.3389/fonc.2021.646110

Purpose: Differentiating lymph node metastases (LNM) from peripheral ganglia by physiological prostate-specific membrane antigen (PSMA) uptake is challenging. Two tracers (^{68}Ga-PSMA-11 and ^{18}F-fluorodeoxyglucose [FDG]) metabolic uptake patterns were evaluated by positron emission tomography-computed tomography (PET-CT), searching for differences that could tell ganglia from LNM.

Methods: Dual ^{68}Ga-PSMA-11 and ^{18}F-FDG PET-CT data of 138 prostate cancer patients acquired from June 2018 to December 2019 were retrospectively evaluated. Ganglia and LNM with PSMA-11 uptake above local background were analyzed by the location and PSMA-11-PET and FDG-PET maximum standardized uptake value (SUVmax).

Results: PSMA-11-positive ganglia (n = 381) and LNM (n = 83) were identified in 138 and 58 patients, respectively. The LNM SUVmax of PSMA-11-PET (16.4 ± 14.8 vs 2.3 ± 0.7, $P < 0.001$) and FDG-PET (3.3 ± 3.2 vs 1.5 ± 0.5, $P < 0.001$) were higher than in ganglia. The probabilities of being an LNM in the low-potential (PSMA-11-PET SUVmax of <4.1 and FDG-PET SUVmax of <2.05), moderate-potential (PSMA-11-PET SUVmax of >4.1 and FDG-PET SUVmax of <2.05, or PSMA-11-PET SUVmax of <4.1 and FDG-PET SUVmax of >2.05), and high-potential (PSMA-11-PET SUVmax of >4.1 and FDG-PET SUVmax of >2.05) groups were 0.9% (3/334), 44.6% (37/83), and 91.5% (43/47), respectively ($P < 0.001$). The cervical and coeliac ganglia had higher PSMA-11 and FDG uptake than the sacral ganglia ($P < 0.001$ for all). LNM PSMA-11 and FDG uptake was similar in these three locations.

Conclusion: The FDG-PET and PSMA-11-PET SUVmax, especially when combined, could well differentiate LNM from ganglia. The tracers uptake differed between cervical/coeliac and sacral ganglia, so the lesion location should be considered during image assessment.

Keywords: ^{68}Ga-PSMA-11, ^{18}F-FDG, ganglia, lymph node metastases, prostate cancer

INTRODUCTION

Prostate cancer is a common malignant tumor in males (1). Despite initial treatment by radical prostatectomy, biochemical recurrence (BCR) remains a major problem (2). The ability to determine the location and degree of recurrence is of great significance for treatment planning. However, conventional imaging techniques, including magnetic resonance imaging (MRI) and computed tomography (CT) (3), have limited sensitivity. Since 2012, the application of ^{68}Ga-prostate-specific membrane antigen (PSMA) positron emission tomography (PET)-CT has significantly improved detection rates in BCR patients (4–7). Various studies showed that 68Ga-PSMA PET-CT detection efficiency is higher than conventional imaging approaches and choline PET (4, 8).

However, PSMA is expressed on prostate cancer cells and many other tissues, both physiologically (9) and pathologically (10). For instance, PSMA is expressed in the salivary glands, submandibular glands, kidneys, spleen, liver, and more. PSMA is also expressed in neovascularization of many solid tumors (11–13). Besides, many studied reported that peripheral nerve ganglia uptake PSMA (14). It has been reported that astrocytes express PSMA physiologically as PSMA is related to their homolog glutamic acid carboxypeptidase III (15, 16). Such a widespread nonspecific PSMA-11 uptake might lead to potential pitfalls in interpreting images.

Therefore, differentiating lymph node metastases from physiological PSMA uptake in peripheral ganglia is a challenge for nuclear medicine physicians. To solve this problem, some strategies have been proposed. For example, performing a careful anatomic correlation by comparing and examining the morphology of the lesions. Banding was correlated with ganglia, while lymph nodes resemble teardrops or nodules (14). Previous studies have shown that ganglia show mild to moderate PSMA-11 uptake and cervical/coeliac ganglia had higher PSMA-11 uptake than sacral ganglia (14). Recently, Alberts et al. found that delayed ^{68}Ga-PSMA PET-CT could be used to differentiate ganglia from lymph node metastases, but the overall diagnostic efficiency was not high, with a sensitivity of 73% and specificity of 65% (17). With such diagnostic efficiency, these methods offer no effective mean to tell lymph node metastases from peripheral ganglia. Therefore, new imaging approaches are needed.

^{18}F-fluorodeoxyglucose (FDG)-PET has been extensively used to differentiate benign from malignant lesions. Studies have also indicated that ^{18}F-FDG has a gain value in partial prostate cancers with a high Gleason grade (18, 19), especially for prostate cancers with negative ^{68}Ga-PSMA PET-CT findings (20, 21). However, studies describing the ^{18}F-FDG uptake pattern for ganglia and whether ^{18}F-FDG PET-CT could be used to differentiate between them and lymph node metastases are lacking. In addition, whether there were ^{18}F-FDG uptake differences of ganglia in different anatomical location were also unknown. Therefore, in this study, we performed dual-tracer (^{68}Ga-PSMA-11 and ^{18}F-FDG) PET-CT to evaluate the metabolic patterns of these tracers according to different anatomical location in lymph node metastases and ganglia. We assumed that the heterogeneous metabolic patterns of ^{68}Ga-PSMA-11 and ^{18}F-FDG could be used to differentiate between lymph node metastases and ganglia, and there were also differences in ^{68}Ga-PSMA-11 and ^{18}F-FDG uptake between cervical/coeliac and sacral ganglia which should be considered for better identification.

METHODS

Participants

The ethics committee of Renji Hospital approved this retrospective study, which used data obtained for clinical purposes. The need for informed consent was waived. The study was performed in accordance with the ethical standards as laid down in the 1964 Declaration of Helsinki and its later amendments. A total of 138 consecutive patients with prostate cancer who underwent both ^{68}Ga-PSMA-11 and ^{18}F-FDG PET-CT between June 2018 and December 2020 were enrolled. The PSMA ligand was ^{68}Ga-PSMA-11. The inclusion criteria were as follows: (a) Prostate cancer patients who underwent ^{68}Ga-PSMA-11 PET-CT and ^{18}F-FDG PET-CT with less than two weeks in between; (b) patients characteristics, including age, Gleason grade score, prostate-specific antigen (PSA) level, and treatment history were available; (c) prostate cancer treatment was not done during the interval between the two scans. The detailed patients' characteristics are listed in **Table 1**.

Image Evaluation

Two nuclear medicine physicians with ten (LX, reader 1) and eight (RC, reader 2) years of experience in PET-CT interpretation evaluated together the image data and resolved any disagreements by discussion till they reached consensus. Regions of interest (ROI) were placed over the selected ganglia or

TABLE 1 | Patients characteristics (n=138).

Characteristics	No. of Patients
Age (y)	
Mean ± SD	69.2 ± 7.4
Range	55-90
Gleason score	
6	4
7	69
8	31
9	31
10	3
Patient type	
Staging before treatment	65
Biochemical recurrence	73
PSA level	
Staging before treatment (IQR)	56.4 (18.5-99.7)
Biochemical recurrence (IQR)	1.1 (0.5-4.1)
PSMA-11-positive ganglia	
No. of patients	138
No. of lesions	381
PSMA-11-positive lymph node metastases	
No. of patients	58
No. of lesions	83

lymph node metastases. The maximum standardized uptake value (SUVmax) was calculated as follows: maximum pixel value in the decay-corrected ROI activity (MBq/kg)/[the injected ^{18}F-FDG or ^{68}Ga-PSMA-11 radioactivity (MBq)/body weight (kg)].

Ganglia and adjacent lymph node metastases were grouped according to their anatomic location: cervical, coeliac, or sacral. The main criterion for ganglia was focal ^{68}Ga-PSMA-11 uptake that projected onto a structure of typical type and location for sympathetic ganglia, as described previously (14). Lesions that were considered to be suggestive for ganglia or lymph node metastases and exhibited increased ^{68}Ga-PSMA-11 tracer uptake relative to local background were counted. To avoid introducing possible bias, the selection criteria for ganglia were as follows: 1) Only the ganglion with the highest PSMA-11 uptake in each anatomical location (cervical, coeliac, or sacral) was selected if more than one PSMA-11-positive ganglion existed. 2) If the anatomical location had no PSMA-11-positive ganglia, it was defined as PSMA-11-negative. The same selection criteria were used to define and select lymph node metastases with increased ^{68}Ga-PSMA-11 uptake relative to local background.

Statistical Analysis

Results are either demonstrated as mean ± SD or as frequencies (%). For comparison of continuous variables, the 2-tailed unpaired Student t test was used. The x2 test was applied to compare nominal variables. All statistical analyses were performed using SPSS 21.0 (IBM Corp., USA), with a two-sided P<0.05 considered statistically significant.

RESULTS

Ganglia Uptake Patterns

We identified 381 PSMA-11-positive ganglia (i.e., cervical, coeliac, or sacral) in all 138 patients in our cohort (100%), and 83 PSMA-11-positive lymph node metastases in 58 patients (42%; **Table 1**). Grouped by anatomical location, PSMA-11-positive uptake was observed in cervical, coeliac, and sacral ganglia at frequencies of 98.6% (136/138 patients), 96.4% (133/138 patients), and 81.2% (112/138 patients), respectively (**Figure 1A**). Cervical and coeliac ganglia had a higher rate of PSMA-11-positive uptake than sacral ganglia (P < 0.001 for both).

Qualitatively, among the 381 PSMA-11-positive ganglia, 13.6% (52/381) were identified as FDG-positive and 86.4% (329/381) as FDG-negative (**Figure 1B**). Quantitatively, the PSMA-11-PET SUVmax ranged from 1.3 to 6.6. The cervical and coeliac ganglia were similar in PSMA-11 uptake (2.5 ± 0.7 vs 2.4 ± 0.8, P = 0.665). However, PSMA-11 uptake in both cervical (2.5 ± 0.7 vs 1.8 ± 0.4, P < 0.001) and coeliac (2.4 ± 0.8 vs 1.8 ± 0.4, P < 0.001) ganglia was significantly higher than in the sacral ganglia (**Figure 3A**). The FDG-PET SUVmax ranged from 0.3 to 3.5. The cervical and coeliac ganglia were similar in FDG uptake (1.6 ± 0.5 vs 1.6 ± 0.4, P = 0.995), but both were significantly higher than in the sacral ganglia (1.6 ± 0.5 vs 1.2 ± 0.4, and 1.6 ± 0.4 vs 1.2 ± 0.4, respectively, P < 0.001 for both; **Figure 3B**). The detailed SUVmax for ganglia and lymph node metastases are listed in **Table 2**. Representative images of ganglia are shown in **Figure 2**.

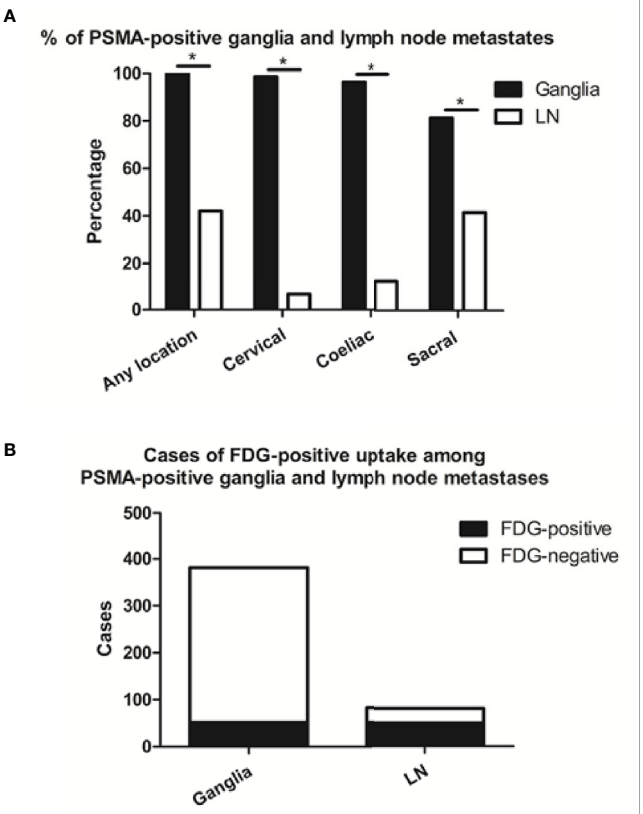

FIGURE 1 | Frequencies of PSMA-11-positive and cases of FDG-positive and -negative ganglia and lymph node (LN) metastases. **(A)** Frequencies of PSMA-11-positive ganglia and lymph node metastases occurring at any location, or limited to the coeliac, cervical, or sacral area on a per-patient-basis. **(B)** Cases of FDG-positive uptake among PSMA-11-positive ganglia and lymph node metastases. Asterisk (*) indicates a significant difference within the same location at P < 0.001.

Lymph Node Metastases Uptake Patterns

PSMA-11-positive lymph node metastases at any anatomical location (cervical, coeliac, or sacral) were detected in 42.0% (58/138) of the patients. Grouped by their anatomical location, PSMA-11-positive cervical, coeliac, and sacral lymph node metastases were observed at frequencies of 6.5% (9/138 patients), 12.3% (17/138 patients), and 41.3% (57/138 patients; **Figure 1A**). Frequencies of PSMA-11-positive ganglia and lymph node metastases differed at all anatomical locations (P < 0.001; **Figure 1A**).

Qualitatively, among the 83 PSMA-11-positive lymph node, 62.7% (52/83) were identified as FDG-positive and 37.3% (31/83) as FDG-negative (**Figure 1B**). FDG-positive rate in PSMA-11-

TABLE 2 | SUVmax of PSMA-11-PET and FDG-PET in ganglia and lymph node metastases.

Parameter		Ganglia				LN			
		Any Location	Cervical	Coeliac	Sacral	Any Location	Cervical	Coeliac	Sacral
PSMA-11	Mean	2.3	2.5	2.4	1.8	16.4	9.7	15.5	17.7
	SD	0.7	0.7	0.8	0.4	14.8	6.6	12.3	16.1
	Median	2.1	2.4	2.3	1.7	10.4	8.7	8.8	11.7
FDG	Mean	1.5	1.6	1.6	1.2	3.3	5.1	3.3	3.1
	SD	0.5	0.5	0.4	0.4	3.2	4	2.4	3
	Median	1.5	1.5	1.6	1.1	2.5	3.9	2.8	2.3

positive lymph node metastases was higher than in PSMA-11-positive ganglia (62.7% vs 13.6%, P < 0.001).

Quantitatively, the PSMA-11-PET SUVmax ranged from 1.0 to 68.2. No difference was observed in PSMA-11 uptake between the cervical, coeliac, and sacral ganglia (P = 0.316). The FDG-PET SUVmax, which ranged from 0.7 to 23.1, was also similar in the three anatomical locations (P = 0.244; **Table 2**). Representative images for lymph node metastasis are shown in **Figure 2**.

Comparison of PSMA-11-PET and FDG-PET SUVmax Between Ganglia and Lymph Node Metastases

As shown in **Figure 3**, PSMA-11-PET SUVmax in lymph node metastases was significantly higher than in ganglia (16.4 ± 14.8 vs 2.3 ± 0.7, $P < 0.001$). Similarly, FDG-PET SUVmax in lymph node metastases was significantly higher than in ganglia (3.3 ± 3.2 vs 1.5 ± 0.5, $P < 0.001$).

We then determined the optimal PSMA-11-PET or FDG-PET SUVmax thresholds for distinguishing between lymph node metastases and ganglia (**Figure 4**). Receiver-operating characteristic (ROC) curve analysis revealed that when the PSMA-11-PET SUVmax cutoff was 4.1, the sensitivity and specificity for identifying a lymph node metastasis were 88.0% (73/83) and 97.1% (370/381), respectively. The area under curve was 0.949 (95% confidence interval [CI]: 0.913-0.985). Similarly, ROC curve analysis revealed that when the FDG-PET SUVmax cutoff was 2.05, the sensitivity and specificity for identifying a lymph node metastasis were 60.2% (50/83) and 88.7% (338/381), respectively. The area under the curve was 0.724 (95% CI: 0.645-0.803). We further compared the diagnostic performance of PSMA-11-PET and FDG-PET for distinguishing between lymph node metastases and ganglia. PSMA-11-PET SUVmax with an AUC of 0.949 showed a better distinguishing performance than FDG-PET SUVmax with an AUC of 0.724 ($P < 0.001$).

Based on the PSMA-11-PET and FDG-PET SUVmax, we divided the lesions into three groups according to the possibility of them being a lymph node metastasis: a low-potential group (PSMA-11-PET SUVmax of <4.1 and FDG-PET SUVmax of <2.05), moderate-potential group (PSMA-11-PET SUVmax of >4.1 and FDG-PET SUVmax of <2.05 or PSMA-11-PET SUVmax of <4.1 and FDG-PET SUVmax of >2.05), and high-potential group (PSMA-11-PET SUVmax of >4.1 and FDG-PET SUVmax of >2.05). The probabilities of being a lymph node metastasis in the low-, moderate-, and high-potential groups were 0.9% (3/334), 44.6% (37/83), and 91.5% (43/47), respectively (P < 0.001; **Table 3**).

Subgroup Analysis According to the Anatomical Location

From the above results, we found that cervical and coeliac ganglia showed higher PSMA-11 and FDG uptake than sacral ganglia (P < 0.001 for all). Lymph node metastases PSMA-11 and FDG uptake were similar in the three anatomical locations. We thus analyzed the lesions according to their anatomical location. With 100% of the lesion being ganglia, we used a PSMA-11-PET SUVmax of <4.1, FDG-PET SUVmax of <2.05 for the cervical and coeliac regions and PSMA-11-PET SUVmax of >4.1, FDG-PET SUVmax of >2.05 for the sacral region.

In the cervical and coeliac regions, the probabilities of being a lymph node metastasis in the low-, moderate-, and high-potential groups were 0% (0/223), 20.8% (11/53), and 78.9% (15/19), respectively ($P < 0.001$; **Table 3**). The probabilities of being a lymph node metastasis in the sacral region in the low-, moderate-, and high-potential groups were 2.7% (3/111), 86.7% (26/30), and 100% (28/28), respectively ($P < 0.001$; **Table 3**).

The Association Between PSMA-11 or FDG Uptake and the Gleason Score and PSA Level in Ganglia and Lymph Node Metastases

We further investigated whether there was a correlation between PSMA-11 and FDG uptake and the Gleason score or PSA level in ganglia and lymph node metastases.

We found no difference in PSMA-11 or FDG uptake between ganglia with high and low Gleason scores ($P > 0.05$ for all, **Figure 5**). Furthermore, no association was found between PSMA-11 or FDG uptake and the PSA level in ganglia of patients evaluated preoperatively (Pearson correlation coefficient between PSMA-11 or FDG uptake and the PSA level: r = 0.115, $P = 0.401$ and r = 0.013, $P = 0.927$, respectively) or following BCR (between PSMA-11 or FDG uptake and the PSA level: r = 0.116, $P = 0.327$ and r = 0.039, $P = 0.745$, respectively).

Similarly, no difference was noted in PSMA-11 or FDG uptake between high and low Gleason scores for lymph node metastases ($P > 0.05$ for both, **Figure 5**). No association was found between PSMA-11 or FDG uptake and the PSA level in lymph node metastases of patients evaluated preoperatively (Pearson correlation coefficient between PSMA-11 or FDG

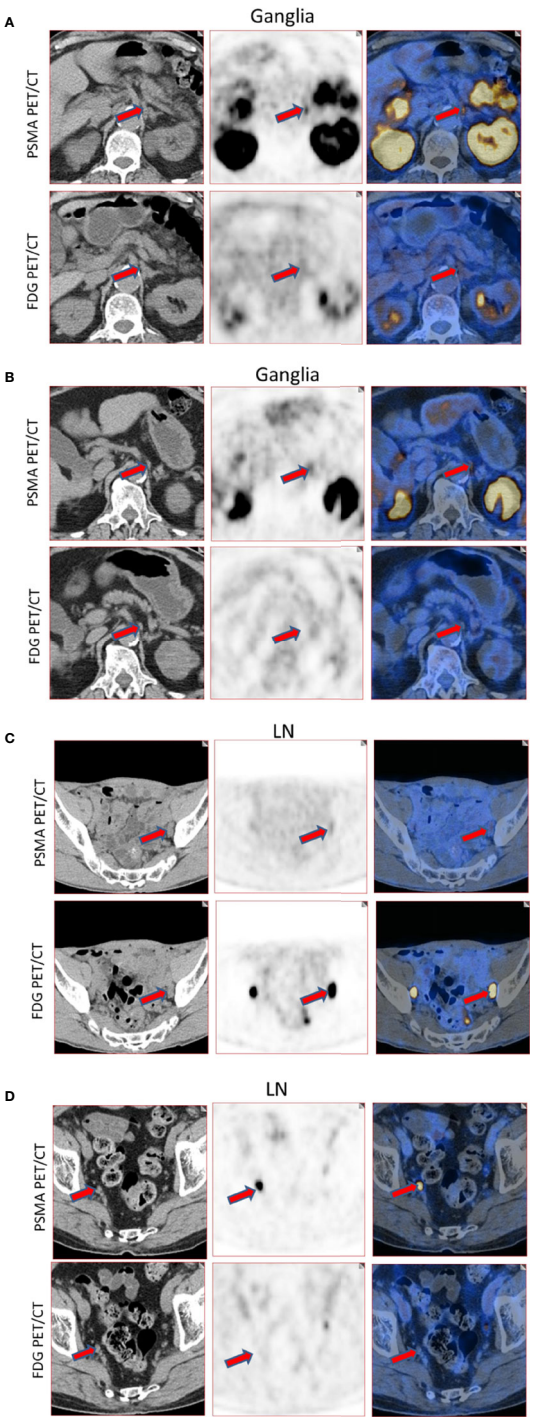

FIGURE 2 | Representative images of PSMA-11-positive ganglia and lymph node metastases. **(A)** FDG-positive celiac ganglia (red arrow, SUVmax of PSMA-11-PET 6.6, SUVmax of FDG-PET 2.9). **(B)** FDG-negative celiac ganglia (red arrow, SUVmax of PSMA-11-PET 3.6, SUVmax of FDG-PET 0.7). **(C)** FDG-positive pelvic lymph node metastasis (red arrow, SUVmax of PSMA-11-PET 3.2, SUVmax of FDG-PET 28.0). Lymph node metastasis was confirmed by postoperative pathology. **(D)** FDG-negative pelvic lymph node metastasis (red arrow, SUVmax of PSMA-11-PET 14.4 and SUVmax of FDG-PET 0.6). Lymph node metastasis was confirmed by postoperative pathology.

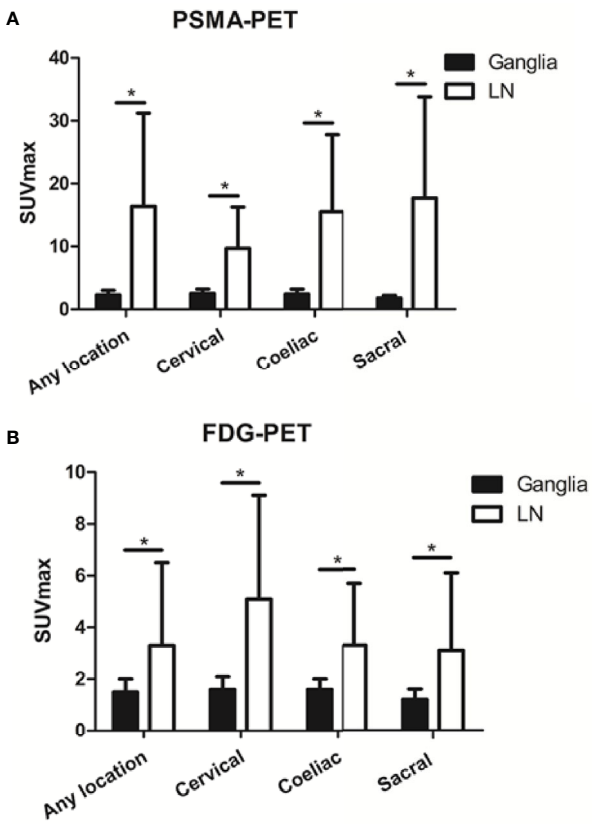

FIGURE 3 | Prostate-specific membrane antigen (PSMA-11) and fluorodeoxyglucose (FDG) uptake in ganglia and adjacent lymph node metastases. **(A)** PSMA-11 uptake in ganglia and adjacent lymph node metastases. **(B)** FDG uptake in ganglia and adjacent lymph node metastases. Asterisk (*) indicates a significant difference within the same location at $P < 0.001$.

uptake and the PSA level: r = 0.251, $P = 0.085$ and r = 0.137, $P = 0.564$, respectively) or following BCR (between PSMA-11 or FDG uptake and the PSA level: r = 0.042, $P = 0.831$ and r = 0.215, $P = 0.273$, respectively).

DISCUSSION

Many studies have indicated the unspecific nature of PSMA-11 expression, and PSMA-11-positive ganglia represent a potential diagnostic pitfall for nuclear medicine physicians. In our study, we analyzed the patterns of ^{68}Ga-PSMA-11 and ^{18}F-FDG tracers uptake by ganglia and lymph node metastases, and whether a dual-tracer PET-CT could be used to tell lymph node metastases and ganglia apart. Our study is the first to describe differences in metabolic patterns in ^{68}Ga-PSMA-11 and ^{18}F-FDG uptake between ganglia and lymph node metastases, and demonstrate that this difference could be used to tell them apart.

In this study, we identified PSMA-11-positive ganglia in 100% of our patients. These included cervical ganglia in 98.6% of the

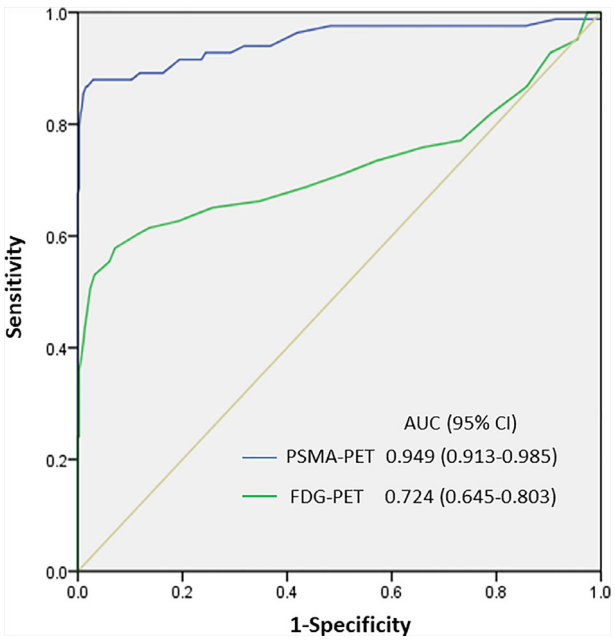

FIGURE 4 | SUVmax of PSMA-11-PET and FDG-PET for distinguishing between lymph node metastasis and ganglia. The area under the curve of PSMA-11-PET was 0.949 (95% confidence interval [CI], 0.913-0.985; $P < 0.001$), and a PSMA-11-PET SUVmax of 4.1 was determined as the optimal threshold for identifying lymph node metastases. With a PSMA-11-PET SUVmax of 4.1, the sensitivity and specificity for identifying lymph node metastases from ganglia were 88.0% (73/83) and 97.1% (370/381), respectively. The area under the curve of FDG-PET was 0.724 (95% CI, 0.645-0.803; $P < 0.001$), and an FDG-PET SUVmax of 2.05 was determined as the optimal threshold for identifying lymph node metastases. With this SUVmax, the sensitivity and specificity for identifying lymph node metastases from ganglia were 60.2% (50/83) and 88.7% (338/381), respectively.

TABLE 3 | Rate of being lymph node metastases or ganglia.

Locaiton	Potential	Total (n)	Being lymph node metastases or ganglia		P value
			Lymph node metastases (%)	Ganglia (%)	
Any location	Low	334	0.9	99.1	<0.001
	Moderate	83	44.6	55.4	
	High	47	91.5	8.5	
	Total	464	17.9	82.1	
Cervical and coeliac	Low	223	0	100	<0.001
	Moderate	53	20.8	79.2	
	High	19	78.9	21.1	
	Total	295	8.8	91.2	
Sacral	Low	111	2.7	97.3	<0.001
	Moderate	30	86.7	13.3	
	High	28	100	0	
	Total	169	33.7	66.3	

patients, coeliac ganglia in 96.4%, and sacral ganglia in 81.2%. These results are similar to the PSMA-11-positive rates reported by Rischpler et al. (14). We observed that lymph node metastases had a significantly higher PSMA-11-PET SUVmax than ganglia, which is consistent with other studies (14, 17). PSMA-11 Vinsensia et al. suggested PSMA-11-PET SUVmax of 2.0 as the threshold for PSMA-11-positive lymph node metastases (22). However, our study demonstrated that 60.9% of the ganglia had a PSMA-11-PET SUVmax higher than 2.0. Furthermore, ganglia and lymph node metastases structures can easily be mistaken visually. In a PET-MRI study of coeliac ganglia, Bialek et al. indicated that about half of the patients had at least one ganglion that was confused with PSMA-11-positive lymph node by shape, size, or PSMA-11 uptake (23). Recently, Alberts et al. indicated that delayed ^{68}Ga-PSMA-11 PET-CT imaging could be used to differentiate ganglia from lymph node metastases, but the overall diagnostic efficiency of predicting lymph node metastases was not high, with sensitivity and specificity of 73% and 65%, respectively (17). The currently available methods efficiency in differentiating ganglion from lymph node metastasis is not high, so new imaging methods are needed to tell them apart.

We found that among the PSMA-11-positive ganglia and lymph node metastases, 62.7% of the lymph node metastases were FDG-positive, while only 13.6% of the ganglia were FDG-positive. ROC analysis indicated that with an SUVmax cut-off of 2.05, the sensitivity and specificity for predicting a lymph node metastasis were 60.2% and 88.7%, respectively. We also found that the absolute PSMA-11-PET SUVmax in lymph node metastases was significantly higher than in ganglia, which is consistent with previous results (17). PSMA-11We found, based on ROC curve analysis, that an SUVmax cut-off of 4.1 had high sensitivity and specificity, and that PSMA-11-PET SUVmax was better than FDG-PET SUVmax at distinguishing between ganglia and lymph node metastases. The relatively low SUVmax of FDG-PET and PSMA-11-PET for ganglia may be attributed to the low ^{18}F-FDG uptake of ganglia and low PSMA-11 expression in ganglia. Because the SUVmax of FDG-PET and PSMA-11-PET for ganglia were lower and narrower that lymph node metastasis, we could distinguish them by the uptake characterization.

We categorized the lesions into three groups based on their potential of being identified as a lymph node metastasis by a combination of PSMA-11-PET and FDG-PET SUVmax. The probability of being a lymph node metastasis was 0.9% in the low-potential group and 91.5% in the high-potential group. Although previous studies indicated that cervical and coeliac ganglia had a higher PSMA-11 uptake than sacral ganglia (14), our study further found that besides PSMA-11 uptake, cervical and coeliac ganglia also had a higher FDG uptake than sacral ganglia. PSMA-11In the sacral region, the probabilities of being a lymph node metastasis in the low-, moderate-, and high-potential groups were 2.7%, 86.7%, and 100%, respectively ($P < 0.001$). PSMA-11In the cervical and coeliac regions, the probabilities of being a lymph node metastasis in the low-, moderate-, and high-potential groups were 0%, 20.8%, and 78.9%, respectively ($P < 0.001$). PSMA-11These results suggest that the pattern of PSMA-11 and FDG uptake by the lesions and their anatomical location should be considered for better differentiation between lymph node metastases and ganglia.

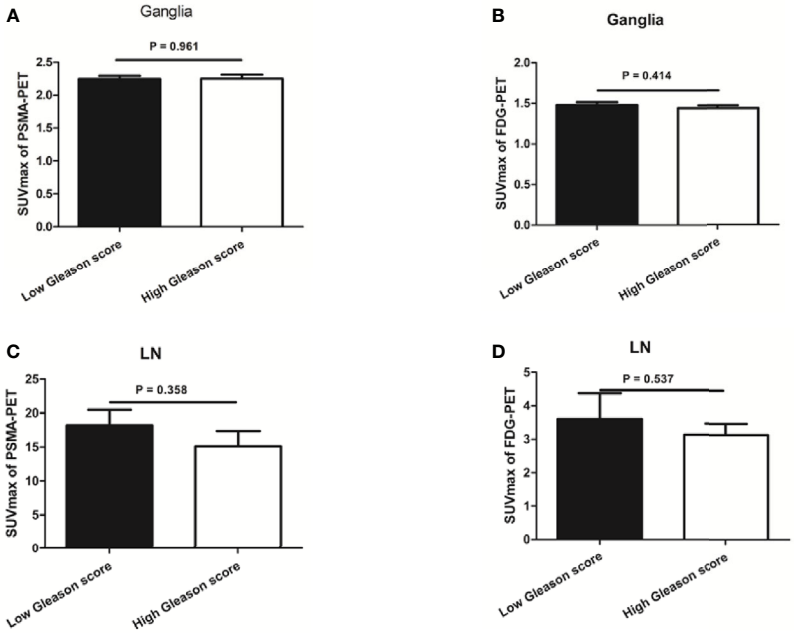

FIGURE 5 | The association between prostate-specific membrane antigen (PSMA-11) or fluorodeoxyglucose (FDG) uptake and Gleason score in ganglia and lymph node (LN) metastases. **(A)** No difference was observed in PSMA-11 uptake between high and low Gleason scores for ganglia (2.3 ± 0.8 vs 2.2 ± 0.7, $P = 0.961$). **(B)** No difference was observed in FDG uptake between high and low Gleason scores for ganglia (1.4 ± 0.4 vs 1.5 ± 0.5, $P = 0.414$). **(C)** No difference was observed in PSMA-11 uptake between high and low Gleason scores for lymph node metastases (15.1 ± 15.0 vs 18.2 ± 13.3, $P = 0.358$). **(D)** No difference was observed in FDG uptake between high and low Gleason scores for lymph node metastases (3.1 ± 2.4 vs 3.6 ± 3.5, $P = 0.537$).

PSA level and Gleason score are independent predictors of PSMA-11 (24) and FDG (18, 19, 25) PET-CT findings. However, PSMA-11no differences were observed in PSMA-11 or FDG uptake between high and low Gleason scores for ganglia. Furthermore, there was also no association between PSMA-11 or FDG uptake and the PSA level for ganglia in patients evaluated preoperatively or following BCR. Similar results were observed with lymph node metastases. Thus, when we differentiate lymph node metastases from ganglia, PSA level and the Gleason score are not risk factors that need to be considered.

Our study has several limitations. The definitions of lymph node metastases and ganglia were made mainly based on their characteristic imaging features, such as typical anatomic location. Pathological evidence was not clinically feasible because of ethical and practical reasons. Although we have established cut-off PSMA-11-PET and FDG-PET SUVmax for telling lymph node metastases from ganglia, this threshold may have been influenced by the PET-CT scanner model, PSMA-11 ligand, scanning procedure, and more. It is essential to establish the optimal SUVmax cut-off in clinical settings according to the actual imaging conditions, and not using PSMA-11-PET SUVmax of 4.1 and FDG-PET SUVmax of 2.05 arbitrarily as the thresholds. Furthermore, the sample size in this study was relatively small, and it was a retrospective study. Therefore, the results could have been influenced by selection bias and should be interpreted carefully. Further prospective studies with more cases are required to confirm our results.

CONCLUSIONS

This is the first study to describe ^{68}Ga-PSMA-11 and ^{18}F-FDG uptake patterns in ganglia and lymph node metastases. It demonstrates that FDG-PET and PSMA-11-PET SUVmax, especially when data from both tracers is combined, could be used to tell lymph node metastases from ganglia. Differences in ^{68}Ga-PSMA-11 and ^{18}F-FDG uptake between cervical/coeliac and sacral ganglia suggest that the anatomical location should be considered for better identification.

DATA AVAILABILITY STATEMENT

The raw data supporting the conclusions of this article will be made available by the authors, without undue reservation.

ETHICS STATEMENT

The studies involving human participants were reviewed and approved by the ethics committee of Renji Hospital. Written informed consent for participation was not required for this study in accordance with the national legislation and the institutional requirements.

AUTHOR CONTRIBUTIONS

RC and JL designed and wrote the experiments. RC, LX, YS, and YW collected and analyzed the data. YZ revised the manuscript. All authors contributed to the article and approved the submitted version.

FUNDING

The study was supported by National Natural Science Foundation of China (no. 81701724, 81771858, 81530053, 81830052, 81602415, and 81771861).

REFERENCES

1. Siegel RL, Miller KD, Jemal A. Cancer statistics, 2020. *CA Cancer J Clin* (2020) 70:7–30. doi: 10.3322/caac.21590
2. Boorjian SA, Eastham JA, Graefen M, Guillonneau B, Karnes RJ, Moul JW, et al. A critical analysis of the long-term impact of radical prostatectomy on cancer control and function outcomes. *Eur Urol* (2012) 61:664–75. doi: 10.1016/j.eururo.2011.11.053
3. Briganti A, Abdollah F, Nini A, Suardi N, Gallina A, Capitanio U, et al. Performance characteristics of computed tomography in detecting lymph node metastases in contemporary patients with prostate cancer treated with extended pelvic lymph node dissection. *Eur Urol* (2012) 61:1132–8. doi: 10.1016/j.eururo.2011.11.008
4. Perera M, Papa N, Roberts M, Williams M, Udovicich C, Vela I, et al. Gallium-68 Prostate-specific Membrane Antigen Positron Emission Tomography in Advanced Prostate Cancer-Updated Diagnostic Utility, Sensitivity, Specificity, and Distribution of Prostate-specific Membrane Antigen-avid Lesions: A Systematic Review and Meta-analysis. *Eur Urol* (2020) 77:403–17. doi: 10.1016/j.eururo.2019.01.049
5. Sprute K, Kramer V, Koerber S, Meneses M, Fernandez R, Soza-Ried C, et al. Diagnostic accuracy of (18)F-PSMA-1007-PET/CT imaging for lymph node staging of prostate carcinoma in primary and biochemical recurrence. *J Nucl Med* (2020) 622. doi: 10.2967/jnumed.120.246363
6. Tan N, Oyoyo U, Bavadian N, Ferguson N, Mukkamala A, Calais J, et al. PSMA-targeted Radiotracers versus (18)F Fluciclovine for the Detection of Prostate Cancer Biochemical Recurrence after Definitive Therapy: A Systematic Review and Meta-Analysis. *Radiology* (2020) 296:44–55. doi: 10.1148/radiol.2020191689
7. Fendler WP, Ferdinandus J, Czernin J, Eiber M, Flavell RR, Behr SC, et al. Impact of (68)Ga-PSMA-11 PET on the Management of recurrent Prostate Cancer in a Prospective Single-Arm Clinical Trial. *J Nucl Med* (2020) 6112. doi: 10.2967/jnumed.120.242180
8. Afshar-Oromieh A, Zechmann CM, Malcher A, Eder M, Eisenhut M, Linhart HG, et al. Comparison of PET imaging with a (68)Ga-labelled PSMA ligand and (18)F-choline-based PET/CT for the diagnosis of recurrent prostate cancer. *Eur J Nucl Med Mol Imaging* (2014) 41:11–20. doi: 10.1007/s00259-013-2525-5
9. Afshar-Oromieh A, Malcher A, Eder M, Eisenhut M, Linhart HG, Hadaschik BA, et al. PET imaging with a [68Ga]gallium-labelled PSMA ligand for the diagnosis of prostate cancer: biodistribution in humans and first evaluation of tumour lesions. *Eur J Nucl Med Mol Imaging* (2013) 40:486–95. doi: 10.1007/s00259-012-2298-2
10. Chang SS. Overview of prostate-specific membrane antigen. *Rev Urol* (2004) 6 Suppl 10:S13–8. doi: 10.1097/01.ju.0000142068.66876.53
11. Kunikowska J, Cieslak B, Gierej B, Patkowski W, Kraj L, Kotulski M, et al. [(68) Ga]Ga-Prostate-Specific Membrane Antigen PET/CT: a novel method for imaging patients with hepatocellular carcinoma. *Eur J Nucl Med Mol Imaging* (2020). doi: 10.1007/s00259-020-05017-0
12. Pozzessere C, Bassanelli M, Ceribelli A, Rasul S, Li S, Prior JO, et al. Renal Cell Carcinoma: the Oncologist Asks, Can PSMA PET/CT Answer? *Curr Urol Rep* (2019) 20:68. doi: 10.1007/s11934-019-0938-9
13. Raveenthiran S, Esler R, Yaxley J, Kyle S. The use of (68)Ga-PET/CT PSMA in the staging of primary and suspected recurrent renal cell carcinoma. *Eur J Nucl Med Mol Imaging* (2019) 46:2280–8. doi: 10.1007/s00259-019-04432-2
14. Rischpler C, Beck TI, Okamoto S, Schlitter AM, Knorr K, Schwaiger M, et al. (68)Ga-PSMA-11-HBED-CC Uptake in Cervical, Celiac, and Sacral Ganglia as an Important Pitfall in Prostate Cancer PET Imaging. *J Nucl Med* (2018) 59:1406–11. doi: 10.2967/jnumed.117.204677
15. Hlouchova K, Barinka C, Klusak V, Sacha P, Mlcochova P, Majer P, et al. Biochemical characterization of human glutamate carboxypeptidase III. *J Neurochem* (2007) 101:682–96. doi: 10.1111/j.1471-4159.2006.04341.x
16. Evans JC, Malhotra M, Cryan JF, O'Driscoll CM. The therapeutic and diagnostic potential of the prostate specific membrane antigen/glutamate carboxypeptidase II (PSMA/GCPII) in cancer and neurological disease. *Br J Pharmacol* (2016) 173:3041–79. doi: 10.1111/bph.13576
17. Alberts I, Sachpekidis C, Dijkstra L, Prenosil G, Gourni E, Boxler S, et al. The role of additional late PSMA-ligand PET/CT in the differentiation between lymph node metastases and ganglia. *Eur J Nucl Med Mol Imaging* (2020) 47:642–51. doi: 10.1007/s00259-019-04552-9
18. Jadvar H. Imaging evaluation of prostate cancer with 18F-fluorodeoxyglucose PET/CT: utility and limitations. *Eur J Nucl Med Mol Imaging* (2013) 40 Suppl 1:S5–10. doi: 10.1007/s00259-013-2361-7
19. Ozturk H, Karapolat I. (18)F-fluorodeoxyglucose PET/CT for detection of disease in patients with prostate-specific antigen relapse following radical treatment of a local-stage prostate cancer. *Oncol Lett* (2016) 11:316–22. doi: 10.3892/ol.2015.3903
20. Perez PM, Hope TA, Behr SC, van Zante A, Small EJ, Flavell RR. Intertumoral Heterogeneity of 18F-FDG and 68Ga-PSMA Uptake in Prostate Cancer Pulmonary Metastases. *Clin Nucl Med* (2019) 44:e28–32. doi: 10.1097/RLU.0000000000002367
21. Parida GK, Tripathy S, Datta Gupta S, Singhal A, Kumar R, Bal C, et al. Adenocarcinoma Prostate With Neuroendocrine Differentiation: Potential Utility of 18F-FDG PET/CT and 68Ga-DOTANOC PET/CT Over 68Ga-PSMA PET/CT. *Clin Nucl Med* (2018) 43:248–9. doi: 10.1097/RLU.0000000000002013
22. Vinsensia M, Chyoke PL, Hadaschik B, Holland-Letz T, Moltz J, Kopka K, et al. (68)Ga-PSMA PET/CT and Volumetric Morphology of PET-Positive Lymph Nodes Stratified by Tumor Differentiation of Prostate Cancer. *J Nucl Med* (2017) 58:1949–55. doi: 10.2967/jnumed.116.185033
23. Bialek EJ, Malkowski B. Celiac ganglia: can they be misinterpreted on multimodal 68Ga-PSMA-11 PET/MR? *Nucl Med Commun* (2019) 40:175–84. doi: 10.1097/MNM.0000000000000944
24. Ceci F, Bianchi L, Borghesi M, Polverari G, Farolfi A, Briganti A, et al. Prediction nomogram for (68)Ga-PSMA-11 PET/CT in different clinical settings of PSA failure after radical treatment for prostate cancer. *Eur J Nucl Med Mol Imaging* (2020) 47:136–46. doi: 10.1007/s00259-019-04505-2
25. Richter JA, Rodriguez M, Rioja J, Penuelas I, Marti-Climent J, Garrastachu P, et al. Dual tracer 11C-choline and FDG-PET in the diagnosis of biochemical prostate cancer relapse after radical treatment. *Mol Imaging Biol* (2010) 12:210–7. doi: 10.1007/s11307-009-0243-y

Conflict of Interest: The authors declare that the research was conducted in the absence of any commercial or financial relationships that could be construed as a potential conflict of interest.

frontiers in Oncology

ORIGINAL RESEARCH
published: 19 April 2021
doi: 10.3389/fonc.2021.664225

Efficacy of PSMA PET-Guided Radiotherapy for Oligometastatic Castrate-Resistant Prostate Cancer

Christoph Henkenberens[1,2], Thorsten Derlin[3], Frank Bengel[3], Tobias L. Ross[3], Markus A. Kuczyk[4], Frank A. Giordano[2], Gustavo R. Sarria[2], Leonard Christopher Schmeel[2], Hans Christiansen[1] and Christoph A. J. von Klot[4]*

[1] Department of Radiotherapy and Special Oncology, Hannover Medical School, Hannover, Germany, [2] Department of Radiation Oncology, University Hospital Bonn, Bonn, Germany, [3] Department of Nuclear Medicine, Hannover Medical School, Hannover, Germany, [4] Department of Urology and Urologic Oncology, Hannover Medical School, Hannover, Germany

OPEN ACCESS

Edited by:
Constantinos Zamboglou, University of Freiburg Medical Center, Germany

Reviewed by:
Frank Wolf, Salzburger Landeskliniken, Austria
Justin Ferdinandus, Essen University Hospital, Germany

***Correspondence:**
Christoph Henkenberens
henkenberens.christoph@mh-hannover.de

Specialty section:
This article was submitted to Cancer Imaging and Image-directed Interventions, a section of the journal Frontiers in Oncology

Received: *04 February 2021*
Accepted: *08 March 2021*
Published: *19 April 2021*

Citation:
Henkenberens C, Derlin T, Bengel F, Ross TL, Kuczyk MA, Giordano FA, Sarria GR, Schmeel LC, Christiansen H and von Klot CAJ (2021) Efficacy of PSMA PET-Guided Radiotherapy for Oligometastatic Castrate-Resistant Prostate Cancer. Front. Oncol. 11:664225. doi: 10.3389/fonc.2021.664225

Purpose: To assess the outcome of radiotherapy (RT) to all PSMA ligand positive metastases for patients with castrate-resistant prostate cancer (mCRPC).

Patients and methods: A total of 42 patients developed oligometastatic mCRPC and received PSMA PET-guided RT of all metastases. The main outcome parameters were biochemical progression-free survival (bPFS), and second-line systemic treatment free survival (SST-FS).

Results: A total of 141 PSMA ligand-positive metastases were irradiated. The median follow-up time was 39.0 months (12-58 months). During the follow-up five out of 42 (11.9%) patients died of progressive mPCa. Five out of 42 (11.9%) patients showed no biochemical responses and presented with a PSA level ≥10% of the baseline PSA at first PSA level measurement after RT and were classified as non-responders. The median PSA level before RT was 4.79 ng/mL (range, 0.4-46.1), which decreased significantly to a median PSA nadir level of 0.39 ng/mL (range, <0.07-32.8; p=0.002). The median PSA level at biochemical progression after PSMA ligand-based RT was 2.75 ng/mL (range, 0.27-53.0; p=0.24) and was not significantly different (p=0.29) from the median PSA level (4.79 ng/mL, range, 0.4-46.1) before the PSMA ligand-based RT. The median bPFS was 12.0 months after PSMA ligand PET-based RT (95% CI, 11.2-15.8) and the median SST-FS was 15.0 months (95% CI, 14.0-21.5).

Conclusion: In well-informed and closely followed-up patients, PSMA PET-guided RT represents a viable treatment option for patients with oligometastatic mCRPC to delay further systemic therapies.

Keywords: PSMA, radiotherapy, castrate-resistant, oligometastases, metastasis-directed therapy

INTRODUCTION

The cornerstone of treatment for metastatic castrate-resistant prostate cancer (mCRPC) is either cytotoxic chemotherapy, androgen biosynthesis inhibition (e.g. abiraterone), androgen receptor inhibition (enzalutamide), or radium-223. Androgen deprivation therapy (ADT) represents the column of systemic therapies, as most of the tumoral burden might remain sensitive to its effects. The escalation of systemic therapies is often associated with a negative impact on quality-of-life (QoL) (1). A small subgroup of patients with oligoprogression, defined as the development or progression of a limited number of lesions, might be controlled by radiotherapy as a metastasis-directed therapy (MDT) when targeting all lesions (2). These patients may continue on ADT for a defined period until further disease progression requires second-line systemic treatment (SST) (3). The recent introduction of prostate-specific membrane antigen (PSMA)-ligand positron emission tomography (PET) has substantially improved the diagnostic accuracy of staging at low prostate-specific antigen (PSA) levels (4–8). This technique yields further refined and well-monitored individualized radio-oncological treatment schemes which aim to improve PSA kinetics, prolong the progression-free survival and potentially defer the initiation of systemic therapies for patients with hormone-sensitive metastatic prostate cancer (mPCA) (9–14). Data on the feasibility and clinical outcome of MDT guided by PSMA-targeted imaging in mCRPC are limited.

Herein, we retrospectively assessed the outcomes of patients with mCRPC treated with PSMA PET-guided radiotherapy (RT) to all PET-positive metastases.

PATIENTS AND METHODS

We retrospectively assessed the clinical outcome of patients treated between June 2014 and May 2019 at a single institution for oligoprogressive PCa among ADT. These patients were classified as early mCRPC and received definitive PSMA PET-guided RT as MDT for all metastases. Criteria for mCRPC were either biochemical progression or radiologic progression according to EAU-ASTRO-SIOG Guidelines (1). No patient received additional systemic second-line treatment like docetaxel, novel androgen axis drug or any other drug. Oligometastatic disease was defined as ≤5 visceral or bone metastases. No limit on lymph node metastases was considered. The patients' characteristics are summarized in **Table 1**.

TABLE 1 | Patient characteristics (n = 42).

Characteristics	Median (range); n (%)
Age at PCa diagnosis	65.5 (49–84)
Initial PSA (ng/ml)	9.8 (3.7–84.5)
Primary therapy	
RPE alone	11 (26.2)
RPE +aRT	13 (31.0)
RPE + sRT	14 (33.3)
EBRT + temporary ADT	4 (9.5)
Initial T stage	
cT1c	5 (11.9)
pT2a,b	4 (8.1)
pT2c	13 (31.0)
pT3a	7 (16.7)
pT3b	11 (26.2)
pT4 a,b	0
unknown	2 (4.8)
Gleason-Score	
7a	8 (19.0)
7b	10 (23.8)
8	13 (31.0)
9	11 (26.2)
Initial N stage	
N0	30 (71.4)
N1	8 (19.0)
Surgical margins	
R0	34 (81.0)
R1	4 (9.5)
unknown	4 (9.5)
Initial risk group	
Low Risk	0
Intermediate Risk	9 (21.4)
High Risk	31 (73.8)
unknown	2 (4.8)
PSA nadir after definitive therapy (ng/ml)	0.07 (<0.07–5.2)
Interval (m) from definitive therapy to PSMA PET	76 (19–178)
PSA level at PSMA ligand PET imaging (ng/ml)	4.79 (0.4–46.1)
Patients with ADT at PSMA ligand PET imaging	42 (100%)
Median Duration of ADT at time of PSMA-PET imaging (m)	40.0 (12–180)
Median PSA dt at time of PSMA-PET imaging (m)	7.6 (3.6–50.5)

ADT, androgen deprivation therapy; aRT, adjuvant radiotherapy; dt, doubling time, EBRT, external beam radiation therapy; m, months; PCa, prostate cance;, PSMA ligand PET, prostate-specific membrane antigen ligand positron emission tomography; PSA, prostate-specific antigen; m, months; RP, radical prostatectomy; sRT, salvage radiotherapy.

PET Imaging

Each patient underwent PET imaging with a ^{68}Gallium-labeled PSMA ligand (15). Imaging acquisition was performed according to the joint EANM and SNMMI guideline (16). PSMA-ligand PET scans were acquired in conjunction with low-dose computed tomography (CT) on a dedicated PET/CT system (Siemens Biograph mCT 128 Flow; Siemens, Knoxville, TN) equipped with an extended field-of-view lutetium oxyorthosilicate PET component, a 128-slice spiral CT component, and a magnetically powered table optimized for continuous scanning. No intravenous contrast material was administered. All patients gave written informed consent before PSMA ligand PET/CT. A positive visual assessment of increased focal tracer uptake higher than the surrounding background activity was used as the criterion for malignancy (6).

Radiotherapy Treatment

Patients with lymph node metastases or relapse in the prostatic fossa were treated with conventionally fractionated RT (CF-RT), and patients with bone metastases were treated with mild hypofractionated RT (HF-RT). In cases of lymph node metastases, the clinical target volume (CTV) encompassed the lymph drainage vessel to the next bifurcation or joint, excluding the whole ipsilateral lymphatic drainage. The prescribed dose was 50.0 Gray (Gy, single dose 2.0 Gy), followed by a sequential CF-RT boost of 10.0 Gy (single dose 2.0 Gy) to the lymph node metastases. Prostate bed relapses were treated with CF-RT doses of 70.0–74.0 Gy (single dose of 2.0 Gy). Bone metastases were treated with HF-RT at single doses of 2.5 Gy to a total of 45.0 Gy. The planning target volume (PTV) for lymph node metastases, bone metastases and local relapse in the prostatic fossa included the CTV plus a 10 mm

safety margin in all directions, accounting for setup errors. Image guidance was conducted at least twice a week with megavoltage cone-beam CT. Visceral metastases were treated with image-guided stereotactic body radiation therapy (SBRT) to a total dose of 37.5 (single dose 12.5 Gy), prescribed to the 67% PTV marginal isodose. The PTV included the internal target volume (ITV) plus a 4 mm safety margin in all directions to account for setup errors.

Follow-Up and Endpoints

All patients had periodic follow-up evaluations, which included PSA measurements every three months. Biochemically progressive disease after RT was defined as two consecutive increases in PSA levels from the nadir PSA level or a PSA level above baseline. Biochemical nonresponse was defined as a ≥10% PSA level elevation three months after RT, in comparison to the baseline PSA level at the time of PSMA ligand PET/CT scan before RT (9, 14). To assess the local failure patterns and rates, the PSMA PET/CT scans underwent a coregistration procedure with the RT treatment plans. Focally increased tracer uptake higher than the surrounding background within the PTV was classified as infield relapse. A second PSMA ligand PET/CT for the assessment of the pattern of relapse was available for 22 of 42 (52.4%) patients. Points of interest included the estimated biochemical progression-free survival (bPFS), second-line systemic treatment free survival (SST-FS), overall survival (OS) and toxicity rates. RT-associated toxicity was analyzed using the National Cancer Institute Common Terminology Criteria for Adverse Events (CTCAE) v4.0 (17).

Statistical Analysis

The statistical analysis was performed with The Jamovi Project (2020), Jamovi (Version 1.6.3) for Windows. Retrieved from https://www.jamovi.org. The paired Student's *t*-test to compare pre-RT with post-RT parametric parameters and the Wilcoxon signed-rank for non-normally distributed data were applied. The estimated survival rates were calculated using the Kaplan–Meier method. Factors for RT treatment failure were analyzed with the log-rank test in univariate analyses, and significant factors were further assessed with multivariate analyses using a binominal logistic regression method to identify independent variables. P-values <0.05 were considered statistically significant. Graphical presentations of the patterns of progression were created using a free software for statistical computing and graphics (R Version 3.0.3).

Ethics Statement

This retrospective study was approved by the local institutional review board (IRB), aligned with the principles of the Declaration of Helsinki. All cases were discussed and approved for RT by the multidisciplinary uro-oncologic board. Informed consent was obtained prior to patients' participation.

RESULTS

Result of PSMA Ligand PET Staging and Therapy for Metastases

Data from a total of 42 patients were analyzed. One hundred and forty-one PSMA ligand-positive metastases were detected and treated with RT: Pelvic nodal metastases accounted for 37.6% (53/141), while 18.4% (26/141) allocated in paraaortic node metastases, 7.8% (11/141) in distant lymph node metastases, 28.4% (40/141) in bone metastases, 1.4% (2/141) in visceral metastases, and 6.4% (9/141) in local prostatic fossa relapses. Regarding distribution patterns, 30.9% of patients (13/42) developed only nodal metastases and 23.8% (10/42) only bone metastases. Additionally, 21.4% (9/42) of patients presented both lymph node and bone metastases, 4.8% (2/42) visceral metastases, 4.8% (2/42) relapse in the prostatic fossa, 4.8% (2/42) relapse in the prostatic fossa and bone metastases, and 9.5% (4/42) relapse in the prostatic fossa and lymph node metastases.

Patterns of Progression and Patient Outcomes

Table 2 summarizes the results for the 22 patients who had a first PSMA ligand PET prior to RT and a restaging PSMA ligand PET after biochemical progression occurred.

The anatomical distributions and migration of metastases are shown in **Figures 1A–C**. Analysis of the RT treatment plans and the second PSMA ligand PET/CT scans resulted in an infield relapse rate of 2.7% (2/73). The two infield relapses occurred in the right iliac lymph nodes and in the spine.

The median follow-up time was 39.0 months (12–58). During the follow-up five (11.9%) patients died of progressive mPCa; in addition, five (11.9%) patients showed no biochemical responses and were classified as non-responders, as a PSA level rise ≥10% above the baseline after first post-RT measurement was evidenced. The median PSA level prior to RT was 4.79 ng/ml (0.4–46.1), which decreased significantly to a median PSA nadir level of 0.39 ng/ml (<0.07–32.8; p = 0.002) following RT. **Figure 2** shows a waterfall plot of the PSA response. The median PSA level at biochemical progression after PSMA PET-guided RT was 2.75 ng/ml (0.27–53.0; p = 0.24), and thus not significantly different (p = 0.29) from the median PSA level (4.79 ng/ml, 0.4–46.1) before the PSMA PET-guided RT. Additionally, 14.3% (6/42) of patients did not show biochemical progression at their

TABLE 2 | Results of first PSMA ligand PET staging prior to PSMA PET-guided radiotherapy and second PSMA ligand PET for restaging after biochemical progression (n = 22).

	First PSMA ligand PET prior to RT	Second PSMA ligand PET after biochemical progression
	N (%)	N (%), p value
No. of PSMA-ligand positive lesions	73 (100)	100 (100); 0.08
Total no. of LNs	54 (73.9)	54 (54.0); 0.32
Pelvic LNs	32 (43.8)	18 (18.0); 0.11
Periaortic/interaortocaval LNs	18 (24.7)	29 (29.0); 0.14
Distant LNs	4 (5.5)	7 (7.0):0.29
Total no. of bone metastases	17 (23.3)	44 (44.0); 0.03
Pelvic bone	12 (16.4)	11 (11.0); 0.59
Extrapelvic bone	5 (5.4)	33 (33.0); 0.01
Prostatic fossa	1 (1.4)	1 (1.0); 0.50
Total no. of visceral metastases	1 (1.4)	1 (1.0); 0.91
	Median (range)	Median (range)
No. irradiated metastases	3 (1–11)	3 (1–13)

LNs, lymph node metastases; PSMA ligand PET, prostate-specific membrane antigen ligand positron emission tomography.

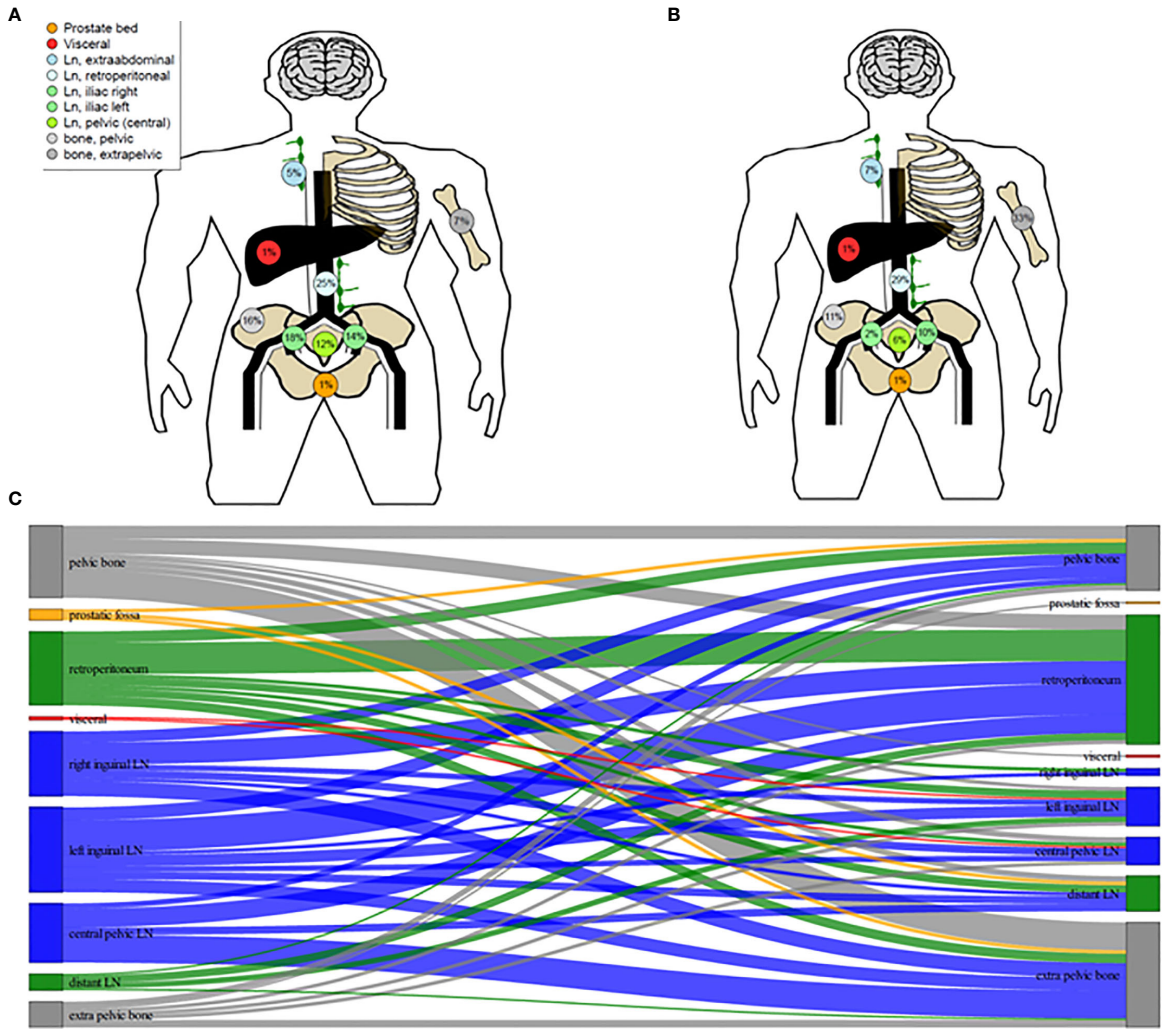

FIGURE 1 | Schematic illustration of ^{68}Ga-PSMA ligand PET/CT distribution of metastases of oligoprogressive prostate cancer under androgen deprivation therapy prior to radiotherapy (RT) **(A)** and distrubution of metastases at further progression after PSMA-guided RT **(B)**. Migration of Metastases **(C)**.

last follow-up. Concerning the 36 patients with biochemical progression, two (5.5%) patients declined SST and chose observation; the patient with the infield lymph node relapse received salvage surgery (1/36, 2.8%). Nine patients (25.0%) received a second PSMA PET-guided RT to all new metastases and SST when further biochemical progression after second PSMA PET-guided RT occurred. Furthermore, 24 patients (66.7%) received SST.

The median bPFS was 12.0 months after PSMA ligand PET-based RT (95% CI, 11.2–15.8; **Figure 3A**), and the median SST-FS was 15.0 months (95% CI, 14.0–21.5; **Figure 3B**). None of the analyzed parameters for bPFS was statistically significant in univariate analyses. The significant parameters in univariate analyses for SST-FS were initial PSA level >10 ng/ml ($p = 0.04$), the number of irradiated metastases ($p = 0.02$) and the peak standardized uptake value (SUVpeak). None of the significant parameters reached significance in multivariate analyses. **Table 3** shows the detailed results of the uni- and multivariate analyses for bPFS and SST-FS.

Toxicity

Acute grade III toxicity was not observed; 4.8% (2/42) of patients developed grade II acute gastrointestinal side effects. Late grade I gastrointestinal toxicity occurred in 2.4% (1/42) of patients. Late grade ≥II toxicities were not observed.

DISCUSSION

The implementation of PSMA ligand-based imaging has substantially improved the diagnostic accuracy of detecting metastatic PCa at low PSA levels (6–8). Although large randomized prospective phase III studies are lacking (12–14, 18),

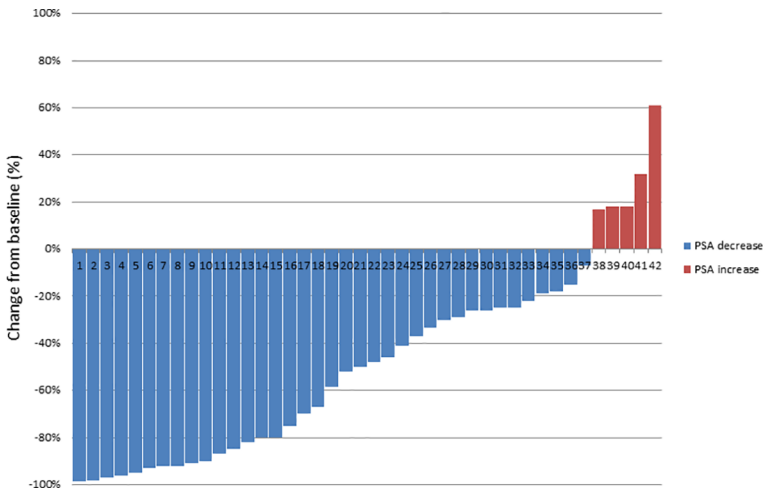

FIGURE 2 | Waterfall plot of best PSA response, based on maximal percentage of PSA change.

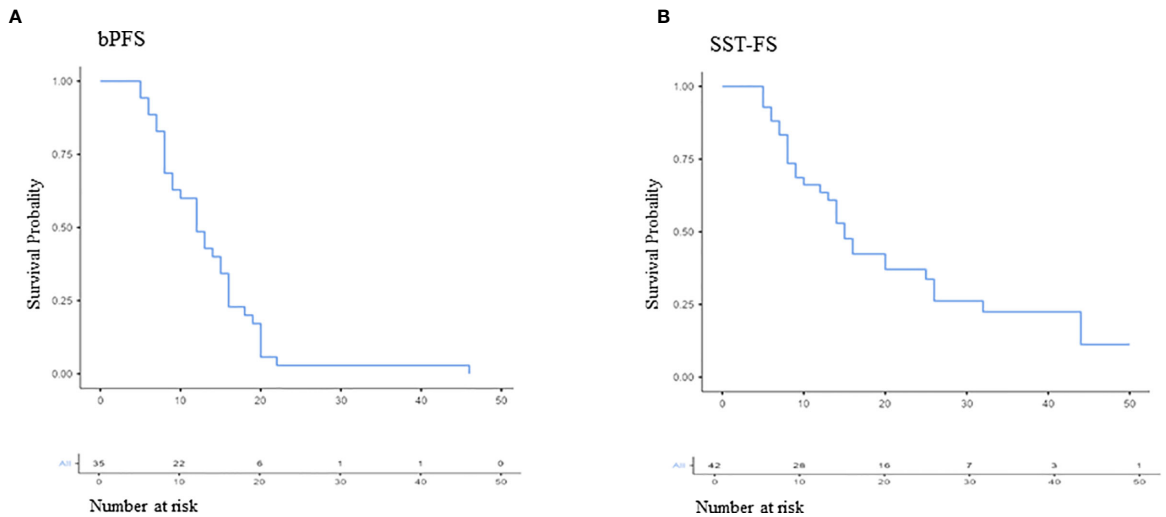

FIGURE 3 | Kaplan–Meier curves of biochemical progression-free survival (bPFS; **A**) and second-line systemic treatment free survival (SST-FS; **B**).

there is a strong consensus among experts that MDT is considered a viable treatment option for well-selected patients, mostly with oligorecurrent PCa (19). However, these trials investigated the potential of MDT to delay the initiation of ADT for asymptomatic hormone-naive metastatic PCa (13, 14, 18). Patients undergoing ADT with increasing PSA levels and detection of a limited number of metastases in PSMA-ligand PET are regarded as early mCRPC and information on MDT in this setting is scarce. Usually, biochemical progression is the trigger for staging imaging, and iconographic progression (in some patients only biochemical progression) is the indication for SST (1). Further systemic therapies are associated with both non-negligible toxicities and increased healthcare expenditures (20). However, a small subgroup of patients might not benefit from SST as the vast majority of disease is still controlled through the ongoing systemic therapy (21). The biological rationale encompasses the evolution of a few cell-line subpopulations within different metastases under the selection pressure of ADT towards a more aggressive phenotype, driving the ominous course of the disease (22). Eradicating these lesions might delay the initiation of SST. Additionally, those large trials which investigated either docetaxel, abiraterone or enzalutamide as SST for mCRPC did not include a sufficient number of participants with low PSA-levels and low tumor burden. It remains, therefore, difficult to draw precise conclusions on the exact benefit and optimal timing of SST for these patients (23–25).

TABLE 3 | Results of first PSMA ligand PET staging prior to PSMA PET-guided radiotherapy and second PSMA ligand PET for restaging after biochemical progression (n = 21).

	SST-FS		bPFS	
	Univariate analysis *p*-value (OR, 95% CI)	**Multivariate analysis *p*-value (OR, 95% CI)**	**Univariate analysis *p*-value (OR, 95% CI)**	**Multivariate analysis *p*-value (OR, 95% CI)**
Initial T stage (≤T2 vs. ≥T3)	0.35 (1.31, 0.67–2.97)	–	0.26 (1.51, 0.74–3.01)	–
Initial N stage (N0 vs. N1)	0.36 (1.63, 0.52–5.75)	–	0.84 (1.02, 0.46–2.26)	–
Initial PSA level in ng/ml	0.69 (1.05, 0.97–1.03)	–	0.39 (1.08, 0.98–1.03)	–
Initial PSA level >20 ng/ml	0.58 (1.12, 0.54–2.98)	–	0.41 (1.34, 0.36–1.52)	–
Initial PSA level >10 ng/ml	0.04 (2.16, 1.20–4.54)	0.98 (0.27–14.60)	0.28 (1.53, 0.69–3.38)	–
PSA nadir after RP	0.40 (1.03, 0.62–1.23)	–	0.46 (0.95, 0.82–1.09)	–
Gleason score	0.29 (1.05, 0.36–3.16)	–	0.86 (1.03, 0.72–1.47)	–
Initial high risk	0.18 (1.63, 0.79–3.36)	–	0.89 (0.95, 0.48–1.88)	–
Duration of ADT	0.22 (1.07, 0.96–1.20)		0.13 (1.19, 0.97–1.20)	
PSA-dt at PSMA PET	0.61 (1.02, 0.97–1.05)	–	0.62 (1.01, 0.96–1.06)	–
PSA at PSMA PET	0.24 (1.03 0.98–1.06)	–	0.95 (1.00, 0.97–1.03)	–
SUVpeak	0.02 (1.21, 1.05–1.31)	0.48 (1.03 0.96–1.10)	0.12 (1.13, 0.87–1.15)	–
No. of irradiated metastases	0.02 (1.26, 1.04–1.40)	0.08 (1.9, 0.93–4.06)	0.14 (1.17, 0.84–1.38)	–
LN metastases only	0.23 (0.64, 0.3–1.35)	–	0.62 (0.90, 0.45–1.81)	–
Extrapelvic disease (LNs and/or bone)	0.53 (1.2, 0.38–1.56)	–	0.61 (1.13, 0.41–1.69)	–

dt, doubling time; LN, lymph node; PSA, prostate-specific antigen; RP, radical prostatectomy; SUV, standardized uptake value.

Based on the biological rationale we retrospectively assessed the clinical outcome of patients with early mCRPC who received RT as MDT to all PSMA positive lesions, and found that the decreased PSA levels lead to a subsequent delay of further systemic therapies. We observed that RT targeting all metastases detected by PSMA-ligand PET postponed the second-line systemic therapies for a median of 15 months with only negligible RT-related side effects. Other reports on MDT for mCRPC have reported similar SST-FS (9, 26–29). However, their outcomes mainly report on patients with both metastatic hormone-sensitive and castration-resistant PCa with limited information on the clinical outcome of patients with mCRPC (27, 28). Furthermore, some patients received RT plus SST which limits a comparison with our results (26). Other retrospective studies assessed the benefit of cytoreductive RT for patients with mCRPC plus abiraterone (30) or for patients with progressive disease among abiraterone or enzalutamide, showing that RT might delay disease progression in both clinical scenarios (31–33). Additionally, there are no data on PSMA-ligand PET for staging purposes prior to RT as MDT for mCRPC.

To our best knowledge, we present the first data including a more homogeneous mCRPC patient cohort staged with PSMA-ligand PET/CT, who received RT to all metastases as MDT to delay the initiation of SST. The observed median SST-FS of 15 months is encouraging, although we found no significant clinical parameter influencing the observed outcome (bPFS and SST-FS). This suggests that clinical parameter do not drive the clinical course, leading to a demand for molecular biomarkers in the presented clinical study (34, 35).

Some limitations to this study should be acknowledged. Its retrospective nature has inherent limitations and might have incurred in selection bias, although the study cohort had a strict follow-up schedule and a PSMA PET-based staging protocol prior to RT was performed fewer metastases should thus have been missed to diagnosis as compared to conventional imaging or choline PET techniques (6–8, 20, 36). There is controversy about the radiation dose, field size, and elective node irradiation when PSMA ligand PET is used for MDT of oligorecurrent mPCa. Data from the choline PET era confirmed that choline PET underestimated the extent of lymph node metastases (37), which is reflected by the fact that approximately two out of three patients treated with SBRT for pelvic lymph node metastases relapsed with lymph node metastases (38, 39), leading to a higher relapse rate than that after elective node irradiation (ENI), although the relapse rate concerning bone and visceral metastases seems to be comparable between SBRT and ENI (40). Additionally the optimal definition of biochemical progression for this emerging clinical scenario does not exist. The PCWG2 (prostate cancer clinical trials working group) definitions for mCRPC were designed to measure outcomes for drug trials that evaluate systemic treatment for mCRPC and "high" PSA levels to improve the alignment of clinical research and practice (41). In our patient cohort the median PSA-level of 4.79 ng/ml was significantly lower than the PSA level in any drug trial on mCRPC. Additionally the PCWG2 definition does not include any information about local therapies. So we used the above mentioned more conservative definition based upon our previous reports, where radiographic clinical progression using PSMA PET showed high concordance with PSA increase (9, 14) allowing refined and well-monitored personalizedradio-oncological treatment concepts. The sample size of 42 patients limited the statistical power. Moreover, the study included a selected cohort with mainly baseline high-risk PCa. In this sense, caution is advised when translating the observed results to clinical practice.

Taken together, the observed clinical results are robust and contribute significantly to set the basis of PSMA guided-RT as MDT in a rapidly evolving clinical field.

CONCLUSION

PSMA PET-guided RT to all enhancing metastases in the mCRPC setting delayed systemic therapies without major

toxicity and represents a promising treatment option. Prospective evaluation is warranted to confirm these findings.

DATA AVAILABILITY STATEMENT

The raw data supporting the conclusions of this article will be made available by the authors, without undue reservation.

ETHICS STATEMENT

The studies involving human participants were reviewed and approved by Medical School Hannover, Ethics Committee. The patients/participants provided their written informed consent to participate in this study.

AUTHOR CONTRIBUTIONS

CH and CK contributed to conception and design of the study. CH and HC enrolled patients. TR, TD, and FB were responsible for conduction and reporting of the PSMA-PET/CTs. MK, FG, GS, and LS wrote and revised sections of the manuscript. All authors contributed to the article and approved the submitted version.

SUPPLEMENTARY MATERIAL

The Supplementary Material for this article can be found online at: https://www.frontiersin.org/articles/10.3389/fonc.2021.664225/full#supplementary-material

REFERENCES

1. Cornford P, Bellmunt J, Bolla M, Briers E, De Santis M, Gross T, et al. EAU-ESTRO-SIOG Guidelines on Prostate Cancer. Part II: Treatment of Relapsing, Metastatic, and Castration-Resistant Prostate Cancer. *Eur Urol* (2017) 71 (4):630–42. doi: 10.1016/j.eururo.2016.08.002
2. Franklin JM, Sharma RA, Harris AL, Gleeson FV. Imaging oligometastatic cancer before local treatment. *Lancet Oncol* (2016) 17(9):e406–14. doi: 10.1016/S1470-2045(16)30277-7
3. Wei XX, Ko EC, Ryan CJ. Treatment strategies in low-volume metastatic castration resistant prostate cancer. *Curr Opin Urol* (2017) 27(6):596–603. doi: 10.1097/MOU.0000000000000436
4. Calais J, Czernin J, Cao M, Kishan AU, Hegde JV, Shaverdian N, et al. ^{68}Ga-PSMA-11 PET/CT Mapping of Prostate Cancer Biochemical Recurrence After Radical Prostatectomy in 270 Patients with a PSA Level of Less Than 1.0 ng/mL: Impact on Salvage Radiotherapy Planning. *J Nucl Med* (2018) 59 (2):230–7. doi: 10.2967/jnumed.117.201749
5. McCarthy M, Francis R, Tang C, Watts J, Campbell A. A Multicenter Prospective Clinical Trial of ^{68}Gallium PSMA HBED-CC PET-CT Restaging in Biochemically Relapsed Prostate Carcinoma: Oligometastatic Rate and Distribution Compared With Standard Imaging. *Int J Radiat Oncol Biol Phys* (2019) 104(4):801–8. doi: 10.1016/j.ijrobp.2019.03.014
6. Schmuck S, Mamach M, Wilke F, von Klot CA, Henkenberens C, Thackeray JT, et al. Multiple Time-Point 68Ga-PSMA I&T PET/CT for Characterization of Primary Prostate Cancer: Value of Early Dynamic and Delayed Imaging. *Clin Nucl Med* (2017) 42(6):e286–e93. doi: 10.1097/RLU.0000000000001589
7. Schmuck S, Nordlohne S, von Klot CA, Henkenberens C, Sohns JM, Christiansen H, et al. Comparison of standard and delayed imaging to improve the detection rate of [^{68}Ga]PSMA I&T PET/CT in patients with biochemical recurrence or prostate-specific antigen persistence after primary therapy for prostate cancer. *Eur J Nucl Med Mol Imaging* (2017) 44(6):960–8. doi: 10.1007/s00259-017-3669-5
8. Schmuck S, von Klot CA, Henkenberens C, Sohns JM, Christiansen H, Wester HJ, et al. Initial Experience with Volumetric ^{68}Ga-PSMA I&T PET/CT for Assessment of Whole-Body Tumor Burden as a Quantitative Imaging Biomarker in Patients with Prostate Cancer. *J Nucl Med* (2017) 58 (12):1962–8. doi: 10.2967/jnumed.117.193581
9. Soldatov A, von Klot CAJ, Walacides D, Derlin T, Bengel FM, Ross TL, et al. Patterns of Progression After ^{68}Ga-PSMA-Ligand PET/CT-Guided Radiation Therapy for Recurrent Prostate Cancer. *Int J Radiat Oncol Biol Phys* (2019) 103(1):95–104. doi: 10.1016/j.ijrobp.2018.08.066
10. Kroeze SGC, Henkenberens C, Schmidt-Hegemann NS, Vogel MME, Kirste S, Becker J, et al. Prostate-specific Membrane Antigen Positron Emission Tomography-detected Oligorecurrent Prostate Cancer Treated with Metastases-directed Radiotherapy: Role of Addition and Duration of Androgen Deprivation. *Eur Urol Focus* (2019) S:2405–4569(19)30270-6. doi: 10.1016/j.euf.2019.08.012
11. Walacides D, Meier A, Knöchelmann AC, Meinecke D, Derlin T, Bengel FM, et al. Comparison of ^{68} Ga-PSMA ligand PET/CT versus conventional cross-sectional imaging for target volume delineation for metastasis-directed radiotherapy for metachronous lymph node metastases from prostate cancer. *Strahlenther Onkol* (2019) 195(5):420–9. doi: 10.1007/s00066-018-1417-9
12. Ost P, Reynders D, Decaestecker K, Fonteyne V, Lumen N, De Bruycker A, et al. Surveillance or Metastasis-Directed Therapy for Oligometastatic Prostate Cancer Recurrence: A Prospective, Randomized, Multicenter Phase II Trial. *J Clin Oncol* (2018) 36(5):446–53. doi: 10.1200/JCO.2017.75.4853
13. Oehus AK, Kroeze SGC, Schmidt-Hegemann NS, Vogel MME, Kirste S, Becker J, et al. Efficacy of PSMA ligand PET-based radiotherapy for recurrent prostate cancer after radical prostatectomy and salvage radiotherapy. *BMC Cancer* (2020) 20:362. doi: 10.1186/s12885-020-06883-5
14. Henkenberens C, Oehus AK, Derlin T, Bengel F, Ross TL, Kuczyk MA, et al. Efficacy of repeated PSMA PET-directed radiotherapy for oligorecurrent prostate cancer after initial curative therapy. *Strahlenther Onkol* (2020) 196 (11):1006–17. doi: 10.1007/s00066-020-01629-5
15. Derlin T, Schmuck S, Juhl C, Zörgiebel J, Schneefeld SM, Walte ACA, et al. PSA-stratified detection rates for [^{68}Ga]THP-PSMA, a novel probe for rapid kit-based ^{68}Ga-labeling and PET imaging, in patients with biochemical recurrence after primary therapy for prostate cancer. *Eur J Nucl Med Mol Imaging* (2018) 45(6):913–22. doi: 10.1007/s00259-017-3924-9
16. Fendler WP, Eiber M, Beheshti M Bomanji J, Ceci F, Cho S, et al. ^{68}Ga-PSMA PET/CT: Joint EANM and SNMMI procedure guideline for prostate cancer imaging: version 1.0. *Eur J Nucl Med Mol Imaging* (2017) 44(6):1014–24. doi: 10.1007/s00259-017-3670-z
17. National Cancer Institute Common Terminology Criteria for Adverse Events (CTCAE)v4.0. Available at: http://ctep.cancer.gov/protocolDevelopment/electronic_applications/ (Accessed 22 October, 2020).
18. Phillips R, Shi WY, Deek M, Radwan N, Lim SJ, Antonarakis ES, et al. Outcomes of Observation vs Stereotactic Ablative Radiation for Oligometastatic Prostate Cancer: The ORIOLE Phase 2 Randomized Clinical Trial. *JAMA Oncol* (2020) 6 (5):650–9. doi: 10.1001/jamaoncol.2020.0147
19. Gillessen S, Attard G, Beer TM, Beltran H, Bossi A, Bristow R, et al. Management of Patients with Advanced Prostate Cancer: The Report of the Advanced Prostate Cancer Consensus Conference APCCC 2017. *Eur Urol* (2018) 73(2):178–211. doi: 10.1016/j.eururo.2017.08.010
20. Wong SE, Everest L, Jiang DM, Saluja R, Chan KKW, Sridhar SS. Application of the ASCO Value Framework and ESMO Magnitude of Clinical Benefit Scale to Assess the Value of Abiraterone and Enzalutamide in Advanced Prostate Cancer. *JCO Oncol Pract* (2020) 16(2):e201–e10. doi: 10.1200/JOP.19.00421
21. Palma DA, Salama JK, Lo SS, Senan S, Treasure T, Govindan R, et al. The oligometastatic state - separating truth from wishful thinking. *Nat Rev Clin Oncol* (2014) 11(9):549–57. doi: 10.1038/nrclinonc.2014.96

22. Ceder Y, Bjartell A, Culig Z, Rubin MA, Tomlins S, Visakorpi T. The Molecular Evolution of Castration-resistant Prostate Cancer. *Eur Urol Focus* (2016) 2(5):506–13. doi: 10.1016/j.euf.2016.11.012
23. Ryan CJ, Smith MR, Fizazi K, Saad F, Mulders PF, Sternberg CN, et al. Abiraterone acetate plus prednisone versus placebo plus prednisone in chemotherapy-naive men with metastatic castration-resistant prostate cancer (COU-AA-302): final overall survival analysis of a randomised, double-blind, placebo-controlled phase 3 study. *Lancet Oncol* (2015) 16 (2):152–60. doi: 10.1016/S1470-2045(14)71205-7
24. Beer TM, Armstrong AJ, Rathkopf DE, Loriot Y, Sternberg CN, Higano CS, et al. Enzalutamide in metastatic prostate cancer before chemotherapy. *N Engl J Med* (2014) 371(5):424–33. doi: 10.1056/NEJMoa1405095
25. Tannock IF, de Wit R, Berry WR, Horti J, Pluzanska A, Chi KN, et al. Docetaxel plus prednisone or mitoxantrone plus prednisone for advanced prostate cancer. *N Engl J Med* (2004) 351(15):1502–12. doi: 10.1056/NEJMoa040720
26. Berghen C, Joniau S, Ost P, Poels K, Everaerts W, Decaestecker K, et al. Progression-directed Therapy for Oligoprogression in Castration-refractory Prostate Cancer. *Eur Urol Oncol* (2019) S2588–9311(19)30138-5. doi: 10.1016/j.euo.2019.08.012
27. Tabata K, Niibe Y, Satoh T, Tsumura H, Ikeda M, Minamida S, et al. Radiotherapy for oligometastases and oligo-recurrence of bone in prostate cancer. *Pulm Med* (2012) 2012:541656. doi: 10.1155/2012/541656
28. Ahmed KA, Barney BM, Davis BJ, Park SS, Kwon ED, Olivier KR. Stereotactic body radiation therapy in the treatment of oligometastatic prostate cancer. *Front Oncol* (2013) 2:215:215. doi: 10.3389/fonc.2012.00215
29. Moyer CL, Phillips R, Deek MP, Radwan N, Ross AE, Antonarakis ES, et al. Stereotactic ablative radiation therapy for oligometastatic prostate cancer delays time-to-next systemic treatment. *World J Urol* (2019) 37(12):2623–9. doi: 10.1007/s00345-018-2477-2
30. Liu Y, Long W, Zhang Z, Mai L, Huang S, Liu B, et al. Cytoreductive radiotherapy combined with abiraterone in metastatic castration-resistance prostate cancer: a single center experience. *Radiat Oncol* (2021) 16(1):5. doi: 10.1186/s13014-020-01732-y
31. Detti B, D'Angelillo RM, Ingrosso G, Olmetto E, Francolini G, Triggiani L, et al. Combining Abiraterone and Radiotherapy in Prostate Cancer Patients Who Progressed During Abiraterone Therapy. *Anticancer Res* (2017) 37 (7):3717–22. doi: 10.21873/anticanres.11744
32. Yildirim BA, Onal C, Kose F, Oymak E, Sedef AM, Besen AA, et al. Outcome of loco-regional radiotherapy in metastatic castration-resistant prostate cancer patients treated with abiraterone acetate. *Strahlenther Onkol* (2019) 195:(10):872–81. doi: 10.1007/s00066-019-01429-6
33. Valeriani M, Marinelli L, Macrini S, Reverberi C, Aschelter AM, De Sanctis V, et al. Radiotherapy in metastatic castration resistant prostate cancer patients with oligo-progression during abiraterone-enzalutamide treatment: a mono-institutional experience. *Radiat Oncol* (2019) 14(1):205. doi: 10.1186/s13014-019-1414-x
34. Karantanos T, Evans CP, Tombal B, Thompson TC, Montironi R, Isaacs WB. Understanding the mechanisms of androgen deprivation resistance in prostate cancer at the molecular level. *Eur Urol* (2015) 67(3):470–9. doi: 10.1016/j.eururo.2014.09.049
35. Attard G, Antonarakis ES. Prostate cancer: AR aberrations and resistance to abiraterone or enzalutamide. *Nat Rev Urol* (2016) 13(12):697–8. doi: 10.1038/nrurol.2016.212
36. Weber M, Hadaschik B, Ferdinandus J, Rahbar K, Bögemann M, Herrmann K, et al. Prostate-specific Membrane Antigen-based Imaging of Castration-resistant Prostate Cancer. *Eur Urol Focus* (2021) S2405-4569(21):00003–1. doi: 10.1016/j.euf.2021.01.002
37. Ost P, Decaestecker K, Lambert B, Fonteyne V, Delrue L, Lumen N, et al. Prognostic factors influencing prostate cancer-specific survival in non-castrate patients with metastatic prostate cancer. *Prostate* (2014) 74(3):297–305. doi: 10.1002/pros.22750
38. Nørgaard M, Jensen AØ, Jacobsen JB, Cetin K, Fryzek JP, Sørensen HT. Skeletal related events, bone metastasis and survival of prostate cancer: a population based cohort study in Denmark (1999 to 2007). *J Urol* (2010) 184 (1):162–7. doi: 10.1016/j.juro.2010.03.034
39. an Leeuwen PJ, Stricker P, Hruby G, Kneebone A, Ting F, Thompson B, et al. $^{(68)}$Ga-PSMA has a high detection rate of prostate cancer recurrence outside the prostatic fossa in patients being considered for salvage radiation treatment. *BJU Int* (2016) 117(5):732–9. doi: 10.1111/bju.13397
40. De Bleser E, Jereczek-Fossa BA, Pasquier D, Zilli T, Van As N, Siva S, et al. Metastasis-directed Therapy in Treating Nodal Oligorecurrent Prostate Cancer: A Multi-institutional Analysis Comparing the Outcome and Toxicity of Stereotactic Body Radiotherapy and Elective Nodal Radiotherapy. *Eur Urol* (2019) 76(6):732–9. doi: 10.1016/j.eururo.2019.07.009
41. Scher HI, Halabi S, Tannock I, Morris M, Sternberg CN, Carducci MA, et al. Prostate Cancer Clinical Trials Working Group. Design and end points of clinical trials for patients with progressive prostate cancer and castrate levels of testosterone: recommendations of the Prostate Cancer Clinical Trials Working Group. *J Clin Oncol* (2008) 26(7):1148–59. doi: 10.1200/JCO.2007.12.4487

Conflict of Interest: The authors declare that the research was conducted in the absence of any commercial or financial relationships that could be construed as a potential conflict of interest.

frontiers in Oncology

ORIGINAL RESEARCH
published: 23 April 2021
doi: 10.3389/fonc.2021.666308

The Heterogeneous Metabolic Patterns of Ganglia in ^{68}Ga-PSMA, ^{11}C-choline, and ^{18}F-FDG PET/CT in Prostate Cancer Patients

Yiping Shi[1†], Jian Guo Wu[2†], Lian Xu[1†], Yinjie Zhu[3], Yining Wang[1], Gan Huang[1], Jianjun Liu[1] and Ruohua Chen[1]*

[1] Department of Nuclear Medicine, Ren Ji Hospital, School of Medicine, Shanghai Jiao Tong University, Shanghai, China, [2] Department of Nuclear Medicine, Second Affiliated Hospital, Nanchang University, Nanchang, China, [3] Department of Urology, Ren Ji Hospital, School of Medicine, Shanghai Jiao Tong University, Shanghai, China

OPEN ACCESS

Edited by:
Xuefeng Qiu,
Nanjing Drum Tower Hospital, China

Reviewed by:
Jie Gao,
Nanjing Drum Tower Hospital, China
Vikas Prasad,
Universitätsklinikum Ulm, Germany

***Correspondence:**
Ruohua Chen
crh19870405@163.com

[†]These authors have contributed equally to this work

Specialty section:
This article was submitted to Cancer Imaging and Image-directed Interventions, a section of the journal Frontiers in Oncology

Received: 10 February 2021
Accepted: 29 March 2021
Published: 23 April 2021

Citation:
Shi Y, Wu JG, Xu L, Zhu Y, Wang Y, Huang G, Liu J and Chen R (2021) The Heterogeneous Metabolic Patterns of Ganglia in ^{68}Ga-PSMA, ^{11}C-choline, and ^{18}F-FDG PET/CT in Prostate Cancer Patients. Front. Oncol. 11:666308. doi: 10.3389/fonc.2021.666308

Purpose: Studies have indicated that PSMA-positive ganglia represent a diagnostic pitfall for nuclear medicine physicians. No studies have described choline and FDG uptake in ganglia, which may be a source of misdiagnosis. Herein, we described the percentage and uptake pattern of ^{68}Ga-PSMA, ^{11}C-choline and ^{18}F-FDG PET/CT in ganglia and evaluated the heterogeneous metabolic patterns of ganglia to differentiate from lymph node metastases (LNM).

Methods: Thirty-nine patients who underwent ^{11}C-choline PET/CT and 120 patients who underwent ^{68}Ga-PSMA PET/CT and ^{18}F-FDG PET/CT were retrospectively analyzed. The prevalence of PSMA-positive, choline-positive and FDG-positive ganglia was determined, the SUVmax of ganglia in different locations were measured, and the configuration was described. The SUVmax cutoff of PSMA-PET, choline-PET and FDG-PET was determined by ROC curve analysis to differentiate ganglia from LNM.

Results: 329 PSMA-positive ganglia were identified in 120 patients, 95 choline-positive ganglia were identified in 39 patients, and 39 FDG-positive ganglia were identified in 34 patients. PSMA-positive uptake was observed in 98.3%, 95.8%, and 80.0% of cervical, coeliac, and sacral ganglia, respectively. Choline-positive uptake was observed in 84.6%, 97.4%, and 61.5% of cervical, coeliac, and sacral ganglia, respectively. FDG-positive uptake was observed in 16.7%, 13.3%, and 2.5% of cervical, coeliac, and sacral ganglia, respectively. Cervical and coeliac ganglia had a higher rate of PSMA-positive uptake than sacral ganglia. Choline uptake was highest in coeliac ganglia followed by cervical and sacral ganglia. PSMA, choline or FDG uptake in LNM was all significantly higher than ganglia. ROC curve analysis revealed that at a 4.1 SUVmax cutoff of PSMA-PET, the sensitivity, specificity and accuracy of LNM identification was 88.4%, 97.9% and 96.2%, respectively. ROC curve analysis revealed that at a 2.35 SUVmax cutoff for choline-PET, the sensitivity, specificity, and accuracy of LNM identification was 95.0%, 92.6% and 93.0%, respectively. ROC curve analysis revealed that at a 2.55 SUVmax cutoff for FDG-PET, the sensitivity, specificity, and accuracy of LNM identification was 77.3%, 87.2%,

and 81.9%, respectively. PSMA-, Choline- and FDG-positive ganglia are mainly band-shaped; most LNMs exhibited nodular and teardrop-shaped configuration.

Conclusion: ^{68}Ga-PSMA and ^{11}C-choline uptake in ganglia was common, and FDG-positive ganglia were observed at lower frequency. Using ^{68}Ga-PSMA, ^{11}C-choline and ^{18}F-FDG uptake and anatomic location and configuration, the differentiation of ganglia from adjacent LNM is feasible.

Keywords: ^{68}Ga-PSMA, ganglia, lymph node metastases, ^{18}F-FDG, ^{11}C-choline

INTRODUCTION

Prostate cancer is a common malignant tumor in males (1). Despite initial treatment, biochemical recurrence (BCR) is a problem after radical prostatectomy (2). The ability to determine the location and degree of recurrence of prostate cancer is important for guiding rescue treatment. However, conventional imaging techniques, including MRI and CT (3), have limited sensitivity. Since 2012, the application of functional positron emission tomography (PET) imaging, such as PSMA or choline PET, has significantly improved prostate cancer detection rates in BCR patients (4–8). PSMA PET has shown advantages in re-staging in BCR patients (9), as well as for the primary staging in initial diagnosed prostate cancer (10). Recently many studies have indicated that PSMA-positive ganglia represent a potential diagnostic pitfall for nuclear medicine physicians (11–14). The morphology and the PSMA uptake of the lesions along with delayed ^{68}Ga-PSMA PET may be used to differentiate ganglia and lymph node metastases (LNM) (11, 12).

Besides ^{68}Ga-PSMA PET, choline PET has also been commonly used to detect biochemical recurrence and has changed the management of BCR patients (15–17). ^{11}C-choline was approved by the U.S. Food and Drug Administration in 2012 under an investigational new-drug application. However, choline-positive ganglia could be an important pitfall in prostate cancers, similar to PSMA-positive ganglia, which has not been reported in previous studies. ^{18}F-FDG is the most widely used tracer in a variety of malignant tumors. ^{18}F-FDG PET has been used in partial prostate cancers with a high Gleason grade, and specifically in prostate cancer patients with negative ^{68}Ga-PSMA PET/CT findings (18–20). However, there have been no studies describing the patterns of FDG uptake in ganglia, either in prostate cancers or other malignant tumors. Therefore, whether there is choline and/or FDG uptake in ganglia, which could be a source of misdiagnosis, remains unclear and needs further investigation. In the present study, we described the percentage and uptake pattern of PSMA, choline and FDG in ganglia and evaluated the heterogeneous metabolic patterns of ganglia in order to differentiate from LNM.

METHODS

Participants

The ethics committee of Renji Hospital approved the present retrospective study, and informed consent was waived. The present study was performed in accordance with the ethical standards as laid down in the 1964 Declaration of Helsinki and its later amendments. A total of 39 patients with prostate cancer who underwent ^{11}C-choline PET/CT between March 2018 and December 2019 and 120 patients with prostate cancer who underwent ^{68}Ga-PSMA and ^{18}F-FDG PET/CT between July 2018 and August 2019 were enrolled. The patients' characteristics, including age, Gleason grade score, PSA level and treatment history, were available for review.

^{11}C-choline PET/CT and ^{18}F-FDG PET/CT

^{68}Ga-PSMA, ^{11}C-choline and ^{18}F-FDG were synthesized by our Radiochemistry Laboratory of Renji Hospital. Patients fasted for four hours before injecting 6.0 MBq/kg of ^{11}C-choline and fasted for six hours before injecting 3.7 MBq/kg of ^{18}F-FDG. The fasting blood glucose was lower than 14.0 mmol/L. Patients were required to rest for 60 minutes before undergoing ^{18}F-FDG PET/CT. The PSMA ligand was ^{68}Ga-PSMA-11. The injected dose of ^{68}Ga-PSMA was 1.85 MBq/kg. ^{68}Ga-PSMA PET/CT was scanned 55 minutes after injecting ^{68}Ga-PSMA. Patients that underwent ^{11}C-choline PET/CT were scanned 20 minutes after ^{11}C-choline injection. PET/CT was carried out by a combined scanner (Biograph mCT). CT images (120 kV automatic milliamp current; 3 mm section thickness) were scanned from the patient's upper thigh to the skull. PET was performed immediately after CT, and the acquisition time of each bed was three minutes.

Image Evaluation

Two nuclear medicine physicians with eight to ten years of experience in PET/CT interpretation evaluated the image data together and resolved any disagreements by consensus. Regions of interest (ROI) were placed over the selected ganglia or lymph nodes metastases. The maximum standardized uptake value (SUVmax) was calculated as follows: maximum pixel value in the decay-corrected ROI activity (MBq/kg)/(the injected ^{68}Ga-PSMA, ^{11}C-choline or ^{18}F-FDG radioactivity (MBq)/body weight (kg)).

Ganglia and adjacent LNM were grouped according to anatomic location, including cervical, coeliac, or sacral plexus. The main criteria for ganglia were focal ^{68}Ga-PSMA, ^{11}C-choline or ^{18}F-FDG that projected onto a structure with typical type and location for sympathetic ganglia as previously described (11). Lesions were counted that were visually considered to be suggestive for ganglia or LNM exhibiting increased ^{68}Ga-PSMA, ^{11}C-choline or ^{18}F-FDG tracer uptake relative to local background. The selected criteria for ganglia to avoid the

introduction of possible bias were as follows: 1) A single ganglia (if more than one PSMA-, choline- or FDG-positive ganglia existed) with the highest ^{68}Ga-PSMA, ^{11}C-choline or ^{18}F-FDG uptake was selected in each of the anatomic locations (cervical, coeliac, or sacral); 2) If the anatomic location had no PSMA-, choline- or FDG-positive ganglia, it was defined as PSMA-, choline- or FDG-negative. In addition, the same selected criteria for definite LNM with increased ^{68}Ga-PSMA, ^{11}C-choline or ^{18}F-FDG uptake relative to local background were selected.

Statistical Analysis

Results are either demonstrated as mean ± SD or as frequencies (%). For comparison of continuous variables, the 2-tailed unpaired Student t test was used. The x2 test was applied to compare nominal variables. All statistical analyses were performed using SPSS 21.0 (IBM Corp., USA), with a two-sided P<0.05 considered statistically significant.

RESULTS

Prevalence of PSMA-Positive, Choline-Positive and FDG-Positive Ganglia

A total of 329 PSMA-positive ganglia were identified in 120 patients, 95 choline-positive ganglia were identified in 39 patients, and 39 FDG-positive ganglia were identified in 34 patients.

On a per-patient basis, 100% (120/120 patients) patients had positive PSMA uptake in ganglia (i.e., cervical, coeliac, or sacral). Grouped by location, PSMA-positive uptake was observed at a frequency of 98.3% (118/120 patients), 95.8% (115/120 patients), and 80.0% (96/120 patients) in cervical, coeliac, and sacral ganglia, respectively. Cervical and coeliac ganglia had a higher rate of PSMA-positive uptake than sacral ganglia (P<0.001 and P<0.001, respectively). Similar frequency of PSMA-positive uptake was observed between cervical and coeliac ganglia (P = 0.365) (**Figure 1**).

On a per-patient basis, 100% (39/39 patients) of patients had positive choline uptake in ganglia (i.e., cervical, coeliac, or sacral). Grouped by location, choline-positive uptake was observed at a frequency of 84.6% (33/39 patients), 97.4% (38/39 patients), and 61.5% (24/39 patients) in cervical, coeliac, and sacral ganglia, respectively (**Figure 1**). The frequency of choline-positive uptake was highest in coeliac ganglia followed by cervical and sacral ganglia (P < 0.05 for all pairs; **Figure 1**).

On a per-patient basis, 28.3% (34/120 patients) of patients had positive FDG uptake in ganglia (i.e., cervical, coeliac, or sacral). Grouped by location, FDG-positive uptake was observed at a frequency of 16.7% (20/120 patients), 13.3% (16/120 patients), and 2.5% (3/120 patients) in cervical, coeliac, and sacral ganglia, respectively. Cervical and coeliac ganglia had a higher rate of FDG-positive uptake than sacral ganglia (P<0.001 and P = 0.002, respectively). Similar frequency of FDG-positive uptake was observed between cervical and coeliac ganglia (P = 0.470) (**Figure 1**).

The frequency of PSMA-positive and choline-positive ganglia per-patient were 100%, but both were significantly higher than the prevalence of FDG-positive (100% vs. 28.3%, and 100% vs. 28.3%, respectively, P < 0.001 for both) (**Figure 1**). Representative PSMA-positive, choline-positive and FDG-positive ganglia were shown in **Figure 2**.

Absolute Uptake of Ganglia

For qualitative analysis, the SUVmax of PSMA-PET ranged from 1.3 to 6.6. No significant difference was observed in PSMA

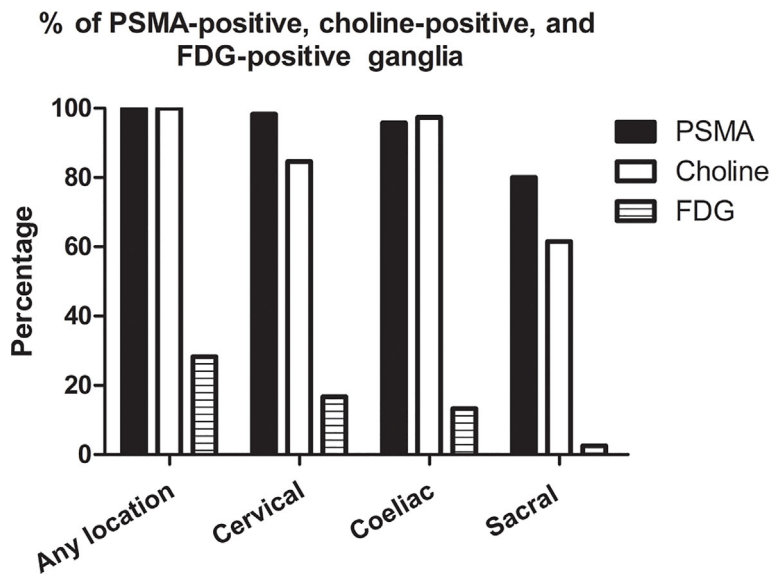

FIGURE 1 | Frequencies of PSMA-positive, choline-positive and FDG-positive ganglia on per-patient-basis.

uptake between ganglia in cervical and coeliac (2.4 ± 0.6 *vs.* 2.4 ± 0.8, P=0.366). However, PSMA uptake in cervical (2.4 ± 0.6 *vs.* 1.8 ± 0.4, P<0.001) and coeliac ganglia (2.4 ± 0.8 *vs.* 1.8 ± 0.4, P<0.001) were both significantly higher than in sacral ganglia (**Figure 3**). For qualitative analysis, the SUVmax of choline-PET ranged from 1.1 to 2.8. choline uptake was highest in coeliac ganglia followed by cervical and sacral ganglia (coeliac was 2.0 ± 0.4; cervical was 1.5 ± 0.3; sacral was 1.4 ± 0.2; P < 0.05 for all pairs). The SUVmax of FDG-PET ranged from 2.0 to 3.5. No significant difference was observed in FDG uptake among cervical, coeliac and sacral ganglia(P =0.915, **Figure 3**).

The SUVmax of choline-PET was lower than the SUVmax of PSMA-PET (1.7 ± 0.4 *vs.* 2.2 ± 0.7, P < 0.001) and SUVmax of FDG-PET (1.7 ± 0.4 *vs.* 2.3 ± 0.3, P < 0.001), and no significant difference was observed between SUVmax of PSMA-PET and FDG-PET (P=0.668). The detailed SUVmax for ganglia are listed in **Table 1**.

Comparison of SUVmax of Choline-PET and FDG-PET Between Ganglia and LNM

On a per-patient basis, PSMA-positive lymph node metastases in any location (i.e., cervical, coeliac, or sacral) were detected in 40.8% (49/120 patients). Grouped by anatomy, PSMA-positive lymph nodes metastases were found at a frequency of 6.7% (8/120 patients), 10.8% (13/120 patients), and 40.0% (48/120 patients) near the typical location of cervical, coeliac, and sacral ganglia, respectively. Frequencies between the occurrence of PSMA-positive ganglia and lymph node metastases were different for any and each separate location (P < 0.001). PSMA uptake in lymph node metastases was significantly higher than in

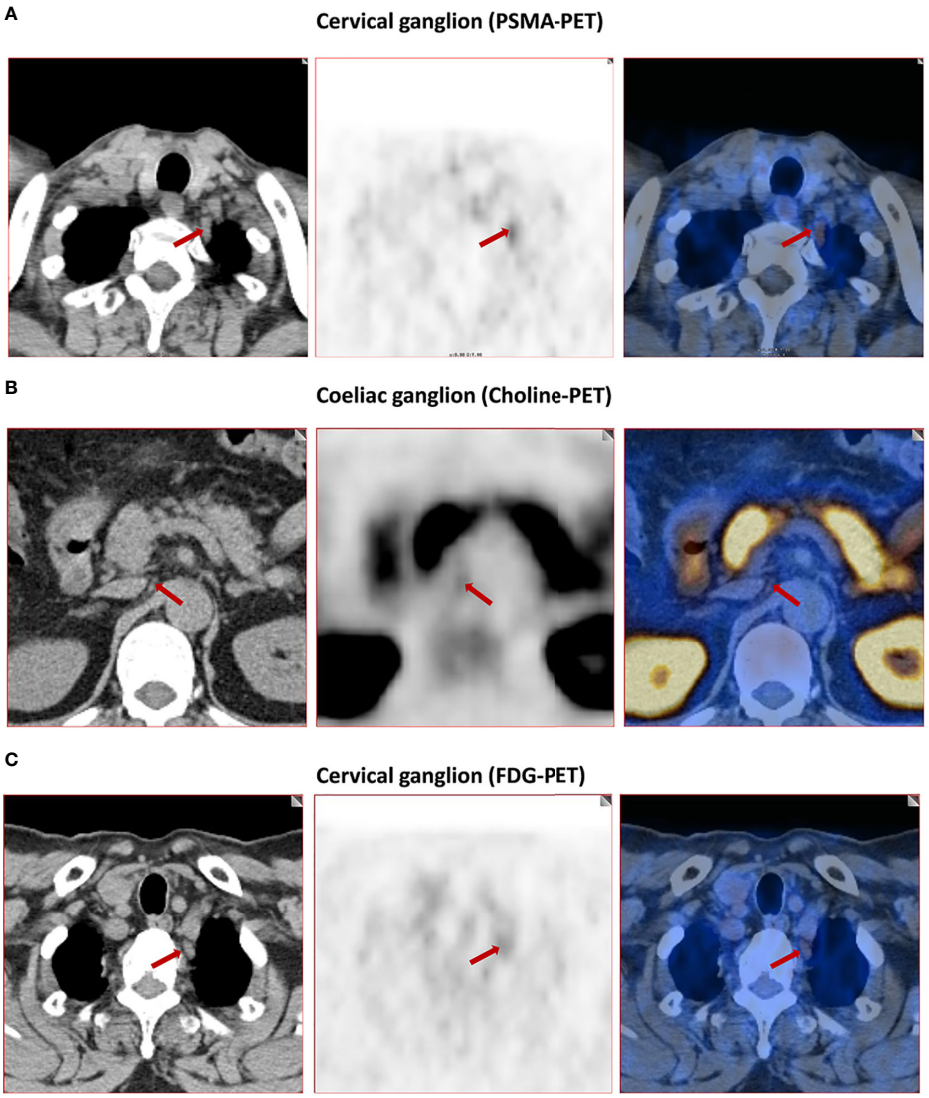

FIGURE 2 | Representative images of PSMA-positive, choline-positive and FDG-positive ganglia. **(A)** PSMA-positive cervical ganglia (red arrow, 4.8 SUVmax for PSMA-PET). **(B)** Choline-positive coeliac ganglia (red arrow, 2.8 SUVmax for choline-PET). **(C)** FDG-positive cervical ganglia (red arrow, 2.9 SUVmax for FDG-PET).

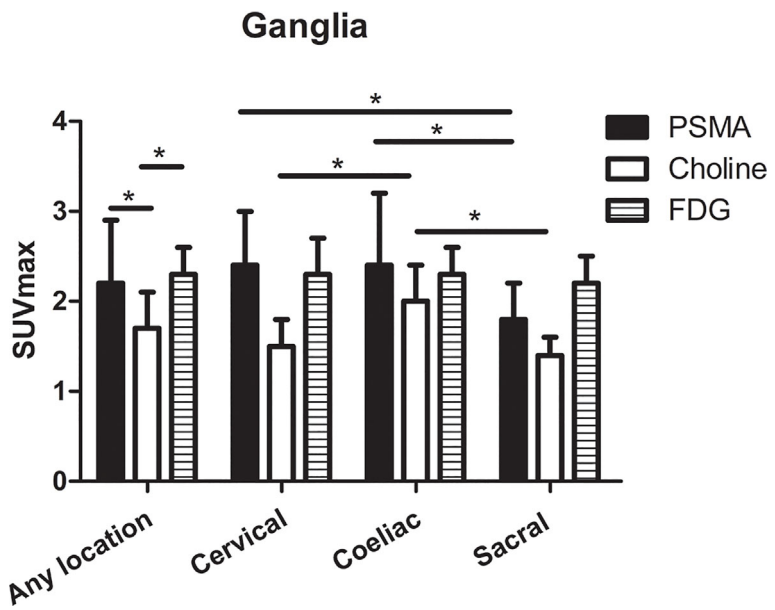

FIGURE 3 | The SUVmax of PSMA-PET, choline-PET and FDG-PET at any location, and cervical, coeliac, and sacral ganglia. *P < 0.05.

TABLE 1 | SUVmax of PSMA-PET, choline-PET and FDG-PET in ganglia.

Parameter		Ganglia Any Location	Cervical	Coeliac	Sacral
PSMA	Mean	2.2	2.4	2.4	1.8
	SD	0.7	0.6	0.8	0.4
	Median	2.1	2.4	2.2	1.7
	Range	1.3-6.6	1.3-4.4	1.3-6.6	1.3-3.3
Choline	Mean	1.7	1.5	2	1.4
	SD	0.4	0.3	0.4	0.2
	Median	1.6	1.5	2	1.4
	Range	1.1-2.8	1.1-2.3	1.4-2.8	1.1-1.7
FDG	Mean	2.3	2.3	2.3	2.2
	SD	0.3	0.4	0.3	0.2
	Median	2.1	2.1	2.1	2.3
	Range	2.0-3.5	2.0-3.5	2.0-2.8	2.0-2.3

ganglia for any location, cervical, coeliac, and sacral locations (any location:19.3 ± 19.0 *vs*. 2.2 ± 0.7, P < 0.001; cervical: 10.7 ± 6.6 *vs*. 2.4 ± 0.6 0.7, P < 0.001; coeliac: 15.1 ± 12.4 *vs*. 2.4 ± 0.8, P < 0.001; sacral: 21.9 ± 20.3 *vs*. 1.8 ± 0.4, P < 0.001) (**Figure 4A**).

Choline-positive LNM in any location was detected in 35.9% (14/39) of patients. Choline-positive LNM was found at a frequency of 5.1% (2/39) of patients at the cervical location, 12.8% (5/39) of patients at the coeliac location, and 33.3% (13/39) of patients at the sacral location. Frequencies in the occurrence of choline-positive ganglia and LNM were significantly different at each location (P < 0.001). Choline uptake in LNM was significantly higher than in ganglia for cervical, coeliac, and sacral locations (any location: 6.6 ± 5.1 *vs*. 1.7 ± 0.4, P < 0.001; cervical: 4.5 ± 0.4 *vs*. 1.5 ± 0.3, P < 0.001; coeliac: 4.4 ± 2.8 *vs*. 2.0 ± 0.4, P < 0.001; sacral: 7.8 ± 5.9 *vs*. 1.4 ± 0.2, P < 0.001) (**Figure 4B**).

FDG-positive LNM at any location (i.e., cervical, coeliac, or sacral) was detected in 25.8% (31/120) of patients. FDG-positive LNM was found at a frequency of 5.0% (6/120) of patients, 6.7% (8/120) of patients, and 25.0% (30/120) of patients near the typical location of cervical, coeliac, and sacral ganglia, respectively. Frequencies in the occurrence of FDG-positive ganglia and LNM were significantly different at each location (P < 0.001). FDG uptake in LNM was significantly higher than in ganglia cervical, coeliac, and sacral locations (any location: 4.9 ± 3.1 *vs*. 2.3 ± 0.3, P < 0.001; cervical: 8.5 ± 3.8 *vs*. 2.3 ± 0.4, P < 0.001; coeliac: 5.1 ± 2.5 *vs*. 2.3 ± 0.3, P < 0.001; sacral: 4.1 ± 2.6 *vs*. 2.2 ± 0.3, P < 0.001) (**Figure 4C**).

ROC Curve Analysis to Differentiate Ganglia From LNM

The optimal SUVmax threshold of PSMA-PET, choline-PET or FDG-PET for distinguishing between LNM and ganglia is shown in **Figure 5**. Receiver-operating characteristic (ROC) curve analysis revealed that at when the SUVmax cutoff of PSMA-

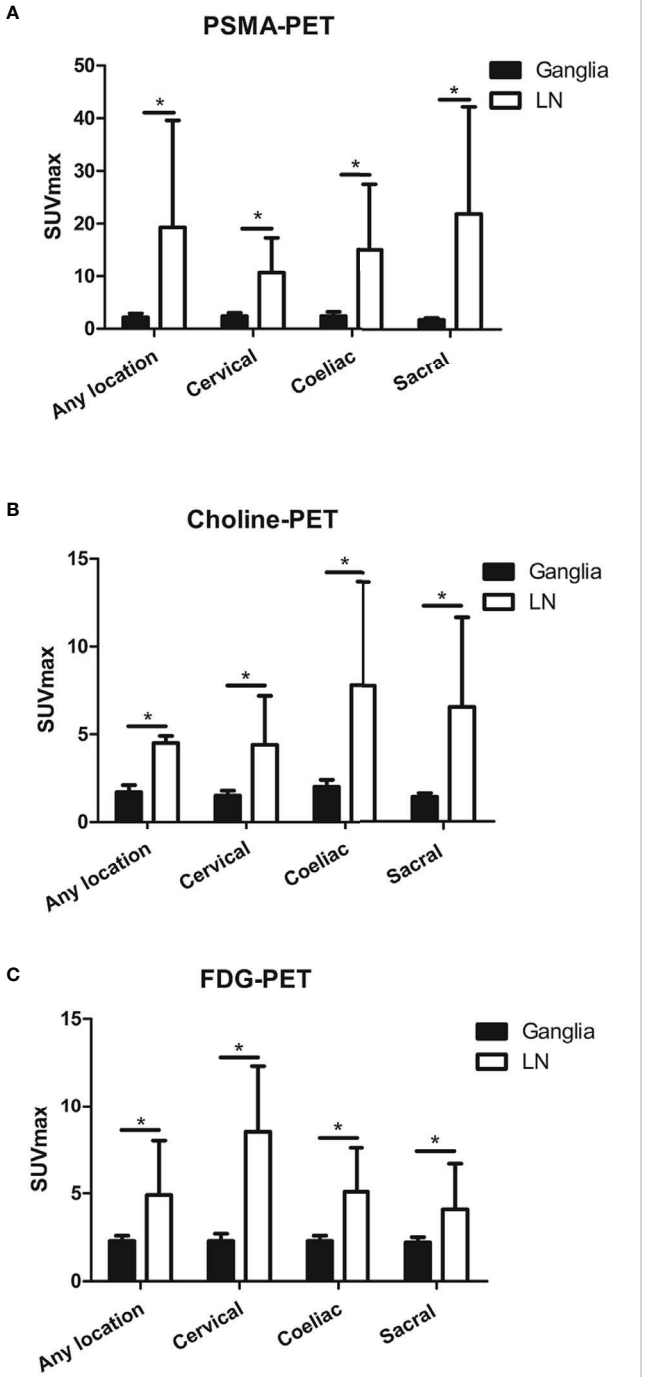

FIGURE 4 | The PSMA, choline and FDG uptake in ganglia and adjacent LNM. **(A)** The PSMA uptake in ganglia and adjacent LNM. **(B)** The choline uptake in ganglia and adjacent LNM. **(C)** The FDG uptake in ganglia and adjacent LNM. *P < 0.05.

PET was 4.1, the sensitivity, specificity and accuracy for identifying lymph node metastasis were 88.4% (61/69), 97.9% (322/329) and 96.2% (383/398), respectively (**Table 2**). And the area under curve was 0.947(95%CI: 0.905-0.989). 2.1% (7/329) of ganglia had a SUVmax of PSMA-PET more than 4.1.

Similarly, ROC curve analysis revealed that when the SUVmax cutoff of choline-PET was 2.35, the sensitivity, specificity, and accuracy for identifying LNM was 95.0% (19/20), 92.6% (88/95), and 93.0% (107/115), respectively. The area under the curve was 0.974 (95%CI: 0.939-1.0). In addition, 7.4% of ganglia showed a SUVmax of choline-PET higher than 2.35.

ROC curve analysis also revealed that at a 2.55 SUVmax cutoff for FDG-PET, the sensitivity, specificity, and accuracy for identifying LNM was 77.3% (34/44), 87.2% (34/39), and 81.9% (68/83), respectively. The area under the curve was 0.876 (95% CI: 0.799-0.954). In addition, 12.8% of ganglia showed a SUVmax of FDG-PET higher than 2.55.

Comparison of Anatomic Morphology Between Ganglia and LNM

We further analyzed the anatomic morphology in ganglia and LNM. In PSMA-positive ganglia, 65.0% exhibited a band-shaped configuration, 28.0% exhibited a teardrop-shaped configuration, and 7.0% exhibited a nodular configuration. In PSMA-positive LNM, only 4.0% exhibited a band-shaped configuration, 19.8% exhibited a teardrop-shaped configuration, and 76.2% exhibited a nodular configuration ($P < 0.001$; **Figure 6A**).

In choline-positive ganglia, 63.1% exhibited a band-shaped configuration, 27.4% exhibited a teardrop-shaped configuration, and 9.5% exhibited a nodular configuration. In choline-positive LNM, only 5.0% exhibited a band-shaped configuration, 20.0% exhibited a teardrop-shaped configuration, and 75.0% exhibited a nodular configuration ($P < 0.001$; **Figure 6B**).

In FDG-positive ganglia, 64.1% exhibited a band-shaped configuration, 30.0% exhibited a teardrop-shaped configuration, and 5.9% exhibited a nodular configuration. In FDG-positive LNM, 4.3% exhibited a band-shaped configuration, 19.8% exhibited a teardrop-shaped configuration, and 75.9% exhibited a nodular configuration ($P < 0.001$; **Figure 6C**).

DISCUSSION

Many studies have indicated that PSMA-positive ganglia represent a potential diagnostic pitfall for nuclear medicine physicians. To solve this problem, some strategies have been proposed, including carefully anatomic correlation and compare and examine the morphology of the lesions (11). Recently, Ian et al. showed that delayed ^{68}Ga-PSMA PET/CT can be used to differentiate between ganglia and LNM (12). The previous studies reporting PSMA uptake by ganglia may help us to differentiate LNM from ganglia. However, choline and ^{18}F-FDG are two additional tracers that are widely used in prostate cancer patients. Nonetheless, there have been no studies describing the patterns of choline and FDG uptake in ganglia.

In the current study, we evaluated the metabolic pattern of ^{68}Ga-PSMA, ^{11}C-choline and ^{18}F-FDG uptake in cervical, coeliac, and sacral ganglia using ^{68}Ga-PSMA, ^{11}C-choline and

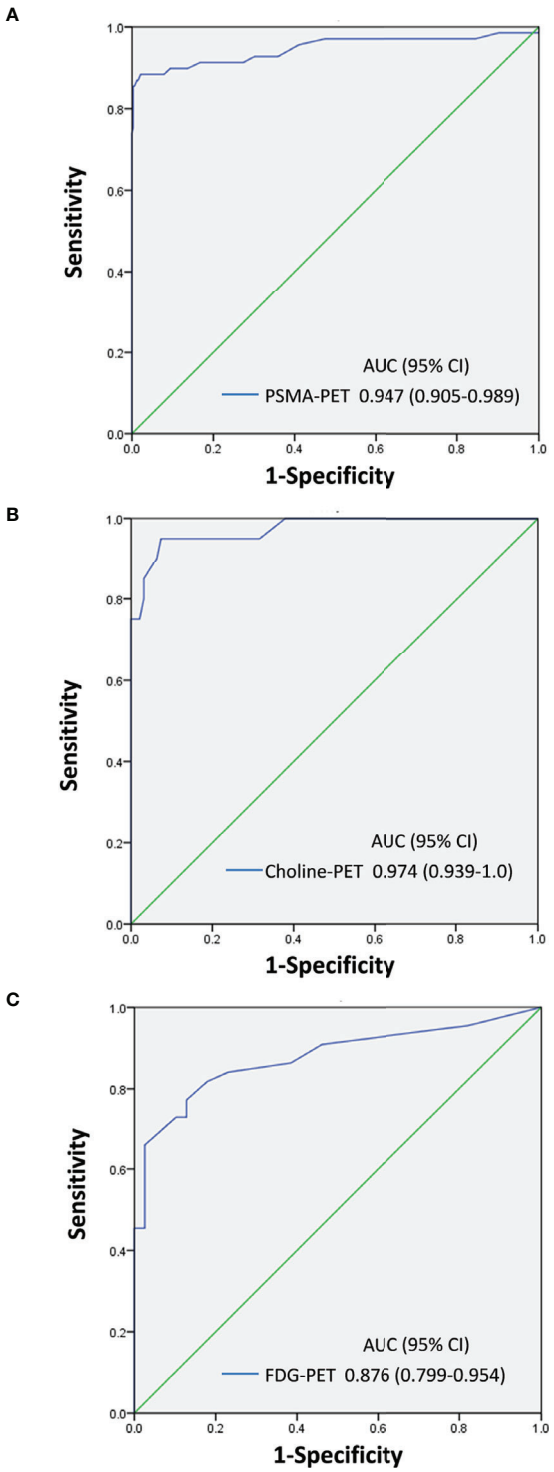

FIGURE 5 | SUVmax of PSMA-PET, choline-PET and FDG-PET for distinguishing between LNM and ganglia. **(A)** PSMA-PET receiver-operating characteristic (ROC) curve analysis showing sensitivity, specificity, and area under curve. **(B)** Choline-PET receiver-operating characteristic (ROC) curve analysis showing sensitivity, specificity, and area under curve. **(C)** FDG-PET receiver-operating characteristic (ROC) curve analysis showing sensitivity, specificity, and area under curve.

TABLE 2 | Identification efficiency between lymph node metastasis and ganglia.

Parameter	Threshold	AUC (95% CI)	Sensitivity	Specificity	Accuracy
PSMA-PET	4.10	0.947(0.905-0.989)	88.4%	97.9%	85.9%
Choline-PET	2.35	0.974(0.939-1.0)	95.0%	92.6%	93.0%
FDG-PET	2.55	0.876 (0.799-0.954)	77.3%	87.2%	81.9%

^{18}F-FDG PET/CT and compared the findings and parameters with LNM. Our study was the first to describe ^{68}Ga-PSMA, ^{11}C-choline and ^{18}F-FDG uptake patterns at different locations (cervical, coeliac, and sacral). Our results showed that ganglia at different location have heterogeneous ^{68}Ga-PSMA, ^{11}C-choline uptake intensity and homogeneous ^{18}F-FDG uptake intensity. In addition, we performed a systematic comparison of the different ganglia and adjacent LNM and demonstrated that ^{68}Ga-PSMA, ^{11}C-choline and ^{18}F-FDG uptake is higher in LNM. In addition, LNM showed a clearly different configuration compared with ganglia. Furthermore, we used ROC curve analysis to differentiate LNM from ganglia and found preferable sensitivity, specificity, and accuracy in ^{68}Ga-PSMA, ^{11}C-choline and ^{18}F-FDG PET/CT.

In this study, we identified PSMA-positive ganglia in 100% of our patients, 98.3% in cervical, 95.8% in coeliac and 80.0% in sacral ganglia, which were similar with the PSMA-positive rates found by Christoph (11). Though lymph node metastases had a statistically significant higher SUVmax of PSMA-PET than ganglia, there was a significant overlap in SUVmax of PSMA-PET between lymph node metastases and ganglia. Vinsensia et al. previously suggested SUVmax 2.0 of PSMA-PET as the threshold for PSMA-positive lymph nodes (21). However, our study demonstrated that 59.9% of ganglia had a SUVmax of PSMA-PET more than 2.0. In the current study, we sought to determine the optimal threshold of SUVmax of PSMA-PET for predicting lymph node metastases. ROC analysis demonstrated that the highest accuracy (96.2%) was obtained with the SUVmax of PSMA-PET 4.1, and the sensitivity and specificity for identifying lymph node metastasis were 88.4%, 97.9%, respectively. As we all known, this is the first study to determine the optimal threshold of SUVmax of PSMA-PET by ROC analysis for identifying lymph node metastases from ganglia, and our diagnostic efficiency is higher than that of other studies (12). When we use 4.1 as the cut-off, only 2.1% of ganglia had a SUVmax of PSMA-PET more than 4.1.

Besides PSMA-positive ganglia which have been described in previous studies, we also investigated in detail the choline and FDG uptake in ganglia which have never been reported before. We identified choline-positive ganglia in 100% of patients, including 84.6% in cervical, 97.4% in coeliac ganglia, and 61.5% in sacral ganglia. Though the frequency of choline-positive ganglia was high, the range of SUVmax of choline-PET in ganglia was narrow, which ranged from 1.1 to 2.8. However, the range of SUVmax of choline-PET in LNM was high, which ranged from 1.8 to 19.0. In addition, choline uptake in LNM was significantly higher than in ganglia for all locations,

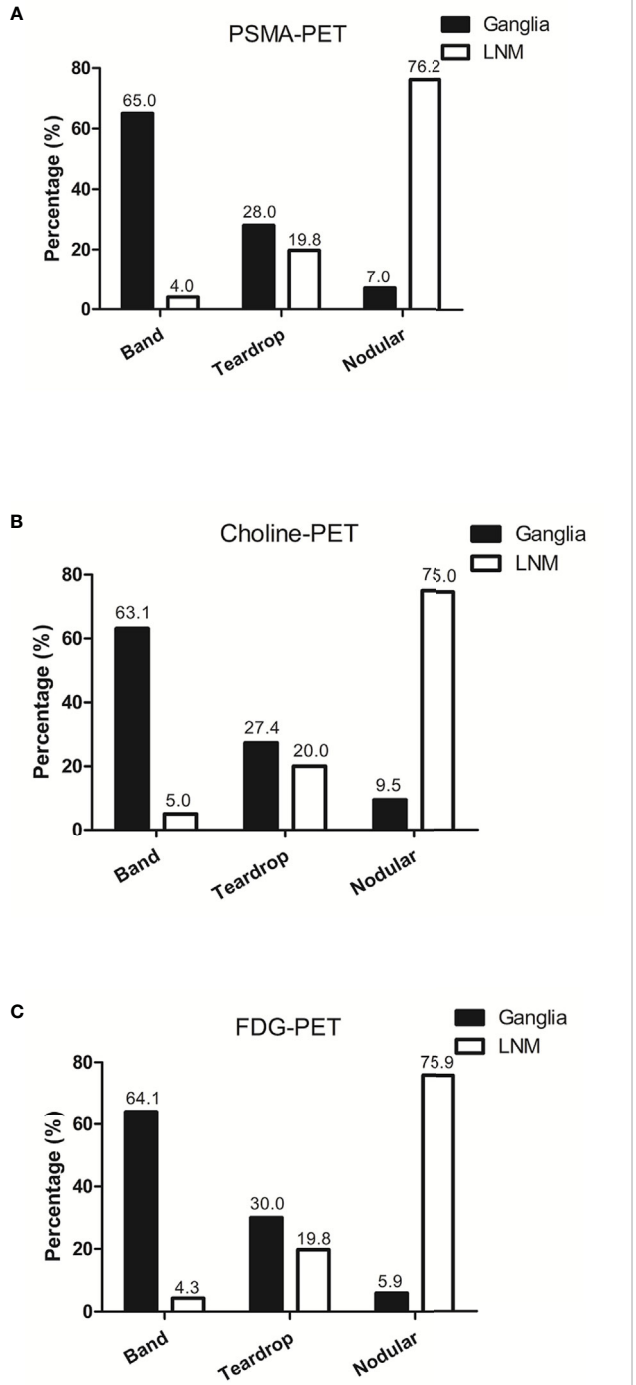

FIGURE 6 | The anatomic morphology of ganglia and LNM in PSMA-PET, choline-PET and FDG-PET. **(A)** The anatomic morphology of ganglia and LNM in PSMA-PET. **(B)** The anatomic morphology of ganglia and LNM in choline-PET. **(C)** The anatomic morphology of ganglia and LNM in FDG-PET.

including cervical, coeliac, and sacral locations. ROC curve analysis revealed that when the SUVmax cutoff of choline-PET was 2.35, it showed preferable sensitivity, specificity, and accuracy for identifying LNM. Only 7.4% of ganglia had a SUVmax of choline-PET higher than 2.35. In addition, choline uptake was highest in coeliac ganglia followed by cervical and sacral ganglia. It should be noted that the SUVmax of sacral ganglia was low (1.7), thus when we differentiated LNM from ganglia in choline-PET, the lesion location was considered and helped us to better distinguish between them. Although the typical location of the ganglia, knowledge about anatomy and disease stage helps in differentiation between LNM and ganglia, the additional SUVmax cut-off value is rarely used. This is mainly due to PSMA is highly sensitive and can also detect LNM as small as 2-3 mm which may show only faint PSMA uptake (hence lower SUVmax). In this LNM with faint PSMA, it is not feasible to differentiate between LNM and ganglia according to the SUVmax.

^{18}F-FDG PET is widely used in many malignant tumors. However, FDG-positive ganglia have not been described in previous studies. In the present study, we identified FDG-positive ganglia in 28.3% of patients, including 16.7% in cervical, 13.3% in coeliac ganglia, and 2.5% in sacral ganglia, which were lower than the frequency of choline-positive ganglia. In addition, choline uptake in LNM was significantly higher than in ganglia for all locations, including cervical, coeliac, and sacral locations. When we used 2.55 SUVmax as a cut-off, 12.8% of ganglia had a SUVmax using FDG-PET of more than 2.55. In addition, though no significant difference was observed in FDG uptake for ganglia in different locations, the frequency of FDG-positive sacral lesion in ganglia was 2.5% but was 25% in LNM. Furthermore, the range of SUVmax of FDG-PET in ganglia was narrow and ranged from 2.0 to 3.5; the maximum of sacral ganglia was 2.3. Lymph nodes are most likely to metastasize into the sacral location and identification is more often required compared with cervical and coeliac location. Therefore, the FDG-PET SUVmax range of sacral ganglia and the FDG-positive rates between ganglia and LNM should be determined, which helped to better distinguish them.

In addition to the ^{68}Ga-PSMA, ^{11}C-choline and ^{18}F-FDG uptake difference, we evaluated the morphology differences between ganglia and LNM. PSMA-, Choline- and FDG-positive ganglia are more often band-shaped. However, most LNMs exhibited nodular configuration or teardrop-shaped configuration. In several lesions with teardrop-shaped structure, ^{68}Ga-PSMA, ^{11}C-choline and ^{18}F-FDG uptake and anatomic location was used to differentiate ganglia from LNM. ^{68}Ga-PSMA, ^{11}C-choline and ^{18}F-FDG uptake characteristics, anatomic location, and configuration can be used to differentiate between ganglia from adjacent LNM.

Although our results indicated different heterogeneous characteristics of tracer uptake in ^{68}Ga-PSMA, ^{11}C-choline or ^{18}F-FDG, the mechanism remains unclear. Many studied reported that peripheral nerve ganglia uptake PSMA (11). It has been reported that astrocytes express PSMA physiologically as PSMA is related to their homologue glutamic acid carboxypeptidase III (22, 23). The uptake of ^{18}F-FDG in ganglia was correlated with the expression level of glucose transporter-1 and glucose transporter-3 (24). Thus, the

heterogeneous metabolic patterns of ganglia may be attributed to the heterogeneous expression of PSMA, glucose transporter-1 and glucose transporter-3 and choline content.

Our study had several limitations. The definition of LNM and ganglia has been mainly based on characteristic imaging features, such as typical anatomic location. However, pathological evidence is not feasible in the clinic because of ethical and practical reasons. The SUVmax cut-off of PSMA-PET, choline-PET and FDG-PET could differentiate LNM from ganglia. However, the SUVmax threshold may be influenced by different PET/CT scanner models, the PSMA or choline ligand, the scan procedure, etc. Therefore, in the clinical setting, it is essential to establish the optimal SUVmax cut-off according to the actual imaging conditions, instead of arbitrarily using the threshold of the current study. In addition, choline-PET and PSMA/FDG-PET were derived from different group of patients, so the comparison between them might be unfair due to the selection bias. Furthermore, the present study had a relatively small sample size and it is a retrospective study. Therefore, the results might have been influenced by selection bias and should be cautiously interpreted. Further prospective studies with more patients are required to confirm our study.

CONCLUSIONS

The current study is the first to describe the patterns of ^{11}C-choline and ^{18}F-FDG uptake in ganglia. ^{68}Ga-PSMA and ^{11}C-choline uptake in ganglia was very common, and FDG-positive ganglia were observed at a lower frequency compared with PSMA-positive and choline-positive ganglia. ^{68}Ga-PSMA, ^{11}C-choline and ^{18}F-FDG uptake characteristics, anatomic location, and configuration may be used to differentiate between ganglia from adjacent LNM.

DATA AVAILABILITY STATEMENT

The raw data supporting the conclusions of this article will be made available by the authors, without undue reservation.

ETHICS STATEMENT

The studies involving human participants were reviewed and approved by RenJi Hospital. Written informed consent for participation was not required for this study in accordance with the national legislation and the institutional requirements.

AUTHOR CONTRIBUTIONS

RC and JL designed and wrote the experiments. YS, JW, LX, YW and GH collected and analyzed the data. YZ revised the manuscript. All authors contributed to the article and approved the submitted version.

FUNDING

This work was supported by grants from the National Natural Science Foundation of China (nos. 81701724, 81771858, 81830052, 81771861), Shanghai Advanced Appropriate Technology Promotion Projects (no. 2019SY029) and JiangXi Provincial Department of Science and Technology (Grant Number: 20161BBG70202 & 20071BBG70050), Jiangxi Provincial Health Commission (Grant Number: 20161071 & 20171090).

REFERENCES

1. Siegel RL, Miller KD, Jemal A. Cancer statistics, 2020. *CA Cancer J Clin* (2020) 70:7–30. doi: 10.3322/caac.21590
2. Boorjian SA, Eastham JA, Graefen M, Guillonneau B, Karnes RJ, Moul JW, et al. A critical analysis of the long-term impact of radical prostatectomy on cancer control and function outcomes. *Eur Urol* (2012) 61:664–75. doi: 10.1016/j.eururo.2011.11.053
3. Briganti A, Abdollah F, Nini A, Suardi N, Gallina A, Capitanio U, et al. Performance characteristics of computed tomography in detecting lymph node metastases in contemporary patients with prostate cancer treated with extended pelvic lymph node dissection. *Eur Urol* (2012) 61:1132–8. doi: 10.1016/j.eururo.2011.11.008
4. Perera M, Papa N, Roberts M, Williams M, Udovicich C, Vela I, et al. Gallium-68 Prostate-specific Membrane Antigen Positron Emission Tomography in Advanced Prostate Cancer-Updated Diagnostic Utility, Sensitivity, Specificity, and Distribution of Prostate-specific Membrane Antigen-avid Lesions: A Systematic Review and Meta-analysis. *Eur Urol* (2020) 77:403–17. doi: 10.1016/j.eururo.2019.01.049
5. Sprute K, Kramer V, Koerber S, Meneses M, Fernandez R, Soza-Ried C, et al. Diagnostic accuracy of (18)F-PSMA-1007-PET/CT imaging for lymph node staging of prostate carcinoma in primary and biochemical recurrence. *J Nucl Med* (2020). doi: 10.2967/jnumed.120.246363
6. Tan N, Oyoyo U, Bavadian N, Ferguson N, Mukkamala A, Calais J, et al. PSMA-targeted Radiotracers versus (18)F Fluciclovine for the Detection of Prostate Cancer Biochemical Recurrence after Definitive Therapy: A Systematic Review and Meta-Analysis. *Radiology* (2020) 296:44–55. doi: 10.1148/radiol.2020191689
7. Fendler WP, Ferdinandus J, Czernin J, Eiber M, Flavell RR, Behr SC, et al. Impact of (68)Ga-PSMA-11 PET on the Management of recurrent Prostate Cancer in a Prospective Single-Arm Clinical Trial. *J Nucl Med* (2020). doi: 10.1055/s-0040-1708125
8. Bravi CA, Fossati N, Gandaglia G, Suardi N, Mazzone E, Robesti D, et al. Long-term Outcomes of Salvage Lymph Node Dissection for Nodal Recurrence of Prostate Cancer After Radical Prostatectomy: Not as Good as Previously Thought. *Eur Urol* (2020) 78:661–9. doi: 10.1016/j.eururo.2020.09.036
9. Morris MJ, Rowe SP, Gorin MA, Saperstein L, Pouliot F, Josephson DY, et al. Diagnostic Performance of (18)F-DCFPyL-PET/CT in Men with Biochemically Recurrent Prostate Cancer: Results from the CONDOR Phase 3, Multicenter Study. *Clin Cancer Res* (2021). doi: 10.1158/1078-0432.CCR-20-4573
10. Malaspina S, Anttinen M, Taimen P, et al. Prospective comparison of (18)F-PSMA-1007 PET/CT, whole-body MRI and CT in primary nodal staging of unfavourable intermediate- and high-risk prostate cancer. *Eur J Nucl Med Mol Imaging* (2021). doi: 10.1007/s00259-021-05296-1
11. Rischpler C, Beck TI, Okamoto S, Schlitter AM, Knorr K, Schwaiger M, et al. (68)Ga-PSMA-HBED-CC Uptake in Cervical, Celiac, and Sacral Ganglia as an Important Pitfall in Prostate Cancer PET Imaging. *J Nucl Med* (2018) 59:1406–11. doi: 10.2967/jnumed.117.204677

12. Alberts I, Sachpekidis C, Dijkstra L, et al. The role of additional late PSMA-ligand PET/CT in the differentiation between lymph node metastases and ganglia. *Eur J Nucl Med Mol Imaging* (2020) 47:642–51. doi: 10.1007/s00259-019-04552-9
13. Krohn T, Verburg FA, Pufe T, Neuhuber W, Vogg A, Heinzel A, et al. [(68)Ga]PSMA-HBED uptake mimicking lymph node metastasis in coeliac ganglia: an important pitfall in clinical practice. *Eur J Nucl Med Mol Imaging* (2015) 42:210–4. doi: 10.1007/s00259-014-2915-3
14. Beheshti M, Rezaee A, Langsteger W. 68Ga-PSMA-HBED Uptake on Cervicothoracic (Stellate) Ganglia, a Common Pitfall on PET/CT. *Clin Nucl Med* (2017) 42:195–6. doi: 10.1097/RLU.0000000000001518
15. Michaud L, Touijer KA, Mauguen A, Zelefsky MJ, Morris MJ, Lyashschenko SK, et al. (11)C-Choline PET/CT in Recurrent Prostate Cancer: Retrospective Analysis in a Large U.S. Patient Series. *J Nucl Med* (2020) 61:827–33. doi: 10.2967/jnumed.119.233098
16. Umbehr MH, Muntener M, Hany T, Sulser T, Bachmann LM. The role of 11C-choline and 18F-fluorocholine positron emission tomography (PET) and PET/CT in prostate cancer: a systematic review and meta-analysis. *Eur Urol* (2013) 64:106–17. doi: 10.1016/j.eururo.2013.04.019
17. Evangelista L, Zattoni F, Guttilla A, Mukkamala A, Calais J, Davenport MS. Choline PET or PET/CT and biochemical relapse of prostate cancer: a systematic review and meta-analysis. *Clin Nucl Med* (2013) 38:305–14. doi: 10.1097/RLU.0b013e3182867f3c
18. Parida GK, Tripathy S, Datta Gupta S, Kumar R, Bal C, Shamim SA. Adenocarcinoma Prostate With Neuroendocrine Differentiation: Potential Utility of 18F-FDG PET/CT and 68Ga-DOTANOC PET/CT Over 68Ga-PSMA PET/CT. *Clin Nucl Med* (2018) 43:248–9. doi: 10.1097/RLU.0000000000002013
19. Perez PM, Hope TA, Behr SC, van Zante A, Small EJ, Flavell RR. Intertumoral Heterogeneity of 18F-FDG and 68Ga-PSMA Uptake in Prostate Cancer Pulmonary Metastases. *Clin Nucl Med* (2019) 44:e28–32. doi: 10.1097/RLU.0000000000002367
20. Jadvar H. Imaging evaluation of prostate cancer with 18F-fluorodeoxyglucose PET/CT: utility and limitations. *Eur J Nucl Med Mol Imaging* (2013) 40 Suppl 1:S5–10. doi: 10.1007/s00259-013-2361-7
21. Vinsensia M, Chyoke PL, Hadaschik B, Holland-Letz T, Moltz J, Kopka K, et al. (68)Ga-PSMA PET/CT and Volumetric Morphology of PET-Positive Lymph Nodes Stratified by Tumor Differentiation of Prostate Cancer. *J Nucl Med* (2017) 58:1949–55. doi: 10.2967/jnumed.116.185033
22. Hlouchova K, Barinka C, Klusak V, Šácha P, Mlčochová P, Majer P, et al. Biochemical characterization of human glutamate carboxypeptidase III. *J Neurochem* (2007) 101:682–96. doi: 10.1111/j.1471-4159.2006.04341.x
23. Evans JC, Malhotra M, Cryan JF, O'Driscoll CM. The therapeutic and diagnostic potential of the prostate specific membrane antigen/glutamate carboxypeptidase II (PSMA/GCPII) in cancer and neurological disease. *Br J Pharmacol* (2016) 173:3041–79. doi: 10.1111/bph.13576
24. Zheng Y, Wang XM. Expression Changes in Lactate and Glucose Metabolism and Associated Transporters in Basal Ganglia following Hypoxic-Ischemic Reperfusion Injury in Piglets. *AJNR Am J Neuroradiol* (2018) 39:569–76. doi: 10.3174/ajnr.A5505

Conflict of Interest: The authors declare that the research was conducted in the absence of any commercial or financial relationships that could be construed as a potential conflict of interest.

frontiers in Oncology

SYSTEMATIC REVIEW
published: 26 April 2021
doi: 10.3389/fonc.2021.649171

Performance of 18F-DCFPyL PET/CT Imaging in Early Detection of Biochemically Recurrent Prostate Cancer: A Systematic Review and Meta-Analysis

Jiale Sun, Yuxin Lin, Xuedong Wei, Jun Ouyang, Yuhua Huang and Zhixin Ling**

Department of Urology, The First Affiliated Hospital of Soochow University, Suzhou, China

OPEN ACCESS

Edited by:
Constantinos Zamboglou, University of Freiburg Medical Center, Germany

Reviewed by:
Marco M. E. Vogel, Technical University of Munich, Germany
Maria Picchio, San Raffaele Hospital (IRCCS), Italy
Nina-Sophie Hegemann, Ludwig Maximilian University of Munich, Germany

***Correspondence:**
Yuhua Huang
sdfyyhyh@163.com
Zhixin Ling
lzx986084954@126.com

Specialty section:
This article was submitted to Cancer Imaging and Image-directed Interventions, a section of the journal Frontiers in Oncology

Received: *04 January 2021*
Accepted: *18 February 2021*
Published: *26 April 2021*

Citation:
Sun J, Lin Y, Wei X, Ouyang J, Huang Y and Ling Z (2021) Performance of 18F-DCFPyL PET/CT Imaging in Early Detection of Biochemically Recurrent Prostate Cancer: A Systematic Review and Meta-Analysis. Front. Oncol. 11:649171. doi: 10.3389/fonc.2021.649171

Background: Prostate-specific membrane antigen (PSMA)-targeted 2-(3-{1-carboxy-5-[(6-[18F] fluoro-pyridine-3-carbonyl)-amino]-pentyl}-ureido)-pentanedioic acid (18F-DCFPyL) positron emission tomography/computed tomography (PET/CT) has shown advantages in primary staging, restaging, and metastasis detection of prostate cancer (PCa). However, little is known about the role of 18F-DCFPyL PET/CT in biochemically recurrent prostate cancer (BRPCa). Hence, we performed a systematic review and meta-analysis to evaluate 18F-DCFPyL PET/CT as first-line imaging modality in early detection of BRPCa.

Methods: A comprehensive literature search of PubMed, Web of Science, Embase, and Cochrane Library was conducted until December 2020. The pooled detection rate on a per-person basis and together with 95% confidence interval (CI) was calculated. Furthermore, a prostate-specific antigen (PSA)-stratified performance of detection positivity was obtained to assess the sensitivity of 18F-DCFPyL PET/CT in BRPCa with different PSA levels.

Results: A total of nine eligible studies (844 patients) were included in this meta-analysis. The pooled detection rate (DR) of 18F-DCFPyL PET/CT in BRPCa was 81% (95% CI: 76.9–85.1%). The pooled DR was 88.8% for PSA $\geq$ 0.5 ng/ml (95% CI: 86.2–91.3%) and 47.2% for PSA $<$ 0.5 ng/ml (95% CI: 32.6–61.8%). We also noticed that the regional lymph node was the most common site with local recurrence compared with other sites (45.8%, 95% CI: 42.1–49.6%). Statistical heterogeneity and publication bias were found.

Conclusion: The results suggest that 18F-DCFPyL PET/CT has a relatively high detection rate in BRPCa. The results also indicate that imaging with 18F-DCFPyL may exhibit improved sensitivity in BRPCa with increased PSA levels. Considering the publication bias, further large-scale multicenter studies are warranted for validation.

Keywords: 18F-DCFPyL, prostate-specific membrane antigen, PET/CT, biochemically recurrent prostate cancer, imaging

INTRODUCTION

Prostate cancer (PCa) is the most common form of malignant tumor among men in the United States and the second most common cause of cancer-related deaths in aging men (1). After patients received the initial treatments, follow-up strategies including physical examination and prostate-specific antigen (PSA) tests were performed to monitor the progression of the disease (2). Despite the high success rate of the primary treatments, PCa recurrence is relatively common, presenting with a sudden rise or persistently elevated PSA levels. For post radical prostatectomy (RP), biochemical recurrence (BCR) is defined as two consecutive PSA values that are >0.2 ng/ml and rising (3). For post external beam radiation therapy (EBRT), BCR is defined as an increase in the PSA level by 2 ng/ml or more above the nadir (4). It is reported that BCR will occur in ∼20–40% of the patients undergoing radical prostatectomy (5–7) and 30–50% of men after EBRT (8). Another study also reported that 13.9% of PCa patients following brachytherapy developed biochemical failure in the first decade of follow-up (9). Although the treatment of men with biochemically recurrent prostate cancer (BRPCa) should be based not only on radiographic characteristics but also on personal clinical, pathologic, and genomic characteristics, and optimal timing of systemic therapy remains controversial (10), the early lesion localization of BRPCa is still essential to define disease distribution that could, in turn, help urologists make further possible clinical decisions including surgery, salvage radiation therapy (RT), androgen deprivation therapy (ADT), or chemotherapy. However, traditional imaging methods such as plain X-ray, CT, MRI, or bone scintigraphy are limited by their low sensitivity while detecting early recurrent disease (11). Developments of imaging techniques may enable urologists to localize recurrence or metastasis sites in BCR patients.

The prostate-specific membrane antigen (PSMA) is specifically highly expressed in the surface of PCa cells (12). Recently, PSMA-targeted positron emission tomography/computed tomography (PET/CT) is increasingly used in PCa diagnostics (13, 14). Moreover, PSMA PET/CT has greater sensitivity and specificity for detecting pelvic nodal or distant metastases than conventional imaging techniques (15). Therefore, PSMA radiopharmaceuticals have been increasingly used to detect small tumor lesions, lymph node, bone, or visceral metastases because of its high sensitivity even at low PSA levels. Several PSMA radioligands such as Gallium-68 (68Ga), Fluorine-18 (18F), Lutetium-177 (177Lu), or Copper-64 (64Cu) are currently available to obtain effective radiotherapeutics for theranostic applications (16–20). 68Ga-PSMA PET/CT was first introduced to predict biochemical recurrence in PCa patients after initial therapy (21, 22). It was reported that lesions suspicious for PCa detected by 68Ga-PSMA PET/CT presented with excellent contrast as early as 1 h post-injection with high detection rates even at low PSA levels (23). However, despite the widespread clinical adoption of this agent, there are some disadvantages related to its short physical half-life (68 min) and decreasing synthesis yields as generators decay. It is also difficult and expensive to comply with good manufacturing practice guidelines, and therefore centralized radiopharmacy production and distribution are constrained (24). By contrast, 18F-labeled PSMA agents seem to have more advantages as they provide a longer half-life, allowing for later facilitating tumor visualization with higher physical spatial resolution (25). The 2-(3-{1-carboxy-5-[(6-[18F] fluoro-pyridine-3-carbonyl)-amino]-pentyl}-ureido)-pentanedioic acid (18F-DCFPyL), as a novel second-generation PSMA agent, binds with higher affinity, thus allowing earlier detection of local recurrence even at a lower PSA level (26, 27). To our knowledge, the value of this kind of radiotracer is still unclear due to the relatively small sizes of the prior studies. Therefore, we performed a meta-analysis to more accurately evaluate the diagnostic performance of 18F-DCFPyL PET/CT in BRPCa patients.

Abbreviations: PSMA, prostate-specific membrane antigen; PET/CT, positron emission tomography/computed tomography; BRPCa, biochemically recurrent prostate cancer; CI, confidence interval; DR, detection rate; PSA, prostate-specific antigen; PCa, prostate cancer; BCR, biochemical recurrence; RP, radical prostatectomy; EBRT, external beam radiation therapy; RT, radiation therapy; PRISMA, Preferred Reporting Items for Systematic Reviews and Meta-analyses; QUADAS-2, quality assessment of diagnostic accuracy studies; 18F-DCFPyL, 2-(3-{1-carboxy-5-[(6-[18F] fluoro-pyridine-3-carbonyl)-amino]-pentyl}-ureido)-pentanedioic acid.

MATERIALS AND METHODS

Search Strategy and Identification of Eligible Studies

Two reviewers (Sun and Lin) searched the online databases PubMed, Web of Science, Embase, and Cochrane Library to identify the relevant articles published until December 2020. The study was reported according to the Preferred Reporting Items for Systematic Reviews and Meta-Analyses (PRISMA) (28), and the following keywords were used: "18F-DCFPyL" OR "2-(3-{1-carboxy-5-[(6-[18F]fluoro-pyridine-3-carbonyl)-amino]-pentyl}-ureido)-pentanedioic acid" AND "Biochemically recurrent prostate cancer." Articles in all languages were considered relevant for review, and the references of pertinent articles were manually screened and checked as well. All prospective or retrospective studies investigating 18F-DCFPyL PET/CT and BRPCa were included. Exclusion criteria were as follows: (I) case series or case reports; (II) review articles and editorial comments; (III) data incomplete or unclear or unusable with our study or major mistakes; (IV) republished literature; (V) studies performed on a per-lesion basis.

Data Extraction

Two reviewers (Sun and Lin) extracted the following information independently from each study, and inconsistencies were resolved by discussion until a consensus was obtained. Extracted data included country, study period, study design, sample size, characteristics of participants, technical aspects, and detection rate (DR) of 18F-DCFPyL PET/CT on a per-person basis. Quality Assessment of Diagnostic Accuracy Studies (QUADAS-2) (29) was used for assessing the quality of articles included in this study.

Statistical Analysis

All statistical analyses were conducted by Stata (version 15; StataCorp, Texas, USA). The heterogeneity between different articles was determined by I^2 index (30). When significant heterogeneity was observed ($I^2 > 50\%$), the random-effect model was applied. Based on our clinical experience, subgroup analysis according to mean/median PSA before 18F-DCFPyL PET/CT scanning was conducted if significant heterogeneity exists. A PSA-stratified performance of detection positivity was obtained to assess the sensitivity of 18F-DCFPyL PET/CT in BRPCa with different PSA levels. Egger's test was conducted to estimate publication bias. All tests with two-sided $P < 0.05$ were considered statistically significant.

RESULTS

Characteristics of Included Studies

As shown in the PRISMA flow diagram (**Figure 1**), nine studies containing 844 patients were finally included for further meta-analysis (31–39). The QUADAS-2 shows that the quality of all articles included was not completely satisfactory because some articles did not detail patient selection information (**Supplementary Materials 1.1**, **1.2**).

Basic characteristics and technical aspects of the involved studies were summarized in **Tables 1**, **2**, respectively. On the whole, all included studies shared a similar type of patients evaluated and detailed techniques of 18F-DCFPyL PET/CT. We

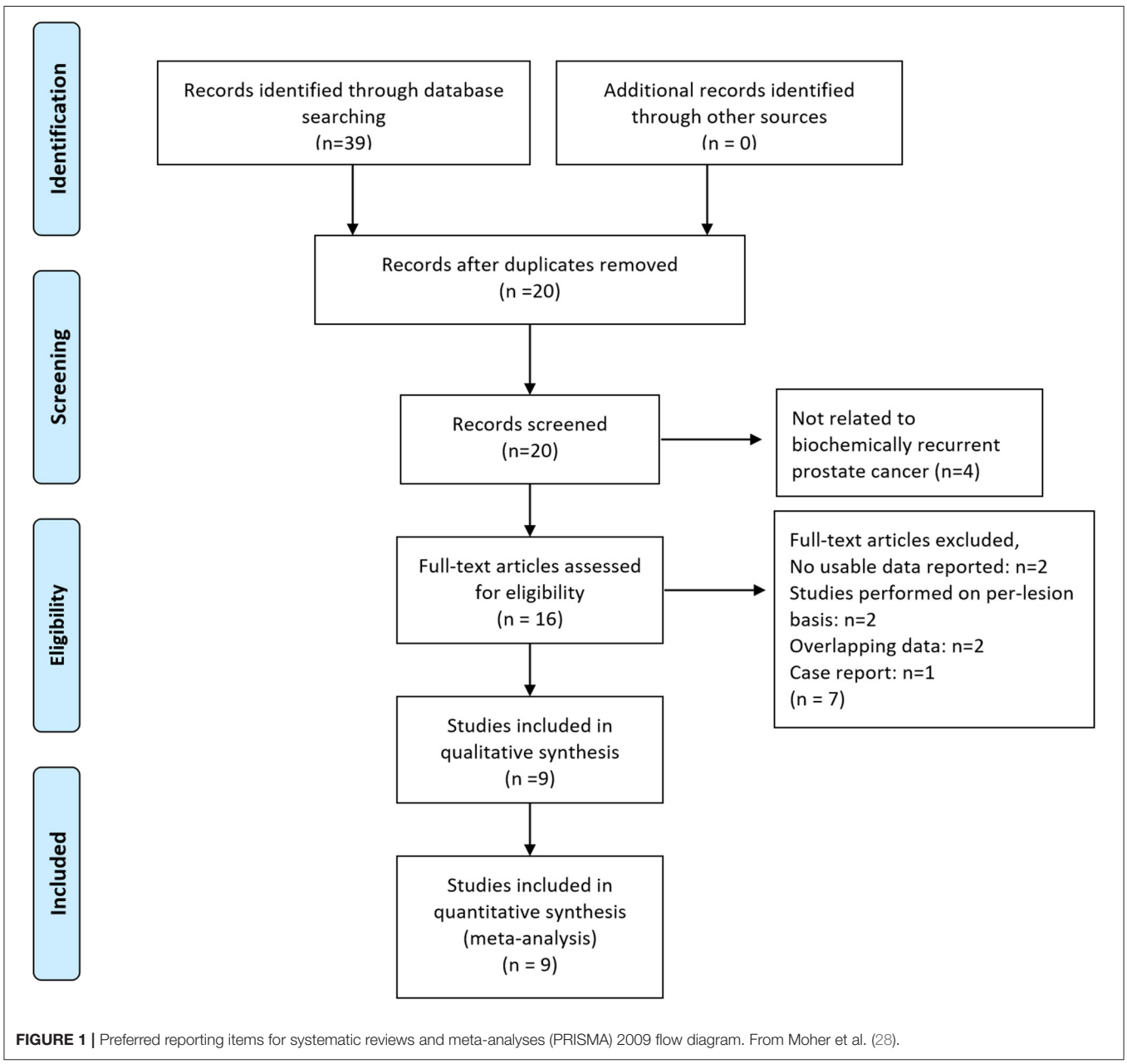

FIGURE 1 | Preferred reporting items for systematic reviews and meta-analyses (PRISMA) 2009 flow diagram. From Moher et al. (28).

TABLE 1 | Summary of the included studies.

References	Study period	Country	Study design	Type of patients evaluated	No. of patients	Mean/median age	Gleason Score	Mean/median PSA values before PET/CT (ng/ml)	Mean/median PSA doubling time before PET/CT (months)
Markowski et al. (31)	NA	USA	Prospective single-center	Patients with BRPCa previously treated with RP.	108	Median: 67 (61–71)	Gleason ≤7 (70.4%) Gleason ≥8 (26.8%) Unknown (2.8%)	Median: 0.7 (0.3–1.8)	NA
Hong et al. (32)	2018–2019	USA	Prospective single-center	Patients with BRPCa previously treated with RP (58.3%) or RT (41.7%) with or without ADT.	72	Mean: 71.5 ± 7.2	Gleason ≤6 (8%) Gleason 7 (51%) Gleason ≥8 (40%)	Median: 3.0 (0.23–698.4) Mean: 15.8 ± 58.2	NA
Wei et al. (33)	2017–2018	Canada	Prospective multicenter	Patients with BRPCa previously treated with RT (100.0%) with or without additional ADT.	79	Median: 75 (51–88)	Gleason ≤6 (29.1%) Gleason 7 (65.9%) Gleason ≥8 (5.1%)	Median: 4.8 (2.1–69)	Median: 14.4 (1.9–48.6)
Jansen et al. (34)	2018–2019	Netherlands	Retrospective single-center	Patients with BRPCa previously treated with RP without ADT.	24	Median: 67 (61–77)	NA	Median: 0.7 (0.4–1.9)	NA
Rowe et al. (35)	NA	USA	Prospective single-center	Patients with BRPCa previously treated with RP.	31	Median: 63 (45–74)	NA	Median: 0.4 (0.2–28.3)	NA
Mena et al. (36)	NA	USA	Prospective single-center	Patients with BRPCa previously treated with RP (42.2%) or RT (30.0%) or RP+RT (27.8%) without ADT.	90	Median: 66 (50–81)	Gleason ≤6 (14.4%) Gleason 7 (35.6%) Gleason≥8 (50.0%)	Median: 2.5 (0.21–35.5)	Median: 7.0 (0.9–75.2)
Rousseau et al. (37)	NA	Canada	Prospective single-center	Patients with BRPCa previously treated with RP (72.3%) or RT (34.6%) with or without additional ADT.	130	Mean: 69.1 ± 6.5	Gleason ≤6 (13%) Gleason 7 (50%) Gleason≥8 (37%)	Mean: 5.2 ± 6.5	Mean: 12.2 ± 11.8
Wondergem et al. (38)	2016–2018	Netherlands	Retrospective multicenter	Patients with BRPCa previously treated with RP or RT with or without ADT.	248	Median: 71 (67–75)	Gleason ≤6 (13%) Gleason 7 (39%) Gleason≥8 (34%) Unknown (14%)	NA	Median: 6 (3–12)
Dietlein et al. (39)	NA	Germany	Retrospective single-center	Patients with BRPCa previously treated with RP (61%) or RT (39%).	62	Mean: 68	Gleason ≤6 (7%) Gleason 7 (56%) Gleason≥8 (37%)	Mean: 3.2	NA

NA, not available; BRPCa, biochemically recurrent prostate cancer; RP, radical prostatectomy; RT = radiation therapy; ADT, androgen deprivation therapy; PET/CT, positron emission tomography/computed tomography.

TABLE 2 | Technical aspects of the included studies.

References	Radiotracer	Hybrid imaging modality	Fasting before radiotracer injection	Mean/median radiotracer injected activity	Time between radiotracer injection and image acquisition	Image analysis	Other imaging performed for comparison
Markowski et al. (31)	18F-DCFPyL	NA	NA	333 MBq	60 min	Visual	NA
Hong et al. (32)	18F-DCFPyL	PET/CT with low-dose CT	NA	338.8 ± 25.3 (270.1–370) MBq	74.4 ± 10.4 min	Visual	CT, mpMRI, bone scan, ^{18}F-NaF PET/CT, and ^{18}F-fluciclovine PET/CT
Wei et al. (33)	18F-DCFPyL	PET/CT with low-dose CT	NA	Mean: 333 MBq (299.7–366.3) MBq	60 ± 10 min	Visual	CT, mpMRI, and bone scan
Jansen et al. (34)	18F-DCFPyL	PET/CT with low-dose CT	NA	Median: 314.4 MBq (257.7–328.6) MBq	120 ± 21 min	Visual	NA
Rowe et al. (35)	18F-DCFPyL	NA	NA	No more than 333 MBq	60 min	Visual and semiquantitative (SUVmax)	NA
Mena et al. (36)	18F-DCFPyL	PET/CT with low-dose CT	NA	Mean: 299.3 MBq (229.4–325.6) MBq	120 min	Visual and semiquantitative (SUVmax, TV, VOI)	NA
Rousseau et al. (37)	18F-DCFPyL	PET/CT with low-dose CT	Yes (at least 4 h)	369.2 ± 47.2 (237–47 × 4) MBq	120 min	Visual and semiquantitative (SUVmax, SUVpeak, SUL, TLG, SUVratio)	NA
Wondergem et al. (38)	18F-DCFPyL	PET/CT with low-dose CT or contrast-enhanced CT	NA	Median: 311 MBq (284–325) MBq	120 min	Visual	NA
Dietlein et al. (39)	18F-DCFPyL	PET/CT with low-dose CT	Yes (at least 4 h)	269.8 ± 81.8 MBq	120 min	Visual and semiquantitative (SUVmax)	^{68}Ga-PSMA-11 PET/CT

NA, not available; PET/CT, positron emission tomography/computed tomography; mpMRI, multiparametric magnetic resonance imaging; 18F-DCFPyL, 2-(3-{1-carboxy-5-[(6-[18F] fluoro-pyridine-3-carbonyl)-amino]-pentyl}-ureido)-pentanedioic acid; MBq, megabecquerel.

TABLE 3 | Main findings of the included studies about 18F-DCFPyL PET/CT in BRPCa patients.

References	Overall DR on a per patient-based analysis	DR in patients with PSA < 0.5 ng/ml	DR in patients with PSA ≥ 0.5 ng/ml	DR in patients with PSA between 0.5 and 1 ng/ml	DR in patients with PSA between 1 and 2 ng/ml	DR in patients with PSA ≥ 2 ng/ml	Local recurrence	Regional lymph node recurrence	Distant lymph node recurrence	Bone	Organ
Markowski et al. (31)	82/108 (75.9%)	26/46 (56.5%)	56/62 (90.3%)	NA	NA	NA	NA	NA	NA	NA	NA
Hong et al. (32)	61/72 (84.7%)	4/8 (50%)	57/64 (89.0%)	9/13 (69%)	5/5 (100%)	43/46 (93.5%)	22/72 (31%)	34/72 (48%)	20/72 (28%)	33/72 (46%)	11/72 (16%)
Wei et al. (33)	69/79 (87.0%)	NA	NA	NA	NA	NA	54/79 (68%)	21/79 (27%)	14/79 (18%)	NA	NA
Jansen et al. (34)	16/24 (66.7%)	NA	NA	NA	NA	NA	NA	NA	NA	NA	NA
Rowe et al. (35)	21/31 (67.7%)	NA	NA	NA	NA	NA	8/31 (25.8%)	14/31 (45.1%)	2/31 (6.5%)	2/31 (6.5%)	0/31 (0%)
Mena et al. (36)	70/90 (77.8%)	10/21 (47.6%)	60/69 (90%)	5/10 (50%)	8/9 (88.9%)	47/50 (94%)	29/90 (32.2%)	39/90 (43.3%)	17/90 (18.8%)	9/90 (10.0%)	5/90 (5.5%)
Rousseau et al. (37)	110/130 (84.6%)	3/5 (60%)	107/125 (85.6%)	18/23 (78.3%)	18/25 (72%)	71/77 (92.2%)	35/130 (26.9%)	57/130 (43.8%)	32/130 (24.6%)	26/130 (20.0%)	3/130 (2.3%)
Wondergem et al. (38)	214/248 (86.3%)	17/29 (59%)	197/217 (90.8%)	20/29 (69%)	35/41 (85%)	142/149 (95%)	92/248 (37.1%)	136/248 (54%)	49/248 (19.8%)	73/248 (29.4%)	12/248 (4.8%)
Dietlein et al. (39)	46/62 (74.2%)	1/8 (12.5%)	45/54 (83.3%)	NA	NA	NA	NA	NA	NA	NA	NA
Pooled values (95% confidence interval)	80.2% (75.6–84.7%)	47.2% (32.6–61.8%)	88.8% (86.2–91.3%)	70.3% (60.2–80.5%)	82.9% (74.5–91.3%)	94.3% (91.8–96.9%)	36.6% (33.1–40.2%)	45.8% (42.1–49.6%)	19.3% (16.2–22.3%)	20.5% (17.3–23.6%)	4.2% (2.6–6.0%)

NA, not available; DR, detection rate; PSA, prostate-specific antigen; BRPCa, biochemically recurrent prostate cancer; 18F-DCFPyL, 2-(3-{1-carboxy-5-[(6-[18F] fluoro-pyridine-3-carbonyl)-amino]-pentyl}-ureido)-pentanedioic acid; PET/CT, positron emission tomography/computed tomography.

also noticed that the mean/median PSA levels of the included BRPCa patients before 18F-DCFPyL PET/CT scanning could be obviously divided into two groups: high-PSA level group (25, 28, 29) and low-PSA level group (26, 27, 30–33).

The main findings of the included studies about 18F-DCFPyL PET/CT in BRPCa patients are shown in **Table 3**. The pooled DR was 88.8% for PSA ≥ 0.5 ng/ml (95% CI: 86.2–91.3%) and 47.2% for PSA < 0.5 ng/ml (95% CI: 32.6–61.8%). The pooled DRs in local recurrence, regional lymph node recurrence, distant lymph node recurrence, bone, and organ were 36.6% (95% CI: 33.1–40.2%), 45.8% (95% CI: 42.1–49.6%), 19.3% (95% CI: 16.2–22.3%), 20.5% (95% CI: 17.3–23.6%), and 4.2% (95% CI: 2.6–6.0%), respectively.

Quantitative Synthesis

The forest plot of the overall DR of 18F-DCFPyL PET/CT in BRPCa was shown in **Figure 2**. The random effect model demonstrated that the pooled overall DR of 18F-DCFPyL PET/CT in BRPCa was 81% (95% CI: 76.9–85.1%). For I^2 = 53.2%, high heterogeneity was found.

In order to identify the source of high heterogeneity, we performed the subgroup analysis (**Figure 3**) according to the PSA level with a cutoff value of 1 ng/ml before 18F-DCFPyL PET/CT scanning. The results revealed that the pooled overall DR in the low-PSA level group was 73% (95% CI: 67–80%), and the pooled overall DR in the high-PSA level group was 84% (95% CI: 77–85%). For $I^2 = 0$ and 28.9%, no high heterogeneity was found.

Lastly, we performed the analysis of detection rate of 18F-DCFPyL PET/CT in BRPCa stratified by different PSA levels (**Figure 4**). The pooled DR was 47.2% for PSA < 0.5 ng/ml (95% CI: 32.6–61.8%), 70.3% for PSA 0.5–1 ng/ml (95% CI: 60.2–80.5%), 82.9% for PSA 1–2 ng/ml (95% CI: 74.5–91.3%), and 94.3% for PSA >2 ng/ml (95% CI: 91.8–96.9%).

Publication Bias

We quantified publication bias by the Egger method. Publication bias was found in the overall DR of 18F-DCFPyL PET/CT in BRPCa (P = 0.021). The Egger graph was shown in **Supplementary Material 2**.

DISCUSSION

Although several meta-analyses have evaluated the diagnostic performance of PET/CT in BRPCa (40–45), to our knowledge, this is the first systematic review that focuses on the role of 18F-DCFPyL PSMA PET/CT in early detection of recurrent lesions in BRPCa patients. Besides, our data include the most up-to-date studies that have been published over the past year. Crocerossa et al. (42) reported that the overall DR of 68Ga-PSMA PET/CT was 72.4%. Fanti et al. (43) reported that the

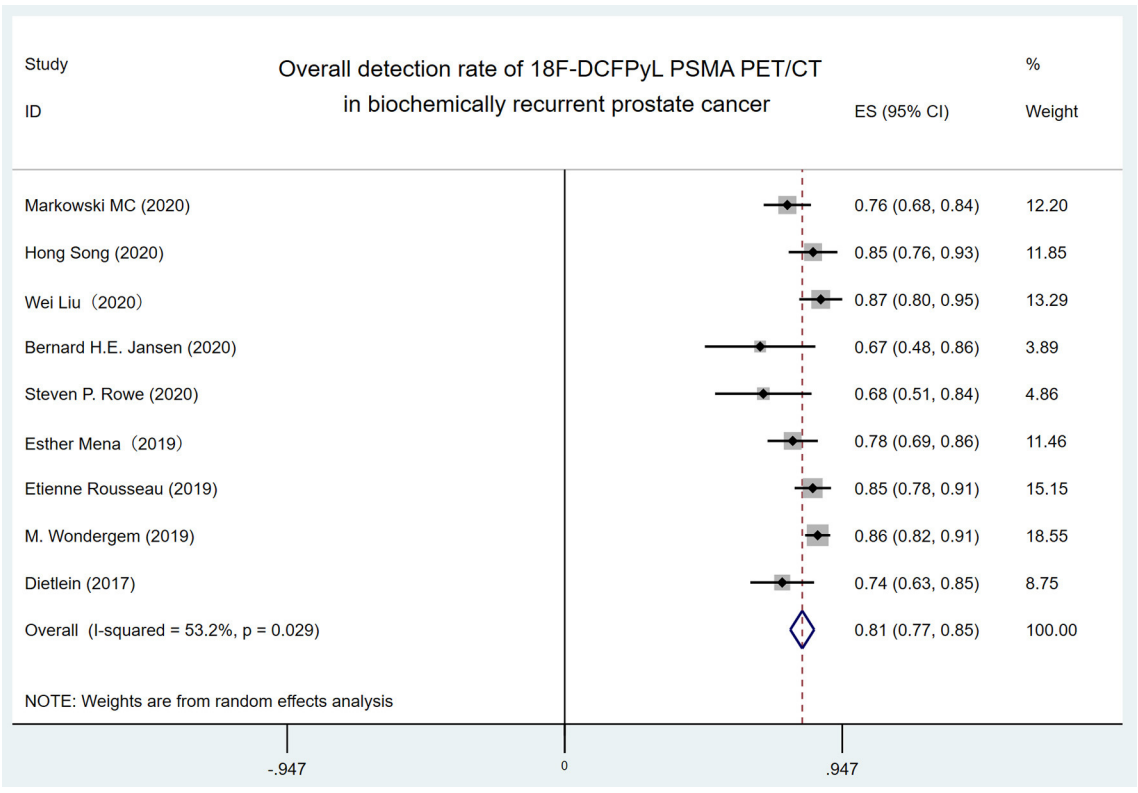

FIGURE 2 | Forest plot for overall detection rate of 18F-DCFPyL PSMA PET/CT in biochemically recurrent prostate cancer. 18F-DCFPyL, 2-(3-{1-carboxy-5-[(6-[18F] fluoro-pyridine-3-carbonyl)-amino]-pentyl}-ureido)-pentanedioic acid; PSMA, prostate-specific membrane antigen; PET/CT, positron emission tomography/computed tomography.

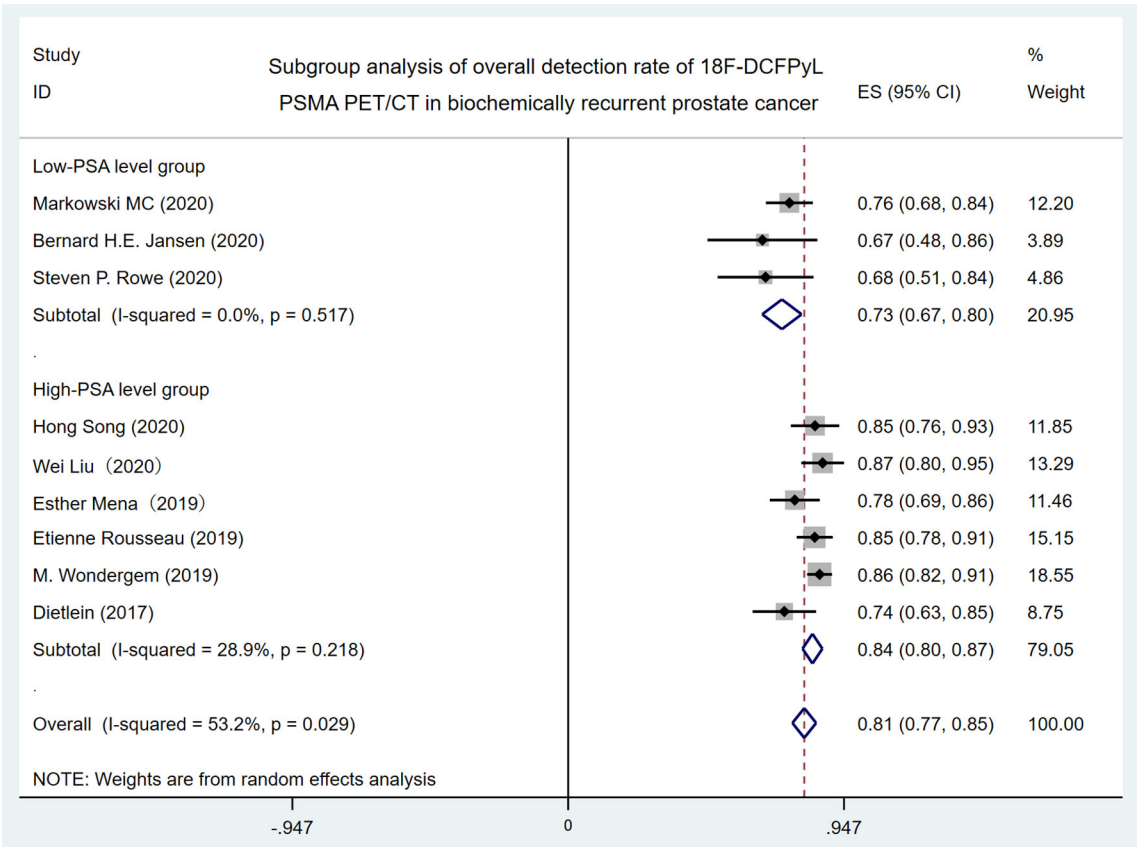

FIGURE 3 | Forest plot for subgroup analysis of overall detection rate of 18F-DCFPyL PSMA PET/CT in biochemically recurrent prostate cancer. 18F-DCFPyL, 2-(3-{1-carboxy-5-[(6-[18F] fluoro-pyridine-3-carbonyl)-amino]-pentyl}-ureido)-pentanedioic acid; PSMA, prostate-specific membrane antigen; PET/CT, positron emission tomography/computed tomography.

overall DR of 11C-choline PET/CT was 62% (95% CI: 53–71%). Von Eyben and Kairemo (44) reported that the overall DR of 18F-fluorocholine PET/CT was 66%, and our result suggests that the overall DR of 18F-DCFPyL PET/CT is 81% (95% CI: 76.9–85.1%). In conclusion, it shows that 18F-DCFPyL PET/CT has a relatively higher overall DR in BRPCa than other techniques mentioned above, which may enable physicians to make earlier clinical decisions for preventing further metastasis. Nevertheless, the results should be prudentially concluded due to the existence of publication bias ($P = 0.021$).

Of all our nine included studies, Jansen et al. (34) and Rowe et al. (35) reported a relatively low overall DR (66.7 and 67.7%, respectively.) in comparison with Song et al. (32), Liu et al. (33), Rousseau et al. (37), and Wondergem et al. (38) (84.7, 87.0, 84.6, and 86.3%, respectively). This is mainly because the participants in the former two studies had lower PSA levels before 18F-DCFPyL PET/CT (0.7 and 0.4 ng/ml, respectively). Another possible reason is that these two studies did not detail the distribution of Gleason scores of their participants. In addition, prior published studies have shown that PSA doubling time was a strong predictor for developing metastatic disease using conventional imaging (46, 47). However, we did not further analyze the association between PSA doubling time and a positive DR, since there were only four of our included studies (33, 36–38) reporting the specific mean/median PSA doubling time before 18F-DCFPyL PET/CT. Lastly, Markowski et al. (31), Jansen et al. (34), and Rowe et al. (35) included patients who were only treated with RP previously. Liu et al. (33) included patients who were only treated with RT previously. Other five studies included patients who were treated with RP or RT previously. Since the definition of BCR after RP is different from that after RT, patients who received different types of therapies could also possibly affect the DR of 18F-DCFPyL PET/CT.

High heterogeneity ($I^2 = 53.2\%$) was found in the overall DR of 18F-DCFPyL PET/CT in BRPCa patients. When the included studies were classified by the mean/median PSA level with 1 ng/ml before 18F-DCFPyL PET/CT scanning in subgroup analysis, the I^2 decreased from 53.2 to 0% and 28.9%, respectively (**Figure 3**). Thus, it shows that the 18F-DCFPyL may exhibit highly consistent sensitivity in BRPCa with higher PSA levels, which is in accordance with our clinical experience.

However, we did not perform a detailed analysis about the DR of 18F-DCFPyL PET/CT in local recurrence, regional lymph node recurrence, distant lymph node recurrence, bone, and

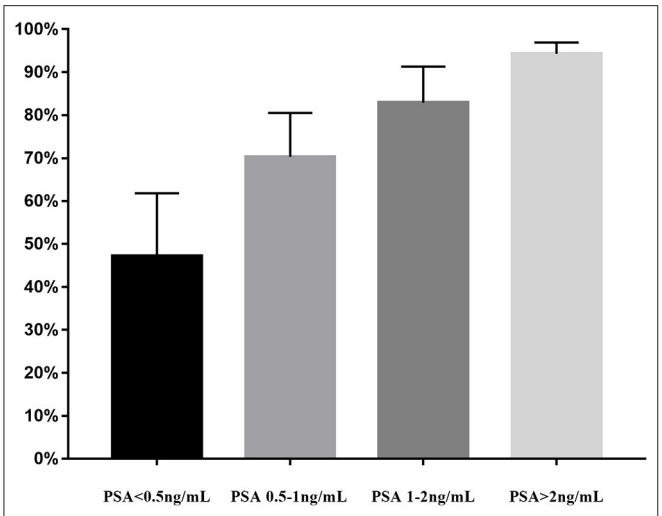

FIGURE 4 | PSA-stratified performance of detection of 18F-DCFPyL PET/CT in biochemically recurrent prostate cancer. PSA, prostate-specific antigen; 18F-DCFPyL, 2-(3-{1-carboxy-5-[(6-[18F] fluoro-pyridine-3-carbonyl)-amino]-pentyl}-ureido)-pentanedioic acid; PSMA, prostate-specific membrane antigen; PET/CT, positron emission tomography/computed tomography.

organ. The reasons are as follows. For one thing, since the place for cancer to metastasize varies between individuals in clinical practice, it is much more reasonable to evaluate DR in recurrent sites on a per-lesion basis. However, all included studies in our meta-analysis only reported DR in recurrent sites on a per-person basis but not on a per-lesion basis. For another, due to the lack of specific corresponding relation between PSA levels and DR in different recurrent sites in our included studies, we could not conduct the analysis of DR in different recurrent sites stratified by different PSA levels.

Treglia et al. (40) previously reported that 18F-labeled PSMA PET/CT had a better DR in BRPCa patients while PSA level was rising. Similarly, our meta-analysis also illustrated a trend that 18F-DCFPyL PSMA PET/CT may exhibit improved sensitivity in BRPCa with increased PSA levels (**Figure 4**). For PSA 1–2 ng/ml and PSA $>$ 2 ng/ml, the overall DR of 18F-DCFPyL PET/CT significantly rose up to 82.9% (95% CI: 74.5–91.3%) and 94.3% (95% CI: 91.8–96.9%), respectively. By contrast, for PSA $<$0.5 ng/ml and 0.5–1 ng/ml, the overall DRs were only 47.2% (95% CI: 32.6–61.8%) and 70.3% (95% CI: 60.2–80.5%), respectively.

Thus, an optimal PSA threshold that would justify 18F-DCFPyL PET/CT imaging is necessary to be established. For 11C-choline PET/CT, Castellucci et al. (48) showed an optimal cutoff point for trigger PSA of 2.43 ng/ml. For 68Ga-PSMA PET/CT, Hope et al. (49) reported an optimal PSA threshold of 1.5 ng/ml. For 18F fluorocholine PET/CT, Gauvin et al. (50) suggested that a trigger PSA of 2.6 ng/ml had a sensitivity of 84% and specificity of 65% for a positive scan. However, the optimal PSA threshold for 18F-DCFPyL PET-CT has not been suggested yet. Our study revealed that the pooled overall DR of 18F-DCFPyL PET/CT was 88.8% for PSA $\geq$ 0.5 ng/ml (95% CI: 86.2–91.3%) and 47.2% for PSA $<$ 0.5 ng/ml (95% CI: 32.6–61.8%). Basing on the above results and considering the high cost of PET/CT scans, we assumed that a PSA threshold of 0.5 ng/ml for 18F-DCFPyL PET/CT might be reasonable and cost-effective. That means 18F-DCFPyL PET/CT could detect recurrent sites in BCR patients at lower PSA levels compared with other targeted radiotracers. Moreover, its higher sensitivity enables urologists to tailor earlier salvage procedures or medical treatment and potentially influence outcome. Nevertheless, our results were based on only nine studies published in recent years. Further large-scale studies are warranted to prove its significant advantages and clinical values.

Over the past decades, a variety of targeted radiotracers including 11C/18F-choline, 18F-fluciclovine, 68Ga-PSMA, and 18F-PSMA have been proposed. In 2012, choline was approved by the U.S. Food and Drug Administration (FDA) as an imaging agent to be used to detect PCa during PET imaging. However, choline is accumulating not only in malignant tissues but also in inflammatory diseases. It means that choline PET/CT imaging may be limited for the differentiation of malignant and benign lesions, which is particularly important in lymph nodes (51). The use of fluciclovine was approved by the U.S. FDA in May of 2016, and its rational biodistribution and slow renal excretion make it suitable for imaging of suspected PCa recurrence following treatment (52). Similarly, a major disadvantage of the 18F-fluciclovine PET tracer is its nonspecific uptake by benign inflammatory prostatic tissue (53). In addition, the review of the data demonstrated lower detection rates of 18F-choline, 18F-fluciclovine for each respective PSA cohort (54). Thus, PCa-specific PET/CT radiotracers such as 68Ga-PSMA and 18F-PSMA seem to show superiority and provide new insight into the early patterns of disease spread. Until now, 68Ga-PSMA is the most commonly used radiotracer in clinical practice (55). It is the first drug for PET imaging of PSMA-positive lesions in men with PCa approved by the U.S. FDA in December of 2020 whether or not the cancer has spread to other parts of the body (56). However, recent years have witnessed the beginning of a shift from 68Ga to 18F-labeled compounds (57). 18F-DCFPyL, the second-generation 18F-labeled PSMA radiotracers, has also received increasing recognition recently since it was proposed (58). Because of the lower positron emission energy of 18F-DCFPyL, the distance to decelerate the positron in human tissue is much shorter in comparison with 68Ga-PSMA, resulting in a higher image resolution. Furthermore, production volume and a longer half-life offer practical advantages over 68Ga-PSMA (10). Given the above diagnostic advantages, the role of 18F-DCFPyL PET/CT may extend beyond BRPCa to the initial staging of high-risk PCa in the future.

The study has several limitations. Firstly, none of the included studies has complete histologic validation. In a lack of histological validation, it cannot be excluded that some lesions detected by 18F-DCFPyL PET/CT may represent false-positive findings. Secondly, we did not further analyze the pooled DR of 18F-DCFPyL PET/CT based on recurrent sites. Thirdly, patients who

receive ADT or not after RP or RT may share different BCR progression, PSA levels, and metastatic sites. All these conditions could possibly affect the DR of 18F-DCFPyL PSMA PET/CT. However, due to the lack of this specific information in our included studies, we could not conduct the subgroup analysis of overall DR divided by patients with or without ADT and it might be a confounder in our study. Lastly, publication bias was observed in our study. Large-scale and well-designed studies are warranted for a valid conclusion.

CONCLUSION

Despite some limitations, our meta-analysis revealed that 18F-DCFPyL PET/CT has a relatively high DR in BRPCa. To prove our results, future large-scale and well-designed studies are needed to provide more powerful evidence.

DATA AVAILABILITY STATEMENT

The original contributions presented in the study are included in the article/**Supplementary Material**, further inquiries can be directed to the corresponding author/s.

AUTHOR CONTRIBUTIONS

JS performed the experiments, analyzed the data, contributed analysis tools, and wrote the paper. YL performed the experiments and prepared figures and/or tables. XW and JO analyzed the data and prepared figures and/or tables. ZL and YH conceived and designed the experiments and reviewed drafts of the paper. All authors contributed to the article and approved the submitted version.

FUNDING

This work was supported by grants from the National Natural Science Foundation of China (No. 82002715), Natural Science Foundation of Jiangsu Province (BK20190170), and science and technology program of Suzhou city (No. SLJ201906).

SUPPLEMENTARY MATERIAL

The Supplementary Material for this article can be found online at: https://www.frontiersin.org/articles/10.3389/fonc.2021.649171/full#supplementary-material

REFERENCES

1. Siegel RL, Miller KD, Jemal A. Cancer statistics, 2020. *CA Cancer J Clin.* (2020) 70:7–30. doi: 10.3322/caac.21590
2. Mottet N, Bellmunt J, Bolla M, Briers E, Cumberbatch MG, De Santis M, et al. EAU-ESTRO-SIOG guidelines on prostate cancer. Part 1: screening, diagnosis, and local treatment with curative intent. *Eur Urol.* (2017) 71:618–29. doi: 10.1016/j.eururo.2016.08.003
3. Cookson MS, Aus G, Burnett AL, Canby-Hagino ED, D'Amico AV, Dmochowski RR, et al. Variation in the definition of biochemical recurrence in patients treated for localized prostate cancer: the American Urological Association Prostate Guidelines for Localized Prostate Cancer Update Panel report and recommendations for a standard in the reporting of surgical outcomes. *J Urol.* (2007) 177:540–5. doi: 10.1016/j.juro.2006.10.097
4. Roach M, 3rd, Hanks G, Thames H, Jr., Schellhammer P, Shipley WU, et al. Defining biochemical failure following radiotherapy with or without hormonal therapy in men with clinically localized prostate cancer: recommendations of the RTOG-ASTRO Phoenix Consensus Conference. *Int J Radiat Oncol Biol Phys.* (2006) 65:965–74. doi: 10.1016/j.ijrobp.2006.04.029
5. Han M, Partin AW, Zahurak M, Piantadosi S, Epstein JI, Walsh PC. Biochemical (prostate specific antigen) recurrence probability following radical prostatectomy for clinically localized prostate cancer. *J Urol.* (2003) 169:517–23. doi: 10.1016/S0022-5347(05)63946-8
6. Freedland SJ, Humphreys EB, Mangold LA, Eisenberger M, Dorey FJ, Walsh PC, et al. Risk of prostate cancer-specific mortality following biochemical recurrence after radical prostatectomy. *JAMA.* (2005) 294:433–9. doi: 10.1001/jama.294.4.433
7. Roehl KA, Han M, Ramos CG, Antenor JA, Catalona WJ. Cancer progression and survival rates following anatomical radical retropubic prostatectomy in 3,478 consecutive patients: long-term results. *J Urol.* (2004) 172:910–4. doi: 10.1097/01.ju.0000134888.22332.bb
8. Kupelian PA, Mahadevan A, Reddy CA, Reuther AM, Klein EA. Use of different definitions of biochemical failure after external beam radiotherapy changes conclusions about relative treatment efficacy for localized prostate cancer. *Urology.* (2006) 68:593–8. doi: 10.1016/j.urology.2006.03.075
9. Lazarev S, Thompson MR, Stone NN, Stock RG. Low-dose-rate brachytherapy for prostate cancer: outcomes at >10 years of follow-up. *BJU Int.* (2018) 121:781–90. doi: 10.1111/bju.14122
10. Spratt DE, McHugh DJ, Morris MJ, Morgans AK. Management of biochemically recurrent prostate cancer: ensuring the right treatment of the right patient at the right time. *Am Soc Clin Oncol Educ Book.* (2018) 38:355–62. doi: 10.1200/EDBK_200319
11. Rowe SP, Mana-Ay M, Javadi MS, Szabo Z, Leal JP, Pomper MG, et al. PSMA-based detection of prostate cancer bone lesions with (1)(8)F-DCFPyL PET/CT: a sensitive alternative to ((9)(9)m)Tc-MDP Bone Scan and Na(1)(8)F PET/CT? *Clin Genitourinary Cancer.* (2016) 14:e115–8. doi: 10.1016/j.clgc.2015.09.011
12. Rajasekaran AK, Anilkumar G, Christiansen JJ. Is prostate-specific membrane antigen a multifunctional protein? *Am J Physiol Cell Physiol.* (2005) 288:C975–81. doi: 10.1152/ajpcell.00506.2004
13. Maurer T, Eiber M, Schwaiger M, Gschwend JE. Current use of PSMA-PET in prostate cancer management. *Nat Rev Urol.* (2016) 13:226–35. doi: 10.1038/nrurol.2016.26
14. Eapen RS, Nzenza TC, Murphy DG, Hofman MS, Cooperberg M, Lawrentschuk N. PSMA PET applications in the prostate cancer journey: from diagnosis to theranostics. *World J Urol.* (2019) 37:1255–61. doi: 10.1007/s00345-018-2524-z
15. Thoma C. PSMA PET-CT outperforms conventional imaging in high-risk prostate cancer. *Nat Rev Urol.* (2020) 17:319. doi: 10.1038/s41585-020-0330-z
16. Diao W, Cao Y, Su D, Jia Z. Impact of (68) Gallium prostate-specific membrane antigen tracers on the management of patients with prostate cancer who experience biochemical recurrence. *BJU Int.* (2021) 127:153–63. doi: 10.1111/bju.15257
17. Ghodsirad MA, Pirayesh E, Akbarian R, Javanmard B, Kaghazchi F, Tavakoli M, et al. Diagnostic utility of lutetium-177 (Lu 177) prostate-specific membrane antigen (PSMA) scintigraphy in prostate cancer patients with PSA rise and negative conventional imaging. *Urol J.* (2020) 17:374–8. doi: 10.22037/uj.v0i0.5451
18. Mirzaei S, Mohammed F, Zandieh S. Theranostics of metastatic prostate cancer applying 64Cu/18F/68Ga PSMA PET-CT and 177Lu radiopharmaceuticals. *Curr Radiopharm.* (2020). doi: 10.2174/1874471013666200908122845. [Epub ahead of print].
19. Paymani Z, Rohringer T, Vali R, Loidl W, Alemohammad N, Geinitz H, et al. Diagnostic performance of [(18)F]Fluorocholine and [(68)Ga]Ga-PSMA PET/CT in prostate cancer: a comparative study. *J Clin Med.* (2020) 9:2308. doi: 10.3390/jcm9072308

20. Kelly JM, Ponnala S, Amor-Coarasa A, Zia NA, Nikolopoulou A, Williams C, et al. Preclinical evaluation of a high-affinity sarcophagine-containing PSMA ligand for (64)Cu/(67)Cu-based theranostics in prostate cancer. *Mol Pharm.* (2020) 17:1954–62. doi: 10.1021/acs.molpharmaceut.0c00060
21. Eiber M, Maurer T, Souvatzoglou M, Beer AJ, Ruffani A, Haller B, et al. Evaluation of hybrid (6)(8)Ga-PSMA ligand PET/CT in 248 patients with biochemical recurrence after radical prostatectomy. *J Nucl Med.* (2015) 56:668–74. doi: 10.2967/jnumed.115.154153
22. Bluemel C, Krebs M, Polat B, Linke F, Eiber M, Samnick S, et al. 68Ga-PSMA-PET/CT in patients with biochemical prostate cancer recurrence negative 18F-choline-PET/CT. *Clin Nucl Med.* (2016) 41:515–21. doi: 10.1097/RLU.0000000000001197
23. Afshar-Oromieh A, Malcher A, Eder M, Eisenhut M, Linhart HG, Hadaschik BA, et al. PET imaging with a [68Ga]gallium-labelled PSMA ligand for the diagnosis of prostate cancer: biodistribution in humans and first evaluation of tumour lesions. *Eur J Nucl Med Mol Imaging.* (2013) 40:486–95. doi: 10.1007/s00259-012-2298-2
24. Ferreira G, Iravani A, Hofman MS, Hicks RJ. Intra-individual comparison of (68)Ga-PSMA-11 and (18)F-DCFPyL normal-organ biodistribution. *Cancer Imaging.* (2019) 19:23. doi: 10.1186/s40644-019-0211-y
25. Kelly J, Amor-Coarasa A, Nikolopoulou A, Kim D, Williams C, Jr., et al. Synthesis and pre-clinical evaluation of a new class of high-affinity (18)F-labeled PSMA ligands for detection of prostate cancer by PET imaging. *Eur J Nucl Med Mol Imaging.* (2017) 44:647–61. doi: 10.1007/s00259-016-3556-5
26. Alexander Drzezga CK, Matthias Schmidt, Georg Kuhnert, Boris Zlatopolskiy, Bernd Neumaier and Markus Dietlein. Application of 18F-labeled PSMA-imaging using [18F]DCFPyL at very low PSA-values may allow curative treatment in recurrent prostate cancer. *J Nucl Med*. (2016) 57(Suppl. 2). Available online at: https://jnm.snmjournals.org/content/57/supplement_2/561
27. Morris MJ, Pouliot F, Saperstein L, Rowe SP, Gorin MA, Josephson DY, et al. A phase III, multicenter study to assess the diagnostic performance and clinical impact of 18F-DCFPyL PET/CT in men with suspected recurrence of prostate cancer (CONDOR). *J Clin Oncol*. (2019) 37(15_Suppl.):TPS5093-TPS. doi: 10.1200/JCO.2019.37.15_suppl.TPS5093
28. Moher D, Liberati A, Tetzlaff J, Altman DG, Group P. Preferred reporting items for systematic reviews and meta-analyses: the PRISMA statement. *PLoS Med.* (2009) 6:e1000097. doi: 10.1371/journal.pmed.1000097
29. Whiting PF, Rutjes AW, Westwood ME, Mallett S, Deeks JJ, Reitsma JB, et al. QUADAS-2: a revised tool for the quality assessment of diagnostic accuracy studies. *Ann Intern Med.* (2011) 155:529–36. doi: 10.7326/0003-4819-155-8-201110180-00009
30. Higgins JP, Thompson SG, Deeks JJ, Altman DG. Measuring inconsistency in meta-analyses. *BMJ.* (2003) 327:557–60. doi: 10.1136/bmj.327.7414.557
31. Markowski MC, Sedhom R, Fu W, Gray JCR, Eisenberger MA, Pomper MG, et al. Prostate specific antigen and prostate specific antigen doubling time predict findings on (18)F-DCFPyL positron emission tomography/computerized tomography in patients with biochemically recurrent prostate cancer. *J Urol.* (2020) 204:496–502. doi: 10.1097/JU.0000000000001064
32. Song H, Harrison C, Duan H, Guja K, Hatami N, Franc BL, et al. Prospective evaluation of (18)F-DCFPyL PET/CT in biochemically recurrent prostate cancer in an academic center: a focus on disease localization and changes in management. *J Nucl Med.* (2020) 61:546–51. doi: 10.2967/jnumed.119.231654
33. Liu W, Zukotynski K, Emmett L, Chung HT, Chung P, Wolfson R, et al. A prospective study of 18F-DCFPyL PSMA PET/CT restaging in recurrent prostate cancer following primary external beam radiotherapy or brachytherapy. *Int J Radiat Oncol Biol Phys.* (2020) 106:546–55. doi: 10.1016/j.ijrobp.2019.11.001
34. Jansen BHE, Jansen RW, Wondergem M, Srbljin S, de Klerk JMH, Lissenberg-Witte BI, et al. Lesion detection and interobserver agreement with advanced image reconstruction for (18)F-DCFPyL PET/CT in patients with biochemically recurrent prostate cancer. *J Nucl Med.* (2020) 61:210–6. doi: 10.2967/jnumed.118.222513
35. Rowe SP, Campbell SP, Mana-Ay M, Szabo Z, Allaf ME, Pienta KJ, et al. Prospective evaluation of PSMA-targeted (18)F-DCFPyL PET/CT in men with biochemical failure after radical prostatectomy for prostate cancer. *J Nucl Med*. (2020) 61:58–61. doi: 10.2967/jnumed.119.226514
36. Mena E, Lindenberg ML, Turkbey IB, Shih JH, Harmon SA, Lim I, et al. (18)F-DCFPyL PET/CT imaging in patients with biochemically recurrent prostate cancer after primary local therapy. *J Nucl Med.* (2020) 61:881–9. doi: 10.2967/jnumed.119.234799
37. Rousseau E, Wilson D, Lacroix-Poisson F, Krauze A, Chi K, Gleave M, et al. A prospective study on (18)F-DCFPyL PSMA PET/CT imaging in biochemical recurrence of prostate cancer. *J Nucl Med*. (2019) 60:1587–93. doi: 10.2967/jnumed.119.226381
38. Wondergem M, Jansen BHE, van der Zant FM, van der Sluis TM, Knol RJJ, van Kalmthout LWM, et al. Early lesion detection with (18)F-DCFPyL PET/CT in 248 patients with biochemically recurrent prostate cancer. *Eur J Nucl Med Mol Imaging.* (2019) 46:1911–8. doi: 10.1007/s00259-019-04385-6
39. Dietlein F, Kobe C, Neubauer S, Schmidt M, Stockter S, Fischer T, et al. PSA-stratified performance of (18)F- and (68)Ga-PSMA PET in patients with biochemical recurrence of prostate cancer. *J Nucl Med*. (2017) 58:947–52. doi: 10.2967/jnumed.116.185538
40. Treglia G, Annunziata S, Pizzuto DA, Giovanella L, Prior JO, Ceriani L. Detection rate of (18)F-labeled PSMA PET/CT in biochemical recurrent prostate cancer: a systematic review and a meta-analysis. *Cancers.* (2019) 11:710. doi: 10.3390/cancers11050710
41. Hope TA, Goodman JZ, Allen IE, Calais J, Fendler WP, Carroll PR. Metaanalysis of (68)Ga-PSMA-11 PET accuracy for the detection of prostate cancer validated by histopathology. *J Nucl Med*. (2019) 60:786–93. doi: 10.2967/jnumed.118.219501
42. Crocerossa F, Marchioni M, Novara G, Carbonara U, Ferro M, Russo GI, et al. Detection rate of prostate specific membrane antigen tracers for positron emission tomography/computerized tomography in prostate cancer biochemical recurrence: a systematic review and network meta-analysis. *J Urol.* (2021) 205:356–69. doi: 10.1097/JU.0000000000001369
43. Fanti S, Minozzi S, Castellucci P, Balduzzi S, Herrmann K, Krause BJ, et al. PET/CT with (11)C-choline for evaluation of prostate cancer patients with biochemical recurrence: meta-analysis and critical review of available data. *Eur J Nucl Med Mol Imaging.* (2016) 43:55–69. doi: 10.1007/s00259-015-3202-7
44. von Eyben FE, Kairemo K. Acquisition with (11)C-choline and (18)F-fluorocholine PET/CT for patients with biochemical recurrence of prostate cancer: a systematic review and meta-analysis. *Ann Nucl Med.* (2016) 30:385–92. doi: 10.1007/s12149-016-1078-7
45. Sathianathen NJ, Butaney M, Konety BR. The utility of PET-based imaging for prostate cancer biochemical recurrence: a systematic review and meta-analysis. *World J Urol.* (2019) 37:1239–49. doi: 10.1007/s00345-018-2403-7
46. Markowski MC, Chen Y, Feng Z, Cullen J, Trock BJ, Suzman D, et al. PSA doubling time and absolute PSA predict metastasis-free survival in men with biochemically recurrent prostate cancer after radical prostatectomy. *Clin Genitourinary Cancer.* (2019) 17:470–5 e1. doi: 10.1016/j.clgc.2019.08.002
47. Pound CR, Partin AW, Eisenberger MA, Chan DW, Pearson JD, Walsh PC. Natural history of progression after PSA elevation following radical prostatectomy. *JAMA.* (1999) 281:1591–7. doi: 10.1001/jama.281.17.1591
48. Castellucci P, Fuccio C, Nanni C, Santi I, Rizzello A, Lodi F, et al. Influence of trigger PSA and PSA kinetics on 11C-Choline PET/CT detection rate in patients with biochemical relapse after radical prostatectomy. *J Nucl Med.* (2009) 50:1394–400. doi: 10.2967/jnumed.108.061507
49. Hope TA, Aggarwal R, Chee B, Tao D, Greene KL, Cooperberg MR, et al. Impact of (68)Ga-PSMA-11 PET on management in patients with biochemically recurrent prostate cancer. *J Nucl Med*. (2017) 58:1956–61. doi: 10.2967/jnumed.117.192476
50. Gauvin S, Cerantola Y, Haberer E, Pelsser V, Probst S, Bladou F, et al. Initial single-centre Canadian experience with 18F-fluoromethylcholine positron emission tomography-computed tomography (18F-FCH PET/CT) for biochemical recurrence in prostate cancer patients initially treated with curative intent. *Can Urol Assoc J.* (2017) 11:47–52. doi: 10.5489/cuaj.4068
51. Huang SM, Yin L, Yue JL, Li YF, Yang Y, Lin ZC. Direct comparison of choline PET/CT and MRI in the diagnosis of lymph node metastases in patients with prostate cancer. *Medicine.* (2018) 97:e13344. doi: 10.1097/MD.0000000000013344
52. Nanni C, Schiavina R, Rubello D, Ambrosini V, Brunocilla E, Martorana G, et al. The detection of disease relapse after radical treatment for

prostate cancer: is anti-3-18F-FACBC PET/CT a promising option? *Nucl Med Commun*. (2013) 34:831–3. doi: 10.1097/MNM.0b013e3283636eaf
53. Schuster DM, Nanni C, Fanti S, Oka S, Okudaira H, Inoue Y, et al. Anti-1-amino-3-18F-fluorocyclobutane-1-carboxylic acid: physiologic uptake patterns, incidental findings, and variants that may simulate disease. *J Nucl Med*. (2014) 55:1986–92. doi: 10.2967/jnumed.114.143628
54. Evans JD, Jethwa KR, Ost P, Williams S, Kwon ED, Lowe VJ, et al. Prostate cancer-specific PET radiotracers: a review on the clinical utility in recurrent disease. *Pract Radiat Oncol*. (2018) 8:28–39. doi: 10.1016/j.prro.2017.07.011
55. Lutje S, Heskamp S, Cornelissen AS, Poeppel TD, van den Broek SA, Rosenbaum-Krumme S, et al. PSMA ligands for radionuclide imaging and therapy of prostate cancer: clinical status. *Theranostics*. (2015) 5:1388–401. doi: 10.7150/thno.13348
56. *FDA Approves First PSMA-Targeted PET Imaging Drug for Men With Prostate Cancer*. (2020). Available online at: https://www.fda.gov/news-events/press-announcements/fda-approves-first-psma-targeted-pet-imaging-drug-men-prostate-cancer
57. Werner RA, Derlin T, Lapa C, Sheikbahaei S, Higuchi T, Giesel FL, et al. (18)F-labeled, PSMA-targeted radiotracers: leveraging the advantages of radiofluorination for prostate cancer molecular imaging. *Theranostics*. (2020) 10:1–16. doi: 10.7150/thno.37894
58. Chen Y, Pullambhatla M, Foss CA, Byun Y, Nimmagadda S, Senthamizhchelvan S, et al. 2-(3-{1-Carboxy-5-[(6-[18F]fluoro-pyridine-3-carbonyl)-amino]-pentyl}-ureido)-pen tanedioic acid, [18F]DCFPyL, a PSMA-based PET imaging agent for prostate cancer. *Clin Cancer Res*. (2011) 17:7645–53. doi: 10.1158/1078-0432.CCR-11-1357

Conflict of Interest: The authors declare that the research was conducted in the absence of any commercial or financial relationships that could be construed as a potential conflict of interest.

frontiers in Oncology

ORIGINAL RESEARCH
published: 10 May 2021
doi: 10.3389/fonc.2021.640467

Combining ^{68}Ga-PSMA-PET/CT-Directed and Elective Radiation Therapy Improves Outcome in Oligorecurrent Prostate Cancer: A Retrospective Multicenter Study

Simon Kirste[1,2], Stephanie G. C. Kroeze[3], Christoph Henkenberens[4], Nina-Sophie Schmidt-Hegemann[5,6], Marco M. E. Vogel[7,8], Jessica Becker[9], Constantinos Zamboglou[1,2], Irene Burger[10], Thorsten Derlin[11], Peter Bartenstein[12], Juri Ruf[13], Christian la Fougère[14,15], Matthias Eiber[16], Hans Christiansen[4], Stephanie E. Combs[7,8], Arndt-Christian Müller[9,15], Claus Belka[5,6], Matthias Guckenberger[3] and Anca-Ligia Grosu[1,2]*

[1] Department of Radiation Oncology, Medical Center—University of Freiburg, Faculty of Medicine, University of Freiburg, Freiburg, Germany, [2] German Cancer Consortium (DKTK), Partner Site Freiburg, Freiburg, Germany, [3] Department of Radiation Oncology, University Hospital Zürich, University of Zurich, Zurich, Switzerland, [4] Department of Radiotherapy and Special Oncology, Medical School Hannover, Hannover, Germany, [5] Department of Radiation Oncology, University Hospital LMU Munich, Munich, Germany, [6] German Cancer Consortium (DKTK), Partner Site Munich, Munich, Germany, [7] Department of Radiation Oncology, Technical University Munich, Munich, Germany, [8] Institute of Radiation Medicine (IRM), Helmholtz Zentrum Munich, Oberschleissheim, Germany, [9] Department of Radiation Oncology, University Hospital Tübingen, Tübingen, Germany, [10] Department of Nuclear Medicine, University Hospital Zürich, University of Zurich, Zurich, Switzerland, [11] Department of Nuclear Medicine, Hannover Medical School, Hannover, Germany, [12] Department of Nuclear Medicine, University Hospital LMU Munich, Munich, Germany, [13] Department of Nuclear Medicine, Medical Center—University of Freiburg, University of Freiburg, Freiburg, Germany, [14] Department of Nuclear Medicine and Clinical Molecular Imaging, University Hospital Tübingen, Tübingen, Germany, [15] German Cancer Consortium (DKTK), Partner Site Tübingen, Tübingen, Germany, [16] Department of Nuclear Medicine, Technical University Munich, Munich, Germany*

Background: In case of oligo-recurrent prostate cancer (PC) following prostatectomy, ^{68}Ga-PSMA-PET/CT can be used to detect a specific site of recurrence and to initiate metastasis-directed radiation therapy (MDT). However, large heterogeneities exist concerning doses, treatment fields and radiation techniques, with some studies reporting focal radiotherapy (RT) to PSMA-PET/CT positive lesions only and other studies using elective RT strategies. We aimed to compare oncological outcomes and toxicity between PET/CT-directed RT (PDRT) and PDRT plus elective RT (eRT; i.e. prostate bed, pelvic or paraaortal nodes) in a large retrospective multicenter study.

Methods: Data of 394 patients with oligo-recurrent ^{68}Ga-PSMA-PET/CT-positive PC treated between 04/2013 and 01/2018 in six different academic institutions were evaluated. Primary endpoint was biochemical-recurrence-free survival (bRFS). bRFS was analyzed using Kaplan–Meier survival curves and log rank testing. Uni- and multivariate analyses were performed to determine influence of treatment parameters.

Results: In 204 patients (51.8%) RT was directed only to lesions seen on ^{68}Ga-PSMA-PET/CT (PDRT), 190 patients (48.2%) received PDRT plus eRT. PDRT plus eRT was associated with a significantly improved 3-year bRFS compared to PDRT alone (53 vs.

OPEN ACCESS

Edited by:
Georgios S. Limouris, National and Kapodistrian University of Athens, Greece

Reviewed by:
Orazio Schillaci, University of Rome Tor Vergata, Italy
Gianluca Ingrosso, University of Perugia, Italy
Barbara Alicja Jereczek-Fossa, University of Milan, Italy
Maarten Donswijk, Antoni van Leeuwenhoek Hospital, Netherlands

***Correspondence:**
Simon Kirste
simon.kirste@uniklinik-freiburg.de

Specialty section:
This article was submitted to Cancer Imaging and Image-directed Interventions, a section of the journal Frontiers in Oncology

Received: *11 December 2020*
Accepted: *09 March 2021*
Published: *10 May 2021*

Citation:
Kirste S, Kroeze SGC, Henkenberens C, Schmidt-Hegemann N-S, Vogel MME, Becker J, Zamboglou C, Burger I, Derlin T, Bartenstein P, Ruf J, la Fougère C, Eiber M, Christiansen H, Combs SE, Müller A-C, Belka C, Guckenberger M and Grosu A-L (2021) Combining ^{68}Ga-PSMA-PET/CT-Directed and Elective Radiation Therapy Improves Outcome in Oligorecurrent Prostate Cancer: A Retrospective Multicenter Study. Front. Oncol. 11:640467. doi: 10.3389/fonc.2021.640467

37%; p = 0.001) and remained an independent factor in multivariate analysis (p = 0.006, HR 0.29, 95% CI 0.12–0.68). This effect was more pronounced in the subgroup of patients who were treated with PDRT and elective prostate bed radiotherapy (ePBRT) with a 3-year bRFS of 61% versus 22% (p <0.001). Acute and late toxicity grade ≥3 was 0.8% and 3% after PDRT plus eRT versus no toxicity grade ≥3 after PDRT alone.

Conclusions: In this large cohort of patients with oligo-recurrent prostate cancer, elective irradiation of the pelvic lymphatics and the prostatic bed significantly improved bRFS when added to ^{68}Ga-PSMA-PET/CT-guided focal radiotherapy. These findings need to be evaluated in a randomized controlled trial.

Keywords: metastasis-directed radiotherapy, oligorecurrent, prostate cancer, elective prostate bed radiotherapy, radiotherapy, elective nodal radiotherapy

INTRODUCTION

Primary, curative treatment of localized prostate cancer (PC) can be performed with either radical prostatectomy (RP) or radiation therapy (RT). In the case of a biochemical relapse after RP, which occurs in up to 50% depending on stage and adverse factors (1, 2), salvage RT of the prostatic bed is performed to achieve long-term disease control in terms of biochemical relapse-free survival (bRFS) as well as cancer specific survival (3).

With the development of improved imaging techniques such as positron emission tomography/computed tomography (PET/CT) it is possible to perform molecular staging before salvage RT and to tailor the radiation volume to the recurrence detected by PET/CT without irradiating elective areas. Furthermore, the implementation of new tracers, such as prostate-specific membrane antigen (PSMA) has significantly improved detection rates for recurrences even at low prostate-specific antigen (PSA) values enabling new treatment concepts (4). The rationale for metastases-directed therapy (MDT) is to eradicate all visible disease locations with high doses to delay the use of androgen-deprivation-therapy (ADT) or even prolong progression-free survival while limiting side effects that could potentially occur by the use of larger radiation treatment fields (5).

Two randomized phase II trials evaluated the role of MDT versus observation in patients with oligo-recurrent PC (6, 7). In the STOMP trial the primary endpoint, median ADT-free survival, was improved from 13 to 21 months with MDT and in the ORIOLE trial MDT was associated with an improved progression-free survival (HR 0.3, 95% CI 0.11–0.81).

In spite of the growing interest in treating oligo-recurrent patients with MDT there is no consensus on the optimal target volumes, doses and techniques for RT in this setting (8). So far, guidelines from different collaborative groups on postoperative RT recommend RT of the prostate bed in case of a biochemical recurrence (9–11). Nevertheless, it remains unclear if the prostate bed or other elective areas should be irradiated in the oligo-metastatic setting.

The aim of this study was to analyze the outcome and toxicity of PET/CT-directed RT (PDRT) versus PDRT plus elective RT (eRT) in oligo-metastatic PC. Specifically, in patients without macroscopically local recurrence after RP, we evaluated the impact of PDRT alone versus elective prostate bed RT (ePBRT) plus PDRT.

METHODS

Patient Population

Data of 394 patients from six different academic centers that were treated with curatively intended salvage RT for oligo-recurrent prostate cancer with PSMA-ligand positive lesions on ^{68}Ga-PSMA-PET/CT were evaluated between April 2013 and January 2018. All patients had prior RP with no evidence of distant metastases at initial diagnosis. According to clinical practice in each institution patients were discussed in a multidisciplinary tumor board before the initiation of oligometastatic treatment. Main inclusion criteria were: biochemical recurrence with either local manifestations (prostate bed), nodal or extra nodal metastases on ^{68}Ga-PSMA-PET/CT; irradiation to all PSMA-ligand positive lesions with curative intent. Any serum prostate specific antigen (PSA) level at the time of ^{68}Ga-PSMA-PET/CT was accepted. In line with the concept of oligo-metastatic disease patients with a maximum of five visceral and/or bone metastases were included. Exclusion criteria were: Recurrences under active ADT, previous chemotherapy for PC or history of previous RT of the prostate bed and/or pelvic lymph nodes after an earlier biochemical recurrence following RP. This retrospective multicenter study was approved by the institutional review board of the principal investigator´s institution and by the respective review boards of collaborating institutions.

^{68}Ga-PSMA-PET/CT and Radiation Therapy (RT)

Pre-RT staging was performed by PET imaging with ^{68}Ga labeled PSMA-11 ligands in conjunction with either contrast-enhanced or low-dose computed tomography with imaging approximately 1 h after intravenous radiotracer administration according to local clinical practice and in accordance with the joint EANM and SNMMI guidelines (12). To reduce activity in the urinary system, furosemide was injected intravenously 30 min prior to

the tracer injection and patients were asked to void prior to the scan. The co-registered PET and CT datasets were analysed using predefined PET window settings (e.g. inverted gray scale, SUV range: 0 to 10). A PSMA-positive lesion was visually defined as focal tracer accumulation greater than normal or physiological local background activity. All lesions were irradiated using conventionally fractionated RT or stereotactic body radiotherapy (SBRT). Dose escalation was performed by a sequential or simultaneous integrated boost technique (SIB).

Treatment technique, target volume concept, dose per fraction, total dose, image guidance and type and length of concomitant ADT treatment were at the discretion of each institution. The prescribed RT dose was converted to EQD2 in Gy using an α/β ratio of 1.5 Gy for prostate cancer. For the purpose of this study two basic target volume concepts were defined: One group that received RT directed to PSMA-expressing lesions only (PDRT) and one group that received PDRT plus RT of elective areas (eRT). Elective areas included the prostate bed, pelvic or paraaortal lymphatics. The respective treatment fields are illustrated in **Figure 1**.

Patients without PET positive local recurrence in the prostate bed were evaluated separately: the group receiving elective prostate bed RT (ePBRT) was compared with patients not receiving ePBRT.

Study End Points and Statistical Analysis

Biochemical recurrence-free survival (bRFS) was the primary endpoint. In accordance with the EAU and ASTRO/AUA guidelines an increase of serum PSA value of ≥0.2 ng/ml above the nadir following definitive treatment of ^{68}Ga-PSMA-PET/CT recurrences was considered an event (9, 13). In case serum PSA-levels did not respond to RT, pre-RT levels with a rise of ≥0.2 ng/ml were used. Time to event was calculated from the last day of RT. BRFS was analyzed using Kaplan–Meier survival curves and log rank testing to compare differences between survival curves. Uni- and backward multivariate analyses were performed to determine influence of treatment parameters on bRFS. A p value of <0.05 was considered statistically significant. Variables included were initial T-, and N-stage, initial risk score, initial resection margins, initial PSA, initial Gleason score, PSA before start of salvage RT, PSA response, local recurrence of the prostate

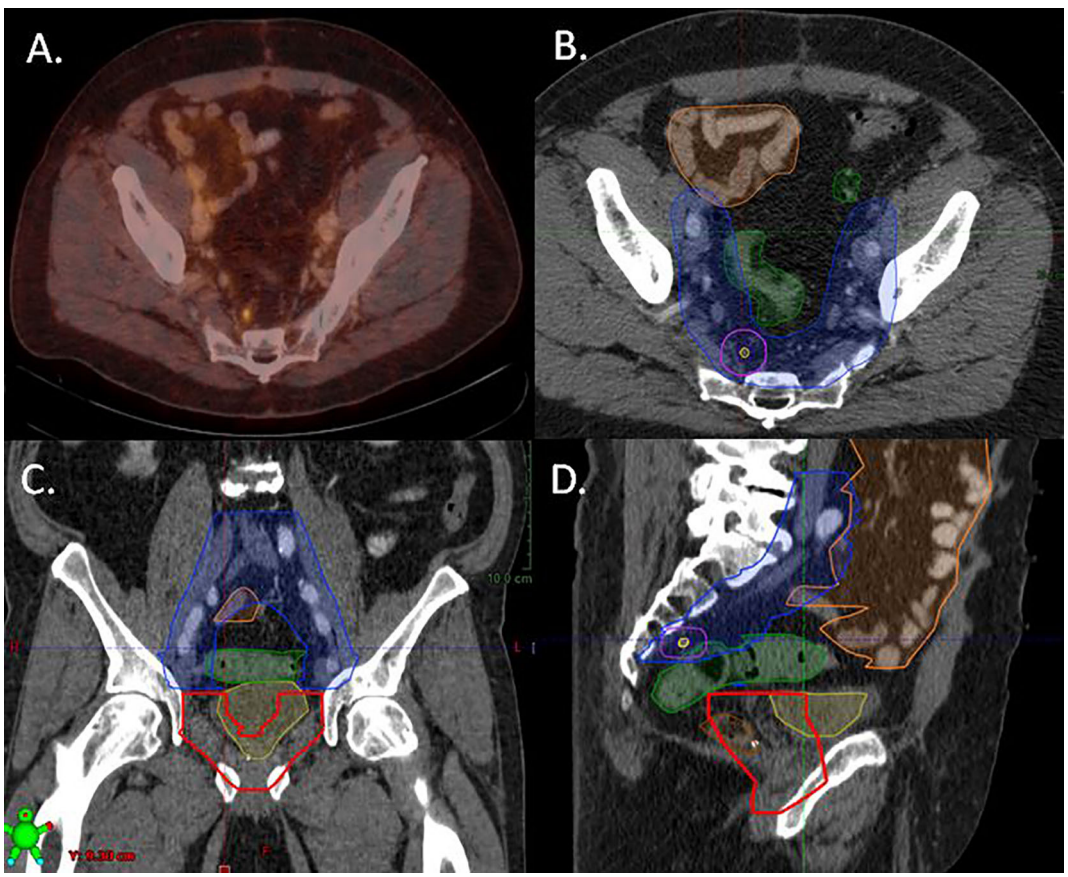

FIGURE 1 | Treatment plan of a patient with a presacral lymph node recurrence on PSMA-PET/CT illustrating the different target volume concepts. The patient was treated with elective prostate bed RT (ePBRT) and elective bilateral lymphatic RT with dose escalation to the PET/CT positive lymph node (PDRT). **(A)** Fused PET/CT image, **(B)** axial plain, **(C)** coronar plain, **(D)** sagittal plain. Yellow line: PSMA-PET/CT positive lymph node; lila line: planning target volume for PSMA-PET/CT positive lymph node; Blue line: elective lymph node RT volume including presacral and bilateral internal iliac nodes; red line: elective prostate bed RT; Green line: organ at risk (sigma); Orange line: organ at risk (small bowel).

bed, N-, and M-stage at time of recurrence, RT of elective areas and additive ADT. Acute and late gastro-intestinal and genito-urinary toxicities were analyzed using the National Cancer Institute Common Terminology Criteria for Adverse Events (CTCAE) v4.03. Survival curves were generated by the Kaplan–Meier method using SPSS v27.0 statistic software package (IBM, USA). Follow-up after RT was done according to the institutions guidelines including regular PSA measurements.

RESULTS

Patient Characteristics

The median age for the whole population at the time of 68Ga-PSMA-PET was 69 years (range, 46–95). The majority of patients (96.1%) had high risk or very high risk features according to D'Amico classification, 162 (41.1%) patients had a Gleason Score of ≥8 and 120 (30.5%) patients presented with lymph node positive disease. Median time to biochemical recurrence after RP was 15 months (range, 0–196). The median PSA value at the time of RT was 1.2 ng/ml (0.04–47.5). Additive ADT was given in 130 patients. Detailed patient characteristics can be found in **Table 1**.

^{68}Ga-PSMA-PET/CT Before Radiation Therapy (RT)

Figure 2 depicts the pre-RT ^{68}Ga-PSMA-PET/CT findings. One hundred and sixteen of 394 patients (29.4%) had a recurrence in the prostate bed, 211 of 394 (53.6%) had a recurrence in lymph nodes and 136 of 394 patients (34.5%) had distant metastases (**Figure 2**). According to ^{68}Ga-PSMA-PET/CT, recurrence was localized in 73 patients in the prostate bed only, in 34 patients in prostate bed and lymph nodes and in 132 patients in lymph nodes only. 134 patients presented with distant metastases and 42 patients with distant metastases and lymph nodes metastases.

Radiation Therapy Target Volume and Dose

Two hundred four patients (51.8%) were treated with PDRT and 190 patients (48.2%) received PDRT plus eRT. Areas of elective RT included the prostate bed in 117 of 190 patients (61.6%), pelvic lymphatics in 163 of 190 patients (85.8%) and paraaortic lymph nodes in 21 of 190 patients (11.1%) (**Table 2**).

In patients without macroscopic recurrence in the prostate bed, elective RT of the prostate bed (ePBRT) was performed with a median dose of 66 Gy (range, 47.5–70 Gy) in single doses of 1.8–2 Gy. If pelvic lymphatics were electively irradiated

TABLE 1 | Patient characteristics.

	Whole cohort n = 394	PDRT n = 204	PDRT plus eRT n = 190
Age at primary treatment (y) (median, range)	66 (46–82)	65.5 (46–81)	66 (46–82)
Initial PSA (ng/ml) (median, range)	11 (2.1–657.20)	9.8 (3.1–657.2)	13.7 (2.8–368)
Initial T stage			
pT1c	8 (2.0)	7 (3.4)	1 (0.5)
pT2a	15 (3.8)	11 (5.4)	4 (2.1)
pT2b	11 (2.8)	7 (3.4)	4 (2.1)
pT2c	126 (32.0)	77 (37.7)	49 (25.8)
pT3a	90 (22.8)	42 (20.6)	48 (25.3)
pT3b	134 (34.0)	57 (27.9)	77 (40.5)
pT4	9 (2.3)	2 (1.0)	7 (3.7)
Tx	1 (0.3)	1 (0.5)	0
Initial N stage			
pN0	261 (66.2)	162 (79.4)	100 (52.6)
pN1	120 (30.5)	35 (17.2)	84 (44.2)
Nx	13 (3.3)	7 (3.4)	6 (3.2)
Initial Gleason score			
6	21 (5.3)	19 (9.3)	2 (1.1)
7a	82 (20.9)	47 (23.0)	36 (18.9)
7b	127 (32.2)	67 (32.8)	60 (31.6)
8	51 (12.9)	23 (11.4)	28 (14.7)
9	108 (27.4)	47 (23.0)	60 (31.6)
10	3 (0.8)	0	3 (1.6)
Unknown	2 (0.5)	1 (0.5)	1 (0.5)
Initial risk group			
Intermediate	14 (3.6)	11 (5.4)	3 (1.6)
High risk	379 (96.1)	192 (94.1)	187 (98.4)
Unknown	1 (0.3)	1 (0.5)	0
Surgical margins			
R0	217 (55.3)	127 (62.3)	90 (47.4)
R1/R2	166 (42.4)	66 (32.4)	100 (52.6)
Rx	11 (2.3)	11 (5.3)	0
Time to biochemical recurrence (mo) (median, range)	15 (0–196)	27 (0–196)	5 (0–166)
PSA at time of MDT (ng/ml) (median, range)	1.2 (0.04–47.5)	1.5 (0.05–47.5)	0.9 (0.04–40.1)

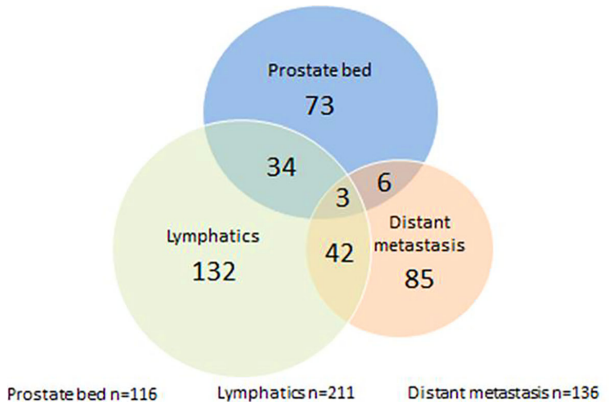

FIGURE 2 | Pre-radiotherapy PSMA-PET/CT findings; n = 394.

TABLE 2 | Patterns of recurrence and elective treatment areas.

PSMA pos. Local recurrence in prostate bed	
no	278 (70.6)
yes	116 (29.4)
PSMA-positive recurrences lymph nodes (n):	
N0	183 (46.4)
N1	211 (53.6)
PSMA-positive distant metastasis (n):	
M0	258 (65.5)
M1a	57 (14.3)
M1b	72 (18.1)
M1c	7 (1.8)
Elective RT volumes:	
no	204 (51.8)
yes	190 (48.2)
Prostate bed only	23 (12.1)
Prostate bed+lymphatics	94 (49.5)
Lymphatics	73 (38.4)
RT technique	
Conventional	205 (52.0)
Conventional with SIB	130 (33.0)
SBRT	38 (9.6)
Conventional with SBRT	21 (5.4)
Elective volume dose (EQD2/1.5 Gy) (median, range)	
Prostate bed	66 (47.5-70)
Pelvic lymphatics	47.5 (42–56)
Additive ADT	
no	262 (66.5%)
yes	130 (33.0%)
unknown	2 (0.5%)

the median dose was 47.5 Gy (range, 36–56/EQD 2/1.5 Gy). ^{68}Ga-PSMA-PET/CT-positive local recurrences within the prostate bed were treated with a median dose of 71.2 Gy (range, 62.6–83/EQD 2/1.5 Gy), PSMA PET-positive pelvic lymph nodes with 59.4 Gy (range, 46–85/EQD 2/1.5 Gy) and paraaortic lymph nodes with 55 Gy (50–99/EQD 2/1.5 Gy).

Most patients were treated with conventionally fractionated RT 205 (52.0%) or conventionally fractionated RT with a simultaneous integrated boost (SIB) technique 130 (33.0%). SBRT was used in 38 (9.6%) and combined SBRT and conventional RT in 21 (5.4%) patients.

Clinical Outcomes

The majority of patients, 364 of 394 (92.4%) showed a decrease of the PSA value 2 months after RT with a median PSA nadir of 0.07 ng/ml (range, 0.01–13.71). Median follow-up was 28 months (range, 1–71). In total, 193 of 394 patients (49.0%) had a biochemical recurrence. Median bRFS was 27 months (**Figure 3**).

Patients who were treated with PDRT had a 3-year bRFS of 37% compared to 53% in patients who received PDRT plus eRT (p = 0.001). Median bRFS was 20 vs. 36 months. Other significant factors in univariate analysis were initial T status, initial lymph node status, Gleason score, local recurrence in the prostate bed, M status at time of ^{68}Ga-PSMA-PET/CT, PSA value at the start of RT, RT technique, additive ADT and area of elective RT. Initial T stage (<T2c vs. ≥T2c; p = 0.035), M status at time of recurrence, PSA value at the start of RT, additive ADT and elective RT (p = 0.005, HR 0.29, 95% CI 0.12–0.68) were independent predictors of bRFS in multivariate analysis (**Table 3**).

In a next step we aimed to analyze the influence of elective prostate bed RT (ePBRT) looking only at 278 patients without ^{68}Ga-PSMA-PET/CT positive prostate bed recurrence. Of these 278 patients, 117 (42.1%) were treated with ePBRT plus PDRT. The 3-year bRFS was 22% and 61% for PDRT only and ePBRT plus PDRT, respectively (p <0.001). Median bRFS was 16 vs. 37 months. This was also significant in multivariate analysis

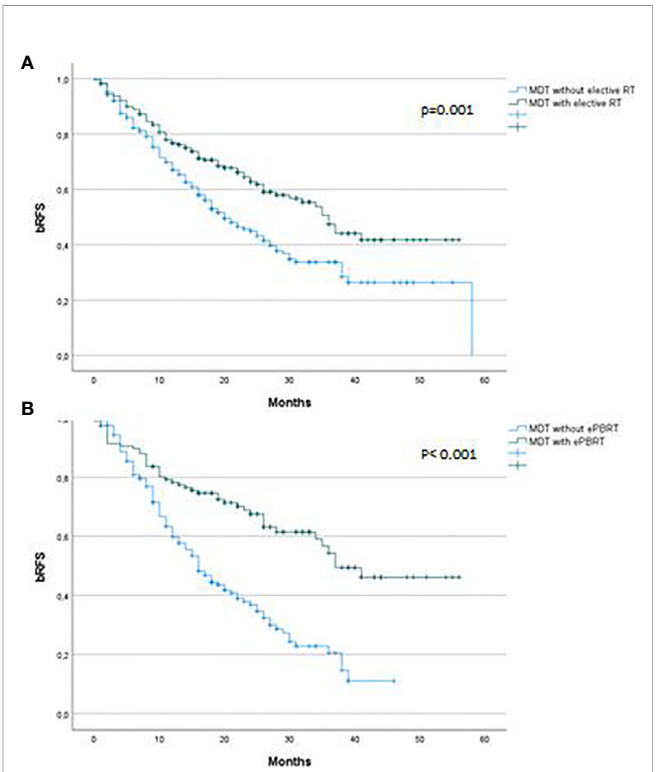

FIGURE 3 | Biochemical recurrence free survival after ^{68}Ga-PSMA-PET CT-directed radiotherapy of prostate cancer recurrences **(A)** stratified by elective RT versus no elective RT, **(B)** stratified by elective RT to prostate bed versus no elective RT to prostate bed. bRFS, Biochemical recurrence free survival; MDT, Metastasis-directed therapy; ePBRT, elective prostate bed radiotherapy.

TABLE 3 | Univariate and multivariate Cox regression analysis determining independent factors influencing biochemical recurrence-free survival for **(A)** whole cohort and **(B)** Prostate bed negative on PSMA-PET/CT.

A. Whole cohort n = 394			
Variables	**Univariate**	**Multivariate**	**HR (95% CI)**
	P value	**P value**	
Time to BR after primary therapy (≤15, >15 mo)	0.677		
Initial T-status (≤T2c, >T2c)	**0.018**	0.020	1.49 (1.07–2.08)
Initial N-status	**0.028**		
Gleason Score (≤7a, 7b, ≥8)	**0.025**		
Initial PSA (≤10ng/ml, 10-20ng/ml, >20ng/ml)	0.121		
Initial risk score	0.689		
Local recurrence prostate bed	**0.003**		
M-status at time of recurrence	**<0.001**	0.001	1.95 (1.32–2.86)
N-status at time of recurrence	0.605		
PSA at time of SRT (≤0.5 ng/ml, >0.5 ng/ml)	**0.005**	0.009	1.53 (1.11–2.10)
Resection margins (R0 vs. R1–2)	0.072		
Additive ADT	**<0.001**	<0.001	0.36 (0.24–0.53)
Elective RT vs. No elective RT	**<0.001**	0.006	0.33 (0.15–0.73)
Area of elective RT (prostate bed, lymphatics)	**<0.001**	0.006	1.76 (1.03–3.83)
Radiotherapy technique (Conventional vs. SBRT)	**<0.001**		
B. Prostate bed negative on PSMA-PET/CT n = 278			
Variables	**Univariate**	**Multivariate**	**HR (95% CI)**
	P value	**P value**	
Time to BR after primary therapy (≤15, >15mo)	0.701		
Initial T-status (≤T2c, >T2c)	**0.035**	0.009	1.67 (1.14–2.44)
Initial N-status	0.063		
Gleason Score (≤7a, 7b, ≥8)	0.31		
Initial PSA (≤10 ng/ml, 10–20 ng/ml, >20 ng/ml)	0.633		
Initial risk score	0.431		
M-status at time of recurrene	**<0.001**	0.002	2.01 (1.32–3.34)
N-status at time of recurrence	**0.036**		-
PSA at time of SRT (≤0.5 ng/ml, >0.5 ng/ml)	**0.001**	0.019	1.56 (1.08–2.25)
Resection margins (R0 vs. R1–2)	0.107		
Additive ADT	**<0.001**	<0.001	0.35 (0.22–0.55)
Elective RT prostate bed	**<0.001**	0.020	0.59 (0.37–0.92)
Radiotherapy technique (Conventional vs. SBRT)	**0.001**		

(p = 0.02, HR 0.59, 95% CI 0.37–0.92). Other factors that were significantly associated with bRFS in univariate analysis were initial T stage, N and M stage at the time of recurrence as well as PSA at the time of sRT (≤0.5 ng/ml vs. ≥0.5 ng/ml), additive ADT and technique of RT (conventional vs. SBRT). In multivariate analysis, in addition to ePBRT and additive ADT (p <0.001), initial T (p = 0.009) and M stage (p = 0.002) were significantly correlated to bRFS. RT dose to the prostate bed or lymph nodes had no influence on bRFS (**Table 3**). We performed an additional analysis excluding M positive patients. Elective RT remained a significant factor for bRFS in this cohort (p = 0,003) with a median bRFS of 41 versus 26 months for elective and no elective RT respectively.

To investigate the impact of elective RT independently of ADT we performed an additional analysis excluding patients who received ADT (n = 130). Median bRFS was 16 versus 28 months for patients receiving PDRT only and ePBRT plus PDRT, respectively (p <0.001) (**Figure 4**).

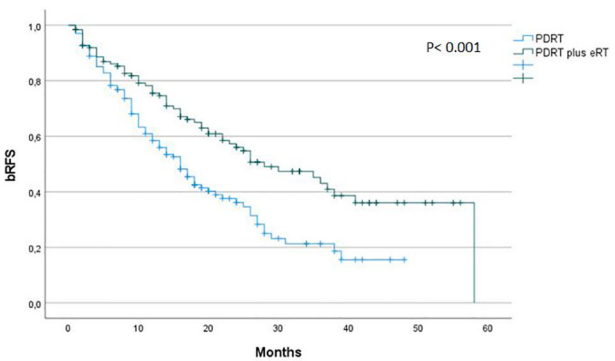

FIGURE 4 | Biochemical recurrence free survival after ^{68}Ga-PSMA-PET CT-directed radiotherapy of prostate cancer recurrences in patients not receiving ADT stratified by elective RT versus no elective RT. bRFS, Biochemical recurrence free survival; PDRT, PET/CT-directed radiotherapy; eRT, elective radiotherapy.

Toxicity

Overall RT was well tolerated with very few acute gastrointestinal (GI) and genitourinary (GU) toxicities. Acute grade 3 toxicity was observed in two patients (diarrhea, lymphedema). Acute grade 2 GI and GU toxicity were observed in 14 and 8.4%, respectively. Late GI toxicity (only grade 2) was observed in 3% and late GU toxicity in 10.9% of patients consisting of seven patients with grade 3 toxicity.

We analyzed if elective RT was associated with an increase in toxicity. Although toxicities were low overall there were significantly more acute (grade 2: 8.8% vs. 31.5%, grade 3: 0% versus 0.4%) and late (grade 2: 1.9% vs. 19.2%, grade 3: 0% versus 3%) GI and GU side effects in patients receiving elective RT (p = 0.001) (**Table 4**).

DISCUSSION

MDT is increasingly investigated as a treatment strategy for oligo-recurrent PC. Still the optimal treatment volume for MDT remains unclear. Some centers implement MDT using a strict definition focally treating lesions detected by PSMA-PET/CT only while other centers are using larger treatment volumes including elective areas (14). Both strategies are not included in current treatment guidelines although a substantial number of international institutions treat patients with MDT as evidenced by a consensus conference of 72 experts in 2019 (15, 16).

To our knowledge, the presented data is the largest study comparing PDRT with PDRT plus elective RT in oligo-recurrent prostate cancer using ^{68}Ga-PSMA-PET/CT as the imaging modality of choice at recurrence. Our study is the first study that looks specifically at elective RT of the prostate bed. Patients receiving PDRT only progressed significantly more often and had a lower 3-year bRFS (22%) than patients receiving PDRT and elective prostate bed RT (ePBRT) (3-year bRFS 61%; p <0.001). This effect proved to be significant in multivariate analysis as well.

A possible explanation for this finding is the limited sensitivity of imaging in the detection of microscopic disease. Though molecular imaging with Choline or PSMA PET/CT has substantially improved detection rates up to 76% for PSA values <1 ng/ml (17), we probably still underestimate the true extent of disease. In a very recent study by Fossati et al. the number of positive lymph nodes found on histology exceeded the number of PET/CT positive lymph nodes (18). This effect was less pronounced for PSMA—than for Choline—PET. The moderate sensitivity of PSMA-PET/CT for the detection of pelvic lymph node metastasis was also shown in series of patients who underwent PET/CT before extended lymph node dissection. The sensitivity ranges from 33–100% and per-node sensitivity is in the range of 24–66% (19). Another demonstration for the underestimation of nodal disease in PET/CT is a study by Rischke et al. (20). In this study patients were treated with additional RT after PET/CT guided salvage lymph node resection. By the addition of RT to the regions with PSMA-expressing lesions on PET/CT, 5-years-PFS was significantly improved from 26.3 to 70.7% indicating remaining micrometastasis after surgery. In analogy to nodal disease, underestimation of subclinical, microscopic disease presumably also occurs in the prostate bed being the location with the highest risk of microscopic disease after radical prostatectomy. In addition to the limited spatial resolution of PET/CT, tracer excretion *via* the bladder with subsequent blurring of the area of the prostatic fossa contributes to the difficult detection of a local recurrence in the prostate fossa.

The majority of data for elective RT comes from small retrospective series (21, 22). PFS rates at 3 years range between 49 and 75% (23). In one study by Tran et al. a 5-year bRFS rate of 43% after elective nodal RT was reported (24). The only prospective trial is the oligo-pelvis–GETUG P07 trial (24). Early toxicity results have been published last year showing low grade 3 toxicity rates even though half of the patients had a re-irradiation of the pelvis (25). Outcome data are not available yet. Comparative data for focal strategies versus elective RT are limited and of retrospective nature. In one study Lepinoy et al. evaluated outcome and toxicity in 62 nodal oligo-recurrent PC patients treated with elective nodal RT (ENRT) or involved node SBRT (26). PFS rate was significantly improved by ENRT (88.3% versus 55.3% at 3-year) while toxicities were similar. The trial that resembles our analysis the most was a large retrospective multicentre analysis by De Bleser and colleagues including 506 pelvic node oligo-recurrent PC patients (27). The primary endpoint was metastasis-free-survival (MFS) after ENRT or SBRT. ENRT was able to improve MFS for patients with a single node while MFS was similar for patients with two to five nodes. Late toxicities were higher in patients who received ENRT (16% vs.

TABLE 4 | Acute and late GI and GU toxicity (≥grade 2) by treatment volume concept according to CTCAE v4.03.

Toxicity	Acute toxicity			
	PDRT n (%)		PDRT + eRT n (%)	
	Grade 2	Grade 3	Grade 2	Grade 3
GU	2 (1.3)	0	31 (13.2)	0
GI	12 (7.5)	0	43 (18.3)	1 (0.4)
Other	0	0	0	1 (0.4)
		Late toxicity		
	PDRT n (%)		PDRT + eRT n (%)	
	Grade 2	Grade 3	Grade 2	Grade 3
GU	1 (0.6)	0	35 (14.9)	7 (3.0)
GI	2 (1.3)	0	10 (4.3)	0
Other	0	0	0	0

PDRT, PET/CT-directed radiotherapy; eRT, elective radiotherapy.

5%). In contrast to our study RT treatment planning was based on Choline-PET/CT in the majority of patients (85%) and prostate bed irradiation was performed in only 60 of 506 patients. Additionally patients with distant metastasis were excluded.

In the current study ADT significantly improved bRFS with a 3-year bRFS rate of 62% versus 34% for patients receiving concurrent ADT to PDRT. This is in accordance with the study by Kroeze et al. with a 2-year PFS rate of 78% versus 53% (28). The additive effect of ADT was seen in patients receiving eRT or not. In patients not receiving eRT median bRFS was 16 versus 30 months for ADT versus no ADT whereas median bRFS in patients who received eRT and no ADT was 26 months. Median bRFS was not reached in the group of patients with eRT and ADT. The role of concurrent ADT in the setting of MDT still needs to be clarified. Potential improvement of survival outcomes must be weighed against increased morbidity and worse quality of life (29). There are two randomized trials showing a benefit for the addition of ADT to RT in the postoperative setting (30, 31). One trial was in the adjuvant setting (RTOG-9601) and the other trial in the salvage setting (GETUG-AFU 16). However, their results are not easily comparable as differently defined patient cohorts were included and both trials did not use pre-RT modern imaging techniques for staging making the results not comparable to the oligo-metastatic state diagnosed by PSMA-PET/CT. So far, results in the oligo-metastatic state are rare and heterogeneous. Most findings come from retrospective, small studies using Choline-PET/CT as imaging modality and varying use and duration of ADT use. The influence of systemic treatment and local treatment remains unclear in this setting. On the other hand an important aim of MDT is to postpone ADT. This was shown by Ost et al. (6). In their study MDT could prolong ADT-free survival by 8 months compared to surveillance alone. In our study the hormone-naive subgroup of patients benefited by adding elective RT areas to PDRT. Median bRFS was 16 versus 28 months in favour of PDRT plus eRT. Further prospective studies assessing the additional benefit of ADT and MDT with or without eRT are required.

Another important parameter for treatment strategy decisions is toxicity. As expected increasing the size of treatment volumes will evidently increase toxicity as shown in a study by Aiter et al. comparing prostate only versus WPRT (32) as well as in a number of other studies (9, 21). PDRT as well as PDRT plus eRT were very well tolerated in our study. Toxicities were mostly mild although PDRT plus eRT was associated with more grade 2 toxicities (8.8% compared to 31.5% and 1.9% vs. 19.2% for acute and late toxicities, respectively) and there were two acute (n = 2; diarrhea and lymphedema) and seven late (n = 7; urinary retention, cystitis) grade 3 events in the PDRT plus eRT group. Toxicity rates are comparable to the results published in the Oligo-pelvis–GETUG P07 trial and the trial by De Bleser et al. showing higher rates of GI and GU toxicity for eRT compared to focal treatment (16% vs. 5%) (33). In summary, toxicity might be slightly higher with larger treatment fields used for eRT but grade 3 toxicity rates were still low and acceptable.

The study has the known limitations inherent to a retrospective analysis, but allows the examination of real-life data in a large cohort of patients. Limitations include the following: the choice for a treatment volume concept, as well as for ADT and follow-up were not standardized and at the discretion of the treating physician implying possible bias. Also, the field for eRT was not standardized leading to potentially different treatment volumes. Further knowledge concerning the extent of the treatment field can be expected by an ongoing prospective multicenter randomized phase II trial treating patients with either MDT and ADT or MDT plus whole pelvis RT and ADT (PEACE V-STORM trial) (34). Results are eagerly awaited and can potentially help to redefine treatment guidelines for salvage RT.

CONCLUSION

^{68}Ga-PSMA-PET-directed RT plus eRT improves bRFS in oligo-recurrent PC patients while slightly increasing side effects. Elective prostate bed irradiation plus PDRT was associated with better bRFS compared to ^{68}Ga-PSMA-PET-directed RT alone. These findings need to be confirmed in a prospective trial.

DATA AVAILABILITY STATEMENT

The raw data supporting the conclusions of this article will be made available by the authors, without undue reservation.

ETHICS STATEMENT

The studies involving human participants were reviewed and approved by Kantonale Ethikkomission Zürich (BASEC-Nr. 2017-01499). The patients/participants provided their written informed consent to participate in this study.

AUTHOR CONTRIBUTIONS

SK, SGK, CH, NS-H, MV, JB, CZ, IB, TD, PB, JR, CL, ME, HC, SC, AM, CB, MG, and AG contributed to the design and implementation of the research. SK, SGK, CH, NS-H, MV, JB, CZ, PB, CL, ME, HC, SC, AM, CB, MG, and AG contributed to data collection and performed the analysis. SK, SGK, CZ, NS, MV, TD, JR, MG, and AG contributed to the writing of the manuscript. All authors contributed to the article and approved the submitted version.

REFERENCES

1. Tilki D, Mandel P, Schlomm T, Chun FK, Tennstedt P, Pehrke D, et al. External validatin of the CAPRA-S score to predict biochemical recurrence, metastasis and mortality after radical prostatectomy in a European cohort. *J Urol* (2015) 193 (6):1970–5. doi: 10.1016/j.juro.2014.12.020
2. Han M, Partin AW, Pound CR, Epstein JI, Walsh PC. Long-term biochemical disease-free and cancer-specific survival following anatomic radical retropubic prostatectomy. The 15-year Johns Hopkins experience. *Urol Clin North Am* (2001) 28(3):555–65. doi: 10.1016/s0094-0143(05)70163-4
3. King CR. The timing of salvage radiotherapy after radical prostatectomy: a systematic review. *Int J Radiat Oncol Biol Phys* (2012) 84(1):104–11. doi: 10.1016/j.ijrobp.2011.10.069
4. McCarthy M, Francis R, Tang C, Watts J, Campbell A. A Multicenter Prospective Clinical Trial of 68Gallium PSMA HBED-CC PET-CT Restaging in Biochemically Relapsed Prostate Carcinoma: Oligometastatic Rate and Distribution Compared With Standard Imaging. *Int J Radiat Oncol Biol Phys* (2019) 104(4):801–8. doi: 10.1016/j.ijrobp.2019.03.014
5. De Bleser E, Tran PT, Ost P. Radiotherapy as metastasis-directed therapy for oligometastatic prostate cancer. *Curr Opin Urol* (2017) 27(6):587–95. doi: 10.1097/MOU.0000000000000441
6. Ost P, Reynders D, Decaestecker K, Fonteyne V, Lumen N, De Bruycker A, et al. Surveillance or Metastasis-Directed Therapy for Oligometastatic Prostate Cancer Recurrence: A Prospective, Randomized, Multicenter Phase II Trial. *J Clin Oncol* (2018) 36(5):446–53. doi: 10.1200/JCO.2017.75.4853
7. Phillips R, Shi WY, Deek M, Radwan N, Lim SJ, Antonarakis ES, et al. Outcomes of Observation vs Stereotactic Ablative Radiation for Oligometastatic Prostate Cancer: The ORIOLE Phase 2 Randomized Clinical Trial. *JAMA Oncol* (2020) 6(5):650–9. doi: 10.1001/jamaoncol.2020.0147
8. De Bruycker A, Lambert B, Claeys T, Delrue L, Mbah C, De Meerleer G, et al. Prevalence and prognosis of low-volume, oligorecurrent, hormone-sensitive prostate cancer amenable to lesion ablative therapy. *BJU Int* (2017) 120 (6):815–21. doi: 10.1111/bju.13938
9. Pisansky TM, Thompson IM, Valicenti RK, D'Amico AV, Selvarajah S. Adjuvant and salvage radiotherapy after prostatectomy: ASTRO/AUA guideline amendment 2018–2019. *J Urol* (2019) 202:533–8. doi: 10.1097/JU.0000000000000295
10. Michalski JM, Lawton C, El Naqa I, Ritter M, O'Meara E, Seider MJ, et al. Development of RTOG consensus guidelines for the definition of the clinical target volume for postoperative conformal radiation therapy for prostate cancer. *Int J Radiat Oncol Biol Phys* (2010) 76(2):361–8. doi: 10.1016/j.ijrobp.2009.02.006
11. Poortmans P, Bossi A, Vandeputte K, Bosset M, Miralbell R, Maingon P, et al. EORTC Radiation Oncology Group. Guidelines for target volume definition in post-operative radiotherapy for prostate cancer, on behalf of the EORTC Radiation Oncology Group. *Radiother Oncol* (2007) 84(2):121–7. doi: 10.1016/j.radonc.2007.07.017
12. Fendler WP, Eiber M, Beheshti M, Bomanji J, Ceci F, Cho S, et al. 68Ga-PSMA PET/CT: Joint EANM and SNMMI procedure guideline for prostate cancer imaging: version 1.0. *Eur J Nucl Med Mol Imaging* (2017) 44(6):1014–24. doi: 10.1007/s00259-017-3670-z
13. Heidenreich A, Bastian PJ, Bellmunt J, Bolla M, Joniau S, van der Kwast T, et al. EAU guidelines on prostate cancer. Part II: treatment of advanced, relapsing, and castration-resistant prostate cancer. *Eur Urol* (2014) 65:467–79. doi: 10.1016/j.eururo.2013.11.002
14. Steuber T, Jilg C, Tennstedt P, De Bruycker A, Tilki D, Decaestecker K, et al. Standard of Care Versus Metastases-directed Therapy for PET-detected Nodal Oligorecurrent Prostate Cancer Following Multimodality Treatment: A Multi-institutional Case-control Study. *Eur Urol Focus* (2019) 5(6):1007–13. doi: 10.1016/j.euf.2018.02.015
15. Cornford P, Bellmunt J, Bolla M, Briers E, De Santis M, Gross T, et al. EAU-ESTRO-SIOG Guidelines on Prostate Cancer. Part II: Treatment of Relapsing, Metastatic, and Castration-Resistant Prostate Cancer. *Eur Urol* (2017) 71 (4):630–42. doi: 10.1016/j.eururo.2016.08.002
16. Gillessen S, Attard G, Beer TM, Beltran H, Bjartell A, Bossi A, et al. Management of Patients with Advanced Prostate Cancer: Report of the Advanced Prostate Cancer Consensus Conference 2019. *Eur Urol* (2020) 77 (4):508–47. doi: 10.1016/j.eururo.2020.01.012
17. Perera M, Papa N, Roberts M, Williams M, Udovicich C, Vela I, et al. Gallium-68 Prostate-specific Membrane Antigen Positron Emission Tomography in Advanced Prostate Cancer-Updated Diagnostic Utility, Sensitivity, Specificity, and Distribution of Prostate-specific Membrane Antigen-avid Lesions: A Systematic Review and Meta-analysis. *Eur Urol* (2020) 77(4):403–17. doi: 10.1016/j.eururo.2019.01.049
18. Fossati N, Scarcella S, Gandaglia G, Suardi N, Robesti D, Boeri L, et al. Underestimation of Positron Emission Tomography/Computerized Tomography in Assessing Tumor Burden in Prostate Cancer Nodal Recurrence: Head-to-Head Comparison of 68Ga-PSMA and 11C-Choline in a Large, Multi-Institutional Series of Extended Salvage Lymph Node Dissections. *J Urol* (2020) 204(2):296–302. doi: 10.1097/JU.0000000000000800
19. Luiting HB, van Leeuwen PJ, Busstra MB, Brabander T, van der Poel HG, Donswijk ML, et al. Use of gallium-68 prostate-specific membrane antigen positron-emission tomography for detecting lymph node metastases in primary and recurrent prostate cancer and location of recurrence after radical prostatectomy: an overview of the current literature. *BJU Int* (2020) 125(2):206–14.
20. Rischke HC, Schultze-Seemann W, Wieser G, Krönig M, Drendel V, Stegmaier P, et al. Adjuvant radiotherapy after salvage lymph node dissection because of nodal relapse of prostate cancer versus salvage lymph node dissection only. *Strahlenther Onkol* (2015) 191(4):310–20. doi: 10.1007/s00066-014-0763-5
21. Fodor A, Berardi G, Fiorino C, Picchio M, Busnardo E, Kirienko M, et al. Toxicity and efficacy of salvage carbon 11-choline positron emission tomography/computed tomography-guided radiation therapy in patients with lymph node recurrence of prostate cancer. *BJU Int* (2017) 119(3):406–13. doi: 10.1111/bju.13510
22. Würschmidt F, Petersen C, Wahl A, Dahle J, Kretschmer M. [18F] fluoroethylcholine-PET/CT imaging for radiation treatment planning of recurrent and primary prostate cancer with dose escalation to PET/CT-positive lymph nodes. *Radiat Oncol* (2011) 6:44. doi: 10.1186/1748-717X-6-44
23. De Bruycker A, Tran PT, Achtman AH, Ost P. GAP6 consortium. Clinical perspectives from ongoing trials in oligometastatic or oligorecurrent prostate cancer: an analysis of clinical trials registries. *World J Urol* (2021) 39(2):317–26. doi: 10.1007/s00345-019-03063-4
24. Tran S, Jorcano S, Falco T, Lamanna G, Miralbell R, Zilli T. Oligorecurrent Nodal Prostate Cancer: Long-term Results of an Elective Nodal Irradiation Approach. *Am J Clin Oncol* (2018) 41(10):960–2.
25. Vaugier L, Palpacuer C, Rio E, Goineau A, Pasquier D, Buthaud X, et al. Early Toxicity of a Phase 2 Trial of Combined Salvage Radiation Therapy and Hormone Therapy in Oligometastatic Pelvic Node Relapses of Prostate Cancer (OLIGOPELVIS GETUG P07). *Int J Radiat Oncol Biol Phys* (2019) 103(5):1061–7. doi: 10.1016/j.ijrobp.2018.12.020
26. Lépinoy A, Silva YE, Martin E, Bertaut A, Quivrin M, Aubignac L, et al. Salvage extended field or involved field nodal irradiation in 18F-fluorocholine PET/CT oligorecurrent nodal failures from prostate cancer. *Eur J Nucl Med Mol Imaging* (2019) 46(1):40–8. doi: 10.1007/s00259-018-4159-0
27. De Bleser E, Jereczek-Fossa BA, Pasquier D, Zilli T, Van As N, Siva S, et al. Metastasis-directed Therapy in Treating Nodal Oligorecurrent Prostate Cancer: A Multi-institutional Analysis Comparing the Outcome and Toxicity of Stereotactic Body Radiotherapy and Elective Nodal Radiotherapy. *Eur Urol* (2019) 76(6):732–9. doi: 10.1016/j.eururo.2019.07.009
28. Kroeze SGC, Henkenberens C, Schmidt-Hegemann NS, Vogel MME, Kirste S, Becker J, et al. Prostate-specific Membrane Antigen Positron Emission Tomography-detected Oligorecurrent Prostate Cancer Treated with Metastases-directed Radiotherapy: Role of Addition and Duration of Androgen Deprivation. *Eur Urol Focus* (2019) 5:S2405-4569(19)30270-6. doi: 10.1016/j.euf.2019.08.012
29. Duchesne GM, Woo HH, King M, Bowe SJ, Stockler MR, Ames A, et al. Health-related quality of life for immediate versus delayed androgen-deprivation therapy in patients with asymptomatic, non-curable prostate cancer (TROG 03.06 and VCOG PR 01-03 [TOAD]): a randomised, multicentre, non-blinded, phase 3 trial. *Lancet Oncol* (2017) 18:1192–201. doi: 10.1016/S1470-2045(17)30426-6
30. Shipley WU, Seiferheld W, Lukka HR, Major PP, Heney NM, Grignon DJ, et al. Radiation with or without Antiandrogen Therapy in Recurrent Prostate Cancer. *N Engl J Med* (2017) 376:417–28.

31. Carrie C, Hasbini A, de Laroche G, Richaud P, Guerif S, Latorzeff I, et al. Salvage radiotherapy with or without short-term hormone therapy for rising prostate-specific antigen concentration after radical prostatectomy (GETUG-AFU 16): a randomised, multicentre, open-label phase 3 trial. *Lancet Oncol* (2016) 17:747–56. doi: 10.1016/S1470-2045(16)00111-X
32. Aizer AA, Yu JB, McKeon AM, Decker RH, Colberg JW, Peschel RE. Whole pelvic radiotherapy versus prostate only radiotherapy in the management of locally advanced or aggressive prostate adenocarcinoma. *Int J Radiat Oncol Biol Phys* (2009) 75(5):1344–9. doi: 10.1016/j.ijrobp.2008.12.082
33. Supiot S, Rio E, Pacteau V, Mauboussin MH, Campion L, Pein F. OLIGOPELVIS - GETUG P07: a multicentre phase II trial of combined salvage radiotherapy and hormone therapy in oligometastatic pelvic node relapses of prostate cancer. *BMC Cancer* (2015) 15:646. doi: 10.1186/s12885-015-1579-0
34. De Bruycker A, Spiessens A, Dirix P, Koutsouvelis N, Semac I, Liefhooghe N, et al. PEACE V - Salvage Treatment of OligoRecurrent nodal prostate cancer Metastases (STORM): a study protocol for a randomized controlled phase II trial. *BMC Cancer* (2020) 20(1):406. doi: 10.1186/s12885-020-06911-4. Published 2020 May 12.

Conflict of Interest: The authors declare that the research was conducted in the absence of any commercial or financial relationships that could be construed as a potential conflict of interest.

frontiers in Oncology

ORIGINAL RESEARCH
published: 14 May 2021
doi: 10.3389/fonc.2021.652678

Influence of Urethra Sparing on Tumor Control Probability and Normal Tissue Complication Probability in Focal Dose Escalated Hypofractionated Radiotherapy: A Planning Study Based on Histopathology Reference

Simon K. B. Spohn[1,2,3†], Ilias Sachpazidis[4†], Rolf Wiehle[4], Benedikt Thomann[4], August Sigle[5], Peter Bronsert[6], Juri Ruf[7], Matthias Benndorf[8], Nils H. Nicolay[1,2], Tanja Sprave[1,2], Anca L. Grosu[1,2], Dimos Baltas[2,4] and Constantinos Zamboglou[1,2,3]*

[1] Department of Radiation Oncology, Medical Center – University of Freiburg, Faculty of Medicine, University of Freiburg, Freiburg, Germany, [2] German Cancer Consortium (DKTK). Partner Site Freiburg, Freiburg, Germany, [3] Berta-Ottenstein-Programme, Faculty of Medicine, University of Freiburg, Freiburg, Germany, [4] Division of Medical Physics, Department of Radiation Oncology, Medical Center - University of Freiburg, Faculty of Medicine, University of Freiburg, Freiburg, Germany, [5] Department of Urology, Medical Center – University of Freiburg, Faculty of Medicine, University of Freiburg, Freiburg, Germany, [6] Institute for Surgical Pathology, Medical Center – University of Freiburg, Faculty of Medicine, University of Freiburg, Freiburg, Germany, [7] Department of Nuclear Medicine, Medical Center – University of Freiburg, Faculty of Medicine, University of Freiburg, Freiburg, Germany, [8] Department of Radiology, Medical Center – University of Freiburg, Faculty of Medicine, University of Freiburg, Freiburg, Germany

Purpose: Multiparametric magnetic resonance tomography (mpMRI) and prostate specific membrane antigen positron emission tomography (PSMA-PET/CT) are used to guide focal radiotherapy (RT) dose escalation concepts. Besides improvements of treatment effectiveness, maintenance of a good quality of life is essential. Therefore, this planning study investigates whether urethral sparing in moderately hypofractionated RT with focal RT dose escalation influences tumour control probability (TCP) and normal tissue complication probability (NTCP).

Patients and Methods: 10 patients with primary prostate cancer (PCa), who underwent 68Ga PSMA-PET/CT and mpMRI followed by radical prostatectomy were enrolled. Intraprostatic tumour volumes (gross tumor volume, GTV) based on both imaging techniques (GTV-MRI and -PET) were contoured manually using validated contouring techniques and GTV-Union was created by summing both. For each patient three IMRT plans were generated with 60 Gy to the whole prostate and a simultaneous integrated boost up to 70 Gy to GTV-Union in 20 fractions by (Plan 1) not respecting and (Plan 2) respecting dose constraints for urethra as well as (Plan 3) respecting dose constraints for planning organ at risk volume for urethra (PRV = urethra + 2mm expansion). NTCP for urethra was calculated applying a Lyman-Kutcher-Burman model. TCP-Histo was calculated based on PCa distribution in co-registered histology (GTV-Histo).

OPEN ACCESS

Edited by:
Tone Frost Bathen,
Norwegian University of Science and Technology, Norway

Reviewed by:
Torgrim Tandstad,
St. Olavs University Hospital, Norway
Ingerid Skjei Knudtsen,
Norwegian University of Science and Technology, Norway
Kathrine Røe Redalen,
Norwegian University of Science and Technology, Norway

***Correspondence:**
Simon K. B. Spohn
Simon.Spohn@uniklinik-freiburg.de

[†]These authors have contributed equally to this work and share first authorship

Specialty section:
This article was submitted to Cancer Imaging and Image-directed Interventions, a section of the journal Frontiers in Oncology

Received: 12 January 2021
Accepted: 08 April 2021
Published: 14 May 2021

Citation:
Spohn SKB, Sachpazidis I, Wiehle R, Thomann B, Sigle A, Bronsert P, Ruf J, Benndorf M, Nicolay NH, Sprave T, Grosu AL, Baltas D and Zamboglou C (2021) Influence of Urethra Sparing on Tumor Control Probability and Normal Tissue Complication Probability in Focal Dose Escalated Hypofractionated Radiotherapy: A Planning Study Based on Histopathology Reference. Front. Oncol. 11:652678. doi: 10.3389/fonc.2021.652678

Complication free tumour control probability (P+) was calculated. Furthermore, the intrafractional movement was considered.

Results: Median overlap of GTV-Union and PRV-Urethra was 1.6% (IQR 0-7%). Median minimum distance of GTV-Histo to urethra was 3.6 mm (IQR 2 – 7 mm) and of GTV-Union to urethra was 1.8 mm (IQR 0.0 – 5.0 mm). The respective prescription doses and dose constraints were reached in all plans. Urethra-sparing in Plans 2 and 3 reached significantly lower NTCP-Urethra ($p = 0.002$) without significantly affecting TCP-GTV-Histo ($p = p > 0.28$), NTCP-Bladder ($p > 0.85$) or NTCP-Rectum ($p = 0.85$), resulting in better P+ ($p = 0.006$). Simulation of intrafractional movement yielded even higher P+ values for Plans 2 and 3 compared to Plan 1.

Conclusion: Urethral sparing may increase the therapeutic ratio and should be implemented in focal RT dose escalation concepts.

Keywords: hypofractionated radiotherapy, PSMA - prostate specific membrane antigen, focal dose escalation, tumor control probability (TCP), NTCP (normal tissue complication probability) model, mpMRI, primary prostate cancer, histopathology

INTRODUCTION

Radiotherapy (RT) of primary Prostate cancer (PCa) is currently experiencing an individualization, utilizing modern imaging techniques for staging and definition of intraprostatic gross tumor volume (GTV). Since an increase in RT dose improves tumor control rates (1), concepts of focal dose escalation have developed to deliver higher doses to the tumor and thereby improving rates of biochemical recurrence (2, 3) without risking higher toxicities by respecting OAR restrictions. Recently the long-term result of the phase III FLAME trial demonstrated that mpMRI-defined focal dose escalation significantly improves biochemical disease free survival (4). Earlier publications from this trial demonstrated the feasibility and reported no significant increase in acute and late toxicities (5). These results are encouraging, that unfavorable intermediate- and high-risk PCa patients, who's proportion is on the rise (6), benefit from these advanced treatments. Besides multiparametric magnetic resonance tomography (mpMRI) being the gold standard for diagnostics in PCa (7), prostate specific membrane antigen positron emission tomography (PSMA-PET) has emerged as a diagnostic tool of high quality (8–13). Recently, the superiority of PSMA-PET for initial staging compared to conventional imaging was prospectively proved, which led to therapy management change in 28% of cases (14). Regarding depiction of the intraprostatic GTV PSMA-PET/CT reveals GTVs more concordant with biopsy reference (9), whereas mpMRI underestimates the true tumor and misses significant tumour lesions (15–17). Previously conducted planning studies from our group and from Goodman et al. demonstrated that despite putative limitations for focal therapy approaches due to larger volumes, boosting of PSMA-PET/CT delineated GTVs is technically feasible (18–20). Bettermann et al. and Eiber et al. could clearly demonstrate that the combined use of mpMRI and PSMA-PET (GTV-Union) significantly improved sensitivity (9, 11). A planning study by Zamboglou et al. revealed significantly increased tissue control probabilities (TCP) for GTV-Union based focal dose escalation compared to GTV-PET or GTV-MRI-based dose escalation (20). Prospective trials will evaluate whether these advances in imaging and diagnostic accuracy can be translated into improved clinical outcomes. A modern approach includes moderately hypofractionated RT (MHRT) to the whole prostate with simultaneously integrated dose escalation to mpMRI- and PSMA-PET/CT-defined GTVs. Although the impact of accountable structures such as bladder, bladder trigone and urethra stay vague, the urethra as a serial organ may be of particular importance in this setting. This planning study aims to investigate whether urethral sparing in MHRT with focal dose escalation delivered to mpMRI and PSMA-PET/CT defined GTVs, influences tumor control probability (TCP) and normal tissue complication probability (NTCP). NTCP was calculated based on the Lyman-Kutcher-Burman (LKB) model with parameters defined by Panettiere et al. (21), TCP was calculated based on 3D dose distribution in co-registered histopathology as standard of reference. Furthermore, the influence of intrafractional movement was assessed (22).

MATERIAL AND METHODS

Patient Cohort

The utilized study cohort consisted of ten (10) patients with primary PCa, who underwent 68Ga-HBED-CC-PSMA (68Ga-PSMA-PET) and mpMRI followed by radical prostatectomy. Patient characteristics are listed in **Table 1**. A written informed consent was obtained from each patient and the institutional review board of the Albert-Ludwigs-University of Freiburg approved the study (No.: 469/14).

PET/CT and MRI Imaging

Diagnostic images were acquired using a diagnostic setup.

TABLE 1 | Patient characteristics.

Patient	Age (y)	PSA (ng/ml)	TNM	Gleason score
1	67	6.07	pT3a pN1 cM0	3+4 (7a)
2	61	10.57	pT2c pN0 cM0	3+4 (7a)
3	73	25.52	pT2c pN0 cM0	3+4 (7a)
4	59	9.15	pT2c pN0 cM0	4+3 (7b)
5	74	8.82	pT2c pN0 cM0	3+4 (7a)
6	74	15	pT2c pN0 cM0	3+4 (7a)
7	76	20.7	pT2c pN0 cM0	4+3 (7b)
8	73	40	pT3a pN1 cM0	4+5 (9)
9	53	16.3	pT3a pN0 cM0	4+4 (8)
10	72	28.9	pT3b pN1 cM0	4+4 (8)

PET/CT scans using the ligand 68Ga-HBED-CC-PSMA (23) were performed in 9 patients with a 64-slice GEMINI TF PET/CT and in 1 patient with a Vereos PET/CT (both Philips Healthcare, USA). The imaging systems were cross-calibrated to ensure the comparability of the quantitative measurements and both scanners fulfilled the requirements indicated in the European Association of Nuclear Medicine (EANM) imaging guidelines and obtained EANM Research Ltd. (EARL) accreditation during acquisition. The spatial resolution in the transverse direction near the centre is 4.8 mm for GEMINI TF (24) and 4.2mm for Vereos (25) Patients underwent the whole-body PET scan starting 1 h after injection andwere asked to urinate prior PET imaging. The uptake of 68Ga-PSMA-HBED-CC was quantified by standardized uptake values (SUV). A detailed description of the used 68Ga-HBED-CC-PSMA PET/CT imaging protocol is described in (26).

MR images were acquired on a 3 Tesla system (5 patients on TrioTim, 1 patient on Magnetom Vida, 1 patient on Skyra, all Siemens, Germany) and on a 1.5 Tesla system (3 patients on Aera, Siemens, Germany). The MR imaging systems were equipped with a surface phased array (Body Matrix) in combination with an integrated spine array coil. No endo-rectal coil was used. Not additional cross-calibration was performed. Essentially, T2-weighted fast spin echo (T2W-TSE) images, diffusion weighted images (DWI) and dynamic contrast-enhanced (DCE) perfusion images were acquired. Apparent diffusion coefficient (ADC) maps were calculated from the DWIs using information from all measured b-values. ADC maps were generated with a monoexponential model as implemented in syngo.via (syngo.via ADC & b-value tool, Siemens Healthcare, Germany). Extrapolated high b-value images (b = 1400 s/mm^2) were calculated with syngo.via using information from all measured b-values. These extrapolated images were considered the high b-value DWIs for prostate MRI reading according to PI-RADS v2.0 (27). MR protocols were heterogeneous in terms of slice thickness, gap between slices and b-values. A detailed description of the used T2w, DWI and DCE MRI imaging protocol can be found in (28).

Contouring

Intraprostatic Tumour Mass

GTV-PET was contoured manually using a validated scaling of SUVmin-max: 0-5 (29) within the prostate using Eclipse™ Treatment Planning System (Varian, USA). GTV-MRI was contoured manually based on MRI T2-w and ADC images, applying imaging criteria PI-RADSv2.0 and considering lesions with a PI-RADS score of ≥ 3 as relevant (27). Final GTVs were the respective consensus contour between two readers with >4 years experience in PET and MRI interpretation. Subsequently careful manual co-registration of *in-vivo* CT and *in-vivo* MRI was performed to transfer GTV-MRI to the corresponding *in-vivo*-CT image and to create GTV-Union composed of the sum of GTV-PET and GTV-MRI. GTV-Union was used based on the benefit in terms of higher sensitivity and complementary information of both techniques (9, 13).

Organs at Risk (OAR), Clinical Target Volume (CTV) and Planning Target Volume (PTV)

Bladder, rectum, femoral head as OAR were contoured based on the planning-CT scan according to RTOG guidelines (30). Urethra was contoured based on the co-registered MRI. Planning organ at risk volume (PRV)-urethra was created from applying 2 mm isotropic extension of urethra according to the hypo-Flame trial (31).

The CTV was created by following the ESTRO-ACROP guidelines (32). CTV1 was defined as the prostate including extracapsular PCa + 3mm isotropic extension (excluding rectum and bladder). CTV_SV was defined as the proximal 1.4 cm and 2.2 cm of the seminal vesicle (SV) in unfavorable intermediate risk and high-risk patients accordingly. In case of tumor infiltration of the SV the respective regions were included in CTV-SV. CTV2 was defined as the prostate and the base of the SV including parts of the SV with visible tumor burden. PTV 1 was created from isotropic 6 mm-extension of CTV1 and 8 mm of CTV_SV, followed by merging both volumes. PTV2 was created from isotropic 6 mm-expansion of CTV2. PTV3 was created from isotropic 2mm-extension of GTV-Union and consequent remove of existing overlaps with organ at risks (OAR) contours. For analysis purposes three different PTV3 were generated: PTV3_1 was defined as the GTV-Union isotropically expanded by 2mm. PTV3_2 was created from the subtraction of urethra from PTV3_1 and finally PTV3_3 was created from the subtraction of PRV-Urethra from PTV_1. See **Figure 1** for illustration of volumes.

Histopathological Co-Registration

PCa lesions in whole mount histopathology were used as standard of reference as previously conducted by our group (9, 33). After fixation, the resected prostate was fixed in a customized localizer with a 4 mm grid and an *ex-vivo* CT scan (16-channel Brilliance Big Bore, Phillips, Germany) was performed. Subsequently, whole-mount step sections were cut every 4 mm using an in–house cutting device to guarantee equal cutting angles between histological and corresponding *ex-vivo* CT slices. Following paraffin embedding, specimens were cut using a Leica microtome. Haematoxylin and eosin staining were performed following routine protocols. A board-certified experienced pathologist marked PCa lesions. Subsequently, histopathological information was digitalized *via* intermediate registration to *ex-vivo* CT using MITK software (MITK Workbench 2015.5.2). Automatic interpolation was performed

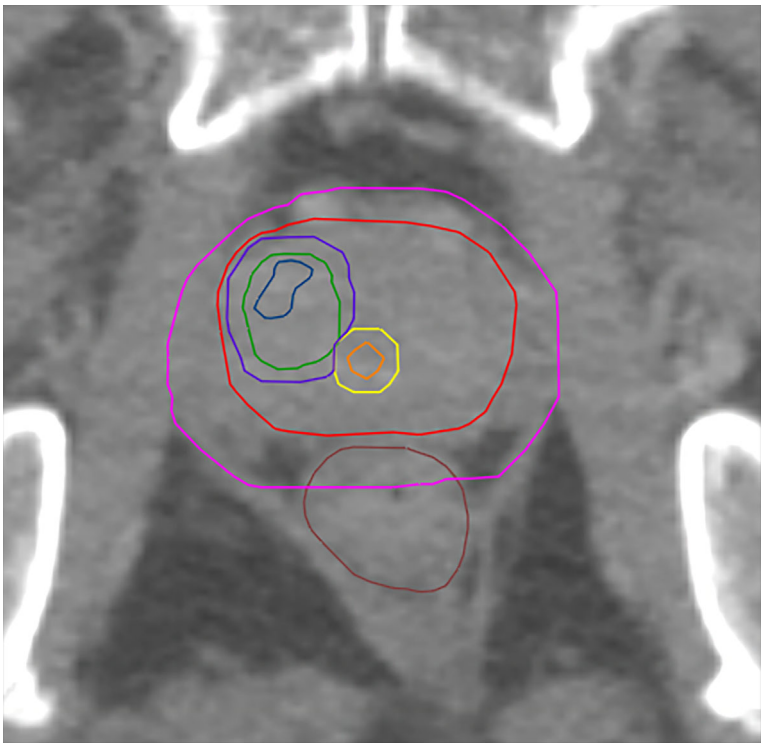

FIGURE 1 | Shows GTV-MRI (blue), GTV-PET (green), urethra (orange) PRV-urethra (yellow), prostate (red), PTV3_3 (boost volume minus PRV-urethra, purple) and PTV1 (pink).

to create GTV-Histo (GTV based on histopathology). Images were transferred to Eclipse™ Treatment Planning System v.15.6 (Varian Medical Systems, USA). *Ex-vivo* CT and *in vivo*-CT (from PSMA-PET/CT scans) were carefully manual co-registered allowing non-rigid deformation and considering the 4mm grid and anatomical landmarks such as urethra and cyst and prostate capsule in particular. Hence, this registration workflow takes into account non-linear shrinkage and distortion of the prostate gland after resection.

Distances to Urethra

Minimum distance of GTV-Histo to urethra was evaluated on each hematoxylin and eosin stained (H&E) slice of the respective patient. Accordingly, minimum distance of GTV-Union to urethra was evaluated on the corresponding CT-slice on the *in vivo* CT.

IMRT Planning

IMRT plans were created in Eclipse™ Treatment Planning System v15.1 (Varian, USA) with a calculation grid size of 1.5 mm. Dose prescription protocols were the following: PTV1 45 Gy in 15 fractions and PTV2 15 Gy in 5 fractions, resulting in 60 Gy for PTV2. A simultaneous integrated boost (SIB) up to 70 Gy for PTV3 for all 20 fractions was prescribed. Adapted from the DELINEATE trial (34) and based on findings from Martinez et al. (1), our dose concept aimed for boost doses near 100 Gy (EQD2, a/b=1.6). For PTV2 D98% was ≥ 58.8 Gy and D2% ≤ 70 Gy, for PTV3 D98% was ≥ 68.6 Gy and D2% ≤ 71.4 Gy. Three different plans were created using three different boost volumes for the simultaneous integrated boost (SIB): The SIB volumes were PTV3_1, PTV3_2 and PTV3_3 for plan 1, 2 and 3 respectively. Dose constraints for organs at risk were considered according to CHHiP-, FLAME- and DELINEATE-trial (5, 34–36). Dose constraints for Urethra and PRV-Urethra were 62.4 Gy for D2%. Details of RT planning prescription doses and OAR constraints can be found in **Supplementary Material 1**.

To evaluate the impact of urethral sparing three different IMRT plans were calculated: (i) Plan 1 without any dose constraints for urethra, (ii) Plan 2 considered the D2% dose constraint for urethra and (iii) Plan 3 considered the D2% dose constraints for PRV-Urethra.

TCP and NTCP Modeling

Structure sets and calculated 3D-dose matrices of the radiotherapy plans were exported as DICOM files. Furthermore, using a Varian ESAPI script (https://varianapis.github.io/), dose matrix voxels for each structure were exported (https://github.com/isachpaz/ESAPICommander). TCP was calculated based on the linear quadratic (LQ) Poisson model (37–41):

$$TCP = e^{-\rho^{cl} \cdot V \cdot e^{-\alpha \cdot EQD0}} \quad \text{Eq. 1}$$

Where ρ_{cl} is the homogeneous clonogenic cell density (# cells/cm^3) in the tumor of volume V. $EQD0$ is the equi-effective dose for 0Gy fractionation given by Eq. 2, and α is the coefficient of LQ-model defining the linear-term of cell killing.

$$EQD0 = D \cdot \left(1 + \frac{d}{\left(\alpha/\beta\right)}\right) \quad \text{Eq. 2}$$

d is the dose per fraction, and D is the total dose delivered in N fractions, $D=N^*d$, where α/β is the *ratio* of linear to quadratic cell killing probability according to the LQ-model.

In the present study, the tumor cell density was set $\rho_{cl}=2.8^*10^8$ cells/cm (42–44). α/β value of 1.6 Gy was assumed, based on the recent meta-analysis results by Vogelius et al., which included studies with mildly- and ultrahypofractionated radiotherapy (45). To account for diversity of published α/β values we performed a robustness analysis for $TCP_{GTV\text{-}Histo}$ with three different parameter sets encompassing the range for α/β described by Vogelius et al. (45). α was each time fitted (**Table 2**), so that 70% $TCP_{GTV\text{-}Histo}$ would be reached in our patient cohort with a conventional dose of 60 Gy in 3 Gy fractions, as we have described in our previous publication (19).

NTCP for bladder and rectum ($NTCP_{Bladder}$, $NTCP_{Rectum}$) were calculated based on the relative seriality model as described by Bostel et al. (46). For bladder a D_{50} of 80.0 Gy as EQD2 for symptomatic contracture and volume loss, a relative seriality parameter value s of 1.3 and γ= 2.59 were used (47). For rectum a D_{50} of 80.0 Gy as EQD2 for severe proctitis/necrosis/stenosis/fistula (2, 47–50), s = 0.75 and γ= 1.79 were considered (47). An α/β value of 3.0 Gy for bladder and rectum was assumed (34). For $NTCP_{Urethra}$ the Lyman-Kutcher-Burman (LKB) model was applied for the endpoint urethral stricture as published by Panitierri et al. (21): D_{50} = 116.7 Gy, m = 0.23, n = 0.3, and α/β = 5.0 Gy. We additionally performed $NTCP_{Urethra}$ calculations for the 68% confident intervals (CI) with a step of 1.0 Gy for D_{50} and a step of 0.01 for m. In total 364 combinations of D_{50} and m were evaluated.

Complication Free Tumour Control Probability P+

In order to account for the injuries or risk for complications to each of the healthy organs (OARs) involved in a given clinical case, the following expression is usually applied for the total probability of injury P_I:

$$P_I = 1 - \prod_{j=1}^{N_{OARs}} w_j \cdot \left(1 - NTCP_j\right) \quad \text{Eq. 3}$$

TABLE 2 | TCP model parameter sets for the robustness analysis.

Parameter set	1	2	3
ρ [x 10^8 cells/cm^3]	2.8	2.8	2.8
α/β (5)	1.2	1.6	2.7
α (5)	0.10099	0.12050	0.15740

where $NTCP_j$ is the probability of injuring the normal tissue (OAR), w_j is a weighting factor expressing the relative clinical importance of each endpoint, and N_{OARs} is the total number of healthy organs involved in the clinical case. The effectiveness of a given dose distribution can be evaluated by the comparison of its advantages in terms of tumour control (benefit B) against its disadvantages considering normal tissues complications (injury I). The probability of complication free tumour control P_+, is defined as

$$P_+ = P(B) - P(B \cap I) = P_B - P_{B \cap I} \quad \text{Eq. 4}$$

where P_B is the probability of getting benefit from the treatment (tumour control, Eq. 1) and P_I is the probability of causing injury to normal tissues (Eq. 3). For the case of complete independency of response of tumor and OARs, P_+ becomes:

$$P_+ = P_B \cdot (1 - P_I) \quad \text{Eq. 5}$$

P_+ is an overall parameter for evaluation of complex dose distributions and treatment localisations and is suggested to support decision on treatment plan selection and treatment adaptation (46, 51–56).

Organ Movement

As previously performed by our group, *TCP* and *NTCP* calculations were calculated with and without movement (22). This was achieved by changing the relative positioning between structure matrix and dose matrix implementing Gaussian filtering of the dose matrix. Based on results of Langen et al. (57) the standard deviation of a three-dimensional Gaussian kernel, was set to 0.92 mm, 1.59 mm and 1.54 mm for left-right, anterior-posterior and cranio-caudal, respectively.

Statistical Analysis

The Sörensen-dice coefficient was calculated for spatial overlap of GTV-Histo with GTV-Union, GTV-PET and GTV-MRI and for spatial overlap of PTV3_1, PTV3_2, PTV3_3 and GTV-Histo.

Statistical analysis of volumes was performed with GraphPad Prism v8.4.2 (GraphPad Sofware, USA). Data normality was tested using the Shapiro-Wilk test. For not normally distributed variables, Friedman test and uncorrected Dunn's test was used for comparison of more than two variables and two-sided Wilcoxon matched-pairs signed rank test was used for comparison of two variables (both at a significance level of 0.05). For normally distributed variables, repeated measures one-way ANOVA with the Geisser-Greenhouse correction and Fisher's LSD was used for comparison of more than two variables and two-sided paired t test was used for comparison of two variables (both at a significance level of 0.05). For statistical analysis of unpaired and not normally distributed data (minimum distance to urethra on H&E slices and CT images) Mann-Whitney test at a significance level of 0.05 was used.

Exploratory statistical analysis of *TCPs*, *NTCPs* and dosimetric analysis was performed with R (version 3.6.2) (58). Wilcoxon matched pairs signed-rank test was used with a significance level of 0.05.

RESULTS

Volumes and Distance of GTVs to Urethra

Median volume for GTV-Histo was 4.5 ml (IQR 1.8 – 6.9ml) and for GTV-Union 5.7 ml (IQR 2.9 – 13.3 ml). Median intersection volume of PRV-Urethra with GTV-Histo was 0.05 ml (IQR 0.00 - 0.25 ml) and with GTV-Union 0.1 ml (IQR 0.00 – 0.88 ml) respectively. Expressed in percentage of the PRV-urethra volume, intersection of GTV-Union with PRV-Urethra was median 1.6% (IQR 0.0 – 6.5%) and maximum 8.5% in patient 10. Please see **Supplementary Table 1** for details.

Median volumes for PTV3_1 was 13.5 ml (IQR 7.0 - 22.6 ml), for PTV3_2 13.2 ml (IQR 6.9 – 22.0 ml) and for PTV3_3 12.8 ml (IQR 6.6 – 20.6 ml), respectively. PTV3_3 was not statistically significantly smaller than PTV3_2 (p = 0.053) but significantly smaller than PTV3_1 (p = 0.031) (**Supplementary Table 2**).

The median intersection volume of GTV-Histo with PTV3_1, PTV3_2 and PTV3_3 was 2.7 ml (IQR 1.5 – 6.3), 2.7 ml (IQR 1.5 – 6.2) and 2.7 ml (1.4 – 5.9), respectively. There was no statistically significant difference between the DSCs for GTV-Histo and the three PTVs (p > 0.96) (**Supplementary Tables 2** and **3**).

Median coverage of GTV-Histo by GTV-Union, GTV-PET and GTV-MRI was 79% (IQR 55 – 97%), 76% (IQR 37 – 83%) and 53% (IQR 13 – 74%). Coverage by GTV-Union was significantly higher than by GTV-PET (p = 0.014) and GTV-MRI (p = 0.004), whereas there was no significant difference between GTV-PET and GTV-MRI (p = 0.058). Median coverage of GTV Histo by PTV3_1, PTV3_2 and PTV3_3 was 90% (IQR 70 – 92%), 89% (IQR 70 – 91%) and 85% (IQR 65 – 88%). Coverage by PTV3_3 was significantly lower than by PTV3_1 (p=0.016) (**Supplementary Tables 3** and **4**).

In 3 patients contact between GTV-Histo and urethra could be observed on H&E slices. In 6 patients contact between GTV-Union and urethra could be observed on *in-vivo* CT slices. Discrepancies between patients with detected contact on slices but without intersection volumes were manually verified. In all cases intersection volumes were present but too small to be quantified in Eclipse™ Treatment Planning System. The median minimum distance of GTV-Histo to urethra on each slice was 3.6 mm (IQR 2.2 – 7.3 mm) and median minimum distance of GTV-Union to urethra was 1.8 mm (IQR 0.0 – 5.0 mm). Distance of GTV-Union to urethra was statistically significantly smaller (p = 0.02). Median minimum distance of GTV-Histo to urethra per patient was 1.9 mm (IQR 0.0 – 3.6 mm) and median minimum distance of GTV-Union to urethra per patient was 0.0 mm (IQR 0.0 – 1.5mm). Again, distance of GTV-Union to urethra was statistically significantly smaller (p = 0.02).

Doses Distribution in Target Volumes

Median D98%, D50% and D2% doses for, PTV3_1-3 (boost volume), GTV-Histo, urethra and PRV-Urethra for plan 1-3 are shown in **Table 3** with and without consideration of the intrafractionary movement, respectively. Without consideration of intrafractionary movement following doses were statistically significant different: For PTV3 D98% of plans 2 and 3 were significantly smaller than for plan 1, whereas D50% showed no significant difference between the three plans. D2% was significantly higher in plans 2 and 3 than in plan 1. For GTV-Histo, only D98% was significantly lower for plan 2 and 3 compared to plan 1. With consideration of intrafractionary movement following doses were statistically significantly different:

For PTV3, D98% and D50% of plan 3 were slightly but significantly smaller compared to plan 1, whereas dose parameters of plan 2 showed no statistical significance to dose parameters of plan 3. D2% was significantly higher in plans 2 and 3 than in plan 1. For GTV-Histo D98% was significantly smaller and D2% significantly higher in plans 2 and 3 compared to plan 1.

Doses for urethra and PRV-urethra were significantly lower in both plan 2 and plan 3 compared to plan 1 in all cases. Furthermore, all doses were significantly lower in plan 3 compared to plan 2 except for D98% with movement. For details about p-values see **Supplementary Table 6**. **Figure 2** shows cumulative dose-volume-histograms for boost volumes, urethra, bladder and rectum without and with movement.

Constraints

All plans complied with the constraints for bladder and rectum.

Without consideration of intrafractional movement, in plan 1 (no dose constraints for urethra considered in optimization) constraints for D2% for urethra were not reached in the majority of the planed cases, 8 out of 10. In plan 2 (respecting dose constraints for urethra), constraints for D2% for PRV-urethra were not reached in 7 patients.

When intrafractional movement is considered, in plan 1 constraints for D2% for urethra were not reached again in in 8 patients. In plan 2, constraints for D2% for urethra were not reached in 4 patients and D2% for PRV-urethra in 7 patients.

In plan 3 urethra- and PRV-Urethra constraints were reached in all patients without and with movement consideration.

TCP/NTCP/P+ Without Intrafractional Movement

Please see **Table 4** for median P_+, $TCP_{GTV\text{-}Histo}$, $NTCP_{Urethra}$, $NTCP_{Bladder}$ and $NTCP_{Rectum}$ as well as p-values. Urethra-sparing resulted in significantly lower $NTCP_{Urethra}$ without significantly affecting $TCP_{GTV\text{-}Histo}$ or $NTCP_{Bladder}$ and $NTCP_{Rectum}$. Consequently, P_+ was statically significantly better for plans respecting urethral sparing. Radiobiological modeling was also performed by assuming α/β values of 1.2 Gy and 2.7 Gy for tumor tissue (see **Supplementary Tables 7** and **8**). Summarized $P+$ shows the same behavior for α/β = 1.2 Gy, whereas for α/β = 2.7 Gy no significant differences between all three plans could be observed. For the calculation of total probability of injury P_I, required for the complication free tumour control P_+ (Eq. 5), all three weighting factors w_j in Eq. 3 for the OARs are set to 1.0 (equal clinical importance). Analysis on patient level revealed, that P+ was higher in plan 2 and plan 3 compared to plan 1 in all patients.

TCP/NTCP/P+ With Intrafractional Movement

Implementation of intrafractional movement into the model yielded in even slightly higher P+ for both urethral sparring plans (**Table 5**).

TABLE 3 | Dose volume parameter values for different volumes without and with consideration of prostate intrafractional movement.

		Without movement			With movement		
		D98%	**D50%**	**D2%**	**D98%**	**D50%**	**D2%**
PTV3_1-3*	Plan 1	67.64 (67.27- 67.93)	70.1 (70.08 - 70.1)	71.86 (71.7 - 72.17)	65.76 (65.1 - 66.03)	69.1 (68.72- 69.33)	71.03 (70.69 - 71.14)
	Plan 2	67.0 (66.88 - 67.22)	70.1 (70.07 - 70.15)	72.23 (72.1 - 72.57)	65.77 (65.05 - 65.87)	69.02 (68.69 - 69.23)	71.13 (70.87 - 71.4)
	Plan 3	67.02 (66.9 - 67.25)	70.14 (70.12 - 70.22)	72.25 (72.13 - 72.59)	65.48 (64.96 - 65.74)	68.94 (68.69 - 69.15)	71.31 (70.89 - 71.55)
GTV-Histo	Plan 1	68.55 (66.6, 69.02)	70.69 (70.53, 70.84)	72.1 (71.79, 72.76)	67.34 (65.57, 68.01)	70.26 (69.48, 70.34)	71.16 (70.82, 71.35)
	Plan 2	66.35 (65.37, 67.82)	70.73 (70.32, 70.94)	72.51 (72.28, 72.87)	67.05 (65.26, 67.22)	69.92 (69.36, 70.45)	71.42 (70.93, 71.71)
	Plan 3	64.51 (64.01, 66.97)	70.6 (70.31, 70.75)	72.63 (72.4, 72.95)	65.71 (64.26, 66.75)	69.92 (69.08, 70.21)	71.64 (70.91, 71.84)
Urethra	Plan 1	59.34 (58.96 - 59.71)	65.95 (62.66 - 66.73)	70.15 (69.66 - 70.69)	57.92 (55.83 - 60.38)	65.45 (62.48 - 66.55)	69.33 (68.74 - 70.27)
	Plan 2	58.27 (57.85 - 58.59)	61.63 (61.34 - 62.4)	66.35 (65.29 - 66.46)	57.79 (56.32 - 59.35)	62.4 (61.57 - 63.65)	66.97 (66.06 - 67.53)
	Plan 3	58.15 (57.49 -58.23)	60.99 (60.54 - 61.58)	64.01 (63.69 - 64.5)	57.64 (56.06 - 59.16)	61.79 (61.22 - 62.51)	65.16 (64.88 - 65.33)
PRV-Urethra	Plan 1	58.69 (58.48- 59.41)	65.47 (62.4 - 66.29)	70.55 (70.06 - 71.24)	55.95 (52.34 - 58.79)	64.95 (62.18 - 66.04)	69.72 (69.16 - 70.46)
	Plan 2	58.24 (57.7 - 58.37)	61.81 (61.2 - 62.73)	68.49 (67.54 - 69.17)	55.94 (53.09 - 58.03)	62.37 (61.2 - 63.63)	68.19 (67.16 - 68.54)
	Plan 3	57.92 (57.37 - 58.32)	60.87 (60.69 - 61.85)	66.62 (66.13 - 66.81)	55.9 (52.85 - 57.75)	61.74 (60.87 - 62.61)	66.53 (66.26 - 66.81)

*Values in parenthesis represent the observed min-max value range. Dosimetry for PTV3_1-3 (boost volume), GTV-Histo, Urethra, and PRV-Urethra is shown. *Plan 1 is based on PTV3_1, plan 2 on PTV3_2 and plan 3 on PTV3_3.*

For median P_+, $TCP_{GTV\text{-}Histo}$, $NTCP_{Urethra}$, $NTCP_{Bladder}$ and $NTCP_{Rectum}$ as well as p-values considering intrafractional movement see **Table 5**. Radiobiological modeling was performed by assuming α/β values of 1.2 Gy and 2.7 Gy for tumor tissue (see **Supplementary Tables 9** and **10**), and summarized P_+ shows again the same behavior for α/β = 1.2 Gy, whereas for α/β = 2.7 Gy no significant differences between all three plans could be observed. Analysis on patient level revealed, that P+ was higher in plan 2 and plan 3 compared to plan 1 in all patients.

Re-run of $NTCP_{Urethra}$, calculation in order to consider uncertainties, showed no deviation from initial outcomes.

DISCUSSION

In the context of focal escalation, the results of our planning study demonstrate that boosting of PSMA-PET/CT and mpMRI defined GTVs using MHRT is technically feasible and prescription doses as well as dose constraints are achieved even when considering organ movement. Furthermore, urethral sparing achieves significantly lower *NTCPs* for urethral toxicities without affecting *TCPs* and *NTCPs* for bladder and rectum, consequently results in a better therapeutic ratio in terms of P_+ and should be implemented in focal RT dose escalation concepts. We discuss the different aspects in the following sections in detail.

Urethra sparing is performed in SBRT and brachytherapy, since higher urethral doses are associated with higher GU toxicities (59, 60). The recently published toxicity reports of the hypoFlame trial suggest that prioritization of OAR constraints yields acceptable toxicities for focal dose escalation using SBRT. At the time of publication, the only published toxicity reports of trials investigating moderately-hyofractionated dose escalation and urethral sparing was the DELINEATE trial, which used MRI-defined boost volumes with dose escalation up to 67 Gy and showed slightly higher, but comparable acute and late GI and GU toxicity rates to dose escalation with conventional fractionation (34). In the cohort receiving focal dose escalated MHRT cumulative grade 2 or worse GU and GI toxicities after 3 years were 22.1% and 14.0%, respectively. The dose regimen chosen in our study utilized a higher prescription dose of 70 Gy for the boost volume defined by validated contouring approaches for GTV definition of PET and mpMRI imaging modalities (29, 61). Not surprisingly, volumes for GTV-Union (median 5.7 ml, IQR 2.9 – 13.3 ml) were significantly larger than GTV-Histo (median 4.5 ml, IQR 1.8 – 6.9 ml, p = 0.01). Consequently, prioritization of maintaining standard toxicity rates is pivotal when boosting larger volumes and therefore we conducted this planning study to evaluate the effect of urethral sparing on *NTCPs* and *TCP* to evaluate its potential in MHRT with focal dose escalation with this novel boost volume definition.

Constraints and prescription doses were achieved for all patients as intended in the respective plans. This also applies when implementing organ movement into the plan evaluation. These results suggest that putative negative consequences in

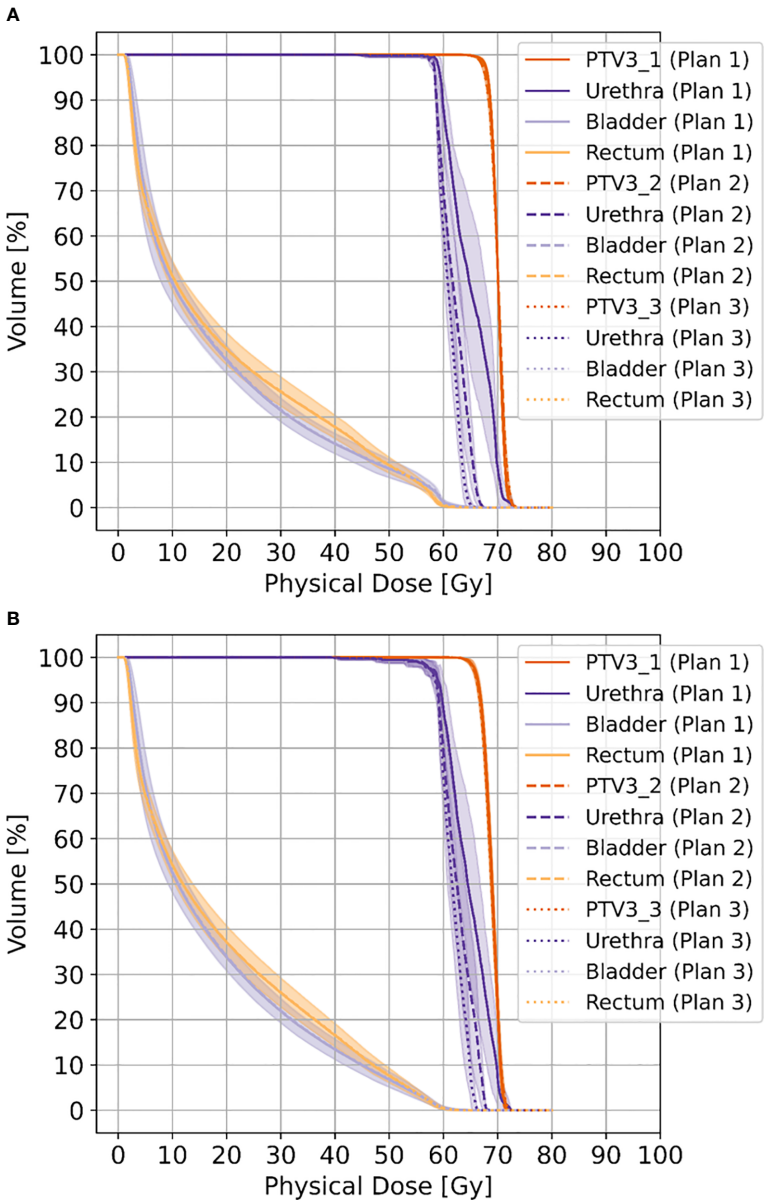

FIGURE 2 | Shows cumulative dose-volume-histograms for boost volumes (PTV3_1-3), urethra, bladder and rectum without movement **(A)** and with movement **(B)**, respectively.

terms of under- or overdosing were not relevant and consequently organ movement did not affect the highly conformal IMRT plans. Furthermore, we confirmed the feasibility of the applied dose and constraint prescription.

To evaluate the impact of urethra-sparing we chose as endpoint for $NTCP_{\mathrm{Urethra}}$ stricture requiring urethrectomy within 4 years based on the LKB model by Panettiere et al. (21). Based on recently published α/β values from Vogelius et al. we used an α/β of 1.6 Gy to calculate the *TCP*. Considering the published range for α/β values, we performed the same analysis with an α/β 1.2 Gy and 2.7 Gy. Application of 1.2 Gy yielded similar results with a significant better *P+* for plan 3 (0.924 and 0.9285 without and with movement, respectively, p = <0.01), whereas application of 2.7 Gy resulted in no significant improvement of P_+ (see **Supplementary Tables 7–10**). However, the mentioned meta-analysis suggests that α/β of 2.7 Gy is likely to be too high, particularly in a setting of hypofractionation. Therefore, we refer on the results derived from α/β of 1.6 in the following. Urethral sparing in IMRT planning significantly reduced the median $NTCP_{Urethra}$ from

TABLE 4 | Median P_+, TCP- and NTCP-values for plans 1-3, as well as p-values for comparison of plan 1 *vs* 2 and 3, respectively, not considering intrafractional movement with α/β 1.6 Gy for tumor tissue and 3 Gy for bladder and rectum.

	P_+	$TCP_{GTV\text{-}Histo}$	$NTCP_{Urethra}$	$NTCP_{Bladder}$	$NTCP_{Recutm}$
Plan 1	0.888	0.997	0.072	0.023	0.009
Plan 2	0.919	0.995	0.047	0.022	0.009
Plan 3	0.919	0.992	0.042	0.023	0.009
			p-value		
Plan 1 *vs* Plan 2	0.006	0.492	0.002	1.0	0.846
Plan 1 *vs* Plan 3	0.006	0.275	0.002	0.846	0.846
Plan 2 *vs* Plan 3	0.922	0.625	0.037	1.0	1.0

The Lyman-Kutcher-Burman model with an α/β of 5 Gy was applied for urethra.

TABLE 5 | Median P_+, TCP- and NTCP-values for plans 1-3, as well as p-values for comparison of plan 1 *vs* 2 and 3, respectively, considering intrafractional movement with α/β 1.6 Gy for tumor tissue and 3 Gy for bladder and rectum.

	P_+	$TCP_{GTV\text{-}Histo}$	$NTCP_{Urethra}$	$NTCP_{Bladder}$	$NTCP_{Recutm}$
Plan 1	0.900	0.995	0.069	0.013	0.006
Plan 2	0.919	0.994	0.051	0.012	0.006
Plan 3	0.923	0.992	0.047	0.012	0.006
			p-value		
Plan 1 *vs* Plan 2	0.027	0.625	0.006	0.922	1.0
Plan 1 *vs* Plan 3	0.020	0.322	0.002	0.846	0.846
Plan 2 *vs* Plan 3	1.0	0.625	0.131	1.0	0.846

A Lyman-Kutcher-Burman model with an α/β of 5 Gy was applied for urethra.

7.2% up to 4.2% (p=0.002) with only minimal and statically not significant reduction of median *TCP* from 99.7% up to 99.2% (p = 0.105). Noteworthy, $NTCP_{Bladder}$ and $NTCP_{Rectum}$ were not affected by urethral sparing, precluding the possibility of improving $NTCP_{Urethra}$ at the costs of other toxicities. Consequently, urethral sparing resulted in significantly better P_+ value (88.8% *vs* up to 91.9%, p = 0.006). Considering that the urethra is a serial organ the minimum distance of urethra to PCa is of particular clinical relevance. Evaluation of minimum distances of GTV-Union to urethra was significantly smaller than GTV-Histo and in 60% of patients, contact of GTV-Union with urethra could be determined, supporting the rationale of urethra sparing. The minimal impact on *TCP* can be attributed to the small intersection of PCa tissue and urethra. Even applying a margin to the urethra resulted in intersection of GTV-Histo and PRV-Urethra of median 0.8% and maximum 6.4%, intersection of GTV-Union with PRV-Urethra was median 1.6% and maximum 8.5%. Considering volume analysis subtraction of PRV-Urethra from PTV3 resulted in slightly, but significantly smaller PTV-volumes, as well as slightly but significantly lower coverage of GTV-Histo. Nevertheless, coverage was still very high (85%) and even though doses partly showed significant differences between IMRT plans, the mentioned differences had no significant consequences on $TCP_{GTV\text{-}Histo}$. Additionally, coverage of GTV-Histo by GTV-Union was statistically significantly higher than by GTV-PET or GTV-MRI, supporting the rationale to implement both imaging modalities in boost volume definition. Overall results of volumetric analysis and TCP/NTCP calculation suggest that boosting of GTV-Union is compatible with sufficient urethra sparing in most cases. A study by Leibovich et al., which found that the mean distance from the urethra to the nearest cancer was 3mm (62). In our study median distance of GTV-Histo to urethra was comparable with 3.6 mm. Even though contact with urethra was detectable in the majority of cases, intersection volumes were very small, supporting the estimation of little consequences of intersection of urethra and GTV.

Comparison of our results with different planning studies is hampered due to lack of data. One other study evaluated $NTCP_{Urethra}$ and showed extremely high NTCP-values >60% by using *TD50* of 70.7 Gy (63). The results of our study are still higher than clinical reported urethral stricture rates after external beam RT (EBRT) ranging between 2-3%, nevertheless applied doses were lower and these studies did not use focal dose escalation (64–66). Considering this aspect our results represent realistic estimations and should be compared with eagerly awaited long term results of clinical trials investigating focal dose escalated EBRT.

Additionally, we simulated intrafractional organ movement in order to evaluate its consequences on IMRT plans and TCP/NTCP calculation. This implementation had slightly positive effects on P_+. Furthermore, urethral sparing did still significantly reduce $NTCP_{Urethra}$ (from 7.2% to 4.3%) without significantly affecting TCP_{Histo}, $NTCP_{Bladder}$ or $NTCP_{Rectum}$. Remarkable $NTCP_{Bladder}$ and $NTCP_{Rectum}$ were even slightly better. These results suggest that intrafractional movement potentially influences positively P_+ and the used margins were adequate to compensate intrafractional movements. This complies with previously reported results by Thomann et al., which demonstrated this effect in cases where boost volumes do not fully comply with GTV-Histo (22). These results are encouraging that urethral sparing might significantly reduce GU toxicities without significantly affecting tumour control, in particular since all patients in our study benefited from urethral sparing in terms of improved P+-values in plan 2 or 3 compared to plan 1. In order to evaluate the clinical benefit of this approach it should be evaluated in clinical trials. This enables to evaluate, whether specific patient subgroups don't benefit from this approach. Likely, in patients with high tumour burden or niches with radio-resistant PCa cells (67) surrounding the urethra, sparing might not be an advantage. Whether a threshold in terms of absolute or relative volume of intersection between PRV-urethra and boost-PTV exist, from which on positive effects are reversed, should be evaluated in further studies and larger cohorts. In this context, individual radiosensitivity might be another important aspect, possibly causing a reduced tumour control with urethral sparing in patients with low radiosensitivity and a negligible impact of urethra sparing in patients with high radiosensitivity due to sufficient dose delivery. We estimated an equal radiosensitivity for all patients in our planning study. To the

best of our knowledge validated surrogate parameters to determine radiosensitivity are missing and our data don't allow do draw conclusions in this regard. Future research might enable to consider this aspect. However, urethra sparing offers another tool for individualizing radiotherapy and acknowledging patients' preferences, for instance a high demand for safety *vs.* tumour control.

Furthermore, adherence to high quality of image acquisition (68), image co-registration (69) as well as accuracy of delineation (29, 70) and radiation delivery (71) is a prerequisite for implementation of this individualized radiotherapy approach. In the context of delineation, progress in diagnostics has to be considered. Regarding PSMA-PET/CT, Fluorine-18-labeled tracers like 18F-PSMA-1007 have been implemented in nuclear medicine practise. Current research shows, that 18F-PSMA-1007 shows very high sensitivities and high specificities (70, 72). Since accurate delineation of boost volumes for focal therapy approaches depends on the applied windowing (73), usage of validated contouring approaches is necessary (13). Whether usage of 18F-PSMA-1007 affects TCP calculation compared to 68Ga-PSMA should be evaluated in future studies.

We acknowledge the limitations of our study. Firstly, it should be mentioned that the NTCP for the urethra was modeled based on a previous publication of Panettieri et al. (21). The analysis was based on 258 which received EBRT and brachytherapy. Thus, without loss of the generality our analysis was based on a parameter-set, which has been modeled with combined treatment. Secondly, we enrolled a relatively small number of patients, which is a result of the elaborate co-registration pathway of the histopathologic specimens. Thirdly, the co-registration between histopathologic 3D-volumes and cross-sectional images bears risks of uncertainty due to non-linear shrinkage of the prostate after prostatectomy and co-registration mismatch susceptibilities. Consequently, coverage of GTV-Histo boost volumes might lack precision. Fourthly, used models for *TCP* and *NTCP* calculation could not be validated with the institutions own experiences, since the follow-up database of patients treated with mildly hypofractionated EBRT was not sufficient. Fifthly, co-registered images were acquired in a diagnostic setup, potentially affecting image registration and dose calculation. Therefore, the included patients, which are part of a larger cohort, were selected in terms of bowel and bladder preparation and positioning enable BRT planning. However, our experiences for image co-registration are in line with a recently published study, demonstrating no significant differences in MRI acquisition in diagnostic and radiotherapy setups (74). Furthermore, different PET/CT and MRI scanners were used. This limitation was considered by cross-calibration of the PET scanners and a reasonable and recommended slice thickness of 3 mm was acquired in all patients.

DATA AVAILABILITY STATEMENT

The raw data supporting the conclusions of this article will be made available by the authors, without undue reservation.

ETHICS STATEMENT

The studies involving human participants were reviewed and approved by Institutional review board of the Albert-Ludwigs-University of Freiburg. The patients/participants provided their written informed consent to participate in this study.

AUTHOR CONTRIBUTIONS

SS, IS, and CZ contributed to conception and design of the study. RW and BT created IMRT plans. MB, IS, and DB implemented intrafractional movement modeling. SS and IS conducted the statistical analysis. AS was involved in surgery indication and prostatectomy. PB conducted the histopathological processing and marking of tumor lesions. JR was responsible for conduction and reporting of the PSMA-PET/CTs. MB was responsible for conduction and reporting of the mpMRIs. TS, NN, DB, and AG supervised the study. SS and IS wrote the first draft of the manuscript. CZ wrote sections of the manuscript. All authors contributed to the article and approved the submitted version.

FUNDING

Ilias Sachpazidis and Constantinos Zamboglou received funding from the "Dekade gegen Krebs" initiative from the BMBF. SS received funding from the EraPERMED Call 2019 (PersoRad, BMBF). Material and publication fee is funded by the EraPERMED Call 2019 (PersoRad, BMBF).

SUPPLEMENTARY MATERIAL

The Supplementary Material for this article can be found online at: https://www.frontiersin.org/articles/10.3389/fonc.2021.652678/full#supplementary-material

REFERENCES

1. Martinez AA, Gonzalez J, Ye H, Ghilezan M, Shetty S, Kernen K, et al. Dose Escalation Improves Cancer-Related Events At 10 Years for Intermediate- and High-Risk Prostate Cancer Patients Treated With Hypofractionated High-Dose-Rate Boost and External Beam Radiotherapy. *Int J Radiat Oncol Biol Phys* (2011) 79(2):363–70. doi: 10.1016/j.ijrobp.2009.10.035
2. Michalski JM, Moughan J, Purdy J, Bosch W, Bruner DW, Bahary JP, et al. Effect of Standard vs Dose-Escalated Radiation Therapy for Patients With Intermediate-Risk Prostate Cancer: The NRG Oncology RTOG 0126 Randomized Clinical Trial. *JAMA Oncol* (2018) 4(6):e180039. doi: 10.1001/jamaoncol.2018.0039
3. Morris WJ, Tyldesley S, Rodda S, Halperin R, Pai H, McKenzie M, et al. Androgen Suppression Combined With Elective Nodal and Dose Escalated

Radiation Therapy (the ASCENDE-RT Trial): An Analysis of Survival Endpoints for a Randomized Trial Comparing a Low-Dose-Rate Brachytherapy Boost to a Dose-Escalated External Beam Boost for High- and Intermediate-risk Prostate Cancer. *Int J Radiat Oncol Biol Phys* (2017) 98 (2):275–85. doi: 10.1016/j.ijrobp.2016.11.026

4. Kerkmeijer LGW, Groen VH, Pos FJ, Haustermans K, Monninkhof EM, Smeenk RJ, et al. Focal Boost to the Intraprostatic Tumor in External Beam Radiotherapy for Patients With Localized Prostate Cancer: Results From the FLAME Randomized Phase III Trial. *J Clin Oncol* (2021) 39(7):787–96. doi: 10.1200/JCO.20.02873
5. Lips IM, van der Heide UA, Haustermans K, van Lin EN, Pos F, Franken SP, et al. Single Blind Randomized Phase III Trial to Investigate the Benefit of a Focal Lesion Ablative Microboost in Prostate Cancer (Flame-Trial): Study Protocol for a Randomized Controlled Trial. *Trials* (2011) 12:255. doi: 10.1186/1745-6215-12-255
6. Ahlering T, Huynh LM, Kaler KS, Williams S, Osann K, Joseph J, et al. Unintended Consequences of Decreased PSA-Based Prostate Cancer Screening. *World J Urol* (2019) 37(3):489–96. doi: 10.1007/s00345-018-2407-3
7. Kasivisvanathan V, Rannikko AS, Borghi M, Panebianco V, Mynderse LA, Vaarala MH, et al. Mri-Targeted or Standard Biopsy for Prostate-Cancer Diagnosis. *New Engl J Med* (2018) 378(19):1767–77. doi: 10.1056/NEJMoa1801993
8. Berger I, Annabattula C, Lewis J, Shetty DV, Kam J, Maclean F, et al. (68)Ga-Psma PET/CT vs. mpMRI for Locoregional Prostate Cancer Staging: Correlation With Final Histopathology. *Prostate Cancer Prostatic Dis* (2018) 21(2):204–11. doi: 10.1038/s41391-018-0048-7
9. Bettermann AS, Zamboglou C, Kiefer S, Jilg CA, Spohn S, Kranz-Rudolph J, et al. [(68)Ga-]Psma-11 PET/CT and Multiparametric MRI for Gross Tumor Volume Delineation in a Slice by Slice Analysis With Whole Mount Histopathology as a Reference Standard - Implications for Focal Radiotherapy Planning in Primary Prostate Cancer. *Radiother Oncol J Eur Soc Ther Radiol Oncol* (2019) 141:214–9. doi: 10.1016/j.radonc.2019.07.005
10. Chen M, Zhang Q, Zhang C, Zhao X, Marra G, Gao J, et al. Combination of (68)Ga-PSMA PET/CT and Multiparameter Mri Improves the Detection of Clinically Significant Prostate Cancer: A Lesion by Lesion Analysis. *J Nucl Med* (2019) 60(7):944–9. doi: 10.2967/jnumed.118.221010
11. Eiber M, Weirich G, Holzapfel K, Souvatzoglou M, Haller B, Rauscher I, et al. Simultaneous 68ga-Psma HBED-CC Pet/Mri Improves the Localization of Primary Prostate Cancer. *Eur Urol* (2016) 70(5):829–36. doi: 10.1016/j.eururo.2015.12.053
12. Scheltema MJ, Chang JI, Stricker PD, van Leeuwen PJ, Nguyen QA, Ho B, et al. Diagnostic Accuracy of (68) Ga-prostate-specific Membrane Antigen (Psma) Positron-Emission Tomography (PET) and Multiparametric (Mp) MRI to Detect Intermediate-Grade Intra-Prostatic Prostate Cancer Using Whole-Mount Pathology: Impact of the Addition of (68) Ga-PSMA PET to Mpmri. *BJU Int* (2019) 124(Suppl 1):42–9. doi: 10.1111/bju.14794
13. Spohn S, Jaegle C, Fassbender TF, Sprave T, Gkika E, Nicolay NH, et al. Intraindividual Comparison Between (68)Ga-PSMA-PET/CT and mpMRI for Intraprostatic Tumor Delineation in Patients With Primary Prostate Cancer: A Retrospective Analysis in 101 Patients. *Eur J Nucl Med Mol Imaging* (2020) 47:2796–803. doi: 10.1007/s00259-020-04827-6
14. Hofman MS, Lawrentschuk N, Francis RJ, Tang C, Vela I, Thomas P, et al. Prostate-Specific Membrane Antigen PET-CT in Patients With High-Risk Prostate Cancer Before Curative-Intent Surgery or Radiotherapy (Propsma): A Prospective, Randomised, Multicentre Study. *Lancet (London England)* (2020) 395(10231):1208–16. doi: 10.1016/S0140-6736(20)30314-7
15. Johnson DC, Raman SS, Mirak SA, Kwan L, Bajgiran AM, Hsu W, et al. Detection of Individual Prostate Cancer Foci Via Multiparametric Magnetic Resonance Imaging. *Eur Urol* (2019) 75(5):712–20. doi: 10.1016/j.eururo.2018.11.031
16. Priester A, Natarajan S, Khoshnoodi P, Margolis DJ, Raman SS, Reiter RE, et al. Magnetic Resonance Imaging Underestimation of Prostate Cancer Geometry: Use of Patient Specific Molds to Correlate Images With Whole Mount Pathology. *J Urol* (2017) 197(2):320–6. doi: 10.1016/j.juro.2016.07.084
17. Sachpazidis I, Mavroidis P, Zamboglou C, Klein CM, Grosu A-L, Baltas D. Prostate Cancer Tumour Control Probability Modelling for External Beam Radiotherapy Based on Multi-Parametric Mri-GTV Definition. *Radiat Oncol* (2020) 15(1):242. doi: 10.1186/s13014-020-01683-4
18. Goodman CD, Fakir H, Pautler S, Chin J, Bauman GS. Dosimetric Evaluation of PSMA Pet-Delineated Dominant Intraprostatic Lesion Simultaneous Infield Boosts. *Adv Radiat Oncol* (2020) 5(2):212–20. doi: 10.1016/j.adro.2019.09.004
19. Zamboglou C, Sachpazidis I, Koubar K, Drendel V, Wiehle R, Kirste S, et al. Evaluation of Intensity Modulated Radiation Therapy Dose Painting for Localized Prostate Cancer Using (68)Ga-HBED-CC Psma-Pet/Ct: A Planning Study Based on Histopathology Reference. *Radiother Oncol* (2017) 123(3):472–7. doi: 10.1016/j.radonc.2017.04.021
20. Zamboglou C, Thomann B, Koubar K, Bronsert P, Krauss T, Rischke HC, et al. Focal Dose Escalation for Prostate Cancer Using (68)Ga-Hbed-Cc PSMA PET/CT and MRI: A Planning Study Based on Histology Reference. *Radiat Oncol* (2018) 13(1):81. doi: 10.1186/s13014-018-1036-8
21. Panettieri V, Rancati T, Onjukka E, Ebert MA, Joseph DJ, Denham JW, et al. External Validation of a Predictive Model of Urethral Strictures for Prostate Patients Treated With HDR Brachytherapy Boost. *Front Oncol* (2020) 10:910. doi: 10.3389/fonc.2020.00910
22. Thomann B, Sachpazidis I, Koubar K, Zamboglou C, Mavroidis P, Wiehle R, et al. Influence of Inhomogeneous Radiosensitivity Distributions and Intrafractional Organ Movement on the Tumour Control Probability of Focused IMRT in Prostate Cancer. *Radiother Oncol* (2018) 127(1):62–7. doi: 10.1016/j.radonc.2018.02.006
23. Eder M, Neels O, Müller M, Bauder-Wüst U, Remde Y, Schäfer M, et al. Novel Preclinical and Radiopharmaceutical Aspects of [68Ga]Ga-PSMA-HBED-CC: A New PET Tracer for Imaging of Prostate Cancer. *Pharmaceuticals (Basel Switzerland)* (2014) 7(7):779–96. doi: 10.3390/ph7070779
24. Surti S, Kuhn A, Werner ME, Perkins AE, Kolthammer J, Karp JS. Performance of Philips Gemini TF Pet/Ct Scanner With Special Consideration for its Time-of-Flight Imaging Capabilities. *J Nucl Med Off Publication Soc Nucl Med* (2007) 48(3):471–80.
25. Rausch I, Ruiz A, Valverde-Pascual I, Cal-González J, Beyer T, Carrio I. Performance Evaluation of the Vereos Pet/Ct System According to the NEMA Nu2-2012 Standard. *J Nucl Med* (2019) 60(4):561–7. doi: 10.2967/jnumed.118.215541
26. Zamboglou C, Carles M, Fechter T, Kiefer S, Reichel K, Fassbender TF, et al. Radiomic Features From PSMA PET for non-Invasive Intraprostatic Tumor Discrimination and Characterization in Patients With Intermediate- and High-Risk Prostate Cancer - a Comparison Study With Histology Reference. *Theranostics* (2019) 9(9):2595–605. doi: 10.7150/thno.32376
27. Weinreb JC, Barentsz JO, Choyke PL, Cornud F, Haider MA, Macura KJ, et al. Pi-Rads Prostate Imaging - Reporting and Data System: 2015, Version 2. *Eur Urol* (2016) 69(1):16–40. doi: 10.1016/j.eururo.2015.08.052
28. Zamboglou C, Wieser G, Hennies S, Rempel I, Kirste S, Soschynski M, et al. Mri Versus ^{6} ^{8}Ga-Psma PET/CT for Gross Tumour Volume Delineation in Radiation Treatment Planning of Primary Prostate Cancer. *Eur J Nucl Med Mol Imaging* (2016) 43(5):889–97. doi: 10.1007/s00259-015-3257-5
29. Zamboglou C, Fassbender TF, Steffan L, Schiller F, Fechter T, Carles M, et al. Validation of Different PSMA-PET/CT-Based Contouring Techniques for Intraprostatic Tumor Definition Using Histopathology as Standard of Reference. *Radiother Oncol* (2019) 141:208–13. doi: 10.1016/j.radonc.2019.07.002
30. Gay HA, Barthold HJ, O'Meara E, Bosch WR, El Naqa I, Al-Lozi R, et al. Pelvic Normal Tissue Contouring Guidelines for Radiation Therapy: A Radiation Therapy Oncology Group Consensus Panel Atlas. *Int J Radiat Oncol Biol Phys* (2012) 83(3):e353–62. doi: 10.1016/j.ijrobp.2012.01.023
31. Draulans C, van der Heide UA, Haustermans K, Pos FJ, van der Voort van Zyp J, De Boer H, et al. Primary Endpoint Analysis of the Multicentre Phase II Hypo-FLAME Trial for Intermediate and High Risk Prostate Cancer. *Radiother Oncol J Eur Soc Ther Radiol Oncol* (2020) 147:92–8. doi: 10.1016/j.radonc.2020.03.015
32. Salembier C, Villeirs G, De Bari B, Hoskin P, Pieters BR, Van Vulpen M, et al. Estro ACROP Consensus Guideline on CT- and MRI-based Target Volume Delineation for Primary Radiation Therapy of Localized Prostate Cancer. *Radiother Oncol J Eur Soc Ther Radiol Oncol* (2018) 127(1):49–61. doi: 10.1016/j.radonc.2018.01.014

33. Zamboglou C, Drendel V, Jilg CA, Rischke HC, Beck TI, Schultze-Seemann W, et al. Comparison of (68)Ga-HBED-CC PSMA-PET/CT and Multiparametric MRI for Gross Tumour Volume Detection in Patients With Primary Prostate Cancer Based on Slice by Slice Comparison With Histopathology. *Theranostics* (2017) 7(1):228–37. doi: 10.7150/thno.16638
34. Murray JR, Tree AC, Alexander EJ, Sohaib A, Hazell S, Thomas K, et al. Standard and Hypofractionated Dose Escalation to Intraprostatic Tumor Nodules in Localized Prostate Cancer: Efficacy and Toxicity in the DELINEATE Trial. *Int J Radiat Oncol* (2020) 106(4):715–24. doi: 10.1016/j.ijrobp.2019.11.402
35. Dearnaley D, Syndikus I, Mossop H, Khoo V, Birtle A, Bloomfield D, et al. Conventional Versus Hypofractionated High-Dose Intensity-Modulated Radiotherapy for Prostate Cancer: 5-Year Outcomes of the Randomised, non-Inferiority, Phase 3 CHHiP Trial. *Lancet Oncol* (2016) 17(8):1047–60. doi: 10.1016/S1470-2045(16)30102-4
36. Wilkins A, Naismith O, Brand D, Fernandez K, Hall E, Dearnaley D, et al. Derivation of Dose/Volume Constraints for the Anorectum From Clinician- and Patient-Reported Outcomes in the CHHiP Trial of Radiation Therapy Fractionation. *Int J Radiat Oncol Biol Phys* (2020) 106(5):928–38. doi: 10.1016/j.ijrobp.2020.01.003
37. Munro TR, Gilbert CW. The Relation Between Tumour Lethal Doses and the Radiosensitivity of Tumour Cells. *Br J Radiol* (1961) 34:246–51. doi: 10.1259/0007-1285-34-400-246
38. Brahme A, Argren AK. Optimal Dose Distribution for Eradication of Heterogeneous Tumors. *Acta Oncol* (1987) 26(5):377–85. doi: 10.3109/02841868709104364
39. Lind BK, Mavroidis P, Hyödynmaa S, Kappas C. Optimization of the Dose Level for a Given Treatment Plan to Maximize the Complication-Free Tumor Cure. *Acta Oncol (Stockholm Sweden)* (1999) 38(6):787–98. doi: 10.1080/028418699432950
40. Wheldon TE, Deehan C, Wheldon EG, Barrett A. The Linear-Quadratic Transformation of Dose–Volume Histograms in Fractionated Radiotherapy. *Radiother Oncol* (1998) 46(3):285–95. doi: 10.1016/S0167-8140(97)00162-X
41. Yorke ED. Modeling the Effects of Inhomogeneous Dose Distributions in Normal Tissues. *Semin Radiat Oncol* (2001) 11(3):197–209. doi: 10.1053/srao.2001.23478
42. van Lin EN, Fütterer JJ, Heijmink SW, van der Vight LP, Hoffmann AL, van Kollenburg P, et al. Imrt Boost Dose Planning on Dominant Intraprostatic Lesions: Gold Marker-Based Three-Dimensional Fusion of CT With Dynamic Contrast-Enhanced and 1H-Spectroscopic Mri. *Int J Radiat Oncol Biol Phys* (2006) 65(1):291–303. doi: 10.1016/j.ijrobp.2005.12.046
43. Casares-Magaz O, van der Heide UA, Rørvik J, Steenbergen P, Muren LP. A Tumour Control Probability Model for Radiotherapy of Prostate Cancer Using Magnetic Resonance Imaging-Based Apparent Diffusion Coefficient Maps. *Radiother Oncol J Eur Soc Ther Radiol Oncol* (2016) 119(1):111–6. doi: 10.1016/j.radonc.2016.02.030
44. Ghobadi G, de Jong J, Hollmann BG, van Triest B, van der Poel HG, Vens C, et al. Histopathology-Derived Modeling of Prostate Cancer Tumor Control Probability: Implications for the Dose to the Tumor and the Gland. *Radiother Oncol J Eur Soc Ther Radiol Oncol* (2016) 119(1):97–103. doi: 10.1016/j.radonc.2016.02.015
45. Vogelius IR, Bentzen SM. Diminishing Returns From Ultrahypofractionated Radiation Therapy for Prostate Cancer. *Int J Radiat Oncol Biol Phys* (2020) 107(2):299–304. doi: 10.1016/j.ijrobp.2020.01.010
46. Bostel T, Sachpazidis I, Splinter M, Bougatf N, Fechter T, Zamboglou C, et al. Dosimetric Impact of Interfractional Variations in Prostate Cancer Radiotherapy—Implications for Imaging Frequency and Treatment Adaptation. *Front Oncol* (2019) 9:(940). doi: 10.3389/fonc.2019.00940
47. Takam R, Bezak E, Yeoh EE, Marcu L. Assessment of Normal Tissue Complications Following Prostate Cancer Irradiation: Comparison of Radiation Treatment Modalities Using NTCP Models. *Med Phys* (2010) 37(9):5126–37. doi: 10.1118/1.3481514
48. Kuang Y, Wu L, Hirata E, Miyazaki K, Sato M, Kwee SA. Volumetric Modulated Arc Therapy Planning for Primary Prostate Cancer With Selective Intraprostatic Boost Determined by 18F-Choline Pet/Ct. *Int J Radiat Oncol Biol Phys* (2015) 91(5):1017–25. doi: 10.1016/j.ijrobp.2014.12.052
49. Liu M, Moiseenko V, Agranovich A, Karvat A, Kwan W, Saleh ZH, et al. Normal Tissue Complication Probability (NTCP) Modeling of Late Rectal Bleeding Following External Beam Radiotherapy for Prostate Cancer: A Test of the QUANTEC-recommended NTCP Model. *Acta Oncol (Stockholm Sweden)* (2010) 49(7):1040–4. doi: 10.3109/0284186X.2010.509736
50. Peeters ST, Hoogeman MS, Heemsbergen WD, Hart AA, Koper PC, Lebesque JV. Rectal Bleeding, Fecal Incontinence, and High Stool Frequency After Conformal Radiotherapy for Prostate Cancer: Normal Tissue Complication Probability Modeling. *Int J Radiat Oncol Biol Phys* (2006) 66(1):11–9. doi: 10.1016/j.ijrobp.2006.03.034
51. Sachpazidis I, Hense J, Mavroidis P, Gainey M, Baltas D. Investigating the Role of Constrained CVT and CVT in HIPO Inverse Planning for HDR Brachytherapy of Prostate Cancer. *Med Phys* (2019) 46(7):2955–68. doi: 10.1002/mp.13564
52. Splinter M, Bostel T, Sachpazidis I, Fechter T, Zamboglou C, Jäkel O, et al. Dosimetric Impact of Interfractional Variations for Post-prostatectomy Radiotherapy to the Prostatic Fossa—Relevance for the Frequency of Position Verification Imaging and Treatment Adaptation. *Fron Oncol* (2019) 9(1191). doi: 10.3389/fonc.2019.01191
53. Mavroidis P, Ferreira BC, Papanikolaou N, Lopes Mdo C. Analysis of Fractionation Correction Methodologies for Multiple Phase Treatment Plans in Radiation Therapy. *Med Phys* (2013) 40(3):031715. doi: 10.1118/1.4792636
54. Roland T, Mavroidis P, Gutierrez A, Goytia V, Papanikolaou N. A Radiobiological Analysis of the Effect of 3D Versus 4d Image-Based Planning in Lung Cancer Radiotherapy. *Phys Med Biol* (2009) 54(18):5509–23. doi: 10.1088/0031-9155/54/18/011
55. Deb P, Fielding A. Radiobiological Model Comparison of 3D Conformal Radiotherapy and IMRT Plans for the Treatment of Prostate Cancer. *Australas Phys Eng Sci Med* (2009) 32(2):51. doi: 10.1007/BF03178629
56. Fernando P, Araceli H. Optimization of Radiotherapy Fractionation Schedules Based on Radiobiological Functions. *Br J Radiol* (2017) 90(1079):20170400. doi: 10.1259/bjr.20170400
57. Langen KM, Willoughby TR, Meeks SL, Santhanam A, Cunningham A, Levine L, et al. Observations on Real-Time Prostate Gland Motion Using Electromagnetic Tracking. *Int J Radiat Oncol Biol Phys* (2008) 71(4):1084–90. doi: 10.1016/j.ijrobp.2007.11.054
58. R Core Team. *R: A Language and Environment for Statistical Computing*. Vienna, Austria: R Foundation for Statistical Computing (2020). Available at: https://www.R-project.org/.
59. Yamada Y, Rogers L, Demanes DJ, Morton G, Prestidge BR, Pouliot J, et al. American Brachytherapy Society Consensus Guidelines for High-Dose-Rate Prostate Brachytherapy. *Brachytherapy* (2012) 11(1):20–32. doi: 10.1016/j.brachy.2011.09.008
60. Zilli T, Jorcano S, Bral S, Rubio C, Bruynzeel AME, Oliveira A, et al. Once-a-Week or Every-Other-Day Urethra-Sparing Prostate Cancer Stereotactic Body Radiotherapy, a Randomized Phase II Trial: 18 Months Follow-Up Results. *Cancer Med* (2020) 9(9):3097–106. doi: 10.1002/cam4.2966
61. Turkbey B, Rosenkrantz AB, Haider MA, Padhani AR, Villeirs G, Macura KJ, et al. Prostate Imaging Reporting and Data System Version 2.1: 2019 Update of Prostate Imaging Reporting and Data System Version 2. *Eur Urol* (2019) 76(3):340–51. doi: 10.1016/j.eururo.2019.02.033
62. Leibovich BC, Blute ML, Bostwick DG, Wilson TM, Pisansky TM, Davis BJ, et al. Proximity of Prostate Cancer to the Urethra: Implications for Minimally Invasive Ablative Therapies. *Urology* (2000) 56(5):726–9. doi: 10.1016/S0090-4295(00)00792-5
63. Wang T, Zhou J, Tian S, Wang Y, Patel P, Jani AB, et al. A Planning Study of Focal Dose Escalations to Multiparametric MRI-Defined Dominant Intraprostatic Lesions in Prostate Proton Radiation Therapy. *Br J Radiol* (2020) 93(1107):20190845. doi: 10.1259/bjr.20190845
64. Mohammed N, Kestin L, Ghilezan M, Krauss D, Vicini F, Brabbins D, et al. Comparison of Acute and Late Toxicities for Three Modern High-Dose Radiation Treatment Techniques for Localized Prostate Cancer. *Int J Radiat Oncol Biol Phys* (2012) 82(1):204–12. doi: 10.1016/j.ijrobp.2010.10.009
65. Moltzahn F, Dal Pra A, Furrer M, Thalmann G, Spahn M. Urethral Strictures After Radiation Therapy for Prostate Cancer. *Investig Clin Urol* (2016) 57(5):309–15. doi: 10.4111/icu.2016.57.5.309

66. King CR, Brooks JD, Gill H, Presti JC. Long-Term Outcomes From a Prospective Trial of Stereotactic Body Radiotherapy for Low-Risk Prostate Cancer. *Int J Radiat Oncol Biol Phys* (2012) 82(2):877–82. doi: 10.1016/j.ijrobp.2010.11.054
67. Lang S, Frame F, Collins A. Prostate Cancer Stem Cells. *J Pathol* (2009) 217 (2):299–306. doi: 10.1002/path.2478
68. Ullrich T, Quentin M, Oelers C, Dietzel F, Sawicki LM, Arsov C, et al. Magnetic Resonance Imaging of the Prostate At 1.5 Versus 3.0t: A Prospective Comparison Study of Image Quality. *Eur J Radiol* (2017) 90:192–7. doi: 10.1016/j.ejrad.2017.02.044
69. Parker CC, Damyanovich A, Haycocks T, Haider M, Bayley A, Catton CN. Magnetic Resonance Imaging in the Radiation Treatment Planning of Localized Prostate Cancer Using Intra-Prostatic Fiducial Markers for Computed Tomography Co-Registration. *Radiother Oncol* (2003) 66 (2):217–24. doi: 10.1016/S0167-8140(02)00407-3
70. Spohn SKB, Kramer M, Kiefer S, Bronsert P, Sigle A, Schultze-Seemann W, et al. Comparison of Manual and Semi-Automatic [18f]Psma-1007 PET Based Contouring Techniques for Intraprostatic Tumor Delineation in Patients With Primary Prostate Cancer and Validation With Histopathology as Standard of Reference. *Front Oncol* (2020) 10:2725. doi: 10.3389/fonc.2020.600690
71. Wegener D, Zips D, Thorwarth D, Weiß J, Othman AE, Grosse U, et al. Precision of T2 Tse MRI-CT-image Fusions Based on Gold Fiducials and Repetitive T2 Tse Mri-MRI-fusions for Adaptive IGRT of Prostate Cancer by Using Phantom and Patient Data. *Acta Oncol* (2019) 58(1):88–94. doi: 10.1080/0284186X.2018.1518594
72. Kuten J, Fahoum I, Savin Z, Shamni O, Gitstein G, Hershkovitz D, et al. Head-to-Head Comparison of (68)Ga-PSMA-11 With (18)F-Psma-1007 PET/CT in Staging Prostate Cancer Using Histopathology and Immunohistochemical Analysis as a Reference Standard. *J Nucl Med Off Publication Soc Nucl Med* (2020) 61(4):527–32. doi: 10.2967/jnumed.119.234187
73. Draulans C, De Roover R, van der Heide UA, Kerkmeijer L, Smeenk RJ, Pos F, et al. Optimal 68Ga-PSMA and 18F-PSMA PET Window Levelling for Gross Tumour Volume Delineation in Primary Prostate Cancer. *Eur J Nucl Med Mol Imaging* (2021) 48:1211–8. doi: 10.1007/s00259-020-05059-4
74. Sabater S, Pastor-Juan MR, Andres I, López-Martinez L, Lopez-Honrubia V, Tercero-Azorin MI, et al. Mri Prostate Contouring is Not Impaired by the Use of a Radiotherapy Image Acquisition Set-Up. An Intra- and Inter-Observer Paired Comparative Analysis With Diagnostic Set-Up Images. *Cancer/Radiothérapie* (2021) 25(2):107–13. doi: 10.1016/j.canrad.2020.05.024

Conflict of Interest: The authors declare that the research was conducted in the absence of any commercial or financial relationships that could be construed as a potential conflict of interest.

frontiers in Oncology

ORIGINAL RESEARCH
published: 21 May 2021
doi: 10.3389/fonc.2021.663631

Feasibility of Different Tumor Delineation Approaches for ^{18}F-PSMA-1007 PET/CT Imaging in Prostate Cancer Patients

*Lena M. Mittlmeier[1], Matthias Brendel[1], Leonie Beyer[1], Nathalie L. Albert[1], Andrei Todica[1], Mathias J. Zacherl[1], Vera Wenter[1], Annika Herlemann[2], Alexander Kretschmer[2], Stephan T. Ledderose[3], Nina-Sophie Schmidt-Hegemann[4], Wolfgang G. Kunz[5], Jens Ricke[5], Peter Bartenstein[1], Harun Ilhan[1] and Marcus Unterrainer[5]**

[1] Department of Nuclear Medicine, University Hospital, Ludwig Maximilian University (LMU) Munich, Munich, Germany, [2] Department of Urology, University Hospital, LMU Munich, Munich, Germany, [3] Department of Pathology, University Hospital, LMU Munich, Munich, Germany, [4] Department of Radiation Oncology, University Hospital, LMU Munich, Munich, Germany, [5] Department of Radiology, University Hospital, LMU Munich, Munich, Germany

OPEN ACCESS

Edited by:
Luigi Aloj,
University of Cambridge,
United Kingdom

Reviewed by:
Vikas Prasad,
Universitätsklinikum Ulm, Germany
Bastiaan Privé,
Radboud University Nijmegen Medical Centre, Netherlands
Aviral Singh,
Central Clinic Bad Berka, Germany

***Correspondence:**
Marcus Unterrainer
marcus.unterrainer@med.uni-muenchen.de

Specialty section:
This article was submitted to Cancer Imaging and Image-directed Interventions, a section of the journal Frontiers in Oncology

Received: 03 February 2021
Accepted: 19 April 2021
Published: 21 May 2021

Citation:
Mittlmeier LM, Brendel M, Beyer L, Albert NL, Todica A, Zacherl MJ, Wenter V, Herlemann A, Kretschmer A, Ledderose ST, Schmidt-Hegemann N-S, Kunz WG, Ricke J, Bartenstein P, Ilhan H and Unterrainer M (2021) Feasibility of Different Tumor Delineation Approaches for ^{18}F-PSMA-1007 PET/CT Imaging in Prostate Cancer Patients. Front. Oncol. 11:663631. doi: 10.3389/fonc.2021.663631

Background: Delineation of PSMA-positive tumor volume on PET using PSMA-ligands is of highest clinical interest as changes of PSMA-PET/CT-derived whole tumor volume (WTV) have shown to correlate with treatment response in metastatic prostate cancer patients. So far, WTV estimation was performed on PET using ^{68}Ga-labeled ligands; nonetheless, ^{18}F-labeled PET ligands are gaining increasing importance due to advantages over ^{68}Ga-labeled compounds. However, standardized tumor delineation methods for ^{18}F-labeled PET ligands have not been established so far. As correlation of PET-based information and morphological extent in osseous and visceral metastases is hampered by morphological delineation, low contrast in liver tissue and movement artefacts, we correlated CT-based volume of lymph node metastases (LNM) and different PET-based delineation approaches for thresholding on ^{18}F-PSMA-1007 PET.

Methods: Fifty patients with metastatic prostate cancer, ^{18}F-PSMA-1007 PET/CT and non-bulky LNM (short-axis diameter ≥10mm) were included. Fifty LNM were volumetrically assessed on contrast-enhanced CT (volumetric reference standard). Different approaches for tumor volume delineation were applied and correlated with the reference standard: I) fixed SUV threshold, II) isocontour thresholding relative to SUV_{max} (SUV%), and thresholds relative to III) liver (SUV_{liver}), IV) parotis ($SUV_{parotis}$) and V) spleen (SUV_{spleen}).

Results: A fixed SUV of 4.0 (r=0.807, r^2 = 0.651, p<0.001) showed the best overall association with the volumetric reference. 55% SUV_{max} (r=0.627, r^2 = 0.393, p<0.001) showed highest association using an isocontour-based threshold. Best background-based approaches were 60% SUV_{liver} (r=0.715, r^2 = 0.511, p<0.001), 80% $SUV_{parotis}$ (r=0.762, r^2 = 0.581, p<0.001) and 60% SUV_{spleen} (r=0.645, r^2 = 0.416, p<0.001). Background tissues SUV_{liver}, $SUV_{parotis}$ & SUV_{spleen} did not correlate (p>0.05 each).

Recently reported cut-offs for intraprostatic tumor delineation (isocontour 44% SUV_{max}, 42% SUV_{max} and 20% SUV_{max}) revealed inferior association for LNM delineation.

Conclusions: A threshold of SUV 4.0 for tumor delineation showed highest association with volumetric reference standard irrespective of potential changes in PSMA-avidity of background tissues (e. g. parotis). This approach is easily applicable in clinical routine without specific software requirements. Further studies applying this approach for total tumor volume delineation are initiated.

Keywords: PSMA, PET, mCRPC, Metastatic castrate-resistant prostate cancer, prostate cancer, whole tumor volume

INTRODUCTION

Prostate-specific membrane antigen (PSMA) targeted positron-emission-tomography (PET)/computed tomography (CT) is increasingly used for prostate cancer (PCa) staging and localization of recurrent and/or advanced disease (1). International PCa guidelines, including the European Association of Urology guideline, recommend PSMA PET/CT and its use, specifically in patients with PSA recurrence after primary therapy. Recently, the proPSMA trial also highlighted the important role of PSMA PET in high-risk patients prior to curative-intent surgery or radiotherapy with superior accuracy and lower costs compared to conventional imaging (2, 3). Furthermore, PCa staging using PSMA PET has significant impact on patient management as demonstrated in several groups (1, 4–8).

Beyond staging, PSMA PET/CT represents a useful tool for response to systemic therapy such as chemotherapy and radioligand therapy using ^{177}Lu-PSMA ligands (1, 9, 10). Here, PSMA PET/CT provides additional information beyond the most commonly used tools for oncological response assessment in clinical trials such as CT, magnetic resonance imaging (MRI), bone scintigraphy and PSA serum levels (9, 11–13). Due to the limited diagnostic and predictive accuracy of morphological criteria, such as Response Evaluation Criteria in Solid Tumors (RECIST), particularly in mCRPC patients, advanced imaging-based response assessment tools with higher accuracy are needed, like it is the case with ^{18}F-FDG-PET/CT in other tumor types like non-small-cell lung cancer (9, 14–16).

In this context, the longitudinal course of the PET-derived whole tumor volume (WTV) during systemic therapies is gaining increasing interest as an additional imaging biomarker for therapy monitoring. Several studies demonstrated that changes of PSMA PET-derived WTV correlate with treatment response (1, 9, 11, 17, 18) and may also serve as prognostic tool for overall survival estimation (1, 19, 20), as recently highlighted by a consensus statement by Fanti et al. (1).

In the field of PSMA ligands, ^{18}F-labeled PSMA ligands will become increasingly important due to their advantages compared to ^{68}Ga-labeled compounds, e. g. longer half-life, a lower positron energy and the possibility of large-batch production (21). While there are already published studies for tracer-specific thresholding and window-level-setting for WTV delineation using ^{68}Ga-labeled ligands, to the best of our knowledge no study so far evaluated different models for WTV estimation using ^{18}F-labeled PSMA ligands hitherto. So far, only two studies focused on intraprostatic tumor delineation using ^{18}F-PSMA-1007, but without application to WTV (21, 22). Hence, we aimed at identifying and comparing different thresholding approaches for tumor delineation on ^{18}F-PSMA-1007 PET/CT in correlation to a direct, CT-based volumetric reference standard.

Even if bone metastases present a common and clinically relevant metastatic spread in PCa patients (23), they are difficult to delineate on CT, mostly deeming them as non-measurable lesions according to RECIST 1.1 (24, 25). Also, lung metastases represent an unideal reference standard, especially due to motion artefacts on PET/CT and unequivocal protocols concerning breath-holding impacting PET imaging. In contrast, LNM represent measurable metastatic sites, especially in case of large extent and non-bulky localization. Therefore, we used large, non-bulky lymph nodes as volumetric reference standard for the evaluation of different threshold approaches for tumor delineation on ^{18}F-PSMA-1007 PET/CT.

MATERIAL AND METHODS

Inclusion Criteria

This retrospective analysis was approved by the institutional ethics committee of the LMU Munich. Criteria for inclusion were I) patients with known or highly suspected (i.e., highly increased PSA value) metastatic prostate cancer; II) ^{18}F-PSMA-1007 PET/CT, III) at least one singular located, non-bulky and PSMA-avid lymph node metastasis with short axis diameter (SAD) ≥ 1.0 cm.

Radiopharmaceutical and Imaging Protocol

A median activity of 247 MBq (range, 192-306 MBq) ^{18}F-PSMA-1007 was injected intravenously in line with previously reported radiosynthesis and administration procedures (26). The patients were premedicated with furosemide (20 mg intravenously), when no contraindication was noted (27). The administration of the radiopharmaceutical was based on an individual patient basis according to the German Pharmaceuticals Act §13(2b). PET was performed from skull base to mid-thigh using a Biograph mCT

scanner or a Biograph 64 PET/CT scanner (Siemens Healthineers Erlangen, Germany). The PET/CT scan was performed 60 min after tracer injection which included a diagnostic, contrast-enhanced CT scan in portal-venous phase (Imeron 350; 1.5 ml/kg body weight; Bracco Imaging, Milano, Italy). Images were reconstructed iteratively using TrueX (three iterations, 21 subsets) with Gaussian post-reconstruction smoothing (2 mm full width at half-maximum). Slice thickness on contrast-enhanced CT was 0.3 cm.

CT Image Analysis

For lymph node analysis, the SAD and the long-axis-diameter (LAD) were assessed. Assessment criterion for lymph node metastases were SAD of at least 1.0 cm, non-bulky, singular located and a distinct localization without contact to other structures. The extent of PSMA-avidity was no criterion for the selection of lymph node metastases. Then, the volume of the respective lymph nodes was manually delineated on a slice-by-slice manner and visually checked for correctness. The respective localizations were determined in each of the selected LNM (one per patient) by two experienced radiologists (WGK, MU) on a dedicated workstation (Siemens Healthineers Erlangen, Germany).

PET Image Analysis

Using a dedicated workstation (Affinity 1.1.4, Hermes Medical Solutions, Stockholm, Sweden) an ellipsoid volume of interest (VOI) was created surrounding the selected lymph node excluding off-target, PSMA-avid lesions. Exclusion of other PSMA-avid lesions was checked visually in order to avoid biased results. In this VOI, different approaches for volumetric delineation of the respective lymph nodes were applied and correlated with the reference standard; the following approaches were used: I) fixed SUV threshold, II) isocontour thresholding relative to SUV_{max} (SUV%) and thresholds relative to III) liver (SUV_{liver}), IV) parotis ($SUV_{parotis}$) and V) spleen (SUV_{spleen}):

I. Fixed SUV thresholds: The following values were applied: SUV 15.0; SUV 10.0; SUV 7.5; SUV 5.0; SUV 4.5; SUV 4; SUV 3.5; SUV 3.0 and SUV 2.5).
II. Isocontour relative to SUV_{max} (SUV%): The following values were applied: 10.0%; 15.0%, 20.0%, 25.0%, 30.0%, 35.0%, 40.0%, 42.0%, 44.0%, 45.0%, 50.0%, 55.0%; 50.0%; 70.0% and 75.0%).
III. Thresholds relative to SUV_{liver}: Background values were derived from a 30 mm-diameter circular reference region of interest (ROI) in the normal inferior right liver lobe in the axial plane excluding blood vessel activity, as described previously (28). The following threshold values were applied: SUV_{liver} minus 45.0%; 50.0%; 55.0%; 60.0%; 70.0% and 75.0%.
IV. Thresholds relative to $SUV_{parotis}$: Values were derived from a cubic 10 x 10 x 10 mm reference ROI in the parotis. The following threshold values were applied: $SUV_{parotis}$ minus 60.0%; 70.0%; 75.0%; 80.0%; 85.0% and 90.0%.
V. Thresholds relative to SUV_{spleen}: Background values were derived from a cubic 30 x 30 x 30 mm reference ROI in the spleen. The following threshold values were applied: SUV_{spleen} minus 40.0%; 50.0%; 55.0%; 60.0%; 65.0% and 70.0%.

Statistical Analyses

Statistical analyses were performed with IBM SPSS® Statistics (version 25, IBM Corp., Armonk, NY). Correlation between CT-measured volumes and the PET-based volumes using different threshold was evaluated using Spearman and Pearson correlation coefficient after testing for normal distribution as determined by the Shapiro-Wilk test. The coefficient of variation (CoV) was used as standardized measure of dispersion of a probability distribution as defined as the ratio of the standard to the mean. Group comparisons of continuous, not normally distributed parameters were compared using the Kruskal-Wallis test. For visualization of correlation, scatter plots and Bland-Altman plots were used. Statistical significance was defined as a two-sided p-value <0.05.

RESULTS

Patients

The median age was 71.0 years (range, 55.8-91.5 years). There was a median PSA of 25.8 ng/ml (range, 0.2 – 1118.0 ng/ml) and a median Gleason score of 9 (range, 6 – 10). Lymph node metastases were present in 50/50 patients (100.0%), tumors at the prostate bed in 28/50 patients (56.0%), bone metastases in 36/50 patients (72.0%) and visceral metastases in 11/50 patients (22.0%). Non PSMA-avid metastatic lesions were present in 0/50 patients (0.0%). Extended patients' specifications including previous therapies are listed in the **Supplementary Table**.

CT Image Analysis

Lymph node size was assessed using the SAD (median 1.4 cm (range, 1.0 – 2.8 cm), LAD (median 1.9 cm; range 1.1 – 3.8 cm) and CT-derived volume (median 3.2 ml; range 1.0 – 23.8 ml). Among the lymph node metastases, 31/50 were located next to the common and internal iliac vessels (62.0%), 6/50 cervical (12.0%), 3/50 mediastinal (6.0%), 3/50 paraaortic and paracaval/interaortocaval (6.0%), 2/50 in the inguinal region (4.0%), 2/50 pararectal (4.0%), 2/50 axillar (4.0%) and1/50 in the retroclavicular region (2.0%).

Volumetric Correlation of Different Delineation Approaches

Results from above mentioned I) fixed SUV thresholds, II) isocontour thresholding relative to SUV_{max} (SUV%), thresholds relative to III) liver (SUV_{liver}), IV) parotis ($SUV_{parotis}$) and V) spleen (SUV_{spleen}) and their correlation to the CT derived volume as reference standard can be found in **Tables 1**–**5**.

I. Fixed SUV thresholds: In I) the highest correlation between CT-derived volume and a fixed threshold could be found with a SUV of 4.0 (r=0.807, r^2 = 0.651, p<0.001). Generally,

it could be shown that higher (e. g. 15.0; 10.0), but also lower fixed SUV values (e. g. 2.5, 5.0 and 4.5) comprised lower correlation to the reference standard (please see **Table 1**), due to a consecutive under- and overestimation of the respective volume.

II. socontour relative to SUV_{max} (SUV%): 55% SUV_{max} showed highest association using an isocontour (r=0.627, r^2 = 0.393, p<0.001). Recently reported isocontour based cut-offs for intraprostatic tumor delineation [i. e. isocontour 20%, 44% and 42% SUV_{max} (21, 22)] revealed inferior association for LNM delineation (please see **Table 2**).

III. Thresholds relative to SUV_{liver}: 60% SUV_{liver} (r=0.715, r^2 = 0.511, p<0.001) showed highest association using thresholds relative to the SUV_{mean} of the liver while lower as well as higher values relative to the liver showed lower correlation to the reference standard (see **Table 3**).

IV. Thresholds relative to $SUV_{parotis}$: 80% $SUV_{parotis}$ (r=0.762, r^2 = 0.581, p<0.001) showed highest association using thresholds relative to the SUV_{mean} of the parotis ($SUV_{parotis}$). Lower values relative to the parotis (e. g. 60% $SUV_{parotis}$), but also higher values (e. g. 90% $SUV_{parotis}$) showed inferior correlation to the volumetric reference standard (see **Table 3**).

V. Thresholds relative to SUV_{spleen}: 60% SUV_{spleen} (r=0.645, r^2 = 0.416, p<0.001) showed highest association using thresholds relative to the SUV_{mean} of the spleen (SUV_{spleen}). Lower as well as higher threshold values showed lower correlations respectively (see **Table 3**).

A patient example applying the best threshold of the different approaches on a single LNM is shown in **Figure 1**. For visualization of the association of the best threshold of the different approaches with the reference standard, correlation plots and the respective Bland-Altman plots are shown in **Figures 2** and **3**.

PSMA-Avidity of Background Tissues

Highest median SUV_{mean} in background tissues was found in the parotid gland followed by the liver and spleen (lowest uptake), i. e. 20.1 (range, 5.8 - 36.3) *vs.* 11.3 (range, 4.2 - 25.5) *vs.* 9.9 (4.7 – 28.7), p<0.001. These uptake values lead to an CoV of 42.6% using SUV_{spleen}, followed by 40.2% using SUV_{liver} and the lowest CoV of 35.6% using $SUV_{parotis}$. PSMA-avidity of background tissues (SUV_{liver}, $SUV_{parotis}$ & SUV_{spleen}) did not show a significant correlation with each other (p>0.05 each) (please see **Table 4**).

TABLE 1 | Correlation with fixed SUV thresholds.

Parameter	r-value	r^2-value	Level of significance
SUV 15.0	0.415	0.172	p<0.001
SUV 10.0	0.575	0.331	p<0.001
SUV 7.5	0.633	0.401	p<0.001
SUV 5.0	0.788	0.621	p<0.001
SUV 4.5	0.802	0.643	p<0.001
SUV 4.0	0.807	0.651	p<0.001
SUV 3.5	0.802	0.643	p<0.001
SUV 3.0	0.800	0.640	p<0.001
SUV 2.5	0.792	0.627	p<0.001

Individual Backwards Thresholding

On an individual, single lymph node basis, threshold values were individually adjusted in order to achieve the very same PET-based volume compared to the CT-based reference standard in each lymph node using a fixed SUV value, as this approach performed best in previous analyses. Here, the same volume compared to the CT-based reference was achieved using a mean SUV of 5.4 ± 2.4, which resulted in a high CoV of 44.4% among the fifty LNM. However, applying these resulting mean values of backwards thresholding to all 50 lymph nodes and correlating these volumes the CT-based volumetric reference (i. e. SUV 5.4 in all 50 lymph nodes), the correlation coefficient was inferior to previous analyses (i. e. r=0.764, r^2 = 0.584, p<0.001) (see **Table 5**).

DISCUSSION

Measuring the volumetric extent of metastatic spread in prostate cancer is of fundamental interest in patients undergoing systemic therapy such as chemotherapy or radioligand therapy (17, 29) with potential impact on clinical decision making (7, 9, 30, 31). Due to its many advantages over ^{68}Ga-labeled ligands, ^{18}F-labeled compounds such as ^{18}F-PSMA-1007 are becoming increasingly important for staging as well as treatment response assessment; in this analysis, we correlated tumor volumes derived from different threshold-based approaches for PET-based delineation with the CT-based, volumetric reference, i. e. the morphological volume of distinct, non-bulky lymph node metastases as derived from hybrid imaging using ^{18}F-PSMA-1007 PET/CT.

Even if bone metastases present a common and clinically relevant metastatic spread in PCa patients (23), they are difficult to delineate on CT resulting in non-measurable lesions according to routine response criteria RECIST 1.1 (24, 25). Also, visceral metastases or lung metastases represent an unideal volumetric reference standard for the current issue, especially due to motion artefacts on PET/CT and unequivocal protocols concerning breath-holding impacting PET imaging. In contrast, LNM represent measurable metastatic sites, especially in case of large extent and non-bulky localization and were primarily evaluated in the current analysis.

In consideration of our results, we can state that a simple fixed SUV of 4.0 as threshold for tumor delineation without reference tissue correlated best with the volumetric reference standard (r=0.807, r^2 = 0.651, p<0.001) even though some of our acquired threshold values also showed comparable, but slightly lower correlation coefficients to the reference standard [e.g. 60% SUV_{liver} (r=0.715, r^2 = 0.511, p<0.001) or 80% $SUV_{parotis}$ (r=0.762, r^2 = 0.581, p<0.001)]. These data are additionally supported by the visual analyses of the respective Bland-Altman plots (see **Figure 2**), where the approach using SUV 4.0 as delineation method also performed best.

TABLE 2 | Isocontour volumetric correlation.

Parameter	r-value	r^2-value	Level of significance
Iso 10%	0.481	0.231	p<0.001
Iso 15%	0.440	0.194	p=0.001
Iso 20%	0.460	0.212	p<0.001
Iso 25%	0.477	0.228	p<0.001
Iso 30%	0.520	0.270	p<0.001
Iso 35%	0.505	0.255	p<0.001
Iso 40%	0.529	0.280	p<0.001
Iso 42%	0.530	0.281	p<0.001
Iso 44%	0.552	0.305	p<0.001
Iso 45%	0.543	0.295	p<0.001
Iso 50%	0.604	0.365	p<0.001
Iso 55%	0.627	0.393	p<0.001
Iso 60%	0.619	0.383	p<0.001
Iso 65%	0.610	0.372	p<0.001
Iso 70%	0.605	0.366	p<0.001
Iso 75%	0.541	0.293	p<0.001

Previously published optimized thresholds for intraprostatic tumor delineation on ^{18}F-PSMA-1007 PET/CT (20%, 42% and 44% isocontour relative to SUV_{max}) showed distinctly lower correlation to the reference standard compared to a fixed SUV of 4.0 (20% SUV%: r=0.460, r^2 = 0.212. 42% SUV%: r=0.530, r^2 = 0.28. 44% SUV%: r=0.552, r^2 = 0.305, p<0.001 each), which indicates that these values seem feasible for delineation of the primary site of prostate cancer, but seem less feasible for delineation of lymph node volumes or even WTV in metastatic prostate cancer patients (22).

Obviously, it can be stated that the identification of the "one" ideal threshold value is a merely impossible task, as, on a cellular level, not all tumor cells can be delineated and be included in the image-derived WTV. However, a uniformly applied approach for PET-based delineation with the nearest approximation to a reference standard might, consequently, also allow a uniform and cross-institutional estimation of a WTV. We identified a simple SUV value of 4.0 as the threshold with the best correlation to the reference standard derived from large LNM. Thresholding using mere SUV values comprises several advantages: no specific software or algorithms are needed to determine WTV on ^{18}F-PSMA-1007 PET/CT, as SUV is a commonly displayed unit in PET imaging. Moreover, no background/reference tissues are needed for WTV estimation making this analysis independent of potential change in PSMA-avidity in the reference tissues potentially changing over time or during systemic therapy, e.g. during ^{177}Lu- or ^{225}Ac-PSMA-radioligandtherapy (32, 33). Of note, we could show that on an inter-individual basis, the most commonly applied reference tissues (i.e. liver, parotis, spleen) do have a high inter-individual variability with CoV values up to 43%. Moreover, the respective PSMA-avidity of all three reference tissues is not correlated with one another on an intra-individual level, so that a general, uniform PSMA-avidity among healthy organs seems unlikely. These findings also support the application of a simple SUV-based approach without reference tissue.

TABLE 3 | Background based volumetric correlations with SUV_{liver}, $SUV_{parotis}$ and SUV_{spleen}.

Parameter	r-value	r^2-value	Level of significance
SUV_{liver}			
45% SUV_{liver}	0.693	0.480	p<0.001
50% SUV_{liver}	0.693	0.480	p<0.001
55% SUV_{liver}	0.711	0.506	p<0.001
60% SUV_{liver}	0.715	0.511	p<0.001
70% SUV_{liver}	0.690	0.467	p<0.001
75% SUV_{liver}	0.697	0.486	p<0.001
$SUV_{parotis}$			
60% $SUV_{parotis}$	0.545	0.297	p<0.001
70% $SUV_{parotis}$	0.666	0.444	p<0.001
75% $SUV_{parotis}$	0.745	0.555	p<0.001
80% $SUV_{parotis}$	0.762	0.581	p<0.001
85% $SUV_{parotis}$	0.650	0.423	p<0.001
90% $SUV_{parotis}$	0.603	0.364	p<0.001
SUV_{spleen}			
40% SUV_{spleen}	0.595	0.354	p<0.001
50% SUV_{spleen}	0.642	0.412	p<0.001
55% SUV_{spleen}	0.639	0.408	p<0.001
60% SUV_{spleen}	0.645	0.412	p<0.001
65% SUV_{spleen}	0.618	0.382	p<0.001
70% SUV_{spleen}	0.618	0.382	p<0.001

When trying to derive an optimal threshold on a backwards step approach, i.e., setting the threshold value to achieve the same volume on PET in every single lymph node, one can state that the reverse deduction of a PET-based threshold is partially limited by the obtained dispersion of threshold-values, i.e., we observed an CoV of around 40% among the resulting threshold values. When directly applying the derived mean SUV value to all lymph nodes and performing a correlation analysis with the CT-based reference standard, a good correlation to the volumetric reference standard was observed, which was, however, still inferior compared to the mere application of a SUV value of 4.0.

Overall, the application of a threshold of SUV 4.0 seems easily applicable in clinical routine, despite a certain blurriness regarding the actual nodal tumor volume. Given the partially extensive WTV in patients prior to systemic therapy, e.g., ^{177}Lu-PSMA radioligand therapy, these small differences in lymph node volumes and small uncertainties in WTV do probably not carry a clinically relevant weight, when the same procedure is applied in a uniform manner consequently, so that the unavoidable blurriness is applied to all studies to the same degree. For potential translation of the derived threshold to other metastases, we included patient examples where the threshold of SUV 4.0 was applied for whole tumor volume delineation (see **Figures 4**, **5**) and showed a direct easy applicability and direct feasibility; nonetheless, further studies evaluating this threshold for WTV delineation and its course during therapy are the logical conclusion of the current analysis.

However, it has to be discussed that metastatic sites without significant PSMA-avidity (e.g. < SUV 4.0) are not included in the whole tumor volume as a consequence. In case of PSMA-negative, but clear metastatic spread on CT imaging (e.g. large bone metastases, bulky lymph nodes, etc.), but very low or even missing PSMA-avidity, a PSMA-derived tumor volume might underestimate the "real" tumor volume. Therefore, more specifically, the term "whole tumor volume" should be noted

TABLE 4 | Correlation of background tissues SUV_{liver}, $SUV_{parotis}$ & SUV_{spleen}.

Parameter	Spleen	Liver	Parotis
SUV_{mean} [median (range)]	9.9 (4.7 - 28.7)	11.3 (4.2 - 25.5)	20.1 (5.8 - 36.3)
Coefficient of variation	42.6%	40.2%	35.6%
Correlation with spleen	–	r=0.082 (p=0.572)	r=0.120 (p=0.406)
Correlation with liver	r=0.082 (p=0.572)	–	r=0.028 (p=0.845)
Correlation with parotis	r=0.120 (p=0.406)	r=0.028 (p=0.845)	–

TABLE 5 | Individual backwards thresholding.

	SUV
Mean ± standard deviation	5.4 ± 2.4
Coefficent of variation (CoV)	44.4%
Correlation to CT reference (SUV 5.4)	r=0.764
Coefficient of determination (SUV 5.4)	r^2 = 0.584
Level of significance (SUV 5.4)	p<0.001

to be the "PSMA-avid whole tumor volume". However, in the concrete case, if there are obvious metastatic sites on CT that are not included in the whole tumor volume due to very low or even missing PSMA-avidity, this fact should lead to e. g. an additional ^{18}F-FDG PET for the evaluation of tumor dedifferentiation; in case of FDG-avid, non-PSMA-avid lesions, ^{18}F-FDG PET imaging might be the superior modality for tumor characterization and, moreover, the application of PSMA-directed therapies should be critically discussed (34, 35).

Moreover, it should be noted that the application of this threshold potentially needs manual refinement, especially in case of close vicinity to areas or physiologically high PSMA-avidity such as the liver or guts, where the application of this threshold would cause a direct inclusion of lesions with physiological PSMA-avidity; however, this phenomenon is common for all PSMA-ligands and, moreover, also other ligands such as ^{18}F-FDG, where areas of high glucose consumptions such as the brain do hamper automated lesion segmentation. E. g. in the rather rare case of liver metastases, the automatic delineation of liver metastases using this threshold SUV 4.0 has to be refined manually, especially, as the radioligand ^{18}F-PSMA-1007 presents with a rather high biliary excretion (36). Nonetheless, in cases with liver metastases from prostate cancer, these cases usually present with generally high tumor burden so that small variabilities in manual refinement of liver metastases do not have a major impact on the absolute whole tumor volume. However, the

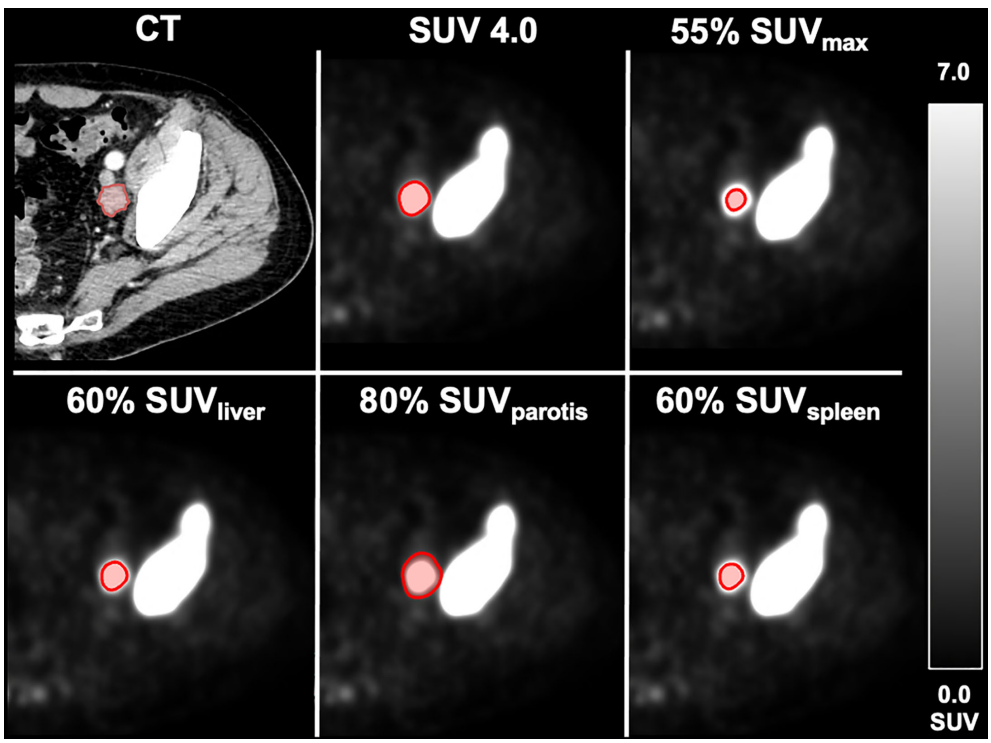

FIGURE 1 | Different delineation methods in an exemplary metastatic patient. Volumetric reference standard 6.3 m; SUV 4.0: 5.5 ml. 55% SUV_{max}: 1.0 ml. 60% SUV_{liver}: 4.5 ml. 80% $SUV_{parotis}$: 6.4 ml. 60% SUV_{spleen}: 4.0 ml.

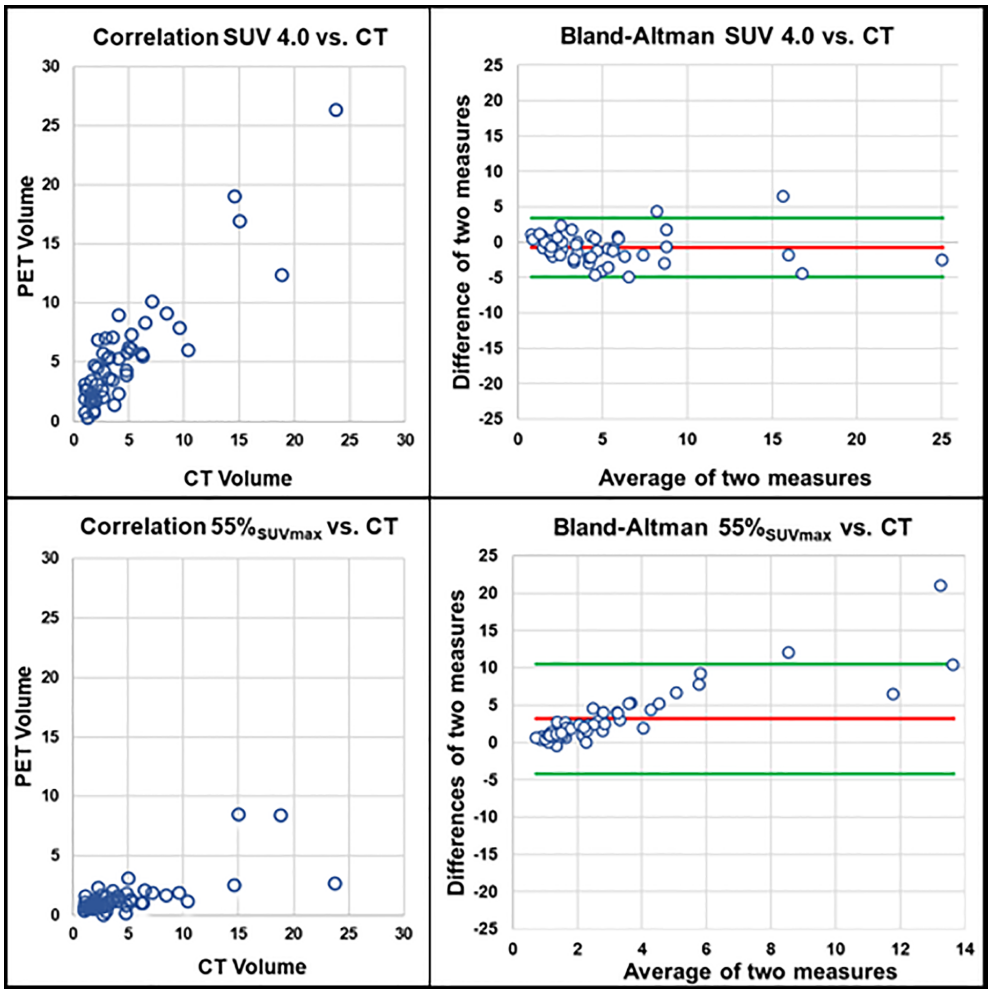

FIGURE 2 | Correlation of PET volumes and CT-based reference standard. Upper row: PET volume SUV 4.0 ($r = 0.807$, $r^2 = 0.651$, $p < 0.001$). Lower row: PET volume isocontour of 55% SUV_{max} ($r = 0.627$, $r^2 = 0.393$, $p < 0.001$); each correlation plot is accompanied by the respective Bland-Altman plot (red line: mean difference of two measures. Green lines: mean difference of two measures ± 1.96 x standard deviation).

issue of delineation of liver metastases is shared by nearly every PSMA-ligand in dependence of the particular degree of biliary excretion.

Moreover, using comparable PET/CT scanners from the same vendor with the same reconstruction algorithms and EARL accreditation, we observed a higher rate of dispersion regarding tumor delineation based on approaches relating to SUV_{max} as reference value, i. e. isocontour delineation. Our proposed delineation method, however, is based on a mere application of SUV values independent of the specific SUV_{max} value within metastatic sites. As also shown for other ligands (37), diverging PET-scanners and reconstruction algorithms do rather affect the reproducibility of SUV_{max} values than significantly lower, mere SUV values within the lesion. Therefore, the proposed delineation method should be more robust and reproducible compared to delineation methods relating to SUV_{max}, as it seems less susceptible to diverging vendors and reconstruction algorithms. Further studies, however, have to address the reproducibility of PET parameters on ^{18}F-PSMA-1007 PET in prostate cancer patients with emphasis on vendors and reconstruction algorithms beyond the scope of the current analysis.

Our analysis has several limitations that need to be considered: Some of the examined lymph nodes might potentially be susceptible to partial volume effect and spillover effects, even though we have chosen lymph nodes with a SAD of at least 1.0 cm (38). Another limitation is the retrospective design of the study as well as the fact that some of the lymph nodes were not histologically proven to be prostate cancer metastases. Nonetheless, our patients were already diagnosed with prostate cancer and presented with significantly increased PSA values and a high PSMA-expression of the lymph nodes, making an unspecifically high PSMA-avidity very unlikely. Moreover, readers were aware of common pitfalls with regard to lymph

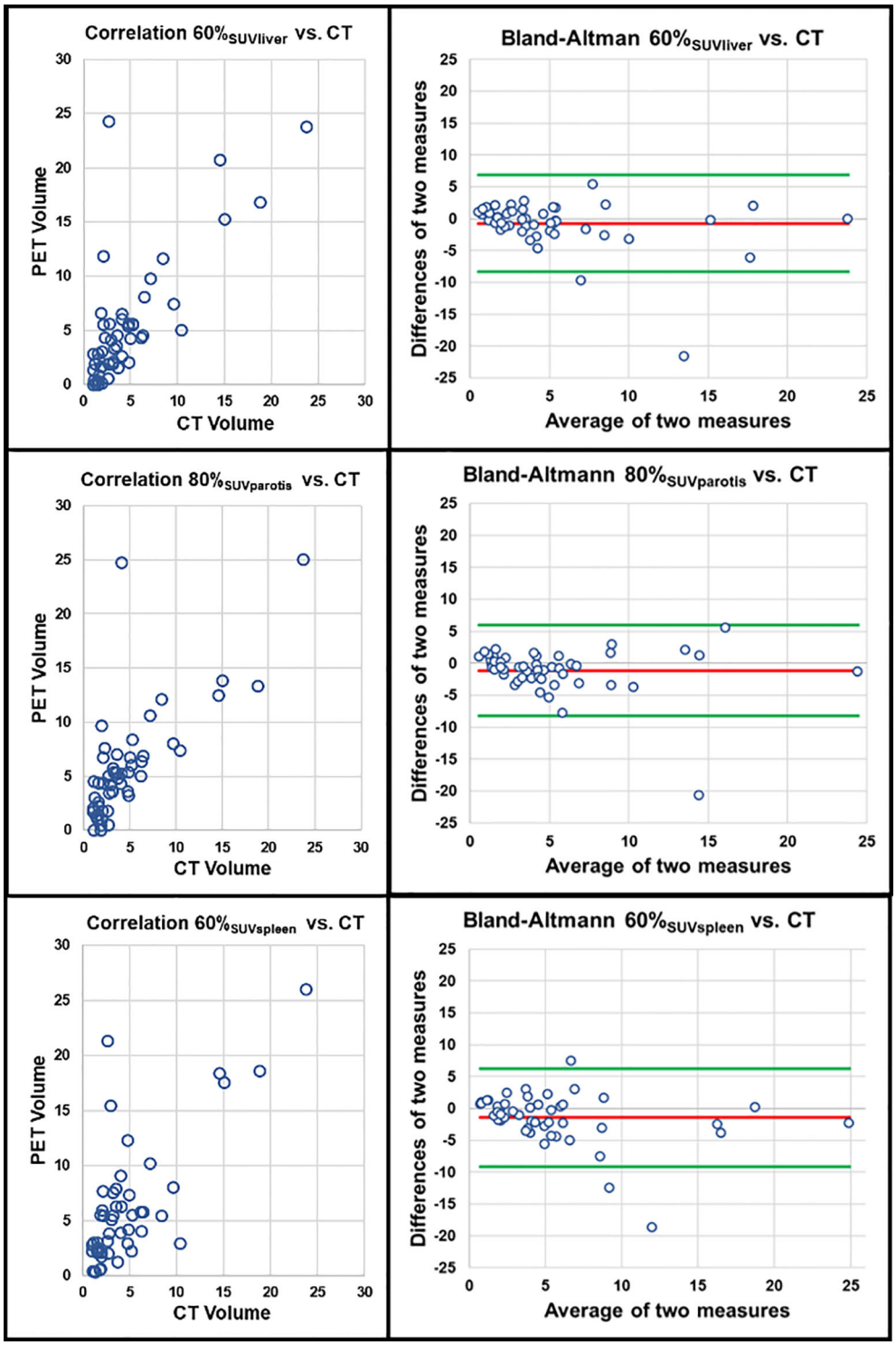

FIGURE 3 | Correlation of PET volumes using background tissue and CT-based reference standard. Upper row: PET volume 60% SUV_{liver} ($r = 0.715$, $r^2 = 0.511$, $p < 0.001$). Middle row: 80% $SUV_{parotis}$ ($r = 0.762$, $r^2 = 0.581$, $p < 0.001$). Lower row: PET volume 60% SUV_{spleen} ($r = 0.645$, $r^2 = 0.412$, $p < 0.001$); each correlation plot is accompanied by the respective Bland-Altman plot (red line: mean difference of two measures. Green lines: mean difference of two measures ± 1.96 x standard deviation).

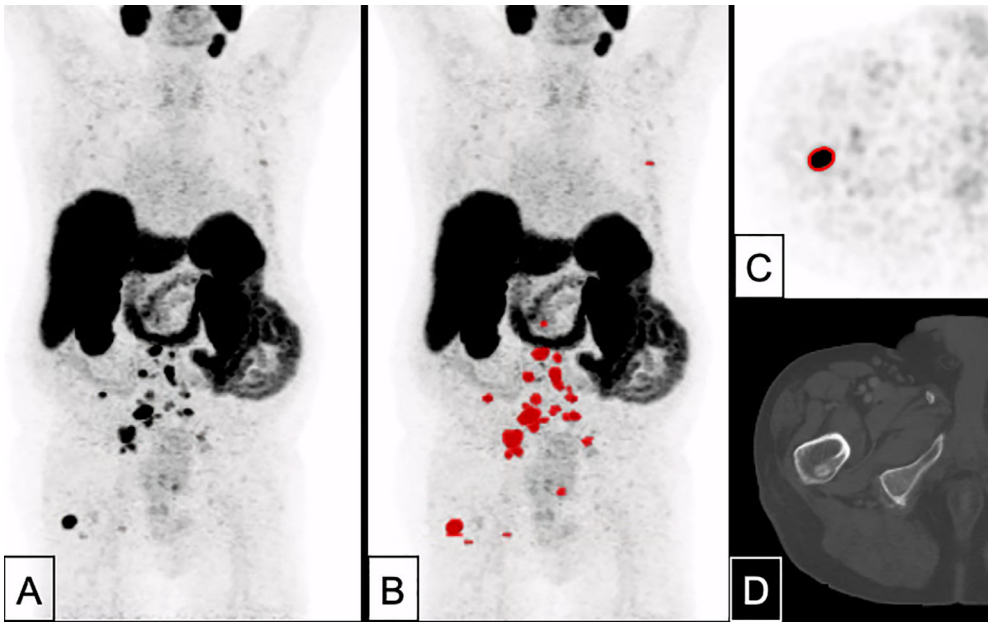

FIGURE 4 | A 82 years-old patient with prostate cancer remnant as well as bone and lymph node metastases (PSA 10.1 ng/ml, Gleason 8). Tumor delineation using a cut-off of SUV 4.0 revealed a WTV of 37.9 ml. **(A)** maximum intensity projection (MIP); **(B)** MIP + WTV (red color); **(C)** delineation of a bone metastasis on PET; **(D)** CT correlate (bone window).

node detection, such as the presence of ganglia (39). In the future, a larger assessment with more patients is warranted to confirm our preliminary results. Additionally, further studies applying our approaches for total tumor volume delineation have to be performed to support our findings. Therefore, the concrete applicability of the currently derived threshold for metastatic sites other than lymph nodes has to be assessed systematically and has to be validated in the specific scenario of therapy monitoring of systemic treatments with assessment of WTV changes over time.

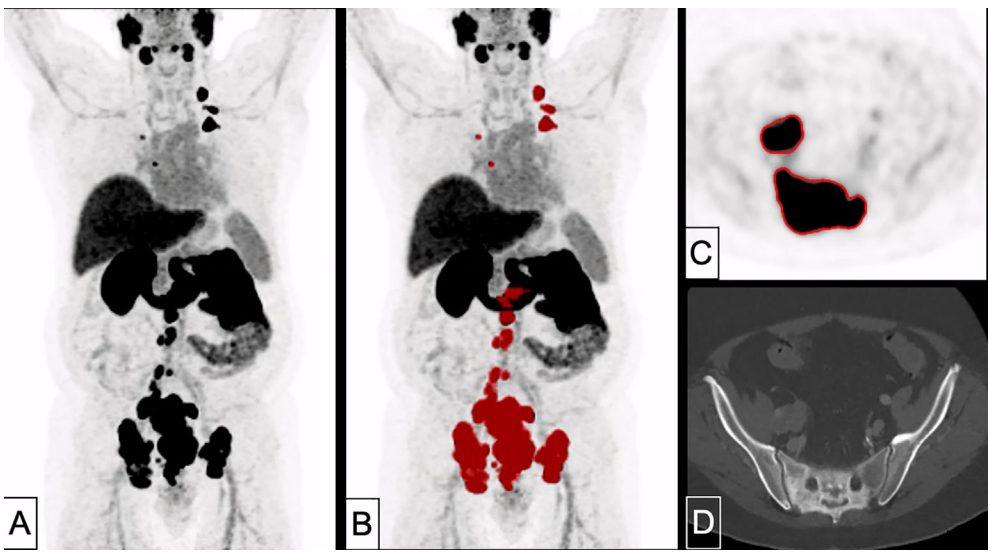

FIGURE 5 | A 70 years-old patient with primary prostate cancer remnant with bone, pleura and lymph node metastases (PSA 78.0 ng/ml, Gleason 10). Tumor delineation using a cut-off of SUV 4.0 revealed a WTV of 586 ml. **(A)**: MIP; **(B)** MIP + WTV (red color); **(C)** delineation of bone and lymph node metastasis on PET; **(D)** CT correlate (bone window).

CONCLUSIONS

A simple threshold of SUV 4.0 for delineation of nodal PCa lesions showed highest association with the volumetric reference standard independent of potential changes of PSMA-avidity in background tissues (e.g. parotis). This approach is easily applicable in clinical routine without specific software requirements. Further studies applying this approach for total tumor volume delineation are underway.

DATA AVAILABILITY STATEMENT

The original contributions presented in the study are included in the article/**Supplementary Material**, further inquiries can be directed to the corresponding author/s.

ETHICS STATEMENT

The studies involving human participants were reviewed and approved by Ethics Committee, LMU Munich. Written informed consent for participation was not required for this study in accordance with the national legislation and the institutional requirements.

AUTHOR CONTRIBUTIONS

Manuscript draft/concept: LM and MU. Clinical management: NA, AT, MZ, VW, AH, AK, SL, and N-SS-H. Image analyses: LM, WK, HI, and MU. Supervision JR and PB. All authors increased the intelectual content of the work. All authors contributed to the article and approved the submitted version.

SUPPLEMENTARY MATERIAL

The Supplementary Material for this article can be found online at: https://www.frontiersin.org/articles/10.3389/fonc.2021.663631/full#supplementary-material

Supplementary Table | Extended patients' characteristics.

REFERENCES

1. Fanti S, Goffin K, Hadaschik BA, Herrmann K, Maurer T, MacLennan S, et al. Consensus Statements on PSMA PET/CT Response Assessment Criteria in Prostate Cancer. *Eur J Nucl Med Mol Imaging* (2021) 48(2):111(9):469–76. doi: 10.1007/s00259-020-04934-4
2. Hofman MS, Murphy DG, Williams SG, Nzenza T, Herschtal A, Lourenco RDA, et al. A Prospective Randomized Multicentre Study of the Impact of gallium-68 Prostate-Specific Membrane Antigen (PSMA) PET/CT Imaging for Staging High-Risk Prostate Cancer Prior to Curative-Intent Surgery or Radiotherapy (proPSMA Study): Clinical Trial Protocol. *BJU Int* (2018) 122 (5):783–93. doi: 10.1111/bju.14374
3. de Feria Cardet RE, Hofman MS, Segard T, Yim J, Williams S, Francis RJ, et al. Is Prostate-specific Membrane Antigen Positron Emission Tomography/ Computed Tomography Imaging Cost-effective in Prostate Cancer: An Analysis Informed by the proPSMA Trial. *Eur Urol* (2021) 79(3):413–18. doi: 10.1016/j.eururo.2020.11.043
4. Bashir U, Tree A, Mayer E, Levine D, Parker C, Dearnaley D, et al. Impact of Ga-68-PSMA PET/CT on Management in Prostate Cancer Patients With Very Early Biochemical Recurrence After Radical Prostatectomy. *Eur J Nucl Med Mol Imaging* (2019) 46(4):901–7. doi: 10.1007/s00259-018-4249-z
5. Hirmas N, Al-Ibraheem A, Herrmann K, Alsharif A, Muhsin H, Khader J, et al. [68 Ga] Psma PET/CT Improves Initial Staging and Management Plan of Patients With High-Risk Prostate Cancer. *Mol Imaging Biol* (2019) 21 (3):574–81. doi: 10.1007/s11307-018-1278-8
6. Hofman MS, Lawrentschuk N, Francis RJ, Tang C, Vela I, Thomas P, et al. Prostate-Specific Membrane Antigen PET-CT in Patients With High-Risk Prostate Cancer Before Curative-Intent Surgery or Radiotherapy (proPSMA): A Prospective, Randomised, Multi-Centre Study. *Lancet* (2020) 395(10231):1208–16.
7. Sonni I, Eiber M, Fendler WP, Alano RM, Vangala SS, Kishan AU, et al. Impact of 68Ga-PSMA-11 PET/CT on Staging and Management of Prostate Cancer Patients in Various Clinical Settings: A Prospective Single Center Study. *J Nucl Med* (2020) 61(8):1153–60. doi: 10.2967/jnumed.119.237602
8. Schmidt-Hegemann N-S, Eze C, Li M, Rogowski P, Schaefer C, Stief C, et al. Impact of 68Ga-PSMA PET/CT on the Radiotherapeutic Approach to Prostate Cancer in Comparison to CT: A Retrospective Analysis. *J Nucl Med* (2019) 60(7):963–70. doi: 10.2967/jnumed.118.220855
9. Grubmüller B, Senn D, Kramer G, Baltzer P, D'Andrea D, Grubmüller KH, et al. Response Assessment Using 68 Ga-PSMA Ligand PET in Patients Undergoing 177 Lu-PSMA Radioligand Therapy for Metastatic Castration-Resistant Prostate Cancer. *Eur J Nucl Med Mol Imaging* (2019) 46(5):1063–72. doi: 10.1007/s00259-018-4236-4
10. Prasad V, Huang K, Prasad S, Makowski MR, Czech N, Brenner W. In Comparison to PSA, Interim Ga-68-PSMA Pet/Ct Response Evaluation Based on Modified Recist 1.1 After 2nd Cycle is Better Predictor of Overall Survival of Prostate Cancer Patients Treated With 177lu-Psma. *Front Oncol* (2021) 11:291. doi: 10.3389/fonc.2021.578093
11. Seitz AK, Rauscher I, Haller B, Krönke M, Luther S, Heck MM, et al. Preliminary Results on Response Assessment Using 68 Ga-HBED-CC-PSMA PET/CT in Patients With Metastatic Prostate Cancer Undergoing Docetaxel Chemotherapy. *Eur J Nucl Med Mol Imaging* (2018) 45(4):602–12. doi: 10.1007/s00259-017-3887-x
12. Seifert R, Seitzer K, Herrmann K, Kessel K, Schäfers M, Kleesiek J, et al. Analysis of PSMA Expression and Outcome in Patients With Advanced Prostate Cancer Receiving 177Lu-PSMA-617 Radioligand Therapy. *Theranostics* (2020) 10(17):7812. doi: 10.7150/thno.47251
13. Sonpavde G, Pond GR, Armstrong AJ, Galsky MD, Leopold L, Wood BA, et al. Radiographic Progression by Prostate Cancer Working Group (PCWG)-2 Criteria as an Intermediate Endpoint for Drug Development in Metastatic Castration-Resistant Prostate Cancer. *BJU Int* (2014) 114(6b):E25–31. doi: 10.1111/bju.12589
14. Cook GJ, Azad G, Padhani AR. Bone Imaging in Prostate Cancer: The Evolving Roles of Nuclear Medicine and Radiology. *Clin Trans Imaging* (2016) 4(6):439–47. doi: 10.1007/s40336-016-0196-5
15. Beer L, Hochmair M, Haug AR, Schwabel B, Kifjak D, Wadsak W, et al. Comparison of RECIST, iRECIST, and PERCIST for the Evaluation of Response to PD-1/PD-L1 Blockade Therapy in Patients With non–Small Cell Lung Cancer. *Clin Nucl Med* (2019) 44(7):535–43. doi: 10.1097/RLU.0000000000002603
16. Rossi G, Baucknehtt M, Genova C, Rijavec E, Biello F, Mennella S, et al. Comparison Between 18F-FDG-PET-and CT-based Criteria in non-Small Cell Lung Cancer (NSCLC) Patients Treated With Nivolumab. *J Nucl Med* (2020) 61(7):990–8. doi: 10.2967/jnumed.119.233056
17. Seifert R, Herrmann K, Kleesiek J, Schafers MA, Shah V, Xu Z, et al. Semi-Automatically Quantified Tumor Volume Using Ga-68-PSMA-11-PET as Biomarker for Survival in Patients With Advanced Prostate Cancer. *J Nucl Med* (2020) 61(12):1786–92. doi: 10.2967/jnumed.120.242057
18. Hartrampf PE, Heinrich M, Seitz AK, Brumberg J, Sokolakis I, Kalogirou C, et al. Metabolic Tumour Volume From PSMA Pet/Ct Scans of Prostate Cancer

Patients During Chemotherapy—Do Different Software Solutions Deliver Comparable Results? *J Clin Med* (2020) 9(5):1390. doi: 10.3390/jcm9051390
19. Seifert R, Kessel K, Schlack K, Weber M, Herrmann K, Spanke M, et al. Psma PET Total Tumor Volume Predicts Outcome of Patients With Advanced Prostate Cancer Receiving [177 Lu] Lu-PSMA-617 Radioligand Therapy in a Bicentric Analysis. *Eur J Nucl Med Mol Imaging* (2021) 48(4):1200–10. doi: 10.1007/s00259-020-05040-1
20. Grubmüller B, Rasul S, Baltzer P, Fajkovic H, D'Andrea D, Berndl F, et al. Response Assessment Using [68Ga] Ga-PSMA Ligand PET in Patients Undergoing Systemic Therapy for Metastatic Castration-Resistant Prostate Cancer. *Prostate* (2020) 80(1):74–82. doi: 10.1002/pros.23919
21. Draulans C, De Roover R, van der Heide UA, Kerkmeijer L, Smeenk RJ, Pos F, et al. Optimal 68 Ga-PSMA and 18 F-PSMA PET Window Levelling for Gross Tumour Volume Delineation in Primary Prostate Cancer. *Eur J Nucl Med Mol Imaging* (2021) 48(4):1211–18. doi: 10.1007/s00259-020-05059-4
22. Spohn SK, Kramer M, Kiefer S, Bronsert P, Sigle A, Schultze-Seemann W, et al. Comparison of Manual and Semi-Automatic [18f] PSMA-1007 Pet Based Contouring Techniques for Intraprostatic Tumor Delineation in Patients With Primary Prostate Cancer and Validation With Histopathology as Standard of Reference. *Front Oncol* (2020) 10. doi: 10.3389/fonc.2020.600690
23. Zacho HD, Nielsen JB, Haberkorn U, Stenholt L, Petersen LJ. 68Ga-PSMA PET/CT for the Detection of Bone Metastases in Prostate Cancer: A Systematic Review of the Published Literature. *Clin Physiol Funct Imaging* (2018) 38(6):911–22. doi: 10.1111/cpf.12480
24. Gupta M, Choudhury PS, Rawal S, Goel HC, Rao SA. Evaluation of RECIST, Percist, EORTC, and MDA Criteria for Assessing Treatment Response With Ga68-PSMA Pet-CT in Metastatic Prostate Cancer Patient With Biochemical Progression: A Comparative Study. *Nucl Med Mol Imaging* (2018) 52(6):420–9. doi: 10.1007/s13139-018-0548-3
25. Schwartz LH, Litière S, de Vries E, Ford R, Gwyther S, Mandrekar S, et al. Recist 1.1—Update and Clarification: From the RECIST Committee. *Eur J Cancer* (2016) 62:132–7. doi: 10.1016/j.ejca.2016.03.081
26. Cardinale J, Schäfer M, Benešová M, Bauder-Wüst U, Leotta K, Eder M, et al. Preclinical Evaluation of 18F-PSMA-1007, a New Prostate-Specific Membrane Antigen Ligand for Prostate Cancer Imaging. *J Nucl Med* (2017) 58(3):425–31. doi: 10.2967/jnumed.116.181768
27. d'Amico A, Gorczewska I, Gorczewski K, Turska-d'Amico M, Di Pietro M. Effect of Furosemide Administration Before F-18 Fluorodeoxyglucose Positron Emission Tomography/Computed Tomography on Urine Radioactivity and Detection of Uterine Cervical Cancer. *Nucl Med Rev* (2014) 17(2):83–6. doi: 10.5603/NMR.2014.0022
28. Eiber M, Herrmann K, Calais J, Hadaschik B, Giesel FL, Hartenbach M, et al. Prostate Cancer Molecular Imaging Standardized Evaluation (PROMISE): Proposed miTNM Classification for the Interpretation of PSMA-ligand Pet/Ct. *J Nucl Med* (2018) 59(3):469–78. doi: 10.2967/jnumed.117.198119
29. Bieth M, Krönke M, Tauber R, Dahlbender M, Retz M, Nekolla SG, et al. Exploring New Multimodal Quantitative Imaging Indices for the Assessment of Osseous Tumor Burden in Prostate Cancer Using 68Ga-PSMA Pet/Ct. *J Nucl Med* (2017) 58(10):1632–7. doi: 10.2967/jnumed.116.189050
30. Grubmüller B, Baltzer P, D'andrea D, Korn S, Haug A, Hacker M, et al. 68 Ga-PSMA 11 Ligand PET Imaging in Patients With Biochemical Recurrence After Radical Prostatectomy–Diagnostic Performance and Impact on Therapeutic Decision-Making. *Eur J Nucl Med Mol Imaging* (2018) 45 (2):235–42. doi: 10.1007/s00259-017-3858-2
31. Grubmüller B, Baltzer P, Hartenbach S, D'Andrea D, Helbich TH, Haug AR, et al. PSMA Ligand PET/MRI for Primary Prostate Cancer: Staging Performance and Clinical Impact. *Clin Cancer Res* (2018) 24(24):6300–7. doi: 10.1158/1078-0432.CCR-18-0768
32. Kratochwil C, Bruchertseifer F, Rathke H, Bronzel M, Apostolidis C, Weichert W, et al. Targeted α-Therapy of Metastatic Castration-Resistant Prostate Cancer With 225Ac-PSMA-617: Dosimetry Estimate and Empiric Dose Finding. *J Nucl Med* (2017) 58(10):1624–31. doi: 10.2967/jnumed.117.191395
33. Rathke H, Kratochwil C, Hohenberger R, Giesel FL, Bruchertseifer F, Flechsig P, et al. Initial Clinical Experience Performing Sialendoscopy for Salivary Gland Protection in Patients Undergoing 225 Ac-PSMA-617 Rlt. *Eur J Nucl Med Mol Imaging* (2019) 46(1):139–47. doi: 10.1007/s00259-018-4135-8
34. Wang B, Liu C, Wei Y, Meng J, Zhang Y, Gan H, et al. A Prospective Trial of 68Ga-PSMA and 18F-FDG PET/CT in Nonmetastatic Prostate Cancer Patients With an Early PSA Progression During Castration. *Clin Cancer Res* (2020) 26(17):4551–8. doi: 10.1158/1078-0432.CCR-20-0587
35. Current K, Meyer C, Magyar CE, Mona CE, Almajano J, Slavik R, et al. Investigating PSMA-Targeted Radioligand Therapy Efficacy as a Function of Cellular Psma Levels and Intratumoral Psma Heterogeneity. *Clin Cancer Res* (2020) 26(12):2946–55. doi: 10.1158/1078-0432.CCR-19-1485
36. Giesel FL, Hadaschik B, Cardinale J, Radtke J, Vinsensia M, Lehnert W, et al. F-18 Labelled PSMA-1007: Biodistribution, Radiation Dosimetry and Histopathological Validation of Tumor Lesions in Prostate Cancer Patients. *Eur J Nucl Med Mol Imaging* (2017) 44(4):678–88. doi: 10.1007/s00259-016-3573-4
37. Filss CP, Albert NL, Böning G, Kops ER, Suchorska B, Stoffels G, et al. O-(2-[18F] Fluoroethyl)-L-Tyrosine PET in Gliomas: Influence of Data Processing in Different Centres. *EJNMMI Res* (2017) 7(1):64. doi: 10.1186/s13550-017-0316-x
38. Cysouw MC, Kramer GM, Hoekstra OS, Frings V, De Langen AJ, Smit EF, et al. Accuracy and Precision of Partial-Volume Correction in Oncological PET/CT Studies. *J Nucl Med* (2016) 57(10):1642–9. doi: 10.2967/jnumed.116.173831
39. Rischpler C, Beck TI, Okamoto S, Schlitter AM, Knorr K, Schwaiger M, et al. 68ga-PSMA-HBED-CC Uptake in Cervical, Celiac, and Sacral Ganglia as an Important Pitfall in Prostate Cancer PET Imaging. *J Nucl Med* (2018) 59 (9):1406–11. doi: 10.2967/jnumed.117.204677

Conflict of Interest: The authors declare that the research was conducted in the absence of any commercial or financial relationships that could be construed as a potential conflict of interest.

frontiers in Oncology

ORIGINAL RESEARCH
published: 01 June 2021
doi: 10.3389/fonc.2021.665304

Changes of Radiation Treatment Concept Based on ^{68}Ga-PSMA-11-PET/CT in Early PSA-Recurrences After Radical Prostatectomy

Dirk Bottke[1†], Jonathan Miksch[2†], Reinhard Thamm[3], Thomas Krohn[4], Detlef Bartkowiak[3], Meinrad Beer[5], Christian Bolenz[6], Ambros J. Beer[2], Vikas Prasad[2] and Thomas Wiegel[3]*

[1] Xcare Praxis für Strahlentherapie, Trier, Germany, [2] Department of Nuclear Medicine, University Hospital of Ulm, Ulm, Germany, [3] Department of Radiation Oncology and Radiotherapy, University Hospital Ulm, Ulm, Germany, [4] Radiologie Aachen Land, Würselen, Germany, [5] Department of Radiology, University Hospital of Ulm, Ulm, Germany, [6] Department of Urology, University Hospital of Ulm, Ulm, Germany

OPEN ACCESS

Edited by:
Trevor Royce, University of North Carolina at Chapel Hill, United States

Reviewed by:
Panayiotis Mavroidis, University of North Carolina at Chapel Hill, United States
Osama Mohamad, University of California, San Francisco, United States

***Correspondence:**
Dirk Bottke
dirk.bottke@x-care.de

[†]These authors share first authorship

Specialty section:
This article was submitted to Cancer Imaging and Image-directed Interventions, a section of the journal Frontiers in Oncology

Received: *07 February 2021*
Accepted: *03 May 2021*
Published: *01 June 2021*

Citation:
Bottke D, Miksch J, Thamm R, Krohn T, Bartkowiak D, Beer M, Bolenz C, Beer AJ, Prasad V and Wiegel T (2021) Changes of Radiation Treatment Concept Based on ^{68}Ga-PSMA-11-PET/CT in Early PSA-Recurrences After Radical Prostatectomy. Front. Oncol. 11:665304. doi: 10.3389/fonc.2021.665304

Background and Purpose: Salvage radiotherapy (SRT) is the main potentially curative treatment option for prostate cancer patients with post-prostatectomy PSA progression. Improved diagnostics by positron emission tomography/computed tomography (PET/CT) can lead to adjustments in treatment procedures (e.g. target volume of radiotherapy, androgen deprivation therapy). We analyzed the impact of ^{68}Ga-PSMA-11-PET/CT on the target volume in early biochemical recurrence (PSA up to 0.5 ng/ml).

Patients and Methods: We retrospectively analyzed 76 patients with biochemical recurrence after radical prostatectomy in whom SRT was planned after ^{68}Ga-PSMA-11-PET/CT. All patients had a PSA ≤0.5 ng/ml. An experienced radiation oncologist determined the radiotherapy concept, first with consideration of the PET/CT, second hypothetically based on the clinical and pathological features excluding PET/CT results.

Results: Without considering the PET/CT, all 76 patients would have been assigned to RT, 60 (79%) to the bed of the prostate and seminal vesicles alone, and 16 (21%) also to the pelvic lymph nodes because of histopathologic risk factors. Uptake indicative for tumor recurrence in ^{68}Ga-PSMA-11-PET/CT was found in 54% of the patients. The median pre-PET/CT PSA level was 0.245 ng/ml (range 0.07–0.5 ng/ml). The results of the PET/CT led to a change in the radiotherapeutic target volume in 21 patients (28%). There were major changes in the target volume including the additional irradiation of lymph nodes or the additional or exclusive irradiation of bone metastases in 13 patients (17%). Minor changes including the additional irradiation of original seminal vesicle (base) position resulted in eight patients (11%).

Conclusion: Using ^{68}Ga-PSMA-11-PET/CT for radiation planning, a change in the treatment concept was indicated in 28% of patients. With PET/CT, the actual extent of

the tumor can be precisely determined even with PSA values of ≤0.5 ng/ml. Thus, the treatment concept can be improved and individualized. This may have a positive impact on progression free survival. Our results warrant further prospective studies.

Keywords: prostate cancer, biochemical recurrence, early salvage radiotherapy, positron emission tomography (PET), PSMA

INTRODUCTION

Radical prostatectomy (RP) is considered to be a standard treatment option for patients with clinically localized prostate cancer (PCa). Nevertheless, up to 50–80% of these men develop biochemical recurrence depending on risk factors such as an advanced pathological stage, a high Gleason score or positive surgical margins (1). In case of PSA recurrence, salvage radiotherapy (SRT) is the only curative option, resulting in approximately 60% of the patients reachieving an undetectable PSA. After 5 years, 80% of these men are free from progression (2). The pre-SRT PSA level is a significant factor of progression, with more favorable results for patients with low PSA levels (0.5 ng/ml or less) (3, 4). Accordingly, European guidelines (EAU) recommend early SRT at a PSA <0.5 ng/ml (5).

At PSA levels <1 ng/ml, most imaging methods are not suitable to detect the correlate for disease progression. Therefore, up to 20% of patients with SRT to the prostate bed (with or without including original seminal vesicle) without morphological correlate will be treated locally without actual local recurrence (2).

Prostate-specific membrane antigen (PSMA) is a cell surface protein with high expression in majority of prostate cancer (6). ^{68}Ga-PSMA has been used since 2012 as PSMA-ligand in recurrent prostate cancer (7–9). Especially at low PSA levels, the detection rate of ^{68}Ga-PSMA-11-PET/CT is significantly higher in comparison to other imaging methods.

In a retrospective analysis of 2,533 patients with biochemical progression after RP, Afshar-Oromieh et al. found that 69% of the patients had at least one positive lesion indicating PCa recurrence. The detection rates were 43% for PSA levels ≤0.2 ng/ml, 58% for PSA >0.2 to ≤0.5 and 72% for PSA >0.5 to ≤1.0. Tumor detection was clearly associated with PSA level and higher Gleason scores (8).

Recently, we reported a detection rate of 50% in 116 patients with PSA levels up to 0.6 ng/ml and in the PSA subgroups 0–0.2, 0.21–0.3, and 0.31–0.6 ng/ml; 24, 57, and 65%, respectively (9).

Bluemel et al. analyzed the impact of ^{68}Ga-PSMA-11-PET/CT in patients with PSA failure and negative F-18-choline-PET/CT. Of 125 patients, 32 patients with negative F-18-choline-PET/CT received an additional ^{68}Ga-PSMA-11-PET/CT, which detected sites of recurrence in 43.8% (10).

This new possibility of precise detection of PSMA-expressing lesions can lead to changes of tumor staging and radiation planning. Data from numerous studies are available, especially on the impact of tumor stage changes on salvage radiotherapy planning (**Table 2**). However, only few data are available for patients with early biochemical recurrence (PSA <0.5 ng/ml) (11).

The goal of this retrospective, single-center analysis was to assess the impact of ^{68}Ga-PSMA-11-PET/CT on the radiotherapeutic treatment concept in biochemical recurrence up to PSA 0.5 ng/ml.

MATERIAL AND METHODS

Patients

In this retrospective analysis, only patients with PSA ≤0.5 ng/ml after RP and having undergone PSMA PET/CT prior to the radiation therapy were included. Patients' data were retrospectively analyzed from the institutional database of the Department of Nuclear Medicine and the Department of Radiation Oncology which are part of the Comprehensive Cancer Center Ulm (CCCU). Overall, 76 patients were found to fulfill the inclusion criteria. For all patients SRT was planned after ^{68}Ga-PSMA-11-PET/CT.

An experienced radiation oncologist determined patient's actual treatment concept with consideration of the PET/CT images. Retrospectively a hypothetical treatment concept (prescription and planning target volume [PTV] contouring) was planned based on the clinical and pathological parameters excluding PET/CT results: In pT2- and pT3a-tumors the PTV included the prostate bed and the basis of the former seminal vesicles. In pT3b-tumors, the bed of seminal vesicles was included, too. Inclusion of regional pelvic lymph nodes was considered in case of histopathologic risk factors (e.g. pN1, Gleason score ≥8).

All patients gave their written informed consent for a retrospective analysis of their data in an anonymized form. The study was approved by the local ethics committee of Ulm University (221/20-FSt/Sta).

Radiopharmaceutical Preparation

The ^{68}Ga-HBED-CC-PSMA complex (ABX GmbH, Radeberg, Germany) was produced as already published. For labeling the 50 mCi (1,850 MBq), iThemba LABS, South Africa ^{68}Ge/^{68}Ga radionuclide generator was used (12, 13).

PET/CT Imaging Protocol and Interpretation

PET/CT images were acquired by a Biograph mCT (40)S in 3D acquisition mode 63.4 ± 11.4 min after intravenous infusion of 160.3 ± 29.4 MBq ^{68}Ga-PSMA-11. Axial, sagittal and coronal slices were reconstructed afterwards. For attenuation correction and anatomical correlation, a low-dose CT was performed. Bed positions were set weight-based taking circa 2.5 min per bed

position for body scan and 2 min for scanning legs. Scans were done from the mid-thighs to the vertex in 5 to 8 bed positions resulting in 15 to 20 min for each scan (170.2 ± 39.7 mAs). Intravenous contrast (80 to 120 ml Ultravist 370, Bayer Schering Pharma, Berlin, Germany) and 15 to 20 mg of furosemide were administered in 71 (93%) and 68 patients (89%) unless contraindicated. For a diagnostic CT, scans were performed 70 s past contrast injection for the venous phase.

TABLE 1 | Patients' characteristics.

Patient number	76
Age (years), median (range)	67 (47–79)
iPSA (ng/ml), median (range)	7.31 (1.93–35.0)
Gleason score n (%)	
Low risk (≤6) (%)	13 (17.1)
Intermediate risk (7) (%)	45 (59.2)
High risk (≥8) (%)	17 (22.4)
Unknown	1 (1.3)
Initial TNM classification n (%)	
≤pT2a (%)	4 (5.3)
pT2b (%)	4 (5.3)
≥pT2c (%)	68 (89.4)
pN0 (%)	69 (90.8)
pN1 (%)	5 (6.6)
cN0	2 (2.6)
cM0	76 (100)
PSA pre-PET/CT	0.245 (0.07–0.5)

A tracer uptake more than the immediate surrounding tissue and not related or explained due to the physiological expression was considered as pathologic. Two experienced nuclear medicine physicians with more than 10 years of experience in PET/CT analyzed the images.

RESULTS

The median PSA level before PET imaging was 0.245 ng/ml (range 0.07–0.5 ng/ml). Median age was 67 years (range 47–79 years). Patient characteristics are shown in **Table 1**.

Pathological tracer uptake as a sign of tumor recurrence in ^{68}Ga-PSMA-11-PET/CT was found in 54% of the patients.

Additional information from ^{68}Ga-PSMA-11-PET/CT lead to adaptation of RT planning in 28% (n = 21) of cases. In the hypothetical scenario without considering PET/CT results all the76 patients would have received RT: 60 (79%) to the bed of the prostate and seminal vesicles alone, and 16 (21%) also to the pelvic lymph nodes because of histopathologic risk factors.

We have defined major and minor changes. Major changes included the additional or exclusive irradiation of lymph nodes or the additional or exclusive irradiation of bone metastases based on the PET/CT. Minor changes included the additional irradiation of original seminal vesicle (base) position (**Figure 1**). Due to PET/CT, major changes were necessary in

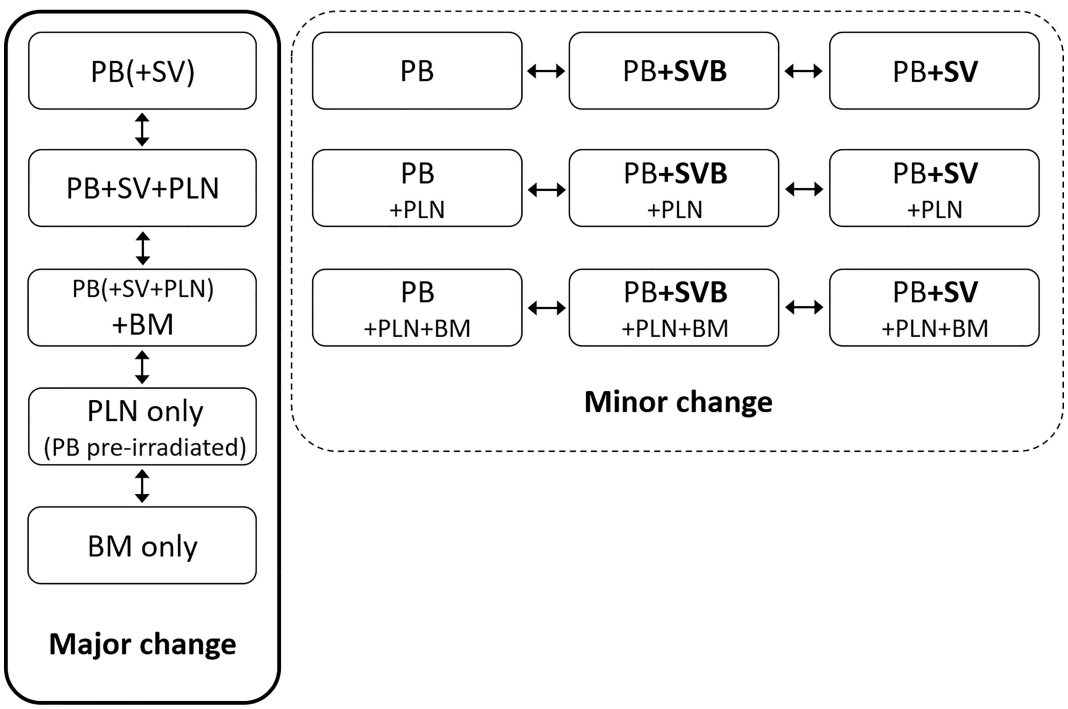

FIGURE 1 | Definition of major and minor changes of radiotherapeutic treatment concept. PB, postoperative prostate bed; SV, original seminal vesicle position; SVB, original seminal vesicle base position; PLN, pelvic lymph nodes; BM, bone metastasis; NC, no change.

13 patients (17%) and minor changes in eight patients (11%) (**Figures 2** and **3**). Postoperative prostate bed ± vesicle base position was irradiated with 72–74 Gy (median 72 Gy) and-positive lymph nodes with 60 Gy (range 50.4–66.6 Gy).

Based on the PET/CT, in six patients (8%), bone metastases were detected and were additionally irradiated with median 45 Gy (range 39–54 Gy).

PSA values 6 months after completion of SRT were available in 54 patients, out of which 47 (87%) patients achieved a PSA response (**Figure 4**).

DISCUSSION

In our retrospective study ^{68}Ga-PSMA-11-PET/CT led to changes of the RT target volume in 28% of patients with PSA ≤0.5 ng/ml after RP.

Detecting the site of prostate cancer recurrence is crucial for a successful treatment planning. In the presence of distant metastases, a prostate bed RT is not indicated. On the other hand, in the event of an exclusive loco-regional recurrence, a long-term ADT could be avoided or at least delayed by SRT. In

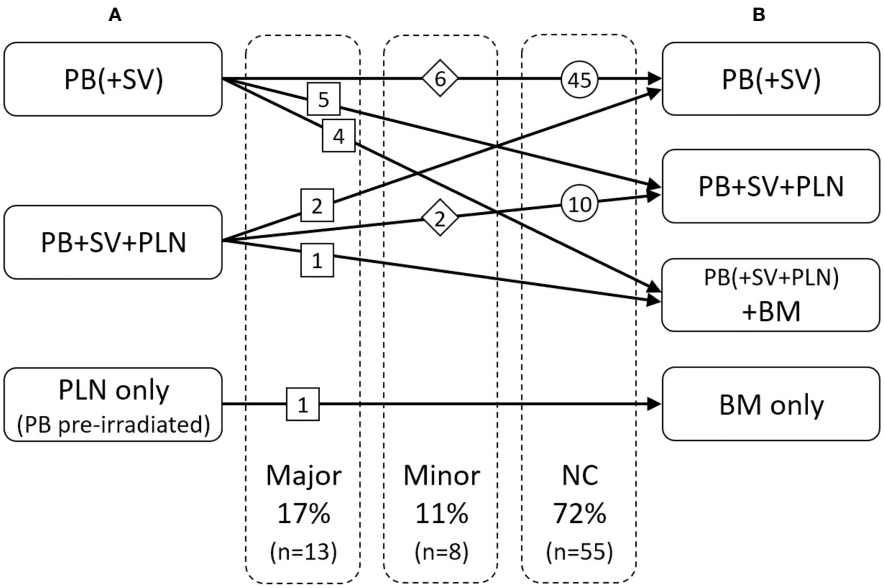

FIGURE 2 | Changes of radiotherapeutic treatment concept: **(A)** based on the clinical and pathological situation without PET/CT, **(B)** with consideration of the PET/CT. PB, postoperative prostate bed; SV, original seminal vesicle position; PLN, pelvic lymph nodes; BM, bone metastasis.

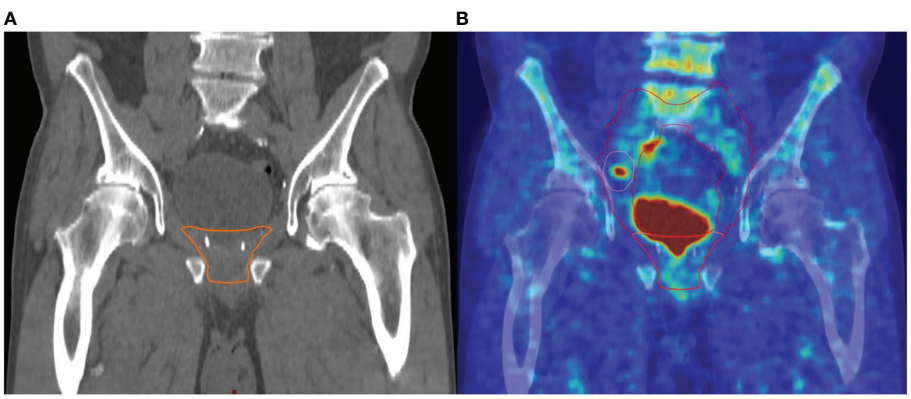

FIGURE 3 | Example of major change of the radiotherapeutic treatment concept: **(A)** target volume without pelvic lymph nodes based on the clinical and pathological situation without PET/CT, **(B)** target volume with consideration of the PET/CT: additional irradiation of pelvic lymph nodes based on a PET/CT-positive right iliac lymph node metastasis.

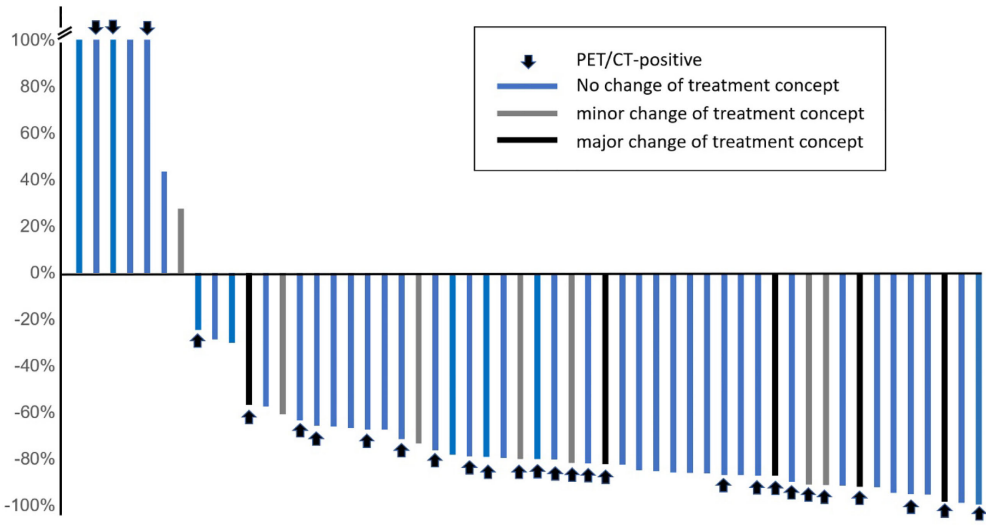

FIGURE 4 | PSA changes after salvage treatment.

the pre-PSMA era, most patients with PSA-failure had to undergo "blind" SRT under the assumption of local recurrence limited to the prostatic bed only.

It is equally imperative to stress that a negative PSMA-PET should not delay early SRT as the sensitivity of PSMA PET/CT for detection of micrometastases is questionable. Therefore, in the absence of any suspicious findings on PSMA-PET/CT, early SRT of the prostate bed should be offered without time delay (14).

On the other side of the spectrum, the possibility to visualize PSMA avid lesions at an early stage prior to the SRT offers the unique possibility of individualization of treatment planning as is shown in our study. ^{68}Ga-PSMA-11-PET/CT led to changes of the radiation concept in 28% of all cases. All patients had a PSA <0.5ng/ml, impressively demonstrating the great potential of this imaging approach.

The impact of PSMA-PET/CT on SRT planning is extensively evaluated in several studies, albeit in heterogeneous patient population as is evident from **Table 2**. In most studies the median PSA value was significantly higher than in our study (median PSA 0.245 ng/ml).

Our results are in line with the retrospective study published by Farolfi et al. (11), to our knowledge the only work that has also studied patients with low PSA limit of 0.5 ng/ml. 119 patients with a median PSA of 0.32 ng/ml (range 0.2–0.5 ng/ml) were evaluated. ^{68}Ga-PSMA-11-PET/CT was positive in 41 patients (34.4%). Pathological PSMA uptake was detected in the prostate bed (three patients), in the pelvic lymph nodes (21 patients), in the retroperitoneal lymph nodes (four patients) and in bone (21 patients). The initial planned radiation concept was changed in 36 patients (30.2%) due to the PET/CT results.

In contrast, a multicenter post-hoc analysis of 270 patients with biochemical recurrence after RP with a PSA ≤1 ng/ml (median 0.48 ng/ml) showed that PSMA-PET/CT had a major impact in 19% of patients (22). A major impact was defined as PSMA-PET/CT-positive disease outside planning target volumes

TABLE 2 | Studies assessing the impact of PSMA-PET/CT on salvage radiotherapy planning.

Authors	Year	n	Median PSA (ng/ml) (range)	PSA limit (ng/ml)	PSMA+	Extra-pelvic PSMA+	Any SRT planning change
Van Leeuwen et al. (15)	2016	70	0.2 (0.05–0.99)	<1	55%	6%	35%
Sterzing et al. (16)	2016	42	2.8 (0.16–113)	None	60%	N/A	61%
Bluemel et al. (17)	2016	45	0.67 (0.10–11.2)	None	54%	9%	42%
Albisinni et al. (18)	2017	48	2.2 (0.72–6.7)	None	N/A	N/A	76%
Habl et al. (19)	2017	83	0.69 (0.09–14.7)	None	71%	10%	57%
Koerber et al. (20)	2018	71	1.2 (0.03–41.24)	None	N/A	51%	54%
Frenzel et al. (21)	2018	75	0.2 (0.02–653.2)	None	N/A	N/A	43%
Farolfi et al. (11)	2019	119	0.32 (0.20–0.50)	<0.5	35%	21%	30%
Calais et al. (22)	2018	270	0.48 (0.03–1.0)	<1	49%	13%	19%
Schmidt-Hegemann et al. (23)	2019	62	0.44 (0.15–6.24)	None	54%	3%	50%
Boreta et al. (24)	2019	125	0.4 (0.28–0.63)	≤2.0	53%	20%	30%
Current study	2020	76	0.25 (0.07–0.50)	<0.5	54%	3%	28%

N/A, not available.

expanded from clinical target volumes (CTV) covering both the prostate bed and pelvic lymph nodes. The two most common PET-positive locations outside the CTV were bone (44%) and lymph nodes (31%). These results show the need for an earlier PSMA-PET/CT (22).

Habl et al. analyzed staging changes due to ^{68}Ga-PSMA-11-PET and its impact on RT procedure in 100 patients after radical prostatectomy. Median PSA level was 1.0 ng/ml (range 0.12–14.7 ng/ml). 29 patients had initial pN1 disease. In 76 patients, at least one pathological PSMA uptake was found. Of these, 80% showed no morphological correlate in the corresponding CT or MRI. The tumor stage was changed in 43% of the patients. Due to the PSMA-PET/CT imaging, initial RT planning was modified in 59% of all cases. An additional simultaneous integrated boost to the prostate bed or lymph nodes was given to 32 and 63%, respectively. Ten patients received stereotactic body radiation therapy to single bone metastases (19).

Our study has some limitations due to the retrospective and monocentric approach. In addition, a biopsy of PET-positive lesions is often not feasible, particularly in patients with recurrent prostate cancer. Therefore, the lack of histological validation is a common limitation in many imaging studies.

Our results showed that ^{68}Ga-PSMA-11-PET/CT is a valuable tool in the RT planning procedure of patients with recurrent PCa after radical prostatectomy even at PSA levels ≤0.5 ng/ml. They support the implementation of this imaging procedure in routine practice for biochemical progression after RP.

However, it remains unclear whether the use of PSMA-PET/CT in planning SRT could improve outcomes.

In September 2018, Calais et al. initiated a randomized phase III trial to determine whether oncological outcomes can be improved by PSMA-PET/CT in patients with early biochemical recurrence following RP. A total of 193 patients will be randomized to standard SRT (without PSMA-PET/CT) or PET scan prior to SRT planning. The primary endpoint is the biochemical progression-free survival after SRT (25).

In the future, the superior soft-tissue contrast of PET/MRI may be able to further improve the detection of pelvic tumor lesions. First results showed that the detection rate was higher than the published results for PET/CT (26). Up to now, however, the availability of PET/MRI is very low.

CONCLUSION

^{68}Ga-PSMA-11-PET/CT showed a high impact on radiation therapy procedure in patients with biochemically recurrent prostate cancer at PSA levels <0.5 ng/ml. With 28% changes in radiotherapy planning, ^{68}Ga-PSMA-11-PET/CT is an important tool in guiding radiation treatment in this patient group. However, clinical data about the outcome of those treated patients have to be awaited.

DATA AVAILABILITY STATEMENT

The raw data supporting the conclusions of this article will be made available by the authors, without undue reservation.

ETHICS STATEMENT

All patients gave their written informed consent for a retrospective analysis of their data in an anonymized form. The study was approved by the local ethics committee of Ulm University (221/20- FSt/Sta).

AUTHOR CONTRIBUTIONS

RT, TW, and AB contributed to conception and design of the study. JM, RT, and DBo organized the database. DBo performed the statistical analysis and wrote the first draft of the manuscript. JM, TK, DBa, MB, CB, AB, VP, and TW wrote sections of the manuscript. All authors contributed to the article and approved the submitted version.

ACKNOWLEDGMENTS

We want to thank the PET-team and Radiopharmacy unit for their excellent work. Ambros Beer, Meinrad Beer and Christian Bolenz are members of the i2SOUL (innovative imaging in surgical oncology Ulm) consortium, which we thank for support.

REFERENCES

1. Wiegel T, Bartkowiak D, Bottke D, Bronner C, Steiner U, Siegmann A, et al. Adjuvant Radiotherapy Versus Wait-and-See After Radical Prostatectomy: 10-Year Follow-Up of the ARO 96-02/AUO AP 09/95 Trial. *Eur Urol* (2014) 66:243–50. doi: 10.1016/j.eururo.2014.03.011
2. Wiegel T, Lohm G, Bottke D, Höcht S, Miller K, Siegmann A, et al. Achieving an Undetectable PSA After Radiotherapy for Biochemical Progression After Radical Prostatectomy Is an Independent Predictor of Biochemical Outcome – Results of a Retrospective Study. *Int J Radiat Oncol Biol Phys* (2009) 73:1009–16. doi: 10.1016/j.ijrobp.2008.06.1922
3. Tendulkar RD, Agrawal S, Gao T, Efstathiou JA, Pisansky TM, Michalski JM, et al. Contemporary Update of a Multi-Institutional Predictive Nomogram for Salvage Radiotherapy After Radical Prostatectomy. *J Clin Oncol* (2016) 34:3648–54. doi: 10.1200/JCO.2016.67.9647
4. Bottke D, Bartkowiak D, Siegmann A, Thamm R, Böhmer D, Budach V, et al. Effect of Early Salvage Radiotherapy At PSA < 0.5 ng/ml and Impact of Post-SRT PSA Nadir in Post-Prostatectomy Recurrent Prostate Cancer. *Prostate Cancer Prostatic Dis* (2019) 22:344–9. doi: 10.1038/s41391-018-0112-3
5. Cornford P, Bellmunt J, Bolla M, Briers E, De Santis M, Gross T, et al. EAU-ESTRO-SIOG Guidelines on Prostate Cancer. Part II: Treatment of Relapsing, Metastatic, and Castration-Resistant Prostate Cancer. *Eur Urol* (2017) 71:630–42. doi: 10.1016/j.eururo.2016.08.002
6. Ghosh A, Heston WD. Tumor Target Prostate Specific Membrane Antigen (PSMA) and Its Regulation in Prostate Cancer. *J Cell Biochem* (2004) 91:528–39. doi: 10.1002/jcb.10661
7. Eiber M, Maurer T, Souvatzoglou M, Beer AJ, Ruffani A, Haller B, et al. Evaluation of Hybrid 68Ga-PSMA Ligand PET/CT in 248 Patients With Biochemical Recurrence After Radical Prostatectomy. *J Nucl Med* (2015) 56:668–74. doi: 10.2967/jnumed.115.154153
8. Afshar-Oromieh A, Holland-Letz T, Giesel FL, Kratochwil C, Mier W, Haufe S, et al. Diagnostic Performance of (68)Ga-PSMA-11 (HBED-CC) PET/CT in Patients With Recurrent Prostate Cancer: Evaluation in 1007 Patients. *Eur J Nucl Med Mol Imaging* (2017) 44:1258–68. doi: 10.1007/s00259-017-3711-7

9. Miksch J, Bottke D, Krohn T, Thamm R, Bartkowiak D, Solbach C, et al. Interobserver Variability, Detection Rate, and Lesion Patterns of (68)Ga-PSMA-11-PET/CT in Early-Stage Biochemical Recurrence of Prostate Cancer After Radical Prostatectomy. *Eur J Nucl Med Mol Imaging* (2020) 47:2339–47. doi: 10.1007/s00259-020-04718-w
10. Bluemel C, Krebs M, Polat B, Linke F, Eiber M, Samnick S, et al. 68Ga-PSMA-PET/CT in Patients With Biochemical Prostate Cancer Recurrence and Negative 18F-Choline-PET/CT. *Clin Nucl Med* (2016) 41:515–21. doi: 10.1097/RLU.0000000000001197
11. Farolfi A, Ceci F, Castellucci P, Graziani T, Siepe G, Lambertini A, et al. (68) Ga-Psma-11 PET/CT in Prostate Cancer Patients With Biochemical Recurrence After Radical Prostatectomy and PSA <0.5 Ng/Ml. Efficacy and Impact on Treatment Strategy. *Eur J Nucl Med Mol Imaging* (2019) 46:11–9. doi: 10.1007/s00259-018-4066-4
12. Eder M, Schäfer M, Bauder-Wüst U, Hull WE, Wängler C, Mier W, et al. 68Ga-Complex Lipophilicity and the Targeting Property of a Urea-Based PSMA Inhibitor for PET Imaging. *Bioconjug Chem* (2012) 23:688–97. doi: 10.1021/bc200279b
13. Schäfer M, Bauder-Wüst U, Leotta K, Zoller F, Mier W, Haberkorn U, et al. A Dimerized Urea-Based Inhibitor of the Prostate-Specific Membrane Antigen for 68Ga-PET Imaging of Prostate Cancer. *EJNMMI Res* (2012) 2:23. doi: 10.1186/2191-219X-2-23
14. Mottet N, Cornford P, van den Bergh RCN, Briers E, De Santis M, Fanti S, et al. *Eau Guidelines on Prostate Cancer* (2020). Available at: https://uroweb.org/guideline/prostate-cancer/.
15. van Leeuwen PJ, Stricker P, Hruby G, Kneebone A, Ting F, Thompson B, et al. (68) Ga-PSMA has a High Detection Rate of Prostate Cancer Recurrence Outside the Prostatic Fossa in Patients Being Considered for Salvage Radiation Treatment. *BJU Int* (2016) 117:732–9. doi: 10.1111/bju.13397
16. Sterzing F, Kratochwil C, Fiedler H, Katayama S, Habl G, Kopka K, et al. (68) Ga-PSMA-11 PET/CT: A New Technique With High Potential for the Radiotherapeutic Management of Prostate Cancer Patients. *Eur J Nucl Med Mol Imaging* (2016) 43:34–41. doi: 10.1007/s00259-015-3188-1
17. Bluemel C, Linke F, Herrmann K, Simunovic I, Eiber M, Kestler C, et al. Impact of (68)Ga-PSMA PET/CT on Salvage Radiotherapy Planning in Patients With Prostate Cancer and Persisting PSA Values or Biochemical Relapse After Prostatectomy. *EJNMMI Res* (2016) 6:78. doi: 10.1186/s13550-016-0233-4
18. Albisinni S, Artigas C, Aoun F, Biaou I, Grosman J, Gil T, et al. Clinical Impact of (68) Ga-Prostate-Specific Membrane Antigen (PSMA) Positron Emission Tomography/Computed Tomography (PET/CT) in Patients With Prostate Cancer With Rising Prostate-Specific Antigen After Treatment With Curative Intent: Preliminary Analysis of a Multidisciplinary Approach. *BJU Int* (2017) 120:197–203. doi: 10.1111/bju.13739
19. Habl G, Sauter K, Schiller K, Dewes S, Maurer T, Eiber M, et al. (68)Ga-PSMA-PET for Radiation Treatment Planning in Prostate Cancer Recurrences After Surgery: Individualized Medicine or New Standard in Salvage Treatment. *Prostate* (2017) 77:920–7. doi: 10.1002/pros.23347
20. Koerber SA, Will L, Kratochwil C, Haefner MF, Rathke H, Kremer C, et al. (68)Ga-PSMA-11 PET/CT in Primary and Recurrent Prostate Carcinoma: Implications for Radiotherapeutic Management in 121 Patients. *J Nucl Med* (2018) 60:234–40. doi: 10.2967/jnumed.118.211086
21. Frenzel T, Tienken M, Abel M, Berliner C, Klutmann S, Beyersdorff D, et al. The Impact of [(68)Ga]PSMA I&T PET/CT on Radiotherapy Planning in Patients With Prostate Cancer. *Strahlenther Onkol* (2018) 194:646–54. doi: 10.1007/s00066-018-1291-5
22. Calais J, Czernin J, Cao M, Kishan AU, Hegde JV, Shaverdian N, et al. (68)Ga-PSMA-11 PET/CT Mapping of Prostate Cancer Biochemical Recurrence After Radical Prostatectomy in 270 Patients With a PSA Level of Less Than 1.0 ng/mL: Impact on Salvage Radiotherapy Planning. *J Nucl Med* (2018) 59:230–7. doi: 10.2967/jnumed.117.201749
23. Schmidt-Hegemann NS, Eze C, Li M, Rogowski P, Schaefer C, Stief C, et al. Impact of (68)Ga-PSMA PET/CT on the Radiotherapeutic Approach to Prostate Cancer in Comparison to CT: A Retrospective Analysis. *J Nucl Med* (2019) 60:963–70. doi: 10.2967/jnumed.118.220855
24. Boreta L, Gadzinski AJ, Wu SY, Xu M, Greene K, Quanstrom K, et al. Location of Recurrence by Gallium-68 PSMA-11 PET Scan in Prostate Cancer Patients Eligible for Salvage Radiotherapy. *Urology* (2019) 129:163–4. doi: 10.1016/j.urology.2018.12.055
25. Calais J, Czernin J, Fendler WP, Elashoff D, Nickols NG. Randomized Prospective Phase III Trial of (68)Ga-PSMA-11 PET/CT Molecular Imaging for Prostate Cancer Salvage Radiotherapy Planning [PSMA-SRT]. *BMC Cancer* (2019) 19:18. doi: 10.1186/s12885-019-5297-x
26. Kranzbühler B, Nagel H, Becker AS, Müller J, Huellner M, Stolzmann P, et al. Clinical Performance of (68)Ga-PSMA-11 PET/MRI for the Detection of Recurrent Prostate Cancer Following Radical Prostatectomy. *Eur J Nucl Med Mol Imaging* (2018) 45:20–30. doi: 10.1007/s00259-017-3850-x

Conflict of Interest: The authors declare that the research was conducted in the absence of any commercial or financial relationships that could be construed as a potential conflict of interest.

frontiers in Oncology

SYSTEMATIC REVIEW
published: 17 June 2021
doi: 10.3389/fonc.2021.684629

The Diagnostic Role of ^{18}F-Choline, ^{18}F-Fluciclovine and ^{18}F-PSMA PET/CT in the Detection of Prostate Cancer With Biochemical Recurrence: A Meta-Analysis

Rang Wang[†], *Guohua Shen*[†], *Mingxing Huang and Rong Tian*[*]

Department of Nuclear Medicine, West China Hospital, Sichuan University, Chengdu, China

OPEN ACCESS

Edited by:
Harun Ilhan, Hospital of the University of Munich, Germany

Reviewed by:
Matthias Miederer, Johannes Gutenberg University Mainz, Germany
Murat Tuncel, Hacettepe University, Turkey

***Correspondence:**
Rong Tian
rongtiannuclear@126.com

[†]*These authors have contributed equally to this work*

Specialty section:
This article was submitted to Cancer Imaging and Image-directed Interventions, a section of the journal Frontiers in Oncology

Received: *23 March 2021*
Accepted: *31 May 2021*
Published: *17 June 2021*

Citation:
Wang R, Shen G, Huang M and Tian R (2021) The Diagnostic Role of ^{18}F-Choline, ^{18}F-Fluciclovine and ^{18}F-PSMA PET/CT in the Detection of Prostate Cancer With Biochemical Recurrence: A Meta-Analysis. Front. Oncol. 11:684629. doi: 10.3389/fonc.2021.684629

Background: Diagnosing the biochemical recurrence (BCR) of prostate cancer (PCa) is a clinical challenge, and early detection of BCR can help patients receive optimal treatment. We conducted a meta-analysis to define the diagnostic accuracy of PET/CT using ^{18}F-labeled choline, fluciclovine, and prostate-specific membrane antigen (PSMA) in patients with BCR.

Methods: Multiple databases were searched until March 30, 2021. We included studies investigating the diagnostic accuracy of ^{18}F-choline, ^{18}F-fluciclovine, and ^{18}F-PSMA PET/CT in patients with BCR. The pooled sensitivity, specificity, and detection rate of ^{18}F-labeled tracers were calculated with a random-effects model.

Results: A total of 46 studies met the included criteria; 17, 16, and 13 studies focused on ^{18}F-choline, fluciclovine, and PSMA, respectively. The pooled sensitivities of ^{18}F-choline and ^{18}F-fluciclovine were 0.93 (95% CI, 0.85–0.98) and 0.80 (95% CI, 0.65–0.897), and the specificities were 0.91 (95% CI, 0.73–0.97) and 0.66 (95% CI, 0.50–0.79), respectively. The pooled detection rates of ^{18}F-labeled choline, fluciclovine and PSMA were 66, 74, and 83%, respectively. Moreover, the detection rates of ^{18}F-labeled choline, fluciclovine, and PSMA were 35, 23, and 58% for a PSA level less than 0.5 ng/ml; 41, 46, and 75% for a PSA level of 0.5–0.99 ng/ml; 62, 57, and 86% for a PSA level of 1.0–1.99 ng/ml; 80, 92, and 94% for a PSA level more than 2.0 ng/ml.

Conclusion: These three ^{18}F-labeled tracers are promising for detecting BCR in prostate cancer patients, with ^{18}F-choline showing superior diagnostic accuracy. In addition, the much higher detection rates of ^{18}F-PSMA showed its superiority over other tracers, particularly in low PSA levels.

Systematic Review Registration: PROSPERO, identifier CRD42020212531.

Keywords: PET/CT, ^{18}F, choline, fluciclovine, prostate-specific membrane antigen, prostate cancer

INTRODUCTION

Prostate cancer (PCa) is one of the most common malignancy in men worldwide and is also the fifth major cause of cancer-related death in men. It is estimated that over 300,000 PCa-related deaths occur in 2018 (1). In addition to its high morbidity and mortality, the recurrence and metastasis of prostate cancer are also troublesome in clinical practice (2, 3).

It is challenging to detect initial recurrence and metastasis after prior treatment because of few obvious characteristics on early recurrent or metastatic lesions. PCa recurrence is usually considered when observing a rise in the serum prostate-specific antigen (PSA) level. This is regarded as biochemical recurrence (BCR) of PCa, and the definition of BCR is a serum PSA level over a threshold of 0.2 ng/ml twice after radical prostatectomy (RP) or an absolute increase in PSA level of 2 ng/ml over the lowest posttreatment PSA level after radiation therapy (RT) (4, 5).

The key issue for patients with BCR is the early and correct identification of recurrent or metastatic disease, which is essential for further devising treatment strategies since treatment varies based on the presence of local recurrence, regional lymph node and distant viscera or bone metastasis (6). Conventional imaging modalities consisting of CT, bone scan, and MRI have been used for patients with advanced PCa, but their roles in detecting minimal or occult lesions are limited (7, 8). These conventional imaging modalities also have low sensitivity and specificity in detecting patients with BCR, especially those with a low PSA level. According to the 2020 American Society of Clinical Oncology (ASCO) guidelines, next-generation imaging (NGI) such as PET/CT, PET/MRI, and whole-body MRI is recommended for use in patients with rising PSA after prior treatment when conventional imaging findings are negative (9). Radioactive tracers such as choline and fluciclovine have been used for prostate cancer staging, restaging, and treatment response evaluation. Meanwhile, prostate-specific membrane antigen (PSMA), a new radiopharmaceutical that binds to prostate cancer-specific target, has demonstrated outstanding detection rate for recurrent or metastatic lesions among patients with BCR.

Choline is an essential element of phospholipids in the cellular wall, and the increased uptake of choline means increased metabolism of the cell membrane components of malignant tumors (10). ^{11}C-choline was approved by the Food and Drug Administration (FDA) in 2012, but its short half-life limits its widespread use in PET/CT centers without onsite cyclotrons. Later, ^{18}F-labeled choline was developed, and its longer half-life has solidified ^{18}F-choline PET/CT as a significant imaging modality in patients with suspected PCa recurrence (11, 12). ^{18}F-Fluciclovine (anti-1-amino-3-^{18}F-fluorocyclobutane-1-carboxylic acid, ^{18}F-FACBC), as a synthetic amino acid that is upregulated in PCa, is an option for molecular imaging in patients with BCR, which was approved by the FDA in 2016 (13, 14). The main advantage of ^{18}F-fluciclovine is its low urinary excretion, which allows for better detection and localization of PCa recurrence in patients with rising PSA level (15). PSMA is a type 2 transmembrane protein that is more highly expressed in the prostate cancer cell membrane than in normal tissues (16–18). Therefore, PSMA has become a promising target for imaging prostate cancer (19). ^{68}Ga-PSMA PET/CT has been proven to improve the detection of metastatic disease and the monitoring of treatment effects in patients with PCa (20). Most recently, ^{68}Ga-PSMA-11, as the first PSMA PET agent, has been approved by the FDA. ^{18}F-labeled PSMA has also begun to be used in clinical practice, and its long half-life and high resolution in PET/CT images have further increased the detection rate of PSMA-targeted imaging in subtle or occult metastases (21, 22). Moreover, ^{18}F-PSMA-1007 PET/CT can differentiate local recurrence from physical uptake in the urinary bladder or ureter due to non-urinary clearance (23, 24).

Some previous studies have compared the diagnostic roles of ^{11}C-choline, ^{18}F-fluciclovine, and ^{68}Ga-PSMA PET/CT in patients with BCR, showing that ^{68}Ga-PSMA PET/CT has a superior detection rate (25). Even so, there have been some clinical challenges existing in ^{68}Ga-PSMA PET/CT due to certain shortcomings including its short half-life, non-ideal energies and the limited availability of ^{68}Ga. Compared with ^{68}Ga and ^{11}C, ^{18}F, as a longer half-life nuclide, has many advantages such centralized production in a cyclotron facility and more favorable positron energies for imaging, thereby motivating the development of ^{18}F-labeled analogs. Currently, growing clinical experience has revealed the high diagnostic accuracy of some ^{18}F-labeled tracers in PCa patients with BCR. However, the effectiveness of ^{18}F-labeled choline, fluciclovine, and PSMA remains unclear because of limited number of studies. Herein, we aimed to perform a meta-analysis to review and compare the diagnostic value of ^{18}F-labeled choline, fluciclovine, and PSMA PET/CT imaging for detecting BCR in patients with PCa, in order to provide better creditability for clinical practice.

METHODS

The Preferred Reporting Items for Systematic Reviews and Meta-analyses (PRISMA) guidelines was used for our study (26). Our review has registered on the international prospective register of systematic reviews (PROSPERO) (CRD 42020198861).

Search Strategy

A literature research was conducted with scientific databases, including PubMed, EMBASE, and Web of Science, until March 30, 2021. A search algorithm was developed based on a combination of keywords ("choline" OR "fluciclovine" OR "FACBC" OR "PSMA" OR "DCFPyL" OR "DCFBC" OR "1007") AND ("prostate cancer" OR "prostate neoplasm") AND ("biochemical recurrence" OR "biochemical failure") AND ("PET/CT" OR "positron emission tomography/computed tomography") AND ("^{18}F" OR "fluorine").

Two authors independently screened and evaluated these studies. The reference lists of all relevant studies were further checked to find more suitable studies. A third author was

responsible for disagreement and solved the controversy between two authors through discussion.

Selection of Studies

Studies using ^{18}F-labeled tracers such as ^{18}F-choline, ^{18}F-fluciclovine, and ^{18}F-PSMA were evaluated. Studies were included according to the following criteria: (a) sample size >10; (b) patients who had evidence of BCR underwent PET/CT; (c) studies evaluating the diagnostic accuracy of ^{18}F-labeled tracers in prostate cancer patients with BCR; (d) histological results, imaging, or clinical follow-up as a reference standard. Studies on other tracers were not included. Abstracts, reviews, and case reports were also not included. If the studies included duplicate patients, we reviewed and included the study with the largest sample or the most recent study performed. The included studies were limited to those published in English.

Quality Assessment

The quality of included studies was critically assessed by two independent authors according to the Quality Assessment of Diagnostic Accuracy Studies-2 (QUADAS-2) tool. This tool comprises four domains (patient selection, index test, reference standard, and flow and timing), and each domain was used to assess the risk of bias. Next, applicability was also considered according to patient selection, the index test, and the reference standard.

Data Extraction

Two authors collected various parameters and outcomes from each eligible study as follows: author, country, publication year, study design, number of patients, age, pre-PET PSA level, reference criteria, scanner model, ligands, and injection dose and the detection rate as well as true positive (TP), false positive (FP), false negative (FN), and true negative (TN) PET/CT with different tracers in patients with BCR. All discrepancies were resolved by consensus and ultimately based on the decision of the third author.

Statistical Analysis

For studies reporting the diagnostic performance of ^{18}F-PSMA, ^{18}F-choline, and ^{18}F-fluciclovine PET/CT in patients with BCR, 2×2 table was used to calculate TP, FP, TN, and FN. The pooled sensitivity and specificity were calculated by a random-effects model. We developed a hierarchical summary receiver operating curve and calculated the area under the curve. We presented forest plots with 95% confidence intervals (CIs) for the sensitivity and specificity of each study. In addition, the detection rates of PET tracers were extracted and pooled using a random-effects model. If possible, subgroup analysis was considered based on different PSA serum values.

Heterogeneity within studies was evaluated using Cochran's Q test and the I^2 statistic (27). An I^2 value greater than 50% was indicative of substantial heterogeneity. The funnel plot test and Egger's test were used to assess the publication bias. All statistical analyses were performed using Stata 15.0 and RevMan 5.3. P-value <0.05 was considered to be statistically significant (28).

RESULTS

The flow chart demonstrates an overview of the search and selection process (**Figure 1**). The initial search yielded 480 studies, of which 95 were duplicates. Subsequently, after reviewing the titles and abstracts, we excluded 238 studies for the following reasons: 170 studies were case reports, reviews, and academic meeting abstracts, 11 were basic studies, five applications in other diseases, and 52 studies used different radiotracers and imaging modalities. Of the remaining studies, 75 studies were not relevant to our aims, and most of them investigated the impact of novel PET/CT tracers in treatment management for patients with PCa or focused on evaluating metastatic disease. In addition, 26 studies did not provide sufficient information and were excluded. Thus, only 46 studies were finally included. Of these, 17 studies focused on the role of ^{18}F-choline PET/CT in prostate cancer patients with BCR (29–45). The numbers of included studies regarding ^{18}F-fluciclovine and ^{18}F-PSMA PET/CT were 16 and 13, respectively (46–74). **Tables 1–3** outline the characteristics of each eligible study.

Quality Assessment

Figures 2A–C show the results of the quality assessment of each eligible study for ^{18}F-choline, ^{18}F-fluciclovine, and ^{18}F-PSMA, respectively. Patient selection was not considered the source of bias because all studies had qualified patient selection criteria. For the index test and reference standard, some studies did not adopt the blinding method when interpreting the positive scan of the PET/CT findings, and we rated these studies as high or unclear levels regarding the risk of bias and applicability concern. Similarly, unclear or high levels were displayed on the applicability concern of flow and timing because of the different follow-up times and multiple reference standards.

Diagnostic Performance of ^{18}F-Choline and ^{18}F-Fluciclovine PET/CT

Seventeen studies reported the diagnostic performance of ^{18}F-choline, and the summary sensitivity and specificity of ^{18}F-choline PET/CT in patients with BCR were 0.93 (95% CI, 0.85–0.96) and 0.91 (95% CI, 0.73–0.97), respectively (**Figure 3**). The summary sensitivity and specificity drawn from studies on ^{18}F-fluciclovine were 0.80 (95% CI, 0.65–0.89) and 0.66 (95% CI, 0.50–0.79), respectively (**Figure 4**). However, the summary sensitivity and specificity were not constructed for ^{18}F-PSMA PET/CT imaging because these studies mostly focused on the detection rate in patients with BCR. Summary receiver operating characteristic (SROC) curves of ^{18}F-choline and ^{18}F-fluciclovine were demonstrated in **Figures 5A, B**.

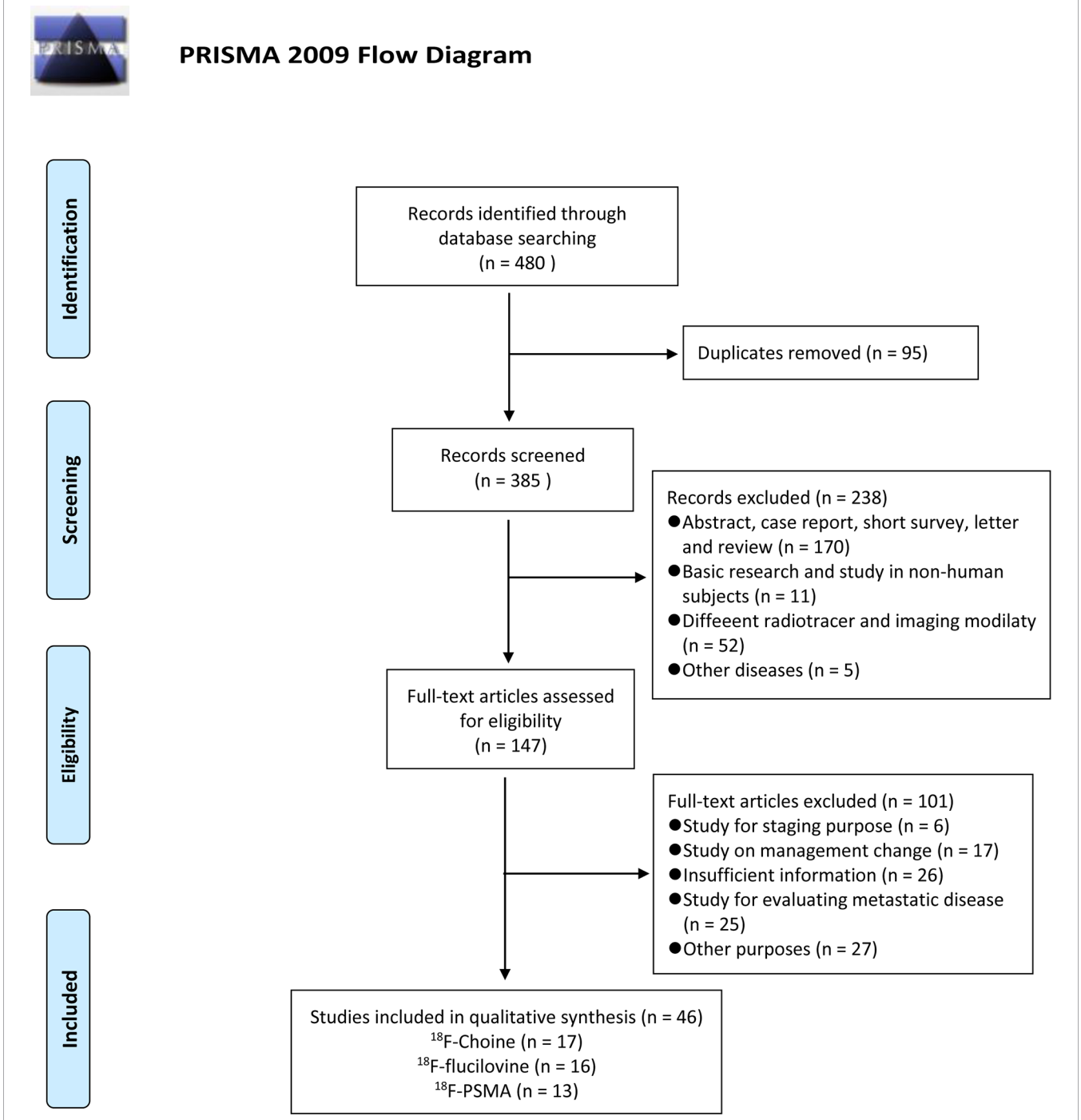

FIGURE 1 | Flow of study search.

Detection Rate of ^{18}F-Choline, ^{18}F-Fluciclovine, and ^{18}F-PSMA PET/CT

The pooled detection rate of ^{18}F-choline PET/CT was 66%, lower than 74% of ^{18}F-fluciclovine PET/CT. In addition, the pooled detection rate of ^{18}F-PSMA PET/CT was 83% (**Figure 6**). Meanwhile, the detection rates of ^{18}F-labeled choline, fluciclovine, and PSMA were 35, 23, and 58% for a PSA level less than 0.5 ng/ml (**Figure 7**); 41, 46, and 75% for a PSA level of 0.5–0.99 ng/ml (**Figure 8**); 62,

TABLE 1 | Study characteristics of ^{18}F-choline PET/CT.

Author	Publication Year	Country	Design	Patients	Mean age/Range	PSA (ng/mL)	Scancer Modality	Ligand	Mean dose	Reference standard
Pelosi	2008	Italy	R	56	67.9 ± 7	4.59 ± 7.87	Discovery ST unit, GE	^{18}F-choline	185–259 MBq	Multiple
Kwee	2012	US	P	50	69.0 ± 8.9	3.2 (0.2–18.2)	Philips Gemini TF-64	^{18}F-fluorocholine	2.6 MBq/kg	Multiple
Panebianco	2012	Italy	P	84	56–72	1.63	Discovery ST, GE	^{18}F-choline	185-259 MBq	Multiple
Schillaci	2012	Italy	P	49	70. 9 ± 7	4.13 ± 4.56	Discovery ST, GE	^{18}F-choline	370 MBq	Biopsy
Detti	2013	Italy	R	170	——	3.5 ± 8.8	PET/CT Philips TOF	^{18}F-fluorocholine	3.7 MBq/kg	Follow-up
Marzola	2013	Italy	R	233	69.4 ± 6.5	7.4 ± 13.6	Discovery STE	^{18}F-fluorocholine	3 MBq/kg	
Piccardo	2014	Italy	P	21	77.2 ± 5.1	5.8 ± 3.4	Discovery ST, GE	^{18}F-choline	3MBq/kg	Multiple
Morigi	2015	Australia	P	38	68(54–81)	1.72 ± 2.54	Philips Ingenuity TF 64	^{18}F-fluorocholine	3.5 MBq/kg	Biopsy
Rodado-Marina	2015	Spain	R	233	68 ± 7.1	5.3 ± 8.7	GE and Siemens equipments	^{18}F-fluorocholine	4 MBq/kg	Multiple
Cimitan	2015	Italy	R	1,000	69.68 ± 7.67	3.30	GE Discovery LS; Siemens Biograph 16 HT or Biograph mCT; GE Discovery ST8,	^{18}F-choline	3.0–3.5 MBq/kg	Multiple
Simone	2015	Italy	P	146	68	0.6 (0.43–0.76)	Siemens Biograph Hi-Rez 16;	^{18}F-choline	4 MBq/kg	Multiple
Emmett	2018	Australia	P	91	64 (59–69)	0.42 (0.29–0.93)	——	^{18}F-choline	3.6 MBq/kg	Multiple
Giovacchini	2019	Italy	R	192	73.2 ± 6.6	9.53 ± 16.70	GE Discovery 710	^{18}F-fluorocholine	3.7 MBq/kg	Multiple
Witkowska-Patena	2019	Poland	P	40	68.6 ± 6.5	0.75 ± 0.6	GE Discovery 710	^{18}F-fluorocholine	248 ± 35 MBq	Multiple
Sánchez	2020	Spain	P	108	69 ± 6.7	4.9 ± 5.2	Siemens Biograph mCT	^{18}F-choline	370 MBq	Multiple
Zattoni	2020	Italy	R	2,798	72 (66.29–77.0)	2.0 (0.1–3.0)	——	^{18}F-choline	2.5-3.7 MBq/kg	
de Leiris	2020	France	R	115	73.2 (56–89)	9.4 (7.1–18.4)	GE Discovery 690	^{18}F-choline	3.7 MBq/kg	Multiple

A multiple reference standards including biopsy, other imaging modalities and follow-up.

TABLE 2 | Study characteristics of ^{18}F-fluciclovine PET/CT.

Author	Publication Year	Country	Design	Patients	Mean age/Range	PSA (ng/mL)	Scancer Modality	Ligand	Mean dose	Reference standard
Schuster	2011	US	P	50	68.3 ± 8.1	6.62 ± 7.63	Discovery DLS, GE	^{18}F-fluciclovine	199.8–484.7 MBq	Multiple
Kairemo	2014	Finland	R	26	68.1 ± 5.8	7.9 ± 14.6	Siemens Biograph	^{18}F-fluciclovine	328 ± 56.8 MBq	Multiple
Nanni	2016	Italy	P	89	69	6.99	Discovery STE, GE	^{18}F-fluciclovine	370 MBq	Follow-up
Odewole	2016	USA	R	53	67.57± 8.03	7.2 ± 8.3	GE Discovery DLS or 690	^{18}F-fluciclovine	358 ± 52.9MBq	Follow-up
Bach-Gansmo	2017	Norway, Italy, UK	R	143	67	5.43	——	^{18}F-fluciclovine	310 MBq	Follow-up
Miller	2017	USA	R	110	67.4 ± 7.37	5.87 ± 7.65	GE Discovery DLS or 690	^{18}F-fluciclovine	370 MBq	Multiple
Akin-Akintayo	2018	USA	P	24	70.8 ± 5.7	8.5 ± 6.1	GE Discovery 690	^{18}F-fluciclovine	370 ± 13 MBq	Biopsy
Jambor	2018	Finland	P	32	65 (49–76)	12 (4.1–35)	GE Discovery 690	^{18}F-fluciclovine	369 ± 10 MBq	Biopsy
Andriole	2019	US	P	213	66.4 ± 7.75	4.24 ± 10.22	——	^{18}F-fluciclovine	370 ± 20% MBq	Multiple
Calais	2019	US	P	50	68 (64–74)	0·48 (0·38–0·83)	Siemens Biograph64 and GE Discovery	^{18}F-fluciclovine	381 MBq	Multiple
England	2019	US	R	28	67.1 (53–77)	0.44(0.1–1)	Siemens Biograph	^{18}F-fluciclovine	370 MBq	Follow-up
Savir-Baruch	2019	US	R	152	68.73 ± 7.92	2.06 (0.006–120)	Philips Ingenuity TF PET/CT	^{18}F-fluciclovine	9.97 ± 1.18mci	——
Teyateeti	2020	US	R	94	65.7 (42.5–80.3)		GE Discovery 710, MI and Siemens Biograph 64	^{18}F-fluciclovine	370 MBq	Multiple
Garza	2021	US	R	78	68.7 (48–87)	0.72(<0.05–1.99)	——	^{18}F-fluciclovine	——	Imaging
Michael	2021	US	R	103	69.79 ± 7.88	5.77 ± 9.98	Siemens Biograph	^{18}F-fluciclovine	10 mci	Imaging
Nakamoto	2021	US	R	165	71.1 ± 8.8	3.1 (1.0–9.6)	GE Discovery 600, 690, or MI	^{18}F-fluciclovine	389 ± 59 MBq	Multiple

A multiple reference standards including biopsy, other imaging modalities and follow-up.

TABLE 3 | Study characteristics of ^{18}F-PSMA PET/CT.

Author	Publication Year	Country	Design	Patients	Mean age/year	PSA (ng/ml)	Scancer Modality	Tracer	Mean dose	Reference standard
Rahbar	2018	Germany	R	100	68.75 ± 7.6	3.3 6 ± 6.11	Siemens Healthcare	^{18}F-PSMA-1007	4 MBq/kg	– –
Eiber	2018	Germany	R	261	72 (49–88)	0.961 (0.01–400.0)	Siemens Biograph mCT	^{18}F-rhPSMA-7	333 ± 44 MBq	– –
Giesel	2018	Germany	R	251	70 (48–86)	1.2 (0.2–228)	Siemens Biograph mCT	^{18}F-PSMA-1007	301 ± 46 MBq	– –
Rousseau	2018	Canada	P	130	69.1 ± 6.5	5.20 ± 6.50	GE Discovery PET/CT 600 or 690	^{18}F-DCFPyL	369.2 ± 47.2 MBq	– –
Wondergem	2019	Netherlands	R	248	71 (67–75)		Philips Ingenuity TF, Siemens Biograph 16	^{18}F-DCFPyL	311 MBq	– –
Mena	2019	USA	P	90	66 (50–81)	2.5 ± 5.9	GE Discovery MI	^{18}F-DCFPyL	299.9 ± 15.5 MBq	– –
Song	2019	USA	P	72	71.5 ± 7.2	3.0 (0.23-698.4)	GE Discovery MI	^{18}F-DCFPyL	338.8 ± 25.3 MBq	– –
Wtkowska-Patena	2019	Poland	P	40	68.6 ± 6.5	0.75 ± 0.6	GE Discovery 710,	^{18}F-PSMA-1007	295.5 ± 14.1 MBq	– –
Rowe	2020	USA	P	31	63 (45–74)	0.4 (0.2–28.3)	GE Discovery RX 64 or Biograph mCT 128	^{18}F-DCFPyL	<333 MBq	– –
Chaussé	2020	Canada	R	93	70.4(51-87)	2.27 (0.07–51.09)	GE Discovery ST	^{18}F-DCFPyL	333 ± 37 MBq	Multiple
Dietlein	2021	Germany	R	70	70.1 ± 5.5			^{18}F-JK-PSMA-7	348 ± 55 MBq	– –
Koschel	2021	Australia	P	98	68.0 (66.0–71.0)	0.32 (0.28–0.36)	GE Discovery 710	^{18}F-DCFPyL	250 ± 50 MBq	Imaging
Perry	2021	New Zealand	R	222	71 (49–89)	0.51 (0.08–58.9)	GE Discovery 690, 710	^{18}F-DCFPyL	250 ± 50 MBq	– –

A multiple reference standards including biopsy, other imaging modalities and follow-up.

57, and 86% for a PSA level of 1.0–1.99 ng/ml (**Figure 9**); 80, 92, and 94% for a PSA level more than 2.0 ng/ml (**Figure 10**).

DISCUSSION

Our meta-analysis included studies investigating the diagnostic roles of three novel ^{18}F-labeled tracers applied in prostate cancer patients with BCR. From our study, the summary sensitivity and specificity of ^{18}F-choline and ^{18}F-fluciclovine PET/CT were 0.93 and 0.91, and 0.80 and 0.66, respectively. For the detection rate, the pooled detection rates of ^{18}F-labeled choline, fluciclovine, and PSMA were 66, 74, and 83%, respectively. Meanwhile, we observed a higher detection rate of biochemically recurrent PCa with ^{18}F-PSMA compared with choline and fluciclovine PET/CT for the different PSA level subgroups.

Multiple PET/CT radiotracers have been developed and experimented in recent years, motivating the wide use of PET/CT or PET/MRI in patients with PCa for staging, restaging, and response evaluation (75, 76). ^{18}F-fluciclovine PET/CT showed a superior advantage over ^{11}C-choline PET/CT in patients with BCR and further aid guiding decision-making in regard to patients' treatment strategy (48, 77). In addition, PSMA PET/CT has shown superior diagnostic accuracy for recurrence and metastases of prostate cancer than fluciclovine and choline. A meta-analysis defined the diagnostic accuracy of PET/CT imaging using ^{11}C-choline, ^{18}F-fluciclovine, or ^{68}Ga-PSMA, showing that ^{68}Ga-PSMA PET/CT has a nearly equal sensitivity but the highest specificity among these tracers for PET/CT imaging in detecting biochemically recurrent PCa (25).

In contrast, our meta-analysis focused on only long-half radionuclides as ^{18}F-labeled tracers and summarized the diagnostic accuracy of ^{18}F-labeled choline, fluciclovine, and PSMA in detecting patients with BCR. Our study revealed that ^{18}F-PSMA had the highest detection rate at different PSA levels, and the detection rate was related to the PSA level. These results were consistent with another meta-analysis that compared the detection rate of biochemically recurrent PCa between PSMA-targeted radiotracers and ^{18}F-fluciclovine, finding that PSMA-targeted radiotracers demonstrate a greater detection rate than ^{18}F-fluciclovine (78). A study compared prospectively paired ^{18}F-fluciclovine and PSMA PET/CT scans for localizing recurrence of PCa after prostatectomy in patients with a PSA level <2.0 ng/ml (55). They found that PSMA PET/CT showed higher detection rates and should be the tracer choice when PET/CT imaging is considered for patients with biochemical recurrence after radical prostatectomy with low PSA concentrations (≤2.0 ng/ml). The same conclusion was drawn from another prospective study paired that compared ^{18}F-PSMA and ^{18}F-fluorocholine PET/CT in patients with BCR (42). The advantage of PSMA-targeted PET/CT imaging could be attributed to the high expression of PSMA in PCa and its metastases.

In late 2020, ^{68}Ga-PSMA-11 became the first PSMA PET tracer to be approved by the FDA, which may facilitate widespread adaptation. Despite this, there also have been some limitations related to ^{68}Ga-PSMA PET/CT because of the short half-life, non-

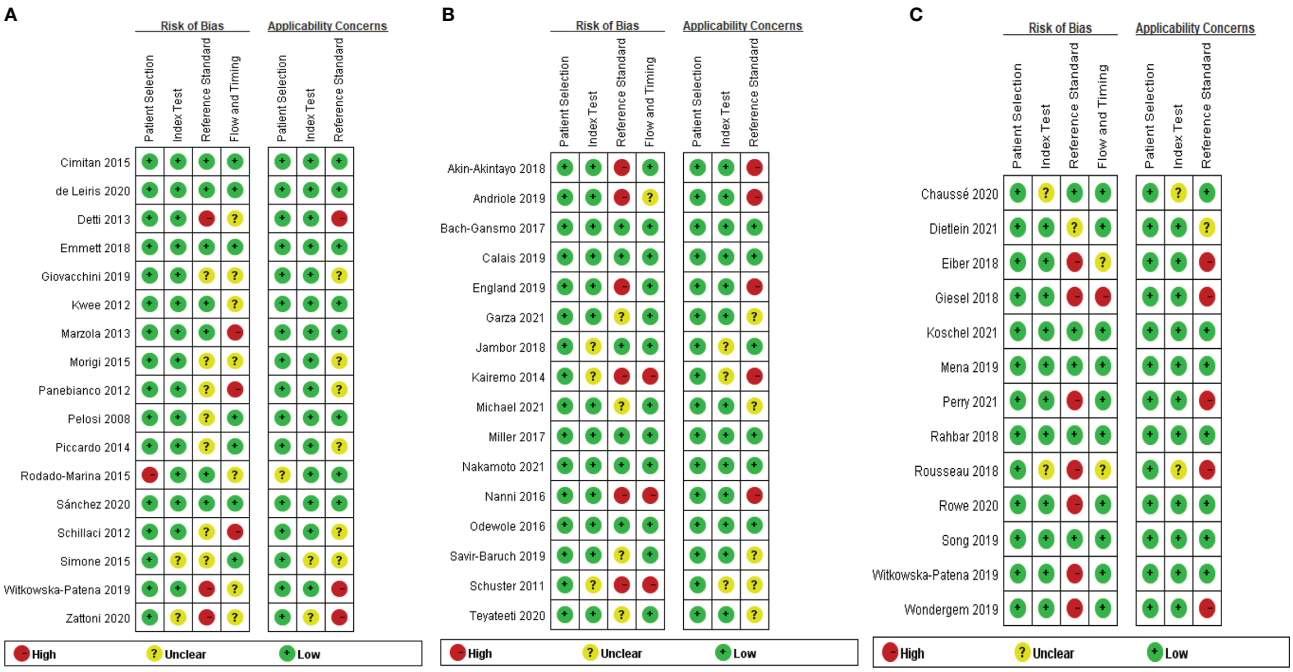

FIGURE 2 | **(A)** Quality Assessment of Diagnostic Accuracy Studies-2 analysis of study bias in ^{18}F-choline cohort. **(B)** Quality Assessment of Diagnostic Accuracy Studies-2 analysis of study bias in ^{18}F-fluciclovine cohort. **(C)** Quality Assessment of Diagnostic Accuracy Studies-2 analysis of study bias in ^{18}F prostate-specific membrane antigen (PSMA) cohort.

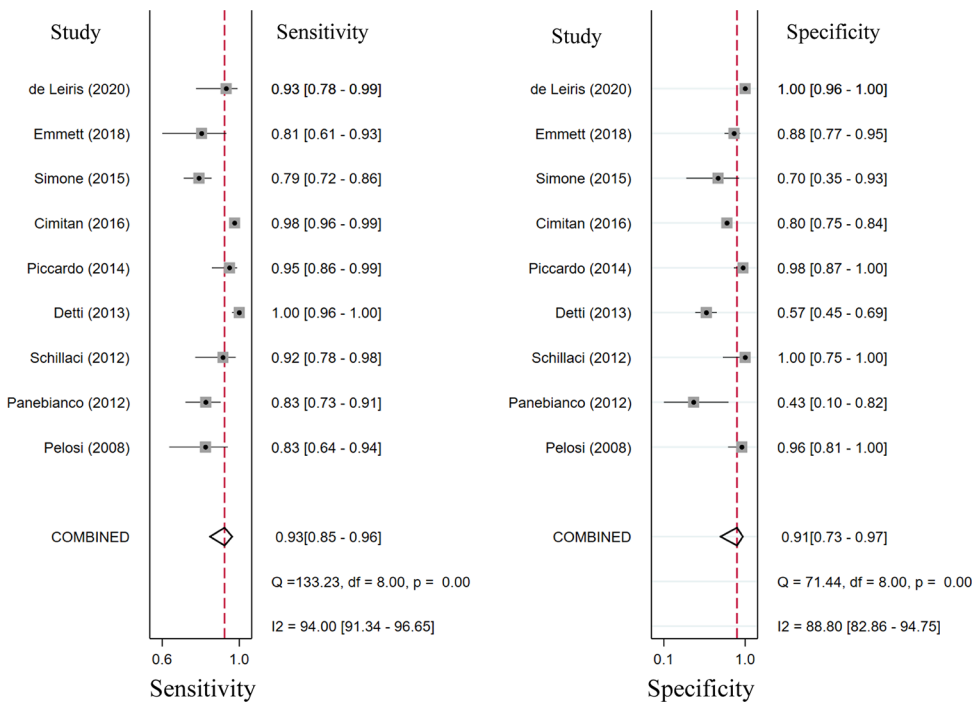

FIGURE 3 | Forest plot of the proportion of ^{18}F-choline positron emission tomography/computed tomography (PET/CT) sensitivity and specificity in prostate cancer patients with biochemical recurrence.

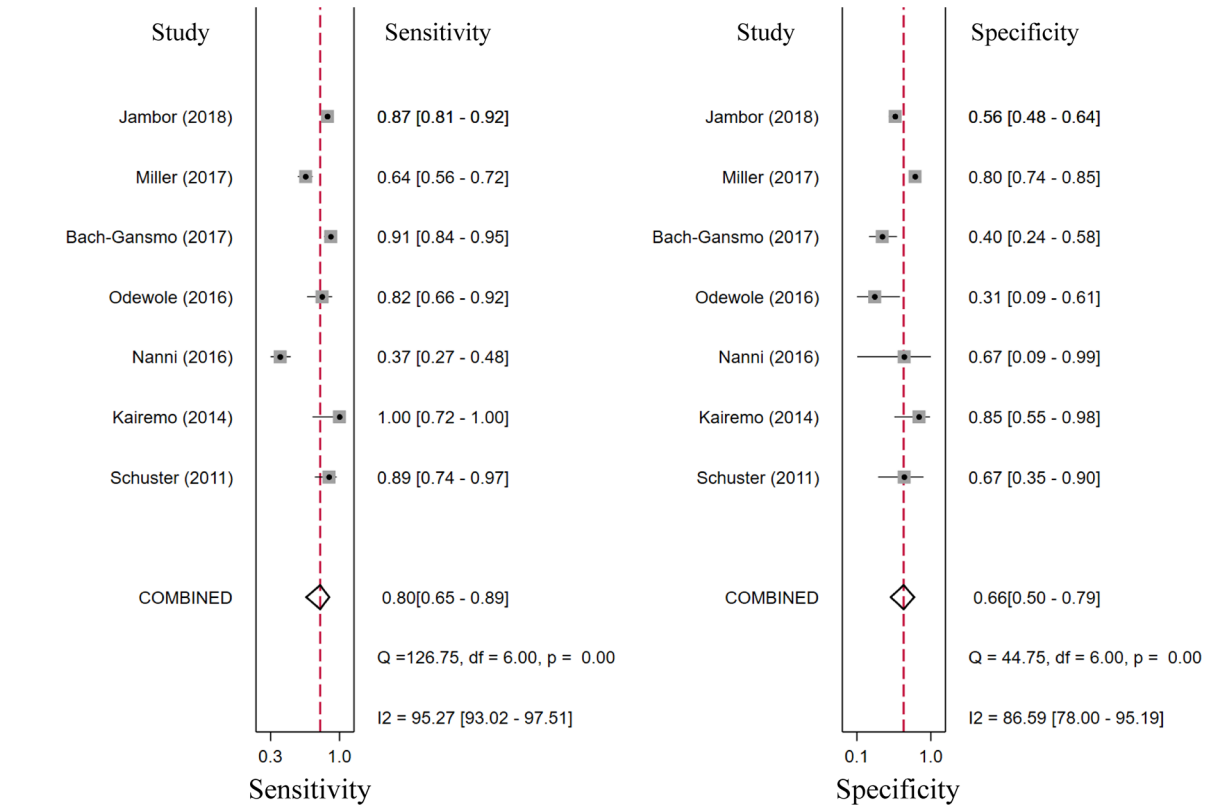

FIGURE 4 | Forest plot of the proportion of ^{18}F-fluciclovine PETCT sensitivity and specificity in prostate cancer patients with biochemical recurrence.

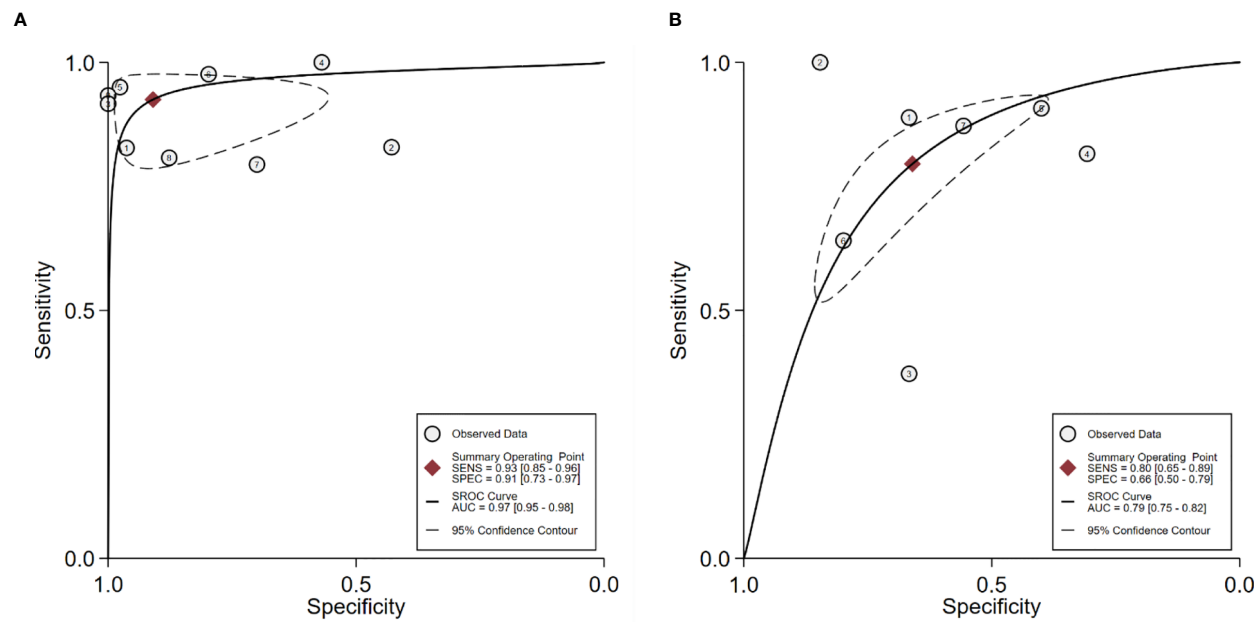

FIGURE 5 | **(A)** SROC curve for the diagnostic accuracy of ^{18}F-choline PET/CT in prostate cancer patients with biochemical recurrence. **(B)** SROC curve for the diagnostic accuracy of ^{18}F-fluciclovine PET/CT in prostate cancer patients with biochemical recurrence. SROC, summary receiver operating characteristic.

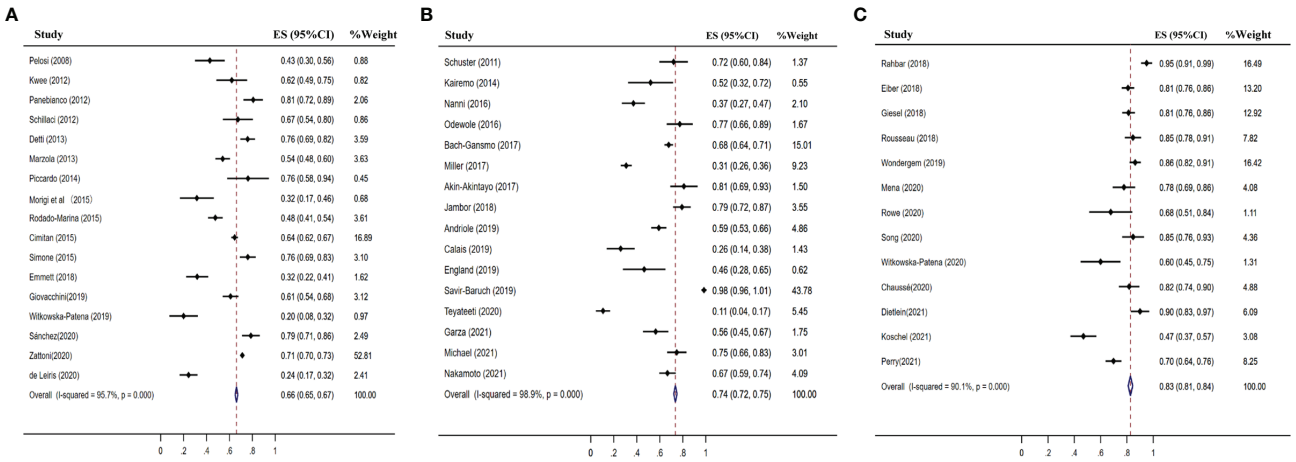

FIGURE 6 | Forest plot of the proportion of ^{18}F-labeled choline **(A)**, fluciclovine **(B)** and PSMA **(C)** PET/CT positivity of prostate cancer patients with biochemical recurrence.

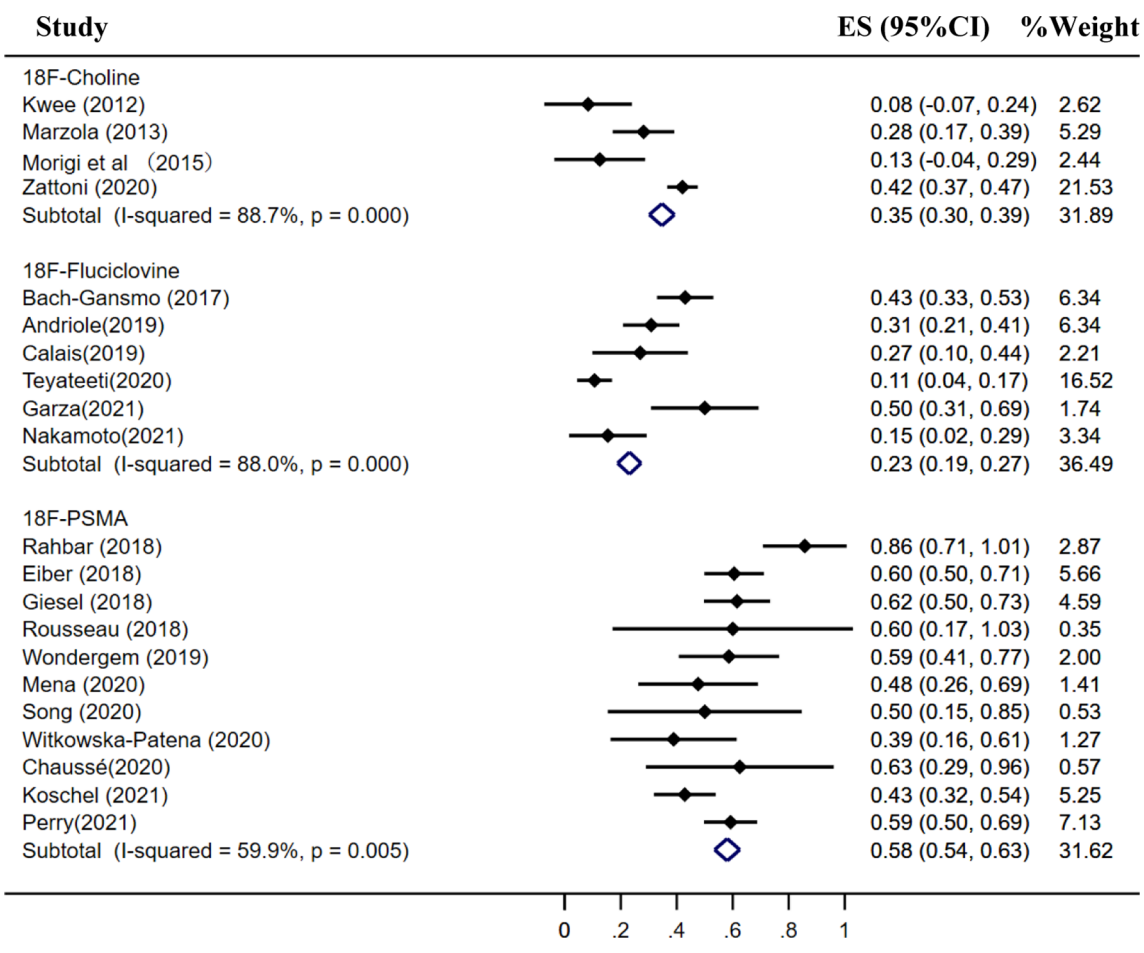

FIGURE 7 | Forest plot of the proportion of ^{18}F-labeled choline, fluciclovine and PSMA positivity of prostate cancer patients with BCR for PSA less than 0.5 ng/ml.

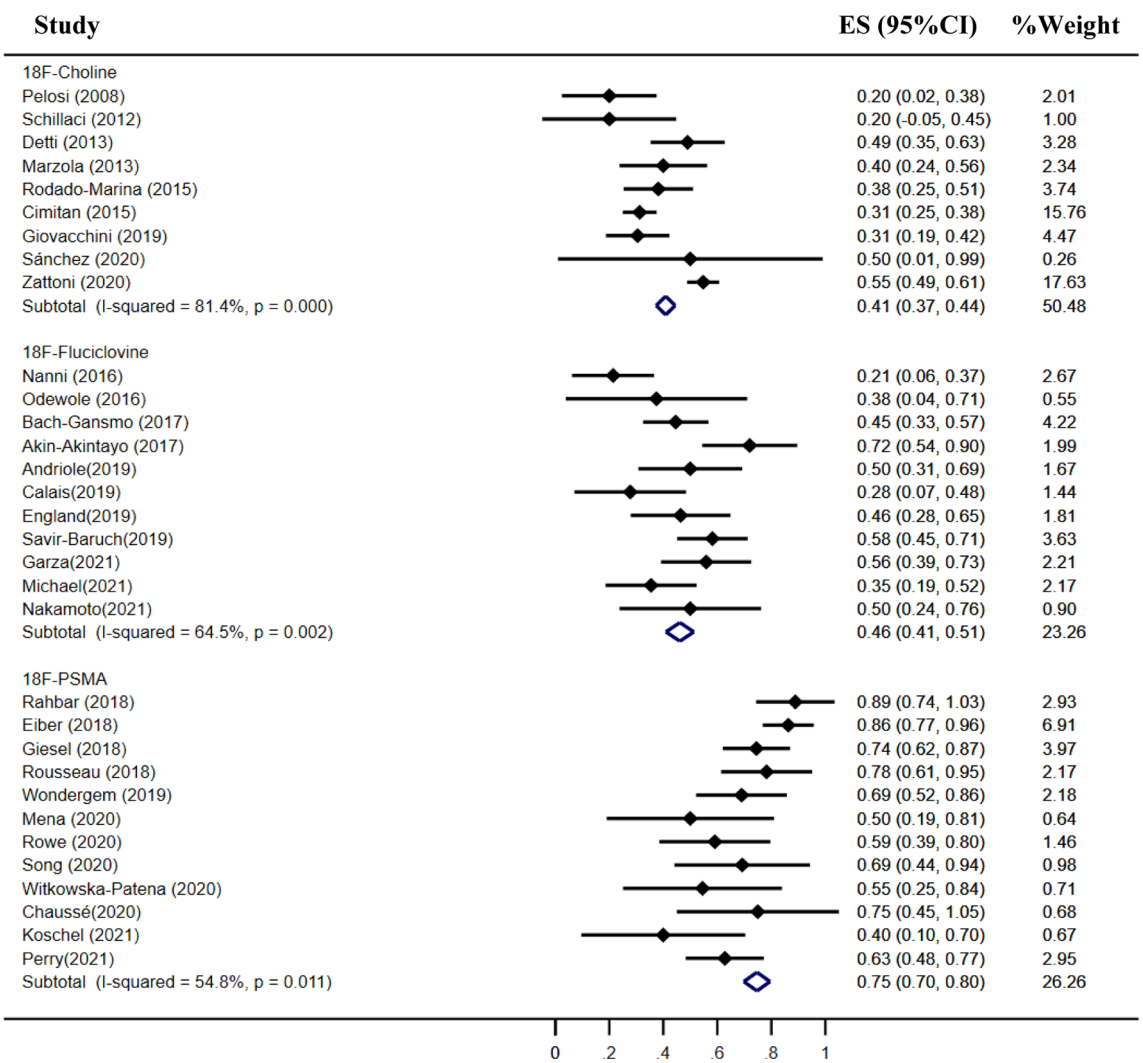

FIGURE 8 | Forest plot of the proportion of ^{18}F-labeled choline, fluciclovine, and PSMA positivity of prostate cancer patients with BCR for PSA 0.5–0.99 ng/ml.

ideal energies, and limited availability of ^{68}Ga, limiting its clinical application in detecting occult or metastatic lesions in the prostate bed (62, 79). However, ^{18}F-PSMA analogs seemed to be more favorable due to their longer half-life and a higher physical spatial resolution (23), and ^{18}F-PSMA-1007, as a second-generation ^{18}F-labeled PSMA tracer, demonstrated high labeling yields, better tumor uptake, and hepatobiliary excretion, making it an ideal PSMA-target tracer for diagnostic imaging in patients with BCR (21, 23). Our meta-analysis found the pooled detection rate with ^{18}F-PSMA of 58% for a PSA level of less than 0.5 ng/ml, 75% for a PSA level of 0.5 to 0.99 ng/ml, and 86% for a PSA level of 1.0 to 1.99 ng/ml. These detection rates are equal or higher than those in recent studies involving ^{68}Ga PSMA PET/CT (80, 81).

Compared with FDA approval of ^{68}Ga-PSMA-11 in late 2020, ^{11}C-choline and ^{18}F-fluciclovine PET/CT have one temporary advantage as they have been granted FDA approval early. They were more accessible and used in the US and Europe. Many studies compared the diagnostic utility of ^{18}F-fluciclovine with ^{11}C-choline PET/CT imaging, showing a better performance in terms of lesion detection rate (48, 82). A recent meta-analysis demonstrated that ^{18}F-fluciclovine had the similar sensitivity and detection rate compared with ^{11}C-choline, but lower specificity than ^{11}C-choline (83). Unlike the short physical half-life of ^{11}C-choline, the radiofluorine of ^{18}F-choline provides a long physical half-life (109.8 min), allowing for centralized manufacture and distribution. These intrinsic advantages of ^{18}F labeling has made ^{18}F-choline PET/CT valuable in staging patients with PCa and detecting recurrently PCa metastases after initial treatment (33, 84). There were limited studies in comparing directly to determine which imaging modality has a better diagnostic efficiency between ^{18}F-choline and ^{18}F-fluciclovine. In our meta-analysis, ^{18}F-choline had a higher sensitivity and

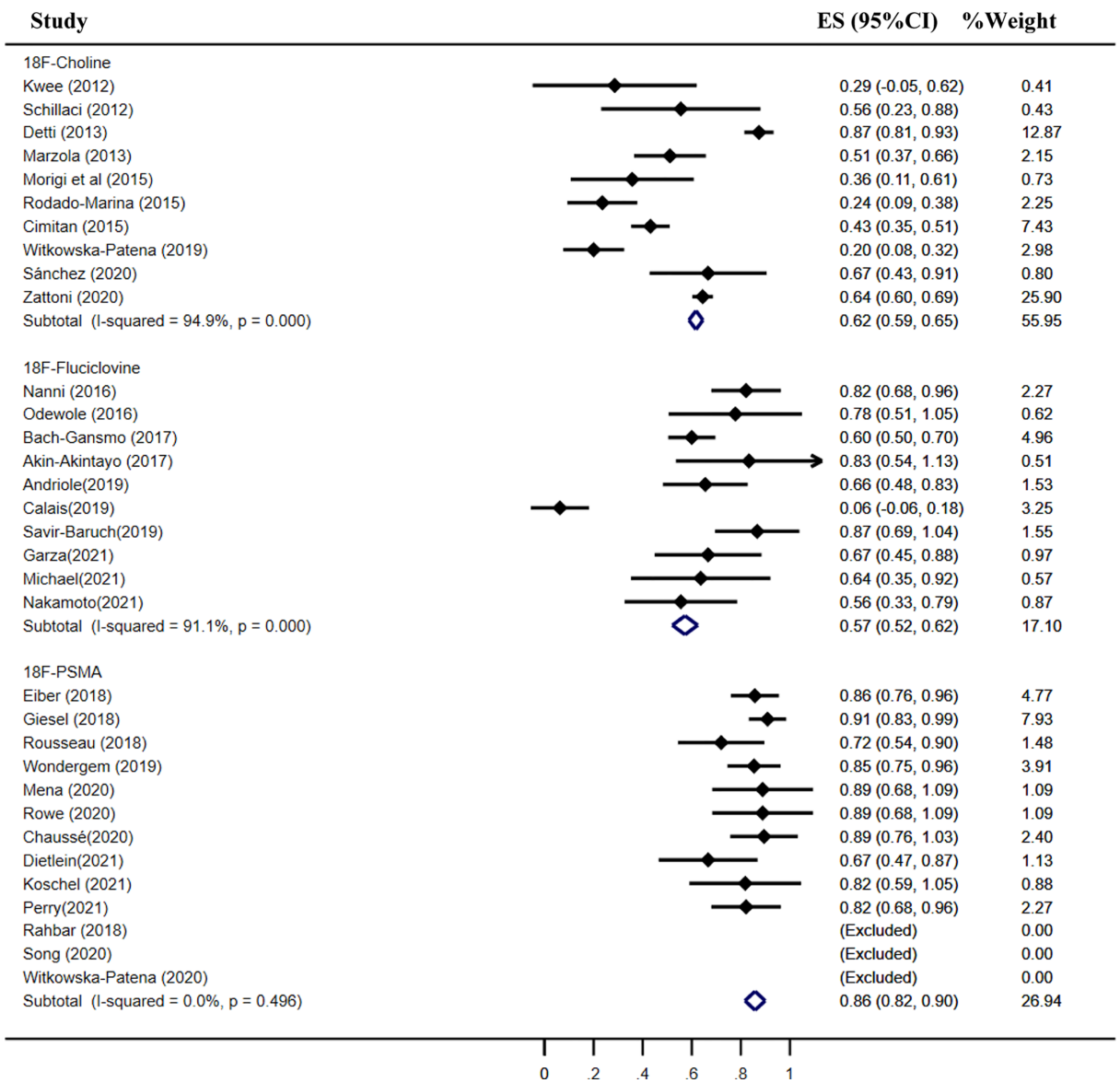

FIGURE 9 | Forest plot of the proportion of ^{18}F-labeled choline, fluciclovine, and PSMA positivity of prostate cancer patients with BCR for PSA 1.0–1.99 ng/ml.

specificity than ^{18}F-fluciclovine through assessing the summary sensitivity and specificity. ^{18}F-choline also has better detection rates than ^{18}F-fluciclovine at PSA levels under 0.5 ng/ml and 1.0–1.99 ng/ml, but the pooled detection rate of ^{18}F-fluciclovine was higher than that of ^{18}F-choline in biochemically recurrent PCa. This difference could be interpreted by different biological processes between amino acid transport and choline expression.

LIMITATIONS

There were several limitations to this study that should be mentioned. First, we only evaluated the diagnostic accuracy of both ^{18}F-choline and ^{18}F-fluciclovine PET/CT in patients with BCR, and the pooled sensitivity and specificity for ^{18}F-PSMA PET/CT were not feasible because of insufficient published data. Second, there were significant heterogeneities among institutions, PET/CT scanners, radiotracers, and prior treatment of patients, which increased the risk of bias and led to significant heterogeneity among ^{18}F-choline, ^{18}F-fluciclovine and ^{18}F-PSMA PET/CT. Third, most of the included studies were retrospective analyses, had small sample sizes, had limited reference standards, and lacked prospective, large sample, and interagent comparison studies. Fourth, there was publication bias according to Egger's test regarding the included studies of ^{18}F-choline,

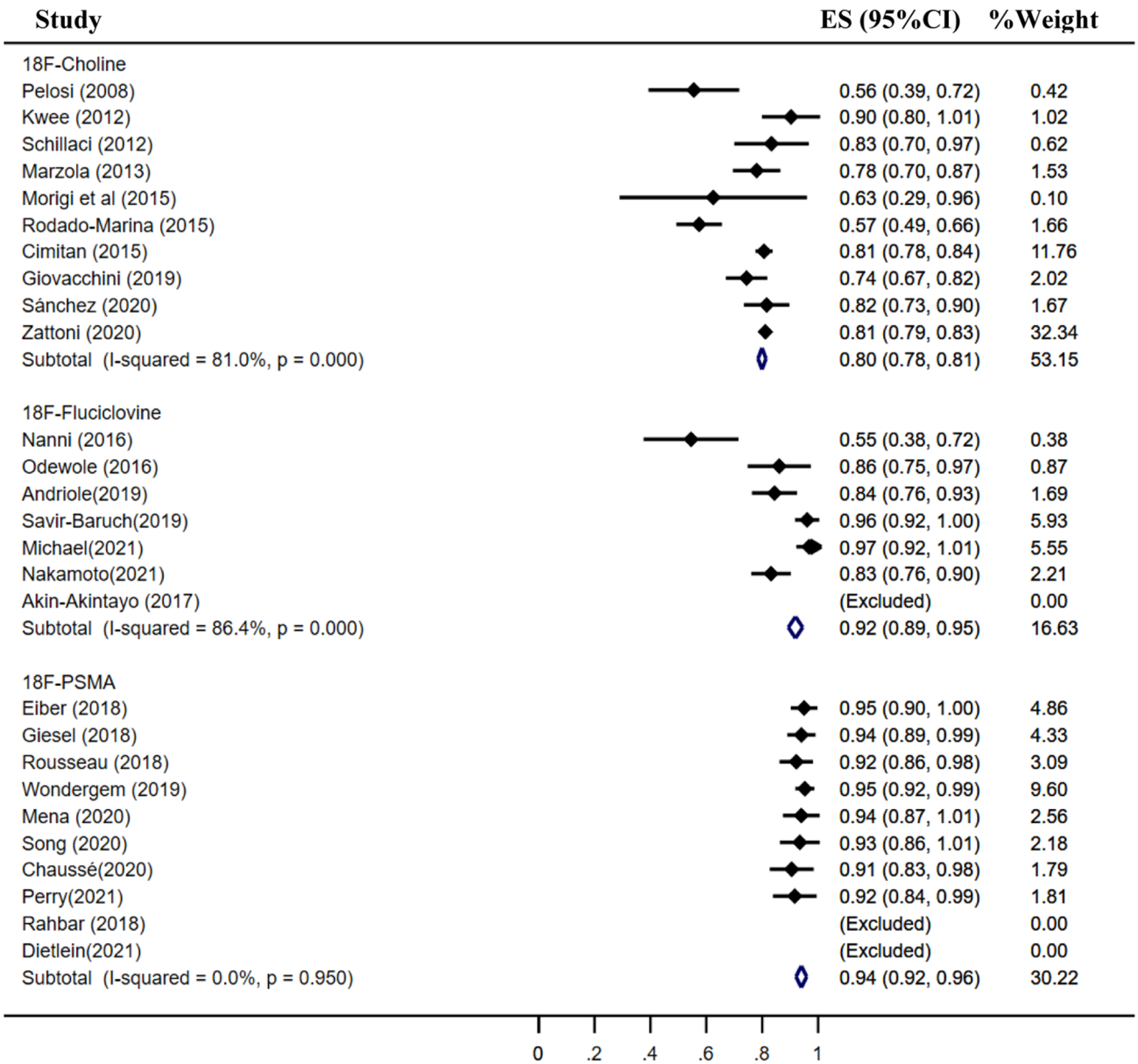

FIGURE 10 | Forest plot of the proportion of ^{18}F-labeled choline, fluciclovine, and PSMA positivity of prostate cancer patients with BCR for PSA more than 2.0 ng/ml.

^{18}F-flocilovine, and ^{18}F-PSMA PET/CT, limiting the interpretation of the data to some degree.

CONCLUSION

PET/CT imaging with ^{18}F-choline, ^{18}F-fluciclovine, and ^{18}F-PSMA is promising in detecting prostate cancer patients with BCR. ^{18}F-PSMA PET/CT demonstrated a significantly higher detection rate over ^{18}F-choline and ^{18}F-fluciclovine for different PSA levels, particularly in PSA level less than 2.0 ng/ml.

DATA AVAILABILITY STATEMENT

The original contributions presented in the study are included in the article/supplementary material. Further inquiries can be directed to the corresponding author.

AUTHOR CONTRIBUTIONS

Conceived and designed the experiments: RW, GS, and RT. Performed the experiments: GS, RW, and MH. Analyzed the

data: RW, GS, and RT. Analyzed tools: GS and MH. Wrote the paper: RW and RT. Provided critical input into the design and drafting of the manuscript: RW, GS, and RT. All authors contributed to the article and approved the submitted version.

FUNDING

This study was supported by the National Natural Science Foundation of China (81971653).

REFERENCES

1. Bray F, Ferlay J, Soerjomataram I, Siegel RL, Torre LA, Jemal A. Global Cancer Statistics 2018: GLOBOCAN Estimates of Incidence and Mortality Worldwide for 36 Cancers in 185 Countries. *CA Cancer J Clin* (2018) 68:394–424. doi: 10.3322/caac.21492
2. Hull GW, Rabbani F, Abbas F, Wheeler TM, Kattan MW, Scardino PT. Cancer Control With Radical Prostatectomy Alone in 1,000 Consecutive Patients. *J Urol* (2002) 167:528–34. doi: 10.1097/00005392-200202000-00018
3. Freedland SJ, Humphreys EB, Mangold LA, Eisenberger M, Dorey FJ, Walsh PC, et al. Risk of Prostate Cancer-Specific Mortality Following Biochemical Recurrence After Radical Prostatectomy. *JAMA* (2005) 294:433–9. doi: 10.1001/jama.294.4.433
4. Kuban DA, Levy LB, Potters L, Beyer DC, Blasko JC, Moran BJ, et al. Comparison of Biochemical Failure Definitions for Permanent Prostate Brachytherapy. *Int J Radiat Oncol Biol Phys* (2006) 65:1487–93. doi: 10.1016/j.ijrobp.2006.03.027
5. Stephenson AJ, Scardino PT, Kattan MW, Pisansky TM, Slawin KM, Klein EA, et al. Predicting the Outcome of Salvage Radiation Therapy for Recurrent Prostate Cancer After Radical Prostatectomy. *J Clin Oncol* (2007) 25:2035–41. doi: 10.1200/JCO.2006.08.9607
6. Fanti S, Minozzi S, Antoch G, Banks I, Briganti A, Carrio I, et al. Consensus on Molecular Imaging and Theranostics in Prostate Cancer. *Lancet Oncol* (2018) 19:e696–708. doi: 10.1016/S1470-2045(18)30604-1
7. Hovels AM, Heesakkers RAM, Adang EM, Jager GJ, Strum S, Hoogeveen YL, et al. The Diagnostic Accuracy of CT and MRI in the Staging of Pelvic Lymph Nodes in Patients With Prostate Cancer: A Meta-Analysis. *Clin Radiol* (2008) 63:387–95. doi: 10.1016/j.crad.2007.05.022
8. Filson CP, Natarajan S, Margolis DJ, Huang J, Lieu P, Dorey FJ, et al. Prostate Cancer Detection With Magnetic Resonance-Ultrasound Fusion Biopsy: The Role of Systematic and Targeted Biopsies. *Cancer* (2016) 122:884–92. doi: 10.1002/cncr.29874
9. Trabulsi EJ, Rumble RB, Jadvar H, Hope T, Pomper M, Turkbey B, et al. Optimum Imaging Strategies for Advanced Prostate Cancer: ASCO Guideline. *J Clin Oncol* (2020) 38:1963–96. doi: 10.1200/JCO.19.02757
10. Zeisel SH. Dietary Choline: Biochemistry, Physiology, and Pharmacology. *Annu Rev Nutr* (1981) 1:95–121. doi: 10.1146/annurev.nu.01.070181.000523
11. Evangelista L, Zattoni F, Guttilla A, Saladini G, Zattoni F, Colletti PM, et al. Choline PET or PET/CT and Biochemical Relapse of Prostate Cancer: A Systematic Review and Meta-Analysis. *Clin Nucl Med* (2013) 38:305–14. doi: 10.1097/RLU.0b013e3182867f3c
12. Krause BJ, Souvatzoglou M, Treiber U. Imaging of Prostate Cancer With PET/CT and Radioactively Labeled Choline Derivates. *Urol Oncol-Seminars Orig Investigations* (2013) 31:427–35. doi: 10.1016/j.urolonc.2010.08.008
13. Oka S, Okudaira H, Yoshida Y, Schuster DM, Goodman MM, Shirakami Y. Transport Mechanisms of Trans-1-Amino-3-Fluoro[1-(14)C] Cyclobutanecarboxylic Acid in Prostate Cancer Cells. *Nucl Med Biol* (2012) 39:109–19. doi: 10.1016/j.nucmedbio.2011.06.008
14. Parent EE, Schuster DM. Update on (18)F-Fluciclovine PET for Prostate Cancer Imaging. *J Nucl Med* (2018) 59:733–9. doi: 10.2967/jnumed.117.204032
15. Bach-Gansmo T, Nanni C, Nieh PT, Zanoni L, Bogsrud TV, Sletten H, et al. Multisite Experience of the Safety, Detection Rate and Diagnostic Performance of Fluciclovine (F-18) Positron Emission Tomography/Computerized Tomography Imaging in the Staging of Biochemically Recurrent Prostate Cancer. *J Urol* (2017) 197:676–82. doi: 10.1016/j.juro.2016.09.117
16. Wright GL Jr, Haley C, Beckett ML, Schellhammer PF. Expression of Prostate-Specific Membrane Antigen in Normal, Benign, and Malignant Prostate Tissues. *Urol Oncol* (1995) 1:18–28. doi: 10.1016/1078-1439(95)00002-y
17. Wright GL Jr., Grob BM, Haley C, Grossman K, Newhall K, Petrylak D, et al. Upregulation of Prostate-Specific Membrane Antigen After Androgen-Deprivation Therapy. *Urology* (1996) 48:326–34. doi: 10.1016/s0090-4295(96)00184-7
18. Perner S, Hofer MD, Kim R, Shah RB, Li H, Möller P, et al. Prostate-Specific Membrane Antigen Expression as a Predictor of Prostate Cancer Progression. *Hum Pathol* (2007) 38:696–701. doi: 10.1016/j.humpath.2006.11.012
19. Eder M, Schafer M, Bauder-Wust U, Hull WE, Wangler C, Mier W, et al. 68Ga-Complex Lipophilicity and the Targeting Property of a Urea-Based PSMA Inhibitor for PET Imaging. *Bioconjug Chem* (2012) 23:688–97. doi: 10.1021/bc200279b
20. Afshar-Oromieh A, Avtzi E, Giesel FL, Holland-Letz T, Linhart HG, Eder M, et al. The Diagnostic Value of PET/CT Imaging With the (68)Ga-Labelled PSMA Ligand HBED-CC in the Diagnosis of Recurrent Prostate Cancer. *Eur J Nucl Med Mol Imaging* (2015) 42:197–209. doi: 10.1007/s00259-014-2949-6
21. Rahbar KA-O, Weckesser M, Ahmadzadehfar H, Schäfers M, Stegger L, Bögemann M. Advantage of (18)F-PSMA-1007 Over (68)Ga-PSMA-11 PET Imaging for Differentiation of Local Recurrence vs. Urinary Tracer Excretion. *Eur J Nucl Med Mol Imaging* (2018) 45:1076–7. doi: 10.1007/s00259-018-3952-0
22. Treglia G, Annunziata S, Pizzuto DA, Giovanella L, Prior JO, Ceriani L. Detection Rate of (18)F-Labeled PSMA PET/CT in Biochemical Recurrent Prostate Cancer: A Systematic Review and a Meta-Analysis. *Cancers (Basel)* (2019) 11:710. doi: 10.3390/cancers11050710
23. Giesel FL, Hadaschik B, Cardinale J, Radtke J, Vinsensia M, Lehnert W, et al. F-18 Labelled PSMA-1007: Biodistribution, Radiation Dosimetry and Histopathological Validation of Tumor Lesions in Prostate Cancer Patients. *Eur J Nucl Med Mol Imaging* (2017) 44:678–88. doi: 10.1007/s00259-016-3573-4
24. Rahbar KA-O, Afshar-Oromieh A, Bögemann M, Wagner S, Schäfers M, Stegger L, et al. (18)F-PSMA-1007 PET/CT at 60 and 120 Minutes in Patients With Prostate Cancer: Biodistribution, Tumour Detection and Activity Kinetics. *Eur J Nucl Med Mol Imaging* (2018) 45:1329–34. doi: 10.1007/s00259-018-3989-0
25. Sathianathen NJ, Butaney M, Konety BR. The Utility of PET-Based Imaging for Prostate Cancer Biochemical Recurrence: A Systematic Review and Meta-Analysis. *World J Urol* (2019) 37:1239–49. doi: 10.1007/s00345-018-2403-7
26. Liberati A, Altman Dg Fau - Tetzlaff J, Tetzlaff J Fau - Mulrow C, Mulrow C Fau - Gøtzsche PC, Gøtzsche Pc Fau - Ioannidis JPA, Ioannidis Jp Fau - Clarke M, et al. The PRISMA Statement for Reporting Systematic Reviews and Meta-Analyses of Studies That Evaluate Health Care Interventions: Explanation and Elaboration. *J Clin Epidemiol* (2009) 62:e1–34. doi: 10.1016/j.jclinepi.2009.06.006
27. Higgins JP, Thompson SG. Quantifying Heterogeneity in a Meta-Analysis. *Stat Med* (2002) 21:1539–58. doi: 10.1002/sim.1186
28. Moses LE, Shapiro D Fau - Littenberg B, Littenberg B. Combining Independent Studies of a Diagnostic Test Into a Summary ROC Curve: Data-Analytic Approaches and Some Additional Considerations. *Stat Med* (1993) 12:1293–316. doi: 10.1002/sim.4780121403
29. Pelosi E, Arena V, Skanjeti A, Pirro V, Douroukas A, Pupi A, et al. Role of Whole-Body 18F-Choline PET/CT in Disease Detection in Patients With Biochemical Relapse After Radical Treatment for Prostate Cancer. *Radiol Med* (2008) 113:895–904. doi: 10.1007/s11547-008-0263-8
30. Kwee SA, Coel MN, Lim J. DR–Detection of Recurrent Prostate Cancer With 18F-Fluorocholine PET/CT in Relation to PSA Level at the Time of Imaging. *Ann Nucl Med* (2012) 26:501–7. doi: 10.1007/s12149-012-0601-8
31. Panebianco V, Sciarra A, Lisi D, Galati F, Buonocore V, Catalano C, et al. Prostate Cancer: 1HMRS-DCEMR at 3T Versus [(18)F]Choline PET/CT in the Detection of Local Prostate Cancer Recurrence in Men With Biochemical Progression After Radical Retropubic Prostatectomy (RRP). *Eur J Radiol* (2012) 81:700–8. doi: 10.1016/j.ejrad.2011.01.095

32. Schillaci O, Calabria F, Tavolozza M, Caracciolo CR, Finazzi Agro E, Miano R, et al. Influence of PSA, PSA Velocity and PSA Doubling Time on Contrast-Enhanced 18F-Choline PET/CT Detection Rate in Patients With Rising PSA After Radical Prostatectomy. *Eur J Nucl Med Mol Imaging* (2012) 39:589–96. doi: 10.1007/s00259-011-2030-7
33. Detti B, Scoccianti S, Franceschini D, Cipressi S, Cassani S, Villari D, et al. Predictive Factors of 18F -Choline PET/CT in 170 Patients With Increasing PSA After Primary Radical Treatment. *J Cancer Res Clin Oncol* (2013) 139:521–8. doi: 10.1007/s00432-012-1354-4
34. Marzola MC, Chondrogiannis S, Ferretti A, Grassetto G, Rampin L, Massaro A, et al. DR–Role of 18F-Choline PET/CT in Biochemically Relapsed Prostate Cancer After Radical Prostatectomy: Correlation With PSA Doubling Time, and Metastatic Distribution. *Clin Nucl Med* (2013) 38:e26–32. doi: 10.1097/RLU.0b013e318266cc38
35. Piccardo A, Paparo F, Piccazzo R, Naseri M, Ricci P, Marziano A, et al. Value of Fused 18F-Choline-PET/MRI to Evaluate Prostate Cancer Relapse in Patients Showing Biochemical Recurrence After EBRT: Preliminary Results. *BioMed Res Int* (2014) 2014:103718. doi: 10.1155/2014/103718
36. Cimitan M, Evangelista L, Hodolič M, Mariani G, Baseric T, Bodanza V, et al. Gleason Score at Diagnosis Predicts the Rate of Detection of 18F-Choline PET/CT Performed When Biochemical Evidence Indicates Recurrence of Prostate Cancer: Experience With 1,000 Patients. *J Nucl Med* (2015) 56:209–15. doi: 10.2967/jnumed.114.141887
37. Morigi JJ, Stricker PD, van Leeuwen PJ, Tang R, Ho B, Quoc N, et al. DR–Prospective Comparison of F-18-Fluoromethylcholine Versus Ga-68-PSMA PET/CT in Prostate Cancer Patients Who Have Rising PSA After Curative Treatment and are Being Considered for Targeted Therapy. *J Nucl Med* (2015) 56:1185–90. doi: 10.2967/jnumed.115.160382
38. Rodado-Marina S, Coronado-Poggio M, García-Vicente AM, García-Garzón JR, Alonso-Farto JC, de la Jara AC, et al. Clinical Utility of (18)F-Fluorocholine Positron-Emission Tomography/Computed Tomography (PET/CT) in Biochemical Relapse of Prostate Cancer After Radical Treatment: Results of a Multicentre Study. *BJU Int* (2015) 115:874–83. doi: 10.1111/bju.12953
39. Simone G, Di Pierro GB, Papalia R, Sciuto R, Rea S, Ferriero M, et al. Significant Increase in Detection of Prostate Cancer Recurrence Following Radical Prostatectomy With an Early Imaging Acquisition Protocol With 18F-Fluorocholine Positron Emission Tomography/Computed Tomography. *World J Urol* (2015) 33:1511–8. doi: 10.1007/s00345-015-1481-z
40. Emmett L, Metser U, Bauman G, Hicks RJ, Weickhardt A, Davis ID, et al. Prospective, Multisite, International Comparison of F-18-Fluoromethylcholine PET/CTand Ga-68-HBED-CC PSMA-11 PET/CT in Men With High-Risk Features and Biochemical Failure After Radical Prostatectomy: Clinical Performance and Patient Outcomes. *J Nucl Med* (2019) 60:794–800. doi: 10.2967/jnumed.118.220103
41. Giovacchini G, Giovannini E, Borsò E, Lazzeri P, Riondato M, Leoncini R, et al. Sensitivity of Fluorine-18-Fluoromethylcholine PET/CT to Prostate-Specific Antigen Over Different Plasma Levels: A Retrospective Study in a Cohort of 192 Patients With Prostate Cancer. *Nucl Med Commun* (2019) 40:258–63. doi: 10.1097/mnm.0000000000000959
42. Witkowska-Patena E, Giżewska A, Dziuk M, Miśko J, Budzyńska A, Walęcka-Mazur A. Head-to-Head Comparison of 18F-Prostate-Specific Membrane Antigen-1007 and 18F-Fluorocholine PET/CT in Biochemically Relapsed Prostate Cancer. *Clin Nucl Med* (2019) 44:e629–e33. doi: 10.1097/rlu.0000000000002794
43. de Leiris N, Leenhardt J, Boussat B, Montemagno C, Seiller A, Phan Sy O, et al. Does Whole-Body Bone SPECT/CT Provide Additional Diagnostic Information Over [18F]-FCH PET/CT for the Detection of Bone Metastases in the Setting of Prostate Cancer Biochemical Recurrence? *Cancer Imaging* (2020) 20:58. doi: 10.1186/s40644-020-00333-y
44. Sánchez N, Valduvieco I, Ribal MJ, Campos F, Casas F, Nicolau C, et al. Diagnostic Utility and Therapeutic Impact of PET/CT 18F-Fluoromethylcholine -Choline in the Biochemical Recurrence of Prostate Cancer. *Rev Esp Med Nucl Imagen Mol* (2020) 39:284–91. doi: 10.1016/j.remn.2020.03.010
45. Zattoni F, Ravelli I, Rensi M, Capobianco D, Borsatti E, Baresic T, et al. 10-Year Clinical Experience With 18F-Choline PET/CT: An Italian Multicenter Retrospective Assessment of 3343 Patients. *Clin Nucl Med* (2020) 45:594–603. doi: 10.1097/rlu.0000000000003125
46. Schuster DM, Savir-Baruch B, Nieh PT, Master VA, Halkar RK, Rossi PJ, et al. Detection of Recurrent Prostate Carcinoma With Anti-1-Amino-3-F-18-Fluorocyclobutane-1-Carboxylic Acid PET/CT and in-111-Capromab Pendetide SPECT/CT. *Radiology* (2011) 259:852–61. doi: 10.1148/radiol.11102023
47. Kairemo K, Rasulova N, Partanen K, Joensuu T. Preliminary Clinical Experience of Trans-1-Amino-3-(18)F-Fluorocyclobutanecarboxylic Acid (Anti-(18)F-FACBC) PET/CT Imaging in Prostate Cancer Patients. *BioMed Res Int* (2014) 2014:305182. doi: 10.1155/2014/305182
48. Nanni C, Zanoni L, Pultrone C, Schiavina R, Brunocilla E, Lodi F, et al. (18)F-FACBC (Anti1-Amino-3-(18)F-Fluorocyclobutane-1-Carboxylic Acid) Versus (11)C-Choline PET/CT in Prostate Cancer Relapse: Results of a Prospective Trial. *Eur J Nucl Med Mol Imaging* (2016) 43:1601–10. doi: 10.1007/s00259-016-3329-1
49. Odewole OA, Tade FI, Nieh PT, Savir-Baruch B, Jani AB, Master VA, et al. Recurrent Prostate Cancer Detection With Anti-3-[18F]FACBC PET/CT: Comparison With CT. *Eur J Nucl Med Mol Imaging* (2016) 43:1773–83. doi: 10.1007/s00259-016-3383-8
50. Akin-Akintayo OO, Jani AB, Odewole O, Tade FI, Nieh PT, Master VA, et al. Change in Salvage Radiotherapy Management Based on(Fluciclovine) PET/CT in Postprostatectomy Recurrent Prostate Cancer. *Clin Nucl Med* (2017) 42:e22–e8. doi: 10.1097/RLU.0000000000001379
51. Bach-Gansmo T, Nanni C, Nieh PT, Zanoni L, Bogsrud TV, Sletten H, et al. Multisite Experience of the Safety, Detection Rate and Diagnostic Performance of Fluciclovine ((18)F) Positron Emission Tomography/Computerized Tomography Imaging in the Staging of Biochemically Recurrent Prostate Cancer. *J Urol* (2017) 197:676–83. doi: 10.1016/j.juro.2016.09.117
52. Miller MP, Kostakoglu L, Pryma D, Yu JQ, Chau A, Perlman E, et al. Reader Training for the Restaging of Biochemically Recurrent Prostate Cancer Using (18)F-Fluciclovine PET/CT. *J Nucl Med* (2017) 58:1596–602. doi: 10.2967/jnumed.116.188375
53. Jambor I, Kuisma A, Kahkonen E, Kemppainen J, Merisaari H, Eskola O, et al. Prospective Evaluation of (18)F-FACBC PET/CT and PET/MRI Versus Multiparametric MRI in Intermediate- to High-Risk Prostate Cancer Patients (FLUCIPRO Trial). *Eur J Nucl Med Mol Imaging* (2018) 45:355–64. doi: 10.1007/s00259-017-3875-1
54. Andriole GL, Kostakoglu L, Chau A, Duan F, Mahmood U, Mankoff DA, et al. The Impact of Positron Emission Tomography With 18F-Fluciclovine on the Treatment of Biochemical Recurrence of Prostate Cancer: Results From the LOCATE Trial. *J Urol* (2019) 201:322–31. doi: 10.1016/j.juro.2018.08.050
55. Calais J, Ceci F, Eiber M, Hope TA, Hofman MS, Rischpler C, et al. Head to Head-FACBC vs PSMA-Restaging-DR 18F-Fluciclovine PET-CT and 68Ga-PSMA-11 PET-CT in Patients With Early Biochemical Recurrence After Prostatectomy: A Prospective, Single-Centre, Single-Arm, Comparative Imaging Trial. *Lancet Oncol* (2019) 20:1286–94. doi: 10.1016/s1470-2045(19)30415-2
56. England JR, Paluch J, Ballas LK, Jadvar H. 18F-Fluciclovine PET/CT Detection of Recurrent Prostate Carcinoma in Patients With Serum PSA </= 1 Ng/Ml After Definitive Primary Treatment. *Clin Nucl Med* (2019) 44:e128–e32. doi: 10.1097/RLU.0000000000002432
57. Savir-Baruch B, Lovrec P, Solanki AA, Adams WH, Yonover PM, Gupta G, et al. Fluorine-18-Labeled Fluciclovine PET/CT in Clinical Practice: Factors Affecting the Rate of Detection of Recurrent Prostate Cancer. *AJR Am J Roentgenol* (2019) 213:851–8. doi: 10.2214/ajr.19.21153
58. Teyateeti A, Khan B, Teyateeti A, Chen B, Bridhikitti J, Pan T, et al. Diagnostic Performance of F-18 Fluciclovine PET/CT in Post-Radical Prostatectomy Prostate Cancer Patients With Rising Prostate-Specific Antigen Level </=0.5 Ng/Ml. *Nucl Med Commun* (2020) 41:906–15. doi: 10.1097/MNM.0000000000001228
59. Garza D, Kandathil A, Xi Y, Subramaniam RM. 18F-Fluciclovine PET/CT Detection of Biochemical Recurrent Prostate Cancer in Patients With PSA Levels <2.00 Ng/Ml. *Nucl Med Commun* (2021). doi: 10.1097/MNM.0000000000001412
60. Michael J, Khandani AH, Basak R, Tan HJ, Royce TJ, Wallen E, et al. Patterns of Recurrence, Detection Rates, and Impact of 18-F Fluciclovine PET/CT on

the Management of Men With Recurrent Prostate Cancer. *Urology* (2021) S0090-4295:00110–2. doi: 10.1016/j.urology.2021.01.038
61. Nakamoto R, Harrison C, Song H, Guja KE, Hatami N, Nguyen J, et al. The Clinical Utility of (18)F-Fluciclovine PET/CT in Biochemically Recurrent Prostate Cancer: An Academic Center Experience Post FDA Approval. *Mol Imaging Biol* (2021). doi: 10.1007/s11307-021-01583-3
62. Rahbar K, Afshar-Oromieh A, Seifert R, Wagner S, Schäfers M, Bögemann M, et al. Diagnostic Performance of (18)F-PSMA-1007 PET/CT in Patients With Biochemical Recurrent Prostate Cancer. *Eur J Nucl Med Mol Imaging* (2018) 45:2055–61. doi: 10.1007/s00259-018-4089-x
63. Eiber M, Kroenke M, Wurzer A, Ulbrich L, Jooß L, Maurer T, et al. 18F-Rhpsma-7 Positron Emission Tomography (PET) for the Detection of Biochemical Recurrence of Prostate Cancer Following Radical Prostatectomy. *J Nucl Med* (2019) 61:696–701. doi: 10.2967/jnumed.119.234914
64. Giesel FL, Knorr K, Spohn F, Will L, Maurer T, Flechsig P, et alDetection Efficacy of (18)F-PSMA-1007 PET/CT in 251 Patients With Biochemical Recurrence of Prostate Cancer After Radical Prostatectomy. *J Nucl Med* 2019) 6460:362–8. doi: 10.2967/jnumed.118.212233
65. Rousseau E, Wilson D, Lacroix-Poisson F, Krauze A, Chi K, Gleave M, et al. A Prospective Study on F-18-Dcfpyl PSMA PET/CT Imaging in Biochemical Recurrence of Prostate Cancer. *J Nucl Med* (2019) 60:1587–93. doi: 10.2967/jnumed.119.226381
66. Wondergem M, Jansen BHE, van der Zant FM, van der Sluis TM, Knol RJJ, van Kalmthout LWM, et al. Early Lesion Detection With (18)F-Dcfpyl PET/CT in 248 Patients With Biochemically Recurrent Prostate Cancer. *Eur J Nucl Med Mol Imaging* (2019) 46:1911–8. doi: 10.1007/s00259-019-04385-6
67. Chausse G, Ben-Ezra N, Stoopler M, Levett JY, Niazi T, Anidjar M, et al. Diagnostic Performance of (18)F-Dcfpyl Positron Emission Tomography/Computed Tomography for Biochemically Recurrent Prostate Cancer and Change-of-Management Analysis. *Can Urol Assoc J* (2020) 15. doi: 10.5489/cuaj.6817
68. Mena E, Lindenberg ML, Turkbey IB, Shih JH, Harmon SA, Lim I, et al. F-18-Dcfpyl PET/CT Imaging in Patients With Biochemically Recurrent Prostate Cancer After Primary Local Therapy. *J Nucl Med* (2020) 61:881–9. doi: 10.2967/jnumed.119.234799
69. Rowe SP, Campbell SP, Mana-Ay M, Szabo Z, Allaf ME, Pienta KJ, et al. Prospective Evaluation of PSMA-Targeted F-18-Dcfpyl PET/CT in Men With Biochemical Failure After Radical Prostatectomy for Prostate Cancer. *J Nucl Med* (2020) 61:58–61. doi: 10.2967/jnumed.119.226514
70. Song H, Harrison C, Duan H, Guja K, Hatami N, Franc BL, et al. Prospective Evaluation of (18)F-Dcfpyl PET/CT in Biochemically Recurrent Prostate Cancer in an Academic Center: A Focus on Disease Localization and Changes in Management. *J Nucl Med* (2020) 61:546–51. doi: 10.2967/jnumed.119.231654
71. Witkowska-Patena E, Giżewska A, Dziuk M, Miśko J, Budzyńska A, Walęcka-Mazur A. Diagnostic Performance of 18F-PSMA-1007 PET/CT in Biochemically Relapsed Patients With Prostate Cancer With PSA Levels ≤ 2.0 Ng/Ml. *Prostate Cancer Prostatic Dis* (2020) 23:343–8. doi: 10.1038/s41391-019-0194-6
72. Dietlein F, Mueller P, Kobe C, Endepols H, Hohberg M, Zlatopolskiy BD, et al. [(18)F]-JK-PSMA-7 PET/CT Under Androgen Deprivation Therapy in Advanced Prostate Cancer. *Mol Imaging Biol* (2021) 23:277–86. doi: 10.1007/s11307-020-01546-0
73. Koschel S, Taubman K, Sutherland T, Yap K, Chao M, Guerrieri M, et al. Patterns of Disease Detection Using [(18)F]Dcfpyl PET/CT Imaging in Patients With Detectable PSA Post Prostatectomy Being Considered for Salvage Radiotherapy: A Prospective Trial. *Eur J Nucl Med Mol Imaging* (2021). doi: 10.1007/s00259-021-05354-8
74. Perry E, Talwar A, Taubman K, Ng M, Wong LM, Booth R, et al. [(18)F] Dcfpyl PET/CT in Detection and Localization of Recurrent Prostate Cancer Following Prostatectomy Including Low PSA < 0.5 Ng/Ml. *Eur J Nucl Med Mol Imaging* (2021) 48:2038–46. doi: 10.1007/s00259-020-05143-9
75. Ghafoor S, Burger IA, Vargas AH. Multimodality Imaging of Prostate Cancer. *J Nucl Med* (2019) 60:1350–8. doi: 10.2967/jnumed.119.228320
76. Wang R, Shen G, Yang R, Ma X, Tian R. (68)Ga-PSMA PET/MRI for the Diagnosis of Primary and Biochemically Recurrent Prostate Cancer: A Meta-Analysis. *Eur J Radiol* (2020) 130:109131. doi: 10.1016/j.ejrad.2020.109131
77. Glaser ZA, Rais-Bahrami S. Fluciclovine Positron Emission Tomography in the Setting of Biochemical Recurrence Following Local Therapy of Prostate Cancer. *Transl Androl Urol* (2018) 7:824–30. doi: 10.21037/tau.2018.07.17
78. Tan N, Oyoyo U, Bavadian N, Ferguson N, Mukkamala A, Calais J, et al. PSMA-Targeted Radiotracers Versus F-18 Fluciclovine for the Detection of Prostate Cancer Biochemical Recurrence After Definitive Therapy: A Systematic Review and Meta-Analysis. *Radiology* (2020) 296:44–55. doi: 10.1148/radiol.2020191689
79. Giesel FL, Kesch C, Yun M, Cardinale J, Haberkorn U, Kopka K, et al. 18F-PSMA-1007 PET/CT Detects Micrometastases in a Patient With Biochemically Recurrent Prostate Cancer. *Clin Genitourin Cancer* (2017) 15:e497–e9. doi: 10.1016/j.clgc.2016.12.029
80. Fendler WP, Calais J, Eiber M, Flavell RR, Mishoe A, Feng FY, et al. Assessment of 68Ga-PSMA-11 PET Accuracy in Localizing Recurrent Prostate Cancer: A Prospective Single-Arm Clinical Trial. *JAMA Oncol* (2019) 5:856–63. doi: 10.1001/jamaoncol.2019.0096
81. Lawhn-Heath C, Flavell RR, Behr SC, Yohannan T, Greene KL, Feng F, et al. Single-Center Prospective Evaluation of (68)Ga-PSMA-11 PET in Biochemical Recurrence of Prostate Cancer. *AJR Am J Roentgenol* (2019) 213:266–74. doi: 10.2214/AJR.18.20699
82. Nanni C, Schiavina R, Brunocilla E, Boschi S, Borghesi M, Zanoni L, et al. 18F-Fluciclovine PET/CT for the Detection of Prostate Cancer Relapse: A Comparison to 11C-Choline PET/CT. *Clin Nucl Med* (2015) 40:e386–91. doi: 10.1097/rlu.0000000000000849
83. Abiodun-Ojo OA, Akintayo AA, Akin-Akintayo OO, Tade FI, Nieh PT, Master VA, et al. (18)F-Fluciclovine Parameters on Targeted Prostate Biopsy Associated With True Positivity in Recurrent Prostate Cancer. *J Nucl Med* (2019) 60:1531–6. doi: 10.2967/jnumed.119.227033
84. Gauvin S, Cerantola Y, Haberer E, Pelsser V, Probst S, Bladou F, et al. Initial Single-Centre Canadian Experience With 18F-Fluoromethylcholine Positron Emission Tomography-Computed Tomography (18F-FCH PET/CT) for Biochemical Recurrence in Prostate Cancer Patients Initially Treated With Curative Intent. *Can Urol Assoc J* (2017) 11:47–52. doi: 10.5489/cuaj.4068

Conflict of Interest: The authors declare that the research was conducted in the absence of any commercial or financial relationships that could be construed as a potential conflict of interest.

frontiers in Oncology

MINI REVIEW
published: 28 July 2021
doi: 10.3389/fonc.2021.722277

Incorporating PSMA-Targeting Theranostics Into Personalized Prostate Cancer Treatment: a Multidisciplinary Perspective

*Thomas S. C. Ng[1], Xin Gao[2], Keyan Salari[3], Dimitar V. Zlatev[3], Pedram Heidari[1] and Sophia C. Kamran[4]**

[1] Division of Nuclear Medicine and Molecular Imaging, Department of Radiology, Massachusetts General Hospital, Harvard Medical School, Boston, MA, United States, [2] Division of Hematology and Oncology, Department of Medicine, Massachusetts General Hospital, Harvard Medical School, Boston, MA, United States, [3] Department of Urology, Massachusetts General Hospital, Harvard Medical School, Boston, MA, United States, [4] Department of Radiation Oncology, Massachusetts General Hospital, Harvard Medical School, Boston, MA, United States

OPEN ACCESS

Edited by:
Trevor Royce, University of North Carolina at Chapel Hill, United States

Reviewed by:
Luca Faustino Valle, University of California, Los Angeles, United States
Simon Spohn, University of Freiburg Medical Center, Germany

***Correspondence:**
Sophia C. Kamran
skamran@mgh.harvard.edu

Specialty section:
This article was submitted to Cancer Imaging and Image-directed Interventions, a section of the journal Frontiers in Oncology

Received: *08 June 2021*
Accepted: *12 July 2021*
Published: *28 July 2021*

Citation:
Ng TSC, Gao X, Salari K, Zlatev DV, Heidari P and Kamran SC (2021) Incorporating PSMA-Targeting Theranostics Into Personalized Prostate Cancer Treatment: a Multidisciplinary Perspective. Front. Oncol. 11:722277. doi: 10.3389/fonc.2021.722277

Recent developments in prostate-specific membrane antigen (PSMA) targeted diagnostic imaging and therapeutics (theranostics) promise to advance the management of primary, biochemically recurrent, and metastatic prostate cancer. In order to maximize the clinical impact of PSMA-targeted theranostics, a coordinated approach between the clinical stakeholders involved in prostate cancer management is required. Here, we present a vision for multidisciplinary use of PSMA theranostics from the viewpoints of nuclear radiology, medical oncology, urology, and radiation oncology. We review the currently available and forthcoming PSMA-based imaging and therapeutics and examine current and potential impacts on prostate cancer management from early localized disease to advanced treatment-refractory disease. Finally, we highlight the clinical and research opportunities related to PSMA-targeted theranostics and describe the importance of multidisciplinary collaboration in this space.

Keywords: PSMA, PET, prostate cancer, radiation, theranostics, therapy, molecular imaging

INTRODUCTION

Prostate cancer is the second most common malignancy in men and the fifth leading cause of cancer-related death worldwide (1). Localized indolent disease has a good prognosis; however, advanced localized, recurrent and metastatic disease often portend poor outcomes (1, 2). Prostate-specific membrane antigen (PSMA) is increasingly appreciated as a promising imaging and therapeutic target for prostate cancer (3). As these agents become FDA-approved and clinically available, opportunities and challenges will arise to incorporate them appropriately into the management armamentarium for prostate cancer. Success in this endeavor will require coordination and collaboration among the clinical stakeholders in prostate cancer management, including imaging physicians, medical oncologists, urologists and radiation oncologists. In this review, we provide a multidisciplinary viewpoint of how PSMA-targeting agents will advance clinical management of prostate cancer. We outline the PSMA-targeted agents for imaging and

therapy and their roles in the management of both localized and metastatic disease. Finally, we identify opportunities for cross-specialty collaboration to advance the utility of PSMA-targeted agents for prostate cancer management.

PSMA: A PROMISING IMAGING/THERAPEUTIC TARGET

PSMA is expressed at 100–1000-fold higher levels in prostate cancer compared to healthy prostate tissue, and importantly, shows highest expression in high-grade and castration-resistant prostate cancer (3, 4). Multiple studies have demonstrated correlation between PSMA expression and prostate cancer aggressiveness (5), Gleason score (6), metastatic potential (7) and castration resistance (8, 9), suggesting that PSMA is a promising imaging/therapeutic target.

PSMA-TARGETED IMAGING AGENTS

The first FDA-approved molecular imaging agent developed to target PSMA was the radiolabeled monoclonal antibody indium-111 (^{111}In)-capromab pendetide (ProstaScint) for single-photon emission computed tomography (SPECT) imaging detection of sites of biochemical recurrence (10). Clinical adoption of ProstaScint has remained low due to the relatively poor resolution of SPECT imaging as well as limited sensitivity due to an unfavorable biodistribution and the antibody targeting an intracellular epitope of PSMA (11–13).

Several SPECT-imaging agents targeting PSMA were developed after ProstaScint, including agents labeled with ^{99m}Tc (14–16) and ^{123}I (17). However, more recent attention has been focused on positron emission tomography (PET) agents, which offer higher sensitivity and spatial resolution compared to SPECT (4, 18).

The pharmacokinetics of small molecules with their fast clearance and good tumor penetration results in a high tumor to background ratio (19). These properties make them ideal as imaging agents. **Table 1** lists the most common PSMA-targeting small molecule agents that are actively used in trials and clinically worldwide. At the time of writing, two of these agents, ^{68}Ga-PSMA-11 and ^{18}F-DCFPyL, have been FDA-approved (but awaiting CMS approval). Beyond favorable imaging profiles (20), these agents have been demonstrated in multiple retrospective and prospective studies to be superior compared to standard cross-sectional imaging, (CT/MRI) (21, 22) nuclear medicine assays (bone scintigraphy) (23, 24), ^{18}F-fluciclovine (25–29), ^{11}C-choline PET/CT (30, 31), and other modalities (32, 33) for characterizing disease burden across the spectrum of the disease (**Figure 1**). Applications include the localized disease setting for both intraprostatic localization and staging (34–36), detection of lesions during biochemical recurrence (22, 37), and for stratification and treatment monitoring in metastatic disease (38). Furthermore, PSMA-targeted imaging has shown synergy with other modalities such as multiparametric prostate MRI (39, 40) and FDG-PET for improved characterization of disease burden (41) and image guidance for bone biopsies (42).

ROLE OF PSMA IMAGING IN LOCALIZED DISEASE

Accurate staging is critical for risk stratification and treatment decisions. Surgery and radiation therapy are curative treatments for localized disease, offer potential cure for biochemically recurrent disease (i.e., salvage radiotherapy or salvage prostatectomy), and can offer durable control in the oligometastatic disease setting. To the extent PSMA imaging can identify micrometastatic disease and reclassify clinical stage, patient selection for local therapies can be expected to improve. Further, the success of radiation largely centers on accurate identification and encompassing of disease within a radiation field in the setting of localized or salvage radiation, or to precisely target disease with stereotactic ablative radiation therapy (SABR) for patients with oligometastatic prostate cancer. Conventional imaging has low sensitivity and low specificity for detection of prostate cancer spread. Thus, PSMA imaging is being explored to determine its role in early stage disease, including for accurate assessment of intraprostatic tumor burden, with higher PSMA uptake previously shown to be associated with histological identification of focal lesions (39, 43, 44). This can guide focal SABR escalation at these sites (45, 46).

High-Risk Disease

Early data exploring the role of PSMA PET/CT in high-risk disease suggest that it can lead to changes in treatment decisions. The proPSMA trial recruited men with high-risk localized prostate cancer randomized to either conventional imaging or PSMA PET/CT as first-line imaging, followed by second-line cross-over imaging for patients with fewer than three distant metastases (21). PSMA PET/CT as first-line imaging led to change in management in 28% of patients (compared to 15% following conventional imaging), half of which comprised a change in surgical or radiotherapy technique. In patients who underwent second-line imaging, PSMA PET/CT similarly led to a change in management in 25% of patients, compared to only 5% following conventional imaging. A separate retrospective study of 138 prostate cancer patients who underwent ^{68}Ga-PSMA-PET/CT imaging at initial diagnosis evaluated the number and anatomical location of PSMA-positive lymph nodes (47). Overall, 441 PSMA-positive lymph node metastases were identified (most frequently of which were internal iliac lymph nodes [25%]). The PSMA-positive lymph nodes were mapped onto a CT planning scan and the standard pelvic radiotherapy fields were overlaid on top for comparison. Extending the cranial border of the pelvic field from L5/S1 to L4/L5 increased accuracy of covering potentially involved nodes. Another recent study used

TABLE 1 | Clinically relevant PSMA-targeted imaging and radio-therapeutic agents (Active at the time of review).

Agent name	Current use	Radioisotope	Target backbone	Notes	Clinical Trials for lesion detection	Therapy-based clinical trials
PSMA-11	Diagnostic	^{68}Ga, ^{18}F	Urea	FDA-approved in 2020, but unclear if there will be reimbursement currently. Kit-based formulation also available.	NCT04846894	NCT04279561 (Androgen receptor inhibitors)
					NCT04831541	NCT03977610 (ADT)
					NCT04462926	NCT04264208 (brachytherapy)
					NCT04216134	NCT03949517 (HIFU, HDR)
					NCT04483414	
					NCT04147494	NCT04794777 (Salvage radiotherapy)
					NCT04279561	NCT04086966 (RT planning)
					NCT04179968	
					NCT03809078 (Surgical guidance)	
					NCT03396874	
					NCT03187990	
					NCT03429244	
					NCT04176497	
					NCT03756077	
					NCT03762759	
PSMA-617	Diagnostic and Therapy	^{68}Ga, ^{64}Cu, ^{177}Lu, ^{225}Ac, ^{44}Sc	Urea	Improved binding affinity and internalization into cells compared to PSMA-11.	NCT04796467	NCT04597411 (225Ac)
					NCT03606837	NCT03805594 (^{177}Lu + pembro)
						NCT04430192
						NCT03780075
						NCT04343885
						NCT03874884
						NCT04663997
						NCT03454750
						NCT04419402
THP-PSMA	Diagnostic	^{68}Ga	Urea	Kit-based formulation, but lower tumor uptake compared to PSMA-11	NCT04158817	
PSMA-I&T	Diagnostic and Therapy	^{68}Ga, ^{177}Lu	Urea	Similar performance characteristics as PSMA-11 and PSMA-617		NCT04188587
						NCT04297410
						NCT04443062
PSMA-I&S	Diagnostic	^{99m}Tc	Urea	SPECT agent	NCT04832958	
					NCT04857502	
					NCT03857113	
^{18}F -DCFBC	Diagnostic	^{18}F	Urea	Poor blood pool clearance		
^{18}F -DCFPyL	Diagnostic	^{18}F	Urea	FDA-approved in 2021, but unclear if there will be reimbursement currently. Similar performance as PSMA-11. Disease detection rate of 59-66% and change in management of 63.9%.	NCT03739684	NCT04457245 (RT)
					NCT03800784	NCT04461509 (HIFU)
					NCT03793543	NCT03253744 (SBRT)
					NCT03824275	NCT03972657 (antiCD28)
					NCT04727736	NCT03525288 (RT)
					NCT04390880	
					NCT03232164	
					NCT03585114	
					NCT03160794	
					NCT03173924	
					NCT02899312	

(Continued)

TABLE 1 | Continued

Agent name	Current use	Radioisotope	Target backbone	Notes	Clinical Trials for lesion detection	Therapy-based clinical trials
					NCT02420977 NCT03594760 NCT03976843 NCT03392181 NCT04017104 NCT04700332 NCT04266392 NCT03718260 NCT03619655 NCT03860987 NCT04030338	
^{18}F -PSMA-1007	Diagnostic	^{18}F	Urea	Reduced renal and increased hepatobiliary excretion compared to other agents, but also increased benign tissue uptake	NCT04487847 NCT04239742 NCT03876912 NCT04794777	
FrhPSMA-7	Diagnostic and Therapy	^{18}F, ^{177}Lu	Urea	Radio hybrid. Low bladder retention, Disease detection rate of 71% at low PSA levels.	NCT04186819 NCT04186845	
CTT1057	Diagnostic	^{18}F	Phosphoramidate	Irreversible binding to PSMA, lower radiation dose to kidneys and salivary glands compared to urea agents. Potentially higher tumor-to-background ratio.	NCT03822871	
J591	Therapy	^{225}Ac, ^{177}Lu	Monoclonal antibody			NCT04576871 NCT04506567 NCT00859781
Rosopatamab	Therapy	^{177}Lu	Monoclonal antibody			NCT04876651

ADT, androgen deprivation therapy; HDR, high dose radiation; HIFU, high intensity frequency ultrasound; RT, Radiation therapy; SBRT, stereotactic body radiation therapy.

data from two prospective trials with PSMA PET/CT imaging in high-risk individuals with cN0M0 disease per conventional imaging to develop a nomogram to help identify high-risk patients who might benefit from the addition of a PSMA PET/CT (48).

Localized Salvage Therapy

Biochemical recurrence after radical prostatectomy or primary radiation can potentially be cured with localized salvage therapy such as pelvic-targeted radiation or salvage prostatectomy (49). Biochemical recurrence can now be detected at earlier PSA

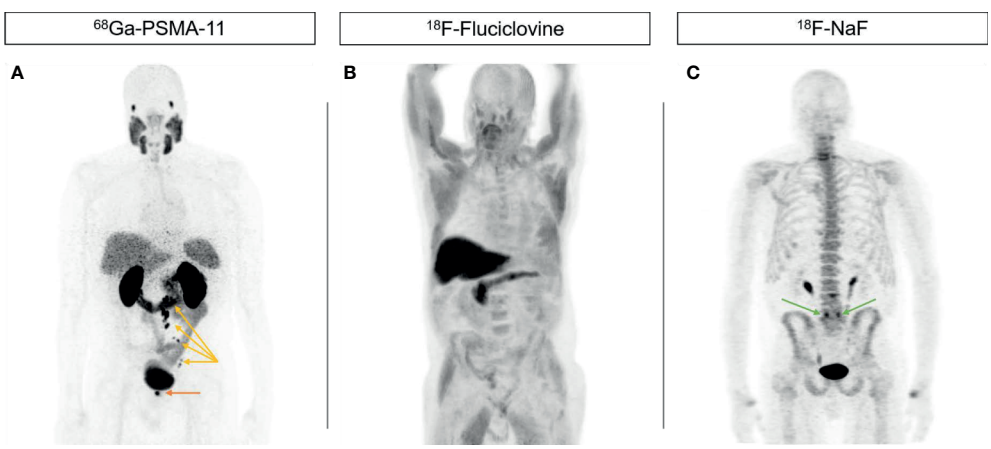

FIGURE 1 | Increased sensitivity of PSMA-targeted imaging compared to current alternatives. 71-year-old male presented initially with T3 N0 M0 Gleason 4 + 5 = 9 PSA 9.42 prostate adenocarcinoma who declined local therapy and was managed with ADT alone, subsequently with castration-resistant progression. **(A)** ^{68}Ga-PSMA-11 PET showing focal uptake in the right prostate bed (orange arrow) as well as left pelvic and retroperitoneal nodes (yellow arrows). **(B)** ^{18}F-Fluciclovine PET do not show any abnormal uptake. **(C)** ^{18}F-NaF PET do not show any abnormal uptake suspicious for metastases. Uptake at L5/S1 facets is due to degenerative change (green arrows).

values, with the definition of failure at 0.2 ng/mL (50). At these low PSA levels, conventional imaging has poor sensitivity for detecting sites of recurrence. PSMA imaging has been shown to be more sensitive in this setting in multiple prospective studies (27, 37, 51–53). The enhanced detection of local and distant lesions with PSMA-targeted imaging has ramifications for treatment planning, including choice of localized *vs.* systemic therapy. For example, a study in 79 radio-recurrent patients using ^{18}F-DCFPyL PET/CT not only showed superior disease detection compared to conventional imaging (87% *vs.* 67% overall, 30% *vs.* 15% for identifying distant metastases), but changed the proposed management in 43% of patients (54). However, it currently remains unknown whether these changes in management are appropriate or will improve overall disease outcomes.

Oligometastatic Disease

The role of surgery and radiation therapy is evolving in the management of low-burden metastatic disease, also known as oligometastatic disease. Early data suggest that aggressive radiation targeted at metastatic lesions may improve outcomes (55–57). PSMA imaging may contribute to increased detection of metastatic disease and thus increased number of patients classified as oligometastatic prostate cancer. A phase II trial evaluating use of metastasis-directed therapy (MDT) to PSMA-defined oligorecurrent prostate cancer demonstrated that, of 37 patients undergoing MDT (stereotactic ablative body radiotherapy [SABR] or surgery), 22% were rendered biochemically disease-free (58). The ORIOLE trial, a randomized phase 2 trial, evaluated men with 1-3 lesions defined on conventional imaging, randomizing to standard-of-care treatment *versus* SABR to all detectable lesions. Patients who underwent SABR also had PSMA PET/CT at baseline and day 180. Overall, 16/36 SABR patients had 1 or more PSMA-positive lesions that were not included as part of the SABR-directed therapy. Of those who had no untreated lesions, the proportion with progression at 6 months was 1/19 (5%) compared to 6/16 (38%) with any untreated lesion. Men who had all PSMA-positive lesions treated were less likely to have new lesions at 6 months (3 of 19, 15.8% *versus* 10 of 16, 62.5%, p=0.006) (59). Taken together, these data support that aggressive metastasis-directed treatment to all PSMA PET-avid lesions may be curative in a subset of patients with low-burden metastatic disease.

Surgical Guidance With PSMA-Imaging

Molecular imaging approaches are increasingly being adopted for surgical guidance (60). Pelvic lymph node dissection (PLND) is the standard approach for nodal staging or management of local lymphatic metastases (61). PSMA-targeted radiolabeled and fluorescent probes are being tested for identifying lymph node metastases intraoperatively during PLND, for confirming appropriate surgical margins, and for correlation with pathological assessment (62–65). These approaches may improve surgical outcomes by increasing the likelihood that all clinically significant disease is resected at the time of surgery.

THERAPEUTIC ROLE OF PSMA IN METASTATIC DISEASE

PSMA-Targeted Radioligand Therapy

Systemically delivered radiotherapies already play a key role in metastatic prostate cancer management, especially with the use of ^{223}Radium for management of osseous lesions (66). PSMA-targeted radiotherapies are poised to offer an even more impactful alternative, being effective for both PSMA-expressing bone and soft tissue metastases (67). To date, the most tested PSMA-targeted agent is ^{177}Lu-PSMA-617, among other agents outlined in **Table 1**, with several clinical studies showing significant treatment response, both by imaging and PSA monitoring (68–70). The largest randomized phase III trial comparing ^{177}Lu PSMA-617 to standard of care alone in 831 patients with advanced metastatic castration-resistant prostate cancer (mCRPC) (VISION) demonstrated that ^{177}Lu PSMA-617 significantly improves overall survival (OS, median, 15.3 *vs.* 11.3 months) and progression-free survival (rPFS, median, 8.7 *vs.* 3.4 months) in patients with PSMA-positive mCRPC (71, 72). Based on the promising results of this trial, regulatory approval for this agent is expected to be imminent. Another randomized phase II trial (TheraP) demonstrated that ^{177}Lu PSMA-617 compared with cabazitaxel in men with mCRPC led to a higher PSA response and fewer grade 3 or 4 adverse effects (73). Several studies have also extended the use of these agents for management of micrometastases in the setting of localized disease (74) and oligometastases (75). Correlation with PSMA imaging is key for patient stratification since patients with high PSMA expression level and low tumor heterogeneity show better outcomes (76, 77).

PSMA radioligand therapy is an area of active investigation, with most notable areas focused on testing various choices of radionuclides and ligands to improve outcomes and reduce toxicity (78). For instance, several radiopharmaceuticals have been engineered to enable radiolabeling of the same ligand using both imaging and therapeutic radionuclides, allowing an accurate pharmacokinetic readout using imaging prior to radioligand therapy (75) (4). Other areas of investigation focus on the development of therapeutic agents with more favorable pharmacokinetics for therapeutic payload delivery such as antibody constructs with longer biological half-lives and different organ toxicity profiles (79, 80). Additionally, the optimal choice of radionuclides is also being assessed. Commonly used radionuclides including ^{177}Lu and ^{90}Y for PSMA-therapy predominantly exert their cytotoxic actions *via* beta particle emission, with spatial range of action on the order of mm. Alpha particles, such a ^{225}Ac or ^{209}Pb, can confer higher linear energy transfer (up to 20x) compared to beta particles, but act on a shorter spatial range (81). ^{225}Ac-PSMA-617 alone or in tandem with ^{177}Lu-PSMA-617 have been studied clinically, with promising results (82). Auger emitters, which impart high energy at a shorter range than alpha particles, may also be useful in the setting of micro-metastases (83). Further preclinical and clinical studies are needed to understand and optimize the interplay between these design parameters, and their effects on efficacy.

PSMA-Targeted Bispecific Agents

Multiple PSMA-targeted bispecific molecules have advanced to early phase clinical evaluation in patients with mCRPC. These antibody-derived bispecific molecules bind to PSMA and a T-cell-specific antigen such as CD3 or CD28, resulting in activation of T-cell response to PSMA-expressing prostate cancer cells. PSMA-targeted bispecific agents are being developed as monotherapies and in combination with immune checkpoint inhibitors.

Pasotuxizumab (AMG 212) is a bispecific T-cell engager (BiTE) engineered to engage PSMA and CD3 and demonstrated reasonable tolerability, immunogenicity, and clinical activity in a phase 1 dose-escalation study in mCRPC patients (84). PSA declines ≥50% (PSA_{50}) occurred in 29% and 19% of patients treated with subcutaneous and intravenous dosing, respectively, including 2 long-term responders (11-17 months to tumor progression). Pasotuxizumab was limited by a short half-life, and a half-life extended anti-PSMA x CD3 BiTE acapatamab (AMG 160) was developed for further clinical evaluation. Preliminary results from the phase 1 study of acapatamab in heavily pretreated mCRPC patients showed promising activity and manageable toxicity (85). PSA_{50} responses were seen in 34% of evaluable patients, including a patient who previously progressed on lutetium-PSMA therapy. Cytokine release syndrome (CRS) was observed in 91% of patients, but most cases were grade 1-2 and decreased in severity after cycle 1. Combination therapy with anti-PD-1 immune checkpoint inhibitors, abiraterone, or enzalutamide is planned (85, 86).

HPN424 is a PSMA-targeting T-cell engager with three binding domains: anti-PSMA, anti-CD3, and anti-albumin for half-life extension (87). Preliminary results from the phase 1/2 study of HPN424 in mCRPC patients demonstrated PSA_{50} responses in 3 (5%) patients. In the highest fixed dose cohort evaluated to date, 3 of 7 patients had PSA declines and 1 patient had a confirmed partial response by RECIST. CRS events occurred in 63% of patients, with 4% of patients experiencing grade 3 CRS. The study continues in dose escalation.

Additional PSMA-targeted bispecific agents are entering the clinical setting. REGN5678 is a first-in-class human IgG4-based bispecific engineered to target PSMA and the T-cell costimulatory receptor CD28, and will be evaluated in a phase 1/2 first-in-human study as monotherapy and in combination with the anti-PD-1 antibody cemiplimab (88). TNB-585 and CCW702 are anti-PSMA x CD3 bispecific agents entering phase 1 evaluation (89, 90).

PSMA-Targeted CAR-T

Chimeric antigen receptor (CAR) T cell therapies are a powerful class of genetically-engineered T cells with synthetic receptors that redirect their specificity, function, and metabolism, and represent a major advancement in the treatment of certain refractory hematologic malignancies (91). Prostate cancer serves as an attractive target for evaluation of CAR-T therapy in solid tumors due to the relative specificity of PSMA as target antigen. An early generation PSMA-targeted CAR-T was evaluated in a small phase 1 study that reported clinical partial responses in 2 of 5 mCRPC patients, with PSA declines of 50% and 70% (92). A second generation PSMA-targeted CAR-T demonstrated evidence of cytokine activation and prolonged stable disease for >6 months in 2 of 7 patients dosed (93).

More modern CAR-T therapies are now entering clinical evaluation for mCRPC patients, with some reporting very preliminary results to date. CART-PSMA-TGFβRDN cells involving autologous T cells engineered to express a dominant negative form of TGFβRII and a CAR with specificity to PSMA reported PSA_{50} decreases in 2 of 3 patients with one-month follow-up, including a patient with >95% PSA decline (94). However, one patient developed grade 2 CRS that progressed to fatal encephalopathy and multi-organ failure despite aggressive immunosuppressive therapy. A second CART-PSMA-TGFβRdn study has reported early results with PSA_{50} decline in 1 of 10 patients (98% decline) and PSA_{30} decline in 3 additional patients (95). Grade 2+ CRS was seen in 5 of 7 patients treated at higher dose. However, the therapy was associated with lethal neurotoxicity and sepsis. P-PSMA-101 is an autologous CAR-T product being evaluated in the U.S. (NCT04249947), while several PSMA-targeted CAR-T products are in clinical trials in China (NCT04053062, NCT04768608, NCT04429451). PSMA-imaging has also been harnessed as a means to track CAR-T trafficking (96).

PSMA-Targeted Antibody-Drug Conjugates

Antibody-drug conjugates (ADCs) comprise a monoclonal antibody binding to a target antigen that is highly specific to tumor cells, a synthetic linker domain, and a potent cytotoxic chemotherapy payload (97). ADCs can deliver chemotherapeutics in a more targeted manner to tumor cells, while sparing normal cells. PSMA represents a rationale target for the development of ADCs.

MLN2704, PSMA ADC, and MEDI3726 are three PSMA-targeted ADCs that have undergone clinical investigation to date. MLN2704 is comprised of a de-immunized anti-PSMA monoclonal antibody (J591) with high affinity to the external domain of PSMA complexed *via* a thiopentanoate linker to maytansinoid-1, a potent anti-microtubule chemotherapeutic (98). PSMA ADC is a fully human immunoglobulin G1 anti-PSMA monoclonal antibody complexed to the anti-mitotic agent monomethyl auristatin E *via* a valine-citrulline linker, which is more stable than thiol linkers in plasma (99). MEDI3726 is comprised of J591 conjugated to the DNA cross-linking agent pyrrolobenzodiazepine (100). These PSMA-targeted ADCs have been evaluated in separate early phase clinical trials in mCRPC patients, with MLN2704 and PSMA ADC treatments associated with PSA_{50} response in 8% and 14% of patients, respectively, while MEDI3726 reported a modest 12% composite response rate involving radiographic, PSA_{50}, and circulating tumor cell (CTC) responses. However, these PSMA-targeted ADCs have been limited by neuropathy, skin toxicities, and cytopenias. Nonetheless, the clinical studies further validate PSMA as a therapeutic target in mCRPC, and future development of

ADCs may focus on improving synthetic linkers that limit deconjugation of the chemotherapeutic payload outside of the tumor microenvironment.

MULTIDISCIPLINARY OPPORTUNITIES AND CHALLENGES IN THE ERA OF PSMA-TARGETED PROSTATE CANCER MANAGEMENT

PSMA-targeted imaging and therapy are poised to play key roles in the management of prostate cancer. Evaluation of their clinical utility will require high-level evidence from prospective clinical studies (101). Precision medicine principles guided by theranostics should be incorporated in the design of these trials, and will require collaboration across radiology/nuclear medicine, urology, medical and radiation oncology. Standardized acquisition methods, and interpretation criteria of PSMA-based imaging exams, such as with recently proposed criteria like the PROMISE staging system (102) or PSMA-RADS (103) will be paramount in this regard. In addition, collaborative efforts at both pre-clinical and clinical levels to examine combination treatments involving the different PSMA-targeting modalities are vital to understanding their optimal role in the treatment armamentarium for prostate cancer.

In summary, exciting opportunities abound with the multiple PSMA-targeted imaging and therapy agents in the clinical pipeline. Collaboration across the different clinical disciplines in the prostate cancer management team will be crucial to maximize the potential of these agents.

AUTHOR CONTRIBUTIONS

All authors contributed to the article and approved the submitted version.

FUNDING

This work is supported in part by a Thrall Innovation Grant from the Department of Radiology, Massachusetts General Hospital (TN) and 1K08CA249047-01(PH).

REFERENCES

1. Rawla P. Epidemiology of Prostate Cancer. *World J Oncol* (2019) 10(2):63–89. doi: 10.14740/wjon1191
2. La Manna F, Karkampouna S, Zoni E, De Menna M, Hensel J, Thalmann GN, et al. Metastases in Prostate Cancer. *Cold Spring Harb Perspect Med* (2018) 9(3):a033688. doi: 10.1101/cshperspect.a033688
3. Chang SS. Overview of Prostate-Specific Membrane Antigen. *Rev Urol* (2004) 6 Suppl 10(Suppl 10):S13–S8.
4. Lawhn-Heath C, Salavati A, Behr SC, Rowe SP, Calais J, Fendler WP, et al. Prostate-Specific Membrane Antigen PET in Prostate Cancer. *Radiology* (2021) 299(2):248–60. doi: 10.1148/radiol.2021202771
5. Gao J, Zhang C, Zhang Q, Fu Y, Zhao X, Chen M, et al. Diagnostic Performance of 68Ga-PSMA PET/CT for Identification of Aggressive Cribriform Morphology in Prostate Cancer With Whole-Mount Sections. *Eur J Nucl Med Mol Imaging* (2019) 46(7):1531–41. doi: 10.1007/s00259-019-04320-9
6. Ross JS, Sheehan CE, Fisher HA, Kaufman RPJr., Kaur P, Gray K, et al. Correlation of Primary Tumor Prostate-Specific Membrane Antigen Expression With Disease Recurrence in Prostate Cancer. *Clin Cancer Res* (2003) 9(17):6357–62.
7. Koerber SA, Boesch J, Kratochwil C, Schlampp I, Ristau J, Winter E, et al. Predicting the Risk of Metastases by PSMA-PET/CT-Evaluation of 335 Men With Treatment-Naïve Prostate Carcinoma. *Cancers (Basel)* (2021) 13 (7):1508. doi: 10.3390/cancers13071508
8. Thang SP, Violet J, Sandhu S, Iravani A, Akhurst T, Kong G, et al. Poor Outcomes for Patients With Metastatic Castration-Resistant Prostate Cancer With Low Prostate-Specific Membrane Antigen (PSMA) Expression Deemed Ineligible for (177)Lu-Labelled PSMA Radioligand Therapy. *Eur Urol Oncol* (2019) 2(6):670–6. doi: 10.1016/j.euo.2018.11.007
9. Fourquet A, Aveline C, Cussenot O, Créhange G, Montravers F, Talbot JN, et al. (68)Ga-PSMA-11 PET/CT in Restaging Castration-Resistant Nonmetastatic Prostate Cancer: Detection Rate, Impact on Patients' Disease Management and Adequacy of Impact. *Sci Rep* (2020) 10(1):2104. doi: 10.1038/s41598-020-58975-8
10. Taneja SS. ProstaScint(R) Scan: Contemporary Use in Clinical Practice. *Rev Urol* (2004) 6 Suppl 10(Suppl 10):S19–28.
11. Schwarzenboeck SM, Rauscher I, Bluemel C, Fendler WP, Rowe SP, Pomper MG, et al. PSMA Ligands for PET Imaging of Prostate Cancer. *J Nucl Med* (2017) 58(10):1545–52. doi: 10.2967/jnumed.117.191031
12. Rauscher I, Maurer T, Souvatzoglou M, Beer AJ, Vag T, Wirtz M, et al. Intrapatient Comparison of 111In-PSMA I&T SPECT/CT and Hybrid 68ga-HBED-CC PSMA PET in Patients With Early Recurrent Prostate Cancer. *Clin Nucl Med* (2016) 41(9):e397–402. doi: 10.1097/rlu.0000000000001273
13. Wallitt KL, Khan SR, Dubash S, Tam HH, Khan S, Barwick TD. Clinical PET Imaging in Prostate Cancer. *Radiographics* (2017) 37(5):1512–36. doi: 10.1148/rg.2017170035
14. Urbán S, Meyer C, Dahlbom M, Farkas I, Sipka G, Besenyi Z, et al. Radiation Dosimetry of Tc99m-PSMA I&S: A Single-Center Prospective Study. *J Nucl Med* (2020) jnumed.120.253476. doi: 10.2967/jnumed.120.253476
15. Vats K, Agrawal K, Sharma R, Sarma HD, Satpati D, Dash A. Preparation and Clinical Translation of 99mtc-PSMA-11 for SPECT Imaging of Prostate Cancer. *MedChemComm* (2019) 10(12):2111–7. doi: 10.1039/C9MD00401G
16. Osborne J, Akhtar NH, Vallabhajosula S, Nikolopoulou A, Maresca KP, Hillier SM, et al. Tc-99m Labeled Small-Molecule Inhibitors of Prostate-Specific Membrane Antigen (PSMA): New Molecular Imaging Probes to Detect Metastatic Prostate Adenocarcinoma (PC). *J Clin Oncol* (2012) 30 (5_suppl):173–. doi: 10.1200/jco.2012.30.5_suppl.173
17. Hillier S, Kern A, Maresca K, Marquis J, Eckelman W, Joyal J, et al. I-123-MIP-1072, a Small-Molecule Inhibitor of Prostate-Specific Membrane Antigen, Is Effective at Monitoring Tumor Response to Taxane Therapy. *J Nucl Med: Off Publication Soc Nucl Med* (2011) 52:1087–93. doi: 10.2967/jnumed.110.086751
18. Rahbar K, Afshar-Oromieh A, Jadvar H, Ahmadzadehfar H. PSMA Theranostics: Current Status and Future Directions. *Mol Imaging* (2018) 17:1536012118776068. doi: 10.1177/1536012118776068
19. Wittrup KD, Thurber GM, Schmidt MM, Rhoden JJ. Chapter Ten - Practical Theoretic Guidance for the Design of Tumor-Targeting Agents. In: Wittrup KD, Verdine GL, eds. *Methods Enzymol*, vol. 503. San Diego: Academic Press (2012). p. 255–68.
20. Rauscher I, Krönke M, König M, Gafita A, Maurer T, Horn T, et al. Matched-Pair Comparison of (68)Ga-PSMA-11 PET/CT and (18)F-PSMA-1007 PET/CT: Frequency of Pitfalls and Detection Efficacy in Biochemical Recurrence After Radical Prostatectomy. *J Nucl Med* (2020) 61(1):51–7. doi: 10.2967/jnumed.119.229187
21. Hofman MS, Lawrentschuk N, Francis RJ, Tang C, Vela I, Thomas P, et al. Prostate-Specific Membrane Antigen PET-CT in Patients With High-Risk Prostate Cancer Before Curative-Intent Surgery or Radiotherapy

(proPSMA): A Prospective, Randomised, Multicentre Study. *Lancet* (2020) 395(10231):1208–16. doi: 10.1016/s0140-6736(20)30314-7
22. Sawicki LM, Kirchner J, Buddensieck C, Antke C, Ullrich T, Schimmöller L, et al. Prospective Comparison of Whole-Body MRI and (68)Ga-PSMA PET/CT for the Detection of Biochemical Recurrence of Prostate Cancer After Radical Prostatectomy. *Eur J Nucl Med Mol Imaging* (2019) 46(7):1542–50. doi: 10.1007/s00259-019-04308-5
23. Acar E, Bekiş R, Polack B. Comparison of Bone Uptake in Bone Scan and Ga-68 PSMA PET/CT Images in Patients With Prostate Cancer. *Curr Med Imaging Rev* (2019) 15(6):589–94. doi: 10.2174/1573405615666190225155254
24. Simsek DH, Sanli Y, Civan C, Engin MN, Isik EG, Ozkan ZG, et al. Does Bone Scintigraphy Still Have a Role in the Era of 68 Ga-PSMA PET/CT in Prostate Cancer? *Ann Nucl Med* (2020) 34(7):476–85. doi: 10.1007/s12149-020-01474-7
25. Tan N, Oyoyo U, Bavadian N, Ferguson N, Mukkamala A, Calais J, et al. PSMA-Targeted Radiotracers Versus 18F Fluciclovine for the Detection of Prostate Cancer Biochemical Recurrence After Definitive Therapy: A Systematic Review and Meta-Analysis. *Radiology* (2020) 296(1):44–55. doi: 10.1148/radiol.2020191689
26. Turkbey B, Choyke PL. 18F-Fluciclovine PET or PSMA PET for Prostate Cancer Imaging? *Nat Rev Urol* (2020) 17(1):9–10. doi: 10.1038/s41585-019-0255-6
27. Pernthaler B, Kulnik R, Gstettner C, Salamon S, Aigner RM. Kvaternik H. A Prospective Head-To-Head Comparison of 18F-Fluciclovine With 68ga-PSMA-11 in Biochemical Recurrence of Prostate Cancer in PET/CT. *Clin Nucl Med* (2019) 44(10):e566–e73. doi: 10.1097/rlu.0000000000002703
28. Calais J, Fendler WP, Herrmann K, Eiber M, Ceci F. Comparison of (68)Ga-PSMA-11 and (18)F-Fluciclovine PET/CT in a Case Series of 10 Patients With Prostate Cancer Recurrence. *J Nucl Med* (2018) 59(5):789–94. doi: 10.2967/jnumed.117.203257
29. Savir-Baruch B, Choyke PL, Rowe SP, Schuster DM, Subramaniam RM, Jadvar H. Role of 18F-Fluciclovine and Prostate-Specific Membrane Antigen PET/CT in Guiding Management of Oligometastatic Prostate Cancer: AJR Expert Panel Narrative Review. *Am J Roentgenol* (2021) 216(4):851–9. doi: 10.2214/AJR.20.24711
30. Treglia G, Pereira Mestre R, Ferrari M, Bosetti DG, Pascale M, Oikonomou E, et al. Radiolabelled Choline Versus PSMA PET/CT in Prostate Cancer Restaging: A Meta-Analysis. *Am J Nucl Med Mol Imaging* (2019) 9(2):127–39.
31. Moghul M, Somani B, Lane T, Vasdev N, Chaplin B, Peedell C, et al. Detection Rates of Recurrent Prostate Cancer: (68)Gallium (Ga)-Labelled Prostate-Specific Membrane Antigen Versus Choline PET/CT Scans. A Systematic Review. *Ther Adv Urol* (2019) 11:1756287218815793. doi: 10.1177/1756287218815793
32. Regula N, Kostaras V, Johansson S, Trampal C, Lindström E, Lubberink M, et al. Comparison of 68Ga-PSMA-11 PET/CT With 11C-Acetate PET/CT in Re-Staging of Prostate Cancer Relapse. *Sci Rep* (2020) 10(1):4993. doi: 10.1038/s41598-020-61910-6
33. Piccardo A, Paparo F, Puntoni M, Righi S, Bottoni G, Bacigalupo L, et al. 64cucl2 PET/CT in Prostate Cancer Relapse. *J Nucl Med* (2018) 59(3):444–51. doi: 10.2967/jnumed.117.195628
34. Hicks RM, Simko JP, Westphalen AC, Nguyen HG, Greene KL, Zhang L, et al. Diagnostic Accuracy of 68Ga-PSMA-11 PET/MRI Compared With Multiparametric MRI in the Detection of Prostate Cancer. *Radiology* (2018) 289(3):730–7. doi: 10.1148/radiol.2018180788
35. Muehlematter UJ, Burger IA, Becker AS, Schawkat K, Hötker AM, Reiner CS, et al. Diagnostic Accuracy of Multiparametric MRI Versus 68Ga-PSMA-11 PET/MRI for Extracapsular Extension and Seminal Vesicle Invasion in Patients With Prostate Cancer. *Radiology* (2019) 293(2):350–8. doi: 10.1148/radiol.2019190687
36. Zhao J, Mangarova DB, Brangsch J, Kader A, Hamm B, Brenner W, et al. Correlation Between Intraprostatic PSMA Uptake and MRI PI-RADS of [(68)Ga]Ga-PSMA-11 PET/MRI in Patients With Prostate Cancer: Comparison of PI-RADS Version 2.0 and PI-RADS Version 2.1. *Cancers (Basel)* (2020) 12(12):3523. doi: 10.3390/cancers12123523
37. Fendler WP, Calais J, Eiber M, Flavell RR, Mishoe A, Feng FY, et al. Assessment of 68Ga-PSMA-11 PET Accuracy in Localizing Recurrent Prostate Cancer: A Prospective Single-Arm Clinical Trial. *JAMA Oncol* (2019) 5(6):856–63. doi: 10.1001/jamaoncol.2019.0096
38. Kuten J, Sarid D, Yossepowitch O, Mabjeesh NJ, Even-Sapir E. [(68)Ga]Ga-PSMA-11 PET/CT for Monitoring Response to Treatment in Metastatic Prostate Cancer: Is There Any Added Value Over Standard Follow-Up? *EJNMMI Res* (2019) 9(1):84. doi: 10.1186/s13550-019-0554-1
39. Spohn S, Jaegle C, Fassbender TF, Sprave T, Gkika E, Nicolay NH, et al. Intraindividual Comparison Between 68Ga-PSMA-PET/CT and mpMRI for Intraprostatic Tumor Delineation in Patients With Primary Prostate Cancer: A Retrospective Analysis in 101 Patients. *Eur J Nucl Med Mol Imaging* (2020) 47(12):2796–803. doi: 10.1007/s00259-020-04827-6
40. Murthy V, Sonni I, Jariwala N, Juarez R, Reiter RE, Raman SS, et al. The Role of PSMA PET/CT and PET/MRI in the Initial Staging of Prostate Cancer. *Eur Urol Focus* (2021) 7(2):258–66. doi: 10.1016/j.euf.2021.01.016
41. Zukotynski KA, Jadvar H, Cho SY, Kim CK, Cline K, Emmenegger U, et al. FDG and PSMA PET in Metastatic Castration-Resistant Prostate Cancer (mCRPC). *J Clin Oncol* (2020) 38(6_suppl):23–. doi: 10.1200/JCO.2020.38.6_suppl.23
42. de Jong AC, Smits M, van Riet J, Fütterer JJ, Brabander T, Hamberg P, et al. (68)Ga-PSMA-Guided Bone Biopsies for Molecular Diagnostics in Patients With Metastatic Prostate Cancer. *J Nucl Med* (2020) 61(11):1607–14. doi: 10.2967/jnumed.119.241109
43. Rahbar K, Weckesser M, Huss S, Semjonow A, Breyholz HJ, Schrader AJ, et al. Correlation of Intraprostatic Tumor Extent With ^{68}Ga-PSMA Distribution in Patients With Prostate Cancer. *J Nucl Med* (2016) 57 (4):563–7. doi: 10.2967/jnumed.115.169243
44. Kostyszyn D, Fechter T, Bartl N, Grosu AL, Gratzke C, Sigle A, et al. Intraprostatic Tumour Segmentation on PSMA-PET Images in Patients With Primary Prostate Cancer With a Convolutional Neural Network. *J Nucl Med* (2020) 62(6):823–8. doi: 10.2967/jnumed.120.254623
45. Zamboglou C, Thomann B, Koubar K, Bronsert P, Krauss T, Rischke HC, et al. Focal Dose Escalation for Prostate Cancer Using (68)Ga-HBED-CC PSMA PET/CT and MRI: A Planning Study Based on Histology Reference. *Radiat Oncol* (2018) 13(1):81. doi: 10.1186/s13014-018-1036-8
46. Zschaeck S, Wust P, Beck M, Wlodarczyk W, Kaul D, Rogasch J, et al. Intermediate-Term Outcome After PSMA-PET Guided High-Dose Radiotherapy of Recurrent High-Risk Prostate Cancer Patients. *Radiat Oncol* (2017) 12(1):140. doi: 10.1186/s13014-017-0877-x
47. Onal C, Ozyigit G, Guler OC, Hurmuz P, Torun N, Tuncel M, et al. Role of 68-Ga-PSMA-PET/CT in Pelvic Radiotherapy Field Definitions for Lymph Node Coverage in Prostate Cancer Patients. *Radiother Oncol: J Eur Soc Ther Radiol Oncol* (2020) 151:222–7. doi: 10.1016/j.radonc.2020.08.021
48. Ma TM, Gafita A, Shabsovich D, Juarez J, Grogan TR, Thin P, et al. Identifying the Best Candidates for Prostate-Specific Membrane Antigen Positron Emission Tomography/Computed Tomography as the Primary Staging Approach Among Men With High-Risk Prostate Cancer and Negative Conventional Imaging. *Eur Urol Oncol* (2021) S2588-9311(21)00030-4. doi: 10.1016/j.euo.2021.01.006
49. Vale CL, Fisher D, Kneebone A, Parker C, Pearse M, Richaud P, et al. Adjuvant or Early Salvage Radiotherapy for the Treatment of Localised and Locally Advanced Prostate Cancer: A Prospectively Planned Systematic Review and Meta-Analysis of Aggregate Data. *Lancet* (2020) 396 (10260):1422–31. doi: 10.1016/s0140-6736(20)31952-8
50. Lowrance W, Breau RH, Chou R, Chapin BF, Crispino T, dreicer R, et al. Advanced Prostate Cancer: AUA/ASTRO/SUO Guideline PART I. *J Urol* (2021) 205(14):14–21. doi: 10.1097/JU.0000000000001375
51. Song H, Harrison C, Duan H, Guja K, Hatami N, Franc BL, et al. Prospective Evaluation of (18)F-DCFPyL PET/CT in Biochemically Recurrent Prostate Cancer in an Academic Center: A Focus on Disease Localization and Changes in Management. *J Nucl Med* (2020) 61(4):546–51. doi: 10.2967/jnumed.119.231654
52. Emmett L, Tang R, Nandurkar R, Hruby G, Roach P, Watts JA, et al. 3-Year Freedom From Progression After (68)Ga-PSMA PET/CT-Triaged Management in Men With Biochemical Recurrence After Radical Prostatectomy: Results of a Prospective Multicenter Trial. *J Nucl Med* (2020) 61(6):866–72. doi: 10.2967/jnumed.119.235028
53. Koschel S, Taubman K, Sutherland T, Yap K, Chao M, Guerrieri M, et al. Patterns of Disease Detection Using [(18)F]DCFPyL PET/CT Imaging in Patients With Detectable PSA Post Prostatectomy Being Considered for

Salvage Radiotherapy: A Prospective Trial. *Eur J Nucl Med Mol Imaging* (2021). doi: 10.1007/s00259-021-05354-8
54. Liu W, Zukotynski K, Emmett L, Chung HT, Chung P, Wolfson R, et al. A Prospective Study of 18F-DCFPyL PSMA PET/CT Restaging in Recurrent Prostate Cancer Following Primary External Beam Radiotherapy or Brachytherapy. *Int J Radiat Oncol Biol Phys* (2020) 106(3):546–55. doi: 10.1016/j.ijrobp.2019.11.001
55. Palma DA, Olson R, Harrow S, Gaede S, Louie AV, Haasbeek C, et al. Stereotactic Ablative Radiotherapy *Versus* Standard of Care Palliative Treatment in Patients With Oligometastatic Cancers (SABR-COMET): A Randomised, Phase 2, Open-Label Trial. *Lancet* (2019) 393(10185):2051–8. doi: 10.1016/s0140-6736(18)32487-5
56. Kamran SC, Zietman AL. Curing Metastatic Disease With Ablative Radiation Therapy: Separating Truth From Wish. *Int J Radiat Oncol Biol Phys* (2020) 107(3):433–6. doi: 10.1016/j.ijrobp.2020.02.468
57. Kamran SC, Efstathiou JA. Current State of Personalized Genitourinary Cancer Radiotherapy in the Era of Precision Medicine. *Front Oncol* (2021) 11:675311. doi: 10.3389/fonc.2021.675311
58. Glicksman RM, Metser U, Vines D, Valliant J, Liu Z, Chung PW, et al. Curative-Intent Metastasis-Directed Therapies for Molecularly-Defined Oligorecurrent Prostate Cancer: A Prospective Phase II Trial Testing the Oligometastasis Hypothesis. *Eur Urol* (2021) S0302-2838(21)00151-2. doi: 10.1016/j.eururo.2021.02.031
59. Phillips R, Shi WY, Deek M, Radwan N, Lim SJ, Antonarakis ES, et al. Outcomes of Observation *vs* Stereotactic Ablative Radiation for Oligometastatic Prostate Cancer: The ORIOLE Phase 2 Randomized Clinical Trial. *JAMA Oncol* (2020) 6(5):650–9. doi: 10.1001/jamaoncol.2020.0147
60. Solomon SB, Cornelis F. Interventional Molecular Imaging. *J Nucl Med* (2016) 57(4):493–6. doi: 10.2967/jnumed.115.161190
61. Bianchi L, Gandaglia G, Fossati N, Suardi N, Moschini M, Cucchiara V, et al. Pelvic Lymph Node Dissection in Prostate Cancer: Indications, Extent and Tailored Approaches. *Urologia* (2017) 84(1):9–19. doi: 10.5301/uro.5000139
62. Maurer T, Graefen M, van der Poel H, Hamdy F, Briganti A, Eiber M, et al. Prostate-Specific Membrane Antigen-Guided Surgery. *J Nucl Med* (2020) 61(1):6–12. doi: 10.2967/jnumed.119.232330
63. Jilg CA, Reichel K, Stoykow C, Rischke HC, Bartholomä M, Drendel V, et al. Results From Extended Lymphadenectomies With [111In]PSMA-617 for Intraoperative Detection of PSMA-PET/CT-Positive Nodal Metastatic Prostate Cancer. *EJNMMI Res* (2020) 10(1):17. doi: 10.1186/s13550-020-0598-2
64. Derks YHW, Löwik DWPM, Sedelaar JPM, Gotthardt M, Boerman OC, Rijpkema M, et al. PSMA-Targeting Agents for Radio- and Fluorescence-Guided Prostate Cancer Surgery. *Theranostics* (2019) 9(23):6824–39. doi: 10.7150/thno.36739
65. van Leeuwen FWB, van Oosterom MN, Meershoek P, van Leeuwen PJ, Berliner C, van der Poel HG, et al. Minimal-Invasive Robot-Assisted Image-Guided Resection of Prostate-Specific Membrane Antigen–Positive Lymph Nodes in Recurrent Prostate Cancer. *Clin Nucl Med* (2019) 44(7):580–1. doi: 10.1097/RLU.0000000000002600
66. Parker C, Nilsson S, Heinrich D, Helle SI, O'Sullivan JM, Fosså SD, et al. Alpha Emitter Radium-223 and Survival in Metastatic Prostate Cancer. *New Engl J Med* (2013) 369(3):213–23. doi: 10.1056/NEJMoa1213755
67. Herrmann K, Schwaiger M, Lewis JS, Solomon SB, McNeil BJ, Baumann M, et al. Radiotheranostics: A Roadmap for Future Development. *Lancet Oncol* (2020) 21(3):e146–e56. doi: 10.1016/S1470-2045(19)30821-6
68. Sun M, Niaz MO, Nelson A, Skafida M, Niaz MJ. Review of 177Lu-PSMA-617 in Patients With Metastatic Castration-Resistant Prostate Cancer. *Cureus* (2020) 12(6):e8921. doi: 10.7759/cureus.8921
69. Privé BM, Peters SMB, Muselaers CHJ, van Oort IM, Janssen MJR, Sedelaar JPM, et al. Lutetium-177-PSMA-617 in Low-Volume Hormone-Sensitive Metastatic Prostate Cancer: A Prospective Pilot Study. *Clin Cancer Res* (2021) 27(13):3595–601. doi: 10.1158/1078-0432.Ccr-20-4298
70. Rasul S, Hacker M, Kretschmer-Chott E, Leisser A, Grubmüller B, Kramer G, et al. Clinical Outcome of Standardized 177Lu-PSMA-617 Therapy in Metastatic Prostate Cancer Patients Receiving 7400 MBq Every 4 Weeks. *Eur J Nucl Med Mol Imaging* (2020) 47(3):713–20. doi: 10.1007/s00259-019-04584-1
71. Sartor O, de Bono J, Chi KN, Fizazi K, Herrmann K, Rahbar K, et al. Lutetium-177–PSMA-617 for Metastatic Castration-Resistant Prostate Cancer. *New Engl J Med* (2021). doi: 10.1056/NEJMoa2107322
72. Sartor AO, Morris MJ, Messman R, Krause BJ. VISION: An International, Prospective, Open-Label, Multicenter, Randomized Phase III Study of 177Lu-PSMA-617 in the Treatment of Patients With Progressive PSMA-Positive Metastatic Castration-Resistant Prostate Cancer (mCRPC). *J Clin Oncol* (2020) 38(6_suppl):TPS259–TPS. doi: 10.1200/JCO.2020.38.6_suppl.TPS259
73. Hofman MS, Emmett L, Violet J, YZ A, Lawrence NJ, Stockler M, et al. TheraP: A Randomized Phase 2 Trial of (177) Lu-PSMA-617 Theranostic Treatment *vs* Cabazitaxel in Progressive Metastatic Castration-Resistant Prostate Cancer (Clinical Trial Protocol ANZUP 1603). *BJU Int* (2019) 124 Suppl 1:5–13. doi: 10.1111/bju.14876
74. Dhiantravan N, Violet J, Eapen R, Alghazo O, Scalzo M, Jackson P, et al. Clinical Trial Protocol for LuTectomy: A Single-Arm Study of the Dosimetry, Safety, and Potential Benefit of ≪Sup<177≪/Sup<Lu-PSMA-617 Prior to Prostatectomy. *Eur Urol Focus* (2021) 7(2):234–7. doi: 10.1016/j.euf.2020.09.021
75. Privé BM, Janssen MJR, van Oort IM, Muselaers CHJ, Jonker MA, de Groot M, et al. Lutetium-177-PSMA-I&T as Metastases Directed Therapy in Oligometastatic Hormone Sensitive Prostate Cancer, a Randomized Controlled Trial. *BMC Cancer* (2020) 20(1):884. doi: 10.1186/s12885-020-07386-z
76. Prasad V, Huang K, Prasad S, Makowski MR, Czech N, Brenner W. In Comparison to PSA, Interim Ga-68-PSMA PET/CT Response Evaluation Based on Modified RECIST 1.1 After 2nd Cycle Is Better Predictor of Overall Survival of Prostate Cancer Patients Treated With 177lu-PSMA. *Front Oncol* (2021) 11:578093. doi: 10.3389/fonc.2021.578093
77. Seifert R, Kessel K, Schlack K, Weber M, Herrmann K, Spanke M, et al. PSMA PET Total Tumor Volume Predicts Outcome of Patients With Advanced Prostate Cancer Receiving [(177)Lu]Lu-PSMA-617 Radioligand Therapy in a Bicentric Analysis. *Eur J Nucl Med Mol Imaging* (2021) 48(4):1200–10. doi: 10.1007/s00259-020-05040-1
78. Czerwińska M, Bilewicz A, Kruszewski M, Wegierek-Ciuk A, Lankoff A. Targeted Radionuclide Therapy of Prostate Cancer-From Basic Research to Clinical Perspectives. *Molecules* (2020) 25(7):1743. doi: 10.3390/molecules25071743
79. Bander NH, Milowsky MI, Nanus DM, Kostakoglu L, Vallabhajosula S, Goldsmith SJ. Phase I Trial of 177Lutetium-Labeled J591, a Monoclonal Antibody to Prostate-Specific Membrane Antigen, in Patients With Androgen-Independent Prostate Cancer. *J Clin Oncol* (2005) 23(21):4591–601. doi: 10.1200/jco.2005.05.160
80. Nauseef JT, Bander NH, Tagawa ST. Emerging Prostate-Specific Membrane Antigen-Based Therapeutics: Small Molecules, Antibodies, and Beyond. *Eur Urol Focus* (2021) 7(2):254–7. doi: 10.1016/j.euf.2021.02.006
81. Kratochwil C, Haberkorn U, Giesel FL. 225Ac-PSMA-617 for Therapy of Prostate Cancer. *Semin Nucl Med* (2020) 50(2):133–40. doi: 10.1053/j.semnuclmed.2020.02.004
82. Khreish F, Ebert N, Ries M, Maus S, Rosar F, Bohnenberger H, et al. (225) Ac-PSMA-617/(177)Lu-PSMA-617 Tandem Therapy of Metastatic Castration-Resistant Prostate Cancer: Pilot Experience. *Eur J Nucl Med Mol Imaging* (2020) 47(3):721–8. doi: 10.1007/s00259-019-04612-0
83. Shen CJ, Minn I, Hobbs RF, Chen Y, Josefsson A, Brummet M, et al. Auger Radiopharmaceutical Therapy Targeting Prostate-Specific Membrane Antigen in a Micrometastatic Model of Prostate Cancer. *Theranostics* (2020) 10(7):2888–96. doi: 10.7150/thno.38882
84. Hummel HD, Kufer P, Grüllich C, Seggewiss-Bernhardt R, Deschler-Baier B, Chatterjee M, et al. Pasotuxizumab, a BiTE(®) Immune Therapy for Castration-Resistant Prostate Cancer: Phase I, Dose-Escalation Study Findings. *Immunotherapy* (2021) 13(2):125–41. doi: 10.2217/imt-2020-0256
85. Tran B, Horvath L, Dorff T, Rettig M, Lolkema MP, Machiels J, et al. Results From a Phase I Study of AMG 160, a Half-Life Extended (HLE), PSMA-Targeted, Bispecific T-Cell Engager (BiTE®) Immune Therapy for Metastatic Castration-Resistant Prostate Cancer (mCRPC). *Ann Oncol* (2020) 31(suppl_4):S507–49. doi: 10.1016/annonc/annonc275
86. Subudhi SK, Siddiqui BA, Maly JJ, Nandagopal L, Lam ET, Whang YE, et al. Safety and Efficacy of AMG 160, a Half-Life Extended BiTE Immune

Therapy Targeting Prostate-Specific Membrane Antigen (PSMA), and Other Therapies for Metastatic Castration-Resistant Prostate Cancer (mCRPC). *J Clin Oncol* (2021) 39(suppl 15; abstr TPS5088). doi: 10.1200/JCO.2021.39.15_suppl.TPS5088

87. de Bono JS, Fong L, Beer TM, Gao X, Geynisman DM, Burris HA, et al. Results of an Ongoing Phase 1/2a Dose Escalation Study of HPN424, a Tri-Specific Half-Life Extended PSMA-Targeting T-Cell Engager, in Patients With Metastatic Castration-Resistant Prostate Cancer (mCRPC). *J Clin Oncol* (2021) 39(suppl 15; abstr 5013). doi: 10.1200/JCO.2021.39.15_suppl.5013
88. Zhang J, Stein MN, Kelly WK, Tsao CK, Falchook GS, Xu Y, et al. A Phase I/II Study of REGN5678 (Anti-PSMAxCD28, a Costimulatory Bispecific Antibody) With Cemiplimab (Anti–PD-1) in Patients With Metastatic Castration-Resistant Prostate Cancer. *J Clin Oncol* (2021) 39(suppl 6; abstr TPS174). doi: 10.1200/JCO.2021.39.6_suppl.TPS174
89. Buelow B, Dalvi P, Dang K, Patel A, Johal K, Pham D, et al. TNB585.001: A Multicenter, Phase 1, Open-Label, Dose-Escalation and Expansion Study of Tnb-585, a Bispecific T-Cell Engager Targeting PSMA in Subjects With Metastatic Castrate Resistant Prostate Cancer. *J Clin Oncol* (2021) 39(suppl 15; abstr TPS5092). doi: 10.1200/JCO.2021.39.15_suppl.TPS5092
90. Markowski MC, Kilari D, Eisenberger MA, McKay RR, Dreicer R, Trikha M, et al. Phase I Study of CCW702, a Bispecific Small Molecule-Antibody Conjugate Targeting PSMA and CD3 in Patients With Metastatic Castration-Resistant Prostate Cancer (mCRPC). *J Clin Oncol* (2021) 39 (suppl 15; abstr TPS5094). doi: 10.1200/JCO.2021.39.15_suppl.TPS5094
91. June CH, Sadelain M. Chimeric Antigen Receptor Therapy. *New Engl J Med* (2018) 379(1):64–73. doi: 10.1056/NEJMra1706169
92. Junghans RP, Ma Q, Rathore R, Gomes EM, Bais AJ, Lo AS, et al. Phase I Trial of Anti-PSMA Designer CAR-T Cells in Prostate Cancer: Possible Role for Interacting Interleukin 2-T Cell Pharmacodynamics as a Determinant of Clinical Response. *Prostate* (2016) 76(14):1257–70. doi: 10.1002/pros.23214
93. Slovin SF, Wang X, Hullings M, Arauz G, Bartido S, Lewis JS, et al. Chimeric Antigen Receptor (CAR+) Modified T Cells Targeting Prostate Specific Membrane Antigen (PSMA) in Patients (Pts) With Castrate Metastatic Prostate Cancer (CMPC). *J Clin Oncol* (2013) 31(suppl; abstr TPS3115). doi: 10.1200/jco.2013.31.15_suppl.tps3115
94. Carabasi MH, McKean M, Stein MN, Schweizer MT, Luke JJ, Narayan V, et al. PSMA Targeted Armored Chimeric Antigen Receptor (CAR) T-Cells in Patients With Advanced mCRPC: A Phase I Experience. *J Clin Oncol* (2021) 39(suppl 15; abstr 2534). doi: 10.1200/JCO.2021.39.15_suppl.2534
95. Narayan V, Barber-Rotenberg J, Fraietta J, Hwang WT, Lacey SF, Plesa G, et al. A Phase I Clinical Trial of PSMA-Directed/Tgfβ-Insensitive CAR-T Cells in Metastatic Castration-Resistant Prostate Cancer. *J Clin Oncol* (2021) 39(suppl 6; abstr 125). doi: 10.1200/JCO.2021.39.6_suppl.125
96. Minn I, Huss DJ, Ahn H-H, Chinn TM, Park A, Jones J, et al. Imaging CAR T Cell Therapy With PSMA-Targeted Positron Emission Tomography. *Sci Adv* (2019) 5(7):eaaw5096–eaaw. doi: 10.1126/sciadv.aaw5096
97. Beck A, Goetsch L, Dumontet C, Corvaïa N. Strategies and Challenges for the Next Generation of Antibody–Drug Conjugates. *Nat Rev Drug Discovery* (2017) 16(5):315–37. doi: 10.1038/nrd.2016.268
98. Milowsky MI, Galsky MD, Morris MJ, Crona DJ, George DJ, Dreicer R, et al. Phase 1/2 Multiple Ascending Dose Trial of the Prostate-Specific Membrane Antigen-Targeted Antibody Drug Conjugate MLN2704 in Metastatic Castration-Resistant Prostate Cancer. *Urol Oncol* (2016) 34(12):530 e15–e21. doi: 10.1016/j.urolonc.2016.07.005
99. Petrylak DP, Vogelzang NJ, Chatta K, Fleming MT, Smith DC, Appleman LJ, et al. PSMA ADC Monotherapy in Patients With Progressive Metastatic Castration-Resistant Prostate Cancer Following Abiraterone and/or Enzalutamide: Efficacy and Safety in Open-Label Single-Arm Phase 2 Study. *Prostate* (2020) 80(1):99–108. doi: 10.1002/pros.23922
100. de Bono JS, Fleming MT, Wang JS, Cathomas R, Miralles MS, Bothos J, et al. Phase I Study of MEDI3726: A Prostate-Specific Membrane Antigen-Targeted Antibody–Drug Conjugate, in Patients With mCRPC After Failure of Abiraterone or Enzalutamide. *Clin Cancer Res* (2021) 27 (13):3602–9. doi: 10.1158/1078-0432.ccr-20-4528
101. Shaygan B, Zukotynski K, Bénard F, Ménard C, Sistani G, Bauman G, et al. Canadian Urological Association Best Practice Report: Prostate-Specific Membrane Antigen Positron Emission Tomography/Computed Tomography (PSMA PET/CT) and PET/magnetic Resonance (MR) in Prostate Cancer. *Can Urol Assoc J* (2021) 15(6):162–72. doi: 10.5489/cuaj.7268
102. Eiber M, Herrmann K, Calais J, Hadaschik B, Giesel FL, Hartenbach M, et al. Prostate Cancer Molecular Imaging Standardized Evaluation (PROMISE): Proposed miTNM Classification for the Interpretation of PSMA-Ligand PET/CT. *J Nucl Med* (2018) 59(3):469–78. doi: 10.2967/jnumed.117.198119
103. Rowe SP, Pienta KJ, Pomper MG, Gorin MA. PSMA-RADS Version 1.0: A Step Towards Standardizing the Interpretation and Reporting of PSMA-Targeted PET Imaging Studies. *Eur Urol* (2018) 73(4):485–7. doi: 10.1016/j.eururo.2017.10.027

Conflict of Interest: The authors declare that the research was conducted in the absence of any commercial or financial relationships that could be construed as a potential conflict of interest.

frontiers in Oncology

ORIGINAL RESEARCH
published: 30 July 2021
doi: 10.3389/fonc.2021.715020

Feasibility and Outcome of PSMA-PET-Based Dose-Escalated Salvage Radiotherapy *Versus* Conventional Salvage Radiotherapy for Patients With Recurrent Prostate Cancer

Marco M. E. Vogel[1,2*], *Sabrina Dewes*[1], *Eva K. Sage*[1], *Michal Devecka*[1], *Kerstin A. Eitz*[1,2,3], *Jürgen E. Gschwend*[4], *Matthias Eiber*[5], *Stephanie E. Combs*[1,2,3] *and Kilian Schiller*[1]

[1] Department of Radiation Oncology, Klinikum rechts der Isar, Technical University of Munich (TUM), Munich, Germany, [2] Institute for Radiation Medicine (IRM), Department of Radiation Sciences (DRS), Helmholtz Zentrum München, Neuherberg, Germany, [3] Deutsches Konsortium für Translationale Krebsforschung (DKTK), Partner Site Munich, Munich, Germany, [4] Department of Urology, Klinikum rechts der Isar, Technical University of Munich (TUM), Munich, Germany, [5] Department of Nuclear Medicine, Klinikum rechts der Isar, Technical University of Munich (TUM), Munich, Germany

Introduction: Prostate-specific membrane antigen-positron emission tomography-(PSMA-PET) imaging facilitates dose-escalated salvage radiotherapy (DE-SRT) with simultaneous-integrated boost (SIB) for PET-positive lesions in patients with prostate cancer (PC). Therefore, we aimed to compare toxicity rates of DE-SRT with SIB to conventional SRT (C-SRT) without SIB and to report outcome.

Materials and Methods: We evaluated 199 patients who were treated with SRT between June 2014 and June 2020. 101 patients received DE-SRT with SIB for PET-positive local recurrence and/or PET-positive lymph nodes. 98 patients were treated with C-SRT to the prostate bed +/– elective pelvic lymphatic pathways without SIB. All patients received PSMA-PET imaging prior to DE-SRT ([68Ga]PSMA-11: 45.5%; [18F]-labeled PSMA: 54.5%). Toxicity rates for early (<6 months) and late (>6 months) gastrointestinal (GI) toxicities rectal bleeding, proctitis, stool incontinence, and genitourinary (GU) toxicities hematuria, cystitis, urine incontinence, urinary obstruction, and erectile dysfunction were assessed. Further, we analyzed the outcome with disease-free survival (DFS) and prostate-specific antigen (PSA) response.

Results: The overall toxicity rates for early GI (C-SRT: 2.1%, DE-SRT: 1.0%) and late GI (C-SRT: 1.4%, DE-SRT: 5.3%) toxicities ≥ grade 2 were similar. Early GU (C-SRT: 2.1%, DE-SRT: 3.0%) and late GU (C-SRT: 11.0%, DE-SRT: 14.7%) toxicities ≥ grade 2 were comparable, as well. Early and late toxicity rates did not differ significantly between DE-SRT *versus* C-SRT in all subcategories ($p>0.05$). PSA response (PSA ≤0.2 ng/ml) in the overall group of patients with DE-SRT was 75.0% and 86.4% at first and last follow-up, respectively.

OPEN ACCESS

Edited by:
Trevor Royce, University of North Carolina at Chapel Hill, United States

Reviewed by:
Pirus Ghadjar, Charité – Universitätsmedizin Berlin, Germany
Luca Nicosia, Sacro Cuore Don Calabria Hospital, Italy
Nina-Sophie Hegemann, Ludwig Maximilian University of Munich, Germany

***Correspondence:**
Marco M. E. Vogel
marco.vogel@tum.de

Specialty section:
This article was submitted to Cancer Imaging and Image-directed Interventions, a section of the journal Frontiers in Oncology

Received: *26 May 2021*
Accepted: *06 July 2021*
Published: *30 July 2021*

Citation:
Vogel MME, Dewes S, Sage EK, Devecka M, Eitz KA, Gschwend JE, Eiber M, Combs SE and Schiller K (2021) Feasibility and Outcome of PSMA-PET-Based Dose-Escalated Salvage Radiotherapy Versus Conventional Salvage Radiotherapy for Patients With Recurrent Prostate Cancer. Front. Oncol. 11:715020. doi: 10.3389/fonc.2021.715020

Conclusion: DE-SRT showed no significantly increased toxicity rates compared with C-SRT and thus is feasible. The outcome of DE-SRT showed good results. Therefore, DE-SRT with a PSMA-PET-based SIB can be considered for the personalized treatment in patients with recurrent PC.

Keywords: simultaneous-integrated boost, relapse, positron emission tomography, prostate-specific membrane antigen, side effects, disease-free survival

INTRODUCTION

Salvage radiotherapy (SRT) is an integral part of prostate cancer (PC) treatment. Approximately one third to one half of the patients undergoing radical prostatectomy (RP) will develop a biochemical relapse (1). Recently, three randomized controlled trials evaluated observation with SRT *versus* adjuvant RT (2–4). The data suggest that observation with SRT can be considered as the standard treatment option for most patients after RP. However, especially for patients with high-risk features adjuvant RT should be discussed as well.

With the introduction of the prostate-specific membrane antigen-positron emission tomography (PSMA-PET) imaging, it quickly became a valid diagnostic tool for patients with PC relapse. PSMA tracers allow for detection rates of 58% at prostate-specific antigen (PSA) levels as low as 0.2 to 1.0 ng/ml for [68Ga]-labeled PSMA, increasing with higher PSA values (5).

Whereas in the past, the radiation oncologist had to treat the prostate bed (PB) and/or the elective pelvic lymph nodes (ePLNs) in cases of SRT mostly without an imaging correlate and based on statistical probabilities, today, RT of the tumor volume visualized by PSMA-PET is possible. The precise imaging allows for treatment of the macroscopic disease [local recurrence or pelvic lymph nodes (LNs)] with higher doses than the elective PB or ePLNs. With modern intensity-modulated RT (IMRT) a simultaneous-integrated boost (SIB) is possible, without prolonging the total treatment time.

However, it remains unknown, if side effects of PSMA-PET-based dose-escalated SRT (DE-SRT) with SIB are increased compared with conventional SRT (C-SRT) without SIB. Therefore, this study aims to compare toxicity of DE-SRT *versus* C-SRT. Further, we report the outcome of patients receiving PSMA-PET-based DE-SRT.

MATERIALS AND METHODS

Patients

We screened 256 patients who were treated between June 2014 and June 2020 at the University Hospital of the Technical University of Munich (TUM). We included patients with relapse after RP who received either DE-SRT with SIB for PET-positive local recurrence or LNs as well as C-SRT without SIB. Patients had a post-RP PSA nadir of <0.1 ng/ml. We excluded patients due to distant metastases or 3-dimensional RT, as well as the use of Choline-PET instead of PSMA-PET or sequential boost techniques. Further, we excluded patients if they showed PET-positive lesions, but no dose escalation was performed. In line with the recent guidelines (6, 7) and to ensure comparability, we excluded patients with doses of EQD2 (1.5 Gy) < 66 Gy to the PB. Patients without follow-up were excluded as well. Analysis was conducted retrospectively and was part of the SIMBA (Simultaneous-Integrated Boost in Salvage Radiotherapy for Patients With Recurrent Prostate Cancer) study. The institutional review board of the Technical University of Munich (TUM) approved the study (No. 564/19-S).

PSMA-PET Imaging

Before DE-SRT, each patient received PET imaging with [68Ga]PSMA-11 (8) or a [18F]-labeled PSMA-ligand ([18F]PSMA-1007 (9), [18F]rhPSMA-7 (10), or [18F]rhPSMA-7.3 (11)). PET acquisition was performed according to the joint EANM and SNMMI guidelines (12). Imaging was acquired in conjunction with either a diagnostic computed tomography (CT) or magnetic resonance imaging (MRI). Intravenous and oral contrast agents were used if the patient had no contraindications both for PET/CT and PET/MRI. When possible, furosemide 20 mg was given to reduce tracer collection in the urinary tract system. One specialist in nuclear medicine and one radiologist or a dual boarded nuclear medicine physician/radiologist interpreted the scans. Focal tracer uptake higher than the surrounding background and not associated with physiologic uptake was considered as suspect.

Radiotherapy

RT was performed with intensity-modulated RT (IMRT) as volumetric arc therapy (VMAT) or helical IMRT. Planning CT and RT were performed with a reproducible comfortably filled bladder and empty rectum. We performed image-guided RT (IGRT) with daily online imaging. Target delineation was conducted using the RTOG (13) or EORTC (14) guideline. Planning target volume (PTV) of the SIBs were generated with an additional margin of 5 to 10 mm to the gross tumor volume (GTV). Indication for additive androgen deprivation therapy was discussed in a multidisciplinary tumor board and recommended thereafter to the patient. When organ at risk constraints allowed, we used the following dose concept: Overall, the PB was irradiated with a total of 68 Gy in 2 Gy single doses (34 fractions). The ePLNs were treated with 50.4 Gy in 1.8 Gy single doses (28 fractions). When patients received RT to the PB and ePLNs we treated the PB for 28 fractions up to 56 Gy and the ePLNs up to 50.4 Gy continuing with the PB only up to the total dose of 68 Gy. In the DE-SRT group, we treated the patients

with an additional SIB to the PET-positive areas (local recurrence and/or LNs). Then the PB was irradiated with 68 Gy in 2 Gy single doses (34 fractions) and a SIB to the local recurrence with 76.5 Gy in 2.25 Gy doses (34 fractions). ePLNs were treated with 50.4 Gy in 1.8 Gy doses (28 fractions) and a SIB to PET positive areas with 58.8 Gy in 2.1 Gy doses (28 fractions) or 61.6 Gy in 2.2 Gy doses (28 fractions). When patients received RT to the PB and ePLNs with SIB we treated the PB and the ePLNs for 28 fractions continuing with the PB only for a total of 34 fractions. However, changes to the total doses of PB, ePLNs, and SIBs were possible and at the discretion of the treating radiation oncologist.

Toxicity

Toxicity of SRT was assessed using the Common Terminology Criteria for Adverse Events (CTCAE) version 5 (15). Follow-up was conducted according to our institutional protocol. First follow-up was performed 4 to 6 weeks after termination of RT, thereafter time intervals increased to 3 and 6 months, before continuing with yearly visits. Outpatient urologic aftercare including PSA tests were recommended every 3 months for the first 2 years, every 6 months for the following 2 years continuing with annual appointments. Side effects before 6 months were classified as early/acute toxicity, whereas late/chronic toxicity was defined as side effects after 6 months. Only newly occurred or worsened side effects were defined as related to RT.

Outcome

We defined PSA response after SRT as a PSA value below or equal 0.2 ng/ml. Disease-free survival (DFS) was defined as either PSA progression (PSA nadir + 0.2 ng/ml and one confirmation value), local relapse, occurrence of metastasis or change/initiation of ADT.

Statistics

To compare baseline characteristics and toxicity in both groups we used a Pearson's chi-square test or an independent-samples median test. Patients without follow-up data were excluded from the evaluation of the respective toxicity endpoint. Toxicity rates were compared by Pearson's chi-square test. For the analysis of DFS, we used Cox regression analysis adjusted for the use of additive ADT.

The median PSA before RT was significantly different. To ensure comparability, we only included patients in the outcome analysis whose PSA levels met the common definition of a relapse of >0.2 ng/ml (16) (n=148). Median time between ADT and last follow-up was 7 months (range: 0–51 months). Since ADT influences the PSA response, we excluded patients with admission of ADT in follow-up after the termination of additive ADT from evaluation of the PSA response. To compare doses with different fractionation schemes, we used the equivalent dose in 2 Gy fractions with an alpha/beta ratio of 1.5 Gy (EQD2, 1.5 Gy). Wherever possible, we report the EQD2 (1.5 Gy). All statistical analyses were performed with SPSS version 21 (IBM, Armonk, USA). A p-value <0.05 was considered as statistically significant.

RESULTS

After screening, we evaluated 199 patients with a median age of 71.0 years (range, 49.0–82.0 years). Median follow-up was 13.6 months (range, 0.4–70.0 months). Complete patient characteristics are shown in **Table 1**.

Patients were treated between 06/2014 und 06/2020 with the median doses shown in **Table 2**.

Toxicity

Baseline toxicity rates are shown in **Table 3**. No significant differences were seen in the pre-RT baseline toxicity.

The overall rate of early gastrointestinal toxicity ≥ grade 2 was 2.1% and 1.0% for the C-SRT and DE-SRT group, respectively. Late gastrointestinal side effects ≥ grade 2 were 1.4% and 5.3% for C-SRT and DE-SRT group. Early genitourinary toxicity ≥ grade 2 occurred in 2.1% and 3.0% of the cases for C-SRT and DE-SRT group. Late genitourinary side effects ≥ grade 2 were seen in 11.0% and 14.7% for patients with C-SRT and DE-SRT, respectively. **Table 4** shows newly occurred or worsened early (<6 months) and late (>6 months) side effects for all patients. No early gastrointestinal or genitourinary fistula was documented. One late genitourinary fistula grade 2 was reported in the DE-SRT group, whereas overall, no late gastrointestinal fistulas were seen. **Table 5** shows the newly diagnosed side effects for the subgroup of patients with C-SRT to the PB only *versus* DE-SRT of the PB with SIB. Toxicity of the remaining patients (PB +ePLNs, PB/SIB + ePLNs, PB + ePLNs/SIB, PB/SIB + ePLNs/SIB, and ePLNs/SIB) is shown in the supplementary files (see **Supplementary Table 1**).

Outcome

We further evaluated the outcome of patients who received DE-SRT and C-SRT. Mean DFS for C-SRT was 41.02 months (95% CI: 30.61–51.43 months) and for DE-SRT 48.12 months (41.86–54.40 months). **Figure 1** shows Cox regression of DFS of the overall group (see **Figure 1A**) and in the subgroup of DE-SRT for the elective PB and local recurrence *versus* C-SRT for PB alone (see **Figure 1B**).

Figure 2 shows a comparison of DFS for patient with *versus* without additive ADT in the DE-SRT group (see **Figure 2A**). Further, we compared DFS of the DE-SRT group with respect to the PET results (Local recurrence only *versus* pelvic LNs and/or local recurrence, see **Figure 2B**). Moreover, we analyzed the DFS in the DE-SRT group for patients with PSA at recurrence <0.5 ng/ml *versus* ≥0.5 ng/ml. There was no significant difference (p=0.39).

We analyzed PSA response for patients who received DE-SRT and C-SRT (see **Table 6**). Overall median PSA at first follow-up was 0.07 ng/ml (range, 0.00–1.09 ng/ml) with a PSA response (≤0.2 ng/ml) of 75.0% for DE-SRT. For C-SRT the overall median PSA at first follow-up was 0.14 ng/ml (range, 0.01–51.72 ng/ml) with a PSA response of 57.5%. Overall median PSA at last follow-up was 0.07 ng/ml (range, 0.00–1.60 ng/ml),resulting in a biochemical response of 86.4% for DE-SRT. For the C-SRT

TABLE 1 | Patient characteristics.

	All patients, n = 199 (%)	C-SRT, n = 98 (%)	DE-SRT, n = 101 (%)	*p*
Age [Years]	71.0 (range: 49.0-82.0)	69.0 (range: 52.0-82.0)	72.0 (range: 49.0-82.0)	0.07
Treatment Fields				
PB	85 (42.7%)	85 (86.7%)	N./a.	*N./a.*
PB + ePLNs	13 (6.5%)	13 (13.3%)	N./a.	
PB/SIB	55 (27.7%)	*N./a.*	55 (54.5%)	
PB/SIB + ePLNs	11 (5.5%)	*N./a.*	11 (10.9%)	
PB + ePLNs/SIB	16 (8.1%)	*N./a.*	16 (15.8%)	
PB/SIB + ePLNs/SIB	15 (7.5%)	*N./a.*	15 (14.8%)	
ePLNs/SIB	4 (2.0%)	*N./a.*	4 (4.0%)	
Postoperative Tumor Classification				
pT1c	1 (0.5%)	1 (1.0%)	0 (0.0%)	0.89
pT2	5 (2.5%)	2 (2.0%)	3 (3.0%)	
pT2a	10 (5.1%)	3 (3.1%)	7 (6.9%)	
pT2b	5 (2.5%)	3 (3.1%)	2 (2.0%)	
pT2c	78 (39.2%)	40 (40.8%)	38 (37.6%)	
pT3	2 (1.0%)	1 (1.0%)	1 (1.0%)	
pT3a	52 (26.1%)	28 (28.6%)	24 (23.7%)	
pT3b	41 (20.6%)	19 (19.4%)	22 (21.8%)	
pT4	2 (1.0%)	1 (1.0%)	1 (1.0%)	
Missing	3 (1.5%)	0 (0.0%)	3 (3.0%)	
Postoperative Nodal Status				
Negative (pN0)	165 (82.9%)	84 (85.7%)	81 (80.2%)	0.65
Positive (pN1)	26 (13.1%)	12 (12.3%)	14 (13.9%)	
Unknown (pNx)	6 (3.0%)	2 (2.0%)	4 (3.9%)	
Missing	2 (1.0%)	0 (0.0%)	2 (2.0%)	
Postoperative Surgical Margin				
Negative (R0)	142 (71.4%)	71 (72.5%)	71 (70.3%)	0.10
Positive (R1)	45 (22.6%)	26 (26.5%)	19 (18.8%)	
Unknown (Rx)	7 (3.5%)	1 (1.0%)	6 (5.9%)	
Missing	5 (2.5%)	0 (0.0%)	5 (5.0%)	
Gleason Score				
ISUP Group 1 (≤6)	12 (6.0%)	9 (9.2%)	3 (3.0%)	0.10
ISUP Group 2 (3 + 4 = 7)	80 (40.2%)	41 (41.8%)	39 (38.6%)	
ISUP Group 3 (4 + 3 = 7)	52 (26.1%)	20 (20.4%)	32 (31.7%)	
ISUP Group 4 (8)	19 (9.6%)	12 (12.3%)	7 (6.9%)	
ISUP Group 5 (9-10)	30 (15.1%)	14 (14.3%)	16 (15.8%)	
Gleason Score 7 without specification	2 (1.0%)	2 (2.0%)	0 (0.0%)	
Missing	4 (2.0%)	0 (0.0%)	4 (4.0%)	
Median time between resection and RT [Months]	37.60 (range: 3.10-293.30)	26.05 (range 3.10-166.30)	51.10 (range:4.60-293.30)	<0.001*
PSA at recurrence [ng/ml]	0.32 (range: 0.02-22.00)	0.21 (range: 0.02-5.64)	0.45 (range:0.02-22.00)	<0.01*
≤0.5 ng/ml	145 (72.9%)	90 (91.8%)	55 (54.5%)	<0.001*
0.5-2.0 ng/ml	37 (18.6%)	5 (5.1%)	32 (31.7%)	
>2.0 ng/ml	17 (8.5%)	3 (3.1%)	14 (13.8%)	
PSMA-PET Imaging				
[^{68}Ga]PSMA-11	70 (35.2%)	24 (24.5%)	46 (45.5%)	<0.001*
[^{18}F]rhPSMA-7	28 (14.1%)	6 (6.1%)	22 (21.8%)	
[^{18}F]rhPSMA-7.3	36 (18.1%)	11 (11.2%)	25 (24.8%)	
[^{18}F]PSMA-1007	10 (5.0%)	2 (2.1%)	8 (7.9%)	
No PET	55 (27.6%)	55 (56.1%)	0 (0.0%)	
Results PSMA-PET Imaging				
Local recurrence (rcT+)	58 (57.4%)	0 (0.0%)	58 (57.4%)	*N./a.*
Lymph node metastasis (rcN+)	18 (17.8%)	0 (0.0%)	18 (17.8%)	
Local recurrence and lymph node metastasis (rcT+ and rcN+)	25 (24.8%)	0 (0.0%)	25 (24.8%)	
Additive ADT				
Yes	40 (20.1%)	12 (12.2%)	28 (27.7%)	0.006*
No	159 (79.9%)	86 (87.8%)	73 (72.3%)	
Median Follow-Up [Months]	13.6 (range: 0.4-70.0)	18.9 (range: 0.4-70.0)	10.7 (range: 0.7-59.4)	0.14

*C-SRT, conventional salvage radiotherapy; DE-SRT, dose-escalated salvage radiotherapy; PB, prostate bed; SIB, simultaneous-integrated boost; ePLNs, elective pelvic lymph nodes; N./a., not applicable; ISUP, International Society of Urological Pathology; PSMA, prostate-specific membrane antigen; RT, radiotherapy; PET, positron emission tomography; Ga, Gallium; F, flour; ADT, androgen deprivation therapy; *significant result.*

TABLE 2 | Radiation doses for conventional salvage radiotherapy (C-SRT) and dose-escalated salvage radiotherapy (DE-SRT).

	C-SRT		DE-SRT	
	Median total dose [Gy]	**Single dose [Gy]**	**Median total dose [Gy]**	**Single dose [Gy]**
PB	68.00 (range: 66.00-70.00)	2.00 (range: 2.00-2.00)	68.00 (range, 68.00–70.00)	2.00 (range, 1.80–2.00)
Elective pelvic LNs	50.40 (range: 50.40-50.40)	1.80 (range: 1.80-1.80)	50.40 (range, 50.40–51.00 Gy)	1.80 (range, 1.50–1.80)
PET-positive LNs	*N./a.*	*N./a.*	58.80 (range, 58.80–61.60)	2.10 (range, 1.80–2.25)
PET-positive LR	*N./a.*	*N./a.*	76.50 (range, 73.10–76.50)	2.25 (range, 2.00–2.25)

PB, prostate bed; LN, lymph node; LR, local recurrence; N./a., not applicable.

TABLE 3 | Baseline toxicity rates of conventional salvage radiotherapy (C-SRT) and dose-escalated salvage radiotherapy (DE-SRT).

	Grade	C-SRT n = 98	DE-SRT n = 101	p
Rectal Bleeding	**0**	98 (100.0%)	101 (100%)	N./a.
Proctitis	**0**	98 (100.0%)	101 (100%)	N./a.
Stool Incontinence	**0**	97 (99.0%)	99 (98.0%)	1.00
	1	1 (1.0%)	2 (2.0%)	
Gastrointestinal Fistula	**0**	98 (100.0%)	101 (100%)	N./a.
Hematuria	**0**	98 (100.0%)	101 (100%)	N./a.
Cystitis	**0**	98 (100.0%)	101 (100%)	N./a.
Urine Incontinence	**0**	67 (68.4%)	56 (55.5%)	0.58
	1	26 (26.5%)	37 (36.6%)	
	2	5 (5.1%)	7 (6.9%)	
	3	0 (0.0%)	1 (1.0%)	
Urinary Obstruction	**0**	97 (99.0%)	101 (100.0%)	0.31
	1	1 (1.0%)	0 (0.0%)	
Genitourinary Fistula	**0**	98 (100.0%)	101 (100%)	N./a.
Erectile Dysfunction	**0**	28 (28.6%)	17 (16.8%)	0.11
	1	16 (16.3%)	15 (14.9%)	
	2	19 (19.4%)	17 (16.8%)	
	3	35 (35.7%)	52 (51.5%)	

Side effects were graded according to the Common Terminology Criteria for Adverse Events (CTCAE) version 5 (15) (N./a., not applicable).

TABLE 4 | Comparison of newly diagnosed or worsened early and late toxicity rates of conventional salvage radiotherapy (C-SRT) *versus* dose-escalated salvage radiotherapy (DE-SRT) in the overall group including all patients.

	Grade	Early Toxicity Rates			Late Toxicity Rates		
		C-SRT (n = 95)	**DE-SRT (n = 99)**	**p**	**C-SRT (n = 73)**	**DE-SRT (n = 75)**	***p***
Rectal Bleeding	**1**	1 (1.1%)	2 (2.0%)	0.51	3 (4.1%)	6 (8.0%)	0.22
	3	1 (1.1%)	0 (0.0%)		0 (0.0%)	2 (2.7%)	
Proctitis	**1**	2 (2.1%)	2 (2.0%)	0.99	2 (2.7%)	7 (9.3%)	0.25
	2	1 (1.1%)	1 (1.0%)		1 (1.4%)	1 (1.3%)	
Stool Incontinence	**1**	0 (0.0%)	2 (2.0%)	0.16	1 (1.4%)	1 (1.3%)	0.61
	2	–	–		0 (0.0%)	1 (1.3%)	
Hematuria	**1**	0 (0.0%)	1 (1.0%)	0.33	3 (4.1%)	2 (2.7%)	0.55
	2	–	–		0 (0.0%)	1 (1.3%)	
Cystitis	**1**	3 (3.2%)	4 (4.0%)	0.74	2 (2.7%)	2 (2.7%)	0.98
Genitourinary Fistula	**2**	–	–	–	0 (0.0%)	1 (1.3%)	0.32
Urine Incontinence	**1**	17 (17.9%)	13 (13.1%)	0.62	21 (28.8%)	23 (30.7%)	0.55
	2	2 (2.1%)	2 (2.0%)		6 (8.2%)	6 (8.0%)	
	3	0 (0.0%)	1 (1.0%)		0 (0.0%)	2 (2.7%)	
Urinary Obstruction	**1**	1 (1.1%)	5 (5.1%)	0.11	5 (6.8%)	3 (4.0%)	0.65
	2	–	–		1 (1.4%)	0 (0.0%)	
	3	–	–		1 (1.4%)	1 (1.3%)	
Erectile Dysfunction	**1**	3 (3.2%)	5 (5.1%)	0.53	4 (5.5%)	3 (4.0%)	0.60
	2	5 (5.3%)	2 (2.0%)		5 (6.8%)	4 (5.3%)	
	3	12 (12.6%)	10 (10.1%)		17 (23.3%)	12 (16.0%)	

Side effects were graded according to the Common Terminology Criteria for Adverse Events (CTCAE) version 5 (15). Only patients with follow-up <6 months (n = 194) were included for analysis of early toxicity. Further, only patients with follow-up >6 months (n = 148) were included for evaluation of late toxicity.

TABLE 5 | Comparison of newly diagnosed or worsened early and late toxicity rates of conventional salvage radiotherapy (C-SRT) to the prostate bed (PB) *versus* dose-escalated salvage radiotherapy (DE-SRT) to the PB and simultaneous-integrated boost (SIB) to a local recurrence.

	Grade	Early Toxicity Rates			Late Toxicity Rates		
		C-SRT PB (n = 82)	DE-SRT PB+SIB (n = 54)	p	C-SRT PB (n = 62)	DE-SRT PB+SIB (n = 40)	*p*
Rectal Bleeding	**1**	1 (1.2%)	1 (1.9%)	0.76	3 (4.8%)	5 (12.5%)	0.16
Proctitis	**1**	2 (2.4%)	1 (1.9%)	0.93	2 (3.2%)	2 (5.0%)	0.86
	2	1 (1.2%)	1 (1.9%)		1 (1.6%)	1 (2.5%)	
Stool Incontinence	**1**	0	1 (1.9%)	0.22	1 (1.6%)	0 (0.0%)	0.33
	2	–	–		0 (0.0%)	1 (2.5%)	
Hematuria	**1**	0	1 (1.9%)	0.22	3 (4.8%)	1 (2.5%)	0.39
	2	–	–		0 (0.0%)	1 (2.5%)	
Cystitis	**1**	3 (3.7%)	1 (1.9%)	0.54	1 (1.6%)	1 (2.5%)	0.75
Urine Incontinence	**1**	14 (17.1%)	7 (13.0%)	0.75	15 (24.2%)	13 (32.5%)	0.39
	2	2 (2.4%)	2 (3.7%)		6 (9.7%)	2 (5.0%)	
	3	–	–		0 (0.0%)	1 (2.5%)	
Urinary Obstruction	**1**	1 (1.2%)	2 (3.7%)	0.33	5 (8.1%)	2 (5.0%)	0.63
	2	–	–		1 (1.6%)	0 (0.0%)	
	3	–	–		1 (1.6%)	0 (0.0%)	
Erectile Dysfunction	**1**	3 (3.7%)	2 (3.7%)	0.90	4 (6.5%)	1 (2.5%)	0.57
	2	3 (3.7%)	1 (1.9%)		4 (6.5%)	1 (2.5%)	
	3	11 (13.4%)	6 (11.1%)		14 (22.6%)	8 (20.0%)	

Side effects were graded according to the Common Terminology Criteria for Adverse Events (CTCAE) version 5 (15). Only patients with follow-up <6 months (n=136) were included for analysis of early toxicity. Further, only patients with follow-up >6 months (n = 102) were included for evaluation of late toxicity.

group overall median PSA at last follow-up was 0.07 ng/ml (range, 0.00–1.40 ng/ml) with a PSA response of 69.6%.

DISCUSSION

The aim of this retrospective study was to compare DE-SRT and C-SRT in terms of toxicity rates. Further, we sought to report outcome data of DE-SRT. To our knowledge, this is the first study which attempted to compare DE-SRT and C-SRT. In all toxicity items (rectal bleeding, proctitis, stool incontinence, hematuria, cystitis, urine incontinence, urinary obstruction, and erectile dysfunction), no significant difference was present neither for early nor for late side effects. One late genitourinary fistula grade 2 was reported in the DE-SRT group. Overall, no gastrointestinal fistulas were seen. The outcome of DE-SRT

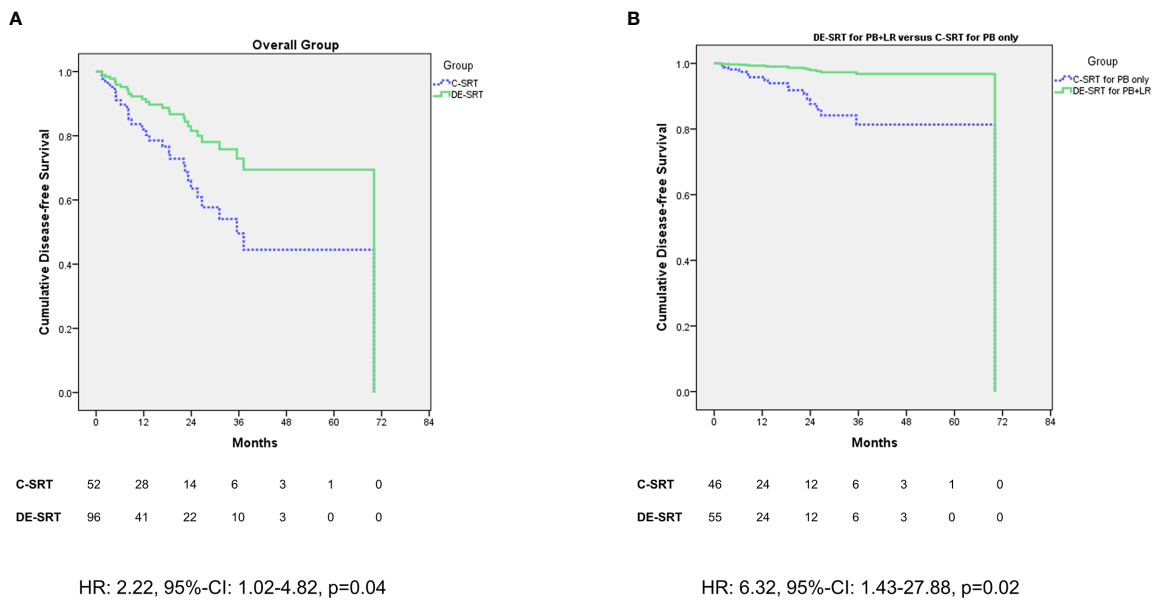

FIGURE 1 | Cox regression (adjusted for the use of additive androgen deprivation therapy) of disease-free survival (DFS) for dose-escalated salvage radiotherapy (DE-SRT) *versus* conventional salvage radiotherapy (C-SRT) in the overall group **(A)** and subgroup of patients with DE-SRT for the prostate bed (PB) and local recurrence *versus* C-SRT for the PB only **(B)** (HR, hazard ratio; 95%-CI, 95%-confidence interval).

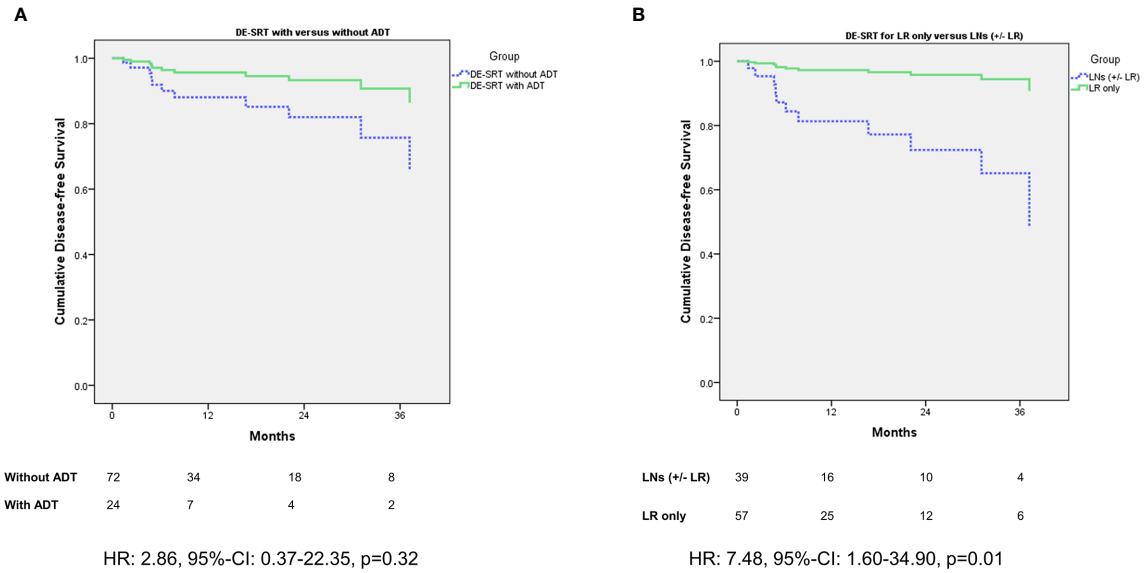

FIGURE 2 | Cox regression of disease-free survival (DFS) for dose-escalated salvage radiotherapy (DE-SRT) in the subgroups of patients with/without additive androgen deprivation therapy (ADT) **(A)** and Cox regression (adjusted for use of additive androgen deprivation therapy) with respect to the PET results **(B)** (LR, local recurrence; LN, pelvic lymph node(s); HR, hazard ratio; 95%-CI, 95%-confidence interval).

seems good with most patients showing a PSA response at first follow-up as well as last follow-up. Patients in the overall group and in the subgroup of C-SRT to the PB *versus* DE-SRT of the PB and a local recurrence showed a significant better outcome in favor of DE-SRT.

Over the last years, the PSMA-PET has become an important diagnostic tool for patients with PC, especially in a recurrence setting. We previously reported the high clinical impact on disease staging and RT management (17). Both the impact as well as the higher diagnostic efficacy compared with other imaging techniques triggered the recommendation of PSMA-PET for patients with biochemical recurrence after prior definitive treatment in the European (18) and German (7) guidelines. With the higher sensitivity of the PSMA-PET dose escalation to specific areas became possible.

The rationale behind the dose escalation derives from the PC dose-response data. The alpha/beta ratio for PC is described to be low (19). A low alpha/beta ratio implies that the target is more resistant to low doses. Therefore, higher total doses and hypofractionated schemes for PC have been increasingly used (20, 21). In the case of SRT, the elective PB and pelvic LNs are commonly treated for microscopic disease spread with doses of 66 to 72 Gy (6, 7) and 45 to 50.4 Gy (22–24), respectively. However, keeping the low alpha/beta ratio in mind: Why should

TABLE 6 | Outcome of dose-escalated (DE-SRT) and conventional (C-SRT) salvage radiotherapy.

	DE-SRT		C-SRT	
PSA Response at 1. FU				
	Overall group		**Overall group**	
Median PSA at 1. FU [ng/ml]	0.07 (0.00–1.09)		0.14 (0.01–51.72)	
PSA at 1. FU ≤0.2 ng/ml	75.0%		57.5%	
	without additive ADT	**with additive ADT**	**without additive ADT**	**with additive ADT**
Median PSA at 1. FU [ng/ml]	0.09 (0.00–1.09)	0.02 (0.00–0.96)	0.16 (0.01–51.72)	0.07 (0.05–0.07)
PSA at 1. FU ≤0.2 ng/ml	69.2%	91.3%	52.8%	100.0%
PSA Response at last FU				
	Overall group		**Overall group**	
Median PSA at last FU [ng/ml]	0.07 (0.00–1.60)		0.07 (0.00–1.40)	
PSA at last FU ≤0.2 ng/ml	86.4%		69.6%	
	without additive ADT	**with additive ADT**	**without additive ADT**	**with additive ADT**
Median PSA at last FU [ng/ml]	0.07 (0.00–1.60)	0.01 (0.00–0.70)	0.10 (0.00–1.40)	0.06 (0.00–0.25)
PSA at last FU ≤0.2 ng/ml	83.1%	95.7%	67.5%	83.3%

Outcome (defined by prostate-specific antigen (PSA) at first and last follow-up (FU) ≤0.2 ng/ml) of the overall group and patients with/without additive androgen deprivation therapy (ADT). Patients with admission of ADT in FU after termination of additive ADT were excluded from this endpoint.

we not treat macroscopic PC in the salvage situation with the same doses as PC in the definitive situation? The European and German guideline recommend an EQD2 of 74 to approximately 80 Gy for definitive treatment of the prostate (6, 7). In our study, we used a median dose of 76.5 Gy in fractions of 2.25 Gy for a local recurrence which translates into an EQD2 (1.5 Gy) of 81.96 Gy and therefore is an appropriate dose for macroscopic PC. The guideline of the Australian and New Zealand Faculty of Radiation Oncology Genito-Urinary group (FROGG) recommends a dose escalation for local recurrence with an EQD2 of 70 to 74 Gy. Dose escalation of pelvic LNs is also recommend; however, the dose remains to be unspecified (25). For DE-SRT of LNs we used a median dose of 58.8 Gy in fractions of 2.10 Gy which translates into an EQD2(1.5Gy) of 62.16 Gy. A meta-analysis by King et al. showed that SRT doses of > 70 Gy are associated with improved relapse-free survival (26). However, most of the data originate from the pre-PSMA-PET era, and therefore, dose escalation for macroscopic tumor was barley possible.

Our data showed no increased toxicity for DE-SRT in comparison to C-SRT in the overall group as well as in the subgroup of patients with SIB to a local recurrence *versus* PB alone. Few retrospective series evaluated toxicity of PSMA-PET-based DE-SRT with a SIB to the macroscopic tumor. Schmidt-Hegemann et al. evaluated the outcome after [68Ga]PSMA-11-PET-based DE-SRT with a SIB or sequential boost with median doses of 70 Gy to the local recurrence, 60 Gy to the PB, 60.8 Gy to PET-positive LNs, and 50.4 Gy to the ePLNs (27). The authors showed acute genitourinary and gastrointestinal toxicity grade 2 in 13% and 16% of the cases, respectively. Late genitourinary and gastrointestinal toxicity grade 2 was documented in 13% and 3% (27).

Zschaeck et al. reported data of 22 patients with [68Ga] PSMA-11-PET-based DE-SRT with 66.6 Gy (1.8 Gy/fraction, EQD2(1.5Gy) = 62.79 Gy) to the PB and a SIB to local recurrences of 74 Gy (2 Gy/fraction, EQD2(1.5Gy)) = 74 Gy) to 77.7 Gy (2.1 Gy/fraction, EQD2(1.5Gy) = 79.2 Gy) (28). The ePLNs were irradiated with 54.0 Gy with a SIB of 66.0 Gy to positive LNs (28). Only 1 patient developed an acute grad 2 cystitis and diarrhea, respectively (28).

Previous series on [18F]Choline-PET-based DE-SRT showed acceptable toxicity rates as well. Wahart et al. evaluated four patients with local recurrence (29). They prescribed 62.7 Gy (1.9 Gy/fraction, EQD2(1.5Gy) = 60.91 Gy) to the PB with a SIB of 69.3 Gy (2.1 Gy/fraction, EQD2(1.5Gy) = 67.32 Gy) to the local recurrence. The authors documented no gastrointestinal toxicity ≥grade 2 and one grade 2 genitourinary toxicity (29). Fodor et al. evaluated 83 patients with LN relapse only on [11C]Choline-PET. The authors treated most of the patients with 51.8 Gy (1.85 Gy/fraction, EQD2(1.5Gy) = 49.58 Gy) to the ePLNs and a SIB with a median dose of 65.5 Gy to the LNs (30). They showed a 3-year rate of ≥ grade 2 rectal and ≥ grade 2 genitourinary toxicity of 6.6% and 26.3%, respectively (30).

The recent SAKK 09/10 evaluated the impact of dose intensified SRT for the whole PB with 64 Gy *versus* 70 Gy on toxicity and outcome. The trial showed similar acute side effects, except for a significantly greater worsening in patient-reported urinary symptoms after 70 Gy (31). However, no SIB was used in the SAKK 09/10 trial. A previous study by Cozzarini et al. evaluated the urinary toxicity for hypofractionated RT to the whole PB after RP (32). Patients with hypofractionated RT showed significantly more late urinary toxicities Grad 3/4 (18.1%) than patients with conventional fractionation (6.9%). These data predate PSMA-PET imaging and therefore a focal treatment to PET-positive areas might accomplish a survival benefit with acceptable toxicity.

PSA response and DFS showed good results for patients with PSMA-PET guided DE-SRT in our cohort of patients. This might be related to the potential of PSMA-PET localizing the site of recurrence, whereas in patients without pre-RT imaging, empiric dose planning was performed. Nevertheless, in 43.9% of the patients in the C-SRT group pre-RT PSMA-PET imaging was negative potentially including a bias. However, even with the high rate of negative PSMA-PETs in the C-SRT group the DFS is reduced which speaks in favor of dose escalation. Additionally, the patients in the DE-SRT group might benefit from a dose escalation for SRT > 70 Gy as described above and was postulated by King et al. (26).

When we stratified for additive ADT in patients with DE-SRT, patients with simultaneous hormonal deprivation showed no significant better DFS (p=0.32). However, the hazard ratio of 2.86 suggests a trend in favor of an additive ADT. This is in line with the data by Shipley et al. (33) and Carrie et al. (34) which suggest additive ADT for patients with SRT. Nevertheless, both trials did not use PSMA-PET imaging for staging before RT, but the underlying principle remains the same: ADT treats the microscopic tumor spread. However, PSMA-PET might help to identify the patients who will benefit from ADT. This should be further investigated.

When comparing sites of relapse (local recurrence only *versus* pelvic LNs and/or local recurrence), the data showed that patients with LNs exhibit a decreased DFS in comparison to patients with local relapse only. Affection of the LNs might indicate wider spread than within patients with confined disease to the PB. Such oligorecurrent patients might benefit from additional ADT (35) and therefore this topic should be further investigated.

Overall, since our data are retrospective and not powered to show superiority the results on outcome must be interpreted cautiously. The small sample size likely leads to large hazard ratios and 95% confidence intervals for the Cox regression analysis. However, the results may be understood as a hint for a better outcome for patients with PSMA-PET guided DE-SRT.

Previous studies have also shown favorable outcome for patients with PSMA-PET guided DE-SRT. Schmidt-Hegemann et al. reported that 78% of the patients reached a PSA ≤ 0.2 ng/ml after PSMA-PET guided DE-SRT (27). This is comparable to our data showing PSA response of ≤ 0.2 ng/ml of 86.4% at last follow-up. Zschaeck et al. showed a median PSA of 0.15 ng/ml at last follow-up, after a median follow-up of 29 months (28). The median PSA at last follow-up in our cohort was 0.07 ng/ml. Emmett et al. evaluated 140 patients with [68Ga]PSMA-11-PET

informed SRT (36). The authors reported the outcome of patients with negative as well as positive PSMA-PET. For patients with local recurrence treatment response was 81% and for patients with LN involvement +/− local recurrence the treatment response was 38.5%. The treatment response was defined as PSA ≤ 0.1 ng/ml and a greater than 50% reduction from pre-RT PSA level. Our data confirm the reduced outcome for patients with LN involvement. Recently, Emmett et al. (37) published data of a prospective trial on [68Ga]PSMA-11-PET-based SRT in 260 patients. External beam RT as well as stereotactic body radiotherapy were allowed. Freedom from progression was defined as PSA not more than 0.2 ng/ml above the post-RT nadir. The overall 3-year freedom from progression was 64.5%, with 79% in patient with local recurrence, and 55% in patients with pelvic LNs (37). Patients with negative PSMA-PET showed the highest rates of freedom from progression with 82.5%. Recently, the EMPIRE-1 trial (38) evaluated [18F]Fluciclovine-PET for salvage RT. Patients received RT directed by conventional imaging (bone scan and CT/MRI) or by PET. The authors reported a significantly improved freedom from biochemical recurrence or persistence. Pernthaler et al. compared [18F]Fluciclovine *versus* [68Ga]PSMA-11 and showed that the overall detection rate for PC recurrence is similar with an advantage for Fluciclovine-PET in terms of local recurrence (39).

Our study has certain limitations. The median follow-up is relatively short, and a future analysis with longer follow-up is planned. Although the groups are well balanced for most factors (see **Table 1**), the retrospective cohort design of our study is a limitation. To supplement the retrospective data, only a prospective randomized controlled trial comparing patients with and without dose escalation would be helpful and therefore should be performed in the future. However, it will remain difficult to justify not performing dose-escalation in PET positive lesions. There was a significant difference in the use of PET imaging in both groups (see **Table 1**). Patients with PET are more likely to be diagnosed with the cause of PSA rise. Therefore, patients with PET are more likely to be in the DE-SRT group. There was an imbalance for coverage of the ePLNs (PB only in 86.7% in C-SRT *versus* 53.9% in DE-SRT group). However, we accounted for that by evaluating the data for the respective subgroups. In our study patients underwent PET with both [68Ga]PSMA-11 and [18F]-labeled PSMA-ligands. This might include a bias; however, this study focused on PSMA-PET-based DE-SRT and current literature indicates relative similar detection efficacy for these different PSMA-ligands (40, 41). Further, there was a significant difference concerning the admission of additive ADT in both groups (see **Table 1**). Additive ADT to SRT is based on two recent publications (33, 34). Patients in the C-SRT group received their treatment earlier than the patients in the DE-SRT group and therefore less patients with additive ADT are in C-SRT group. This might be a bias for the outcome analysis; however, we accounted for this fact by evaluating the outcome for patients with additive ADT as well as without ADT and used adjusted Cox regression analysis. Moreover, patients in the C-SRT group had a significantly shorter time from RP to RT as well as a lower PSA before SRT (see **Table 1**). To account for that, we only included patients with PSA >0.2 ng/ml at relapse for the outcome analysis.

Currently, data of a phase III trial on [68Ga]PSMA-11-PET/CT-based SRT after RP are on the way (NCT03582774). The trial compares standard SRT to PSMA-PET-based SRT. A focal dose escalation to the PSMA-positive lesions may be performed on the discretion of the treating radiation oncologist if feasible (42).

CONCLUSION

PSMA-PET-based DE-SRT with SIB is feasible and showed no significantly increased toxicity rates compared with C-SRT. Further, DE-SRT showed good results in terms of PSA response and DFS. Therefore, PSMA-PET-based DE-SRT can be considered as part of the personalized cancer management of patients with PSMA-PET positive local pelvic relapse.

DATA AVAILABILITY STATEMENT

The raw data supporting the conclusions of this article will be made available by the authors, without undue reservation.

ETHICS STATEMENT

The studies involving human participants were reviewed and approved by the institutional review board of the Technical University of Munich (TUM). Written informed consent for participation was not required for this study in accordance with the national legislation and the institutional requirements.

AUTHOR CONTRIBUTIONS

All authors contributed to the study conception and design. Material preparation, data collection, and analysis were performed by MV. The first draft of the manuscript was written by MV and all authors commented on previous versions of the manuscript. All authors contributed to the article and approved the submitted version.

SUPPLEMENTARY MATERIAL

The Supplementary Material for this article can be found online at: https://www.frontiersin.org/articles/10.3389/fonc.2021.715020/full#supplementary-material

REFERENCES

1. Fichtner J. The Management of Prostate Cancer in Patients With a Rising Prostate-Specific Antigen Level. *BJU Int* (2000) 86(2):181–90. doi: 10.1046/j.1464-410x.2000.00701.x
2. Kneebone A, Fraser-Browne C, Duchesne GM, Fisher R, Frydenberg M, Herschtal A, et al. Adjuvant Radiotherapy *Versus* Early Salvage Radiotherapy Following Radical Prostatectomy (TROG 08.03/ANZUP RAVES): A Randomised, Controlled, Phase 3, Non-Inferiority Trial. *Lancet Oncol* (2020) 21(10):1331–40. doi: 10.1016/s1470-2045(20)30456-3
3. Parker CC, Clarke NW, Cook AD, Kynaston HG, Petersen PM, Catton C, et al. Timing of Radiotherapy After Radical Prostatectomy (RADICALS-RT): A Randomised, Controlled Phase 3 Trial. *Lancet (London England)* (2020) 396(10260):1413–21. doi: 10.1016/s0140-6736(20)31553-1
4. Sargos P, Chabaud S, Latorzeff I, Magné N, Benyoucef A, Supiot S, et al. Adjuvant Radiotherapy *Versus* Early Salvage Radiotherapy Plus Short-Term Androgen Deprivation Therapy in Men With Localised Prostate Cancer After Radical Prostatectomy (GETUG-AFU 17): A Randomised, Phase 3 Trial. *Lancet Oncol* (2020) 21(10):1341–52. doi: 10.1016/s1470-2045(20)30454-x
5. Perera M, Papa N, Christidis D, Wetherell D, Hofman MS, Murphy DG, et al. Sensitivity, Specificity, and Predictors of Positive (68)Ga-Prostate-Specific Membrane Antigen Positron Emission Tomography in Advanced Prostate Cancer: A Systematic Review and Meta-Analysis. *Eur Urol* (2016) 70(6):926–37. doi: 10.1016/j.eururo.2016.06.021
6. Mottet N, van den Bergh RCN, Briers E, Cornford P, De Santis M, Fanti S, et al. *Eau - ESTRO - ESUR - SIOG Guidelines on Prostate Cancer 2020. European Association of Urology Guidelines. 2020 Ed.* Arnhem, The Netherlands: European Association of Urology Guidelines Office (2020).
7. Leitlinienprogramm Onkologie (Deutsche Krebsgesellschaft DK, AWMF). *Interdisziplinäre Leitlinie Der Qualität S3 Zur Früherkennung, Diagnose Und Therapie Der Verschiedenen Stadien Des Prostatakarzinoms, Langversion 5.1, AWMF Registernummer: 043/022ol* (2019). Available at: http://www.leitlinienprogramm-onkologie.de/leitlinien/prostatakarzinom/ (Accessed 2020-04-05).
8. Eder M, Schafer M, Bauder-Wust U, Hull WE, Wangler C, Mier W, et al. 68Ga-Complex Lipophilicity and the Targeting Property of a Urea-Based PSMA Inhibitor for PET Imaging. *Bioconjugate Chem* (2012) 23(4):688–97. doi: 10.1021/bc200279b
9. Cardinale J, Martin R, Remde Y, Schäfer M, Hienzsch A, Hübner S, et al. Procedures for the GMP-Compliant Production and Quality Control of [(18)F]PSMA-1007: A Next Generation Radiofluorinated Tracer for the Detection of Prostate Cancer. *Pharmaceuticals (Basel Switzerland)* (2017) 10(4):77. doi: 10.3390/ph10040077
10. Wurzer A, Di Carlo D, Schmidt A, Beck R, Eiber M, Schwaiger M, et al. Radiohybrid Ligands: A Novel Tracer Concept Exemplified by (18)F- or (68)Ga-Labeled rhPSMA Inhibitors. *J Nucl Med* (2020) 61(5):735–42. doi: 10.2967/jnumed.119.234922
11. Wurzer A, Di Carlo D, Herz M, Richter A, Robu S, Schirrmacher R, et al. Automated Synthesis of [(18)F]Ga-rhPSMA-7/-7.3: Results, Quality Control and Experience From More Than 200 Routine Productions. *EJNMMI Radiopharm Chem* (2021) 6(1):4. doi: 10.1186/s41181-021-00120-5
12. Fendler WP, Eiber M, Beheshti M, Bomanji J, Ceci F, Cho S, et al. (68)Ga-Psma PET/CT: Joint EANM and SNMMI Procedure Guideline for Prostate Cancer Imaging: Version 1.0. *Eur J Nucl Med Mol Imaging* (2017) 44(6):1014–24. doi: 10.1007/s00259-017-3670-z
13. Michalski JM, Lawton C, El Naqa I, Ritter M, O'Meara E, Seider MJ, et al. Development of RTOG Consensus Guidelines for the Definition of the Clinical Target Volume for Postoperative Conformal Radiation Therapy for Prostate Cancer. *Int J Radiat Oncol Biol Phys* (2010) 76(2):361–8. doi: 10.1016/j.ijrobp.2009.02.006
14. Poortmans P, Bossi A, Vandeputte K, Bosset M, Miralbell R, Maingon P, et al. Guidelines for Target Volume Definition in Post-Operative Radiotherapy for Prostate Cancer, on Behalf of the EORTC Radiation Oncology Group. *Radiother Oncol* (2007) 84(2):121–7. doi: 10.1016/j.radonc.2007.07.017
15. National Cancer Institute. *Common Terminology Criteria for Adverse Events Version 5.0* (2017). Available at: https://ctep.cancer.gov/protocoldevelopment/electronic_applications/docs/CTCAE_v5_Quick_Reference_8.5x11.pdf.
16. Cornford P, Bellmunt J, Bolla M, Briers E, De Santis M, Gross T, et al. Eau-Estro-Siog Guidelines on Prostate Cancer. Part II: Treatment of Relapsing, Metastatic, and Castration-Resistant Prostate Cancer. *Eur Urol* (2017) 71(4):630–42. doi: 10.1016/j.eururo.2016.08.002
17. Habl G, Sauter K, Schiller K, Dewes S, Maurer T, Eiber M, et al. (68) Ga-PSMA-PET for Radiation Treatment Planning in Prostate Cancer Recurrences After Surgery: Individualized Medicine or New Standard in Salvage Treatment. *Prostate* (2017) 77(8):920–7. doi: 10.1002/pros.23347
18. Mottet N, Bellmunt J, Bolla M, Briers E, Cumberbatch MG, De Santis M, et al. Eau-Estro-Siog Guidelines on Prostate Cancer. Part 1: Screening, Diagnosis, and Local Treatment With Curative Intent. *Eur Urol* (2017) 71(4):618–29. doi: 10.1016/j.eururo.2016.08.003
19. Vogelius IR, Bentzen SM. Meta-Analysis of the Alpha/Beta Ratio for Prostate Cancer in the Presence of an Overall Time Factor: Bad News, Good News, or No News? *Int J Radiat Oncol Biol Phys* (2013) 85(1):89–94. doi: 10.1016/j.ijrobp.2012.03.004
20. Dearnaley D, Syndikus I, Mossop H, Khoo V, Birtle A, Bloomfield D, et al. Conventional *Versus* Hypofractionated High-Dose Intensity-Modulated Radiotherapy for Prostate Cancer: 5-Year Outcomes of the Randomised, Non-Inferiority, Phase 3 CHHiP Trial. *Lancet Oncol* (2016) 17(8):1047–60. doi: 10.1016/s1470-2045(16)30102-4
21. Catton CN, Lukka H, Gu CS, Martin JM, Supiot S, Chung PWM, et al. Randomized Trial of a Hypofractionated Radiation Regimen for the Treatment of Localized Prostate Cancer. *J Clin Oncol* (2017) 35(17):1884–90. doi: 10.1200/jco.2016.71.7397
22. Warde P, Mason M, Ding K, Kirkbride P, Brundage M, Cowan R, et al. Combined Androgen Deprivation Therapy and Radiation Therapy for Locally Advanced Prostate Cancer: A Randomised, Phase 3 Trial. *Lancet (London England)* (2011) 378(9809):2104–11. doi: 10.1016/s0140-6736(11)61095-7
23. Lawton CA, DeSilvio M, Roach M3rd, Uhl V, Kirsch R, Seider M, et al. An Update of the Phase III Trial Comparing Whole Pelvic to Prostate Only Radiotherapy and Neoadjuvant to Adjuvant Total Androgen Suppression: Updated Analysis of RTOG 94-13, With Emphasis on Unexpected Hormone/Radiation Interactions. *Int J Radiat Oncol Biol Phys* (2007) 69(3):646–55. doi: 10.1016/j.ijrobp.2007.04.003
24. Roach M3rd, DeSilvio M, Lawton C, Uhl V, Machtay M, Seider MJ, et al. Phase III Trial Comparing Whole-Pelvic *Versus* Prostate-Only Radiotherapy and Neoadjuvant *Versus* Adjuvant Combined Androgen Suppression: Radiation Therapy Oncology Group 9413. *J Clin Oncol* (2003) 21(10):1904–11. doi: 10.1200/jco.2003.05.004
25. Lieng H, Hayden AJ, Christie DRH, Davis BJ, Eade TN, Emmett L, et al. Radiotherapy for Recurrent Prostate Cancer: 2018 Recommendations of the Australian and New Zealand Radiation Oncology Genito-Urinary Group. *Radiother Oncol* (2018) 129(2):377–86. doi: 10.1016/j.radonc.2018.06.027
26. King CR. The Dose-Response of Salvage Radiotherapy Following Radical Prostatectomy: A Systematic Review and Meta-Analysis. *Radiother Oncol* (2016) 121(2):199–203. doi: 10.1016/j.radonc.2016.10.026
27. Schmidt-Hegemann N-S, Stief C, Kim T-H, Eze C, Kirste S, Strouthos I, et al. Outcome After PSMA PET/CT Based Salvage Radiotherapy in Patients With Biochemical Recurrence After Radical Prostatectomy: A Bi-Institutional Retrospective Analysis. *J Nucl Med* (2018) 60(2):227–33. doi: 10.2967/jnumed.118.212563
28. Zschaeck S, Wust P, Beck M, Wlodarczyk W, Kaul D, Rogasch J, et al. Intermediate-Term Outcome After PSMA-PET Guided High-Dose Radiotherapy of Recurrent High-Risk Prostate Cancer Patients. *Radiat Oncol* (2017) 12(1):140. doi: 10.1186/s13014-017-0877-x
29. Wahart A, Guy JB, Vallard A, Geissler B, Ben Mrad M, Falk AT, et al. Intensity-Modulated Salvage Radiotherapy With Simultaneous Integrated Boost for Local Recurrence of Prostate Carcinoma: A Pilot Study on the Place of PET-choline for Guiding Target Volume Delineation. *Br J radiol* (2016) 89(1058):20150579. doi: 10.1259/bjr.20150579
30. Fodor A, Berardi G, Fiorino C, Picchio M, Busnardo E, Kirienko M, et al. Toxicity and Efficacy of Salvage Carbon 11-Choline Positron Emission Tomography/Computed Tomography-Guided Radiation Therapy in Patients With Lymph Node Recurrence of Prostate Cancer. *BJU Int* (2017) 119(3):406–13. doi: 10.1111/bju.13510
31. Ghadjar P, Hayoz S, Bernhard J, Zwahlen DR, Hölscher T, Gut P, et al. Acute Toxicity and Quality of Life After Dose-Intensified Salvage Radiation Therapy

for Biochemically Recurrent Prostate Cancer After Prostatectomy: First Results of the Randomized Trial SAKK 09/10. *J Clin Oncol* (2015) 33 (35):4158–66. doi: 10.1200/jco.2015.63.3529
32. Cozzarini C, Fiorino C, Deantoni C, Briganti A, Fodor A, La Macchia M, et al. Higher-Than-Expected Severe (Grade 3-4) Late Urinary Toxicity After Postprostatectomy Hypofractionated Radiotherapy: A Single-Institution Analysis of 1176 Patients. *Eur Urol* (2014) 66(6):1024–30. doi: 10.1016/j.eururo.2014.06.012
33. Shipley WU, Seiferheld W, Lukka HR, Major PP, Heney NM, Grignon DJ, et al. Radiation With or Without Antiandrogen Therapy in Recurrent Prostate Cancer. *N Engl J Med* (2017) 376(5):417–28. doi: 10.1056/NEJMoa1607529
34. Carrie C, Hasbini A, de Laroche G, Richaud P, Guerif S, Latorzeff I, et al. Salvage Radiotherapy With or Without Short-Term Hormone Therapy for Rising Prostate-Specific Antigen Concentration After Radical Prostatectomy (GETUG-AFU 16): A Randomised, Multicentre, Open-Label Phase 3 Trial. *Lancet Oncol* (2016) 17(6):747–56. doi: 10.1016/s1470-2045(16)00111-x
35. Kroeze SGC, Henkenberens C, Schmidt-Hegemann NS, Vogel MME, Kirste S, Becker J, et al. Prostate-Specific Membrane Antigen Positron Emission Tomography-Detected Oligorecurrent Prostate Cancer Treated With Metastases-Directed Radiotherapy: Role of Addition and Duration of Androgen Deprivation. *Eur Urol Focus* (2019) 7(2):309–16. doi: 10.1016/j.euf.2019.08.012
36. Emmett L, van Leeuwen PJ, Nandurkar R, Scheltema MJ, Cusick T, Hruby G, et al. Treatment Outcomes From (68)Ga-PSMA PET/CT-Informed Salvage Radiation Treatment in Men With Rising Psa After Radical Prostatectomy: Prognostic Value of a Negative Psma Pet. *J Nucl Med* (2017) 58(12):1972–6. doi: 10.2967/jnumed.117.196683
37. Emmett L, Tang R, Nandurkar R, Hruby G, Roach P, Watts JA, et al. 3-Year Freedom From Progression After (68)Ga-Psma PET/CT-Triaged Management in Men With Biochemical Recurrence After Radical Prostatectomy: Results of a Prospective Multicenter Trial. *J Nucl Med* (2020) 61(6):866–72. doi: 10.2967/jnumed.119.235028
38. Jani AB, Schreibmann E, Goyal S, Halkar R, Hershatter B, Rossi PJ, et al. 18f-fluciclovine-PET/CT Imaging *Versus* Conventional Imaging Alone to Guide Postprostatectomy Salvage Radiotherapy for Prostate Cancer (EMPIRE-1): A Single Centre, Open-Label, Phase 2/3 Randomised Controlled Trial. *Lancet* (2021) 397(10288):1895–904. doi: 10.1016/S0140-6736(21)00581-X
39. Pernthaler B, Kulnik R, Gstettner C, Salamon S, Aigner RM, Kvaternik H. A Prospective Head-to-Head Comparison of 18F-Fluciclovine With 68Ga-PSMA-11 in Biochemical Recurrence of Prostate Cancer in PET/CT. *Clin Nucl Med* (2019) 44(10):e566–e73. doi: 10.1097/rlu.0000000000002703
40. Rauscher I, Krönke M, König M, Gafita A, Maurer T, Horn T, et al. Matched-Pair Comparison of (68)Ga-PSMA-11 PET/CT and (18)F-PSMA-1007 PET/CT: Frequency of Pitfalls and Detection Efficacy in Biochemical Recurrence After Radical Prostatectomy. *J Nucl Med* (2020) 61(1):51–7. doi: 10.2967/jnumed.119.229187
41. Kroenke M, Mirzoyan L, Horn T, Peeken JC, Wurzer A, Wester HJ, et al. Matched-Pair Comparison of (68)Ga-PSMA-11 and (18)F-Rhpsma-7 PET/CT in Patients With Primary and Biochemical Recurrence of Prostate Cancer: Frequency of non-Tumor Related Uptake and Tumor Positivity. *J Nucl Med* (2020) 41(7). doi: 10.2967/jnumed.120.251447
42. Calais J, Czernin J, Fendler WP, Elashoff D, Nickols NG. Randomized Prospective Phase III Trial of 68Ga-PSMA-11 PET/CT Molecular Imaging for Prostate Cancer Salvage Radiotherapy Planning [PSMA-SRT]. *BMC Cancer* (2019) 19(1):18. doi: 10.1186/s12885-018-5200-1

Conflict of Interest: ME reports an advisory role for Blue Earth Diagnostics, Point Biopharma, Telix and Janssen and patent application for rhPSMA.

The remaining authors declare that the research was conducted in the absence of any commercial or financial relationships that could be construed as a potential conflict of interest.

Publisher's Note: All claims expressed in this article are solely those of the authors and do not necessarily represent those of their affiliated organizations, or those of the publisher, the editors and the reviewers. Any product that may be evaluated in this article, or claim that may be made by its manufacturer, is not guaranteed or endorsed by the publisher.

frontiers in Oncology

ORIGINAL RESEARCH
published: 02 August 2021
doi: 10.3389/fonc.2021.722430

Establishing a Provincial Registry for Recurrent Prostate Cancer: Providing Access to PSMA PET/CT in Ontario, Canada

Sympascho Young[1], *Ur Metser*[2], *Golmehr Sistani*[3], *Deanna L. Langer*[4] *and Glenn Bauman*[1]*

[1] London Regional Cancer Program, Department of Oncology, Western University and London Health Sciences Centre, London, ON, Canada, [2] Joint Department of Medical Imaging, Princess Margaret Hospital, University Health Network, Mount Sinai Hospital, Women's College Hospital and University of Toronto, Toronto, ON, Canada, [3] Department of Medical Imaging, London Health Sciences Center and Western University, London, ON, Canada, [4] Clinical Institutes and Quality Programs, Ontario Health (Cancer Care Ontario), Toronto, ON, Canada

OPEN ACCESS

Edited by:
Xuefeng Qiu,
Nanjing Drum Tower Hospital, China

Reviewed by:
Salvatore Annunziata,
Catholic University of the Sacred Heart, Italy
Gad Abikhzer,
Jewish General Hospital, Canada

***Correspondence:**
Glenn Bauman
glenn.bauman@lhsc.on.ca

Specialty section:
This article was submitted to Cancer Imaging and Image-directed Interventions, a section of the journal Frontiers in Oncology

Received: 08 June 2021
Accepted: 19 July 2021
Published: 02 August 2021

Citation:
Young S, Metser U, Sistani G, Langer DL and Bauman G (2021) Establishing a Provincial Registry for Recurrent Prostate Cancer: Providing Access to PSMA PET/CT in Ontario, Canada. Front. Oncol. 11:722430. doi: 10.3389/fonc.2021.722430

Prostate Specific Membrane Antigen (PSMA) positron emission tomography/computed tomography (PET/CT) is becoming established as a standard of care for the (re)staging of high-risk primary and prostate cancer recurrence after primary therapy. Despite the favorable performance of this imaging modality with high accuracy in disease detection, the availability of PSMA PET/CT varies across jurisdictions worldwide due to variability in the selection of PSMA PET/CT agent, regulatory approvals and funding. In Canada, PSMA based radiopharmaceuticals are still considered investigational new drug (IND), creating limitations in the deployment of these promising imaging agents. While regulatory approval rests with Health Canada, as a single payer health system, funding for Health Canada approved drugs and devices is decided by Provincial Health Ministries. Ontario Health (Cancer Care Ontario) (OH-CCO) is the agency of the Ministry of Health (MOH) in Ontario responsible for making recommendations to the MOH around the organization and funding of cancer services within Ontario (population of 15 million), and the PET Steering Committee of OH-CCO is responsible for providing recommendations on the introduction of new PET radiopharmaceuticals and indications. For Health Canada approved PET radiopharmaceuticals like 18F-FDG, OH-CCO (on behalf of the MOH) provides coverage based on levels of evidence and specific PET Registries are established to aid in real-world evidence collection to inform OH-CCO regarding emerging PET applications. In the case of PSMA PET/CT, adapting this model to an IND PSMA PET/CT agent, 18F-DCFPyL, necessitated the creation of a hybrid Registry-Study model to leverage the existing OH-CCO Registry structure while respecting the need for a Health Canada Clinical Trials Application (CTA) for the deployment of this agent in the province. Within the first 2 years of the registry, over 1700 men have been imaged resulting in a change in management (compared to pre-PET management plans) in over half of the men imaged. In this article, we describe the organization and deployment of the PSMA PET/CT (PREP) Registry throughout the province to provide access for men with

suspected prostate cancer recurrence along with key stakeholder perspectives and preliminary results.

Keywords: PSMA - prostate specific membrane antigen, registry, prostate cancer, biochemical failure (BF), positron emission tomography (PET), Ontario (Canada), health policy, healthcare funding

INTRODUCTION

Ontario has a publicly funded health care system with a proven track record in clinical trials, health services research and evidence-based medicine (1). Two decades ago, when FDG PET was rapidly adopted as a new clinical tool in various jurisdictions worldwide, Ontario adopted a more cautious approach (2). To address limitations in the literature that PET scanning impacted patient management decisions and outcomes, several high-quality randomized clinical trials were launched. As evidence matured, funding for PET as an insured service was provided for the specific clinical indications where PET was clinically beneficial and had advantages over other testing. An initial government advisory board became the Ontario Steering Committee for PET Evaluation ("PET Steering Committee"), which was initially assigned the task of reviewing of the literature and generating some of the needed evidence by undertaking a series of trials. For indications where the existing evidence for the use of PET was limited but compelling (e.g., retrospective studies suggestive of impact to care), PET Cancer Registries were established (2). The registries facilitated real-world evaluation and evidence-building in the Ontario context for specific clinical indications, enabling access to PET scanning for patients while collecting a minimum dataset (such as pre- and post-PET stage, pre- and post-scan intended treatment) that could then be linked to provincial administrative databases to determine a change in management decisions, actual treatment delivered, and patient outcomes after the provision of PET (3). While praised as an evidence-based approach to ensure funded interventions demonstrate clear benefits to patients, this model has also been criticized by others as perhaps too rigorous (unreasonable to expect diagnostic tests to show impact on clinical outcomes where downstream management strategies might diverge quickly confounding the influence of imaging on outcomes) and that the time it takes to acquire high-level evidence may limit patient access to new PET technologies (2).

The present provincial PET Steering Committee, currently an Ontario Health (Cancer Care Ontario) (OH-CCO) committee, has a mandate to provide recommendations on the clinical indications for use, quality criteria, and distribution and access to PET scan services. The Committee continues to assess potential PET indications through multiple mechanisms, including: 1) proactive systematic literature reviews supported by the Program in Evidence-Based Care (cancercareontario.ca/en/guidelines-advice), which involve reviews of all clinical practice guidelines as well as primary literature of high-quality PET trials; 2) ongoing evidence-building through PET Registries; 3) provincial-level support for clinical trials, including a limited number of randomized controlled trials (NCT02751710, NCT02462239) if PET Registry-type data would not suffice to address questions of utility or outcome. When identified, new potential PET indications are discussed together with disease-site experts from the relevant OH-CCO Ontario Cancer Advisory Committees to determine whether the available evidence is sufficient to make a recommendation for funding of the new indication as an insured service or whether further data is needed through a clinical trial or PET cancer registry.

In 2016, ^{18}F-DCFPyL, an ^{18}F-labeled second generation PSMA tracer, became available for use in Ontario through clinical trials (4). Multiple investigator-led trials evaluating the use of PSMA PET in prostate cancer were launched, predominantly for restaging men at the time of biochemical failure (NCT02856100, NCT02793284). Awareness of the availability of PSMA PET in these trials and the increasing reports of lesion-directed therapy, radiotherapy, and surgery, for patients with oligometastatic disease, also led to increased demand for access to PSMA PET outside of these trials. This, along with emerging reports in the literature on the diagnostic accuracy and clinical impact of PSMA PET (5–8), incentivized the development of a prospective Provincial PSMA PET Registry Study in collaboration with the provincial Genitourinary Advisory Committee at OH-CCO. This Registry Study would utilize existing provincial infrastructure to support access to PSMA PET for recurrent prostate cancer, compliant within the Health Canada regulatory framework, in several scenarios of suspected persistent or limited recurrent disease after primary therapy at various decision points in the disease trajectory. In addition to patient access, the design supports consistent, large scale real-world data collection to inform where PSMA PET is the most impactful in detecting sites of disease recurrence and guiding management; this data, in turn, can be leveraged to refine which indications are recommended for routine funding.

METHODS

Establishing the Registry Study

In order to establish the Registry Study, a common provincial clinical trial protocol was developed (**Supplementary Material**s) with co-primary investigators from Nuclear Medicine, Radiation Oncology and Uro-Oncology. The protocol provided for investigation of PSMA PET/CT across a variety of clinical scenarios in the setting of prostate cancer recurrence after primary therapy, after PET/CT directed therapy, or through an access cohort for PET/CT-assisted decision making in scenarios not covered by the other cohorts. Minimum sample sizes for each cohort were determined based on performance for lesion detection by PSMA PET/CT as reported in the literature. Among the provincial cancer centers that had expressed the interest and

capacity to participate in the Registry Study, a lead center and overall project coordinator at that center were identified to initiate the regulatory approval process for the Province. From the clinical protocol, the lead center obtained a Health Canada CTA for the use of the PET/CT tracer and the protocol was submitted by the lead center to the Ontario Cancer Research Ethics Board (OCREB), a centralized Ethics Review board that is recognized as "Board of Record" by all the participating sites. Following OCREB approval for the lead center, other individual sites applied through OCREB for approval as a participating center with a site Principle Investigator.

Each participating center assigned a multidisciplinary group of collaborators and a local lead investigator, recruited study coordinators for screening, consenting and scheduling patients and for maintaining all regulatory and other study documents in collaboration with the study sponsor. The new registry utilized experience from prior registries as well as the expertise built through investigator-led PSMA PET trials, existing PET/CT infrastructure in the province, and centralized radiopharmaceutical production. ^{18}F-labeled PSMA radiopharmaceuticals were chosen instead of ^{68}Ga due to its advantages in the setting of a large multicenter registry (in a province more than 1.5 times the size of the state of Texas). First, ^{18}F-labeled radiopharmaceuticals are produced at a cyclotron facility, rather than with a ^{68}Ge/^{68}Ga generator. This enables central radiopharmaceutical production and participation of multiple PET centers without needing to procure multiple generators and/or rely on local radiopharmaceutical production. Second, the larger volume of radiopharmaceutical produced in a cyclotron along with the longer half-life of ^{18}F compared to ^{68}Ga (110 minutes vs 68 minutes, respectively) facilitates distribution to distant centers across the province. Patients are booked for PSMA PET after securing a dose on a provincial roster for upcoming radiopharmaceutical production days. The number of production days is adjusted according to demand. For those centers located within Southern Ontario, distribution of radiopharmaceutical by land transportation was feasible with central production occurring in the morning, followed by transportation of the radiopharmaceutical and imaging at the regional PET centers occurring in early to late afternoon. One site (Ottawa) was primarily served *via* air transport, but had land transportation as a back-up option if required. One site in Northern Ontario (Thunder Bay site) was supplied exclusively by air transportation.

In order to gauge the effectiveness of PSMA PET/CT compared to conventional imaging, the initial phase of the Registry Study required all men to be staged with conventional imaging (bone scan and CT) prior to PSMA PET/CT. Men were eligible for PSMA PET/CT if the conventional imaging demonstrated either no lesions, equivocal lesions or less than four metastases (oligometastatic disease). Reads were conducted by local readers with no centralized read, however informal support for challenging cases was provided through peer-to-peer consultation. Post-PSMA PET/CT results were provided back to the referring physicians and completion of a change in management questionnaire based on the PSMA PET/CT results was required. Information sent back centrally to OH-CCO included standardized reporting of the PSMA PET/CT and post management questionnaires. Existing provincial payment mechanisms for PET/CT were utilized to reimburse participating centers for the costs of conducting the PSMA PET/CT (tracer and technical costs and physician reads). Recognizing the additional workload associated with the Registry Study required in order to be compliant with Health Canada regulatory requirements, participating centers received support for related activities (e.g. patient eligibility and consent, documentation, data submission). Phase II of the Registry Study was launched in September 2020 and removed the requirement for pre-PET/CT conventional imaging for men with PSA <10 ng/ml at the time of imaging given the low yield of conventional imaging at lower PSA levels (9).

Key Stakeholder Interviews

Given the unique "hybrid" nature of the registry study, we conducted targeted structured interviews with key stakeholders (investigators, administrative personnel, study personnel, patients) to identify benefits and strengths of this hybrid approach as well as identify gaps and weaknesses after completion of the first phase of the Registry Study. Interviews were conducted through videoconferencing using a semi-structured interview guide. Interviews were recorded and reviewed for coding and qualitative analysis.

RESULTS

Accrual and Preliminary Study Results

After receiving regulatory approvals from OCREB and Health Canada, the PSMA-PET for Recurrent Prostate Cancer (PREP) registry was launched in September 2018 and included 5 participating PET centers across the province (**Figure 1**). Men were eligible for enrollment based on predefined clinical scenarios/cohorts (**Table 1**). Recruitment to the registry study was swift with over 1700 patients scanned in the first 21 months (Phase I of the registry) (**Figure 2**). The majority of referrals were from urology and radiation oncology, with a minority of referrals from medical oncology. In October 2020, Phase II of the Registry was launched; the major refinement being removing the requirement for restaging CT and Bone Scan for men with PSA < 10 at the time of enrollment. There was one adverse event reported during Phase I of the Registry, this was deemed unrelated to the radiotracer itself. A small percentage of cases (<5%) planned scans needed to be rescheduled because of a failure of production run of tracer from the centralized distribution site. Among successful production runs, there was one instance of a missed sterility test which resulted in the need to reschedule the planned scans as the product was not administered.

Overall, nearly two-thirds of PSMA PET scans were positive, including > 60% of studies performed in patients with negative CT and bone scintigraphy. As reported in prior studies, the detection rate of PSMA PET increased with level of serum PSA at time of inclusion. Nearly a third of patients had evidence of locoregional failure on PET. A quarter of patients had

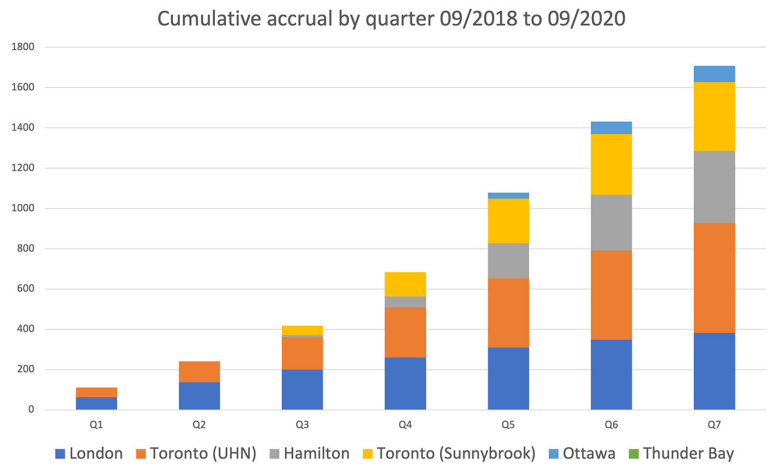

FIGURE 1 | Location of participating PREP Centers.

TABLE 1 | PREP Registry Cohorts.

Cohort	Description
1	Men with node positive disease or detectable PSA within 3 months of prostatectomy
2	Men with biochemical failure (PSA >0.1ng/ml) post prostatectomy
3	Men with biochemical failure (PSA >0.1ng/ml) post prostatectomy following adjuvant or salvage pelvic radiotherapy
4	Men with biochemical failure post prostatectomy and salvage hormone therapy (with or without salvage/adjuvant radiotherapy)
5	Evaluation of response among men with PSMA PET/CT directed treatment
6	Men with biochemical failure (PSA >2.0ng/ml/Phoenix criteria) post radiotherapy
7	Access cohort for PSMA PET/CT assisted decision making in men not meeting criteria for Cohorts 1-6

oligometastatic disease, defined as up to 4 sites of disease, and nearly 10% had extensive metastases detected on PET. The high detection rate of additional disease by PSMA PET in men with suspected low volume metastatic disease resulted in frequent changes in management.

Stakeholder Feedback

Seventeen key stakeholders (5 referring physicians from urology and radiation oncology, 4 nuclear medicine physicians, 6 research coordinators and 2 patients) were interviewed. Participant responses were grouped into themes, which are described below.

Successes of the Study

Physicians, study coordinators and patients were overwhelmingly positive about the value of PSMA PET/CT scans. Physicians expressed that the access to PSMA PET/CT scans has been "game changing" and given valuable information, clarity and more assurance in managing recurrent prostate cancer. One urologist (referring physician #4) revealed that it has changed prostate cancer management at their center to such a degree that "We now basically have PSMA PET rounds instead of tumor boards. We're discussing the significant of PSMA studies for every patient case." When inquired about PSMA's impact on prostate cancer management, he described that "It feels like we have to start over and figure out how to manage prostate cancer again. I thought I knew how to manage prostate cancer until PSMA PET came along." From the perspective of nuclear physicians, several noted that the Registry Study also provided an excellent opportunity to develop and enhance their skills in interpreting PSMA PET/CT. Nuclear physicians were able to easily integrate PSMA PET into existing PET/CT workflows. Patients accessing the registry were similarly positive, felt well-supported by staff and describe the intake process as efficient. For one patient, "the test took only two hours, and was easier or comparable to CT, nuclear, and MRI tests experiences that I've received recently. Further, having more confidence in the fidelity of the results, it is allowing me to explore my continuing treatment strategies and paths forward with better information on the state of my disease." (Patient #2) Another patient commented that PSMA PET "highlighted some cancerous cells were lurking [in my lungs] and allowed my doctor the ability to plan a course of treatment very quickly." (Patient #3).

Overall, referring physicians and study coordinators acknowledge that enrolling patients in the Registry study involved some paperwork, though attitudes towards the paperwork were mixed. Most referring physicians felt that it was relatively straight-forward to enroll patients, "not onerous" and that they received plenty of support from the lead study site when they encountered issues. One urologist commented "it's nothing, it takes a couple of seconds." On the other hand, there were physicians who resented the additional paperwork involved and felt the Registry Study was "cumbersome for the value of the science" and a limiting factor for patient access. After enrolling patients, physicians agreed unanimously that imaging results were easily viewable in the existing electronic medical records (EMR) at their centers.

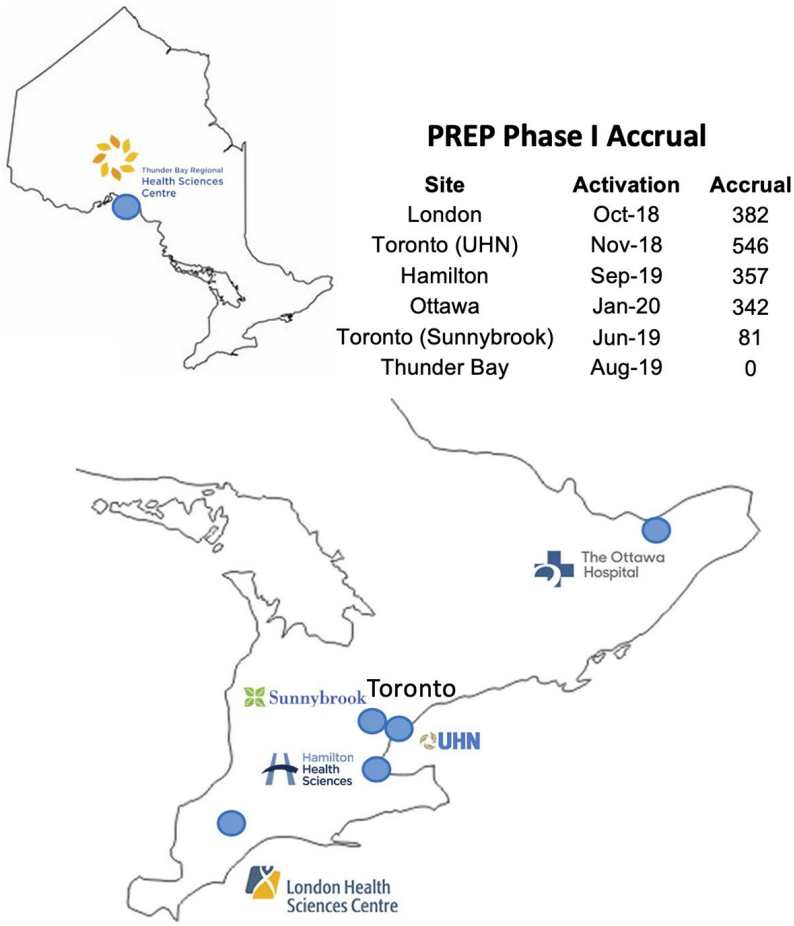

FIGURE 2 | Accrual by quarter across PREP Centers.

Drawbacks of a Study Approach

Though stakeholders were generally positive about the study, with most physicians recognizing that the registry study served in part to improve provincial access to PSMA PET, there was still the feeling that Ontario lagged behind certain parts of the world in respect to PSMA PET. One of the criticisms was a sense that there is already enough international evidence supporting the use of PSMA PET in these patient populations, and thus limited benefit in gathering additional registry-style data at the cost of introducing barriers for both physicians and patients. Other respondents, however, welcomed the registry study as generating needed information: "The most important thing that will come from this study is defining the population of men that PSMA PET/CT scans are most beneficial for, and the PSA thresholds when the scan is beneficial." One urologist felt the study approach was a way for Ontario to "limit [expenses and] access to PSMA PET by creating hurdles" for clinicians to order the test, perhaps not realizing that without the Registry study framework in place to address Health Canada regulatory requirements, the provision of PSMA PET as a clinical service would not be possible.

One of the barriers of the study approach was that due to the ethical policies around clinical study consenting, physicians at most centers could not obtain consent from their own patients. As a result, study coordinators were required to obtain consent from patients. Paperwork requiring details of prior treatments, radiation, and post-imaging forms were sometimes described as "cumbersome" and "tedious" by busy clinicians. On the other hand, study coordinators mentioned that often spent considerable time tracking down physicians for post management forms and to "make sure all of our referral forms are filled in correctly." The requirement for a bone and CT scan within 3 months of the PSMA PET were also seen unanimously as a barrier by referring physicians and study coordinators, which led to additional costs of "unnecessary scans" and delays in the ability to enroll patients on trial, as wait-times for conventional imaging could add weeks or months to accessing PSMA PET/CT. Phase II of PREP was able to mitigate this concern, as the bone scan and CT criteria was removed.

Access to Regional Cancer Centers

Another drawback of the study approach is that only physicians who were co-investigators of the study could enroll patients onto

the registry. At participating centers, most physicians in either radiation oncology or urology were involved as co-investigators of the study and could directly enroll patients. However, physicians in non-participating centers could not directly enroll their patients and were required to refer patients to co-investigators of the study in order for their patients to be enrolled. As a result, one or two physicians at each center are referred the majority of these patients and facilitate scans for them. This supports broader patient access, but was identified to be inefficient for patients, their referring physicians, and the designated co-investigators at each center.

Production and Distribution of Radiopharmaceuticals

Central production of radiopharmaceuticals was identified to have both advantages and disadvantages. While central production offered the advantages of greater production efficiency, cost-effectiveness and easier licensing, it also made the supply chain more vulnerable to transportation and production issues. For instance, since the entire province was supplied by a single cyclotron, when radiopharmaceutical production issues inevitably occurred, all participating centers were affected and scans across the province had to be cancelled. These uncommon but last-minute cancellations of scans led to additional patient frustration and anxiety.

In addition, distribution from a central source made the supply chain vulnerable to transportation challenges. For the Thunder Bay site, distribution through commercial air travel created additional several months-long delays in setting up the study, as additional waivers had to be obtained from the Ministry of Transportation to enable delivery. Unfortunately, this delay led to "a lot of upset and anxious patients because they had signed the consent forms and were waiting and waiting to get the scan to direct their cancer treatment … and for several months, [physicians] could not offer patients the scan and we had to refer patients to Toronto." (Radiation oncologist, referring physician #5).

With any new supply chain, estimating and developing an appropriate production capacity is challenging. When the study was first activated, there was high patient enrollment but inadequate radiopharmaceutical production and distribution capacity. A study coordinator commented that even in the first month of the study, "we were already starting to get a backlog of patients" due to lack of radiopharmaceutical supply. Over time, additional production days were added at the cyclotron to accommodate clinical need. Study coordinators are now satisfied with the supply: "wait times are caught up" and "the access radiopharmaceuticals is no longer limiting the amount of scans per month."

Patients Wait Times

Wait times for scans were dependent on both radiopharmaceutical availability as well as PET scanner availability. As previously noted, availability of ^{18}F-DCPyL was more of a limiting factor early on in PREP, and impacted by both the number of production days supported and the occurrence of production issues leading to cancelled bookings. As a Registry Study, PSMA PET scans were also provided during regular clinical hours (i.e., there were not additional dedicated hours), and these scans needed to be incorporated as part of clinical demand. As such, wait times for PSMA PET were also subject to the regular operating pressures experienced by the participating PET centers, and prioritized accordingly. Notably, at two of the centers (London and Hamilton), PET scanners were down for a number of weeks, creating a backlog of patient scans. Wait times for PSMA PET scans have been 6-8 weeks on average for patients in the London, Hamilton, Toronto and Ottawa centers. For reference, these are longer than wait times for FDG PET scans in Ontario, given the difference in clinical urgency compared to most routine PET scans as well as dictated in part by having limited PSMA scan days each week.

Impact of the COVID-19 Pandemic

At most centers, the enrollment of patients onto the Registry Study was not significantly impacted by the restrictions to clinical trial activities during the pandemic as the Registry was regarded as "clinically essential" research. However, the pandemic's impact was felt disproportionately at the Thunder Bay site, as it affected the availability and predictability of commercial air travel, leading to frequent cancellations and inability to reliably transport radiopharmaceuticals by air. Radiopharmaceutical availability was described as a "gong show" and both anxiety-provoking for patients who had to be constantly rescheduled and frustrating for research coordinators and physicians. Unfortunately, Thunder Bay was forced to cancel scans altogether on January 29th, 2021 and stop further accrual of patients due to the state of air travel. Patients already enrolled had to either travel to Toronto or out of the country for scans, or simply decided to go ahead with treatment based on results of conventional imaging. A physician at Thunder Bay observed that "central production and distribution are not a sustainable setup if the trial will go on for several years. It puts us at the mercy of available transportation, which is an ever-changing situation with COVID." (Radiation oncologist, referring physician #5). Though unfortunate, this experience is similar to others in Europe and Asia, where the pandemic also heavily impacted nuclear medicine departments and delayed radiopharmaceutical supply (10).

Finance and Funding Process

The hybrid Registry-Study model proved challenging in terms of the flow of funding. Consistent with the Ontario Ministry of Health (MOH) directive that guides transfer of funding for organizations such as OH-CCO, funding was provided to participating sites for specific deliverables (e.g., fulfilling Health Canada regulatory and ethics board requirements, volume funding for the PSMA PET scans, data submission), rather than for identified roles or units of time, etc. And, as these PSMA PET scans were provided as part of the overall provincial PET program, funding was managed *via* the existing agreements supporting clinical PET scanning services. Agreements are also issued for each fiscal year, with execution occurring within-year; funding is then initiated at the time of execution, to be retroactive to the beginning of fiscal. Several stakeholders, including

physicians and study coordinators, commented that this approach – which differs from that of traditional clinical trials – led to operational challenges. All participating sites had dedicated research units with well-defined processes, including approaches for budgeting and contract format expectations (e.g., total-budget over multiple years, versus annual agreements) for costs associated with the conduct of individual cancer clinical trials. Funding was also managed at the level of the institution versus research unit, and did not include delineated budgets for research study coordinators or other resources. Internal institutional processes were also needed to manage transfers between departments which, from the perspective of the research units, made it "difficult to follow where the money [for research] went." This led to difficulties in getting approvals to hire and pay for coordinators, and, at one site an experienced investigator who was interested in leading the study at their site was unable to do so due to because of issues related to funding and processes. In one of the years of the Registry study there was a significant delay in issuing the agreement and subsequent delay in the release of funds and transfer to the research unit. At one site this caused significant challenges in managing staffing from within the designated budget at the institution; a nuclear physician commented that "The funding for our research coordinator was still missing after a year; if not for alternate sources of funding, our research coordinator would not have been paid." The unique needs of a Registry study utilizing an IND agent added consenting and regulatory requirements that fell outside the usual functions of the PET centers and added to the complexity of budgeting and funding of PREP activities.

Limitations of ^{18}F-DCFPyL Radiopharmaceutical

Generally, performance of ^{18}F-DCFPyL within PREP was on par with results reported for ^{18}F-DCFPyL by other institutions and other PSMA PET agents like ^{68}Ga-PSMA. Both radiation oncologists and nuclear physicians observed that the pharmacokinetics of the specific PSMA agent, ^{18}F-DCFPyL, had limitations for use in the PREP indications as the primary route of GU excretion could interfere with detecting local recurrences (prostate bed and prostate). Adopting PSMA agents with hepatic excretion was felt to be potentially helpful for the future, particularly for those patients with earlier recurrence.

Nuclear Medicine Physician Training for Interpreting PSMA PET/CT Scans

For nuclear medicine (NM) physicians, the Registry also provided an opportunity to enhance their skills in interpreting PSMA PET/CT. In general, each center had at least one NM physician who had prior exposure to PSMA PET/CT interpretation, either through past practice at a center with PSMA PET/CT, through participation in prior PSMA PET/CT clinical trials, or in the review of PSMA PET/CT for patients from their center referred out of province for imaging. These individuals helped organize local initiatives such as peer to peer mentoring through grand rounds, case discussion forums or encouraging the adoption of online training to ensure other members gained proficiency in scan interpretation. PSMA lectures at conferences (regional and national) helped all teams to become more familiar with PSMA PET imaging and investigators taking part in the Registry were involved in helping organize these conferences.

Unexpected Impacts

An unexpected clinical impact of PSMA PET scans was noted among men with biochemical failure post-radical prostatectomy and negative or equivocal scans. These patients were often reluctant to undergo salvage treatment (standard of care), and have opted instead to be followed with surveillance. One urologist explained "you cannot get patients to do salvage radiotherapy, because they'll say "What are you going to radiate? There's nothing on the PET scan!" And then you'll have to teach them about sensitivity/specificity which may be difficult to accomplish in a clinic visit. It is easier to see these patients in close follow-up rather than send them for salvage RT." The urologist also predicted that with more patients undergoing PSMA PET scans at low PSAs, "I'll bet salvage radiotherapy rates are going to go down significantly." Given that failure free survival from salvage RT are highest among those patients with absent or prostate fossa restricted PSMA PET/CT uptake (11), this strategy may not be the most appropriate. Further research and education of both clinicians and patients regarding this clinical scenario are important.

An unexpected system level impact of the study is that it created a useful pipeline and network between treating physicians, nuclear medicine physicians and PET centers that did not previously exist in Ontario. This has created an infrastructure for the development of future projects, such as the CPD-002 (NCT04644822) and PATRON trials (NCT04557501).

DISCUSSION

This paper has outlined the process and initial outcomes of launching a Registry study within the province of Ontario, Canada. The PREP registry was launched as a pragmatic response in order to (1): Enable access to advanced prostate cancer imaging with PMSA PET/CT on a provincial scale (multi-center across Ontario) (2) build evidence to inform the most appropriate and impactful indications for PSMA PET and (3) support the nuclear medicine community in gaining experience with this radiopharmaceutical (12). Based our stakeholder feedback conducted, though there were challenges, the Registry successfully addressed all three aims.

With regards to access, PSMA PET is currently not standard of care in Canada, and aside from access through the PREP registry, there are no prostate cancer-specific PET radiopharmaceuticals approved for routine clinical use by Health Canada. This is similar to much of the world currently, in that access to PSMA PET is still limited and only available through clinical studies. As the evidence continues to build, policies are quickly changing. For example, in the United States, the first PSMA PET radiotracer 18F-DCPyL was approved by the FDA for commercial use on May 27, 2021 based on findings

from prospective phase 2/3 trials OSPREY and CONDOR (13, 14).

Australia, one of the world leaders in PET, took a different approach to regulating radiopharmaceuticals. When PET/CT imaging was initially registered with the Australian Therapeutic Goods Administration (TGA), it came with the approval to use any PET radiopharmaceuticals (15). As a result, new radiopharmaceuticals do not go through the same regulatory mechanisms as other pharmaceuticals (15). This regulatory landscape allowed early roll out and adoption of PSMA PET technology by Australian physicians, as early as 2014. By 2015, PSMA PET became the primary mode of primary and secondary staging of prostate cancer (>90% of all patients) at an Australian center, despite a lack of clinical evidence supporting its use at the time (16). This approach has both pros and cons, and balancing the tradeoffs between the benefits of early adoption and threshold of evidence required is something that every public-health system must decide for itself. However, in this case Australia's regulatory policies have clearly allowed the advantage of early adoption and widespread access of a valuable diagnostic modality. In a cost-effectiveness analysis of the proPSMA study, PSMA PET was modeled to be more cost effective than CT and bone scans in the Australian setting (17). Similarly, in Germany, a permissive regulatory environment has fostered an environment favoring innovation in PSMA based theranostics, however, there is variable access to these agents both by indication and by jurisdiction (18). Whether the same economics hold true in Canada remains to be seen and the PATRON (NCT04557501) trial plans to conduct a cost-effectiveness analysis in the Canadian setting as well as tracking clinical impact of PET informed treatment.

Beyond regulatory approval, in order for patients to access PSMA PET in a single-payer public healthcare system such as Canada's, there needs to be a funding mechanism to support clinical use in the appropriate indications. In Canada, such funding is organized at the provincial level, and for PET in Ontario, OH-CCO reviews and recommends funding through an evidence-based process in order to maximize health care investment in areas where there is strong evidence supporting clinical impact and patient and/or system benefit; the Ministry of Health, in turn, must prioritize investments across the health-care system. In considering radiopharmaceuticals such as PSMA PET-based agents, generating evidence to satisfy both regulatory and funding decisions can be challenging. Regulatory decisions for a new diagnostic agent/test are based primarily on considerations of safety and test accuracy. In the case of prostate cancer, patterns of disease recurrence tend to be in locations that are less accessible to biopsy (i.e., pelvic or para-aortic lymph nodes, bone) and, as a consequence, reliance on clinical surrogates such as correlative imaging or response to therapeutic interventions may be necessary (19). In order for PSMA PET to be approved for funding, more stringent levels of evidence may be necessary, such as clinical trials that demonstrate an impact on patient outcomes, consider cost efficacy and/or benefits over other testing. Such endpoints are challenging to demonstrate in prostate cancer, where a long natural history and multiple therapeutic interventions can obscure the long-term impact of early diagnostic decision points on endpoints like metastases free or overall survival. Nevertheless, randomized trials examining clinical endpoints like biochemical disease-free survival after PET directed salvage therapy post prostatectomy are underway (Quebec phase II trial NCT03525288 and pan-Canadian PATRON trial NCT04557501, Swedish trial NCT04794777, Netherland's trial PERYTON NCT04794777, and UCLA's PSMA SRT NCT03582774) and may provide the evidence base to inform funding decisions.

In an effort to gather real world evidence using a cost-effective strategy, the PREP Registry Study utilized existing PET Registry processes managed by OH-CCO as part of the provincial PET program. Many of the identified challenges and barriers stemmed from the hybrid Registry Study model of PREP, which was necessitated by the absence of Health Canada approval for PSMA agents and requirement of a Health Canada CTA. Previous (and ongoing) OH-CCO Registries building evidence for emerging clinical evidence for indications of FDG PET did not encounter the same challenges, primarily because FDG is approved by Health Canada. However, the clinical data collection for FDG PET Registries that is required to strengthen and build evidence in the Ontario setting of care - aligned with the goal of data collection in PREP - can also be perceived as a burden for busy clinicians and PET administrative teams. Although overall positively received as an approach to bring PSMA PET scans to patients, the hybrid model also created inherent challenges identified through our stakeholder interviews in activating and conducting the Registry. While funding was provided to support sites in meeting the trial requirements for the PSMA PET scans to occur, clinical trial functions such as trial activation and regulatory approvals like REB submissions and patient enrollment and consenting were often managed outside of clinical operations, through separate clinical trial research units (CRUs). Achieving the goals of the Registry study, including meeting regulatory and clinical requirements aligned with funding deliverables, thus required significant collaboration between research and clinical departments. The funding approach employed by OH-CCO provides for flexibility in how sites accomplish the goals, but internal agreement on roles and reimbursement for the CRUs for their contributions to the PREP registry tasks needed to be organized on a per-center level. In many cases this created delays in trial activation in some centers due to negotiations between the PET centers and the CRUs. Additionally, Health Canada regulations required referral of patients to centers participating in the PET Registry Study, even for regions with local access to PET/CT. This requirement created additional hurdles for access for men outside of the PREP Centers and additional workload for the PREP Centers themselves as men referred for PSMA PET/CT would need to be consented by physicians at the PREP Centre for the Registry study. While telemedicine was utilized in many centers to address this hurdle, this inefficiency will persist as long as Health Canada approved PSMA PET radiopharmaceuticals are not available.

The use of 18F-DCFPyL allowed for a model of large-scale centralized production and distribution (20), which was successful for the most part with meeting demand. Though it led to ease of production and cost savings, this model was not without challenges. In particular, the Thunder Bay site in Northern Ontario faced logistical challenges due to the impact of the COVID-19 pandemic on commercial air travel and transport of the radiopharmaceutical agents. An advantage of local production of radiopharmaceuticals, whether by a local cyclotron or generator, is that it could lead to more stable and reliable delivery by removing the uncertainties of transport logistics and potentially serving as a backup redundant source in the event of production issues at other facilities. A center in Italy faced with the challenge of not having an on-site cyclotron demonstrated that it was feasible to synthesize 18F-PSMA-1007 from 18F- imported from different external suppliers (21). However in the case of Ontario, the absence of local cyclotrons was not the reason for a centralized production model. This model was also a requirement due to existing licensing and regulatory approvals. Licensing for 18F-DCFPyL was held by the CPDC (Centre for Probe Development and Commercialization), which had Health Canada approvals for production at the Toronto CanProbe facility (Canadian Molecular Probe Consortium, a joint venture between the University Health Network (UHN) and the CPDC). Given the complexities and costs of licensing requirements and clinical use approvals, there continues to be regulatory barriers in the way of local production despite the availability of a cyclotron in Thunder Bay. Whether centralized or decentralized production best fits the geography and needs of a jurisdiction is an important question to be considered when deciding between 68Ga and 18F-based radiopharmaceuticals.

Challenges aside, stakeholder feedback was overall positive regarding the impact of PSMA PET/CT on the care of men enrolled on the Registry. The rates of detection and management change in the Registry were consistent with the experiences in other jurisdictions (5, 6, 22) and stakeholder feedback affirmed the clinical value of PSMA PET/CT studies. Additionally, the Registry consent provides for data linkage to other provincial administrative databases, providing opportunities to explore other downstream care impacts of PSMA PET/CT such as patterns of salvage radiotherapy utilization for biochemical failure post radical prostatectomy, as well as developing predictive models to improve the pre-test probability of an informative PSMA PET/CT to encourage appropriate utilization. Finally, the Registry study is providing a valuable opportunity for nuclear medicine physicians throughout the Province to gain experience with this new PET imaging modality. Existing peer to peer networks are being leveraged among nuclear medicine physicians for knowledge dissemination and shortening of learning curves.

Future Directions

As the PREP registry study further accrues patients, we hope to understand and build evidence on the most appropriate and impactful indications for PSMA PET. Currently, there is strong global evidence supporting the use of PSMA PET in the biochemical recurrent setting (23). The evidence for PSMA PET in other indications is not as clear (12). Through PREP, we seek to continue to assess the use of PSMA PET in other indications, for example, in primary staging of medium or high-risk prostate cancer or in primary detection of tumor in complex cases where there exists clinical suspicion for prostate cancer despite a negative conventional workup, including multiparametric prostate MRI and systematic biopsies. PREP includes an adjudicated "decision making" access cohort as it is acknowledged that patients outside of the PREP defined cohorts (**Table 1**) may also benefit from PSMA PET informed decision making.

Though the PREP registry has provided many men in Ontario with the access to PSMA PET scans, the ultimate goal is to build adequately robust evidence for Health Canada approval and provincial funding for the appropriate indications. Likely, the first indication to gain Health Canada approval will be men with biochemically recurrent prostate cancer – once that happens, OH-CCO can transition this aspect of the registry into a funded clinical service. However, support for additional indications will require prospective data demonstrating improved clinical outcomes from PET-directed therapy. Such randomized trials are beginning to read out (24); for example, ongoing trials in Ontario are evaluating metastasis directed and PET-guided treatments in recurrent and high risk prostate cancer. Of note, the Canadian PATRON (NCT04557501) trial is assessing whether PSMA PET-guided intensification of therapy would improve clinical outcomes compared to the current standard of care, in both the biochemical recurrence and primary staging settings. As the clinical evidence base supporting the use of PSMA PET/CT develops, building distributed provincial radiopharmaceutical production and PET/CT scanning capacity to meet new indications will be necessary to meet future need and ensure equitable access province wide.

CONCLUSION

In summary, the PREP registry study was launched in Ontario in 2018 as a pragmatic response to enable access to PSMA PET/CT imaging on a provincial scale, to build evidence and inform appropriate indications for PSMA PET, and to support the nuclear medicine community in gaining experience with the novel 18F-DCFPyL PSMA radiopharmaceutical. Through key stakeholder interviews, we elicited the successes, barriers and logistics of developing a provincial registry, including the challenges of radiopharmaceutical production and distribution, funding models and the impact of the pandemic. We share these results for other provinces and countries seeking to improve access to novel PET imaging for their patients. Overall, we demonstrate that the PREP registry has been a successful endeavor in providing access and real-world experience of a promising advanced prostate cancer imaging modality in Canada. Many of the lessons learned from this registry may be

applicable to the introduction of novel radiopharmaceuticals in other jurisdictions.

DATA AVAILABILITY STATEMENT

The data that support the findings of this study are available from the corresponding author (GB) upon reasonable request.

ETHICS STATEMENT

Health Canada CTA approval obtained for clinical use of the PSMA PET/CT radiotracer. Clinical protocol approved by the Ontario Cancer Research Ethics Board (OCREB ID 1398).

AUTHOR CONTRIBUTIONS

GB and UM conceived and designed the Registry Study. SY and GS designed interview guides, conducted key stakeholder interviews and engaged in qualitative data analysis. The manuscript was drafted by SY, GB, and UM and edited by all authors. All authors contributed to the article and approved the submitted version.

FUNDING

The PREP Registry is funded by Cancer Care Ontario, an agency of the Ontario Ministry of Health.

ACKNOWLEDGMENTS

We would like to acknowledge all the PREP Registry co-investigators, study coordinators, nuclear medicine physicians and PET technicians who have contributed their hard work and expertise to the Registry Study and their perspectives in key stakeholder interviews, including but not limited to: Dr. Marlon Hagerty, Dr. Lawrence Klotz, Dr. Joseph Chin, Dr. Nicholas Power, Dr. Luke Lavallée, Dr. Katherine Zukotynski, Dr. Patrick Veit-Haibach, Catherine Hildebrand, Stephanie Horst, Linda Chan, Lori-Ann Moon, Camilla Tajzler, David Yachnin, and Douglas Hussey.

SUPPLEMENTARY MATERIAL

The Supplementary Material for this article can be found online at: https://www.frontiersin.org/articles/10.3389/fonc.2021.722430/full#supplementary-material

REFERENCES

1. MacNeil M, Koch M, Kuspinar A, Juzwishin D, Lehoux P, Stolee P. Enabling Health Technology Innovation in Canada: Barriers and Facilitators in Policy and Regulatory Processes. *Health Policy (New York)* (2019) 123(2):203–14. doi: 10.1016/j.healthpol.2018.09.018
2. Evans WK, Laupacis A, Gulenchyn KY, Levin L, Levine M. Evidence-Based Approach to the Introduction of Positron Emission Tomography in Ontario, Canada. *J Clin Oncol* (2009) 27(33):5607–13. doi: 10.1200/JCO.2009.22.1614
3. Metser U, Prica A, Hodgson DC, Mozuraitis M, Eberg M, Mak V, et al. Effect of PET/CT on the Management and Outcomes of Participants With Hodgkin and Aggressive non-Hodgkin Lymphoma: A Multicenter Registry. *Radiol [Internet]* (2019) 290(2):488–95. doi: 10.1148/radiol.2018181519
4. Chen Y, Pullambhatla M, Foss CA, Byun Y, Nimmagadda S, Senthamizhchelvan S, et al. 2-(3-{1-Carboxy-5-[(6-[18F]fluoro-pyridine-3-carbonyl)-amino]-pentyl}-ureido)-pentanedioic Acid, [18F]DcfpyL, a PSMA-based PET Imaging Agent for Prostate Cancer. *Clin Cancer Res [Internet]* (2011) 17(24):7645–53. doi: 10.1158/1078-0432.CCR-11-1357
5. Treglia G, Annunziata S, Pizzuto DA, Giovanella L, Prior JO, Ceriani L. Detection Rate of 18 F-Labeled Psma PET / CT in Review and a Meta-Analysis. *Cancers (Basel)* (2019) 11(5):1–14. doi: 10.3390/cancers11050710
6. Han S, Woo S, Kim YJ, Suh CH. Impact of 68Ga-PSMA PET on the Management of Patients With Prostate Cancer: A Systematic Review and Meta-Analysis. *Eur Urol [Internet]* (2018) 74(2):179–90. doi: 10.1016/j.eururo.2018.03.030
7. Calais J, Fendler WP, Eiber M, Gartmann J, Chu FI, Nickols NG, et al. Impact of 68 Ga-PSMA-11 PET/CT on the Management of Prostate Cancer Patients With Biochemical Recurrence. *J Nucl Med* (2018) 59(3):434–41. doi: 10.2967/jnumed.117.202945
8. Fendler WP, Calais J, Eiber M, Flavell RR, Mishoe A, Feng FY, et al. Assessment of 68Ga-PSMA-11 PET Accuracy in Localizing Recurrent Prostate Cancer: A Prospective Single-Arm Clinical Trial. *JAMA Oncol* (2019) 5(6):856–63. doi: 10.1001/jamaoncol.2019.0096
9. Hövels AM, Heesakkers RAM, Adang EM, Jager GJ, Strum S, Hoogeveen YL, et al. The Diagnostic Accuracy of CT and MRI in the Staging of Pelvic Lymph Nodes in Patients With Prostate Cancer: A Meta-Analysis. *Clin Radiol [Internet]* (2008) 63(4):387–95. doi: 10.1016/j.crad.2007.05.022
10. Annunziata S, Bauckneht M, Albano D, Argiroffi G, Calabrò D, Abenavoli E, et al. Impact of the COVID-19 Pandemic in Nuclear Medicine Departments: Preliminary Report of the First International Survey. *Eur J Nucl Med Mol Imaging [Internet]* (2020) 47(9):2090–9. doi: 10.1007/s00259-020-04874-z
11. Emmett L, Tang R, Nandurkar R, Hruby G, Roach P, Watts JA, et al. 3-Year Freedom From Progression After 68ga-Psma PET/CT-Triaged Management in Men With Biochemical Recurrence After Radical Prostatectomy: Results of a Prospective Multicenter Trial. *J Nucl Med* (2020) 61(6):866–72. doi: 10.2967/jnumed.119.235028
12. Trabulsi EJ, Rumble RB, Jadvar H, Hope T, Pomper M, Turkbey B, et al. Optimum Imaging Strategies for Advanced Prostate Cancer: Asco Guideline. *J Clin Oncol* (2020) 38(17):1963–96. doi: 10.1200/JCO.19.02757
13. Pienta KJ, Gorin MA, Rowe SP, Carroll PR, Pouliot F, Probst S, et al. A Phase 2/3 Prospective Multicenter Study of the Diagnostic Accuracy of Prostate Specific Membrane Antigen PET/CT with 18 F-DCFPyL in Prostate Cancer Patients (OSPREY). *J Urol* (2021) 206(1). doi: 10.1097/JU.0000000000001698
14. Morris MJ, Rowe SP, Gorin MA, Carroll PR, Saperstein L, Pouliot F, Josephson D, et al. Diagnostic Performance of 18 F-DCFPyL-PET/CT in Men With Biochemically Recurrent Prostate Cancer: Results from the CONDOR Phase III, Multicenter Study. *Clin Cancer Res* (2021) 27(13). doi: 10.1158/1078-0432.CCR-20-4573
15. Woo H. *From the Desk of the Associate Editor: PSMA PET/CT in the Assessment of Intra-Prostate Prostate Cancer* (2018). Available at: https://www.urotoday.com/journal/prostate-cancer-and-prostatic-diseases/from-the-editor/105176-from-the-desk-of-the-associate-editor.html.
16. Haran C, McBean R, Parsons R, Wong D. Five-Year Trends of Bone Scan and Prostate-Specific Membrane Antigen Positron Emission Tomography Utilization in Prostate Cancer: A Retrospective Review in a Private Centre. *J Med Imaging Radiat Oncol [Internet]* (2019) 63(4):495–9. doi: 10.1111/1754-9485.12885
17. de Feria Cardet RE, Hofman MS, Segard T, Yim J, Williams S, Francis RJ, et al. Is Prostate-specific Membrane Antigen Positron Emission Tomography/

Computed Tomography Imaging Cost-effective in Prostate Cancer: An Analysis Informed by the proPSMA Trial. *Eur Urol [Internet]* (2021) 79 (3):413–8. doi: 10.1016/j.eururo.2020.11.043

18. Hope T. *Thomas Hope - The Accidental Journey of Shpherding Psma PET Imaging in Prostate Cancer to the Clinic in the United States* (2021). Available at: https://www.urotoday.com/video-lectures/imaging-prostate-cancer/video/1944-the-accidental-journey-of-shepherding-psma-pet-imaging-in-prostate-cancer-to-the-clinic-in-the-united-states-thomas-hope.html.
19. De Visschere PJL, Standaert C, Fütterer JJ, Villeirs GM, Panebianco V, Walz J, et al. A Systematic Review on the Role of Imaging in Early Recurrent Prostate Cancer. *Eur Urol Oncol* (2019) 2(1):47–76. doi: 10.1016/j.euo.2018.09.010
20. Bouvet V, Wuest M, Jans HS, Janzen N, Genady AR, Valliant JF, et al. Automated Synthesis of [18F]Dcfpyl Via Direct Radiofluorination and Validation in Preclinical Prostate Cancer Models. *EJNMMI Res [Internet]* (2016) 6(1):1–15. doi: 10.1186/s13550-016-0195-6
21. Di Iorio V, Boschi S, Sarnelli A, Cuni C, Bianchini D, Monti M, et al. [18f]F-Psma-1007 Radiolabelling Without an On-Site Cyclotron: A Quality Issue. *Pharmaceuticals* (2021) 14(7):599. doi: 10.3390/ph14070599
22. Sonni I, Eiber M, Fendler WP, Alano RM, Vangala SS, Kishan AU, et al. Impact of 68Ga-PSMA-11 PET/CT on Staging and Management of Prostate Cancer Patients in Various Clinical Settings: A Prospective Single-Center Study. *J Nucl Med [Internet]* (2020) 61(8):1153–60. doi: 10.2967/jnumed.119.237602
23. Young S, Liu W, Zukotynski K, Bauman G. *Prostate-Specific Membrane Antigen Targeted PET/CT for Recurrent Prostate Cancer: A Clinician's Guide. Expert Rev Anticancer Ther* (2021).
24. Jani A, Schreibmann E, Goyal S, Halkar R, Hershatter B, Rossi PJ, et al. 18F-Fluciclovine-PET/CT Imaging Versus Conventional Imaging Alone to Guide Postprostatectomy Salvage Radiotherapy for Prostate Cancer (EMPIRE-1): A Single Centre, Open-Label, Phase 2/3 Randomised Controlled Trial. *Lancet* (2021) 397(10288). doi: 10.1016/S0140-6736(21)00581-X

Conflict of Interest: UM is a consultant for POINT Biopharma Inc. SY holds common shares in Lantheus Holdings Inc.

The remaining authors declare that the research was conducted in the absence of any commercial or financial relationships that could be construed as a potential conflict of interest.

Publisher's Note: All claims expressed in this article are solely those of the authors and do not necessarily represent those of their affiliated organizations, or those of the publisher, the editors and the reviewers. Any product that may be evaluated in this article, or claim that may be made by its manufacturer, is not guaranteed or endorsed by the publisher.

frontiers in Oncology

ORIGINAL RESEARCH
published: 01 October 2021
doi: 10.3389/fonc.2021.723536

A Multi-Institutional Analysis of Prostate Cancer Patients With or Without 68Ga-PSMA PET/CT Prior to Salvage Radiotherapy of the Prostatic Fossa

Nina-Sophie Schmidt-Hegemann[1†], Constantinos Zamboglou[2,3,4†], Reinhard Thamm[5], Chukwuka Eze[1], Simon Kirste[2], Simon Spohn[2], Minglun Li[1], Christian Stief[6], Christian Bolenz[7], Wolfgang Schultze-Seemann[8], Peter Bartenstein[9], Vikas Prasad[10], Ute Ganswindt[11], Anca-Ligia Grosu[2,3], Claus Belka[1,12], Benjamin Mayer[13] and Thomas Wiegel[5]*

[1] Department of Radiation Oncology, University Hospital, Ludwig-Maximilians Universität (LMU) Munich, Munich, Germany, [2] Department of Radiation Oncology, Medical Center – University of Freiburg, Faculty of Medicine, University of Freiburg, Freiburg, Germany, [3] German Cancer Consortium Deutsches Konsortium für Translationale Krebsforschung (DKTK), Partner Site Freiburg, Freiburg, Germany, [4] Berta-Ottenstein-Programme, Faculty of Medicine, University of Freiburg, Freiburg, Germany, [5] Department of Radiation Oncology, University Hospital Ulm, Ulm, Germany, [6] Department of Urology, University Hospital, LMU Munich, Munich, Germany, [7] Department of Urology, University of Ulm, Ulm, Germany, [8] Department of Urology, Medical Center – University of Freiburg, Faculty of Medicine, University of Freiburg, Freiburg, Germany, [9] Department of Nuclear Medicine, University Hospital, LMU Munich, Munich, Germany, [10] Department of Nuclear Medicine, University of Ulm, Ulm, Germany, [11] Department of Therapeutic Radiology and Oncology, Innsbruck Medical University, Innsbruck, Austria, [12] German Cancer Consortium (DKTK), Partner Site Munich, Munich, Germany, [13] Institute for Epidemiology and Medical Biometry, Ulm University, Ulm, Germany

OPEN ACCESS

Edited by:
Tone Frost Bathen,
Norwegian University of Science and Technology, Norway

Reviewed by:
Andreas J. Tulipan,
Oslo University Hospital, Norway
Fangyu Peng,
University of Texas Southwestern Medical Center, United States

***Correspondence:**
Nina-Sophie Schmidt-Hegemann
Nina-Sophie.Hegemann@med.uni-muenchen.de

[†]These authors have contributed equally to this work

Specialty section:
This article was submitted to Cancer Imaging and Image-directed Interventions, a section of the journal Frontiers in Oncology

Received: 10 June 2021
Accepted: 14 September 2021
Published: 01 October 2021

Citation:
Schmidt-Hegemann N-S, Zamboglou C, Thamm R, Eze C, Kirste S, Spohn S, Li M, Stief C, Bolenz C, Schultze-Seemann W, Bartenstein P, Prasad V, Ganswindt U, Grosu A-L, Belka C, Mayer B and Wiegel T (2021) A Multi-Institutional Analysis of Prostate Cancer Patients With or Without 68Ga-PSMA PET/CT Prior to Salvage Radiotherapy of the Prostatic Fossa. Front. Oncol. 11:723536. doi: 10.3389/fonc.2021.723536

Introduction: 68Ga-PSMA PET/CT is associated with unprecedented sensitivity for localization of biochemically recurrent prostate cancer at low PSA levels prior to radiotherapy. Aim of the present analysis is to examine whether patients undergoing postoperative, salvage radiotherapy (sRT) of the prostatic fossa with no known nodal or distant metastases on conventional imaging (CT and/or MRI) and on positron emission tomography/computed tomography (68Ga-PSMA PET/CT) will have an improved biochemical recurrence-free survival (BRFS) compared to patients with no known nodal or distant metastases on conventional imaging only.

Material and Methods: This retrospective analysis is based on 459 patients (95 with and 364 without 68Ga-PSMA PET/CT). BRFS (PSA < post-sRT Nadir + 0.2 ng/ml) was the primary study endpoint. This was first analysed by Kaplan-Meier and uni- and multivariate Cox regression analysis for the entire cohort and then again after matched-pair analysis using tumor stage, Gleason score, PSA at time of sRT and radiation dose as matching parameters.

Results: Median follow-up was 77.5 months for patients without and 33 months for patients with 68Ga-PSMA PET/CT. For the entire cohort, tumor stage (pT2 vs. pT3-4; p= <0.001), Gleason score (GS ≤ 7 vs. GS8-10; p=0.003), pre-sRT PSA (<0.5 vs. ≥0.5ng/ml; p<0.001) and sRT dose (<70 vs. ≥70Gy; p<0.001) were the only factors significantly

associated with improved BRFS. This was not seen for the use of 68Ga-PSMA PET/CT prior to sRT (p=0.789). Matched-pair analysis consisted of 95 pairs of PCa patients with or without PET/CT and no significant difference in BRFS based on the use of PET/CT was evident (p=0.884).

Conclusion: This analysis did not show an improvement in BRFS using 68Ga-PSMA PET/CT prior to sRT neither for the entire cohort nor after matched-pair analysis after excluding patients with PET-positive lymph node or distant metastases a priori. As no improved BRFS resulted with implementation of 68Ga-PSMA PET in sRT planning, sRT should not be deferred until the best "diagnostic window" for 68Ga-PSMA PET/CT.

Keywords: prostate, cancer, PSMA PET/CT, biochemical recurrence, radiotherapy

INTRODUCTION

More than half of the men with adverse pathologic features of their prostate cancer will experience biochemical failure, defined by a rise in serum prostate-specific antigen (PSA) level, after radical prostatectomy (RP) (1). In all major guidelines on salvage radiotherapy (sRT) it is advocated that postoperative radiotherapy should be administered at a low level of PSA recurrence (2, 3).

So far, treatment of patients with biochemically recurrent prostate cancer after RP has been guided for years by nomograms to estimate freedom from biochemical failure and distant metastases following postprostatectomy sRT (4). These nomograms demonstrated, that low pre-RT PSA, low Gleason score 6-7, positive surgical margins and high PSA doubling time >10 months are associated with the highest progression-free probability with a known superiority of early sRT at lower PSA levels compared to all other mentioned parameters (4).

Advances in novel positron emission tomography (PET) radiotracers for prostate cancer, above all ^{68}Gallium-labeled ligands of the prostate-specific membrane antigen (68Ga-PSMA) are associated with unprecedented sensitivity for localization of biochemically recurrent prostate cancer at low PSA levels as shown by several meta-analyses of retrospective studies (5) and lately by a prospective multicentre trial including 635 patients (6). Consequently, 68Ga-PSMA PET/CT has a high impact on the management of biochemically recurrent prostate cancer as assessed by several retrospective and prospective analyses leading to changes in treatment in more than half of patients with biochemical recurrence (7, 8). Hypothetically, 68Ga-PSMA PET/CT's high impact and subsequently individualization of treatment could possibly translate into improved biochemical recurrence free and ultimately overall survival. This has been analysed so far by a few studies mostly without a comparator group of patients treated without prior 68Ga-PSMA PET/CT (9, 10).

Currently, a Phase III trial (NCT03582774) explicitly analysing the oncologic benefit of an additional 68Ga-PSMA PET/CT prior to sRT is underway with the aim to prove that the incorporation of 68Ga-PSMA PET/CT in sRT planning will improve 5-year BRFS by 20% (11). With the results of this trial not to be expected within the next few years, a matched pair analysis of patients with and without 68Ga-PSMA PET/CT prior to sRT of the prostate fossa was undertaken. The aim of this matched pair analysis was to examine whether patients undergoing sRT of the prostate fossa with no known nodal or distant metastases on conventional imaging (CT and/or MRI) and on 68Ga-PSMA PET will have an improved biochemical recurrence-free survival compared to patients with no known nodal or distant metastases on conventional imaging only.

MATERIAL AND METHODS

Patient Population

From 1998 - 2017, a total of 672 consecutive patients were referred for sRT after RP due to persistent or rising PSA at the Radiation Oncology departments of four university hospitals. Patients with pathologic lymph nodes at time of RP, distant or lymph node metastases in 68Ga-PSMA PET, androgen deprivation therapy (ADT) before or simultaneously with sRT, prior history of RT or incomplete documentation were excluded. All patients received sRT of the prostatic bed only. Thus, the following analysis is based on 459 patients. Of this cohort, 364/459 (79%) patients were treated without a 68Ga-PSMA PET and 95/459 (21%) received a 68Ga-PSMA PET/CT prior to sRT. This retrospective analysis was performed in compliance with the principles of the Declaration of Helsinki and its subsequent amendments (12) and was approved by the local Ethics Committee of the respective medical university centers. The requirement to obtain informed consent was waived.

Statistical Analysis

Biochemical recurrence-free survival (BRFS), defined as PSA < post-radiotherapy Nadir + 0.2 ng/ml from the last day of sRT, was the primary outcome. The effect of 68Ga-PSMA PET/CT and other important clinical parameters on BRFS was first analysed by means of Kaplan-Meier analysis using the log-rank test as well as by uni- and multivariable Cox regression analyses for the entire cohort. Multivariable Cox-regression analysis was used to identify predictors of BRFS after sRT. The effect of 68Ga-PSMA PET/CT on BRFS was then additionally assessed after a propensity score (PS) matching (1:1 ratio) has been conducted using tumor stage (pT2 *vs.* pT3-4), Gleason score (GS ≤ 7 *vs.* GS8-10), PSA at time of sRT (<0.5 *vs.* ≥0.5 ng/ml) and radiation dose (<70 *vs.* ≥70 Gy) as matching variables. The PS was calculated using a logistic regression model

and the final matching was done using the calculated PS as a measure of distance within an optimal matching approach (13). Differences in BRFS after the PS-matching were assessed by means of a Cox proportional hazards model using a robust sandwich covariance matrix estimator to account for the clustered structure introduced by the PS-matching. Differences between subgroups were compared using Mann-Whitney-U, Student's t- and Chi-square test with a p-value of <0.05 considered statistically significant.

RESULTS

Patients' Characteristics and Outcome for the Entire Cohort

Patients had primarily pT2 prostate cancer (52% of the pre-68Ga-PSMA PET patients and 61% of patients with 68Ga-PSMA PET). Patient cohorts differed significantly regarding Gleason score and surgical margins with a higher percentage of 68Ga-PSMA PET patients with a Gleason Score ≥ 7 (93% *vs.* 64%; p<0.001) and surgically negative resection margins (69% *vs.* 47%; p<0.001). Further, 68Ga-PSMA PET-patients had a significantly higher median pre-SRT PSA levels (0.33 ng/ml *vs.* 0.29 ng/ml; p<0.007) compared to patients of the pre-68Ga-PSMA PET era. Median follow-up was 77.5 months (range 0-157) for patients without and 33 months (range 3-63) for patients with 68Ga-PSMA PET/CT. Thirty-one patients (33%) had evidence of PET-positive local recurrence. Patients' characteristics are listed in **Table 1**.

For the entire cohort, no difference in BRFS (**Figure 1**) depending on the use of 68Ga-PSMA PET was observable (2-year BRFS 84.1% for non-PET-group *vs.* 85.6% for PET-group and 3-year BRFS 76.6% *vs.* 77.8%, p=0.884, respectively). A multivariable cox regression analysis (**Table 2**) was conducted to assess whether there was an association between tumour or treatment specific variables and BRFS. Overall, tumor stage (pT2 *vs.* pT3-4; p<0.001), Gleason score (GS ≤ 7 *vs.* GS8-10; p=0.003), PSA at time of sRT (<0.5 *vs.* ≥0.5ng/ml; p<0.001) and radiation dose (<70 *vs.* ≥70Gy; p<0.001) were the only factors significantly associated with BRFS. No significant association was observed for the use of 68Ga-PSMA PET/CT prior to sRT (p=0.789), initial PSA (<10 ng/ml *vs.* ≥ 10 ng/ml; p=0.508), surgical margins (R0 *vs.* R1; p=0.055) and post-prostatectomy PSA (<0.1 ng/ml *vs.* ≥ 0.1 ng/ml; p=0.192).

Patient Characteristics and Outcome After Propensity Score Matching

Propensity score matching based on tumor stage (pT2 *vs.* pT3-4), Gleason score (GS ≤ 7 *vs.* GS8-10), PSA at time of sRT (<0.5 *vs.* ≥0.5 ng/ml) and radiation dose (<70 *vs.* ≥70 Gy) resulted in 95 patient pairs. Assessment of both the area of common support of the PS distributions in PET and no PET patient groups as well as the absolute standardized difference (ASD) after the matching was done revealed perfectly balanced comparison groups. The common support area nearly reached 100% overlapping, and

TABLE 1 | Patient characteristics.

Factor	no PSMA-PET/CTN=364	PSMA-PET/CTN=95	p-value
Year of RP	1989 - 2015	2000 - 2017	
Median FU (range)	77.5 months (0 - 157)	33 months (3 - 63)	<0.001*
iPSA ng/ml			
Mean (SD)	12.2 (10.0)	12.8 (12.2)	0.814*
Median (IQR)	9.2 (6.2 - 14.3)	10.2 (6.0 - 14.4)	
Tumor stage			
pT2	190 (52%)	58 (61%)	0.123**
pT3-4	174 (48%)	37 (39%)	
Gleason score			
GS ≤6	132 (36%)	7 (7%)	<0.001**
GS 7	160 (44%)	63 (67%)	
GS 8-10	72 (20%)	25 (26%)	
Surgical margins			
R0	172 (47%)	65 (69%)	<0.001**
R1	160 (44%)	26 (27%)	
Rx	32 (9%)	4 (4%)	
Post-RP PSA nadir			
<0.1 ng/ml	288 (79%)	75 (79%)	0.970**
≥0.1 ng/ml	76 (21%)	20 (21%)	
Time between surgery and PSA recurrence	12 (0-149)	25 (0-137)	<0.001*
Pre-SRT PSA ng/ml			
Mean (SD)	0.52 (0.84)	0.54 (0.67)	0.007 *
Median (IQR)	0.29 (0.15 - 0.51)	0.33 (0.23 - 0.51)	
SRT dose Gy			
Mean (SD)	69.3 (2.6)	69.2 (3.0)	0.796***
Median (IQR)	70.2 (66.6 – 72.0)	70.2 (66.0 – 72.0)	

**Mann-Whitney-U test; **Chi-square test; ***Student's t-test.*

RP, radical prostatectomy; iPSA, initial PSA; GS, Gleason Score; SRT, salvage radiotherapy; SD, standard deviation; IQR, inter quartile range.

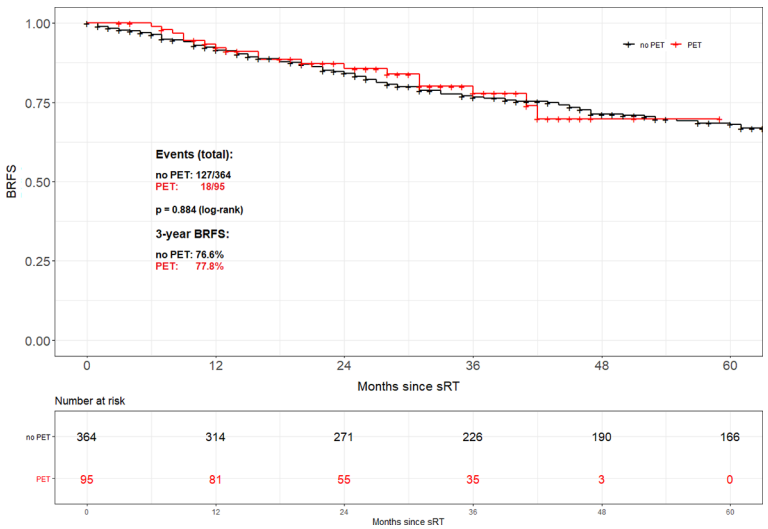

FIGURE 1 | Biochemical recurrence-free survival according to the use of PSMA PET/CT for the entire cohort.

TABLE 2 | Multivariable Cox Regression Analysis on factors associated with biochemical recurrence free survival after SRT.

Factor	HR (95% CI)	p
PSMA-PET/CT (no*/yes)	1.07 (0.64 - 1.79)	0.789
iPSA 10 (<10*/≥10 ng/ml)	1.13 (0.79 - 1.60)	0.508
Tumor stage (pT2*/pT3-4)	2.29 (1.60 - 3.27)	<0.001
Gleason score (GS ≤ 7*/GS8-10)	1.77 (1.22 - 2.57)	0.003
Surgical margins (R0*/R1)	0.72 (0.52 - 1.01)	0.055
Post-RP PSA nadir (<0.1*/≥0.1 ng/ml)	1.28 (0.88 - 1.87)	0.192
Pre-SRT PSA (<0.5*/≥0.5 ng/ml)	2.00 (1.39 - 2.86)	<0.001
SRT dose (<70*/≥70 Gy)	0.54 (0.39 - 0.76)	<0.001

**State of reference.*

HR, Hazard Ratio; CI, confidence interval; iPSA, initial PSA; GS, Gleason Score; RPE, radical prostatectomy; SRT, salvage radiotherapy.

ASD values for all variables in the PS model were <0.1. Consequently, there was almost no pair of case and control patient which differed in any value of all the matching variables. Overall, no difference in BRFS based on the use of 68Ga-PSMA PET/CT prior to sRT (3-year BRFS 77.8% *vs.* 79.4%; p=0.802) could be found (**Figure 2**). Equally no difference in BRFS was evident when comparing patients with PET-positive local recurrences within the prostatic fossa to patients without PET/CT prior to sRT or a negative PET/CT (p=0.805) (**Figure 3**). Patients with PET-positive local recurrence had significantly higher median pre-sRT PSA values compared to PET-negative patients and patients without a PET/CT (0.46ng/ml *vs.* 0.29 ng/ml *vs.* 0.24ng/ml, p= 0.001).

DISCUSSION

The introduction of 68Ga-PSMA PET/CT imaging has substantially improved the detection and localization of macroscopic disease in patients with biochemical recurrence after RP. 68Ga-PSMA PET/CT allows for an individualization of treatment in terms of irradiation volumes, applied overall dose and concomitant ADT (14–16). This has led to a surge in the use of 68Ga-PSMA PET/CT particularly across Europe compared to the United States, where 68Ga-PSMA PET has been approved by the US Food and Drug Administration for institutional use at the University of California, Los Angeles (UCLA) and the University of California, San Francisco (UCSF). Only recently, a phase III trial corroborated the high detection rates of 68Ga-PSMA PET/CT at low PSA levels in patients with biochemical recurrence ranging from 38% for a PSA level <0.5 ng/ml to 57% for 0.5 to <1.0 ng/ml (6). Consequently, the European guidelines on prostate cancer cautiously recommend to perform a PSMA PET/CT post-prostatectomy at PSA levels >0.2 ng/ml (3).

To assess the oncologic benefit of 68Ga-PSMA PET/CT in patients with or without a PET-positive local recurrence within the prostatic fossa and with prior exclusion of patients with PET-positive lymph node or distant metastases, a matched pair analysis of patients treated with sRT of the prostate fossa without *vs.* patients with 68Ga-PSMA PET/CT prior to sRT was undertaken. For the entire cohort, no significant difference in BRFS between patients with or without 68Ga-PSMA PET/CT was observed, although the two cohorts differed significantly with more adverse features in the 68Ga-PSMA PET cohort, namely higher Gleason score, higher pre-sRT PSA and higher percentage of patients with R0-resection being present. Subsequently, not 68Ga-PSMA PET/CT but pre-sRT PSA (<0.5 *vs.* ≥0.5 ng/ml), tumor stage (pT2 *vs.* pT3-4), Gleason score (GS ≤ 7 *vs.* GS8-10), and radiation dose (<70 *vs.* ≥70 Gy) were the only factors significantly associated with BRFS. Several retrospective studies have affirmed the prognostic role of the pre-sRT PSA level with a potential chance of cure in more than 60% of patients treated before PSA rises >0.5ng/ml (4, 17, 18). Likewise, the association of dose-escalation in the sRT setting with relapse-free survival was previously confirmed in multiple

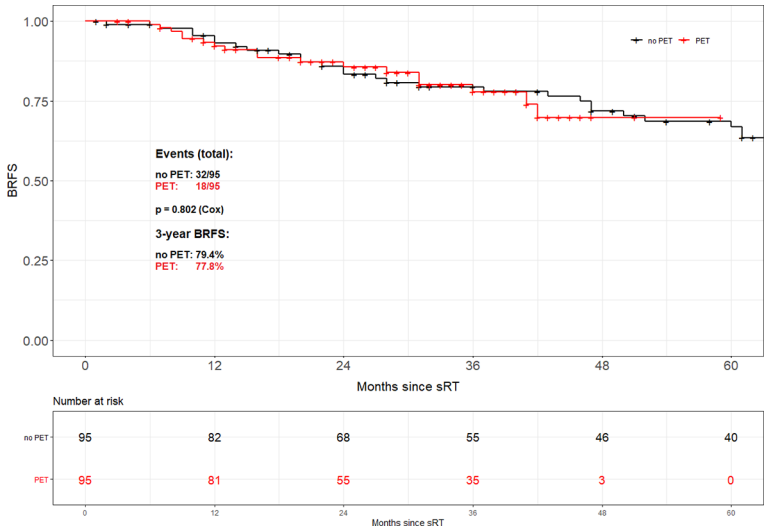

FIGURE 2 | Biochemical recurrence-free survival according to the use of PSMA PET/CT after propensity score matching.

retrospective analyses with the oncologic results of the SAKK 09/10, a phase III trial on the potential benefit of dose-escalation still pending (19, 20).

After matching according to these factors with an overall 95 pairs of patients again no difference in BRFS was evident, nor was a significant difference in BRFS seen when comparing patients with a PET-positive local recurrence to patients without 68Ga-PSMA PET.

Once again, this underlines the significant influence of pre-sRT PSA on BRFS after sRT with higher PSA-levels correlating with macroscopic local and/or lymph node recurrences and diminished BRFS rates. Thus, based on these findings in a selective cohort of patients with exclusion of patients with 68Ga-PSMA PET-positive lymph node or distant metastases a priori, the current analysis supports the recommendations by several guidelines on prostate cancer that PSMA PET/CT should be performed in patients with PSA >0.2 ng/ml and sRT should not be postponed until a PSMA PET-positive result is observed (3, 21).

This is especially true as in contrast to the pre-PSMA PET era, when the 3 major studies on adjuvant radiotherapy were initially published (1, 22, 23) a certain reluctance can nowadays be observed among urologists but as well radiation oncologists to perform adjuvant radiotherapy in men with adverse pathologic features.

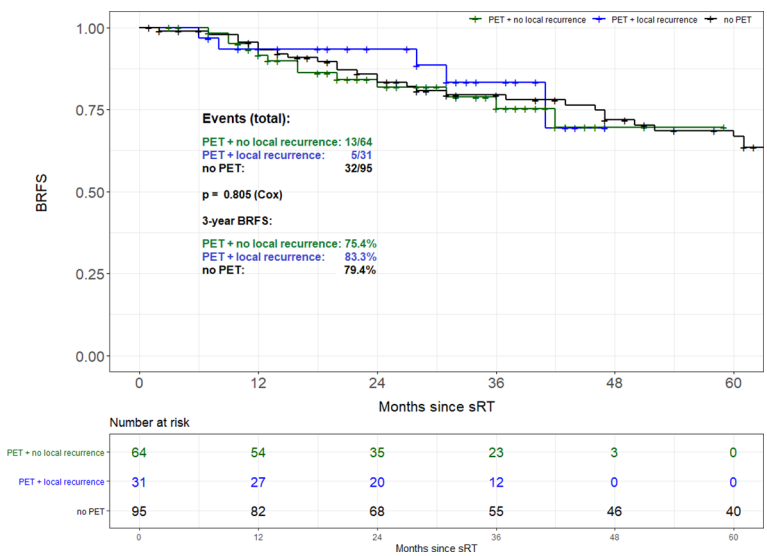

FIGURE 3 | Biochemical recurrence-free survival of patients with PET-positive local recurrence vs. patients without PET/CT.

This tendency most likely stems from an increase in RT-associated side effects e.g. urinary incontinence or erectile dysfunction when applying early postoperative RT in comparison to sRT (24). In addition, no difference in 5-year BRFS and even 8-year metastasis-free or overall survival was observed in retrospective studies initiating sRT at low PSA levels (25, 26).

A further increase of sRT will most likely be observed based on the latest results of the three randomised studies RADICALS-RT, RAVES and GETUG-AFU 17 all comparing adjuvant radiotherapy to a policy of early sRT triggered at low PSA failures of maximum 0.2ng/ml after RP (27). All three only recently published studies indicate the possibility of an observation policy with sRT after RP as long as sRT is initiated at low PSA levels (28–30).

With a known better outcome for patients receiving early sRT at PSA levels ≤ 0.5 ng/ml (4), the fundamental maxim of sRT might as such be "the earlier, the better" (4). In particular, Bartkowiak et al. advocate for very early sRT at PSA levels of 0.2 ng/ml or less (18) with a known risk for further metastases at a PSA level of 0.4 ng/ml and rising (31). The significance of an early sRT start at low PSA-levels is further depicted in the work by Shelan et al. showing that even dose-escalated sRT with short-course ADT in patients with macroscopic local recurrences after RP leads to inferior tumor control compared to early sRT (32).

Thus, not surprisingly, the present data reveal that not the availability of a 68Ga-PSMA PET/CT is decisive for BRFS after sRT but the initiation of sRT at low PSA-levels with patients treated without a PSMA PET having significantly lower PSA levels prior to sRT. This underlines the dilemma of modern imaging with 68Ga-PSMA PET/CT, which so far has a superior detection of relapses than any other imaging modality for prostate cancer but is still not sensitive enough for the low PSA levels associated with the highest chance of long-term BRFS after sRT. Nevertheless, with growing body of evidence PSMA PET will maintain its dominant role in staging patients at initial diagnosis before curative-intent surgery or radiotherapy, as seen in proPSMA trial, at the time of postoperative PSA relapse as well as in the treatment setting of metastatic castration-resistant prostate cancer patients who do receive [(177) Lu]-PSMA-617 radionuclide treatment (6, 33, 34).

The present study has several limitations mainly due to its retrospective nature. Based on varying institutional policies, the treatment protocols and the follow-up procedure were not identical for all patients. The influence of 68Ga-PSMA PET might therefore be disguised by the comparably high overall median dose in the sRT setting of 70.2 Gy in both cohorts. For the cohort of patients without 68Ga-PSMA PET/CT the precise staging method (CT and/or MRI) was not known for each patient. A further shortcoming of the present analysis that precludes drawing final conclusions is the relatively short follow-up of patients with 68Ga-PSMA PET/CT. We tried to overcome these issues by performing a matched-pair analysis with a reasonably high number of 95 patient pairs for statistical analyses. To avoid further biases, patients with ADT were excluded resulting in a BRFS free of the influence of ADT.

CONCLUSION

This multi-institutional analysis did neither confirm an improvement in BRFS for the entire cohort nor after matched-pair analysis nor for patients with PET-positive local recurrences using 68Ga-PSMA PET/CT prior to sRT compared to a pre-PSMA PET cohort after excluding patients with PET-positive lymph node or distant metastases a priori. Overall, the significance of a low PSA before the initiation of sRT was reconfirmed in the present analysis. As no improved BRFS resulted with implementation of 68Ga-PSMA in sRT planning, sRT should not be deferred until the best "diagnostic window" for PSMA PET/CT. Further advances in PSMA PET/CT like the recent emergence of Fluorine-18 tracers with promising detection rates of 61.5% for patients with PSA values as low as 0.2 - 0.5 ng/ml might further influence BRFS rates post-sRT (35).

DATA AVAILABILITY STATEMENT

The raw data supporting the conclusions of this article will be made available by the authors, without undue reservation.

ETHICS STATEMENT

The studies involving human participants were reviewed and approved by approval number of the University of Ulm (391/15), approval number of the University of Freiburg (519/17), approval number of the University of Munich (17-765)]. Written informed consent for participation was not required for this study in accordance with the national legislation and the institutional requirements.

AUTHOR CONTRIBUTIONS

All authors contributed to the study conception and design. Material preparation, data collection and analysis were performed by N-SS-H, CZ, BM, and TW. The first draft of the manuscript was written by N-SS-H, CZ, BM, and TW. All authors commented on previous versions of the manuscript. All authors contributed to the article and approved the submitted version.

REFERENCES

1. Wiegel T, Bartkowiak D, Bottke D, Bronner C, Steiner U, Siegmann A, et al. Adjuvant Radiotherapy Versus Wait-And-See After Radical Prostatectomy: 10-Year Follow-Up of the ARO 96–02/AUO AP 09/95 Trial. *Eur Urology* (2014) 66(2):243–50. doi: 10.1016/j.eururo.2014.03.011
2. Pisansky Thomas M, Thompson Ian M, Valicenti Richard K, D'Amico Anthony V, Selvarajah S. Adjuvant and Salvage Radiotherapy After Prostatectomy: ASTRO/AUA Guideline Amendment 2018-2019. *J Urol* (2019) 202(3):533–8. doi: 10.1097/JU.0000000000000295
3. Mottet N, Cornford P, van den Bergh RCN. EAU - EANM - ESTRO - ESUR – SIOG Guidelines on Prostate Cancer. *Eur Assoc Urol* (2020).

4. Tendulkar RD, Agrawal S, Gao T, Efstathiou JA, Pisansky TM, Michalski JM, et al. Contemporary Update of a Multi-Institutional Predictive Nomogram for Salvage Radiotherapy After Radical Prostatectomy. *J Clin Oncol* (2016) 34(30):3648–54. doi: 10.1200/JCO.2016.67.9647
5. von Eyben FE, Picchio M, von Eyben R, Rhee H, Bauman G. 68Ga-Labeled Prostate-Specific Membrane Antigen Ligand Positron Emission Tomography/Computed Tomography for Prostate Cancer: A Systematic Review and Meta-Analysis. *Eur Urol Focus* (2018) 4(5):686–93. doi: 10.1016/j.euf.2016.11.002
6. Fendler WP, Calais J, Eiber M, Flavell RR, Mishoe A, Feng FY, et al. Assessment of 68Ga-PSMA-11 PET Accuracy in Localizing Recurrent Prostate Cancer: A Prospective Single-Arm Clinical Trial. *JAMA Oncol* (2019) 5(6):856–63. doi: 10.1001/jamaoncol.2019.0096
7. Han S, Woo S, Kim YJ, Suh CH. Impact of 68Ga-PSMA PET on the Management of Patients With Prostate Cancer: A Systematic Review and Meta-Analysis. *Eur Urol* (2018) 74(2):179–90. doi: 10.1016/j.eururo.2018.03.030
8. Fendler WP, Ferdinandus J, Czernin J, Eiber M, Flavell RR, Behr SC, et al. Impact of 68Ga-PSMA-11 PET on the Management of Recurrent Prostate Cancer in a Prospective Single-Arm Clinical Trial. *J Nucl Med* (2020). doi: 10.1016/S2666-1683(20)33398-X
9. Schmidt-Hegemann N-S, Stief C, Kim T-H, Eze C, Kirste S, Strouthos I, et al. Outcome After PSMA PET/CT–Based Salvage Radiotherapy in Patients With Biochemical Recurrence After Radical Prostatectomy: A 2-Institution Retrospective Analysis. *J Nucl Med* (2019) 60(2):227–33. doi: 10.2967/jnumed.118.212563
10. Zschaeck S, Wust P, Beck M, Wlodarczyk W, Kaul D, Rogasch J, et al. Intermediate-Term Outcome After PSMA-PET Guided High-Dose Radiotherapy of Recurrent High-Risk Prostate Cancer Patients. *Radiat Oncol* (2017) 12(1):140. doi: 10.1186/s13014-017-0877-x
11. Calais J, Czernin J, Fendler WP, Elashoff D, Nickols NG. Randomized Prospective Phase III Trial of (68)Ga-PSMA-11 PET/CT Molecular Imaging for Prostate Cancer Salvage Radiotherapy Planning [PSMA-SRT]. *BMC Cancer* (2019) 19(1):18–8. doi: 10.1186/s12885-018-5200-1
12. Association GAotWM. World Medical Association Declaration of Helsinki: Ethical Principles for Medical Research Involving Human Subjects. *J Am Coll Dent* (2014) 81(3):14–8.
13. Mayer B, Tadler S, Rothenbacher D, Seeger J, Wöhrle J. A Hierarchical Algorithm for Multicentric Matched Cohort Study Designs. *Curr Med Res Opin* (2020) 36(11):1889–96. doi: 10.1080/03007995.2020.1808453
14. Afshar-Oromieh A, Holland-Letz T, Giesel FL, Kratochwil C, Mier W, Haufe S, et al. Diagnostic Performance of (68)Ga-PSMA-11 (HBED-CC) PET/CT in Patients With Recurrent Prostate Cancer: Evaluation in 1007 Patients. *Eur J Nucl Med Mol Imaging* (2017) 44(8):1258–68. doi: 10.1007/s00259-017-3711-7
15. Farolfi A, Ceci F, Castellucci P, Graziani T, Siepe G, Lambertini A, et al. 68Ga-PSMA-11 PET/CT in Prostate Cancer Patients With Biochemical Recurrence After Radical Prostatectomy and PSA <0.5 Ng/Ml. Efficacy and Impact on Treatment Strategy. *Eur J Nucl Med Mol Imaging* (2019) 46(1):11–9. doi: 10.1007/s00259-018-4066-4
16. Müller J, Ferraro DA, Muehlematter UJ, Garcia Schüler HI, Kedzia S, Eberli D, et al. Clinical Impact of 68Ga-PSMA-11 PET on Patient Management and Outcome, Including All Patients Referred for an Increase in PSA Level During the First Year After its Clinical Introduction. *Eur J Nucl Med Mol Imaging* (2019) 46(4):889–900. doi: 10.1007/s00259-018-4203-0
17. Stish BJ, Pisansky TM, Harmsen WS, Davis BJ, Tzou KS, Choo R, et al. Improved Metastasis-Free and Survival Outcomes With Early Salvage Radiotherapy in Men With Detectable Prostate-Specific Antigen After Prostatectomy for Prostate Cancer. *J Clin Oncol* (2016) 34(32):3864–71. doi: 10.1200/JCO.2016.68.3425
18. Bartkowiak D, Thamm R, Bottke D, Siegmann A, Böhmer D, Budach V, et al. Prostate-Specific Antigen After Salvage Radiotherapy for Postprostatectomy Biochemical Recurrence Predicts Long-Term Outcome Including Overall Survival. *Acta Oncologica* (2018) 57(3):362–7. doi: 10.1080/0284186X.2017.1364869
19. King CR. The Timing of Salvage Radiotherapy After Radical Prostatectomy: A Systematic Review. *Int J Radiat OncologyBiologyPhysics* (2012) 84(1):104–11. doi: 10.1016/j.ijrobp.2011.10.069
20. Ghadjar P, Hayoz S, Bernhard J, Zwahlen DR, Hölscher T, Gut P, et al. Acute Toxicity and Quality of Life After Dose-Intensified Salvage Radiation Therapy for Biochemically Recurrent Prostate Cancer After Prostatectomy: First Results of the Randomized Trial SAKK 09/10. *J Clin Oncol* (2015) 33(35):4158–66. doi: 10.1200/JCO.2015.63.3529
21. Wirth M, Berges R, Fröhner M, Miller K, Rübben H, Stöckle M, et al. *Interdisziplinäre Leitlinie Der Qualität S3 Zur Früherkennung, Diagnose Und Therapie Der Verschiedenen Stadien Des Prostatakarzinoms*, Vol. 5.0. (2018).
22. Thompson IM, Tangen CM, Paradelo J, Lucia MS, Miller G, Troyer D, et al. Adjuvant Radiotherapy for Pathological T3N0M0 Prostate Cancer Significantly Reduces Risk of Metastases and Improves Survival: Long-Term Followup of a Randomized Clinical Trial. *J Urol* (2009) 181(3):956–62. doi: 10.1016/j.juro.2008.11.032
23. Bolla M, van Poppel H, Tombal B, Vekemans K, Da Pozzo L, de Reijke TM, et al. Postoperative Radiotherapy After Radical Prostatectomy for High-Risk Prostate Cancer: Long-Term Results of a Randomised Controlled Trial (EORTC Trial 22911). *Lancet* 380(9858):2018–27. doi: 10.1016/S0140-6736(12)61253-7
24. Zaffuto E, Gandaglia G, Fossati N, Dell'Oglio P, Moschini M, Cucchiara V, et al. Early Postoperative Radiotherapy is Associated With Worse Functional Outcomes in Patients With Prostate Cancer. *J Urology 2017/03/01* (2017) 197(3 Part 1):669–75. doi: 10.1016/j.juro.2016.09.079
25. Fossati N, Karnes RJ, Boorjian SA, Moschini M, Morlacco A, Bossi A, et al. Long-Term Impact of Adjuvant Versus Early Salvage Radiation Therapy in Pt3n0 Prostate Cancer Patients Treated With Radical Prostatectomy: Results From a Multi-Institutional Series. *Eur Urol* (2016). doi: 10.1016/j.eururo.2016.07.028
26. Briganti A, Wiegel T, Joniau S, Cozzarini C, Bianchi M, Sun M, et al. Early Salvage Radiation Therapy Does Not Compromise Cancer Control in Patients With Pt3n0 Prostate Cancer After Radical Prostatectomy: Results of a Match-Controlled Multi-Institutional Analysis. *Eur Urology* (2012) 62(3):472–87. doi: 10.1016/j.eururo.2012.04.056
27. Vale CL, Fisher D, Kneebone A, Parker C, Pearse M, Richaud P, et al. Adjuvant or Early Salvage Radiotherapy for the Treatment of Localised and Locally Advanced Prostate Cancer: A Prospectively Planned Systematic Review and Meta-Analysis of Aggregate Data. *Lancet* (2020). doi: 10.1016/S0140-6736(20)31952-8
28. Kneebone A, Fraser-Browne C, Duchesne GM, Fisher R, Frydenberg M, Herschtal A, et al. Adjuvant Radiotherapy Versus Early Salvage Radiotherapy Following Radical Prostatectomy (TROG 08.03/ANZUP RAVES): A Randomised, Controlled, Phase 3, non-Inferiority Trial. *Lancet Oncol* (2020) 21(10):1331–40. doi: 10.1016/S1470-2045(20)30456-3
29. Parker CC, Clarke NW, Cook AD, Kynaston HG, Petersen PM, Catton C, et al. Timing of Radiotherapy After Radical Prostatectomy (RADICALS-RT): A Randomised, Controlled Phase 3 Trial. *Lancet* (2020). doi: 10.1016/S0140-6736(20)31553-1
30. Sargos P, Chabaud S, Latorzeff I, Magné N, Benyoucef A, Supiot S, et al. Adjuvant Radiotherapy Versus Early Salvage Radiotherapy Plus Short-Term Androgen Deprivation Therapy in Men With Localised Prostate Cancer After Radical Prostatectomy (GETUG-AFU 17): A Randomised, Phase 3 Trial. *Lancet Oncol* (2020) 21(10):1341–52. doi: 10.1016/S1470-2045(20)30454-X
31. Stephenson AJ, Kattan MW, Eastham JA, Dotan ZA, Bianco FJ, Lilja H, et al. Defining Biochemical Recurrence of Prostate Cancer After Radical Prostatectomy: A Proposal for a Standardized Definition. *J Clin Oncol* (2006) 24(24):3973–8. doi: 10.1200/JCO.2005.04.0756
32. Shelan M, Odermatt S, Bojaxhiu B, Nguyen DP, Thalmann GN, Aebersold DM, et al. Disease Control With Delayed Salvage Radiotherapy for Macroscopic Local Recurrence Following Radical Prostatectomy. *Front Oncol* (2019) 9:12. doi: 10.3389/fonc.2019.00012
33. Hofman MS, Lawrentschuk N, Francis RJ, Tang C, Vela I, Thomas P, et al. Prostate-Specific Membrane Antigen PET-CT in Patients With High-Risk Prostate Cancer Before Curative-Intent Surgery or Radiotherapy (proPSMA): A Prospective, Randomised, Multicentre Study. *Lancet* (2020) 395(10231):1208–16. doi: 10.1016/S0140-6736(20)30314-7
34. Kratochwil C, Fendler WP, Eiber M, Baum R, Bozkurt MF, Czernin J, et al. EANM Procedure Guidelines for Radionuclide Therapy With 177Lu-Labelled PSMA-Ligands (177Lu-PSMA-RLT). *Eur J Nucl Med Mol Imaging* (2019) 46(12):2536–44. doi: 10.1007/s00259-019-04485-3

35. Giesel FL, Knorr K, Spohn F, Will L, Maurer T, Flechsig P, et al. Detection Efficacy of 18F-PSMA-1007 PET/CT in 251 Patients With Biochemical Recurrence of Prostate Cancer After Radical Prostatectomy. *J Nucl Med* (2019) 60(3):362–8. doi: 10.2967/jnumed.118.212233

Conflict of Interest: The authors declare that the research was conducted in the absence of any commercial or financial relationships that could be construed as a potential conflict of interest

Publisher's Note: All claims expressed in this article are solely those of the authors and do not necessarily represent those of their affiliated organizations, or those of the publisher, the editors and the reviewers. Any product that may be evaluated in this article, or claim that may be made by its manufacturer, is not guaranteed or endorsed by the publisher.

frontiers in Oncology

SYSTEMATIC REVIEW
published: 20 October 2021
doi: 10.3389/fonc.2021.737989

Head-to-Head Comparison of ^{68}Ga-PSMA-11 PET/CT and Multiparametric MRI for Pelvic Lymph Node Staging Prior to Radical Prostatectomy in Patients With Intermediate to High-Risk Prostate Cancer: A Meta-Analysis

Xueju Wang[1†], *Qiang Wen*[2†], *Haishan Zhang*[3*] *and Bin Ji*[2*]

[1] Department of Pathology, China-Japan Union Hospital of Jilin University, Changchun, China, [2] Department of Nuclear Medicine, China-Japan Union Hospital of Jilin University, Changchun, China, [3] Department of Surgery, China-Japan Union Hospital of Jilin University, Changchun, China

Purpose: To compare the diagnostic performance of ^{68}Ga-PSMA-11 PET/CT and mpMRI for pelvic lymph node staging prior to radical prostatectomy in prostate cancer (PCa) patients based on per patient data.

Methods: PubMed and Embase databases were searched until October 2020 for eligible studies evaluating head-to-head comparison of ^{68}Ga-PSMA-PET/CT and mpMRI for the detection of pelvic lymph node metastases (PLNMs) using pelvic lymph node dissection (PLND) as gold standard. The pooled sensitivity, specificity, and area under the summary receiver-operating characteristics curve (AUC) were determined for the two imaging modalities.

Results: Nine studies with 640 patients were included. The pooled sensitivity, specificity, and AUC for ^{68}Ga-PSMA-11 PET/CT vs. mpMRI were 0.71 (95% CI: 0.48–0.86) vs. 0.40 (95% CI: 0.16–0.71), 0.92 (95% CI: 0.88–0.95) vs. 0.92 (95% CI: 0.80–0.97), and 0.92 (95% CI: 0.88–0.95) vs. 0.82 (95% CI: 0.79–0.86), respectively. There was substantial heterogeneity for both imaging modalities, and meta-regression analysis revealed that the number of patients, prevalence of PLNMs, PSA level, reference standard, and risk classification might be the potential causes of heterogeneity.

Conclusion: This meta-analysis of head-to-head comparison studies confirms that there is a trend toward a higher sensitivity and diagnostic accuracy of ^{68}Ga-PSMA-11 PET/CT compared to mpMRI for the detection of PLNMs in PCa patients. Nevertheless, according to current guidelines, PLND still needs to be recommended in case of negative results from ^{68}Ga-PSMA-11 PET/CT due to significant risk of malignancy.

Keywords: ^{68}Ga-PSMA-11 PET/CT, multiparametric MRI, pelvic lymph node metastases, sensitivity, diagnostic accuracy

OPEN ACCESS

Edited by:
Trevor Royce,
University of North Carolina at Chapel Hill, United States

Reviewed by:
Orhan K. Oz,
University of Texas Southwestern Medical Center, United States
Ameya Puranik,
Tata Memorial Hospital, India

***Correspondence:**
Bin Ji
jibin1983104@163.com;
jibin@jlu.edu.cn
Haishan Zhang
hszhang@jlu.edu.cn

†These authors have contributed equally to this work

Specialty section:
This article was submitted to Cancer Imaging and Image-directed Interventions, a section of the journal Frontiers in Oncology

Received: *08 July 2021*
Accepted: *24 September 2021*
Published: *20 October 2021*

Citation:
Wang X, Wen Q, Zhang H and Ji B (2021) Head-to-Head Comparison of ^{68}Ga-PSMA-11 PET/CT and Multiparametric MRI for Pelvic Lymph Node Staging Prior to Radical Prostatectomy in Patients With Intermediate to High-Risk Prostate Cancer: A Meta-Analysis. Front. Oncol. 11:737989. doi: 10.3389/fonc.2021.737989

INTRODUCTION

Correct lymph node staging is crucial to identify prostate cancer (PCa) patients with poor prognosis who would benefit from additional therapies (1, 2). Pelvic lymph node dissection (PLND) represents the gold standard, but it is impeded by increased risk of complications such as lymphedema and venous thromboembolism as well as longer hospital stay (3, 4). Although cross-sectional abdominopelvic imaging has been recommended for patients with intermediate to high-risk PCa across guidelines, conventional imaging techniques only have modest diagnostic accuracy (4–7).

In recent years, positron emission tomography (PET) techniques with PSMA ligands have emerged as a promising tool for PCa detection, tumor staging, and treatment planning (8). Among them, ^{68}Ga-PSMA-11 and ^{18}F-DCFPyL have been consecutively approved by the FDA for patients with primary and recurrent PCa (9, 10). Nevertheless, although ^{18}F-based tracers offer important advantages such as higher production capacity, longer physical half-life, and minimal radiotracer accumulation in the bladder (11–13); up until now, ^{68}Ga-PSMA-11 is still worldwide the most commonly used and provides the absolute majority of evidence in the literature for PSMA imaging. Importantly, many accuracy studies and two previous meta-analyses have reported favorable diagnostic performance of ^{68}Ga-PSMA-11 PET/CT for the detection of pelvic lymph node metastases (PLNMs) in intermediate to high-risk PCa (14–17).

Multiparametric MRI (mpMRI), which combines T2-weighted imaging (T2WI), diffusion weighted imaging (DWI), and dynamic contrast-enhanced (DCE) sequence, has been the leading imaging modality in the primary PCa detection and localization in the last decade. Several previous studies have compared it with ^{68}Ga-PSMA-11 PET/CT for pelvic lymph node staging prior to radical prostatectomy. However, the results were variable and sometimes conflicting (18–32). Therefore, to clarify their relative effectiveness, in the present study, we sought to compare the diagnostic performance of these two imaging modalities by summarizing the most recent evidence in the literature. To reduce interstudy heterogeneity, only studies in which both modalities were performed in the same population were included.

MATERIAL AND METHODS

This study was conducted according to the Preferred Reporting Items for Systematic Reviews and Meta-Analyses guidelines (33).

Search Strategy

We comprehensively searched all available literature until October 2020 in the PubMed and Embase databases using an algorithm based on a combination of terms: (1) "Gallium Radioisotopes" (Mesh) OR Ga OR gallium; (2) "68Ga-PSMA" (Supplementary Concept) OR PSMA OR "prostate specific membrane antigen"; (3) "Positron Emission Tomography" (Mesh) OR PET OR "positron emission tomography"; (4) "Multiparametric Magnetic Resonance Imaging" (Mesh) OR mpMRI OR "Magnetic Resonance Imaging" (Mesh) OR "magnetic resonance imaging" OR MRI; (5) prostat*; (6) "Prostatic Neoplasms" (Mesh) OR pCa OR cancer* OR tumor* OR carcinoma; (7) "Lymph Nodes" (Mesh) OR "lymph node*" OR "lymph nodal" OR "locoregional." The reference lists of identified publications were also hand-searched for potentially relevant studies.

Inclusion and Exclusion Criteria

Studies were eligible for inclusion if all the following criteria applied: (a) the diagnostic performance of ^{68}Ga-PSMA-11 PET/CT and mpMRI for pelvic lymph node staging prior to radical prostatectomy in PCa patients were clearly identified in the study or subset of the study; (b) the data were sufficient (i.e., patient number above 9) to construct a 2×2 contingency table; (c) the reference standard was histopathology confirmation from PLND, which should be clearly stated in the article. The exclusion criteria were (a) duplicated articles; (b) abstract, editorial comments, letters, case reports, review, or meta-analyses; and (c) clearly irrelevant titles and abstracts.

Using the aforementioned inclusion and exclusion criteria, two researchers independently screened titles and abstracts of the retrieved articles and then evaluated the full-text version of the remaining articles to determine their eligibility for inclusion. Disagreements between the researchers were resolved by consensus.

QUALITY ASSESSMENT

Two researchers independently assessed the quality of the included studies based on the Quality Assessment of Diagnostic Accuracy Studies (QUADAS-2) tool. Each study was evaluated based on the following domains: patient selection, index test, reference standard, and flow and timing. These domains were then evaluated according to the risk of bias and were rated regarding applicability as "high," "low," or "unclear." Disagreements between the researchers were resolved by consensus.

Data Extraction

Two researchers independently conducted data extraction for all included articles. The extracted data included the first author, study characteristics (year, country, study design, prevalence of PLNMs, extracted lymph node number, and reference standard), patient characteristics (number of patients, age, PSA level, and D'Amico risk stratification), and technical aspects (field strength and MRI sequence for mpMRI; injection dose, uptake time, and image analysis for ^{68}Ga-PSMA-11 PET/CT). For each study, the absolute numbers of true-positive, true-negative, false-positive, and false-negative data for mpMRI and ^{68}Ga-PSMA-11 PET/CT were extracted on a per-patient basis. Disagreements between the researchers were resolved by consensus.

Statistical Analysis

The pooled sensitivity and specificity for ^{68}Ga-PSMA-11 PET/CT and mpMRI were presented as estimates with 95% confidence intervals (CIs) by using random-effect analysis. The summary receiver-operating characteristic (SROC) curves were constructed, and the area under the curve (AUC) was calculated.

Heterogeneity among pooled studies was assessed by use of Cochrane Q and I^2 statistics. Values of I^2 equal to 25, 50, and

75% were assumed to represent low, moderate, and high heterogeneity, respectively. In case of substantial heterogeneity, meta-regression analysis was performed to explore the potential source of heterogeneity and the covariates were (1) number of patients included (>40 vs. ≤40); (2) ethnicity (Asian vs. the rest); (3) prevalence of PLNMs (>20% vs. ≤20%); (4) extracted lymph node number (>10 vs. ≤10); (5) reference standard (PLND vs. extended PLND); (6) PSA (>10 vs. ≤10); (7) D'Amico risk stratification (high risk vs. intermediate and high risk); (8) PET image analysis (visual vs. quantitative); (9) field strength (1.5 T vs. 3.0 T); and (10) MRI sequence (T2WI, DWI, and DCE vs. DWI and DCE). Publication bias was assessed by Deeks' funnel plot. All analyses were conducted with Stata 15.1 (Stata Corporation).

RESULTS

Literature Search and Study Selection

The initial search retrieved 414 articles, and 398 were excluded upon review of titles and abstracts. The remaining 16 articles were carefully assessed by full text, and another seven were excluded for the following reasons: insufficient reference standard (n = 2); data not retrievable for analysis (n = 2); not evaluated in the same patient population (n = 1); with only nodal-based data (n = 1); and tracers other than ^{68}Ga-PSMA-11 (n =1). Finally, nine articles including patient-based data on the head-to-head comparison of diagnostic performance of ^{68}Ga-PSMA-11 PET/CT and mpMRI were eligible for further analysis. A PRISMA flow diagram of the study selection process is shown in **Figure 1**.

Study Description and Quality Assessment

The study and patient characteristics of the nine articles comprising 640 patients are summarized in **Table 1**. The range of the prevalence of PLNMs for the included studies was 4% to 58.3%, and the median was 25%. The technical aspects of ^{68}Ga-PSMA-11 PET/CT and mpMRI were presented in **Table 2**.

The results of summary risk of bias and applicability concerns of each study are shown in **Figure 2**. The quality of the included studies was considered satisfactory.

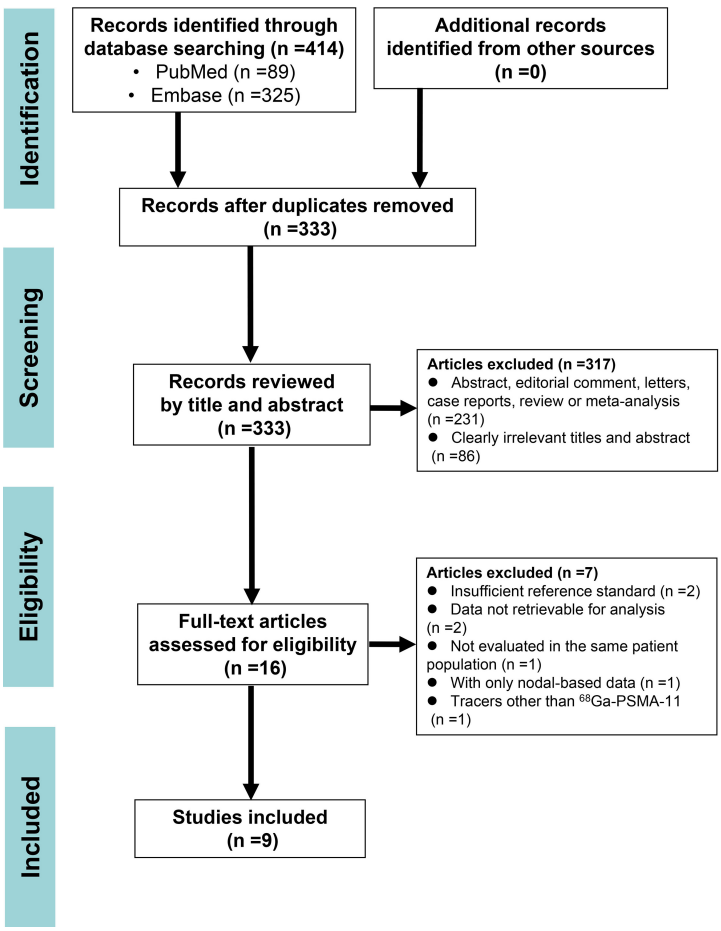

FIGURE 1 | The PRISMA flow diagram of study selection.

TABLE 1 | Study and patient characteristics of the included studies.

Author	Year	Country	Study characteristics				Patient characteristics			
			Study design	Prevalence of PLNMs	No. of extracted lymph node	Reference standard	No. of patients	Age (median, range)	PSA (median, range)	D'Amico risk stratification
Frumer et al. (28)	2020	Israel	Retro	13.5%	Median 9 Range 6–14	PLND	89	67 (64–70)	8.5 (5–15)	Intermediate 40; high risk 49
Franklin et al. (32)	2020	Australia	Retro	24.5%	Median 16 Range 1–53	PLND	233	68 (48–81)	7.4 (1.5–72.0)	Low risk 2; intermediate 90; high risk 141
Kulkarni et al. (26)	2020	India	Retro	45.7%	NA	PLND	35	NA	NA	Intermediate and high risk
Pallavi et al. (31)	2020	India	Pro	24.1%	NA	NA	29	NA	NA	NA
Van Leeuwen et al. (24)	2019	Netherlands and Australia	Retro	36.4%	Median 16 Range 12–21	ePLND	140	NA	9.4	Intermediate 30; high risk 110
Yilmaz et al. (23)	2019	Turkey	Retro	20.0%	NA	rPLND	10	NA	NA	Low risk 3; intermediate 15; high risk 6
Berger et al. (21)	2018	Australia	Retro	4%	Median 12 Range 3–22	PLND	50	649 ± 5.6	10.6 ± 8.1	NA
Gupta et al. (20)	2017	India	Retro	58.3%	Median 20	ePLND	12	61 (46–76)	24.3 (8.7–200.6)	High risk 12
Zhang et al. (19)	2017	China	Retro	35.7%	Median 7 Range 2–15	PLND	42	69 (55–82)	37.25 (7.2–348.)	Intermediate 17; high risk 25

NA, not available.

Diagnostic Performance of ^{68}Ga-PSMA-11 PET/CT for PLNMs

The pooled sensitivity and specificity for ^{68}Ga-PSMA-11 PET/CT were 0.71 (95% CI: 0.48–0.86) with moderate heterogeneity (75%) and 0.92 (95% CI: 0.88–0.95) with moderate heterogeneity (54%), respectively (**Figure 3**). **Figure 4** shows the SROC curve and the AUC for ^{68}Ga-PSMA-11 PET/CT was 0.92 (95% CI: 0.89–0.94).

Meta-regression analysis was performed to explore the sources of heterogeneity, and we identified that prevalence of PLNMs ($p = 0.01$ for specificity), PSA level ($p < 0.001$ for sensitivity and $p < 0.001$ for specificity), risk classification ($p < 0.001$ for sensitivity), and reference standard ($p < 0.001$ for specificity) were possible causes of heterogeneity for ^{68}Ga-PSMA-11 PET/CT. No publication bias was found ($p = 0.15$).

Diagnostic Performance of mpMRI for PLNMs

The pooled sensitivity and specificity for mpMRI were 0.40 (95% CI: 0.16–0.71) with high heterogeneity (86%) and 0.92 (95% CI: 0.80–0.97) with high heterogeneity (92%), respectively (**Figure 3**). **Figure 4** shows the SROC curve and the AUC for mpMRI was 0.82 (95% CI: 0.79–0.86).

Meta-regression analysis revealed that number of patients ($p < 0.001$ for specificity) and PSA level ($p < 0.001$ for sensitivity) were possible causes of heterogeneity. No publication bias was found ($p = 0.87$).

DISCUSSION

The present meta-analysis pooled patient-based data from nine studies which compared ^{68}Ga-PSMA-11 PET/CT and mpMRI in the same population. It was found that the former had higher sensitivity (0.71 vs. 0.40), similar specificity (0.92 vs. 0.92), and higher AUC (0.92 vs. 0.82) as compared with the latter. The resulting relativeness was in agreement with those (sensitivity, 0.65 vs. 0.41; specificity, 0.94 vs. 0.92; AUC, 0.92 vs. 0.83) from a previous meta-analysis, in which indirect comparisons (not in the same population) were made by including 13 studies (29). The higher trend of sensitivity and diagnostic accuracy of ^{68}Ga-PSMA-11 PET/CT over mpMRI for pelvic lymph node staging prior to radical prostatectomy in patients with intermediate to high-risk PCa were thus confirmed based on the most recent evidence. To better illustrate the imaging features of mpMRI and 68Ga-PSMA PET/CT in characterizing lymph node metastases, an example of one patient who had underwent both imaging modalities was shown in **Figure 5**.

Different interpreting strategies for small PLNMs between the two imaging modalities across the included studies might help to explain the better performance of ^{68}Ga-PSMA-11 PET/CT. While most of the mpMRI interpretations used the short-axis diameter of more than 10 or 8 mm as a determining factor for malignancy, all PET/CT interpretations decided PLNMs solely based on PSMA uptake, irrespective of the small size of lymph nodes. Thus, some small PLNMs without significant

TABLE 2 | Technical aspects of ^{68}Ga-PSMA-11 PET/CT and mpMRI scans.

Author	Year	mpMRI		^{68}Ga-PSMA-PET/CT		
		Field strength	MRI sequence	Injection dose	Uptake time (min)	Image analysis
Frumer et al. (28)	2020	3.0 or 1.5 T	T2WI, DWI, DCE	3–5 mCi	50–60	Visual
Franklin et al. (32)	2020	3.0 T	T2WI, DWI, DCE	Mean, 200 MBq	45–60	Visual
Kulkarni et al. (26)	2020	3.0 T	T2WI, DWI, DCE	3–4.5 mCi	60	Visual
Pallavi et al. (31)	2020	3.0 T	T2WI, DWI	Mean, 1.76 MBq/kg	60	Visual
Van Leeuwen et al. (24)	2019	3.0 or 1.5 T	T2WI, DWI, DCE	2.0 MBq/kg or 100 MBq	60 or 45	NA
Yilmaz et al. (23)	2019	3.0 T	T2WI, DWI, DCE	Median, 175 MBq	60	Quantitative
Berger et al. (21)	2018	3.0 T	T2WI, DWI	NA	60	Quantitative
Gupta et al. (20)	2017	1.5 T	T2WI, DWI	2 MBq/kg	60	Visual
Zhang et al. (19)	2017	3.0 T	T2WI, DWI, DCE	Median 131.7 MBq	60	Visual

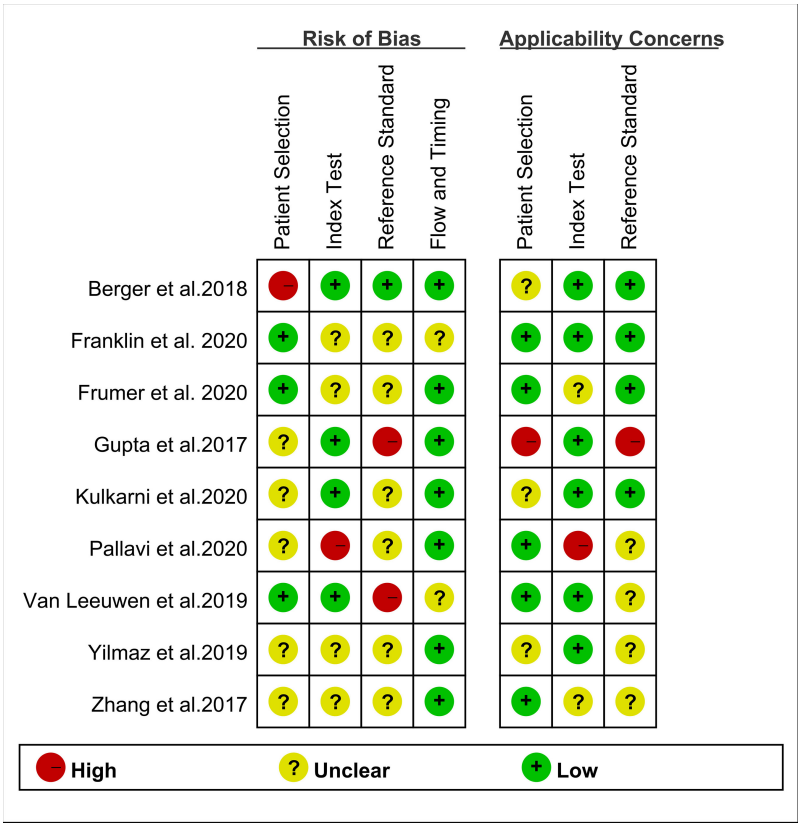

FIGURE 2 | Summary risk of bias and applicability concerns of the included studies.

anatomical characteristics might be only detected by PET/CT. In a study of 240 patients, Franklin et al. found that the median diameter of avid lymph nodes on ^{68}Ga-PSMA PET/CT were 7.0 mm (range, 0.5–40 mm), in comparison to 11.7 mm (range, 2.2–20 mm) for mpMRI. The per-patient sensitivity of PET/CT and mpMRI in this study was 48.3% and 22.4%, respectively (32).

Nevertheless, ^{68}Ga-PSMA-11 PET/CT still missed as many as 29% of the PLNMs identified by PLND according to the result of our meta-analysis. In a study of 140 patients, Van Leeuwen et al. reported that no lymph nodes detected < 2 mm and only 27% of the lymph node metastases 2 and 4 mm were detected by preoperative ^{68}Ga-PSMA-PET/CT (24). In a larger study of 208 patients, Yaxley et al. found that 85.4% of histologically positive LNs ≤ 5 mm in maximal diameter were missed by preoperative ^{68}Ga-PSMA PET/CT (34). It seems that the resolution of ^{68}Ga-PSMA PET/CT is still not sufficient to detect many microscopic diseases seen at histopathology, particularly those with a diameter <5 mm. However, since it has been reported that the presence of microscopic diseases is associated with late disease recurrence, similar to PLNMs with large diameter, the clinical impact of these radiographically

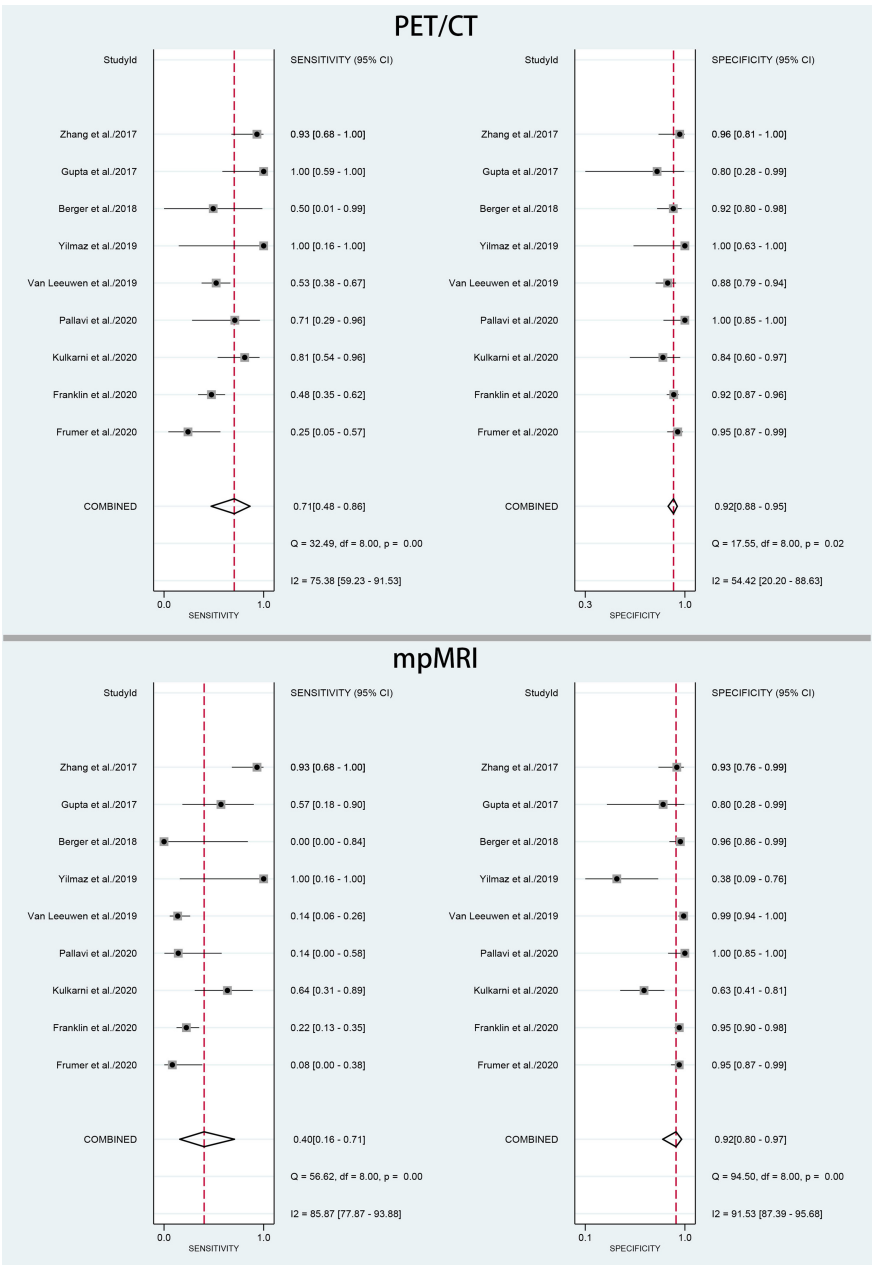

FIGURE 3 | Forest plot of pooled sensitivity and specificity of ^{68}Ga-PSMA-PET/CT and mpMRI for the detection of pelvic lymph node metastases prior to radical prostatectomy in PCa patients.

undetected microscopic diseases could be significant (35, 36). Therefore, despite its known limitations and complications, PLND remains necessary in that it could reveal microscopic diseases that might lead to early initiation of salvage radiotherapy and androgen deprivation therapy, which would eventually result in improved long-term local pelvic control and improved biochemical-free progression (2, 37).

On the other hand, according to the current EAU or NCCN guidelines, if the risk of a PLNM is >5% or >2%, respectively, PLND is recommended at the time of radical prostatectomy (38, 39). Based on the results of this meta-analysis, Fagan's nomogram indicated that when the pretest probability (prevalence of PLNMs) was assumed to be 25%, which is the medium value of our included studies, the negative posttest probability (the probability of being malignancy when the test is negative) decreased to 10% for ^{68}Ga-PSMA-11 PET/CT and 22% for mpMRI (**Figure 6**). Thus, negative test results from both imaging modalities leaves a residual malignancy risk of above 5%. In this regard, PLND still needs to

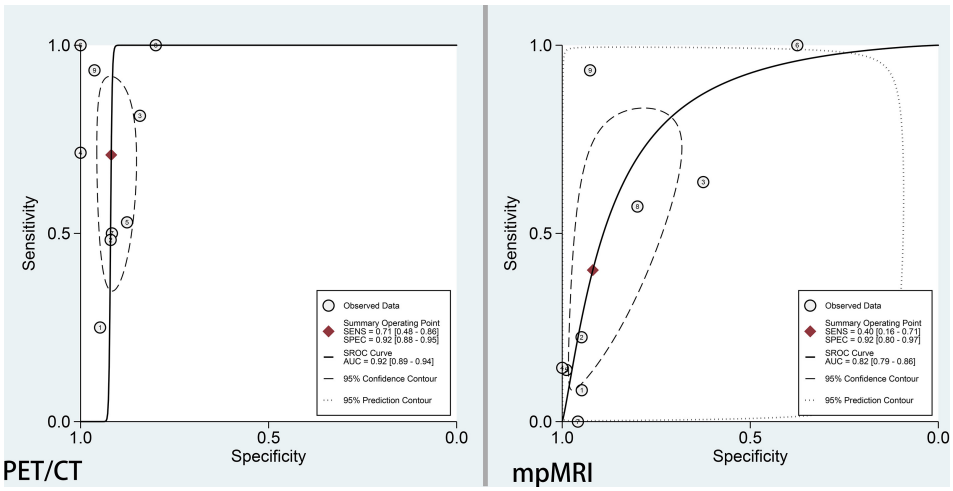

FIGURE 4 | SROC curve of ^{68}Ga-PSMA-PET/CT and mpMRI for the detection of pelvic lymph node metastases prior to radical prostatectomy in PCa patients.

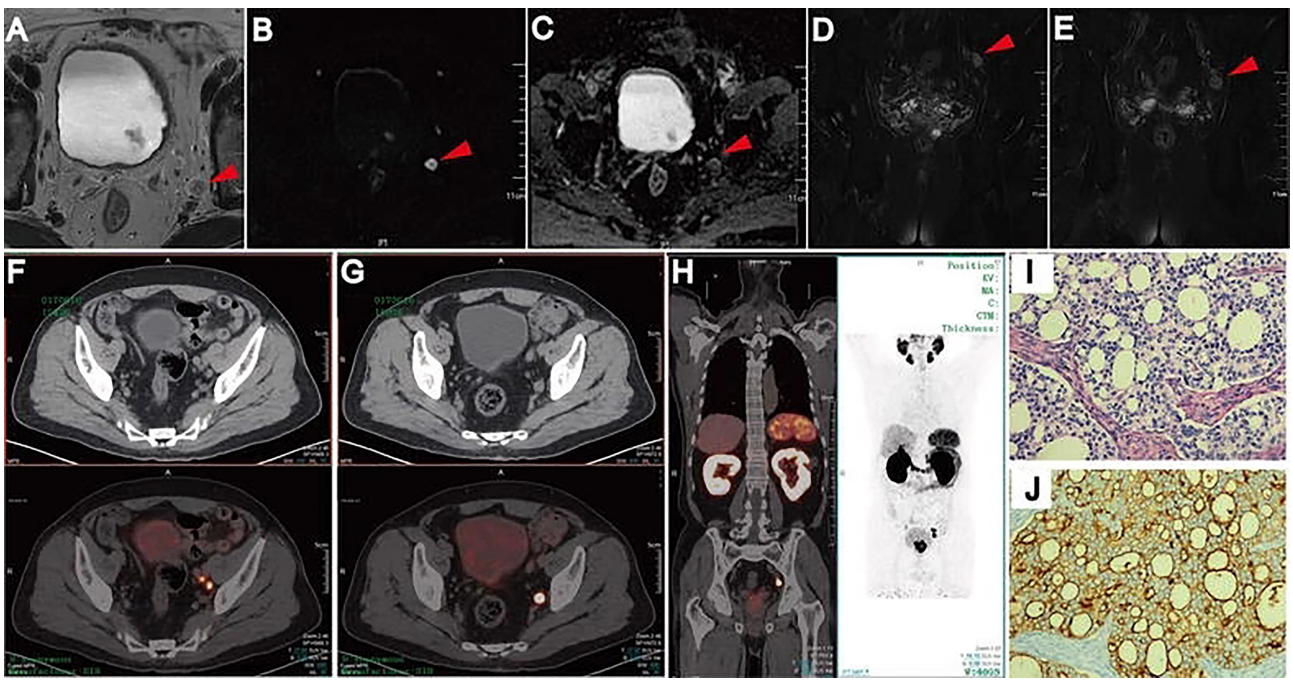

FIGURE 5 | Lymph node metastases on pelvic mpMRI and 68Ga-PSMA PET/CT. Axial T2WI **(A)**, DWI **(B)**, ADC **(C)**, and coronal Fat suppression T2WI **(D, E)**. Fused 68Ga-PSMA PET/CT **(F–H)** images were taken from left internal iliac and obturator fossa regions with histopathologically proven disease (HE staining, **(I)** PSMA IHC staining, **(J)**. Reproduced with permission from **Figure 2** of Zhang et al. (19).

be recommended if ^{68}Ga-PSMA PET/CT or mpMRI did not identify any suspicious lymph nodes.

In recent years, researchers have begun to incorporate ^{68}Ga-PSMA PET/CT and mpMRI parameters into comprehensive preoperative algorithms to evaluate the risk of PLNMs. Franklin et al. found that the combination of a negative ^{68}Ga-PSMA PET/CT, ISUP biopsy grade <4 and PIRADS <4 prostate mpMRI, or an ISUP grade 5 with PIRADS <3 on mpMRI was associated with a <5% risk of PLNMs (32). Ferraro et al. devised a model based on visual lymph node status on ^{68}Ga-PSMA PET/CT, total PSMA uptake of the primary tumor, PSA, and Gleason score, which showed a tendency to improve patient selection for PLND overprediction models using clinical risk factors (40). It is hoped that future nomograms incorporating not only clinical risk

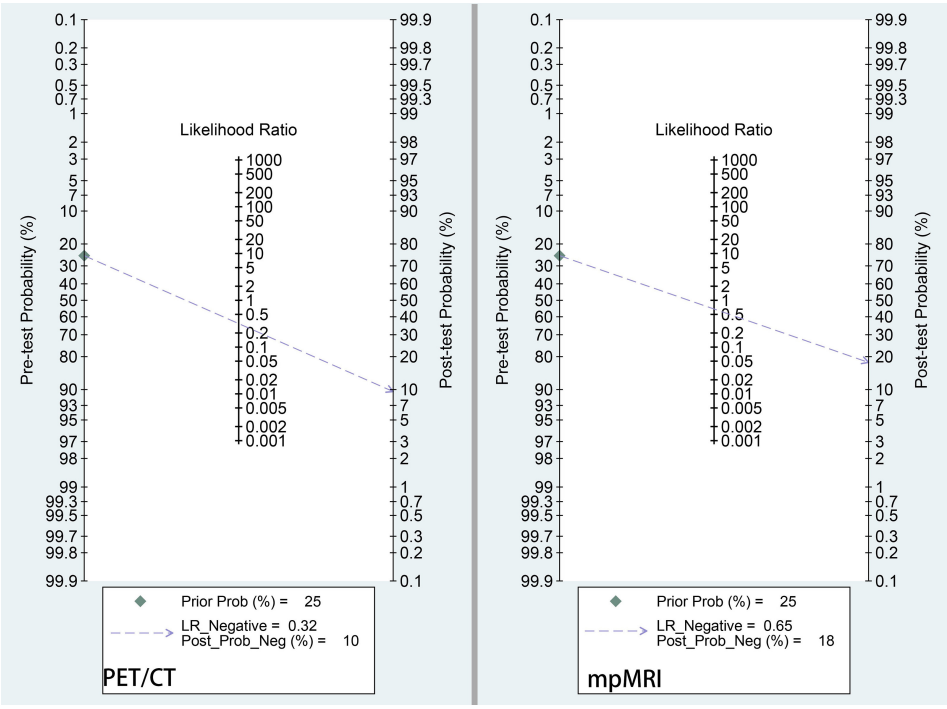

FIGURE 6 | Fagan nomogram of pretest probability and negative posttest probability for ^{68}Ga-PSMA-PET/CT and mpMRI. The pretest probability was set at 25%.

factors but also data from modern imaging modalities will help to more appropriately select candidates for PLND. Moreover, hybrid PET/MRI modality may offer incremental value for preoperative detection of PLNMs. In a 2018 study, Thalgott et al. demonstrated that ^{68}Ga-PSMA-11 PET/MRI even had a specificity of 100% in this setting (41).

Major limitations of our study include small sample size and heterogeneous study and patient characteristics and technical aspects of the included studies. We tried our best to perform subgroup analyses and found that number of patients, prevalence of PLNMs, PSA level, reference standard, and risk classification might be the sources of heterogeneity for the two imaging modalities. Besides, we only analyzed patient-based data in the present meta-analysis, because in clinical practice, it is difficult to precisely associate either PET or MRI findings with the histological results in a node-to-node manner and patients with one positive PLNM could provide enough prognostic information to alter patient management (34).

In conclusion, this meta-analysis of head-to-head comparison studies confirms that there is a trend toward a higher sensitivity and diagnostic accuracy of ^{68}Ga-PSMA-11 PET/CT compared to mpMRI for the detection of PLNMs in PCa patients. Nevertheless, according to current guidelines, PLND still needs to be recommended in case of negative results from ^{68}Ga-PSMA-11 PET/CT due to significant risk of malignancy. Hybrid PET/MRI modality exploiting both the superb molecular information from ^{68}Ga-PSMA-11 PET and the high local contrast of MRI may represent a future direction.

DATA AVAILABILITY STATEMENT

The original contributions presented in the study are included in the article/supplementary material. Further inquiries can be directed to the corresponding authors.

AUTHOR CONTRIBUTIONS

JB and HZ conceived and designed the study, which were proofed by JB. XW, QW, and FT collected and analyzed the data. XW and QW wrote the manuscript. All authors contributed to the article and approved the submitted version.

REFERENCES

1. Messing EM, Manola J, Yao J, Kiernan M, Crawford D, Wilding G, et al. Immediate Versus Deferred Androgen Deprivation Treatment in Patients With Node-Positive Prostate Cancer After Radical Prostatectomy and Pelvic Lymphadenectomy. *Lancet Oncol* (2006) 7(6):472–9. doi: 10.1016/s1470-2045(06)70700-8
2. Abdollah F, Karnes RJ, Suardi N, Cozzarini C, Gandaglia G, Fossati N, et al. Impact of Adjuvant Radiotherapy on Survival of Patients With Node-Positive Prostate Cancer. *J Clin Oncol* (2014) 32(35):3939–47. doi: 10.1200/jco.2013.54.7893

3. Briganti A, Chun FK, Salonia A, Suardi N, Gallina A, Da Pozzo LF, et al. Complications and Other Surgical Outcomes Associated With Extended Pelvic Lymphadenectomy in Men With Localized Prostate Cancer. *Eur Urol* (2006) 50(5):1006–13. doi: 10.1016/j.eururo.2006.08.015
4. Mottet N, van den Bergh RCN, Briers E, Van den Broeck T, Cumberbatch MG, De Santis M, et al. EAU-EANM-ESTRO-ESUR-SIOG Guidelines on Prostate Cancer-2020 Update. Part 1: Screening, Diagnosis, and Local Treatment With Curative Intent. *Eur Urol* (2021) 79(2):243–62. doi: 10.1016/j.eururo.2020.09.042
5. Carroll PH, Mohler JL. NCCN Guidelines Updates: Prostate Cancer and Prostate Cancer Early Detection. *J Natl Compr Canc Netw* (2018) 16(5s):620–3. doi: 10.6004/jnccn.2018.0036
6. Sanda MG, Cadeddu JA, Kirkby E, Chen RC, Crispino T, Fontanarosa J, et al. Clinically Localized Prostate Cancer: AUA/ASTRO/SUO Guideline. Part I: Risk Stratification, Shared Decision Making, and Care Options. *J Urol* (2018) 199(3):683–90. doi: 10.1016/j.juro.2017.11.095
7. Hövels AM, Heesakkers RA, Adang EM, Jager GJ, Strum S, Hoogeveen YL, et al. The Diagnostic Accuracy of CT and MRI in the Staging of Pelvic Lymph Nodes in Patients With Prostate Cancer: A Meta-Analysis. *Clin Radiol* (2008) 63(4):387–95. doi: 10.1016/j.crad.2007.05.022
8. de Kouchkovsky I, Aggarwal R, Hope TA. Prostate-Specific Membrane Antigen (PSMA)-Based Imaging in Localized and Advanced Prostate Cancer: A Narrative Review. *Transl Androl Urol* (2021) 10(7):3130–43. doi: 10.21037/tau-20-1047
9. Hennrich U, Eder M. [(68)Ga]Ga-PSMA-11: The First FDA-Approved (68) Ga-Radiopharmaceutical for PET Imaging of Prostate Cancer. *Pharmaceuticals (Basel)* (2021) 14(8):713. doi: 10.3390/ph14080713
10. Song H, Iagaru A, Rowe SP. FDA Approves (18)F-DCFPyL PET Agent in Prostate Cancer. *J Nucl Med* (2021) 62(8):11n. doi: 10.2967/jnumed.121.262989
11. Grünig H, Maurer A, Thali Y, Kovacs Z, Strobel K, Burger IA, et al. Focal Unspecific Bone Uptake on [(18)F]-PSMA-1007 PET: A Multicenter Retrospective Evaluation of the Distribution, Frequency, and Quantitative Parameters of a Potential Pitfall in Prostate Cancer Imaging. *Eur J Nucl Med Mol Imaging* (2021). doi: 10.1007/s00259-021-05424-x
12. Sun J, Lin Y, Wei X, Ouyang J, Huang Y, Ling Z. Performance of 18F-DCFPyL PET/CT Imaging in Early Detection of Biochemically Recurrent Prostate Cancer: A Systematic Review and Meta-Analysis. *Front Oncol* (2021) 11:649171. doi: 10.3389/fonc.2021.649171
13. Wondergem M, van der Zant FM, Broos WA, Knol RJ. Matched-Pair Comparison of (18)F-DCFPyL PET/CT and (18)F-PSMA-1007 PET/CT in 240 Prostate Cancer Patients; Inter-Reader Agreement and Lesion Detection Rate of Suspected Lesions. *J Nucl Med* (2021) 62(10):1422–1429. doi: 10.2967/jnumed.120.258574
14. Erdem S, Simsek DH, Degirmenci E, Aydin R, Bagbudar S, Ozluk Y, et al. How Accurate Is (68)Gallium-Prostate Specific Membrane Antigen Positron Emission Tomography/Computed Tomography [(68)Ga-PSMA PET/CT] on Primary Lymph Node Staging Before Radical Prostatectomy in Intermediate and High Risk Prostate Cancer? A Study of Patient- and Lymph Node- Based Analyses. *Urol Oncol* (2021) S1078–1439(21):00307–0. doi: 10.1016/j.urolonc.2021.07.006
15. Esen T, Falay O, Tarim K, Armutlu A, Koseoglu E, Kilic M, et al. (68)Ga-PSMA-11 Positron Emission Tomography/Computed Tomography for Primary Lymph Node Staging Before Radical Prostatectomy: Central Review of Imaging and Comparison With Histopathology of Extended Lymphadenectomy. *Eur Urol Focus* (2021) 7(2):288–93. doi: 10.1016/j.euf.2021.01.004
16. Tu X, Zhang C, Liu Z, Shen G, Wu X, Nie L, et al. The Role of (68)Ga-PSMA Positron Emission Tomography/Computerized Tomography for Preoperative Lymph Node Staging in Intermediate/High Risk Patients With Prostate Cancer: A Diagnostic Meta-Analysis. *Front Oncol* (2020) 10:1365. doi: 10.3389/fonc.2020.01365
17. Peng L, Li J, Meng C, Li J, You C, Tang D, et al. Can (68)Ga-Prostate Specific Membrane Antigen Positron Emission Tomography/Computerized Tomography Provide an Accurate Lymph Node Staging for Patients With Medium/High Risk Prostate Cancer? A Diagnostic Meta-Analysis. *Radiat Oncol* (2020) 15(1):227. doi: 10.1186/s13014-020-01675-4
18. Tulsyan S, Das CJ, Tripathi M, Seth A, Kumar R, Bal C. Comparison of 68Ga-PSMA PET/CT and Multiparametric MRI for Staging of High-Risk Prostate Cancer68ga-PSMA PET and MRI in Prostate Cancer. *Nucl Med Commun* (2017) 38(12):1094–102. doi: 10.1097/mnm.0000000000000749
19. Zhang Q, Zang S, Zhang C, Fu Y, Lv X, Zhang Q, et al. Comparison of (68)Ga-PSMA-11 PET-CT With mpMRI for Preoperative Lymph Node Staging in Patients With Intermediate to High-Risk Prostate Cancer. *J Transl Med* (2017) 15(1):230. doi: 10.1186/s12967-017-1333-2
20. Gupta M, Choudhury PS, Hazarika D, Rawal S. A Comparative Study of (68) Gallium-Prostate Specific Membrane Antigen Positron Emission Tomography-Computed Tomography and Magnetic Resonance Imaging for Lymph Node Staging in High Risk Prostate Cancer Patients: An Initial Experience. *World J Nucl Med* (2017) 16(3):186–91. doi: 10.4103/1450-1147.207272
21. Berger I, Annabattula C, Lewis J, Shetty DV, Kam J, Maclean F, et al. (68)Ga-PSMA PET/CT vs. mpMRI for Locoregional Prostate Cancer Staging: Correlation With Final Histopathology. *Prostate Cancer Prostatic Dis* (2018) 21(2):204–11. doi: 10.1038/s41391-018-0048-7
22. Meißner S, Janssen JC, Prasad V, Diederichs G, Hamm B, Brenner W, et al. Accuracy of Standard Clinical 3T Prostate MRI for Pelvic Lymph Node Staging: Comparison to (68)Ga-PSMA PET-Ct. *Sci Rep* (2019) 9(1):10727. doi: 10.1038/s41598-019-46386-3
23. Yilmaz B, Turkay R, Colakoglu Y, Baytekin HF, Ergul N, Sahin S, et al. Comparison of Preoperative Locoregional Ga-68 PSMA-11 PET-CT and mp-MRI Results with Postoperative Histopathology of Prostate Cancer. *Prostate* (2019) 79(9):1007–17 doi:10.1002/pros.23812
24. van Leeuwen PJ, Donswijk M, Nandurkar R, Stricker P, Ho B, Heijmink S, et al. Gallium-68-Prostate-Specific Membrane Antigen [(68) Ga-PSMA] Positron Emission Tomography (PET)/computed Tomography (CT) Predicts Complete Biochemical Response From Radical Prostatectomy and Lymph Node Dissection in Intermediate- and High-Risk Prostate Cancer. *BJU Int* (2019) 124(1):62–8. doi: 10.1111/bju.14506
25. Çelen S, Gültekin A, Özlülerden Y, Mete A, Sağtaş E, Ufuk F, et al. Comparison of 68Ga-PSMA-I/T PET-CT and Multiparametric MRI for Locoregional Staging of Prostate Cancer Patients: A Pilot Study. *Urol Int* (2020) 104(9-10):684–91. doi: 10.1159/000509974
26. Kulkarni SC, Sundaram PS, Padma S. In Primary Lymph Nodal Staging of Patients With High-Risk and Intermediate-Risk Prostate Cancer, How Critical Is the Role of Gallium-68 Prostate-Specific Membrane Antigen Positron Emission Tomography-Computed Tomography? *Nucl Med Commun* (2020) 41(2):139–46. doi: 10.1097/mnm.0000000000001110
27. Arslan A, Karaarslan E, Güner AL, Sağlıcan Y, Tuna MB, Kural AR. Comparing the Diagnostic Performance of Multiparametric Prostate MRI Versus 68ga-PSMA PET-CT in the Evaluation Lymph Node Involvement and Extraprostatic Extension. *Acad Radiol* (2020) S1076–6332(20):30427–X. doi: 10.1016/j.acra.2020.07.011
28. Frumer M, Milk N, Rinott Mizrahi G, Bistritzky S, Sternberg I, Leibovitch I, et al. A Comparison Between (68)Ga-Labeled Prostate-Specific Membrane Antigen-PET/CT and Multiparametric MRI for Excluding Regional Metastases Prior to Radical Prostatectomy. *Abdom Radiol (NY)* (2020) 45 (12):4194–201. doi: 10.1007/s00261-020-02640-1
29. Wu H, Xu T, Wang X, Yu YB, Fan ZY, Li DX, et al. Diagnostic Performance of (68)Gallium Labelled Prostate-Specific Membrane Antigen Positron Emission Tomography/Computed Tomography and Magnetic Resonance Imaging for Staging the Prostate Cancer With Intermediate or High Risk Prior to Radical Prostatectomy: A Systematic Review and Meta-Analysis. *World J Mens Health* (2020) 38(2):208–19. doi: 10.5534/wjmh.180124
30. Petersen LJ, Nielsen JB, Langkilde NC, Petersen A, Afshar-Oromieh A, De Souza NM, et al. (68)Ga-PSMA PET/CT Compared With MRI/CT and Diffusion-Weighted MRI for Primary Lymph Node Staging Prior to Definitive Radiotherapy in Prostate Cancer: A Prospective Diagnostic Test Accuracy Study. *World J Urol* (2020) 38(4):939–48. doi: 10.1007/s00345-019-02846-z
31. Pallavi UN, Gogoi S, Thakral P, Malasani V, Sharma K, Manda D, et al. Incremental Value of Ga-68 Prostate-Specific Membrane Antigen-11 Positron-Emission Tomography/Computed Tomography Scan for Preoperative Risk Stratification of Prostate Cancer. *Indian J Nucl Med* (2020) 35(2):93–9. doi: 10.4103/ijnm.IJNM_189_19
32. Franklin A, Yaxley WJ, Raveenthiran S, Coughlin G, Gianduzzo T, Kua B, et al. Histological Comparison Between Predictive Value of Preoperative 3-T

Multiparametric MRI and (68) Ga-PSMA PET/CT Scan for Pathological Outcomes at Radical Prostatectomy and Pelvic Lymph Node Dissection for Prostate Cancer. *BJU Int* (2021) 127(1):71–9. doi: 10.1111/bju.15134
33. Liberati A, Altman DG, Tetzlaff J, Mulrow C, Gøtzsche PC, Ioannidis JP, et al. The PRISMA Statement for Reporting Systematic Reviews and Meta-Analyses of Studies That Evaluate Health Care Interventions: Explanation and Elaboration. *J Clin Epidemiol* (2009) 62(10):e1–34. doi: 10.1016/j.jclinepi.2009.06.006
34. Yaxley JW, Raveenthiran S, Nouhaud FX, Samartunga H, Yaxley AJ, Coughlin G, et al. Outcomes of Primary Lymph Node Staging of Intermediate and High Risk Prostate Cancer With (68)Ga-PSMA Positron Emission Tomography/Computerized Tomography Compared to Histological Correlation of Pelvic Lymph Node Pathology. *J Urol* (2019) 201(4):815–20. doi: 10.1097/ju.0000000000000053
35. Pagliarulo V, Hawes D, Brands FH, Groshen S, Cai J, Stein JP, et al. Detection of Occult Lymph Node Metastases in Locally Advanced Node-Negative Prostate Cancer. *J Clin Oncol* (2006) 24(18):2735–42. doi: 10.1200/jco.2005.05.4767
36. Conti A, Santoni M, Burattini L, Scarpelli M, Mazzucchelli R, Galosi AB, et al. Update on Histopathological Evaluation of Lymphadenectomy Specimens From Prostate Cancer Patients. *World J Urol* (2017) 35(4):517–26. doi: 10.1007/s00345-015-1752-8
37. Touijer KA, Karnes RJ, Passoni N, Sjoberg DD, Assel M, Fossati N, et al. Survival Outcomes of Men With Lymph Node-Positive Prostate Cancer After Radical Prostatectomy: A Comparative Analysis of Different Postoperative Management Strategies. *Eur Urol* (2018) 73(6):890–6. doi: 10.1016/j.eururo.2017.09.027
38. Mottet N, Bellmunt J, Bolla M, Briers E, Cumberbatch MG, De Santis M, et al. EAU-ESTRO-SIOG Guidelines on Prostate Cancer. Part 1: Screening, Diagnosis, and Local Treatment With Curative Intent. *Eur Urol* (2017) 71(4):618–29. doi: 10.1016/j.eururo.2016.08.003
39. Mohler JL, Antonarakis ES, Armstrong AJ, D'Amico AV, Davis BJ, Dorff T, et al. Prostate Cancer, Version 2.2019, NCCN Clinical Practice Guidelines in Oncology. *J Natl Compr Canc Netw* (2019) 17(5):479–505. doi: 10.6004/jnccn.2019.0023
40. Ferraro DA, Muehlematter UJ, Garcia Schüler HI, Rupp NJ, Huellner M, Messerli M, et al. (68)Ga-PSMA-11 PET has the Potential to Improve Patient Selection for Extended Pelvic Lymph Node Dissection in Intermediate to High-Risk Prostate Cancer. *Eur J Nucl Med Mol Imaging* (2020) 47(1):147–59. doi: 10.1007/s00259-019-04511-4
41. Thalgott M, Düwel C, Rauscher I, Heck MM, Haller B, Gafita A, et al. One-Stop-Shop Whole-Body (68)Ga-PSMA-11 PET/MRI Compared With Clinical Nomograms for Preoperative T and N Staging of High-Risk Prostate Cancer. *J Nucl Med* (2018) 59(12):1850–6. doi: 10.2967/jnumed.117.207696

Conflict of Interest: The authors declare that the research was conducted in the absence of any commercial or financial relationships that could be construed as a potential conflict of interest.

Publisher's Note: All claims expressed in this article are solely those of the authors and do not necessarily represent those of their affiliated organizations, or those of the publisher, the editors and the reviewers. Any product that may be evaluated in this article, or claim that may be made by its manufacturer, is not guaranteed or endorsed by the publisher.

Advantages of publishing in Frontiers

OPEN ACCESS
Articles are free to read for greatest visibility and readership

FAST PUBLICATION
Around 90 days from submission to decision

HIGH QUALITY PEER-REVIEW
Rigorous, collaborative, and constructive peer-review

TRANSPARENT PEER-REVIEW
Editors and reviewers acknowledged by name on published articles

Frontiers
Avenue du Tribunal-Fédéral 34
1005 Lausanne | Switzerland

Visit us: www.frontiersin.org
Contact us: frontiersin.org/about/contact

REPRODUCIBILITY OF RESEARCH
Support open data and methods to enhance research reproducibility

DIGITAL PUBLISHING
Articles designed for optimal readership across devices

FOLLOW US
@frontiersin

IMPACT METRICS
Advanced article metrics track visibility across digital media

EXTENSIVE PROMOTION
Marketing and promotion of impactful research

LOOP RESEARCH NETWORK
Our network increases your article's readership